IAEA-TECDOC-1070

Techniques for high dose dosimetry in industry, agriculture and medicine

Proceedings of a symposium held in Vienna, 2–5 November 1998

INTERNATIONAL ATOMIC ENERGY AGENCY IAEA

The originating Section of this publication in the IAEA was:

Dosimetry and Medical Radiation Physics Section
International Atomic Energy Agency
Wagramer Strasse 5
P.O. Box 100
A-1400 Vienna, Austria

TECHNIQUES FOR HIGH DOSE DOSIMETRY IN INDUSTRY,
AGRICULTURE AND MEDICINE
IAEA, VIENNA, 1999
IAEA-TECDOC-1070
ISSN 1011–4289

Printed by the IAEA in Austria
March 1999

The IAEA does not normally maintain stocks of reports in this series.
However, copies of these reports on microfiche or in electronic form can be obtained from

INIS Clearinghouse
International Atomic Energy Agency
Wagramer Strasse 5
P.O. Box 100
A-1400 Vienna, Austria
E-mail: CHOUSE@IAEA.ORG
URL: http://www.iaea.org/programmes/inis/inis.htm

Orders should be accompanied by prepayment of Austrian Schillings 100,–
in the form of a cheque or in the form of IAEA microfiche service coupons
which may be ordered separately from the INIS Clearinghouse.

FOREWORD

A code of practice for the radiation sterilization of medical products was formulated in the mid-1960s as a result of an IAEA panel meeting. Today, radiation processing is an expanding technology offering potential technological advantages as well as safety and economy. Examples of the application of radiation in industry, agriculture and medicine include the sterilization of health care products, the irradiation of food, quarantine procedures and disease control, radiation therapy, polymer treatment, rubber vulcanization, the treatment of sewage sludge and stack gases, and biomass conversion.

In radiation processing, it is important that the irradiated products are reliable and safe. For processes that impact directly on public health, dosimetry provides a formal means of regulation. For other applications, measurements are indispensable for process control to improve quality and the measurements have to be standardized. Thus, dosimetry is an essential part of quality standards for radiation processes. In the developing world, establishment of such quality standards is only in the embryonic stage, and the IAEA should and does play a role in the development and implementation of these standards.

The IAEA initiated a programme of high dose dosimetry in 1977 to accomplish dose standardization on an industrial scale, to promote dosimetry as a quality control measure in radiation processing, and to help develop new dosimetry techniques. Since dosimetry has such a key role in these processes, the IAEA organized this international symposium to provide a forum for presentation and discussion of up-to-date developments in this field.

Since the International Symposium on High Dose Dosimetry for Radiation Processing held in 1990 the field of dosimetry has deepened and broadened. There is a definite shift towards quality assurance, which calls for dependable dosimetry systems with well established traceability to national or international standards. Also, many new applications of radiation have been developed and for these new and innovative dosimetry methods are needed. This symposium has provided a forum for the discussion of many of these developments and consideration of the outstanding issues in these vital areas.

The Scientific Secretary of the symposium and IAEA officer responsible for this publication was K. Mehta of the Division of Human Health.

EDITORIAL NOTE

In preparing this publication for press, staff of the IAEA have made up the pages from the original manuscripts as submitted by the authors. The views expressed do not necessarily reflect those of the IAEA, the governments of the nominating Member States or the nominating organizations.

Throughout the text names of Member States are retained as they were when the text was compiled.

The use of particular designations of countries or territories does not imply any judgement by the publisher, the IAEA, as to the legal status of such countries or territories, of their authorities and institutions or of the delimitation of their boundaries.

The mention of names of specific companies or products (whether or not indicated as registered) does not imply any intention to infringe proprietary rights, nor should it be construed as an endorsement or recommendation on the part of the IAEA.

The authors are responsible for having obtained the necessary permission for the IAEA to reproduce, translate or use material from sources already protected by copyrights.

CONTENTS

INFLUENCE QUANTITIES IN DOSIMETRY (Session 4)

MEDICAL AND OTHER APPLICATIONS (Session 5)

PROCESS VALIDATION (Session 6)

CALIBRATION AND TRACEABILITY (Session 7)

DOSIMETRY STANDARDS AND INTERCOMPARISIONS (Session 8)

OVERVIEW

(Session 1)

Chairperson

P. ANDREO
International Atomic Energy Agency

Invited Paper

RADIATION PROCESSING DOSIMETRY – PAST, PRESENT AND FUTURE

W.L. McLAUGHLIN
Ionizing Radiation Division, Physics Laboratory,
National Institute of Standards and Technology,
Gaithersburg, Maryland,
United States of America

Abstract

Since the two United Nations Conferences were held in Geneva in 1955 and 1958 on the Peaceful Uses of Atomic Energy and the concurrent foundation of the International Atomic Energy Agency in 1957, the IAEA has fostered high-dose dosimetry and its applications. This field is represented in industrial radiation processing, agricultural programmes, and therapeutic and preventative medicine. Such dosimetry is needed specifically for pest and quarantine control and in the processing of medical products, pharmaceuticals, blood products, foodstuffs, solid, liquid and gaseous wastes, and a variety of useful commodities, e.g. polymers, composites, natural rubber and elastomers, packaging, electronic, and automotive components, as well as in radiotherapy. Improvements and innovations of dosimetry materials and analytical systems and software continue to be important goals for these applications. Some of the recent advances in high-dose dosimetry include tetrazolium salts and substituted polydiacetylene as radiochromic media, on-line real-time as well as integrating semiconductor and diamond-detector monitors, quantitative label dosimeters, photofluorescent sensors for broad dose range applications, and improved and simplified parametric and computational codes for imaging and simulating 3D radiation dose distributions in model products. The use of certain solid-state devices, e.g. optical quality LiF, at low (down to 4K) and high (up to 500 K) temperatures, is of interest for materials testing. There have also been notable developments in experimental dose mapping procedures, e.g. 2D and 3D dose distribution analyses by flat-bed optical scanners and software applied to radiochromic and photofluorescent images. In addition, less expensive EPR spectrometers and new EPR dosimetry materials and high-resolution semiconductor diode arrays, charge injection devices, and photostimulated storage phosphors have been introduced.

1. INTRODUCTION

In 1956, a series of articles began to appear in microbiology journals, e.g. *J. Bacteriol.; Virol.; Appl. Microbiol.*, on the effects of ionizing radiation on the survival of micro-organisms. Ten years later, the first recommended "Code of Practice for the Sterilization of Medical Products" was formulated as a result of an IAEA panel meeting. It was published the following year as a document appended to the Proceedings of the IAEA Symposium on *Radiosterilization of Medical Products* [1]. In reviewing this Code of Practice, L. O. Kallings of the National Bacteriology Laboratory of Sweden observed that "Dosimetry should be the backbone of the control procedures on commissioning [radiation sterilization and processing] or where-ever the process parameters are altered [and] the dose distribution in a standard package has to be evaluated [2].

From the period of the two UN *Peaceful Uses of Atomic Energy* conferences in Geneva in 1955 and 1958 and since its foundation in 1957, the IAEA has supported broad and definitive world-wide programmes in industrial processing (e.g. sterilization and chemical processes), medical treatments (e.g. disease control and radiotherapy), environmental applications (e.g. waste mediation

and recycling), and agricultural measures (e.g. food irradiation and pest control), involving mainly high-power electron accelerator beams and large gamma-radiation sources. Radiation measurements continue to play a vital role in all these applications. This is reflected in the IAEA Symposia dedicated to dosimetry [3 – 7], as well as in numerous expert missions and training courses for Member States and Regional Areas, professional exchanges, and co-ordinated research projects. An example of the early interest in radiation processing and its control is the IAEA meeting held in Warsaw in September, 1959, on "Applications of Large Radiation Sources in Industry and Especially Chemical Processes". This took place during the exciting period when electron accelerators were first commissioned for sterilization of surgical sutures at the 6 MeV, 4 kW Linac at Ethicon, Inc. NJ, USA [8], and for other sterilization and radiation processing purposes at the 10 MeV, 10 kW Linac at Risø, Denmark, at the 3 MeV, 6 kW van de Graaff accelerator at Leybold's Hochvakuum Anlagen in Cologne, Germany, and at the 3 MeV 20 kW DC Dynamitron accelerator at Radiation Dynamics, Inc. in Westbury LI NY, USA. Almost simultaneously large gamma-ray sources were being commissioned for processing also at Ethicon, Inc., at the UK Atomic Energy Authority at Wantage, at Conservatome in Dagneux near Lyon, France, and at Gamma Sterilization Pty, Ltd. in Dandenong near Melbourne, Australia.

Since then, significant advances in radiation processing are represented by major commercial successes with sterilization, wire and cable manufacturing, heat-shrinkable film and tubing production, and polymer, elastomer and composite cross-linking. In addition, radiation applied to quarantine control of meats, seafood, grains, and produce, and to various foods and to pollution abatement is promising. Dosimetry helps achieve and maintain good manufacturing practice and to satisfying regulatory requirements, any major radiation application affecting public health and safety.

2. DOSIMETRY SYSTEMS

From the beginning of this decade, when the IAEA Symposium on *High-Dose Dosimetry for Radiation Processing* was held in Vienna [7], notable progress has been made in several key areas. Many involve the development of numerous standard guides and practices developed by the American Society for Testing and Materials (ASTM)[9, 10]. A number of new advances are featured in the present symposium, and lead us to the future of dosimetry for industry, agriculture, and medicine on an international scale.

Table I lists some of the successful and established dosimetry systems for reference and/or routine radiation processing applications. Also listed are the analytical methods, approximate useful ranges of absorbed dose, and the ASTM Standard Practice numbers. Table II presents some newer dosimeters, detectors, and dose monitoring systems that show promise for the future. The latest developments of many from both groups are included in these proceedings.

A number of these novel dosimetry systems constitute significant advances in practical radiation processing, providing more efficient and accurate means of assuring that a given process is meeting specifications. A sampling of new dosimetry developments is listed as follows:

- *Free-radical systems* – polyolefins or silicone as binders for EPR analysis of alanine in the form of pellets or thin films [11, 12].
- *Radiochromic films or solutions* – Tetrazolium salts for liquid or film systems for broad dose range applications [13-15] and GafChromic film systems for relatively low doses (radiotherapy, blood irradiation, insect population control, food irradiation) [16-18], as measured spectrophotometrically.
- *Dye solutions and films* – Aqueous alcohol or polyvinyl alcohol solutions of methylene blue, methyl orange, or congo red, which bleach upon irradiation and are measured with a spectrophotometer or densitometer. These may be used for either large-scale liquid-phase dosimetry or for inexpensive routine processing dosimetry [19-21].

TABLE I. DOSIMETRY SYSTEMS FOR RADIATION PROCESSING [9, 56, 57]

System	Method of Analysis	Useful Dose Range, kGy	ASTM Practice No.
Calorimeters	heat meas. by thermistor or thermocouple	0.001 – 50	E 1631
Fricke solution	UV spectrophotometry	0.02 – 0.40	E 1026
Dichromate sol.	UV or vis. spectrophotometry	2.0 - 50	E 1401
Ceric – cerous sol.	UV or vis. spectrophotometry electrochem. potentiometry	0.5 – 50	E 1205
Radiochromic sol.	vis. spectrophotometry	0.01 – 40	E 1540
Ethanol chlorobenzene sol.	vis.spectrophot or HF conduct.	0.02 – 2000	E 1538
Alanine pellets or film	EPR spectrometry	0.001 – 100	E 1607
Polymethylmethacrylate	vis. spectrophotometry	0.1 – 100	E 1276
Radiochromic film	vis. spectrophot. or densitometry	0.1 – 100	E 1276
Cellulose triacetate film	UV or vis. spectrophotometry	5 – 1000	E 1650
Lithium fluoride crystal	UV or vis. spectrophotometry	0.5 – 20,000	-----
Radiochromic optical waveguide	vis. spectrophot., densitometry or photometry	0.01 – 10	E 1310

TABLE II. NOVEL APPROACHES TO DOSIMETRY AND DOSE MONITORING

System	Sensor Components	Method of Analysis	Useful Dose Range, kGy
Radiochromic poly-diacetylene film	substit. polydiactylene coating on film	vis. spectrophot.	0.001 – 50
Tetrazolium salt in polymer	tetrazolium chloride in polyvinyl alcohol	vis. spectrophot. or densitometry	1 – 50
Tetrazolium salt solution	tetrazolium chloride in aqueous alcohol	vis. spectrophot.	1 – 100
Bleachable dye solution	methylene blue, congo red, etc. in aqueous alcohol	vis. spectrophot.	0.05 – 30
Optically stimulated luminescent film	inorganic salts in polymer	vis. spectrofluorimetry	0.01 – 100
Polyethylene film	low- or high-density polyethylene	Fourier-transform IR spectrophot.	0.01 – 1000
Inorganic crystals	SiO_2, Al_2O_3, or $CaSO_4$:Dy in polymer	EPR spectrometry	0.01 – 10,000
Bipolar; MOSFET; or p-FET transistors	silicon- or rare-earth-base devices	electrical load (voltage) signal	0.001 – 100
Diamond probe, film or disk	diamond (carbon) crystal or sintered film	electrical load (current) signals	dose-rate meas. up to 10^3 Gy/min

- *Photoluminescent systems* – Sunna dosimeter films for single-point or 2D imaging, readout by spectrofluorimetry, phosphor imaging systems or semiconductor micro-diode arrays [22-25].
- *Opaque radiochromic labels* – Diffuse reflection spectrophotometric readout of colour-changing labels and opalescent media (e.g. dyed paper or coated films) [25-28].
- *Optical waveguides* – Radiochromic fibre optics for food irradiation dosimetry or for real-time dose monitoring [29].
- *Polymers* – Polyethylene film readout by ultraviolet (UV) or Fourier transform infrared (FTIR) spectrophotometry [30, 31].
- *Semiconductor or solid-state chips* – bipolar, p-FET, or MOSFET transistors, diamond detectors, or pure LiF crystals, as active or passive dosimeters for broad dose and dose-rate ranges [32-36].
- *Conductimetric systems* – Liquid solutions or solid matrices which can be readout by high-frequency (oscillometric) or steady-state conductimetry [25].

3. STANDARDIZATION AND TRACEABILITY

The Bureau International des Poids et Mesures (BIPM) in Sevres near Paris has recently announced plans to coordinate a high-dose dosimetry intercomparison for national standards laboratories. This will expand its scope beyond radiotherapy-level doses to those of interest here, especially for radiation processing with ionizing photons and electrons.

National and reference standard transfer dosimetry systems, such as calorimeters and dedicated chemical systems (e.g. Fricke, dichromate, ethanol-chlorobenzene, and alanine), have undergone significant advances. Examples of new calorimeters for electron beam calibrations are the portable graphite system at NPL (UK) [37], graphite, water, and polystyrene calorimeters for day-to-day routine monitoring of beam parameters, supplied by Risø National Laboratory (Denmark) [38], and modular graphite calorimeters developed at NIST (USA) [39]. The alanine/EPR system has also been further refined for transfer reference and routine dosimetry of gamma rays, electrons, and heavy particles, for doses ranging from radiotherapy levels and food irradiation to the highest sterilizing doses [40].

4. PROCESS VALIDATION AND VERIFICATION

As essential dosimetric components of the commissioning and implementing of radiation processes, important developments have been made in experimental dose-mapping procedures [41, 42], and mathematical modeling of dose distributions and minimum and maximum doses in irradiated products [43-46]. Some of the available computational codes for mathematical modeling of processing facility design, dose mapping, and dose prediction are shown in Table III.

TABLE III. AVAILABLE COMPUTATIONAL SOFTWARE CODES FOR MATHEMATICAL MODELING (EMPHASIS IS GIVEN TO THOSE IN BOLDFACE) [43 - 46]

ADEPT	EZTRAN	
GEANT	ZTRAN	
EDMULT	TIGER	
ETRAN	ACCEPT	
EGS4	CLYTRAN	**ITSv3.0**
CEPXS/ONELD	XGEN	
SANDYL	**MCNP4A&B**	

Studies of the effects on high-dose dosimeters of various influence parameters, e.g. dose rate, temperature, relative humidity, ambient light, storage conditions, have been made [47].

Novel methods to measure doses within liquid, grain, aerosol, or sludge flow systems have been devised, involving powder/EPR analysis, dye film, or electronic sensors [19, 48-50]. Quantitative label dosimeters are finally reaching a viable stage for routine use in radiation processing, especially for food and pharmaceutical processing [26-28].

5. KEY LITERATURE SOURCES

The scientific journal, *Radiation Physics and Chemistry* (RPC), published by Elsevier Science Ltd., Amsterdam, publishes monthly international peer-reviewed articles on radiation processing and dosimetry related to this field. The IAEA symposia proceedings and other technical documents, the ASTM standard guides and practices [9], the reports of the Panel on Gamma and Electron Irradiation [51], the Newsletter of the Association Internationale d'Irradiation Industrielle (AIII) [52], International Standards Organization (ISO) standards and technical reports [53], European Committee for Standardization (CEN) standards [54], technical information reports of the US Association for the Advancement of Medical Instrumentation (AAMI) [55], and the series of ten (so far) proceedings of the International Radiation Processing Meetings (which began in 1977 and are published by RPC), continue to provide essential recognition and processing guidelines to practitioners and users of high-dose dosimetry. The widely used *Manual on Food Irradiation Dosimetry* was published in 1977 by the IAEA [56] and is presently being revised. A comprehensive text covering dosimetry for radiation processing is found in reference [57].

REFERENCES

[1] IAEA, "Recommended Code of Practice for Radiosterilization of Medical Products", *Radiosterilization of Medical Products*, Proc. Symp., Budapest, June 1967 and Panel Meeting Results, Vienna, Dec. 1966, IAEA STI/PUB/157, Vienna (1967) 422 –431.

[2] KALLINGS, L.O., "Review of the Code of Practice for Radiosterilization of Medical Products", *loc. cit.*, 433 – 442.

[3] IAEA, *Dosimetry in Agriculture, Industry, Biology, and Medicine*, Proc. Symp., Vienna, April 1972, IAEA STI/PUB/311, Vienna (1973).

[4] IAEA, *Biomedical Dosimetry*, Proc. Symp., Vienna, April 1974, IAEA STI/PUB/401, Vienna (1981).

[5] IAEA and WHO, *Biomedical Dosimetry: Physical Aspects, Instrumentation, Calibration*, Proc. Symp. Paris, October 1980, IAEA STI/PUB/567, Vienna (1981).

[6] IAEA, *High-Dose Dosimetry*, Proc. Symp. Vienna, October 1984, IAEA STI/PUB/671, Vienna (1985).

[7] IAEA, *High Dose Dosimetry for Radiation Processing*, Proc. Symp. Vienna, November 1990, IAEA STI/PUB/846, Vienna (1991).

[8] ARTANDI, C., VAN WINKLE, W., "Electron-beam sterilization of surgical sutures", *Nucleonics* **17** (3) (1959) 86-90.

[9] ASTM, *Annual Book of ASTM Standards*, Section 12, Vol. **12.02**, Nuclear, Solar, and Geothermal Energy, American Society for Testing and Materials, West Conshohocken PA, USA 19428 (1998).

[10] FARRAR IV, H., "Dosimetry standards for radiation processing" (1998) these Proceedings, Paper IAEA-SM-356/R7.

[11] JANOVSKÝ, I., "Progress in alanine film/ESR dosimetry, *High Dose Dosimetry for Radiation Processing* (Proceedings of Symposium, Vienna, 1990) IAEA STI/PUB/846, International Atomic Energy Agency, Vienna (1991) pp. 173 – 187.

[12] UREÑA-NUÑEZ, F., FLORES, M.J., ZUAZUA, M.P., SECKER, D.A., COOGAN, J.J., ROSOCHA, L.A., "Use of alanine-silicone pellets for electron dosimetry. Determination of a three-dimensional dose profile of an irradiation chamber", *Appl. Radiat. Isotopes* **46** (1995) 813 - 818.

[13] KOVÁCS, A., WOJNÁROVITS, L., McLAUGHLIN, W.L., EBRAHIM EID, S.E., MILLER. A., "Radiation- chemical reaction of 2,3,5-triphenyl-tetrazolium chloride in liquid and solid state", *Radiation Chemistry* (Prceedings of 8th Tihany Symposium, Balatonszeplak, Hungary, 1994); *Radiat. Phys. Chem.* **47** (1996) 483 - 486.

[14] AL-SHEIKHLY, A. McLAUGHLIN, W.L., CHRISTOU, A., KOVACS, A., "Radiochromic blue tetrazolium film dosimeter" (1998) these Proceedings, Paper IAEA-SM-356/62.

[15] PIKAEV, A.K., KRIMINSKAYA, Z.K. "Use of tetrazolium salts in dosimetry of ionizing radiation", (Proceedings of 10th International Meeting on Radiation Processing, Anaheim CA, 1997); *Radiat. Phys. Chem.* **52** (1998) 555 – 561.

[16] McLAUGHLIN, W.L., PUHL, J.M., AL-SHEIKHLY, M., CHRISTOU, C.A., MILLER, A., KOVÁCS, A., WOJNÁROVITS, L., LEWIS, D.F., "Novel radiochromic films for clinical dosimetry", *Solid State Dosimetry (*Proceedings 11th International Conference, Part II, Budapest, 1995); *Radiat. Prot. Dosimetry* **66** (1996) 263-268.

[17] McLAUGHLIN, W.L., O'HARA, K.P., "The importance of reference standard and routine absorbed-dose measurements in blood irradiation", (Proceedings of AABB Annual Meeting, Orlando FL, 1996) American Association of Blood Banks, 8101 Glenbrook Rd., Bethesda MD, 20814 (1996).

[18] WALKER, M.L., DICK, C.E., McLAUGHLIN, W.L., "Remote real-time dose measurements of gamma-ray photon beams with radiochromic sensors ", *Nucl. Instr. Meth. Phys. Res.* **B79** (1993) 835-837.

[19] KOVÁCS, A., WOJNÁROVITS, L., KURUCZ, C., AL-SHEIKHLY, M., McLAUGHLIN, W.L., "Large-scale dosimetry using dilute methylene blue dye in aqueous solution", (Proceedings 11th International Meeting on Radiation Processing, Anaheim CA, 1997); *Radiat. Phys. Chem.* **52** (1998) 539-542.

[20] CHUNG, W.H., MILLER, A., "Film dosimeters based on methylene blue and methyl orange in polyvinyl alcohol", *Nucl. Technol.* **106** (1994) 261-264.

[21] KHAN, H.M., ANWER, M., "Characterization of aqueous solution of congo red for food irradiation dosimetry" (1998) these Proceedings, Paper IAEA-SM-356/22.

[22] McLAUGHLIN, W.L., MILLER, S.D., SAYLOR, M.C., KOVÁCS, A., WOJNÁROVITS, L., "A preliminary communication on an inexpensive mass-produced high-dose polymeric dosimeter based on optically-stimulated luminescence", *Radiat. Phys. Chem.* (1999) in press.

[23] McLAUGHLIN, W.L., PUHL, J.M., KOVÁCS, A., BARANYAI, M., SLEZSÁK, I., SAYLOR, M.C., SAYLOR, S.A., MILLER, S.D., MURPHY, M., "Work in progress. Sunna Dosimeter: An integrating photoluminescent film and reader system", Proceedings 9th Int. Sympos. on Radiation Chemistry, Tata, Hungary, 1998; R*adiat. Phys. Chem.* (1999) in press.

[24] KOVÁCS, A., BARANYAI, M., WOJNÁROVITS, L., SLESZÁK, I., McLAUGHLIN, W.L., MILLER, S.D., "Applicability of a polymeric dosimeter film based on optically stimulated luminecence for process control" (1998) these Proceedings, Paper IAEA-SM-356/27.

[25] SLEZSÁK, I., KOVÁCS, A., McLAUGHLIN, W.L., MILLER, S.D., "Development of oscillo-metric, fluorimetric and photometric evaluation methods for process control in radiation processing" (1998) these Proceedings, Paper IAEA-SM-356/28.

[26] EHLERMANN, D.A.E., "Validation of a label dose meter with regard to dose assurance in critical applications as quarantine control" (1998) these Proceedings, Paper IAEA-SM-356/38.

[27] ABDEL-FATTAH, A.A., EL-KELENY, M., ABDEL-REHIM, F., "Development of a radiation-sensitive indicator", *Radiat. Phys. Chem.* **48** (1996) 497 – 503.

[28] VARMA, S.S., DONAHUE, J.M. "A new radiochromic film for dosimetry during interventional procedures", Paper WIP-D-4 of AAPM Annual Meeting Works in Progress, San Antonio, TX (1998) available from Advanced Materials, International Specialty Products, Inc., 1361 Alps Rd., Wayne, NJ, 07470, USA

[29] AL-SHEIKHLY, M., McLAUGHLIN, W.L., HSU, C.-K., CHRISTOU, A., "Radiochromic gel-core fluorinated-polyethylene-polypropylene fiber optics for distributed sensing of X and gamma rays", (Proceedings of Photonics West, San Jose CA 1997).

[30] ABDEL-FATTAH, A.A., EBRAHEEM, S., ALI, Z.I., ABDEL-REHIM, F. "Ultraviolet and infrared spectral anaysis of irradiated polyethylene films: Correlation and possible application for large-dose radiation dosimetry", *J. Appl. Polymer Sci.* **67** (1998) 1837-1851.

[31] McLAUGHLIN, W.L., SILVERMAN, J., AL-SHEIKHLY, M., CHAPPAS, W.J., LIU ZHAN-JUN, MILLER, A., BATSBERG-PEDERSEN, W., "High-density polyethylene dosimetry by transvinylene FTIR analysis", *Radiat. Phys. Chem.* (1999) in press.

[32] HARTSHORN, A. MACKAY, G., SPENDER, M., THOMSON, I., "Absorbed dose mapping in self-shielded irradiators using direct reading MOSFET dosimeters", (abstract published in Proceedings of Health Physics Society Annual Meeting, Boston, July, 1995), full monograph available from Thomson and Nielsen Electronics, 25E Northside Rd., Nepean, Ontario, Canada K2H 8S1.

[33] FUOCHI, P.G., LAVALLE, M., GOMBIA, E., MOSCA, R., KOVÁCS, A., VITANZA, A., PATTI, A., "On the use of a bipolar power transistor as routine dosimeterin radiation processing" (1998) these Proceedings, Paper IAEA- SM-356/47.

[34] BUEHLER, M.G., MARTIN, D.P., "p-FET dosimeters for the radiation sterilization industry", *EMI Tech. Note No. 1,* (1998) 1-4.

[35] SHU, D., KUZAY, T.M., FANG YUE, BARRAZA, J., CUNDIFF, T., "Synthetic diamond-based position-sensitive photoconductive detector development for the Advanced Photon Source", *J. Synchrotron Radiat.* **5** (1998) 636 –638.

[36] McLAUGHLIN, W.L., "Colour centres in LiF for measurement of absorbed doses up to 100 Mgy", *Radiat. Prot. Dosimetry* **66** (1966) 197-200.

[37] McEWEN, M.R., DUANE, S., "Development of a portable graphite calorimeter for photons and electrons" (1998) these Proceedings, Paper IAEA-SM-356/55.

[38] MILLER, A., KOVÁCS, A,, "Calorimeters for documentation of radiation processing" (1998) these Proceedings, Paper IAEA-SM-356/59.

[39] McLAUGHLIN, W.L., WALKER, M.L., HUMPHREYS, J.C., "Calorimeters for calibration of high-dose dosimeters in high-energy electron beams", (Proceedings of 9th International Meeting on Radiation Processing, Istanbul, 1994); *Radiat. Phys. Chem.* **46** (1995) 1235 – 1242.

[40] REGULLA, D.F., 'EPR dosimetry- present and future"(1998) these Proceedings, paper IAEA-SM-356/R4.

[41] MILLER, A. "Scanner dosimetry system", Risø National Laboratory Report, Roskilde, Denmark (1997), private communications

[42] WALKER, M.L., McLAUGHLIN, W.L., PUHL, J.M., GOMES, P., "Radiation-field mapping of insect irradiation cannisters", *Appl. Radiat. Isotopes* **48** (1997) 117 – 125.

[43] WEISS, D.E., KENESK, R.P., "Complete model description of an electron beam using ACCEPT monte carlo simulation code", (Proceedings of *RadTech '94 North America UV/EB Conf. and Exhibition,* Vol. 1 (1994) pp. 130 - 149.

[44] SAYLOR, M.C., BARYSCHPOLEC, S.W., HURWITZ, L.M., McLAUGHLIN, W.L., "Radiation process data, analysis, and interpretation", *Sterilization of Medical Products,* Vol. **6** (MORRISSEY, R.F., Ed.) Polysciences Publications Inc., Morin Heights, Canada (1993) pp. 240 – 260.

[45] HENDRICKS, J.S., "MCNP – A General Monte Carlo Code", Transports Methods Group, Los Alamos Laboratory (1997).

[46] FLOYD, J.E., CHAPPAS, W.J. "Dose-depth simulations in standard construction geometries", *Radiat. Phys. Chem.* **48** (1996) 179 --194.

[47] CHU, R.D. "Variation of influence quantities in industrial irradiators and their effect on dosimetry performance"(1998) these Proceedings, Paper IAEA-SM-356/R3.

[48] NABLO, S.V., WOOD Jr., J.C., DESROSIERS, M.F., NAGY, V.Y., "A fluidized bed process for electron sterilization of powders, *Radiat. Phys. Chem.* (1999) in press.

[49] EHLERMANN, D.A.E., "The suitability of intrinsic and added materials as dose meters for radiation processing of particulate foods", *Radiat. Phys. Chem.* **36** (1990) 609 – 612; see also EHLERMANN, D.A.E., DELINCEE, H., "Dosimetry and process control for radiation processing of bulk quantities of particulate foods" (Proceedings 7th International Meeting on Radiation Processing, Noordwijkerhout, Netherlands, 1989); *Radiat. Phys. Chem.* **35** (1990) 836 – 840.

[50] BENNY, P.G., BHATT, B.C., "Investigation of TL properties of sand collected from sludge as an 'in situ' dosimeter", *Appl. Radiat. Isotopes* **47** (1996) 115 – 121; see also BENNY, P.G., BHATT, B.C., SHAH, M.R., "TL dosimetry using extracted and cleaned sand to measure gamma-ray dose rate at a liquid sludge irradiation facility", *Radiat. Phys. Chem.* **49** (1997) 377 – 381.

[51] Panel on Gamma & Electron Irradiation, "Guidance notes on the dosimetric aspects of dose-setting methods", *Panel Guidance Note,* 525 Chesham House, 29-30 Warwick St., London, W1R 5RD, UK (Dec. 1996).

[52] AIII, *Newsletter,* No. **25,** Vols. **1** and **2**, Association Internationale d'Irradiation Industrielle, 59 Route de Paris, 69260 Carbonnièrres-les Bains, France, (1992).

[53] ISO, "Sterilization of health care products – Requirements for validation and routine control – Radiation sterilization", International Organization for Standardization, Case Postale 56, CH-1211, Geneve 20, Switzerland (1995).

[54] CEN, "Sterilization of medical devices – Validation and routine control of sterilization by irradiation" *European Standard* **EN 552**, European Committee for Standardization, Central Secretariat: rue de Stassart 36, B-1050 Brussels, Belgium (1994).

[55] AAMI, "Dosimetry for monitoring gamma irradiation sterilization of medical products", *AAMI-TIR-5* Association for the Advancement of Medical Instrumentation, 3330 Washington Blvd., Suite 4001, Arlington VA, USA (1989).

[56] CHADWICK, K.H., EHLERMANN, D.A.E., McLAUGHLIN, W.L., *Manual of Food Irradiation Dosimetry,* Technical Reports Series 178, IAEA STI/DOC/10/178, Vienna (1978).

[57] McLAUGHLIN, W.L., BOYD, A.W., CHADWICK, K.H., McDONALD, J.C:, MILLER, A., *Dosimetry for Radiation Processing,* Taylor and Francis, London (1989)

HIGH-DOSE DOSIMETRY PROGRAMME OF THE IAEA

XA9949699

K. MEHTA
Dosimetry and Medical Radiation Physics Section,
International Atomic Energy Agency,
Vienna

Abstract

The high-dose dosimetry programme was initiated by the International Atomic Energy Agency in 1977. Like any other Agency programme, this one has various activities. These cover: research contracts and research agreements, co-ordinated research projects (CRP), training courses, and laboratory-based activities. The Agency's dose quality audit service (International Dose Assurance Service, IDAS), initiated in 1985, is one of the key elements of the programme. At earlier times, the technical part was operated through a laboratory in Germany. However, after purchasing the Bruker ESR spectrometer, the entire service has been operated from the Agency since 1992. This audit service has served well the needs of various institutes around the world involved with radiation processing. We have had two Co-ordinated Research Projects (the second one is in its last year) over the last several years. Both were/are aimed at standardization of dosimetry for radiation processing. Nine or ten participants of each CRP were about evenly distributed between the developed and developing Member States. In collaboration with the Food and Environmental Protection Section and the Industrial Applications and Chemistry Section, the Dosimetry and Medical Radiation Physics Section has participated in several training courses; these have been mainly regional courses. This collaboration has worked well since such courses combine specific radiation processing applications with the needs of good dosimetry and process control. Also, the Agency has organised several dose intercomparisons in recent time. The activities of the high-dose dosimetry programme since the last symposium (November 1990) are reviewed here.

1. INTRODUCTION

For any industry, development and implementation of standards are very much necessary and they indicate a level of maturity. Measurements are needed for process control to improve quality, and these measurements should be standardized. For radiation processing applications, it is important that the irradiated products are reliable and safe; and this is essential for regulated products. With this in mind the Agency initiated the programme of high-dose dosimetry in 1977. This was necessary since there was no concerted international effort then to achieve standardization of dosimetry for industrial processes. One may argue that it was too early since the industry was still nascent. On the other hand, such a programme can help to start a new industry on a good foundation and help achieve its full potential.

The purpose of this programme is to accomplish standardization of dose at an industrial scale, to promote dosimetry as a quality control measure in radiation processing, and to help develop new dosimetry techniques. This programme has come a long way and I would like to believe that it has had some contribution towards helping industry to establish itself in a confident manner in developing Member States through its various activities. Since the initiation of the programme, other national and international organisations such as International Standards Organization (ISO), European Committee for Standardization (CEN), American Society for Testing and Material (ASTM), and Association for the Advancement of Medical Instrumentation (AAMI) have been actively involved in several aspects of dosimetry for radiation processing, either through development of standard practices and guidelines for dosimetry systems [1] or through providing recommendations for process control for the radiation processes [2-4]. The Agency has been aware of these development, and has tried to support their effort

by disseminating these standards and recommendations and helping their implementation through various activities, such as research contracts and training courses.

Like any other Agency programme, the high-dose dosimetry programme has various activities. Systematic effort has been put in order to achieve the set goals by means of scientific meetings, research support, dose intercomparisons, training courses and workshops, and dose quality audit service from the Agency Dosimetry Laboratory. These are summarized and reviewed in Table I. This list includes activities since the last dosimetry symposium organised by the Agency in 1990. The activities till that point in time were described by Nam [5] at that symposium.

The two previous symposia organised by the Agency in 1984 [6] and 1990 [7] were very successful in that they brought together researchers and facility operators from around the world to discuss and exchange information. This present symposium is expected to achieve similar results.

TABLE I. ACTIVITIES OF THE HIGH-DOSE DOSIMETRY PROGRAMME

1977	Initiation
1984	International Symposium on High Dose Dosimetry
1985-91	IDAS (at GSF, Germany)
1990	International Symposium on High Dose Dosimetry for Radiation Processing
1992	IDAS to Agency Dosimetry Laboratory
1988-99	2 CRPs (high-dose)
1994-95	Calibration laboratories intercomparison
1998	CRP (EPR on biodosimetry) initiated
1998	International Symposium on Techniques for High-Dose Dosimetry in Industry, Agriculture and Medicine

2. REVIEW OF THE PROGRAMME

The Agency generally conducts reviews and audits of its various programmes and activities to assure that they are implemented as intended, to check their effectiveness and to review them for any modifications needed in view of the changing requirements of Member States. In line with this policy, the Agency has an established Standing Advisory Group that regularly reviews and evaluates the work of the Dosimetry and Medical Radiation Physics Section. Since 1990, this committee has met four times to review the dosimetry programme of the Agency. Initially, this Group did not include specifically the expertise for high-dose dosimetry; and hence their effort was augmented by other expert meetings. Two such meetings were convened in Vienna:

- to review the International Standardization and Quality Assurance of High-Dose Dosimetry, 8-10 March 1993; and
- to review the purpose, operation and future of the IDAS, 31 October - 3 November 1994.

Since 1995, the membership of the Standing Advisory Group was expanded to specifically include an individual with high-dose dosimetry experience.

The recommendations emanating from these meetings have helped the programme to keep focused and to modify the programme as required to reflect the needs of Member States.

3. INTERNATIONAL DOSE ASSURANCE SERVICE (IDAS)

This dose quality audit service was initiated in 1985 [5] with an objective of assisting Member States to establish reliable dosimetry system(s) in their radiation facilities. This service provides an independent check on the entire dose measurement system, i.e. dosimeters, measuring equipment,

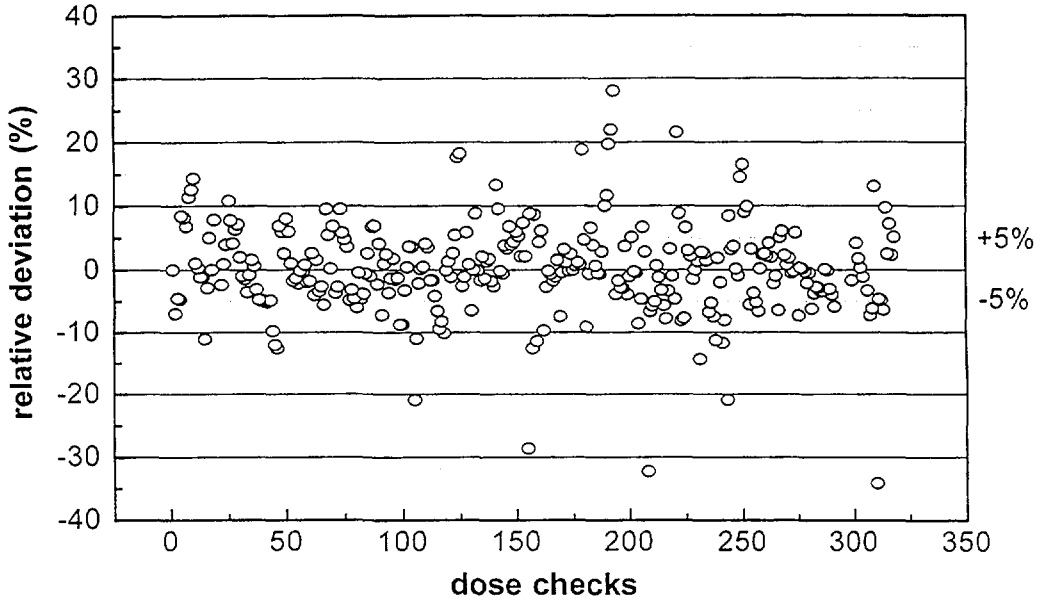

FIG. 1. Relative deviations for all audit checks since 1992. The acceptance limit is ±5 %; about 60 % of the results are within these limits.

procedure for the use of the system, data transfer procedures, skill of the technical staff, etc. From 1985 till 1991 the technical operation of the service was provided by a German laboratory (GSF, Neuherberg) under a contract with the Agency, while the administration was managed by the then Dosimetry Section of the Agency. However, after acquiring the ESR spectrometer and training the staff in the ESR techniques, the entire service has been operated from the Agency since 1992.

This transition involved the establishment of the alanine-ESR dosimetry system at the Agency Dosimetry Laboratory. This required selection and purchase of the alanine dosimeters, commissioning of the ESR spectrometer, characterisation of the dosimetry system, establishing an in-house calibration facility, etc. The Agency's reference dosimetry system presently in use for IDAS is described elsewhere in this proceedings [8].

The start was slow but in recent years it has shown moderate growth. Till 2 years ago, the cost of the service was $100 per dose check for all participants, which is the same since the beginning of the service. Also, every new participant was required to be nominated by the relevant national authority. It was perceived that these may be the factors that were hindering the wider use of the service. The Agency now offers this service at no cost to a non-commercial institute for one dose check per year. Also, the initiation requirements are relaxed for these participants. This has resulted in a significant increase in the use of the service by Member States.

Since 1992 the IDAS has provided more than 300 dose checks. Figure 1 shows the relative deviations[1] between the Agency dose values based on alanine-ESR and the participants' dose values based on their dosimetry system for all the dose checks since 1992. The acceptance limit of ±5 % is shown by the two dotted lines. About 60% of the checks fall within these limits. It is the presence of the remaining 40 % that indicates the necessity of this service. To evaluate the performance of the service we have followed the relative deviation values for multiple participation. These values should decrease with time for institutes with multiple participation. Such a trend, if it exists, is very weak. We believe that the reasons for this tendency include: rotation of the staff at the institute/facility resulting in insufficient trained staff, and cost of repairing/calibrating the analysis equipment. However, this does indicating the continuous need of such a dose quality audit service.

[1] relative deviation (%) = 100x(participant's dose value-IAEA dose value)/(IAEA dose value)

The current IDAS service is limited to ^{60}Co gamma rays. The alanine dosimeters used for IDAS are not really suitable for electrons. A field study was however conducted to check the usefulness/suitability of these dosimeters for electrons. It was concluded from this study that under certain limiting conditions the current dosimeters may be used for electron-IDAS for energies higher than 8 MeV.

4. RESEARCH ACTIVITIES AND SUPPORT

The Agency's formal method of supporting research activities in Member States is through awarding research contracts and research agreements; some of these are single contracts (self-standing) while others are part of Co-ordinated Research Projects (CRP).

In the review period, 12 single research contracts were awarded in the field of high-dose dosimetry. Half of these were related to development of alanine dosimetry and the other half for development of several other types of dosimeters.

There were two CRPs related to high-dose dosimetry during this period; out of these one is now complete. This completed CRP on *Development of Quality Control Dosimetry Techniques for Particle Beam Radiation Processing* consisted of 10 participants and resulted in various advancement in electron dosimetry systems, including [9]:

- alanine was established as a reliable reference and routine dosimeter;
- calorimetry systems were modified; polystyrene was shown to be a good absorber, modular multi-element system was developed for measuring depth dose and thus electron energy; and
- on-line process control devices were developed for monitoring various beam parameters, such as electron beam energy and scan width.

The primary conclusion of this CRP was that alanine-ESR is a reliable transfer dosimeter for electron beams.

The second CRP is still active and is on *Characterization and Evaluation of High-Dose Dosimetry Techniques for Quality Assurance in Radiation Processing*. It has two objectives: (i) to understand and evaluate the influence of various external parameters on the performance of routine dosimeters currently in use, and (ii) to develop reference and transfer dosimetry technique for electrons of energy less than 4 MeV [10]. The research carried out by some of the participants so far indicate that:

- alanine film (100 - 300 μm) is suitable as a reference dosimeter; it may be analysed with ESR spectrometry or with DRS (diffuse reflection spectrometry); and
- for routine dosimetry, there are several choices that are being pursued: thin calorimeters, thin films or coatings (radiochromic, alanine, optically stimulated luminescence systems), and flat bags containing dosimetric material (glutamine powder, ECB).

Several other participants carried out research aimed at understanding:

- the effect of irradiation temperature on alanine-PS and glutamine dosimeters;
- the combined effect of temperature and dose rate for PMMA GammaChrome YR and FWT;
- the effect of various storage conditions and relative humidity during irradiation on new PVG films.

5. INTERCOMPARISONS

Since 1990, the Agency has organised three intercomparisons: two of which were part of the two CRPs and the third one was amongst several calibration laboratories.

5.1. CRP intercomparison - electron beam

The first intercomparison was under the electron CRP [9] mentioned above where the objectives were (i) to demonstrate that laboratories possessing well-characterised electron beams can administer a

consistent absorbed dose with acceptable uncertainties for typical radiation processing dose range, and (ii) to evaluate the suitability of alanine as a transfer dosimeter. There were nine participants and irradiation was carried out at three dose levels: 10, 30 and 50 kGy. The results demonstrated that consistency between the participants was achievable at the 5-7% level. It was felt that with the chosen transfer dosimetry system and the wide range of irradiation facilities and conditions, including beam qualities, consistency at this level was the best which can be obtained. It was concluded that the main factors contributing to the differences between the laboratories were likely to be related to the traceability of the dose at the point of measurement and the effect of irradiation temperature.

5.2. CRP intercomparison - ^{60}Co gamma rays

The second intercomparison was part of the currently active CRP [10] where the objective was to ensure that all doses quoted by the CRP participants are in agreement, thus increasing the credibility of the results and of the conclusions based on the research. There were nine participants and one dose level: 15 kGy. The analyses showed that for the seven participants the mean and standard deviation for the dose ratio (laboratory/IAEA) were 0.995 and 1.9%. The remaining two participants were quite outside the acceptance limit. This pointed out the necessity of participating in such intercomparisons frequently.

5.3. Calibration laboratories intercomparison - ^{60}Co gamma rays

The third intercomparison was organised in collaboration with the Bureau International des Poides et Mesures (BIPM) [11]. The participants were internationally recognised calibration laboratories of Member States, several being Primary Standard Dosimetry Laboratories. The dose levels selected for the exercise were 15 and 45 kGy. The focused objective was to examine to which degree there was an agreement between the various calibration laboratories in administering prescribed absorbed doses (to water) in a standard dosimeter holder geometry. Figure 2 shows the results for 15 kGy for all the nine participants. Each point is the mean value of the set of 5 dosimeters. The results were quite similar for the two dose levels. The standard deviation of the population shown is 1.96 % for 15 kGy and 2.15% for 45 kGy. The mean total uncertainty of the ratio as reported by the participants is about 1.6%, close to the experimental value of about 2%. Thus, the results of the comparison are consistent with the uncertainties estimated by the various laboratories.

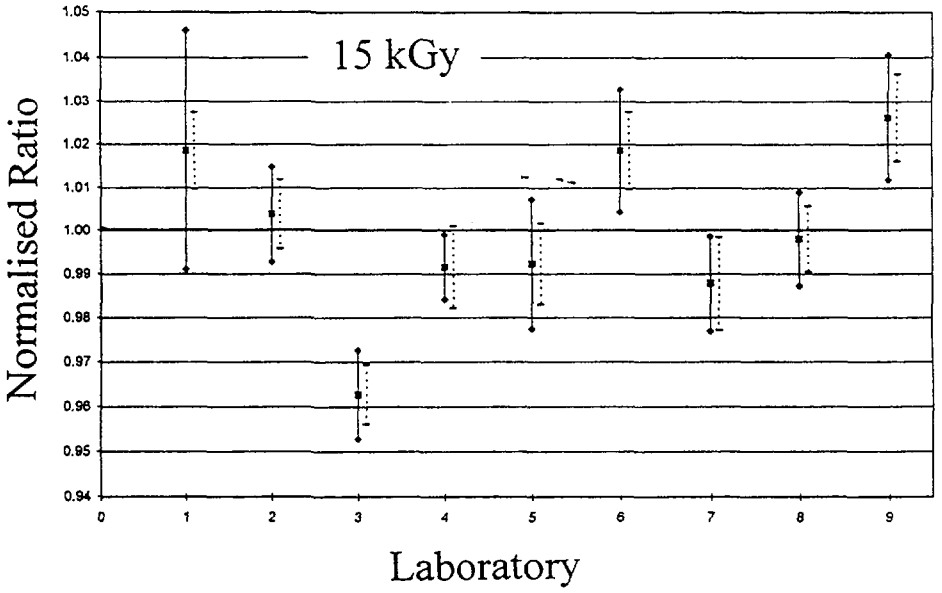

FIG. 2. The participant/Agency dose ratio, where the value is the mean of the five dosimeters in a set. The solid error bars show the combined uncertainty values quoted by the participants, the dashed bars are the statistical uncertainty in the Agency measurements.

TABLE II. TRAINING COURSES/WORKSHOPS WITH SUPPORT FROM THE DOSIMETRY AND MEDICAL RADIATION PHYSICS SECTION

Course Title	Date	Place	Organised by	DMRP support
Workshop on process control and quality assurance for radiation processing	Sept 1993	Prague, Czech Repub.	IAC	technical officer
Regional (ARCAL) workshop on industrial gamma and electron beam processing: Process control and dosimetry	May 1994	Sao Paulo, Brazil	IAC	technical officer
Regional (ARCAL) training course on radiation sterilization: Standards and regulations, process validation and dose setting	May 1994	Buenos Aires, Argentina	IAC	lectures and laboratory
Regional training course on radiation sterilization - validation, routine control and application of ISO standards	July 1994	Bangkok, Thailand	IAC	lectures and laboratory
Workshop on dosimetry techniques for process control in food irradiation for AFRA	August 1995	Pretoria, South Africa	FEP	lectures and laboratory
General training course on food irradiation	March 1996	Cairo, Egypt	FEP	lectures and laboratory
UNDP/RCA/IAEA regional training course on process and quality control in radiation processing	August 1996	Takasaki, Japan	IAC	technical officer
Regional training course on radiation sterilization - Regulations and international standards for process validation	Novem. 1996	Santiago, Chile	IAC	technical officer
Regional workshop on food irradiation process control	Aug/Sept 1997	Teheran, Iran	FEP	lectures and laboratory
National training course on dosimetry and quality assurance in radiation processing	Novem. 1997	Seoul, Korea	DMRP	technical officer

6. ESR DOSIMETRY TECHNIQUES

ESR analysis technique has found its applications in various field. At the Agency in recent times, the following activities were pursued in the application of this analysis method to two dose ranges other than those suitable for radiation processing:

- alanine-ESR for dose levels suitable for radiotherapy, and
- biodosimetry for dose reconstruction.

6.1. Radiotherapy

In April 1997, the Agency convened a consultants' meeting (a) to review the work being pursued in this field at various laboratories; (b) to evaluate the applicability of the alanine-ESR dosimetry system to radiotherapy; and (c) to recommend the role of the Agency. Following the recommendations of the consultants [12], a CRP on 'Alanine-ESR dosimetry for radiotherapy' was proposed and was approved by the Agency. However, because of the budget constraint its implementation is pending an extra-budgetary support.

6.2. Dose reconstruction

A CRP on 'EPR biodosimetry' was initiated earlier this year with 9 participants. The objectives of the CRP are (a) to review the available methods for EPR biodosimetry technology for dose reconstruction (retrospective dosimetry), and (b) to investigate the influence of various parameters on the analyses. This technique is of particular interest in case of exposure to relatively low doses or when the results of conventional dosimetry are not available (for example, in accidental circumstances) or when there are conflicting dose estimates. The final goal of the CRP is to make recommendations for the most suitable procedures of practical use.

7. COLLABORATION WITH OTHER DIVISIONS

The Dosimetry and Medical Radiation Physics (DMRP) Section has close collaboration with several other Sections and Divisions within the Agency. As regards to high-dose programme, the closest relations are with Food and Environmental Protection Section (FEP) and the Industrial Applications and Chemistry Section (IAC). These are the two main sections of the Agency that deal with applications of radiation that has a strong dosimetry component. The continuous contacts consist of consultation on several activities, such as research contracts, CRP, expert missions, purchase of equipment,, etc. However, the major collaboration has been in the form of support that the DMRP Section has provided to these sections in the training courses and workshops. Table II lists the training courses/workshop that were formally organised by these sections and where the DMRP Section provided a significant level of assistance at various levels: as lecturers and for laboratory exercises related to dosimetry, assistance in the organisation, and sometimes acting as the technical officer. The collaboration has worked well since such courses combine specific radiation processing applications with the needs of good dosimetry and process control.

8. CONCLUSIONS

I hope this symposium like the previous two would provide the forum for exchanging information and for discussion. We are facing the dawn of the next century and with that several new applications of radiation. The typical example are in the field of environment, such as sludge treatment, elimination of nitrogen oxides and sulphur oxides from gaseous effluents, etc. Also with further globalisation, the need for reliable process validation and process control for the irradiated products for the international trade is ever increasing. I hope that this symposium would provide a stimulus for the future development of dosimetry techniques needed for the new applications and the new challenges.

REFERENCES

[1] ASTM, *Annual Book of ASTM Standards,* Section 12, Vol. **12.02**, Nuclear, Solar, and Geothermal Energy, American Society for Testing and Materials, West Conshohocken PA, USA 19428 (1998)

[2] ISO, "Sterilization of health care products – Requirements for validation and routine control – Radiation sterilization", International Organization for Standardization, Case Postale 56, CH-1211, Geneve 20, Switzerland (1995).

[3] CEN, "Sterilization of medical devices – Validation and routine control of sterilization by irradiation" *European Standard* **EN 552**, European Committee for Standardization, Central Secretariat: rue de Stassart 36, B-1050 Brussels, Belgium.

[4] Codex Alimentarius Commission, Codex General Standard for Irradiated Foods and Recommended International Code for the Operation of Radiation Facilities Used for the Treatment of Foods, CAC/Vol. XV-Ed .1, 1984

[5] NAM J.W. Standardization and Assurance of High Doses: An IAEA Activity on Dosimetry for Radiation Processing (IAEA-SM-314/62), Proceedings of the International Symposium on High Dose Dosimetry for Radiation Processing, 5-9 November 1990, Vienna, Austria, 1991

[6] International Atomic Energy Agency, Proceedings of the International Symposium on High-Dose Dosimetry, 8-12 October 1984, Vienna, Austria, 1985

[7] International Atomic Energy Agency, Proceedings of the International Symposium on High Dose Dosimetry for Radiation Processing, 5-9 November 1990, Vienna, Austria, 1991

[8] MEHTA K., GIRZIKOWSKY R., IAEA Reference Dosimeter: Alanine-ESR, These Proceedings, Paper No: IAEA-SM-356/63.

[9] INTERNATIONAL ATOMIC ENERGY AGENCY, Report on the 3rd RCM for the CRP on *Development of Quality Control Dosimetry Techniques for Particle Beam Radiation Processing,* Riso National Laboratory, Denmark, 24-28 April 1995

[10] INTERNATIONAL: ATOMIC ENERGY AGENCY, Report on the 2nd RCM for the CRP on *Characterization and Evaluation of High-Dose Dosimetry Techniques for Quality Assurance in Radiation Processing,* Vienna, 6-10 October 1997

[11] MEHTA K. and GIRZIKOWSKY R., IAEA *High-Dose Intercomparison in ^{60}Co Field,* Proceedings of the International Conference on Biodosimetry and 5th International Symposium on ESR Dosimetry and Applications, 22-26 June 1998, Moscow/Obninsk, Russia

[12] INTERNATIONAL ATOMIC ENERGY AGENCY, Report on consultants' meeting on *Alanine dosimetry for radiotherapy*, Vienna, 28-30 April 1997

DEVELOPMENT OF DOSIMETRY TECHNIQUES — I

(Session 2)

Chairperson

A. KOVÁCS
Hungary

A REAL-TIME LOW ENERGY ELECTRON CALORIMETER

N. MOD ALI*, F.A. SMITH
Physics Department,
Queen Mary and Westfield College,
University of London,
London, United Kingdom

Abstract

A real-time low energy electron calorimeter with a thin film window has been designed and fabricated to facilitate a reliable method of dose assessment for electron beam energies down to 200 keV. The work was initiated by the Radiation Physics Group of Queen Mary and Westfield College in collaboration with the National Physical Laboratory (NPL), Teddington. Irradiations were performed on the low and medium electron energy electron accelerators at the Malaysian Institute for Nuclear Technology Research (MINT). Calorimeter response was initially tested using the on-line temperature measurements for a 500-keV electron beam. The system was later redesigned by incorporating a data-logger to use on the self-shielded 200-keV beam. In use, the final version of the calorimeter could start logging temperature a short time before the calorimeter passed under the beam and continue measurements throughout the irradiation. Data could be easily retrieved at the end of the exposure.

1. INTRODUCTION

The calorimeter consists of a graphite core of diameter 50 mm and thickness 2 mm, embedded in a graphite scatter ring. Two 0.5-mm diameter glass bead thermistors are inserted in the absorber disc and connected to opposite arms of a DC bridge. Thermal insulation above the graphite core is achieved by a 1-mm thick of polystyrene foam, and a 8-μm thick aluminised mylar film is stretched across the aluminium ring. These minimize the upward heat losses from the core, mostly caused by the compressed air cooling of the accelerator window. For the purpose of calibration, the design also provided an opportunity to insert thin film dosimeters between the polystyrene foam and the aluminized mylar film. The entire graphite core plus the scatter ring rests on a 13-mm thick polystyrene foam block held securely within a PVC casing of dimensions 140 mm x 140 mm x 17 mm (Fig. 1).

Calorimeter response was initially tested using the on-line temperature measurements on the MINT 500-keV electron beam. For these measurements, the thermistor was connected via the high quality co-axial cables directly to a Wheatstone DC bridge circuit and the real-time temperature measurements were made by recording the out-of-balance voltage on digital voltmeters. Voltages were then down-loaded via a Tastronic IEEE 488-R232 converter into a computer memory for analysis.

The system was then redesigned for used with the MINT 200-keV self-shielded accelerator which does not permit on-line measurements. A commercially available voltage data-logger was used and the device set to start logging a short time before the calorimeter passed under the beam. Data were recovered after the calorimeter had emerged from the irradiation. The bridge, lithium batteries and voltage data-logger were all contained within the same box as the calorimeter itself (Fig. 2).

---

* Present address: Mint-Tech Park (MINT), Block 43, Jalan Dengkil, 43000 Kajang, Selangor, Malaysia.

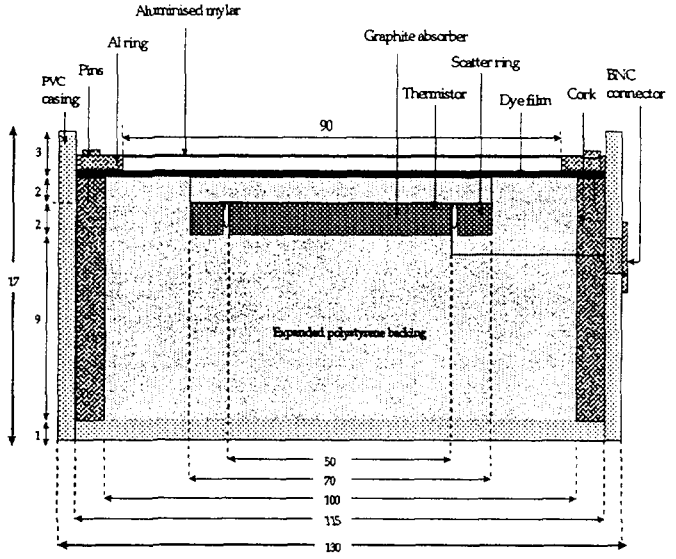

FIG.1. Schematic cross-section of a low energy calorimeter

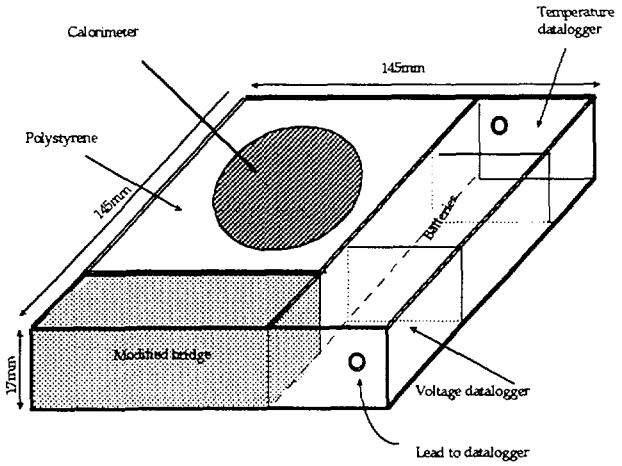

FIG.2. Diagram of the calorimeter with the data-logger system

2. APPLICATIONS

2.1. Calibration of accelerator output

Typical temperature-time plots for the data-logger system at 200 keV and the on-line system at 500 keV are shown in Fig. 3. A slow temperature drift before the irradiation begins (period I) is followed by a rapid rise during irradiation (period II) and then a slow cooling after the end of the irradiation (period III). The shape of the post-irradiation curve depends on the difference between the calorimeter core and the ambient temperature, the cooling rate being smaller at 200 keV than it was at 500 keV.

The temperature rise, ΔT in the graphite core was determined from the extrapolation to the mid-irradiation time, of both the pre- and post- irradiation parts of the curve. Values of ΔT at typical conveyor speeds and beam currents for the 200-and 500-keV beams are shown in Fig. 4. These can be used firstly to relate the accelerator output to the beam settings of energy, beam current and conveyor speed, and secondly, to determine the total absorbed dose in the calorimeter core using Eq. (1):

$$D_{graphite} = \frac{E}{m} = c_g . \Delta T \qquad (1)$$

where, E is the deposited energy, ΔT is the temperature rise induced by the radiation, m and c_g are the mass and specific heat of the graphite core, respectively.

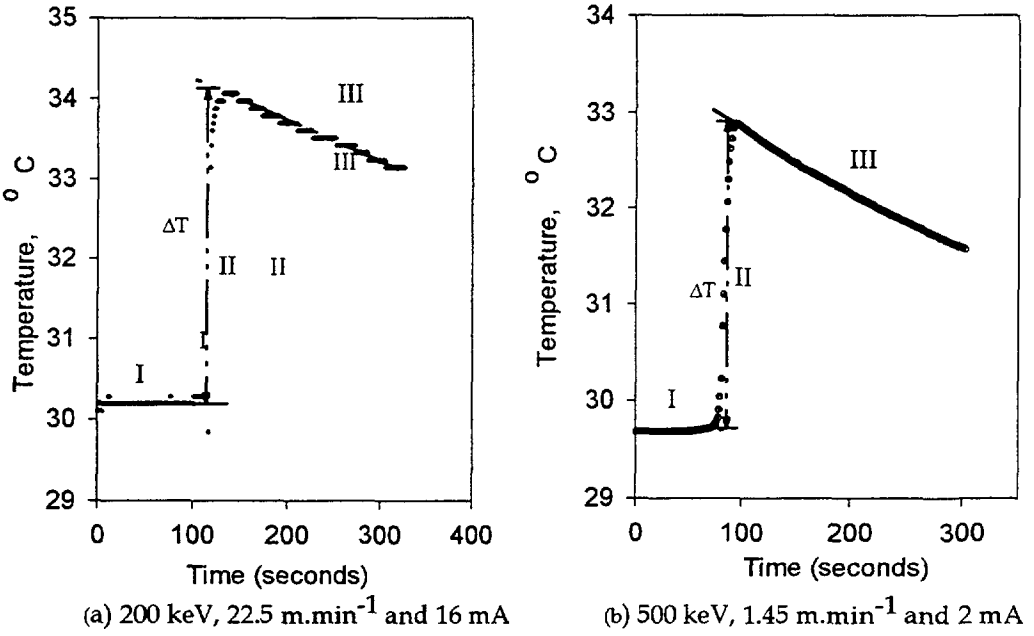

(a) 200 keV, 22.5 m.min^{-1} and 16 mA (b) 500 keV, 1.45 m.min^{-1} and 2 mA

FIG.3. Temperature-time pattern using (a) the data-logger system at 200 keV and (b) the on-line system at 500 keV at the stated values of conveyor speed and beam current.

2.2. Calibration of thin film dosimeter

In order to establish a procedure for the calibration of the thin film dosimeters for low energy irradiations, films of cellulose triacetate (CTA) and blue cellophane (BC) were arranged in a stack between the thin aluminised mylar window and the calorimeter core. Both film materials were irradiated at 200 and 500 keV and the difference of temperature rise recorded with and without the insertion of the film stacks. This provided an accurate determination of absorbed dose by the films (Figs 3 and 5). A calibration factor could then be determined to relate the radiation-induced absorbance of the film to the total dose deposited in the film.

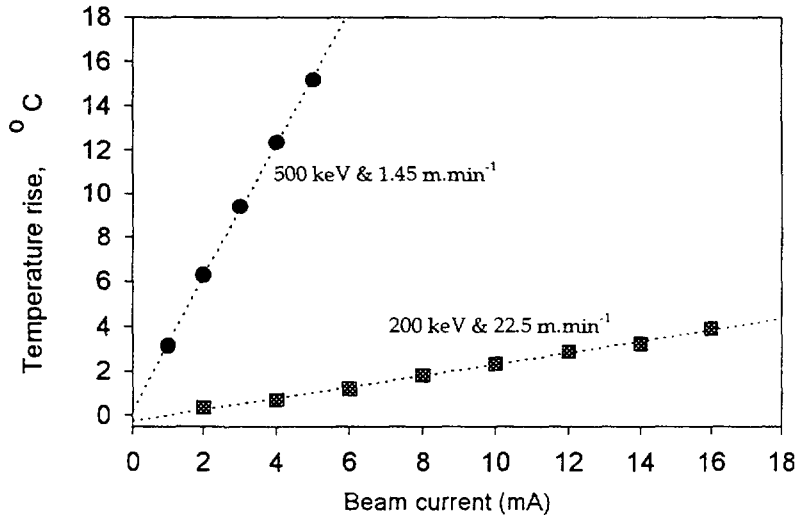

FIG.4. Relation between temperature rise and beam current for 200-keV and 500-keV electrons at the stated conveyor speeds

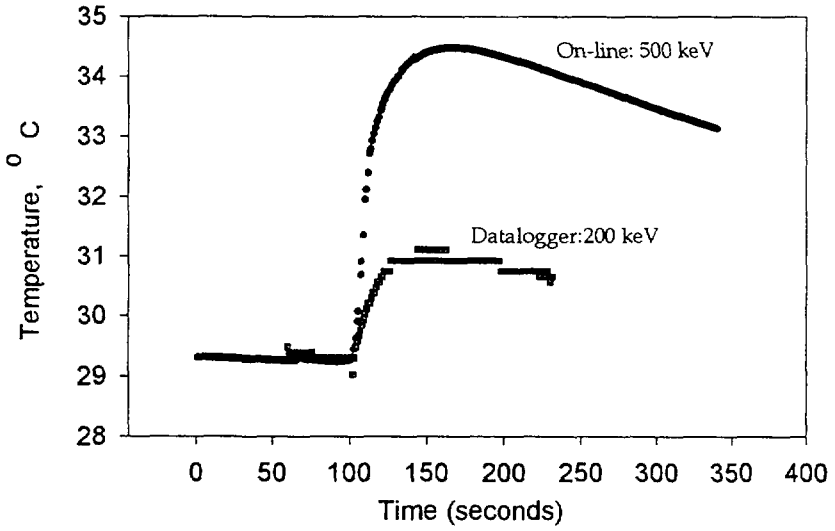

FIG.5. Typical temperature-time pattern with film stack with (a) 500 keV, m.min^{-1} and 3 mA (20 pieces of BC) and (b) 200 keV, 22.5 m.min^{-1} and 12 mA (5 pieces of BC).

Film response was expressed as the net change in the absorbance per unit film thickness and when plotted against absorbed dose gave the calibration curves for CTA and BC films at 200 and 500 keV (Fig. 6). There is a linear response of the CTA film at both energies although the smaller electron penetration at 200 keV gives a smaller range of absorbed dose even for beam currents up to 18 mA (~1 kGy) (Fig. 6a). The 500-keV beam requires beam currents only up to 5 mA to achieves doses up to 4 kGy. A measured calibration factor of 0.0062 ± 0.0002 kGy^{-1} was found to be in good agreement with measurements at other institutions [1,2,3] made under different conditions. A slight non-linearity was observed in the calibration curve for the BC film (Fig. 6b). Although a second order polynomial could be fitted without difficulty, the absorbance was found to be much higher than that obtained using higher energy electrons and photons [4].

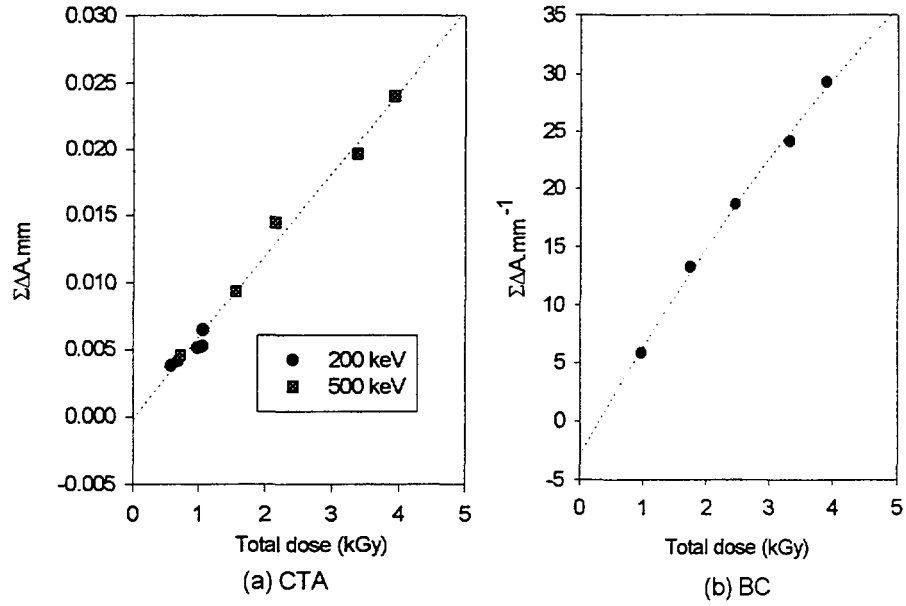

FIG.6. Calibration curve for (a) CTA and (b) BC film dosimeter.

3. CONCLUSIONS AND FUTURE WORK

The simple and accurate method of dose determination using the real-time low energy calorimeter provides a reliable method of dosimetric calibration and standardization for low energy electron beam facilities. The advantages of the calorimeter are that:

- it permits use on either on-line and off-line facilities
- it is suitable for daily use since the data can be retrieved at any time after it comes from the beam
- it provides for a precise calibration of the beam and film dosimeters under actual irradiation conditions

ACKNOWLEDGEMENTS

The authors wish to thank the Malaysian Government for the award of a scholarship to NMA, and Dr. David Burns, Dr. Peter Sharpe, Mr. Alan Dusatouy and Mr Malcolm McEwen for assistance both with the calorimeter development and the data interpretation. The work forms part of the thesis (Low Energy Electron Calorimetry for Industrial Processing) presented by NMA to the University of London for the award of the Ph.D degree (1998).

REFERENCES

[1] SUNAGA.H., TANAKA, R., MOD ALI, N AND YOTSUMOTO, K.(1995). Radiat. Phys. Chem. **46,** pp 1283-1286.

[2] JANOVSKY, I AND MILLER, A. (1987). Appl. Radiat. Isot. **38,** pp 931-937

[3] GEHRINGER, P., PROKSCH, E. AND ESCHWEILER, H. (1985). Proc.High Dose Dosimetry Symp. Vienna 333-344.

[4] MCLAUGHLIN, W.L., HUMPHREYS J.C., RADAK, B.B., MILLER, A. AND OLEJNIK, T.A. (1979) Radiat. Phys. Chem. **14,** pp 535-550.

A SIMPLE READER FOR LABEL DOSIMETERS IN QUARANTINE AND OTHER APPLICATIONS*

D.A.E. EHLERMANN, B. BAUER
Institute of Process Engineering, Federal Research Centre for Nutrition, Karlsruhe, Germany

Abstract

A commercially available 'label dosimeter' is intended for visual evaluation. The physical changes in colour and brightness are the basic changes on which subjective judgement relies. Change in brightness was chosen as the parameter of objective evaluation and a reader was developed. After test of an experimental set-up a prototype reader was developed and finally converted into an electronic hand-held instrument. This allows for reading of the code of a 'label dosimeter' giving information about its 'decision function' and the associated threshold dose value, reading the optical response of the particular 'label dosimeter' and converting this into a judgement about acceptance or rejection of the product lot under inspection. At present, such 'label dosimeters' are manufactured only for a limited set of threshold dose values. For commercial scale and international trade applications a wide range of such 'label dosimeters' need to be utilized. The electronic instrument developed in this study would allow for a great variety of such 'label dosimeters' to be evaluated by objective means and the results be recorded and transmitted for further evaluation by control authorities.

1. INTRODUCTION

The commercial availability of label dosimeters [1] and the proof of their general suitability in commercial practices [2, 3] has fostered interest in instrumental read-out systems of such labels. Such equipment could supplement the visual judgement of an inspector upon entry of the irradiated item into a quarantine-protected area. The judgement by the inspector is whether or not the label 'indicates' that a threshold dose was surpassed. The design of a prototype-reader relied on previously reported measurements of 'colour' in standardized (CIE-Lab) coordinates [2]. It could be shown that the trace of changes in the ab-chromaticity space is a straight line; ie the relative components of 'red' and 'yellow' are unchanged, saturation of colour decreases from bright to black. At a given illumination with yellow-red light, hence, the change of the CIE-brightness ordinate L is a good measure of the radiation effect. The validity of the concept, however, that a dose reading at a reference position can render information about the adherence to a required minimum dose as in applications of quarantine and insect disinfestation needs further evaluation [4].

2. MATERIALS AND METHODS

Label dosimeters (provided by courtesy of International Speciality Products (ISP) Inc., Wayne NJ, USA) were irradiated at several doses around the nominal threshold value [2]. In a first approach, the readings using an experimental set-up were compared with the results of colorimetric measurement of brightness L. Illumination was from a light-emitting-diode (LED) at 615 nm and reflected light was detected by use of a photodiode (Fig. 1). The response function for the several types of 'label dosimeters' was then incorporated into a dedicated processor; a reader was added for the type coding of such labels. Finally a display was designed giving a complete report of the measurements taken together with a proposed judgement of the compiled results. The prototype was further miniaturized for ease of practical utilization and converted into a hand-held reader (Fig. 2). An interface was added in order to allow for transfer of the collected data to a central documentation and evaluation system.

*Work partially supported by IAEA Research Agreement No. 7776/CF under FAO/IAEA Co-ordinated Research Programme on 'Standardized Methods to Verify Absorbed Dose of Irradiated Fresh and Dried Fruits and Tree Nuts in Trade'.

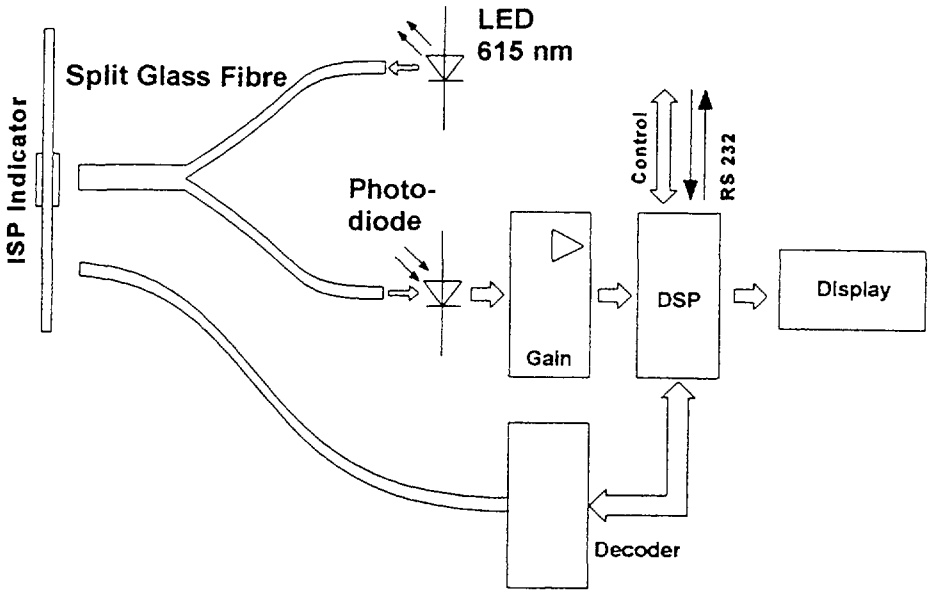

FIG. 1: Schematic diagram of the prototype reader for label dose-indicators

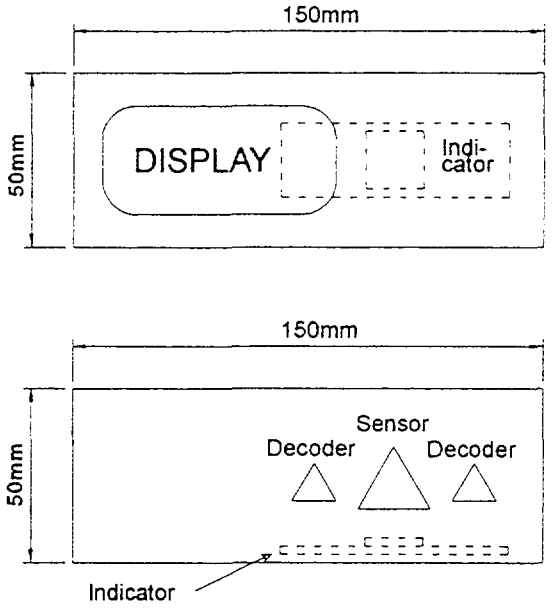

FIG. 2: Design of a miniaturized, hand-hold label indicator reader for routine applications

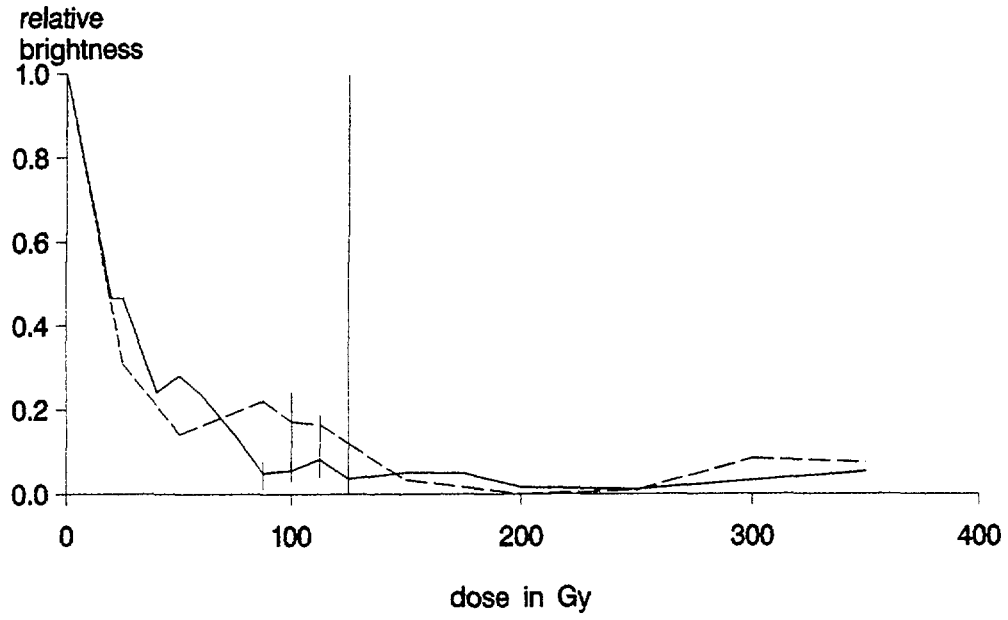

FIG. 3: Comparison of CIE-L brightness (solid line) and photo-diode (prototype reader, dashed line) signal for indicator nominal dose of 125 Gy; respective raw data normalized to range 0 - 1; fine vertical line indicator threshold; max/min of repeated measurements indicated

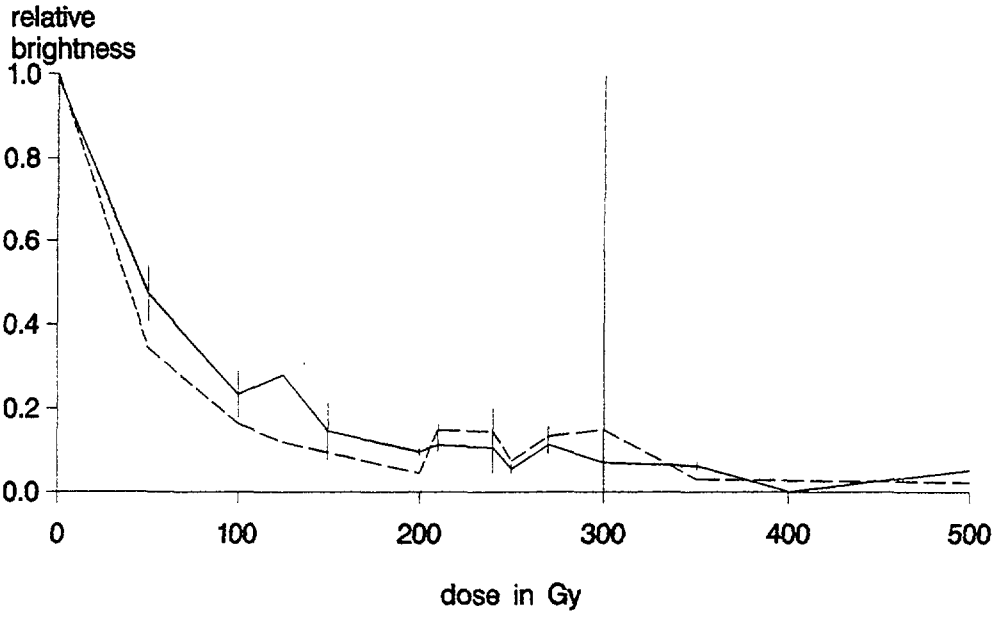

FIG. 4: Comparison of CIE-L brightness (solid line) and photo-diode (prototype reader, dashed line) signal for indicator nominal dose of 300 Gy; respective raw data normalized to range 0 - 1; fine vertical line indicator threshold; max/min of repeated measurements indicated

3. RESULTS AND DISCUSSION

In a first step, reading the labels with a trichromatic colorimeter was compared to the results of the experimental set-up. For this purpose data were normalized for initial (unirradiated) brightness to 100 % and for the asymptotic brightness value at higher doses to 0 % (Figs 3 and 4). Essentially both curves are identical; however, with the prototype reader only one indicator per dose step could be evaluated and repeatability is not shown in the figures.

The response function allowed for setting a threshold value for intensity of reflected light which was related to required minimum value of dose at the reference position. It should be noted that the 'label dosimeters' as presently manufactured show saturation (complete darkening) only at dose levels considerably higher nominal dose value. This finding implies that for the built-in decision function, the range of expected signals at the intended minimum dose together with appropriate tolerance limits must always be considered. From this observation a modified prototype was developed. This includes - for a range of several labels and stored on ROM - the respective response curves, the appropriate decision function, a code reader for identifying the type and kind of the label. The display is a YES/NO for acceptance of the product lot under investigation; however, the complete detailed measurement results are readable from an interface to a computer. It is intended to miniaturize the whole set-up (Fig. 2) in order to obtain a hand-held reader for field use. For data collection, this instrument can also be coupled to a computer.

From the experience in the simulated commercial scale experiments [4] it was concluded that graded set of such 'label dosimeters' would be needed which are not yet commercially available; for example, for the reported experiments (with a minimum target dose of 300 Gy in several configuration/geometries of product) at 420, 430, 490, and 940 Gy nominal dose. However, their design principle [1] allows for easy adjustment during manufacturing; it is only a question of economics whether such fine grades could be offered.

REFERENCES

[1] LEWIS, D.F., LISTL, C.A. (1992) Radiation Dose Indicator, US Patent No. 5084623

[2] EHLERMANN, D.A.E. (1997) Validation of a Label Dosimeter for Food Irradiation Applications by Subjective and Objective Means, Appl. Radiat. Isot. **48**, 1197-1201

[3] RAZEM, D. (1997) Dosimetric Performance of and Environmental Effects on STERIN Irradiation Indicator Labels, Radiat. Phys. Chem. **49**, 491-495

[4] EHLERMANN, D.A.E. Validation of a Label Dose Meter with Regard to Dose Assurance in Critical Applications as Quarantine Control. These Proceedings, paper no: IAEA-SM-356/38

[5] EHLERMANN, D.A.E. (to be published) Process control and dosimetry applied to establish a relation between reference dose measurements and actual dose distribution, in: Final report of FAO/IAEA Co-ordinated Research Programme on 'Standardized Methods to Verify Absorbed Dose of Irradiated Fresh and Dried Fruits and Tree Nuts in Trade'

DEVELOPMENT OF TL AND PTTL FROM NATURAL QUARTZ FOR HIGH-DOSE DOSIMETRY IN RADIATION PROCESSING

XA9949702

Muhammad FATHONY
Centre for Standardisation and Radiation Safety Research,
National Atomic Energy Agency of Indonesia,
Jakarta, Indonesia

Abstract

It is well understood that the effectiveness of radiation processing depends on the proper application of dose and its measurement. Thermoluminescence (TL) and its further methods, phototransfer thermoluminescence (PTTL), are of special interest to be applied for high-dose dosimetry. TL in natural quartz is based on the emission of light upon heating the quartz specimen – following the absorption of radiation – up to a maximum temperature, say ~ 500 °C in a TL reader system. PTTL is, however, the regeneration of TL by exposing the TL specimen, which had been previously readout, with UV light that enables one to re-observe the TL information. Some important dosimetric characteristics of TL and PTTL in natural quartz are presented and discussed. These include, for example, TL and PTTL glow-curves, TL and PTTL dose-response linearity, and repeated cycles of the PTTL, with special attention on suggestion of their use for high-dose dosimetry in radiation processing. In addition, the TL and PTTL mechanism to explain the results are also described briefly. Overall performance of TL and PTTL in natural quartz exhibit desirable dosimetric characteristics suitable for high-dose measurements.

1. INTRODUCTION

Radiation processing is a rapidly developing technology with numerous applications in, for example, medical product sterilisation, polymer modification, and food treatment. Food processing with radiation, for instance, could have its greatest impact in the developing countries like Indonesia. The effectiveness of the process, however, depends on the proper application of dose and its measurement [1-4]. Some conventional high-dose dosimeters, e.g. calorimeters, alanine/electron spin resonance (ESR) systems, liquid solutions (Fricke, ceric-cerous, dichromate), and polymer systems (polymethyl methacrylate, cellulose triacetate, radiochromic films and optical waveguides) are generally adequate for most reference and routine radiation processing measurement purposes [2].

Among various dosimetric methods commonly applied for high doses, thermoluminescence (TL) method is of special interest. Further method of TL, that is phototransfer thermoluminescence (PTTL), can also contribute some additional advantages for high-dose dosimetry. TL and PTTL in common natural materials, e.g. natural quartz, provide a useful method for the direct measurement of absorbed radiation [5-7]. TL in natural quartz is based on a physical phenomenon of the visible light emission upon heating the quartz specimen – following the absorption of radiation – up to a maximum temperature, say ~ 500 °C in a TL reader system. PTTL is, however, the regeneration of TL by exposing TL specimen – previously readout -- with UV light that enables one to observe the TL information. The facts showed that the TL as well as PTTL output is proportional to the radiation absorbed by the materials [5-7].

TL as well as PTTL in quartz is much less known than that in the more intensively studied alkali halides (e.g. LiF) for radiation dosimetry. However quartz has become a TL (now also PTTL) material which is of practical use, especially in the field of dating. Quartz has been much less exploited in the

field of TL dosimetry compared to its application in dating. However, it should be recognised that the use of quartz in TL dating in recording the natural dose received by a pottery sample is a good example of the application of quartz in the field of dosimetry using TL. Another advantage of quartz is that it is a unique material, which is extremely stable and normally very pure [7].

This report presents some important dosimetric characteristics of TL and PTTL in natural quartz, with special attention on suggestion of its use for high-dose dosimetry in radiation processing. In addition, the TL and PTTL mechanism to explain the results are also described briefly.

2. MATERIALS AND METHODS

Crystals of natural quartz were first washed with 25% HNO_3 in an ultrasonic bath overnight for removing inorganic dissolvable impurities (if present). The crystals were then crushed and sieved to yield powder of grain size ≤ 63 μm, followed by annealing at 500 °C for 1 h in an oven to remove the natural dose. The powdered samples were then prepared for gamma irradiation from ^{60}Co (~ 18.5 TBq). The sample irradiation was carried out in an electronic equilibrium condition. Before and after irradiation, the samples were kept in a black plastic box to avoid sunlight or room light.

The treated samples were then divided into aliquots weighing ~ 5 mg each, and deposited on aluminium planchets by the acetone sedimentation technique. The samples were then taken for TL readout up to a temperature of 500 °C. For PTTL measurements, the samples were then illuminated with UV light centred at 254 nm or 366 nm, for 1 min using two 8-watt lamps (at 11 cm from the samples). Following this, the PTTL glow-curves were readout with the TL reader as done before. Four planchets were prepared in every case for repeated measurements. TL and PTTL dose responses were observed in terms of the integration area under the glow-peaks of the glow-curves.

3. RESULTS

Both TL and PTTL glow-curves from natural quartz having been irradiated with 100 Gy of gamma rays from ^{60}Co can be seen in Fig.1. TL in natural quartz was found to consist of four main peaks: 110 °C, 160 °C, 235 °C, and 325 °C. Most natural quartz exhibits these four peaks, however, sometimes the last peak is not present. These TL peak temperatures are approximate values. The exact positions are, in fact, highly variable depending upon various factors: e.g. radiation dose, previous sample treatment, and impurities present. Among TL peaks, the 110 °C peak seems to be the most dominant. This peak corresponds to the shallow traps, which are the most sensitive ones to trap electrons. The PTTL glow-curve consists of three main peaks: 110 °C, 160 °C, and 235 °C. The last peak of TL (325 °C) did not appear because there are probably no more electrons within this trap to transfer. This was in agreement with Ref. [7]. As also explained by some authors (see Refs [5-7]), the mechanism of TL and PTTL in this case can be explained respectively as follows:

- In TL process, the irradiation of the crystals excites the electrons from the valence to the conduction band, in accordance with the energy band theory model of crystalline solids. Some of the excited electrons are trapped in the local trapping levels within the forbidden band. In the TL reader, the previously irradiated samples are heated up to a certain temperature at which the trapped electrons acquire sufficient energy to release into the conduction band, from where the electrons recombine at a luminescence centre with the emission of light. The TL data is normally displayed in terms of the plot of luminescence intensity vs temperature – a glow-curve. The temperature at which the peak maximum appears is related to the trap depth. The area under each peak is related to the number of filled traps, which, in turn, is related to the amount of radiation initially imparted to the quartz sample.

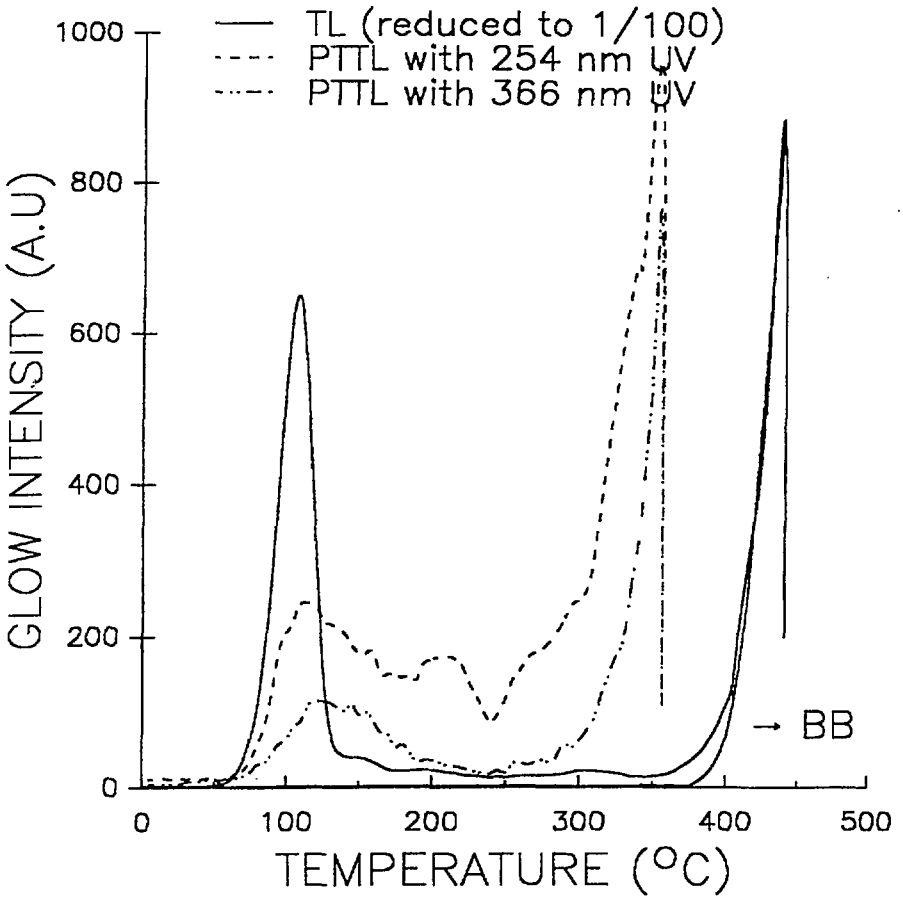

FIG. 1. Glow-curves of TL and PTTL from natural quartz irradiated at 100 Gy with gamma rays from ^{60}Co. PTTL was carried out with exposing the natural quartz samples with 254 nm and/or 366 nm UV

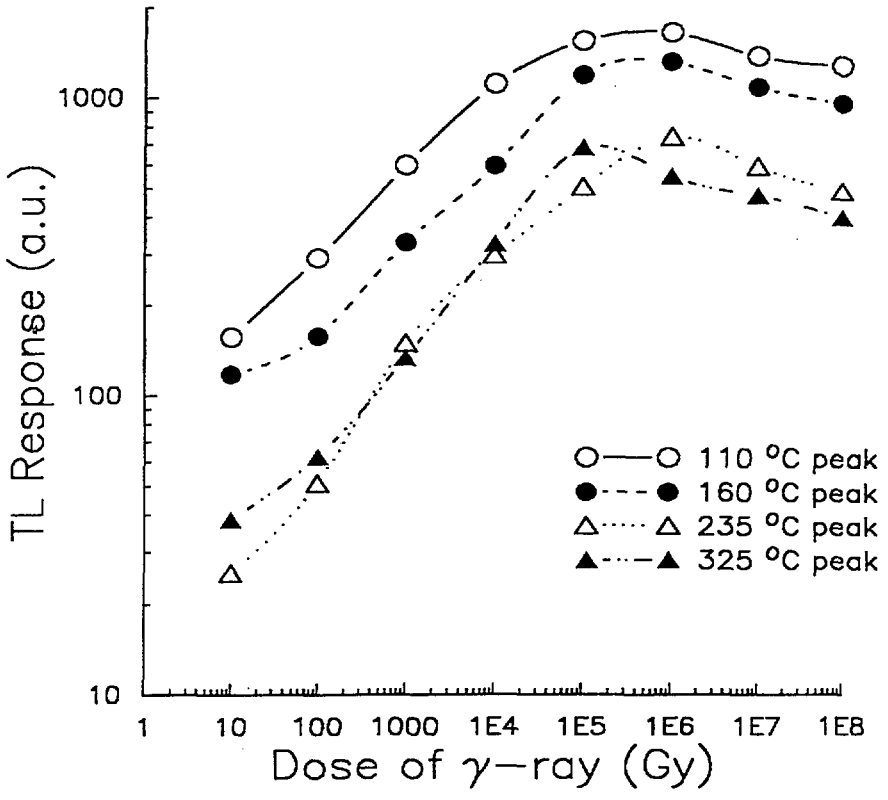

FIG. 2. TL responses of natural quartz irradiated with various doses of gamma ray from ^{60}Co. TL responses are linear up to the dose of 100 kGy, whereas beyond this point they seem to fall down.

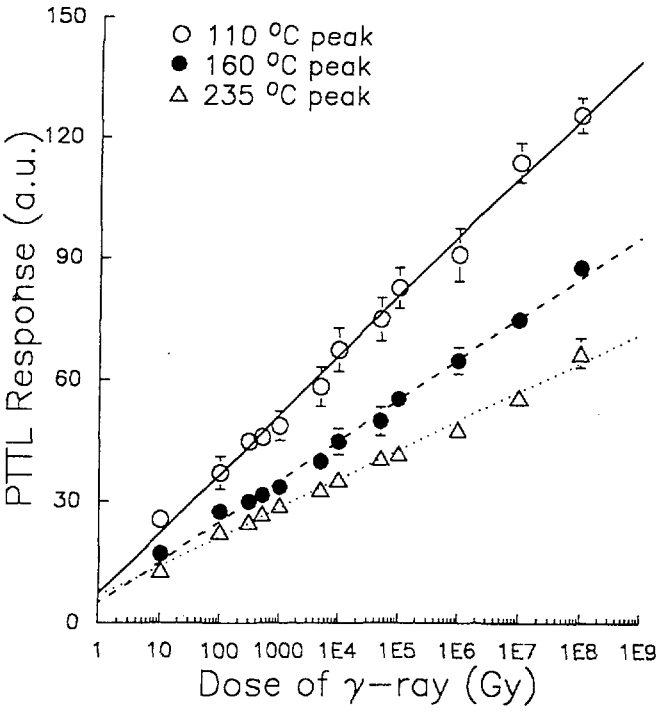

FIG. 3. PTTL responses of natural quartz irradiated with various doses of gamma ray from ^{60}Co. PTTL responses are linear up to the dose of 100 MGy. PTTL was carried out with 254 nm UV exposure for 1 min.

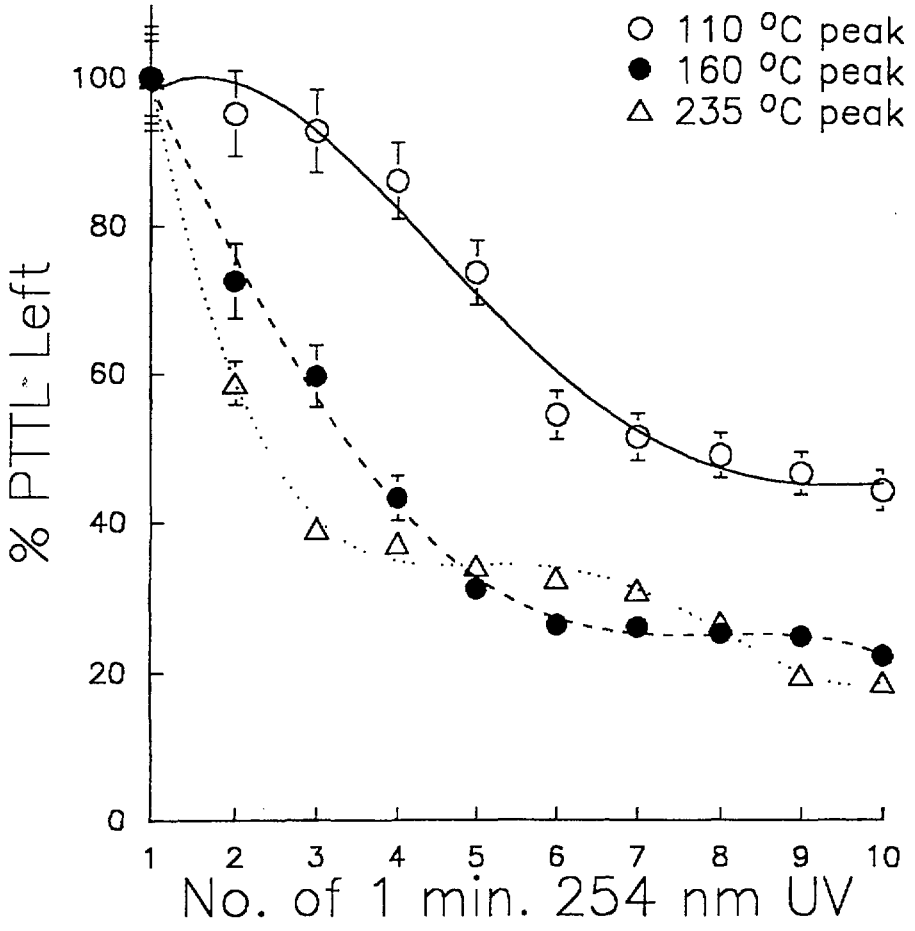

FIG. 4. Repeated cycles of PTTL with 1 min 254 nm UV exposure. The PTTL response rapidly decreases for about five UV exposures. Thereafter, it decreases slowly.

- PTTL is the transfer of electrons from more stable ('donor') traps, usually deeper trapping levels, to the shallow ones. The shallow trapping levels are more usable as normally used in TL observation. The electron transferring was carried out with exposing the samples under UV light. This showed that the trapped electrons absorb enough energy (from UV) to be transferred to the shallow traps which had been emptied during the TL observation (reading). In this PTTL process, the dominant peak, 110 °C, may become an 'acceptor peak', whereas the other higher temperature ones may become a 'donor peak'. This mechanism is also in good agreement with Refs [5-7].

TL responses against various gamma-ray doses were found to be linear from the dose of 10 Gy to 100 kGy for all the four TL peaks (note that both the axes represent log-values of the parameters). However, beyond 100 kGy the responses start to saturate or even to fall down, as shown in Fig. 2. The linear region is in agreement with the requirements of the IAEA TRS No.178 [4]. The saturated region as explained by Ref. [6] was probably due to the radiation damage in the natural quartz crystals. This shortcoming, however, can be overcome with the use of PTTL method, where the results can be seen in Fig. 3.

In Fig.3, it is seen that the PTTL response is linear from the gamma dose of 10 Gy up to 100 MGy. As has been mentioned above, this linearity is due to the fact that the deeper trapping levels are more stable than the shallow ones. Ref. [7] has shown that these trapping levels have low fading and bleaching behaviour. Furthermore, the high doses that cannot be observed by the normal TL method can be handled by the PTTL method. The linearity performance of PTTL dose-response is much better than that of the TL. Moreover, the PTTL range of linearity is much longer than that of the TL.

In addition, last but not the least, in order to regenerate TL by using the PTTL method, the samples that had been previously TL readout, can be exposed with the UV light repeatedly, say up to 10 times, for 1 min each time. Figure 4 shows that the PTTL response left in the sample decreases rapidly up to five exposures, thereafter it falls slowly. This fact has supported the prediction that the electron transfer takes place very rapidly while the electron population in the deeper traps is high enough. It could be postulated that there would be very little electron transferring after ten processes of PTTL, because the electron population in the deep trapping level is very little by then. If there is still some response, it could be considered as a black body radiation.

4. CONCLUSION

Both TL and PTTL glow-peaks of glow-curves resulting from the irradiated natural quartz can easily be observed. The linearity of TL responses with gamma dose showed that the TL method could be used to measure dose for radiation processing applications. The PTTL method, furthermore, can be used to regenerate TL information above. Also, the PTTL dose-response linearity is better than that of the TL one, and also over a larger dose range. In order to regenerate TL by using the PTTL method, the samples that had been previously TL readout, can be exposed with the UV light repeatedly. This performance of the natural quartz is a desirable dosimetric characteristic for radiation processing dosimetry.

REFERENCES

[1]. FARRAR, H. (1991), *Proc. Symp. on High Dose Dosimetry for Radiation Processing*, IAEA, Vienna 5-9 November 1990, pp.29-35.

[2]. MILLER, A. (1991), *Proc. Symp. on High Dose Dosimetry for Radiation Processing*, IAEA, Vienna 5-9 November 1990, pp.37-43.

[3]. EHLERMANN, D.A.E (1991), *Proc. Symp. on High Dose Dosimetry for Radiation Processing*, IAEA, Vienna 5-9 November 1990, pp.45-54.
[4]. IAEA-Vienna (1977), Technical Report Series No.178.
[5]. FATHONY, M. AND DURRANI, S.A (1992), *TL and PTTL characteristics of quartz irradiated with Au heavy ions*, Darmstadt-Germany GSI Reports 92-1, pp.249.
[6]. FATHONY, M. AND DURRANI, S.A (1993), *Sensitization of TL and PTTL in natural quartz with Xe heavy-ion predose*, Darmstadt-Germany GSI Reports 93-1, pp.299.
[7]. FATHONY, M. (1992), *Dosimetric Characteristics Studies of Phototransfer Thermoluminescence in Natural Quartz*, PhD Thesis, University of Birmingham, Birmingham, U.K.

NEW GENERATION OF SELF-CALIBRATED SS/EPR DOSIMETERS: ALANINE/EPR DOSIMETERS*

N.D. YORDANOV, V. GANCHEVA
Institute of Catalysis,
Bulgarian Academy of Sciences,
Sofia, Bulgaria

Abstract

A new type of solid state/EPR dosimeters is described. Principally, it contains radiation sensitive diamagnetic material, some quantity of EPR active, but radiation insensitive, substance (for example Mn^{2+}/MgO) and a binding material. In the present case alanine is used as a radiation sensitive substance. With this dosimeter, the EPR spectra of alanine and Mn^{2+} are simultaneously recorded and the calibration graph represents the ratio of alanine versus Mn^{2+} EPR signal intensity as a function of absorbed dose. In this way the reproducibility of the results is expected to be improved significantly including their intercomparison among different laboratories. Homogeneity of the prepared dosimeters and their behaviour (fading of EPR signals with time, influence of different meteorological conditions) show satisfactory reproducibility and stability with time. Because two different EPR active samples are recorded simultaneously, the influence of some instrument setting parameters (microwave power, modulation amplitude and modulation frequency) on the ratio $I_{alanine}/I_{Mn}$ is also investigated.

1. INTRODUCTION

The increased applications of ionising radiation processing need a reliable reference and transfer dosimetry system. Since the first proposal of powder alanine as a radiation detector [1] this idea has been developing [2-6] and as a result currently many types of alanine dosimeters of different size and shape are available [7], even commercially [8, 9]. They consist of powder L-α- or DL-α-alanine and some binding material - paraffin, cellulose, polymer or silicon. The reason for the growing interest of using these types of dosimeters is that the free radicals induced by high energy radiation in alanine are very stable and the intensity of their EPR signal increases linearly over a wide range of absorbed doses. On the other hand, the size of dosimeter is small, they can be easily transported, a non-destructive reading is used for the estimation of the dose and they could be kept as a document,.

However, there are various sources of uncertainties in the evaluation of absorbed dose with the described dosimeters, the main of which is the necessity to calibrate each EPR spectrometer and to prepare calibration graph for each batch of dosimeters available in the appropriate laboratory before their use. All this is connected with very large discrepancies in the results obtained by different labs and even on different spectrometers in one lab. In order to improve the accuracy of the estimation of the absorbed dose and to facilitate the comparison of the results obtained in different laboratories and EPR spectrometers, we have recently proposed a new type of solid state/EPR dosimeter [10, 11]. Besides L-α-alanine powder as a radiation sensitive material and paraffin as a binder, it contains MgO doped with Mn^{2+}, acting as an internal standard. The preliminary EPR studies from this laboratory show that Mn^{2+} magnetically diluted in MgO is radiation insensitive material in the dose interval 1 - 50 000 Gy [12]. Thus, in this type of solid state (SS)/EPR dosimeters the EPR spectra of alanine and Mn^{2+} are simultaneously recorded and the calibration graph represents the ratio of alanine versus Mn^{2+} EPR signal intensity as a function of absorbed dose.

*Work partially supported by IAEA research contract No. 8745.

The aim of this work is to extend the investigations on the behaviour of such dosimeters with respect to their homogeneity, influence of some meteorological factors and EPR signal fading with time after irradiation. On the other hand since two different EPR active samples are simultaneously recorded the influence of some instrument setting parameters on the ratio $I_{alanine}/I_{Mn}$ was studied in order to choose the most appropriate values of them, making the determination of absorbed dose more accurate.

2. EXPERIMENTAL

All chemicals were purchased from Merck and used without treatment.

The internal standard of Mn^{2+} magnetically diluted in MgO has been prepared as described [12].

The set of dosimeters was prepared by mixing and homogenization of L-α-alanine (75% w/w), Mn^{2+} magnetically diluted in MgO (15% w/w) and paraffin (10% w/w), used as a binding material. The dosimeters were extruded from this mixture in the form of cylinders with a diameter of 3 mm and a length of 10 mm.

The dosimeters were irradiated with γ-rays in the dose region 100-50 000 Gy on the irradiation unit "Isledovatel" (former USSR) with a dose rate of 1.8 kGy/h. The gamma irradiation was performed in air and at room temperature.

The EPR spectra were recorded on a Bruker ER200D SRC spectrometer at room temperature in a form of first derivative.

Typically all measurements were performed at least 72 hours after irradiation.

3. RESULTS AND DISCUSSION

3. 1. Internal radiation insensitive standard

Mn^{2+} was chosen as an internal standard because it fulfils the requirements for such material [12], namely: our previous studies had shown that at room temperature the host lattice (MgO) is EPR silent; there are no changes in the intensity and other EPR parameters of the Mn^{2+} spectrum after γ-irradiation with doses up to 100 kGy [12]; Mn^{2+} EPR lines are not overlapping with the central part of alanine EPR spectrum; Mn^{2+} lines are narrow, easily and unambiguously distinguished from those of alanine.

3. 2. Radiation detector

Figure 1 shows an EPR spectrum typical of the new generation of alanine dosimeters.

After irradiation, only changes in the intensity of the alanine EPR spectrum occur, whereas the intensity of Mn^{2+} EPR signal remains constant. Thus the ratio $I_{alanine}/I_{Mn}$ will dependent only on the absorbed dose and will be fully independent of the spectrometer used. Therefore, it is obvious that recording spectra under these conditions will permit to find with high accuracy the exact dependence of the alanine EPR response, represented by the ratio $I_{alanine}/I_{Mn}$, on the absorbed dose from high energy radiation.

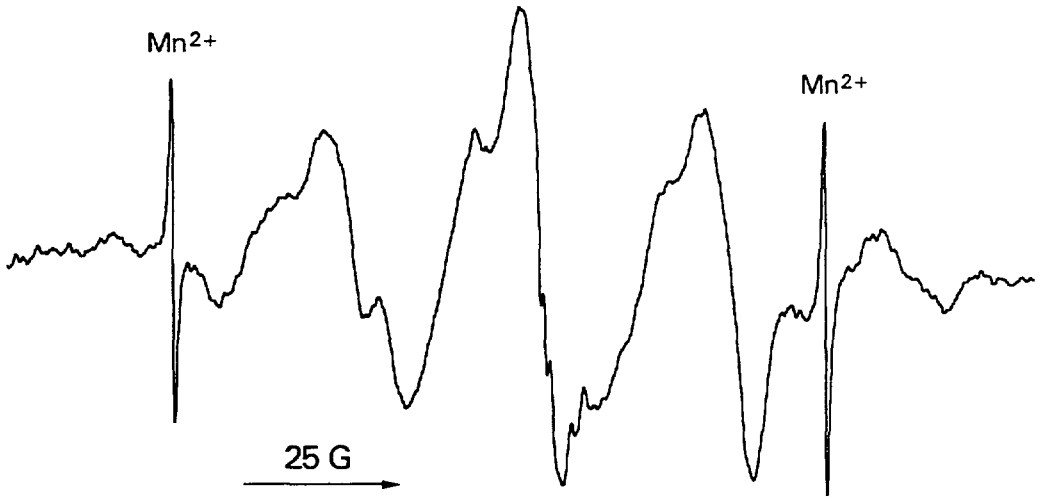

FIG. 1. Typical EPR spectrum of self-calibrated alanine/EPR dosimeter.

3. 3. Dose response

Figure 2 shows a plot of the intensity of the central line of alanine EPR spectrum of dosimeters irradiated with different doses as a function of absorbed dose. This calibration graph may be used only for the present batch of dosimeters and for the EPR spectrometer for which it is prepared. For other spectrometers and/or other dosimeter batches different calibration graphs will be valid.

Figure 3 shows the plot of response of the new type of alanine dosimeter. In it not the intensity of alanine versus absorbed dose, but the ratio between the intensity of the alanine EPR signal and the averaged intensity of the third and fourth Mn^{2+} lines versus absorbed dose is plotted. The simultaneous recording of the spectrum of the radiation sensitive material and of the standard under the same experimental conditions strongly reduces the uncertainties in the dose estimations with these dosimeters. Moreover, this calibration curve is independent of the spectrometer and depends only on the absorbed dose. The response of the described dosimeters for γ-rays in the range of absorbed dose of 100 - 50 000 Gy is found to exhibit excellent linearity and reproducibility within 1%.

On the other hand, using this new type of alanine dosimeters there is no need for each laboratory to prepare its own set of standard samples irradiated in advance with known doses for the calibration of the dosimetry system. It may be expected that the producers of these new type of dosimeters will supply the users with information about the value of the response $(I_{alanine}/I_{Mn})/Gy$ for each batch, which will be characteristic for the dosimeters. In this way, the accuracy of dose estimation will be increased and the results obtained at different laboratories will become comparable. The alternative is to apply the method of the "additional dose" in order to find the response $(I_{alanine}/I_{Mn})/Gy$ with one dosimeter of the batch.

3. 4. Influence of EPR recording conditions

Because after irradiation the described dosimeters contain two EPR active materials, the EPR instrument settings parameters and conditions for simultaneous recording of undistorted spectra of both substances become important. However, it is worth to note that in order to get higher sensitivity it is also possible after inserting the dosimeter in the EPR cavity to record consecutively two separate spectra - one for Mn^{2+} and another for alanine free radical with different EPR instrument settings parameters. In view of this, both possibilities were studied and in the following we describe the EPR instrument setting conditions for simultaneous undisturbed recording of the spectra of both the substances, and also the conditions when the consecutive procedure is used.

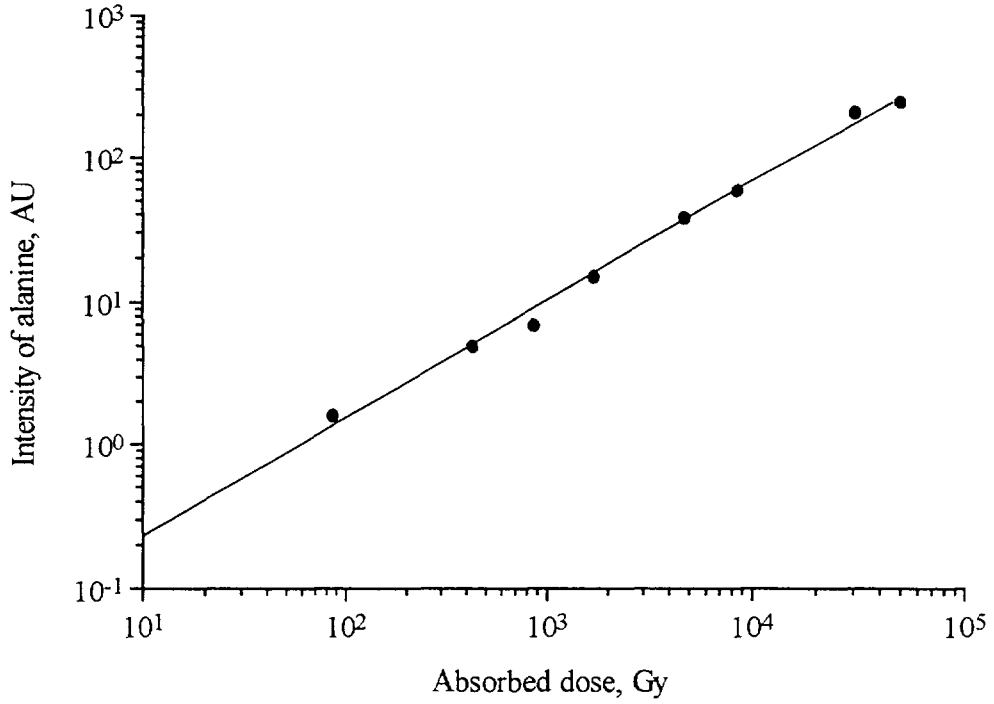

FIG. 2. EPR calibration curve for alanine dosimeters irradiated with γ-rays

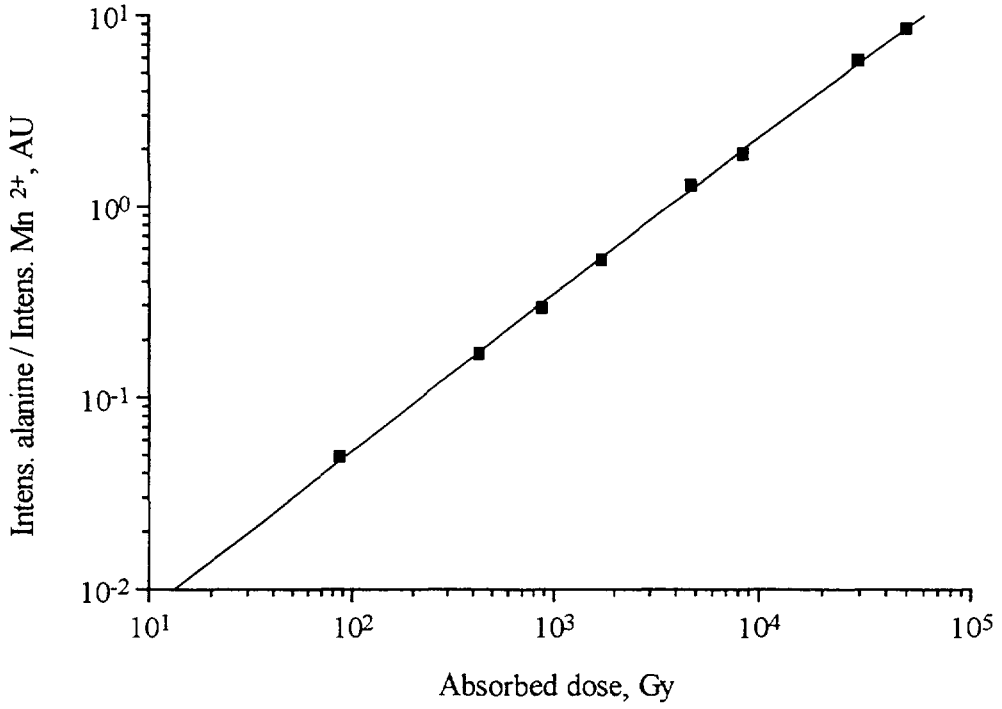

FIG. 3. Dose response curve for the new type solid state alanine dosimeters

3. 4. 1. Microwave power

Figure 4 shows the ratio of the peak-to-peak EPR signal height of the central hyperfine line of alanine and those of Mn^{2+} as a function of the square root of microwave power, P, for irradiated dosimeters. The averaged peak-to-peak intensity of the third (g^{III} = 2.0330) and fourth (g^{IV} = 1.9810) Mn^{2+} lines was taken as a measure of the peak-to-peak intensity of Mn^{2+}. As seen this ratio remains unchanged up to about P = 1 mW and then significantly increases. This effect may be explained with the fact that at P ≥ 1 mW the EPR spectrum of Mn^{2+} is under saturation and thus it is no longer linearly dependent on $P^{1/2}$. Under the same experimental conditions the EPR response of alanine is still in linear dependence of $P^{1/2}$. Therefore, the microwave power must be less than 1 mW for simultaneous recording of the particularly reported SS/EPR dosimeters. On the other hand, separate EPR measurements of Mn^{2+} (at P ≤ 1 mW) and alanine (P ≥ 1 mW) will increase the sensitivity of the estimations.

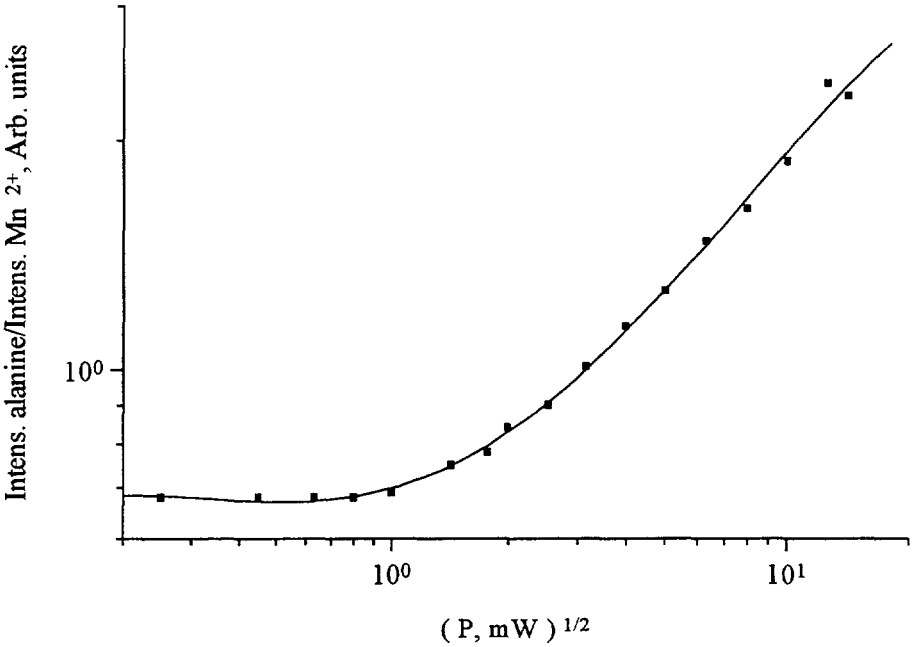

FIG. 4. The ratio of the EPR signal intensity of alanine and Mn^{2+} recorded simultaneously as a function of the square root of microwave power, P.

3. 4. 2. Modulation amplitude

The ratio $I_{alanine}/I_{Mn}$ as a function of the modulation amplitude is plotted in Fig. 5 for the case of simultaneous reading. There is a flat region up to 0.5 G, and after that the ratio $I_{alanine}/I_{Mn}$ increases. This effect is due to the differences in the EPR line widths of alanine and Mn^{2+}/MgO. The present results show that working in the range 0.1 - 0.5 G will assure linear response of the ratio $I_{alanine}/I_{Mn}$ versus absorbed dose of high energy radiation in the case of simultaneous recording. However, to increase the sensitivity it is possible to record two separate spectra - one with modulation amplitude up to 0.5 G for recording of unperturbed Mn^{2+} line and another with c.a. 5 G for alanine.

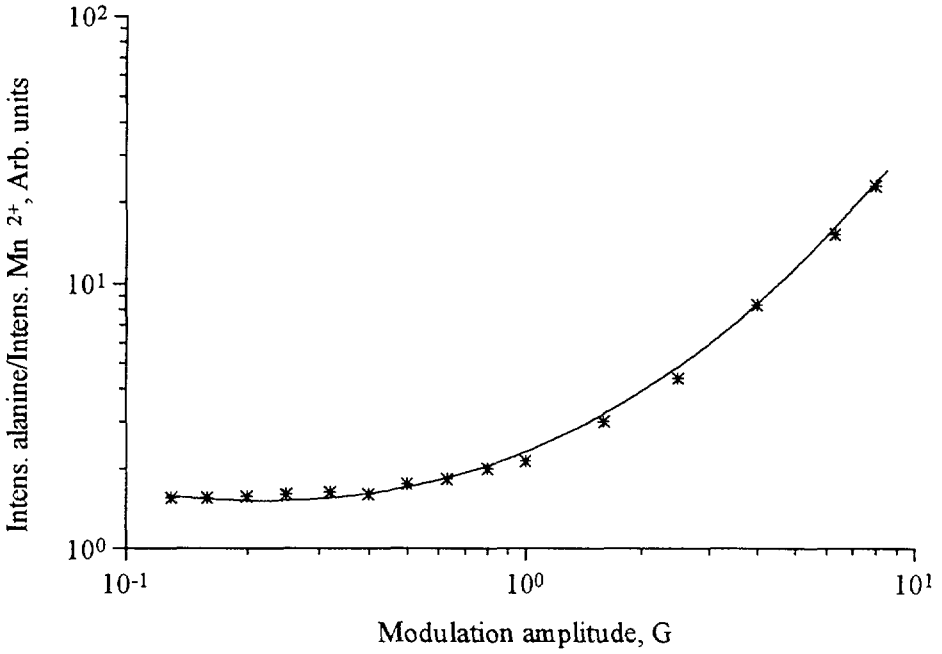

FIG. 5. The ratio of alanine and Mn^{2+} EPR signal intensity as a function of modulation amplitude, A.

3. 4. 3. Modulation frequency

The EPR spectra of irradiated alanine dosimeters were recorded at the modulation frequency of 12.5 kHz and 100 kHz. It was found that the modulation frequency changes only the absolute value of the peak-to-peak height of both signals, but not their ratio.

3. 5. Homogeneity test

Three randomly selected dosimeters from a batch of 50 dosimeters were irradiated at the same dose of c.a. 3 kGy and then were measured by the described simultaneous procedure (*vide supra*). After three consecutive measurements of the EPR spectrum of each of the dosimeters including the procedure inserting-removing-inserting of the dosimeter in the cavity of the EPR spectrometer the deviation was found to be within ±2%.

3. 6. Fading characteristics under storage conditions

The behaviour of the described self-calibrated dosimeters with time after irradiation was studied in respect to the EPR signals fading. The results show that the ratio $I_{alanine}/I_{Mn}$ remains unchanged over a two year period. Thus, after the first recording of the ratio $I_{alanine}/I_{Mn}$, the dosimeter may be kept as a document and it is very easy to re-check at any time without additional calibration graphs. The reproducibility of the data was found to be in the frame of 1%.

3.7. Influence of some meteorological factors

The studies on the behaviour of the ratio $I_{alanine}/I_{Mn}$ was done at different meteorological factors, such as temperature (270 - 330 K) and humidity (40 - 95%). It was found that they do not affect the ratio $I_{alanine}/I_{Mn}$. Moreover, it was found that there is no influence on the ratio $I_{alanine}/I_{Mn}$ even in the cases when dosimeters were kept in water for one hour.

4. CONCLUSIONS

The main conclusion is that the described self-calibrated SS/EPR dosimeter with alanine as a radiation sensitive material is promising, specially in respect to the significant improvement of the reproducibility of the estimations by different EPR spectrometers and laboratories, and the insensitivity of the estimations on external meteorological factors. It makes the analysis more accurate especially in transfer dosimetry, where the data obtained from different laboratories must be compared. Because the fading of the EPR signals is not significant for the present self-calibrated dosimeters, it is possible to repeat very easily the measurements after unlimited (up to now for 2 years) period of time without applying any corrections.

ACKNOWLEDGEMENTS

The financial support from the IAEA (project 8745/RB) and the National Foundation "Scientific Research" (project MY-X-04) are gratefully acknowledged.

REFERENCES

[1] BRADSHAW, W.W., CADENA, D.G., CRAWFORD, G.W., SPETZLER, H. A.W., The use of alanine as a solid radiation dosimeter, Radiat. Res. **17** (1962) 11-21.

[2] BERMANN, F., De CHOUDENCE, H., DESCOURS, S., "Application a la dosimetrie de la measure par resonance paramagnetique electronique des radicaux librescrees dans les acides amines" Advances in Physical and Biological Radiation Detectors (Proc. Symp. Vienna, 1970), STI/PUB/1269, IAEA, Vienna (1971) 311-325

[3] REGULLA, D.F., DEFFNER, U., Dosimetry by ESR spectroscopy of alanine, Int. J. Appl. Radiat. Isot. **33** (1982) 1101-1114

[4] BARTOLOTTA, A., INDOVINA, F.L., ONORI, S., ROSATI A., Dosimetry for cobalt-60 gamma rays with alanine, Radiat. Prot. Dosim. **9** (1984) 277-281

[5] HANSEN, J.W., OLSEN, K.J., WILLE, M., The alanine radiation detector for high and low-LET dosimetry, Radiat. Prot. Dosim. **19** (1987) 43-47

[6] KOJIMA, T., TANAKA, R., MORITA, Y., SEGUCHI, T., Alanine dosimeters using polymers as binders, Appl. Radiat. Isot. **37** (1986) 517-520

[7] McLAUGHLIN, W.L., ESR dosimetry, Radiat. Prot. Dosim. **47** (1993) 255-262

[8] KOJIMA, T., HARUYAMA, Y., TACHIBANA, H., TANAKA, R., Fading characteristics of an alanine-polystyrene dosimeter, Appl.Radiat. Isot.**43** (1992) 863-867

[9] CONINCKX, F., SCHONBACHER, H., Experience with a new polimer-alanine dosimeter in a high-energy particle accelerator environment, Appl. Radiat. Isot. **44** (1993) 67-71

[10] YORDANOV, N.D., GANCHEVA, V., Selfcalibrated dosimeters for determination of high-energy dose on the base of Solid State/EPR spectrometry (submitted for Bulg. Patent)

[11] YORDANOV, N.D., GANCHEVA, V., Selfcalibrated alanine/EPR dosimeters: A new generation of Solid State/EPR dosimeters, J. Radioanalyt. Nucl. Chem. (in press)

[12] YORDANOV, N.D., GANCHEVA, V., PELOVA, V., Studies on some materials suitable for use as internal standards in high energy EPR dosimetry, (submitted)

CHARACTERIZATION OF AQUEOUS SOLUTION OF CONGORED FOR FOOD IRRADIATION DOSIMETRY

Hasan M. KHAN, Mohammad ANWER
Radiation Chemistry Laboratory,
National Centre of Excellence in Physical Chemistry,
University of Peshawar,
Peshawar, Pakistan

Abstract

Aqueous solution of congored has been investigated spectrophotometrically for possible applications in food irradiation dosimetry. Absorption spectra of the solution showed two absorption bands with peaks at 346 and 498 nm. Radiation induced bleaching of the dye was measured at the wavelengths of maximum absorbance (346 and 498 nm) as well as at several other wavelengths (491, 540 and 570 nm). At 498 nm, the decrease in absorbance of the dosimeter was linear with respect to the absorbed dose from 50 to 600 Gy. At the other peak wavelength (346 nm), the response was linear up to 400 Gy, however, the upper limit was increased to 600 Gy when the response was measured at longer wavelengths (491, 540 or 570 nm). If the negative logarithm of the absorbance (-log A) at these wavelengths is plotted versus absorbed dose, a linear response was observed from 50 to 1200 Gy. Post-irradiation stability of dosimetric solution was studied at room temperature and showed almost stable response up to 50 days when stored in dark. The response was found almost stable for 50 days when the solution after irradiation was exposed to white fluorescent light or to diffused sunlight inside the laboratory. The aqueous congored solution is unstable when exposed to direct sunlight, showing rapid decrease in absorbance for the first few hours followed by a slower decrease. The results suggest that the aqueous congored dosimeter with linear response up to 1200 Gy is suitable for a number of food irradiation applications, such as, sprout inhibition of potatoes, onion and garlic and for ripening delay and ripening stimulation of fruits and vegetables.

1. INTRODUCTION

Developing countries have special interest in food irradiation technology to reduce devastating loses of food during harvest and storage as well as to control the causes of foodborne diseases. Recently authorities in Pakistan have cleared a number of food items for radiation treatment. For commercialisation of food irradiation, a reliable dosimetry system is necessary for quality assurance and to satisfy regulatory requirements. Several chemical dosimeters as well as dye or leuco dye solutions have been used for food irradiation dosimetry over a wide range of doses [1-4]. These dyes systems have advantage of being easily commercially available, relatively inexpensive and the solution can be easily prepared, handled and measured spectophotometricaly. We have earlier reported the dosimetric characteristics of some aqueous solutions that can be used for food irradiation dosimetry [5,6]. In the present paper, we have investigated the dosimetric properties of aqueous solution of congored with possible applications in low-dose food irradiation dosimetry.

2. EXPERIMENTAL PROCEDURES

Congored ($C_{32}H_{22}N_6Na_2O_6S_2$, FW 696.68) was purchased from E. Merck (Germany) and was used as received. For the preparation of congored solution, 0.0597 g of the compound was dissolved in triply distilled water to prepare one litre of 100 μmol L^{-1} solution at natural pH (*ca.* 9.5). The solution was saturated with oxygen by passing oxygen through the solution for about 30 minutes.

The cobalt-60 gamma rays source (Issledovatel, former USSR) of the Nuclear Institute for Food and Agriculture (NIFA), Tarnab, was used for irradiations. To get reliable and reproducible results, all the samples were irradiated at a fixed position in the radiation field. The dose rate at the selected irradiation position was determined using Fricke dosimetry solution or GAF films [7,8]. Typical dose rates at the calibrated position was 39 Gy/minute.

Irradiation of solutions were carried out as follows: 9 ml of solution was taken in a Pyrex glass tube with a ground stopper. The tubes were placed in the radiation field at a fixed position with the help of a stand and were irradiated for predetermined interval of time. For each absorbed dose, at least three samples were irradiated in order to calculate an average value and standard deviation. All irradiations were carried out in the presence of air at room temperature (*ca.* 25 °C). Before and after irradiation, the dosimetric solutions were protected from light. Absorbance measurements were made using a Varian DMS-200 UV-VIS spectrophotometer. Radiation induced absorption changes were determined against unirradiated solution as blank unless specified.

3. RESULTS AND DISCUSSION

3.1. Absorption spectra of unirradiated and irradiated solutions

In order to select a suitable wavelength for dosimetric characterization, absorption spectra of the unirradiated solution as well as the irradiated solution were determined in the spectral range of 320 nm to 700 nm. The absorption spectra of oxygen saturated aqueous congored solutions (pH 9.5) before and after irradiation for different absorbed doses of gamma rays (50 to 1200 Gy) are shown in Fig.1. The spectra show that the maximum in the absorbance lies at 498 nm and 346 nm which are comparable to the reported values (*i.e.* 497 nm) [9]. The spectra also show that there is a decrease in the absorbance of the irradiated solution over all the wavelength range (320 to 586 nm) as the absorbed dose is increased. The 498 nm absorbance peak almost disappears at high absorbed doses. Therefore, wavelengths of maximum absorption (*i.e.* 346 and 498 nm) should be suitable wavelengths for dosimetric characterization. In the present study, the measurements have been made at these peak wavelengths as well as at three other wavelengths (*i.e.* 491, 540 and 570 nm).

3.2. Response curves and useful dose range

Response curves (plot of change in absorbance of the irradiated solution at a selected wavelength versus absorbed dose) were determined to find out the useful dose range of the 100 μmol L^{-1} aqueous congored solution. Fig. 2, shows a typical response curve at 498 and 540 nm, where the response of the dosimeter with respect to absorbed dose was linear in the range of 50 to 600 Gy. At other peak wavelength, *i.e.* at 346 nm, the response showed linearity up to an absorbed dose of 400 Gy. However, this dose range can be increased up to 600 Gy, if analysed at other wavelengths *i.e.* 491 and 570 nm. The response deviates from linearity at higher doses. Thus the useful dose range for the congored dosimeter is from 50 to 400 Gy at 346 nm and from 50 to 600 Gy if measurements are made at longer wavelengths (491, 498, 540 or 570 nm).

However, when negative logarithm of the absorbance (-log A) is plotted against absorbed dose at these wavelengths, a linear response is observed at all these wavelengths up to 1200 Gy as shown in Figs 3 and 4. This wide range makes the use of this dosimeter suitable for a number of low-dose food irradiation applications [10].

3.3. Pre-irradiation shelf-life

Aqueous solution of congored (100 μmol L^{-1}) at pH 9.5 or at pH 7.0 were stored at room temperature either in the dark or under room fluorescent light or in a refrigerator (*ca.* 7 °C). Absorption spectra of these solutions were determined at different times after the preparation of solution. It was

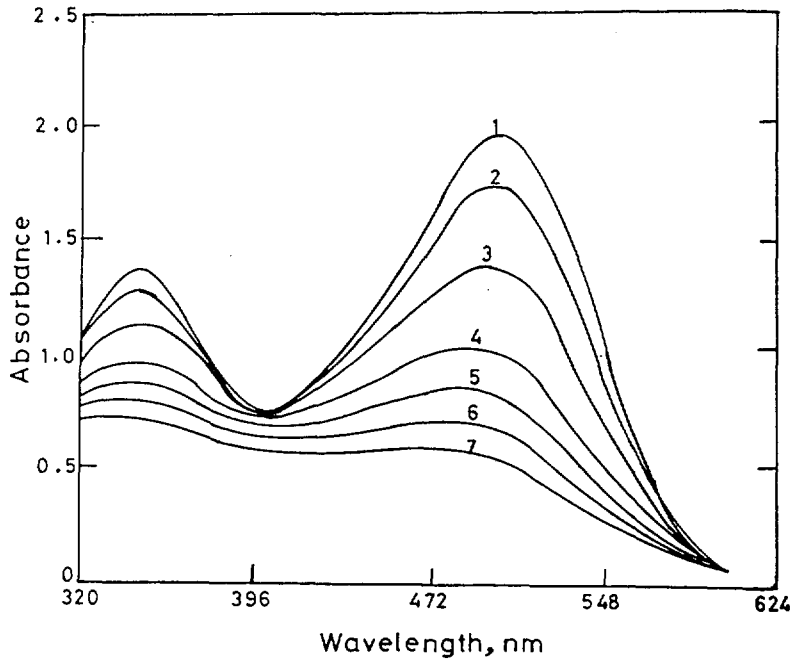

FIG. 1. Absorption spectra of 100 μmol L^{-1} aqueous solution of congored versus water. The numbers beside the curves indicate absorbed dose. 1: unirradiated; 2: 100 Gy; 3: 300 Gy; 4: 600 Gy; 5: 800 Gy; 6: 1000 Gy; 7: 1200 Gy.

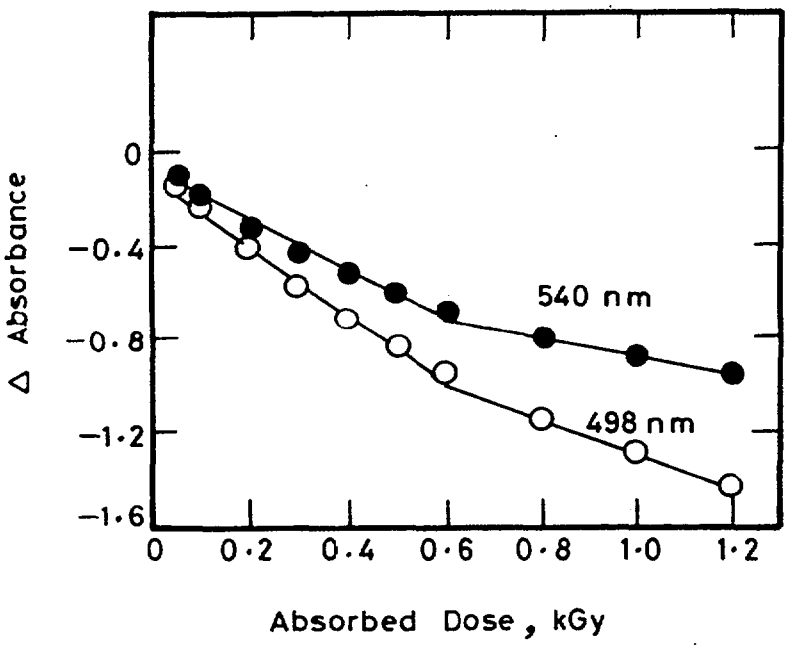

FIG. 2. Response curve for aqueous congored solution at 498 and 540 nm.

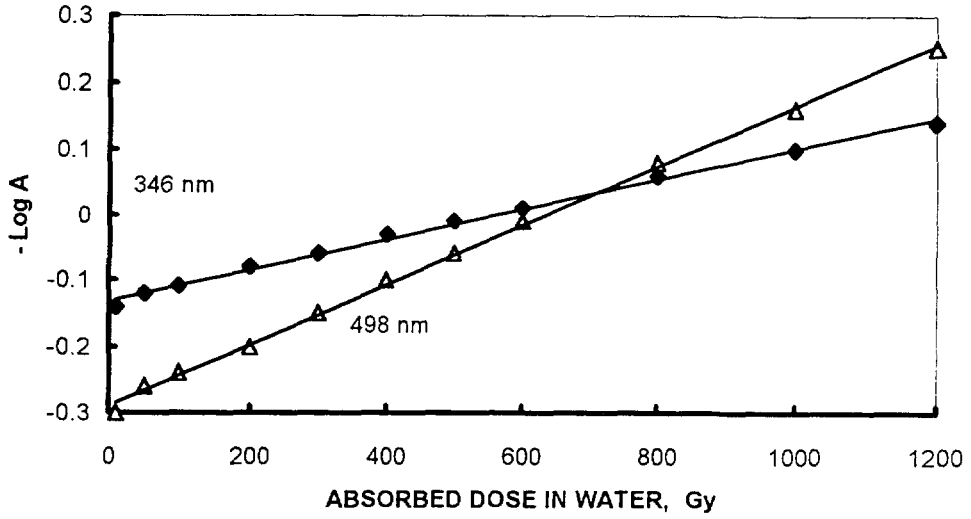

FIG. 3. Radiation response function (in terms of negative logarithm of absorbance) versus absorbed dose in water for 100 μmol L^{-1} aqueous solution of congored measured at 346 and 498 nm.

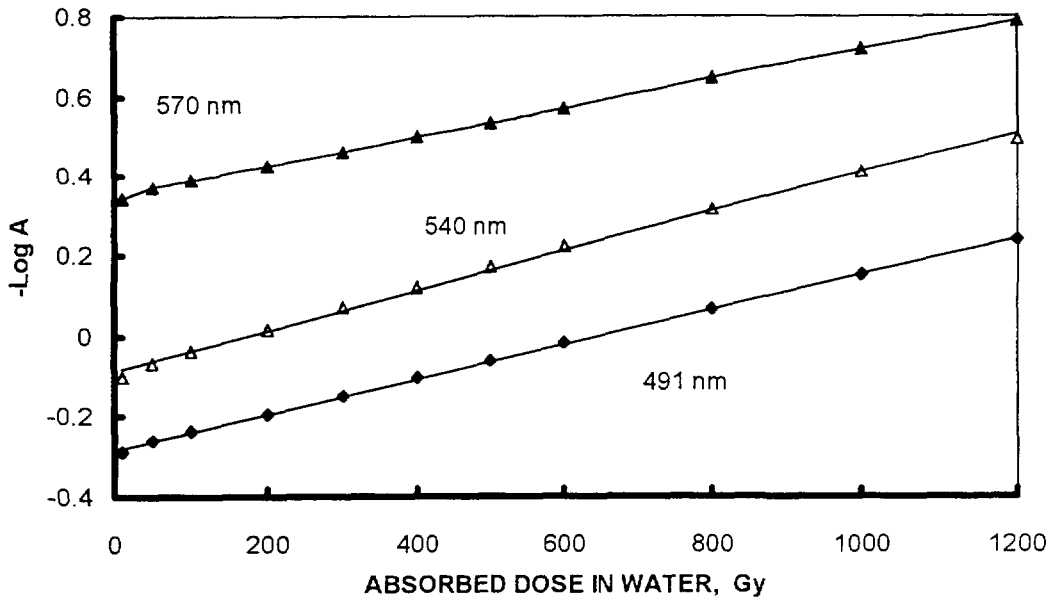

FIG. 4. Radiation response function (in terms of negative logarithm of absorbance) versus absorbed dose in water for 100 μmol L^{-1} aqueous solution of congored measured at 491, 540 and 570 nm.

observed that there was no change in the absorption characteristics of the solutions for a storage period of 22 days either in the dark or in fluorescent light at both the pH values. However, when stored in a refrigerator, the stock solution of the congored was quite stable up to 65 days.

The foregoing results suggests that stock solution of congored at natural pH 9.5 can be stored up to three weeks either in the dark or in fluorescent light and for more than two months in a refrigerator and, therefore, preparation of fresh solution is not necessary for daily experiments.

3.4. Post-irradiation stability

Stability of the dosimetric solution during post-irradiation storage in dark was checked for a storage period of about 50 days at all the selected wavelengths (*i.e.* 346, 491, 498, 540 and 570 nm).

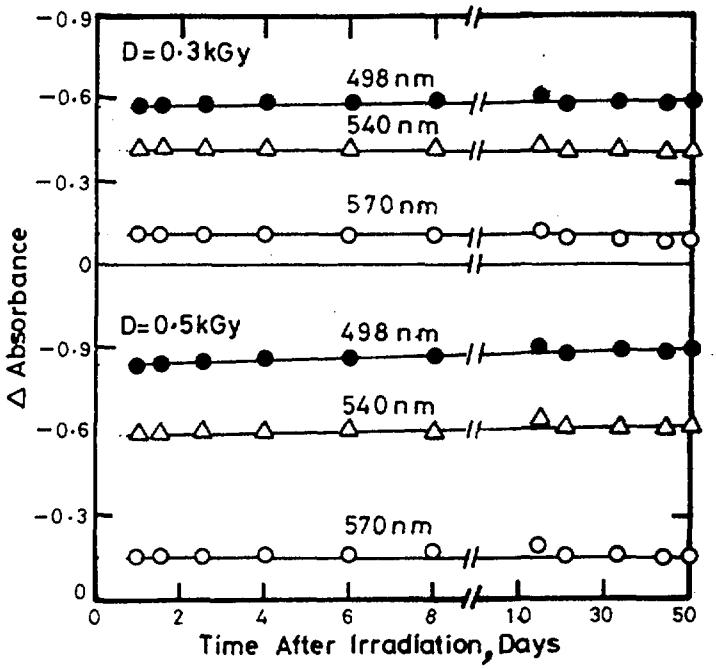

FIG. 5. Stability of response of aqueous congored solution during post-irradiation storage in dark.

Two sets of dosimetric solutions were irradiated to absorbed doses of 300 or 500 Gy in stoppered Pyrex glass tubes. After irradiation, the dosimetric solutions were wrapped in black polyethylene bags to protect them from light and stored at room temperature (*ca.* 25 °C). The response of the dosimeter was measured at different intervals of time and representative results are presented in Fig. 5 for three wavelengths at both the absorbed doses. It was concluded that the radiation induced absorbance remained stable for a storage period of 50 days at 346, 540 and 570 nm. However, at 491 and 498 nm there was a slow and continuous decrease in absorbance with time for both the absorbed doses. This effect was less pronounced for absorbed dose of 300 Gy as compared to 500 Gy.

3.5. Post-irradiation stability under different light conditions

In many dosimeters, the change in absorbance due to irradiation is not stable and is generally affected by a number of environmental factors during post-irradiation storage, such as, light, temperature and humidity conditions. In order to check the effects of various light conditions, which the dosimeter may encounter during commercial irradiation, the solutions were irradiated to 300 or 500 Gy and stored either in white fluorescent light, in diffused sunlight inside the laboratory or under direct sunlight.

In order to check the effect of fluorescent light on aqueous congored dosimeter, the solutions after irradiation were stored at room temperature under fluorescent light until spectral analysis. Fig. 6 shows the effect of fluorescent light on the response of dosimeter for three wavelengths (498, 540 and 570 nm). The results showed that the response of the dosimeter was almost stable at 346, 540 and 570 nm for both the absorbed doses over a storage period of 50 days while around the peak of broad absorbance band (491 and 498 nm), there was a slow and continuous decrease in absorbance with time, similar to the behaviour for storage in dark.

Similarly, two sets of congored solutions irradiated to dose levels of 300 and 500 Gy were exposed to diffused sunlight inside the laboratory. The results were similar to that observed for storage in dark or in fluorescent light described above.

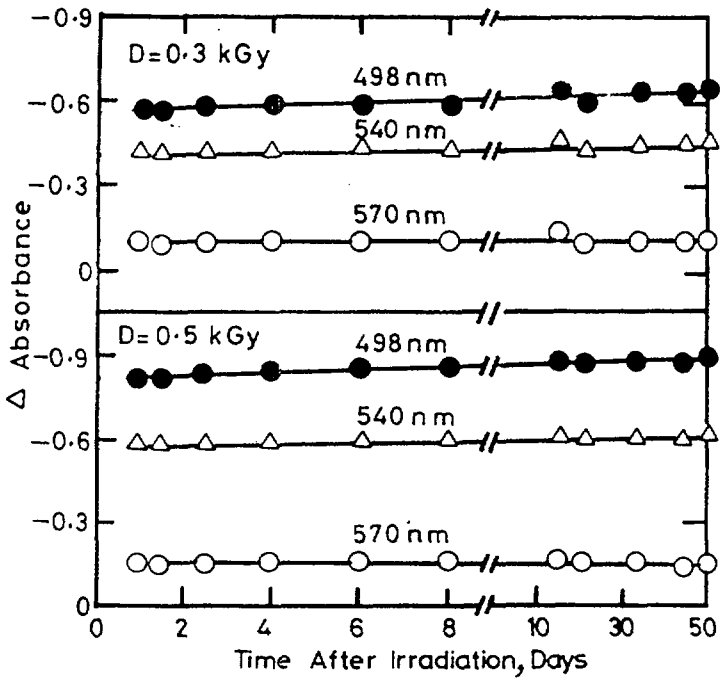

FIG. 6. Stability of response of aqueous congored solution during post-irradiation storage in room fluorescence light.

To check the behaviour of the dosimeter under direct sunlight, irradiated solutions were exposed to direct sunlight and the response of the solutions were measured at all the selected wavelengths. The results indicated a significant bleaching at all the wavelengths with some rapid decrease in the absorbance within first few hours after exposure to direct sunlight followed by a slow and steady decrease in the response at all the wavelengths. It is noteworthy that exposure to direct sunlight results in a drastic decrease in response similar to that observed in several other aqueous dosimetry solutions, such as ferrous-cupric sulphate, coumarine and triphenylmethane solutions [3,5,6].

The foregoing results suggested that the response of the aqueous congored dosimeter is somewhat unstable in direct sunlight. Therefore, the dosimetric solution should not be exposed to direct sunlight, however exposure to room fluorescent light or diffused sunlight does not affect the stability of the response during post-irradiation storage.

4. CONCLUSIONS

It can be concluded that aqueous solution of congored with a linear dose response from 50 to 1200 Gy can be used as a dosimeter for a number of low-dose food irradiation applications, such as sprout inhibition of potatoes, onion and garlic (up to 150 Gy), for ripening delay and ripening stimulation of fruits and vegetables (100 to 1000 Gy) and to control insect infestation of dates, beans, pulses, rice and wheat during storage (1000 Gy). The response of the dosimeter is stable in dark, in diffuse sunlight or in room fluorescence light for about seven weeks, however, the solution should be protected from direct sunlight.

ACKNOWLEDGEMENT

We are grateful to the NIFA authorities for permission to use radiation facilities.

REFERENCES

[1] McLAUGHLIN, W.L., BOYD, A.W., CHADWICK, K.H., McDONALD, J.C., MILLER, A. "Dosimetry for Radiation Processing", Taylor and Francis, London (1989), ch 8.

[2] EL-ASSAY, N.B., ROUSHDY, H.M., RAGEH, M., McLAUGHLIN, W. L., LEVINE,H, "γ-Ray dosimetry using pararosaniline cynide in dimethyl sulfoxide solutions", *Int. J. Appl. Radiat. Isot.* **33** (1982) 641-645.

[3] EL-ASSAY, N.B., YUN-DONG, C.,WALKER, M.L., AL-SHEIKHLY, M., McLAUGHLIN, W.L., "Anionic triphenylmethane dye solutions for low-dose food irradiation dosimetry", *Radiat. Phys. Chem.* **46** (1995) 1189-1197.

[4] KOVACS, A.., WOJNAROVITS, L., KURUCTZ, C.,ALSHEIKHLY, M., McLAUGHLIN, W. L., "Large scale dosimetry using dilute methylene blue dye in aqueous solution", *Radiat. Phys. Chem.* **52** (1998) 539-542.

[5] KHAN, H.M., ANWER, M., "Stability of response of the ferrous-cupric sulfate dosimeter at different temperature", *J. Radioanal. Nucl. Chem., Lett.* **173** (1993) 199-206.

[6] KHAN, H.M., ANWER, M., "Effect of temperature and light on the response of an aqueous coumarin dosimeter", *J. Radioanal. Nucl. Chem., Lett.* **200** (1995) 521-527.

[7] SEHESTED, K. "The Fricke dosimeter", Manual on radiation dosimetry (HOLM, N. W., BERRY, R. J., Ed.) Marcel Dekker, New York, (1970) 313-317.

[8] McLAUGHLIN, W. L., CHEN, Y., SOARES, C. G., MILLER, A., VAN DYKE, G., LEWIS, D. F., "Sensitometry of the response of a new radiochromic film dosimeter to gamma radiation and electron beams", *Nucl. Instr. Methods Phys. Res.* **A302** (1991) 165-176.

[9] ALDRICH, Handbook of Fine Chemicals (1992-93) p 179, 333.

[10] CHADWICK, K.H., EHLERMANN, D.A.E., McLAUGHLIN, W.L., "Manual of Food Irradiation Dosimetry", IAEA Technical Report Series No.178, Vienna (1977).

A POLYMERIC DOSIMETER FILM BASED ON OPTICALLY-STIMULATED LUMINESCENCE FOR DOSE MEASUREMENTS BELOW 1 kGy

A. KOVÁCS, M. BARANYAI, L. WOJNÁROVITS
Institute of Isotopes and Surface Chemistry, Chemical Research Center,
Hungarian Academy of Sciences, Budapest, Hungary

I. SLEZSÁK
Z. Bay Applied Research Foundation, Budapest, Hungary

W.L. McLAUGHLIN
Ionising Radiation Division, Physics Laboratory,
National Institute of Standards and Technology,
Gaithersburg, Maryland,
United States of America

S.D. MILLER
Sunna Systems Corporation,
Richland, Washington,
United States of America

A. MILLER
High-Dose Reference Laboratory, Risø National Laboratory,
Roskilde, Denmark

P.G. FUOCHI, M. LAVALLE
Institute of Photochemistry and High Energy Radiation,
Bologna, Italy

Abstract

A new potential dosimetry system "Sunna" containing a microcrystalline dispersion of an optically-stimulated fluor in a plastic matrix has been recently developed to measure and image high doses. Our previous investigations have revealed that the new dosimeter system is capable of measuring absorbed doses in the dose range of 1-100 kGy. The optically-stimulated luminescence (OSL) analysis is based on the blue light stimulation of the colour center states produced upon irradiation, and the intensity of the resulting red-light emission is used to measure absorbed dose. This analysis is carried out with a simple table-top fluorimeter developed for this purpose having also the ability to calculate the mathematical formula of the calibration function. The Sunna dosimeter was recently investigated for potential use in lower dose range below 1 kGy. These investigations have shown that the film is suitable for measuring doses in the range of 1-1000 Gy for both electron and gamma radiation. To test the applicability of the film, its reproducibility, stability, sensitivity to ambient and UV light and irradiation temperature were measured. The stability of the dosimeter was investigated by monitoring the change of the OSL signal with storage time after irradiation. Further experiments proved the homogeneity of the film with respect to thickness variation, and limited differences in its response were found between batches.

1. INTRODUCTION

Upon irradiation of alkali halide crystals (e.g. LiF), various types of stable absorption bands appear in the crystal lattice as "damage" centers. By photoexcitation of some of these centres increasing luminescence is produced with increasing radiation dose. Optically stimulated luminescence (OSL) dosimetry, by applying inorganic solid-state fluors distributed in a matrix, is a well-known method to

measure small absorbed doses [1]. The readout method uses excitation of the fluor by relatively short wavelength light (e.g. blue light, 450 nm) and the resulting emission intensity is measured by a photodetector at higher wavelengths (670 nm). The OSL method has the advantage that the emission centers are not removed by the readout procedure; thus the irradiated samples can be read several times making possible e.g. archival dosimetry application.

A new OSL based dosimeter system, the Sunna dosimeter film, has been developed recently with the primary aim of measuring doses in the sterilization range. Detailed investigations have revealed that this dosimeter film is capable of measuring doses in the range of 1-100 kGy [2]. Due to irradiation temperature and dose rate effects on the film, however, for higher doses (> 5 kGy), the optical absorption evaluation method with short-wavelength ultraviolet densitometry or spectrophotometry appears to be more suitable than the OSL evaluation. In the lower dose range (< 5 kGy), however, this method is not sensitive enough, thus the potential use of OSL analysis was investigated.

The aim of the present work was to study the applicability of the Sunna "N" film with OSL readout with respect to the characteristics of the film radiation temperature dependence and response to gamma radiation and electrons. In addition, a new OSL readout instrument is introduced.

2. EXPERIMENTAL

There are different types of the Sunna dosimeter films containing the same fluor (LiF), but incorporated into different types or different thicknesses of polymer host material. In the case of the Sunna "N" type film, it is polyethylene with a thickness of 0.24 mm or 0.40 mm. The size of the film is 1cm x 3cm which fits into the hinged holder of the OSL reader. The reader is the Sunna Fluorimeter(type FR-2141, produced by Sensolab, Ltd. God, Hungary). It is a simple table-top fluorimeter, coupled with a PC, designed to measure the dosimeter film. The irradiated samples are excited with a pulsed light source of wavelength of around 450 nm. The emitted fluorescing light is measured by photometric reading at around 670 nm, and its value (mV) can be related to the absorbed dose (kGy) by means of a calibration function that has been entered previously into the memory of the reader using a set of "standard" irradiated OSL dosimeter samples. The calibration function (a third-order polynomial) is stored in the Word Perfect for Windows software in the memory of the reader for absorbed dose determinations of dosimeter samples irradiated to unknown doses. The calculated dose values are then stored in the memory of the reader.

The gamma irradiations were carried out with the Gammacell type ^{60}Co facility of Riso National Laboratory (Roskilde, Denmark; dose rate in the irradiation position: 1.8 kGy/h), and with the pilot scale ^{60}Co irradiation facility of the Institute of Isotopes Ltd. Co. (Budapest, Hungary; dose rate in the irradiation position: 1.0 kGy/h and 18 kGy/h). The electron irradiations were performed with the 10-MeV linear accelerator (2-μs pulses of 4 Gy/pulse with 50 Hz repetition rate) of the Institute of Photochemistry and High Energy Radiation Research of the C.N.R. (Bologna, Italy).

The absorbed dose in the case of the gamma irradiations at the Institute of Isotopes and Surface Chemistry was measured with the oscillometric ethanol-monochlorobenzene dosimetry system, while in the case of electron irradiations the dose per pulse value was determined with super Fricke dosimeter solution.

3. RESULTS AND DISCUSSION

3.1. Dose response with gamma and electron irradiation

In order to study the dose response of the Sunna "N" type dosimeter film, the fluorimeter, originally developed for dose measurements in the 1-100 kGy range, was modified to enhance the system sensitivity for measuring doses below 1 kGy. The Sunna films were irradiated in the dose range of 1-1000 Gy using both gamma and electron irradiation. The dose response of the dosimeter film for

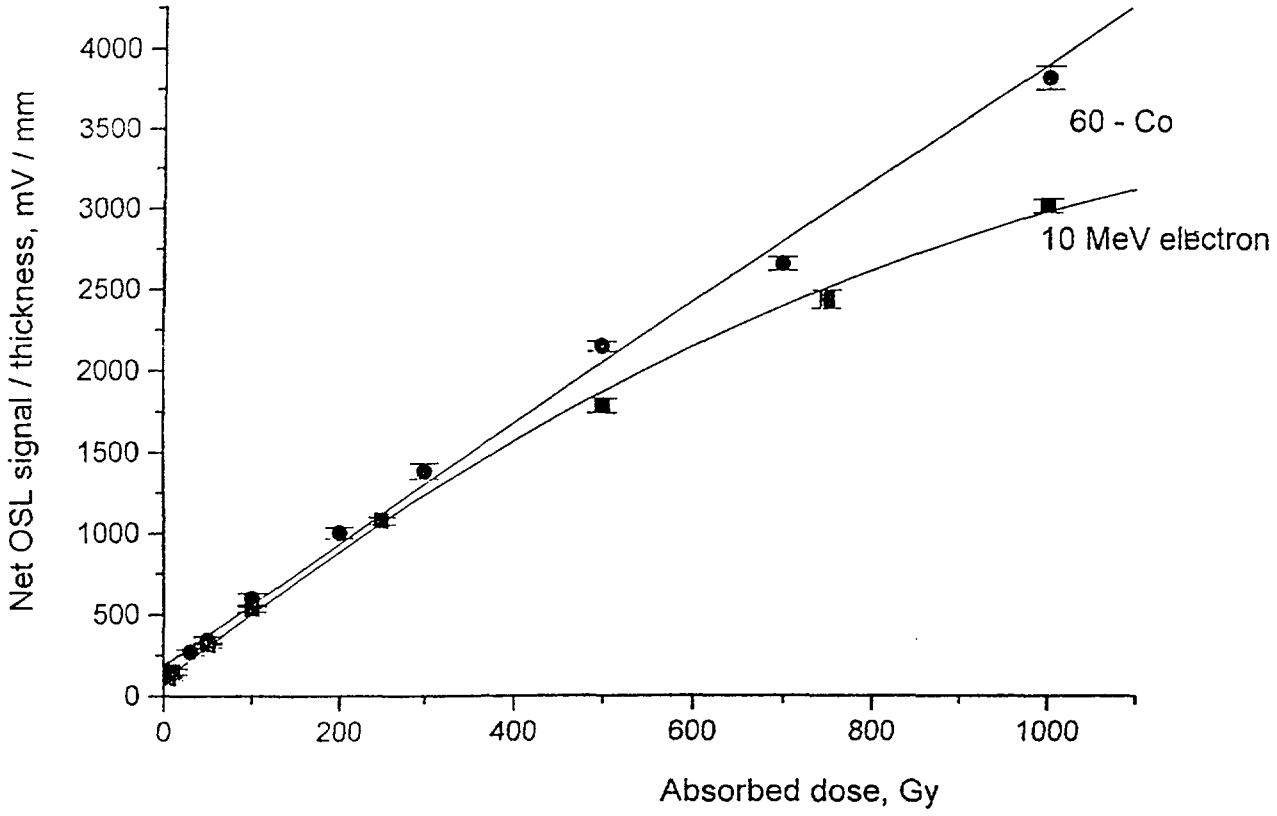

FIG. 1. Dose response of the gamma and electron irradiated Sunna "N" dosimeter film (error bar: 1 standard deviation)

the two types of irradiation is shown on Fig. 1. The net OSL signal was divided by the thickness of the film, and this value is plotted as a function of absorbed dose.

When studying the dose response of the Sunna "N" film below 1 kGy it was found that with the present film and the reader doses from about 1 Gy can be measured with a reproducibility of less than ±5 % (1 σ). The response function can be described with a second-order polynomial for both types of radiation. The response of the film is not the same (see Fig. 1.), i.e. it is less sensitive for electron irradiation (high dose rate) than with gamma radiation (low dose rate), and this effect becomes more pronounced with increasing dose.

When studying the effect of gamma-ray dose rate in the range of 0.18-18 kGy/h, no difference in the response of the films was observed in the case of the films irradiated up to a dose of 1000 Gy. When comparing the response of the films irradiated to the same dose with electron and gamma irradiation, however, it was found that the electron irradiated film samples had approximately 20 % less response.

3.2. Effect of irradiation temperature

In order to check the effect of irradiation temperature on the response of the Sunna "N" film - especially in light of the previous observations of significant temperature dependence at doses above 5 kGy [3] - the dosimeter samples were irradiated in the temperature range of 10-60 °C at doses of 100 Gy, 500 Gy and 1000 Gy. Similar effect was observed at all three doses as shown in Fig. 2 for 1000 Gy.

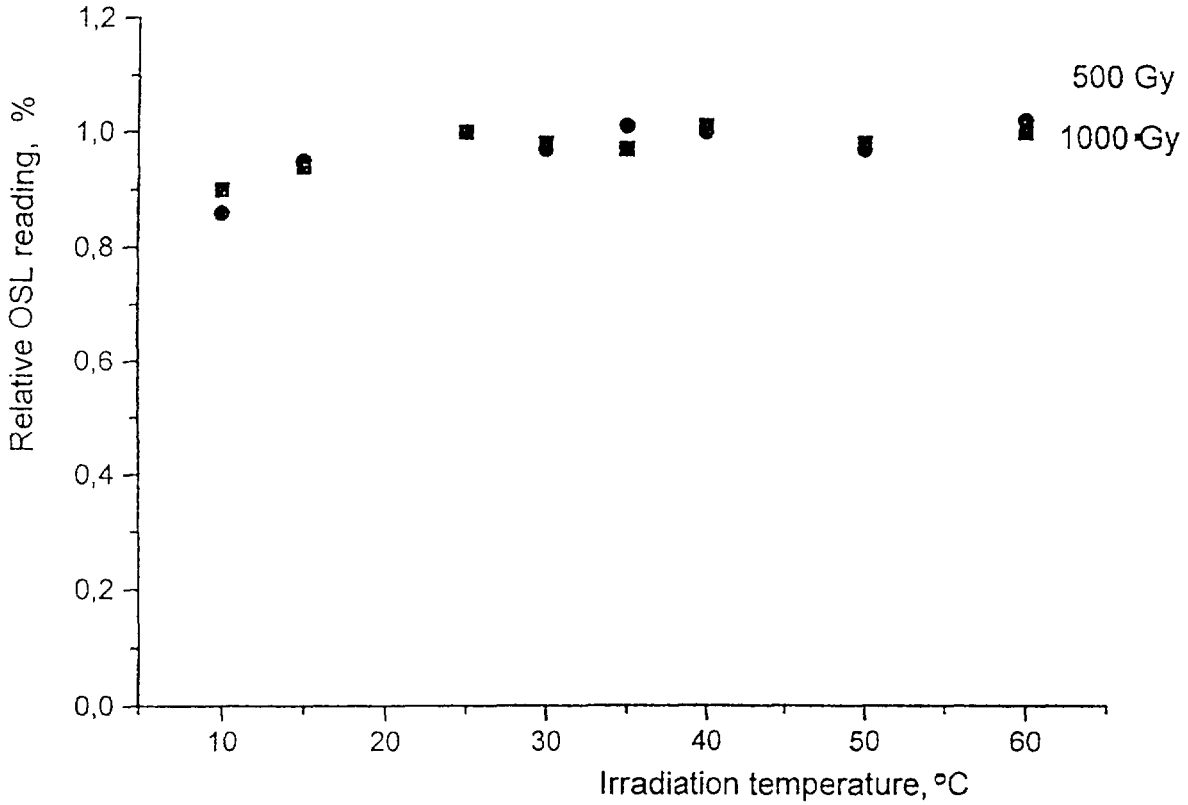

FIG. 2. Effect of irradiation temperature on the dose response of the Sunna "N" film (All data are normalized to the OSL value measured at 25 °C)

As seen, there is almost no effect of the irradiation temperature in the temperature range of 15-60 °C, but below 15 °C a lower dose response was found. This observation is also supported by our preliminary results carried out in the temperature range of -30 to +10 °C, where the dose response at low temperatures showed a significant decrease compared to the results measured at room temperature.

3.3. Stability of the OSL reading

The stability of the OSL reading after irradiation has been studied in order to determine the most suitable timing for readout, both for calibration and routine measurement. Immediately after irradiation, a significant increase in the OSL signal was observed in the first 4 hours, then the signal becomes stable. The long time stability, on the other hand, has shown that the OSL signal increases - although to a much smaller extent - during the first two days after irradiation. In order to improve the post irradiation stability of the film, the irradiated film samples were heated after irradiation at 60 °C for 15 minutes. According to our preliminary investigations this heat treatment resulted in the disappearance of the post irradiation change, i.e. the OSL response of the films irradiated to 500 Gy and 1000 Gy was almost constant for hours after irradiation (Fig. 3.).

With respect to the stability in the presence of ambient light, the Sunna "N" film samples were exposed to different intensities of UV radiation using different types of UV lamps. The OSL signal of the films was measured before and after exposure and no change in the reading was observed, indicating the absence of the effect of light on the dosimeter film.

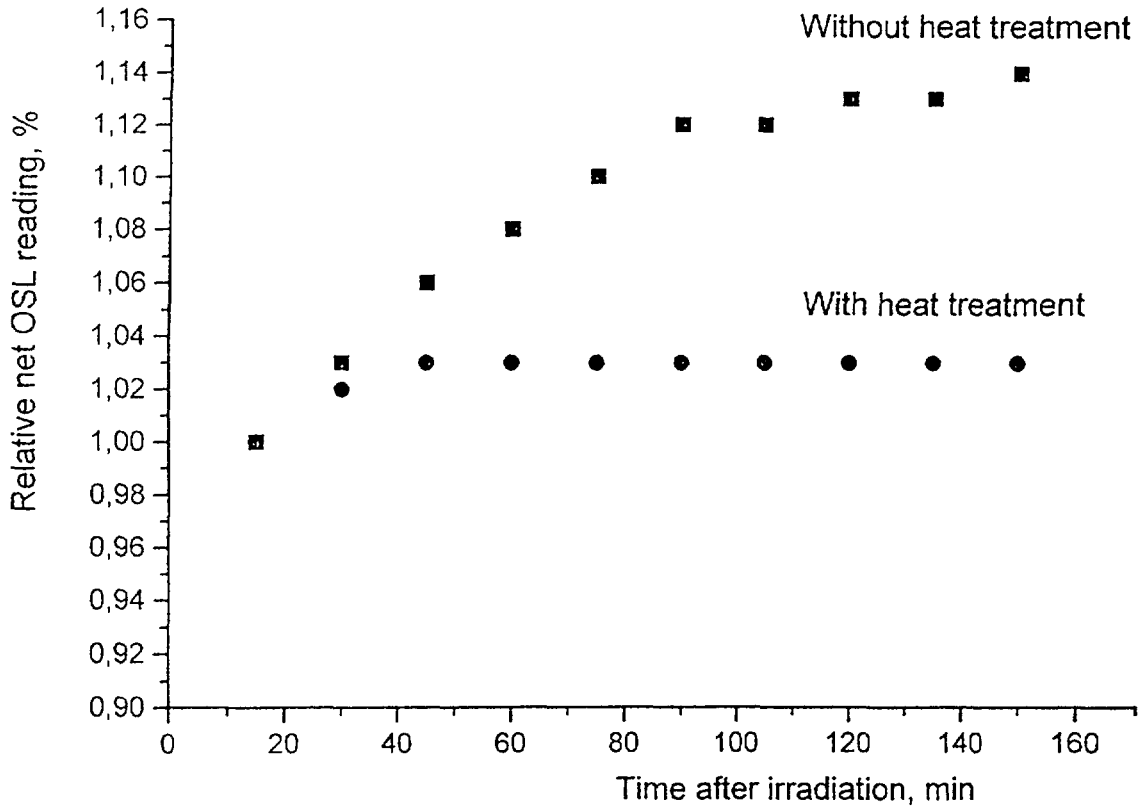

FIG. 3. Change of OSL signal of films irradiated to 1000 Gy with and without post-irradiation heat treatment(OSL readings are normalized to the value measured soon after irradiation).

4. CONCLUSIONS

The Sunna "N" type films studied earlier for high-dose applications using the OSL evaluation method have been investigated with respect to their potential use for measuring doses below 1 kGy. By modifying the fluorimeter that was originally designed for high doses, it was possible to carry out dose determination in the range of 1-1000 Gy.

The dose response functions of the gamma and electron irradiated Sunna "N" films were different for the two types of radiation, gamma-rays and electrons, but each can be described by a second-order polynomial in the dose range of 1-1000 Gy. It means consequently, that these types of films must be calibrated separately both for gamma and electron irradiation.

No irradiation temperature effect was observed on these dosimeter films in the temperature range of 15-60 °C, but below 15 °C decreasing signal of the OSL response was found with decreasing temperature. There is no dose rate effect in the case of gamma irradiation in the range of 0.18-18 kGy/h. At very high dose rates of electron irradiation, however, smaller response compared to gamma irradiation dose rate was observed.

No effect of UV radiation on the stability of the response of the dosimeter film was found. It was shown, however, that post-irradiation heat treatment of the irradiated films eliminates the change (increase) of OSL response of the films thus increasing their post-irradiation instability.

ACKNOWLEDGEMENT

The present work was carried out with the support of the Hungarian National Research Fund (contract No.: T 017089) and in the frame of the Joint US - Hungarian Research Fund No. 508.

REFERENCES

[1] MILLER, S.D., ESCHBACH, P.A., Optimized readout system for cooled optically stimulated luminescence, Radiation Effects Defects Solids, (1991), 119-121.

[2] McLAUGHLIN, W.L., MILLER, S.D., SAYLOR, M.C., KOVACS, A., WOJNAROVITS, L., A preliminary communication on an inexpensive mass-produced high-dose polymeric dosimeter based on optically-stimulated luminescence, Radiat. Phys. Chem. (in press).

[3] McLAUGHLIN, W.L., PUHL, J.M., KOVACS, A., BARANYAI, M., SLEZSAK, I., SAYLOR, M.C., SAYLOR, S.A., MILLER, S.D., MURPHY, M., Work in progress, Sunna Dosimeter: An integrating photoluminescent film and reader system, Radiat. Phys. Chem. (in press).

RADIOCHROMIC BLUE TETRAZOLIUM FILM DOSIMETER

M. AL-SHEIKHLY*, W.L. McLAUGHLIN***, A. CHRISTOU*, A. KOVÁCS***

*Department of Materials and Nuclear Engineering, University of Maryland, College Park, Maryland, United States of America

**Ionizing Radiation Division, Physics Laboratory, National Institute of Standards and Technology, Gaithersburg, Maryland, United States of America

***Institute of Isotopes and Surface Chemistry, Chemical Research Center, Hungarian Academy of Sciences, Budapest, Hungary

Abstract

The colourless radiochromic chloride salt of blue tetrazolium (BT^{2+}) is reduced radiolytically to the deep violet-coloured formazan. Dosimeter films of this radiation sensor can be produced by dissolving polyvinyl alcohol (PVA) in a heated aqueous solution of the salt, and, upon cooling, by casting the solution on a horizontal glass plate. In the present development, the resulting flexible transparent film is readily stripped from the plate, with a thickness of 0.045 mm. Upon irradiation with gamma rays or electron beams, a permanent image is produced with a broad absorption band in the visible spectrum. The radiation response is approximately a linear function in terms of the increase in optical absorbance (ΔA) measured at λ_{max} = 552 nm wavelength versus absorbed dose (D) over the range 5 to 50 kGy. The radiochromic image has a relatively high spatial resolution and can be used to register dose distributions and beam profiles. The value of ΔA shows a gradual increase for the first 24 hours after irradiation but is stable thereafter. The variation of response with irradiation temperature is negligible over the temperature range -20 °C to +30 °C, but displays a pronounced positive temperature dependence at higher temperatures. The response to gamma radiation shows negligible dose-rate dependence as long as the radiochromic sensor concentration in the PVA matrix is sufficiently high (> 6 % by weight).

1. INTRODUCTION

The ditetrazolium chloride salt, $C_{40}H_{32}Cl_2N_8O_2$ is referred to in dye literature as *blue tetrazolium* (BT^{2+}) [1,2]. It has been used histochemically and cytochemically as a biological stain with oxidative enzyme systems, especially nicotinamide coenzyme-formed dehydrogenase reactions, for the past 50 years [3,4]. BT^{2+} is an analogue of the more familiar mono-tetrazolium form, in particular the triphenyl-tetrazolium chloride (TTC) salt, used as a radiochromic dosimeter by means of radiolytic reduction to triphenyl-formazan pigment. Slightly soluble in aqueous or alcohol solution and in hydrogels, BT^{2+} forms a nearly colourless, pale yellow medium. When irradiated with short-wave ultraviolet or ionizing radiation, however it is reduced irreversibly to a deep-violet di-formazan pigment. This reaction is similar to radiation chemical reactions studied by pulse radiolysis of other tetrazolium salt solutions, e.g. the mono-form 2,3,5-triphenyl-tetrazolium chloride [5-7]. Aqueous solutions of BT^{2+} have recently been investigated at the University of Maryland and NIST by pulse radiolysis [8], which gave results similar to those reported by Bielski's group at Brookhaven National Laboratory with another aqueous di-tetrazolium, nitro blue tetrazolium (NBT^{2+})[9]. It is shown that the reactions of BT^{2+} or NBT^{2+} with the hydrolytic hydrated electron and hydrogen atom proceed by rapid reduction at a rate constant of about 10^{10} $M^{-1}s^{-1}$, with protonation occurring at the nitrogen closest to the unsubstituted phenyl group. This reaction involves the step-wise addition of four electrons and the formation of two transient tetrazole ring-shared free radicals, $BT^{\cdot}$ or $NBT^{\cdot}$ and the mono-formazan, MF, leading to the opening of one of the rings to a formazan cation centre MF^{+} and an intermediate tetrazolium centre consisting of

the tetrazolinyl radical. These can be further reduced radiolytically to the stable hydophobic product, di-formazan (DF) [8].

This reduction occurs via the two intermediate tetrazolinyl radicals shared by the di-tetrazole ring nitrogens, by the pH-dependent second-order disproportionation reaction producing mono-formazan and the *blue tetrazolium* cation cited below.

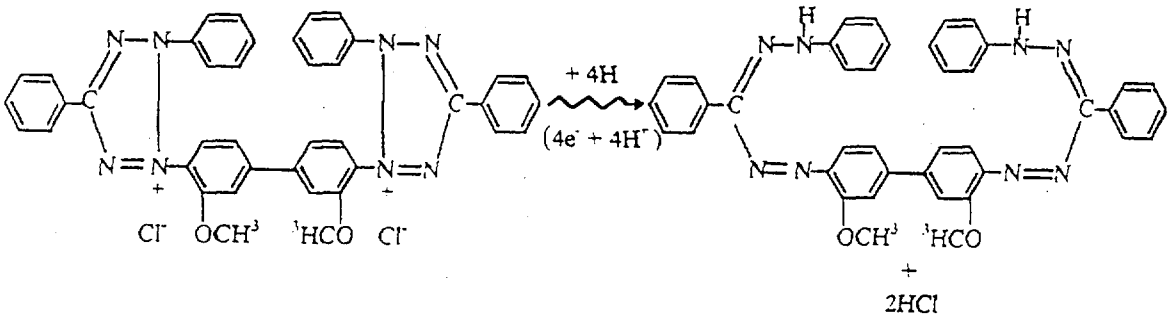

The aim of the present study is to evaluate a polymeric film containing BT^{2+} as a radiochromic dosimeter. The effects of BT^{2+} concentration, absorbed dose and dose rate, storage conditions, and irradiation temperature on dosimeter performance are investigated by gamma-ray sensitometry.

2. EXPERIMENTAL PROCEDURES

The blue tetrazolium salt (MW 727.66) was used as received from Aldrich Chemical Co., Inc.[1] without further purification. Polyvinyl alcohol (PVA) (99.7 % mol hydrolyzed; average MW 108,000) from Polysciences, Inc.[1] was used as the film-formulator host material. Dextrose (MW 180,162) from Fisher Scientific Co. Inc.[1] was used as the precursor to the reducing radicals. Water purified by the Millipore Milli-Q system[1] was used as the solvent for both the BT^{2+} salt and PVA.

The PVA (2.5 g) was slowly dissolved in 50 mL of deionized water at 90 °C. The solution was kept well stirred in a 100-mL volumetric flask in which a pre-dissolved aliquot of BT^{2+} in water at a specific ultimate concentration value was added, in order to form a specific weight percentage (6.7 wt%) of radiochromic dye in the PVA solution. Stirring of this solution was continued at 60 °C for 30 minutes, to prevent precipitation of the polymer and in order to achieve a uniform viscous medium. This solution was then poured onto a horizontal glass plate and allowed to dry at room temperature for two days in a draft-free darkened room. The resulting non-tacky, flexible, colourless film could then be stripped from the glass surface and cut into 1 cm x 1 cm dosimeter film samples having a relatively uniform thickness of 0.045 ($\pm$ 0.005) mm (1σ).

For gamma-ray irradiations, the films were held between 5-mm thick polystyrene layers, in order to maintain approximate electron equilibrium conditions simulating water for 1.25 MeV photons. The gamma-ray irradiations were made at a series of absorbed doses in water over a dose range of 1 to 75 kGy. The film sandwich assembly was placed for irradiation in an annular geometry using a thermostated shielded arrangement of twelve equally-spaced ^{60}Co source rods. Two Nordion International Gammacell Model 220 (GC-45 and GC-232) irradiators[1] were used, supplying absorbed dose rates in water of 0.95 and 3.15 Gy s^{-1}, respectively.

[1] The mention of commercial products in this paper does not imply recommendation or endorsement by the University of Maryland or the National Institute of Standards and Technology, nor does it imply that the products identified are necessarily the best available for the purpose.

Before and after irradiation of the films, their absorption spectra and absorbance values at specific wavelengths were measured with a double-beam Cary Model 3E spectrophotometer (Varian Australia Pty. Ltd.)[1]. For each measurement series, a stack of five 10 mm x 10 mm pieces of the film were irradiated together, and then were measured spectrophotometrically individually at room temperature. For both unirradiated and irradiated films at each dose, the average of the absorbance values of the five replicate film samples was used.

3. RESULTS

The gamma-ray response characteristics of the PVA film dosimeter containing 6.7 wt% BT^{2+} are shown in Fig. 1. The response curve measured spectrophotometrically at λ = 552 nm is presented on the left. The radiation-induced absorption spectra, where the ordinate on the left is given as the increase in

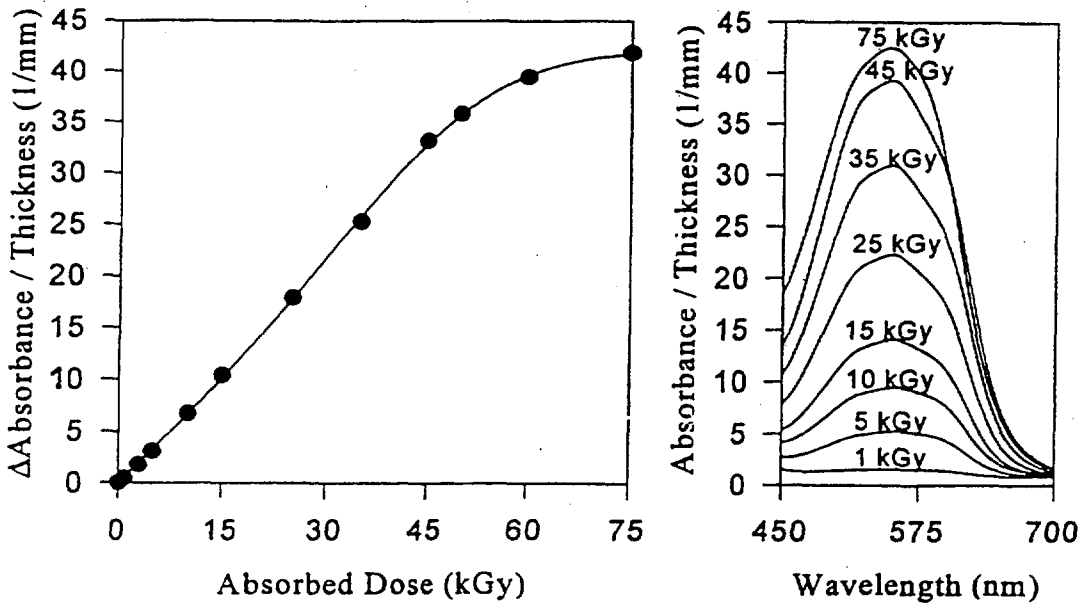

FIG.1. PVA films (6.7 wt% BT^{2+}) exposed to gamma radiation from a ^{60}Co source: left – the calibration curve in terms of increase in absorbance per unit thickness of the film at 552 nm wavelength as a function of absorbed dose in water; right – the radiation-induced absorption spectra.

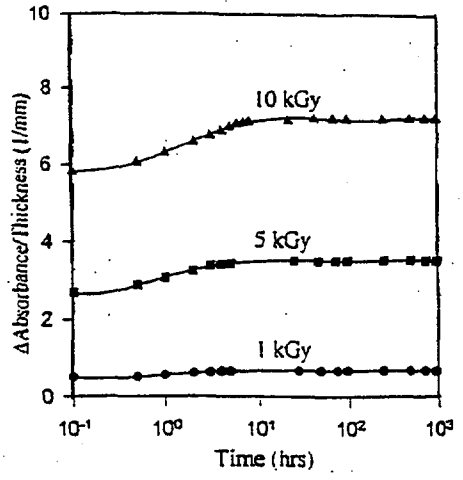

FIG.2 Stability of ΔA/l readings of BT^{2+} films stored in the dark at room temperature after irradiation to three different doses

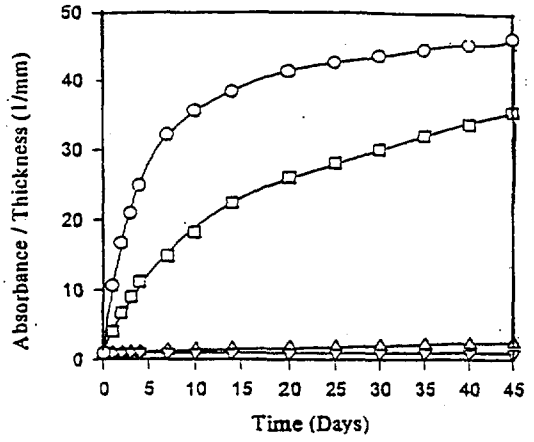

FIG.3. Instability of un-irradiated BT^{2+} films under different storage conditions.
o direct sunlight; □ in the shade
Δ white fluorescent light; ▽ in the dark

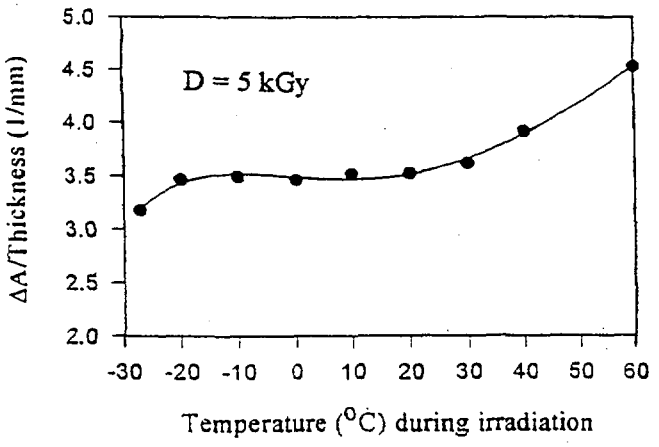

FIG.4. Variation in ΔA/l at 552 nm as a function of irradiation temperature for gamma-irradiated BT^{2+} radiochromic film.

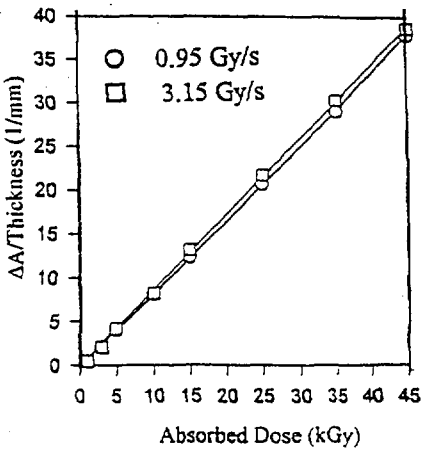

FIG.5. Gamma-ray response of the BT^{2+} radiochromic film at two dose rates.

absorbance per unit film thickness, $\Delta A/l$ are on the right. The irradiations were made at a temperature of 25 °C. The response curve in Fig. 1 is approximately linear in the dose range up to about 50 kGy, but it tends toward saturation at higher doses.

In order to study post-irradiation stability properties, the PVA-BT^{2+} films were irradiated with gamma rays to three doses, and then values of ΔA at 552 nm wavelength were monitored at different times after the end of irradiation. Between each ΔA reading, the films were stored in the dark at room temperature. Figure 2 shows that, at a dose of 10 kGy, the absorbance continues to increase by about 20 percent for about the first eight hours after irradiation and then becomes stable. The time for reaching a stable ΔA value is somewhat shorter at the lower doses.

In another stability study, the effects of ambient light conditions were investigated, as shown in Fig. 3. Here, the sensitivity of these films to the ultraviolet component of daylight is revealed by the increase in absorbance per unit film thickness. This indicates that the films should not be handled under bright light conditions, i.e. direct or indirect (shade) sunlight.

The irradiation temperature dependence of the film response to gamma radiation at a dose of 5 kGy was also studied over the temperature range -30 °C to +60 °C. The results shown in Fig. 4 indicate that, whereas a positive temperature coefficient is found at temperature extremes below -20 °C and above +30 °C, the response is relatively temperature-independent between -20 °C and +30 °C.

The film response was also studied at two absorbed dose rates 0.95 and 3.15 Gy/s. The results are shown for PVA film containing 6.7 wt% BT^{2+} (see Fig. 5) in terms of the increase in absorbance per unit film thickness measured at λ = 552 nm wavelength and as a function of absorbed dose administered at the two dose rates. The sensitivity at the lower dose rate is slightly less than that at the higher dose rate, but the difference is within the estimated uncertainty of the absorbance readings of the film dosimeter, i.e., within $\pm$ 4% (1σ).

4. CONCLUSION

Radiochromic PVA – BT^{2+} films, with sensor concentrations of 6.7 wt %, are shown to be useful for routine gamma-ray dosimetry in the absorbed dose range of approximately 1 to 50 kGy, when measured at the peak of the radiation-induced absorption band.

The radiochromic response is dependent on extremes of irradiation temperature below -20 °C and above +30 °C. They must be shielded from direct or indirect sunlight because of their intrinsic sensitivity to ultraviolet light. Even when stored in the dark, they require several hours delay before readout because of a slow transient increase in absorbance immediately after irradiation. Further studies should be made with gamma radiation over broader ranges of dose rate and with electron beams at much higher dose rates, as well as with ultraviolet radiation curing sources, in order to expand the potential uses of this system for radiation processing applications.

ACKNOWLEDGEMENT

Part of the present work was carried out with funding by the Joint US – Hungary Research Fund No. 508 and the Hungarian National Research Fund No. T 017 089.

REFERENCES

[1] GLENNER, G.G., "Formazans and tetrazolium salts", Chapt. 9 in *H. J. Conn's Biological Stains* 9th Edition (LITTLE, R.D., Ed.) Sigma Chemical Co., St. Louis MO (1990) pp. 229 - 230.

[2] GREEN, F.J., *The Sigma-Aldrich Handbook of Stains, Dyes and Indicators*, Aldrich Chemical Co., Milwaukee WI (1991) pp. 146 - 147.

[3] RUTENBERG, A.M., GOFSTEIN, R., SELIGMAN, A.M., "Preparation of a new tetrazolium salt which yields a blue pigment on reduction, and its use in the demonstration of enzymes in normal and neoplastic tissues", *Cancer Res.* **10** (1950) 113 - 121.

[4] FARBER, E., STERNBERG, W.H., DUNLAP, C.E. "Histochemical localization of specific oxidative enzymes. I. Tetrazolium stains for diphosphopyridine nucleotide diaphorase and triphosphopyridine nucleotide diaphorase", *J. Histochem. Cytochem.* **4** (1956) 254 - 265.

[5] KRIMINSKAYA, Z.K., DYUMAEV, K.M., VISHCHPANOVA, L.S., IVANOV, Yu. V., PIKAEV, A.K., "Pulse radiolysis of aqueous solutions of tetrazolium salts", *High Energy Chem.* **22** (1988) 10 - 14.

[6] KOVÁCS, A., WOJNÁROVITS, L., McLAUGHLIN, W.L., EBRAHIM EID, S.E., MILLER, A. "Radiation-chemical reaction of 2,3,5-triphenyl-tetrazolium chloride in liquid and solid state", (Proceedings 8th Tihany Symposium, Balatonszeplak, Hungary , 1994); *Radiat. Phys. Chem.* **47** (1995) 483 - 486.

[7] KOVÁCS, A., WOJNÁROVITS, L., EL-ASSY, N.B., AFEEFY, H.Y., AL-SHEIKHLY, M., WALKER, M.L., McLAUGHLIN, W.L., "Alcohol solutions of triphenyl-tetrazolium chloride as high-dose radiochromic dosimeters", (Proceedings 10th Int. Meeting on Radiation Processing, Part II, Istanbul, 1994); *Radiat. Phys. Chem.* **46** (1995) 1217 -1225.

[8] SADEGHI, A., AL-SHEIKHLY, M., McLAUGHLIN, W.L., "On the mechanisms of radiation-induced reduction of ditetrazolium salt in aqueous solution", *Radiat. Phys. Chem.* (1999) in press.

[9] BIELSKI, B.H.J., SCHIUE, G.G., BAJUK, S., "Reduction of nitro blue tetrazolium by CO_2^- and O_2^- radicals", *J. Phys. Chem.* **84** (1980) 830 - 833.

DEVELOPMENT OF DOSIMETRY TECHNIQUES — II

(Session 3)

Chairperson

D. RAŽEM
Croatia

SAND AS *IN SITU* TL DOSIMETER IN RADIATION HYGIENISATION OF SEWAGE SLUDGE

XA9949707

P.G. BENNY
Isotope Division, Bhabha Atomic Research Centre,
Mumbai

B.C. BHATT
Radiological Physics and Advisory Division,
Bhabha Atomic Research Centre,
Mumbai

India

Abstract

Recently, we have investigated the thermoluminescence (TL) properties of the sand, collected from the sewage sludge, after various extensive cleansing procedures. In the present studies, the sand separated from the sludge was used to estimate irradiation dose to sludge at Sludge Hygienisation Research Irradiator (SHRI), Vadodara, India. A dose vs TL response calibration curve was established for the 220°C TL peak for the hydrogen peroxide (H_2O_2)-treated and HF-treated sludge sand samples collected from the unirradiated batch. This was used to estimate the dose absorbed in the corresponding batch of the irradiated sludge. Similar curve was plotted for the 370°C TL peak for the HF-treated sand samples for its application as an in-situ dosimeter. Using this method, the absorbed dose rate delivered to the sludge during irradiation at SHRI was estimated to be 0.49 ± 0.02 kGy per hour. Also, the saturation levels of the TL response curves for these peaks are reported here.

1. INTRODUCTION

A Sludge Hygienisation Research Irradiator (SHRI) has been set up at Vadodara, India, for disinfection of liquid sewage sludge by subjecting it to irradiation in the dose range of 3-4 kGy using ^{60}Co gamma rays. The irradiation vessel is an integral part of the irradiator system that houses the planar grid assembly of sources with a total activity of 1.8 x 10^{15} Bq (its full capacity is 1.85 x 10^{16} Bq). The digested sludge is fed by gravity into the irradiation vessel in a batch of 3 m^3 volume. The sludge in the irradiation vessel is then kept under constant recirculation to prevent settling during the radiation exposure. At the end of the pre-determined exposure time, the sludge is drained into a storage tank from where it is pumped into drying beds for further use. Initially, the gamma-ray dosimetry of the facility was being done by introducing various encapsulated dosimeters (such as TLDs, chemical dosimeters and radiochromic films) at the inlet of the sludge irradiator and retrieving them after a predetermined irradiation period at the outlet [1]. It is normally desired that these dosimeter capsules have nearly the same flow dynamics as that of the sludge being treated for a true representation of the dose absorbed in the sludge. This is often difficult to achieve for a variety of reasons including the mis-match of the density between the sludge and the dosimeter. This necessitated development of an alternative approach using the thermoluminescent characteristics of the sand in the sludge itself. In the sand samples treated with either hydrogen peroxide (H_2O_2) or hydrofluoric acid (HF), there is a prominent TL peak at about 220°C after gamma irradiation for dosimetry purpose; a TL peak at about 370°C was also observed in irradiated HF-treated sand samples. As we have reported earlier, the sensitivity of 220°C TL peak of H_2O_2-treated as well as HF-treated sand samples is good up to a dose of 6 kGy [2]. The post-irradiation fading of this peak in these samples is negligible. Therefore, these sludge sand samples could be considered for use as *in situ* TL dosimeters for radiation disinfection of sewage sludge.

The present paper reports on the estimated gamma-ray doses using H_2O_2- and HF-treated sand samples separated from the irradiated sludge at the SHRI facility. Also it reports dose vs TL response of 220°C and 370°C peaks in the HF-treated sand and 220°C peak in the H_2O_2-treated sand in the dose range of 0.25 kGy to 18 kGy in order to test saturation effects in the respective TL peaks in the two samples.

2. EXPERIMENTAL

The procedure is to collect 15 L each of unirradiated and irradiated sludge samples. These are allowed to settle and the settled portion is collected. These samples are subjected to the cleansing process as described by us in an earlier publication in order to separate H_2O_2-treated and HF-treated sand samples [2]. The unirradiated samples of a particular batch are used for calibration for the corresponding irradiated samples. All irradiated samples are given a post-irradiation annealing of 120°C for 20 min to erase the influence of low-temperature TL peaks.

All the TL measurements (peak height as well as area under the TL glow peak) of H_2O_2- and HF-treated sand samples were taken at a heating rate of 10°C/s, using a Harshaw 3000A TLD reader coupled to a flow chart recorder. For each measurement, 5 mg of the sand sample was used. All TL results reported for 220°C peak in this work are on the basis of measurements of TL peak area taken between 25 and 275°C for the HF-treated, and between 25 and 325°C for the H_2O_2-treated samples. Dosimetric measurements were also made using 370°C TL peak (peak height) in HF-treated sand samples. Each experimental point represents average of six measurements with standard deviation (1σ) less than 5%.

The dose vs TL intensity response curves were plotted for both the types of treated samples in the dose range of 0.25 - 18 kGy using a laboratory ^{60}Co gamma-ray source at a dose rate of 10.3 Gy/min, as calibrated with a Fricke chemical dosimeter.

3. RESULTS

Fig. 1 shows the dose vs TL intensity calibration curves for 220°C and 370°C peaks in the HF-treated sand samples in the dose range of 0.25 -18 kGy. It is seen that the response curve of 220°C peak does not saturate up to 6 kGy. Beyond the dose of 6 kGy, it decreases slowly up to the studied dose of 18 kGy. Similarly dose vs TL intensity response curve of 370°C peak does not saturate up to 10 kGy;

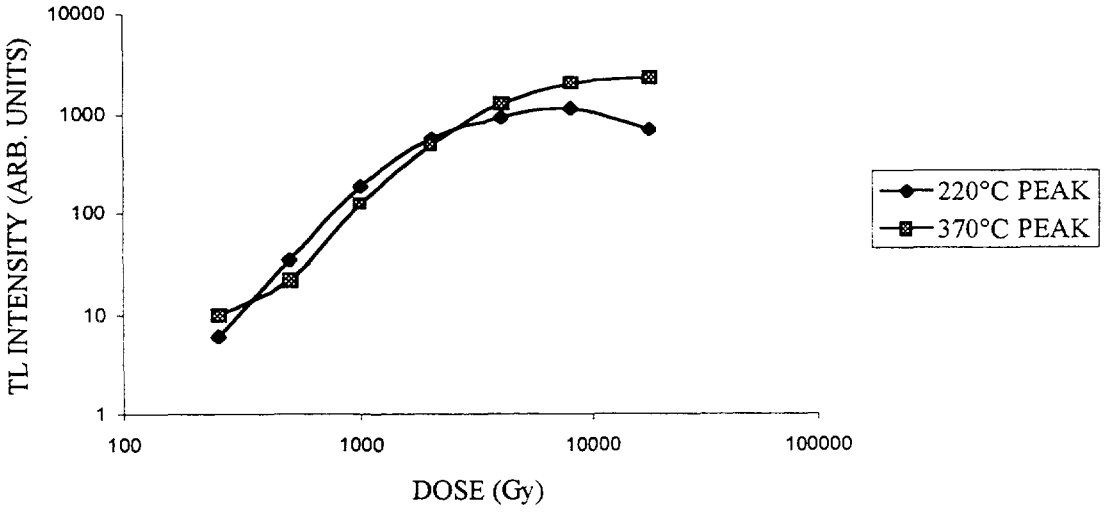

FIG. 1. Dose vs TL response curve of 220°C and 370°C peaks in HF treated sand

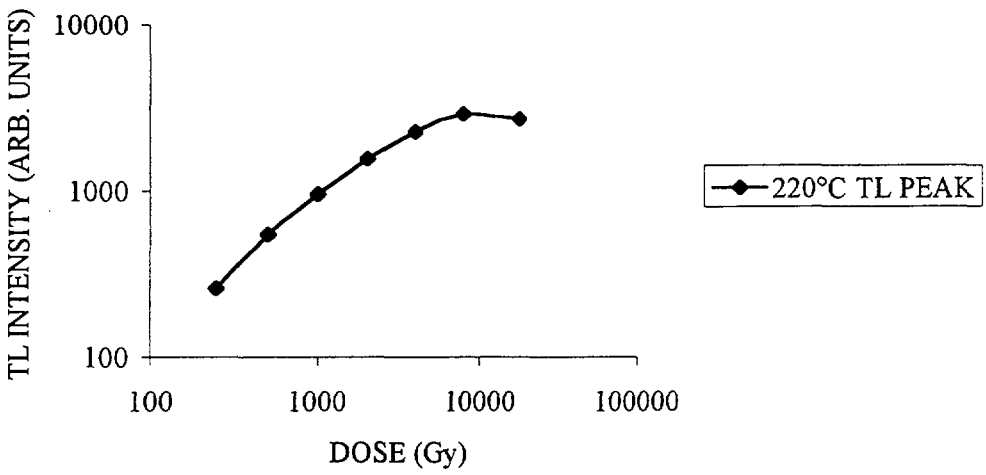

FIG. 2. Dose vs TL response curve of 220°C peak in H2O2 treated sand

TABLE I. ESTIMATED ABSORBED DOSE IN THE IRRADIATED SLUDGE SAMPLES BY USING H_2O_2- AND HF-TREATED SAND SAMPLES

Sand dosimeter	Estimated absorbed dose (kGy) for different periods of irradiation		
	2h	4h	6h
H_2O_2 - treated (220°C)	0.90 ± 0.03	1.90 ± 0.07	2.80 ± 0.21
HF-treated (220°C)	0.96 ± 0.04	2.00 ± 0.06	3.00 ± 0.04
HF-treated (370°C)	1.00 ± 0.05	2.00 ± 0.06	3.00 ± 0.02

beyond which it decreases slowly. In the dose range 1 - 10 kGy, the maximum measurement uncertainties in the individual calibrations were within ±5%; however, at lower doses uncertainties were higher than ±5%. Fig. 2 shows similar dose vs TL intensity calibration curve for the H_2O_2- treated samples. In this case also the response curve does not saturate up to 6 kGy; beyond which it decreases slowly. Thus, these dose vs TL intensity calibration curves can be used to estimate the dose to the irradiated sludge.

Table I shows the results for the estimated absorbed dose in the sludge for the samples irradiated for three different periods. The estimated dose rate for the sludge irradiator was found to be 0.49 ± 0.02 kGy per hour.

4. DISCUSSION AND CONCLUSIONS

It was observed that the dose vs TL intensity curves of 220°C peak in the H_2O_2- and HF-treated sand samples do not show saturation up to 6 kGy. Therefore, they can be used as *in situ* TL dosimeters for radiation hygienisation of sewage sludge. The dose normally given to sludge is about 3-4 kGy. The 370°C TL peak in the HF-treated samples does not saturate even up to the studied dose of 10 kGy. Therefore, the dose response of 370°C TL peak can also be used for estimating the dose given during radiation disinfection of sewage sludge in addition to the 220°C TL peak. Use of such *in situ* TL dosimeters (separated from the irradiated sludge) has many advantages over other external dosimeters

as explained earlier. Using these dosimeters, the estimated dose rate for the sludge irradiator facility was found to be 0.49 ± 0.02 kGy per hour (see Table I). In order to minimise uncertainties introduced due to batch-to-batch variations in TL sensitivity, it is recommended that a separate calibration be drawn for each batch. This is done by taking sludge samples at the inlet of the irradiator facility as well as at the outlet on completion of the irradiation. Since both the types of samples (H_2O_2- and HF-treated) show room-light-induced as well as sunlight-induced TL fading, care should be taken to protect the sand samples from exposure to room-light or sunlight during collection of sludge samples at the inlet as well as at the outlet of the irradiator, and also during cleaning, irradiation and TL readout of the sand samples.

REFERENCES

[1] BENNY, P.G., SHAH, M.R., "Problems in dosimetry at Sludge Hygienisation Research Irradiator (SHRI), Baroda", Nuclear Energy Programme - Achievements and Prospects in Medicine, Industry and Agriculture (Proc. Symp. Indian Nuclear Society, Bombay, 1992), pp. 119-121.

[2] BENNY, P.G., BHATT, B.C., Investigation of TL properties of Sand collected from Sewage Sludge as an 'In-Situ' dosimeter in Radiation Disinfection, Appl. Radiat. Isotopes 47 (1996) 115-121.

XA9949708

ULTRAVIOLET AND INFRARED SPECTRAL ANALYSIS OF POLY(VINYL)BUTYRAL FILMS: CORRELATION AND POSSIBLE APPLICATION FOR HIGH-DOSE RADIATION DOSIMETRY

S. EBRAHEEM, M. EL-KELANY, W. BESHIR, A.A. ABDEL-FATTAH
National Centre for Radiation Research and Technology,
Cairo, Egypt

Abstract

A detailed study was performed to develop the dosimetric characteristics of poly(vinyl)butyral film (PVB), to be used as a film dosimeter for high-dose gamma radiation dosimetry. The useful dose range of this polymeric film extends up to 350 kGy. Correlations were established between the absorbed dose of gamma radiation and the radiation-induced changes in PVB measured by means of ultraviolet (UV) and Fourier Transform Infrared (FTIR) spectrophotometry. The results showed a significant dependence of the response on the selected readout tool of measurements whether FTIR (at 1738 and 3400 cm^{-1}) or UV (at 275 and 230 nm), as well as on the quantity used for calculation. The effect of relative humidity during irradiation on dosimeter performance as well as the post-irradiation stability at different storage conditions are also discussed.

1. INTRODUCTION

According to extensive studies of the radiation effects on polymers [1,2], irradiation of polymer film in air induces the oxidation of the polymer and the production of carbonyl groups. The magnitude of the oxidation process depends not only on the structure of polymer but also on the type of ionizing radiation; more specifically, the dose rate. Hence, it would be expected that oxidation processes predominate for irradiation with gamma rays which are characterized by their slow rate. On the contrary, for irradiation with accelerated electrons, which are known to have very high dose rates, processes other than oxidation, such as inter-molecular and disproportion reactions would predominate. In the polymeric film dosimeters, the radiation-induced signal depends on the absorbed dose of ionizing radiation by the dosimeter and may also depend on the dose rate or fractionation of dose [3], on the temperature during the irradiation and handling, on the presence or absence of oxygen in the surrounding atmosphere or in the dosimeter [3], and on the ambient humidity or rather on the amount of water in the dosimeter [4,5].

2. EXPERIMENTAL

The film used in this investigation was prepared using poly(vinylbutyral) (PVB), (Pioloform BM18, average molecular weight of about 36,000, product of Wacker Co., USA). 5g of PVB was dissolved in 100 mL of n-butanol at about 50 °C and kept well stirred at that temperature for about 24 h. 30 mL, of this solution, poured onto a 15x15 cm glass plate and dried at room temperature for about 48 h. After drying, the film was stripped from the glass plate, then cut into 1x1 cm pieces and stored for different investigations. The thickness of the obtained film was found to be 50±5 mm (1s).

A Uvikon 860 spectrophotometer was used for scanning the absorption spectra and measuring the optical density at λ_{max} of the different film dosimeters. Also, Mattson 1000 Fourier Transform Infrared (FTIR) spectrometer (Unicam) was used for measuring and scanning the infrared absorption spectra at resolution of 4 cm^{-1}. High signal-to-noise spectra were obtained by collection of hundred scans for each sample. The resultant digitilized spectra were stored for further data processing. Irradiation was carried out in the ^{60}Co gamma chamber 4000 A (product of Bhabha Atomic Research Center, India). Dose rate of (2.17) kGy/h was used as checked by Fricke dosimetry [5].

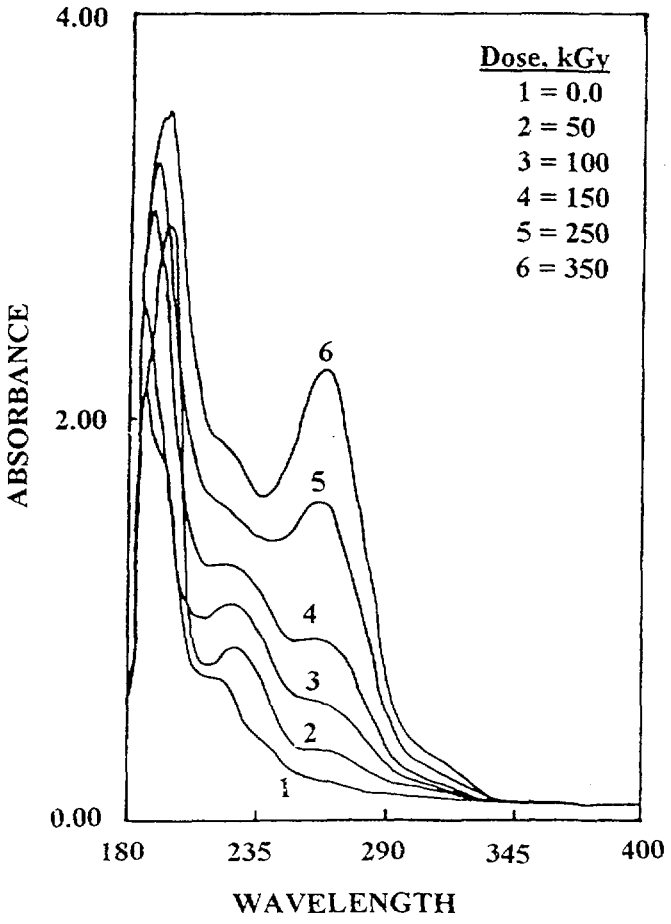

FIG. 1. UV-absorption spectra of PVB films, unirradiated and irradiated to different absorbed doses.

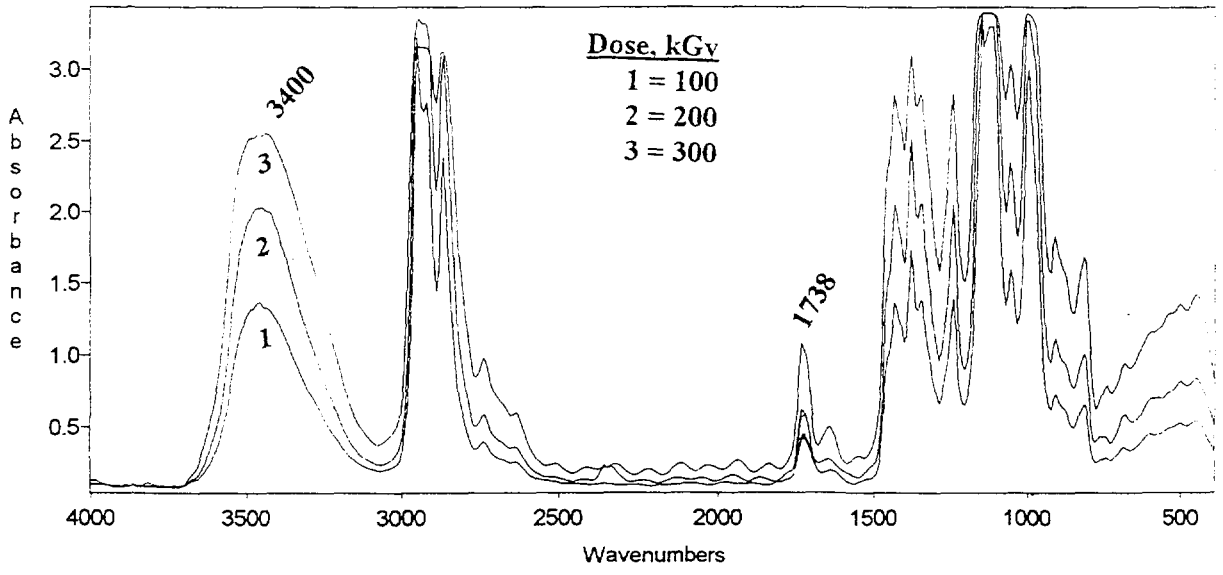

FIG. 2. FTIR-difference spectrum of PVB films irradiated to different absorbed doses.

3. RESULTS AND DISCUSSION

3.1. Absorption spectra

The ultraviolet spectrophotometric scan in the wavelength range between 180 and 400 nm of PVB films was recorded before and after g-irradiation to different doses and are shown in Fig. 1. It can be seen that the UV-spectrum of the unirradiated film has a main absorption bands peaking at 188 nm, which may be attributed to n-s* transition of non-bonding electrons of the (C-O-C) group. Upon irradiation, two absorption bands at 230 and 275 nm wavelengths were developed. The absorption band at 230 nm is related to the presence of a ketonic carbonyl group due to the oxidation of PVB upon gamma irradiation in air, while the other absorption band at 275 nm is indicative of the presence of conjugated double bonds of polymers [6]. Despite the experimental finding of the increase of absorption at 188 nm with the irradiation dose, it cannot be used for quantitative estimation of absorbed dose. This is due to its unstability at fixed wavelength as can be seen in Fig. 1. Careful examination as well as preliminary experimentation has shown that absorption bands at higher wavelengths (230, 275) may be used for dosimetry studies.

Oxidation products of irradiated PVB were also identified and quantified by FTIR spectroscopy. Figure 2 shows the IR difference spectra of films irradiated to different doses, obtained by subtracting the spectrum of the unirradiated film from that of the same film after irradiation. Changes due to irradiation can be seen, these changes are mainly represented by the appearance of three absorption bands, the first at about 3400 cm^{-1} which is attributed to the formation of hydrogen bonded -OH groups, the second at 1738 cm^{-1} wavenumber which is attributed to the stretching vibration of ketonic carbonyl groups and the third at 1190 cm^{-1} which is probably due to the -C-O- absorption of the peroxide cross-links [6,7].

3.2. Responce curves

The response curves of PVB films obtained by using the UV-spectrophotometric quantities ($\Delta A \cdot mm^{-1}$) and (A_i/A_o) at 230 and 275 nm wavelength, as a function of absorbed dose are shown in Figs. 3 and 4, respectively; where ($\Delta A \cdot mm^{-1}$) is the change in absorbance before and after irradiation

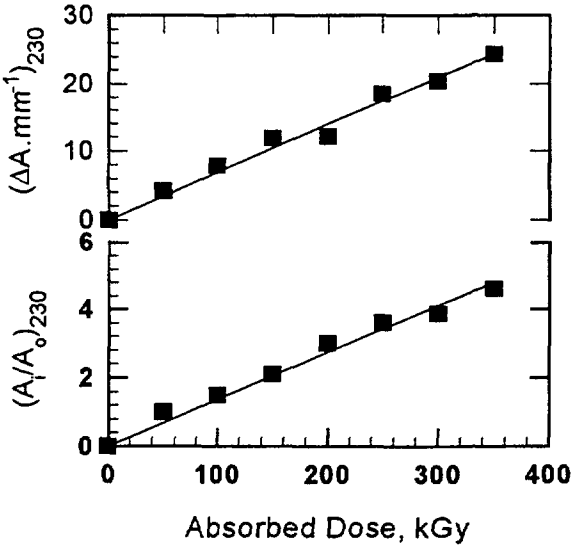

FIG. 3. Radiation response curves of PVB films, in terms of change in UV-spectrophotometric quantities $(\Delta A.mm^{-1})_{230}$ and $(A_i/A_o)_{230}$ as a function of absorbed dose.

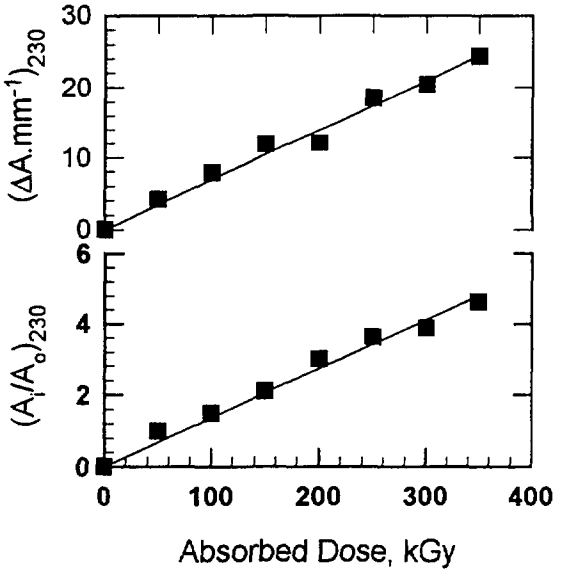

FIG. 4. Radiation response curves of PVB films, in terms of change in UV-spectrophotometric quantities $(\Delta A.mm^{-1})_{275}$ and $(A_i/A_o)_{275}$ as a function of absorbed dose.

divided by thickness of the film, and A_o and A_i are the optical densities at 230 and 275 nm wavelengths for the unirradiated and irradiated films, respectively.

It can be seen that, the response curves of both quantities ($\Delta A \cdot mm^{-1}$) and (A_i/A_o) obtained at 230 and 275 nm wavelength are linear and can be represented by Eq. (1):

$$Y = a + bD \tag{1}$$

where, Y is ($\Delta A \cdot mm^{-1}$) or (A_i/A_o), D is the absorbed dose in kGy, a and b are constants. The constants a and b as well as the correlation coefficients for the response curves are given in Table I.

TABLE I. THE CONSTANTS A AND B AND THE CORRELATION COEFFICIENTS (r^2) OF THE UV RESPONSE CURVES.

constants	$(\Delta A.mm^{-1})_{275}$	$(A_i/A_o)_{275}$	$(\Delta A.mm^{-1})_{230}$	$(A_i/A_o)_{230}$
a	-3.679	0.117	1.017	0.371
b	0.097	0.024	0.066	0.012
r^2	0.991	0.989	0.979	0.989

The response functions of PVB films for ^{60}Co irradiation using the FTIR spectroscopy were established by plotting the IR-spectrometric quantities ($DA \cdot mm^{-1}$) and (A_i/A_o) at 1738 and 3400 cm^{-1} as a function of absorbed dose (see Fig. 5), where ($DA \cdot mm^{-1}$) is the radiation-induced peak absorbance divided by thickness (in mm) and A_o and A_i are the peak absorbances before and after irradiation, respectively. From Fig. 5, it can be seen that the response curves for 1738 cm^{-1} are linear throughout the

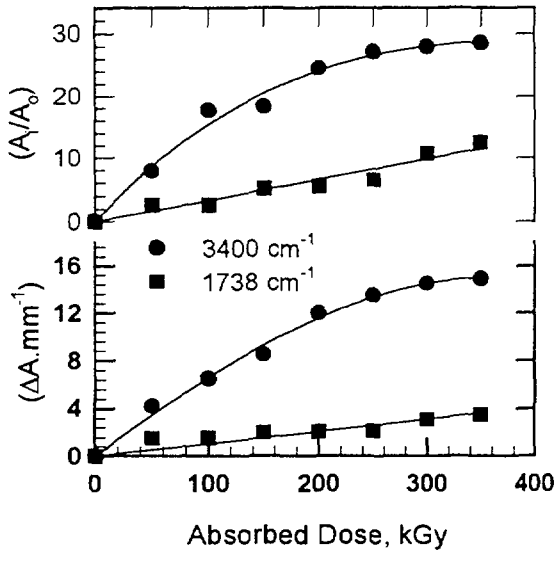

FIG. 5. Radiation response curves of PVB films, in terms of the change of FTIR-spectrophotometric quantities ($\Delta A.mm^{-1}$) and (A_i/A_o) as a function of absorbed dose. Wavenumbers of analysis are indicated.

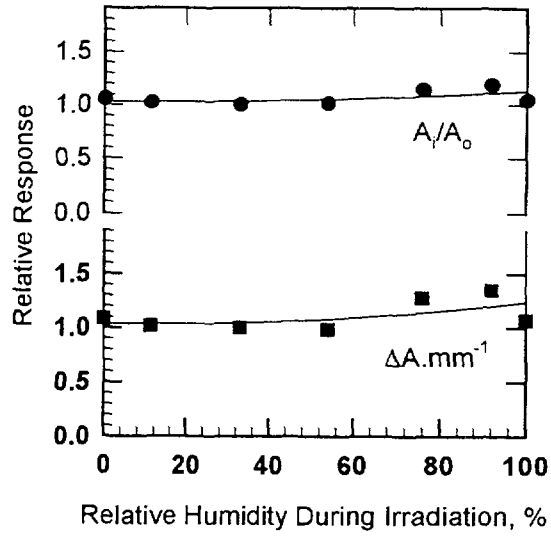

FIG. 6. Relative change of UV spectrophotometric quantities ($\Delta A.mm^{-1}$) and (A_i/A_o), relative to that value at 33% RH, as a function of percentage relative humidity during irradiation. Absorbed doae = 150 kGy

whole dose range, and follow the general linear Eq. (1). While those for 3400 cm^{-1} are non-linear, where they follow the third-order polynomial equation which can be represented by Eq. (2).

$$Y = a + bD + cD^2 + dD^3 \quad (2)$$

The constants *a, b, c* and *d* as well as the correlation coefficients for the response curves are given in Table II.

TABLE II. THE CONSTANTS a, b, c and d AND THE CORRELATION COEFFICIENTS (r^2) OF THE FTIR- RESPONSE CURVES

constants	$(\Delta A.mm^{-1})_{1738}$	$(\Delta A.mm^{-1})_{3400}$	$(A_i/A_o)_{1738}$	$(A_i/A_o)_{3400}$
a	0.548	0.281	-0.141	0.38
b	0.0081	0.0665	0.0333	0.01954
c	-------	$-2.3x10^{-5}$	-------	-0.0043
d	-------	$-1.4x\ 10^{-7}$	-------	$3x10^{-7}$
r^2	0.900	0.994	0.942	0.986

3.3 Radiation-chemical yield

The radiation-chemical yields of the ketonic carbonyl group and the hydroxyl group produced in irradiated PVB films were evaluated from the increment of the IR-absorbance (DA_{1738}) at 1738 cm^{-1} and (DA_{3400}) at 3400 cm^{-1}, respectively. Using the reported molar extinction coefficient e_{1738} = 111 $L.mol^{-1}.cm^{-1}$ and e_{3400} = 138 $L.mol^{-1}.cm^{-1}$ [8], G(>C=O) was found to be 0.81 mmol/J and G(>C-OH) was found to be 4.86 mmol/J.

3.4 Relative humidity during irradiation

To investigate the effect of relative humidity (RH) during irradiation on the response of PVB films, the latter were irradiated to an absorbed dose of 150 kGy (dose rate = 2.17 $kGy.h^{-1}$) at different relative humidities by suspending films (five films per each relative humidity) over different saturated salt solutions in tightly enclosed glass tube [5,6], except for the two extreme values of relative humidity. The 0% RH value was obtained with films suspended over dried silica gel and 100% RH was attained with films suspended over water. The mean temperature during gamma ray irradiation was about 35°C. The films were stored before irradiation for 48 hours under the same relative humidity conditions as when irradiated, so that equilibrium moisture in the PVB films could be established before irradiation. Immediately after the irradiation, the dosimeters were removed from the tube and then readout spectrophotometrically at room temperature.

Figure 6 shows the relative variation of response as a function of percent relative humidity, in terms of both UV-quantities [$(\Delta A.mm^{-1})_{275}$ and $(A_i/A_o)_{275}$] relative to that value at 33% RH. It was found that, in the intermediate range of 10-60% RH, the responses of all spectrophotometric quantities are not influenced by the change in relative humidity during irradiation. As a conclusion, PVB films can be used for routine high-dose dosimetry in the 10-60% R.H. range without any correction. Irradiation at relative humidities higher than 60% should be avoided, otherwise correction is needed.

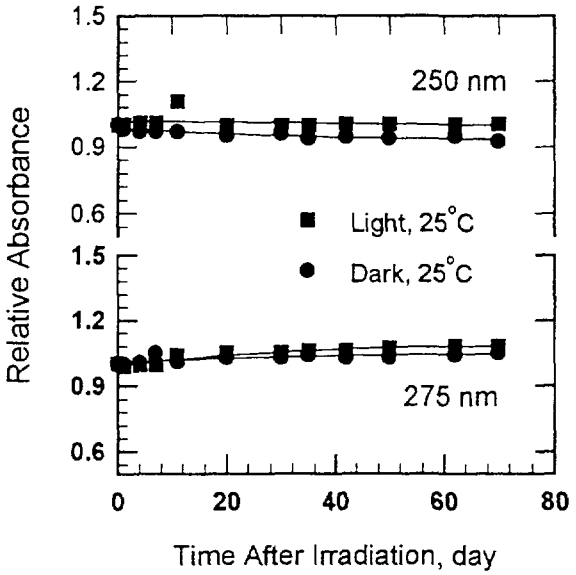

FIG. 7. Relative change of the UV-spectrophotometric quantities ($\Delta A \cdot mm^{-1}$), at λ_{250} and λ_{275}, as a function of storage time after irradiation to a dose of 150 kGy of films stored at different conditions.

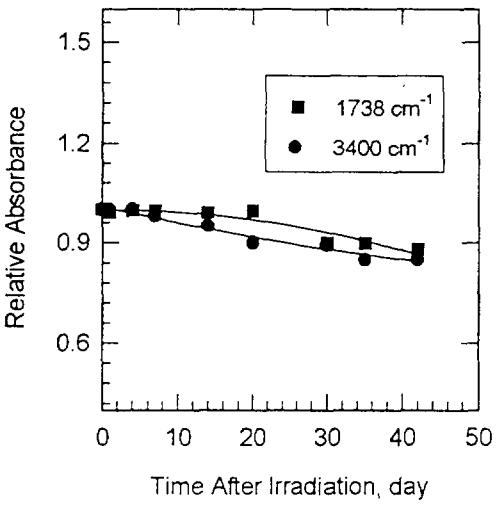

FIG. 8. Relative change of the FTIR-spectrophotometric quantities, $(\Delta A \cdot mm^{-1})_{1738}$ and $(\Delta A \cdot mm^{-1})_{3400}$ as a function of storage time after irradiation to a dose of 400 kGy of films stored at different conditions.

3.5 Post irradiation stability

A study of the stability of the radiation-induced changes in PVB films was made over a period of 70 days between irradiation (D = 150 kGy) and readout by means of ultraviolet spectrophotometery at 230 and 275 nm. After irradiation, the films were stored, at ambient relative humidity (35-40 % RH), under different storage conditions namely, normal laboratory illumination plus daily incident daylight at 25 °C and dark at 25 °C.

Figures 7 and 8 show the stability results in relative absorbance as a function of storage time between irradiation and readout at 230 and 275 nm, 1738 cm^{-1} and 3400 cm^{-1}, respectively. In all figures, the values of relative response are normalized to the values of both quantities obtained immediately after irradiation (zero storage time).

The results given in the last two figures indicate that further oxidation processes may take place within the bulk of the polymer on storing after irradiation.

REFERENCES

[1] R.J. WOODS, A. K. PIKEAV, Applied Radiation Chemistry: Radiation Processing, Wiley, New York, 1994.

[2] J.W.T. SPINKS, J. WOODS, *An Introduction to Radiation Chemistry,* (Wiley & Sons Inc., New York, 1964).

[3] W.L. MCLAUGHLIN, A.W. BOYD, K.H. CHADWICK, J.C. MCDONALD, A. MILLER, *Dosimetry for Radiation Processing*, (Taylor and Francis, London, 1989).

[4] W.L. MCLAUGHLIN, J.M. PUHL, A. MILLER, *Proceedings of 9th Int. Meeting on Radiation Processing,* Sept. 12-16, 1994, Istanbul.

[5] I. JANOVSKY, K. MEHTA, *Radiat. Phys. Chem.*, **43** (1994) 407.

[6] A.A. ABDEL-FATTAH, S. EBRAHEEM, Z. I. ALI, F. ABDEL-REHIM, *Appl. Poly. Scie.*, **67** (1998) 1837.

[7] ASTM (American Society for Testing and Materials), Standard Practice E 1707 (1995).

[8] Encyclopedia of Polymer Science and Technology, **14** (1992) 229-230

A SET OF DOSIMETRY SYSTEMS FOR ELECTRON BEAM IRRADIATION

Min LIN, Jingwen LIN, Yundong CHEN, Huazhi LI, Zhenhong XIAO
Radiometrology Center,
China Institute of Atomic Energy

Juncheng GAO
Ionizing Radiation Division,
National Institute of Metrology

Beijing, China

Abstract

To follow the rapid development of radiation processing with electron beams, it is urgent to set up a set of dosimetric standards to provide Quality Assurance (QA) of electron beam irradiation and unify the values of the quality of the absorbed dose measurements for electron beams. This report introduces a set of dosimetry systems established in Radiometrology Center of China Institute of Atomic Energy (RCCIAE), which have been or will be used as dosimetric standards in the Nuclear Industry System (NIS) in China. For instance, the potassium (silver) dichromate and ceric-cerous sulfate dosimetry systems will be used as standard dosimeters, while alanine-ESR dosimetry system as a transfer dosimeter, and FJL-01 CTA as a routine dosimeter.

1. INTRODUCTION

In recent years, the radiation processing with gamma rays and electron beams have been extensively developed in China. So far in the last decade, more than 100 ^{60}Co gamma irradiation facilities and more than 40 electron beam irradiation facilities have been set up, which are now widely used in industry, medicine and agriculture. With the rapid development of radiation processing, it is realised that accurate and reliable high-dose measurements are very essential.

From 1980's, RCCIAE has done much work for gamma ray and electron beam irradiation. To begin with, four types of liquid chemical dosimetry systems were studied and set up for gamma ray irradiation in RCCIAE. As no dosimetric standard was established for electron beam irradiation till 1994, RCCIAE has placed extra effort to develop a set of dosimetry systems suitable for measuring the absorbed dose for electron beams. First, two liquid chemical dosimetry systems were established as standard dosimeters, they are the potassium (silver) dichromate and the ceric-cerous sulfate dosimeters. At the same time, RCCIAE also began to study a low-cost and mass-producible dosimetry system cellulose triacetate (CTA) thin film dosimeter to meet the requirement of routine quality control for electron beam irradiation. Right after these works, another mass-producible dosimetry system alanine-PE thin film dosimeter was developed, which is expected to be used as transfer dosimeter for electron beams. In the following, the three levels of dosimetry systems are described.

2. LIQUID CHEMICAL DOSIMETRY SYSTEMS

The liquid chemical dosimetry is a basic method for measuring the absorbed dose for gamma ray and electron beam irradiation, which is based on proportional relationship between radiation-induced variation of optical absorbance at a given wavelength and absorbed dose. The liquid chemical dosimeters can be used to measure the absolute absorbed dose at a given location.

Though the G value of the Fricke dosimeter does not change with dose rate up to 1×10^{6} Gy·s^{-1}, it's small dose range makes it unsuitable for electron beam irradiation. Similar to the Fricke dosimeter,

the ceric-cerous sulfate dosimeter is also not dose rate dependent under 1×10^6 Gy·s^{-1}. It was also shown that no effect of dose rate occurred in the dichromate dosimeter containing silver ions up to 4 μs, 600 Gy pulse [1]. Thus in 1994, after the four types of aqueous chemical dosimetry systems for gamma rays had been approved by the National Institute of Metrology (NIM) [2,3,4], RCCIAE tried to extend two liquid chemical dosimetry systems - the potassium (silver) dichromate and ceric-cerous sulfate dosimeters to electron beam irradiation.

Different to the dosimeters for gamma rays, the dosimetric solutions were sealed in self-made and mass-producible coin-shaped containers, which were made of polystyrene with 1mm in the incident window, 2 mm in the back, 46 mm in o.d., 40 mm in i.d. and 7 mm in height, see Fig. 1 of Ref. [2]. The total volume of the dosimeter is about 4 ml. It has good rigidity and is easy to handle.

The composition of the two dosimetry systems are shown as follows:

- Potassium (silver) dichromate dosimeter:
  2 mmol·L^{-1} $K_2Cr_2O_7$ and 0.5 mmol·L^{-1} $Ag_2Cr_2O_7$ in 0.1 mol·L^{-1} $HClO_4$
- Ceric-cerous sulphate dosimeter:
  0.01 mol·L^{-1} Ce^{4+} and 0.004 mol·L^{-1} Ce^{3+}

The two dosimetry systems were calibrated against the Fricke dosimeter made in RCCIAE with ^{60}Co gamma rays. The Fricke dosimeter was traceable to the national dosimetry standard of the NIM. Before irradiation, the coin-shape dosimeters were placed in the specially designed phantoms to prevent from back and side scattering of the secondary electrons. Dose response of the two dosimetry systems, irradiated with electron beams (linear accelerator, 12 MeV, 100 μA, dynamic irradiation with 1.4 m·min^{-1} of the conveyor speed), was measured at 25.0±0.1 °C by spectrophotometry (Cary-3E, VARIAN) at 440 nm for the potassium (silver) dichromate dosimeter and 318 nm for the ceric-cerous sulfate dosimeter. Figure 1 shows the dose response curves of the two dosimetry systems for the coin-shaped and rod-shaped (glass ampoules). The precision were within ±1 % (at 68 % confidence level).

To study the difference in the G values for the two dosimetry systems between gamma rays and electron beams, a series of comparisons with the water calorimeter, made in China Institute of Engineering Physics (CIEP), was conducted with 12 MeV (100 μA, dynamic irradiation with 1.4 m·min^{-1} of the conveyor speed) and 4 MeV (100 μA, stationary irradiation) electron beams. The

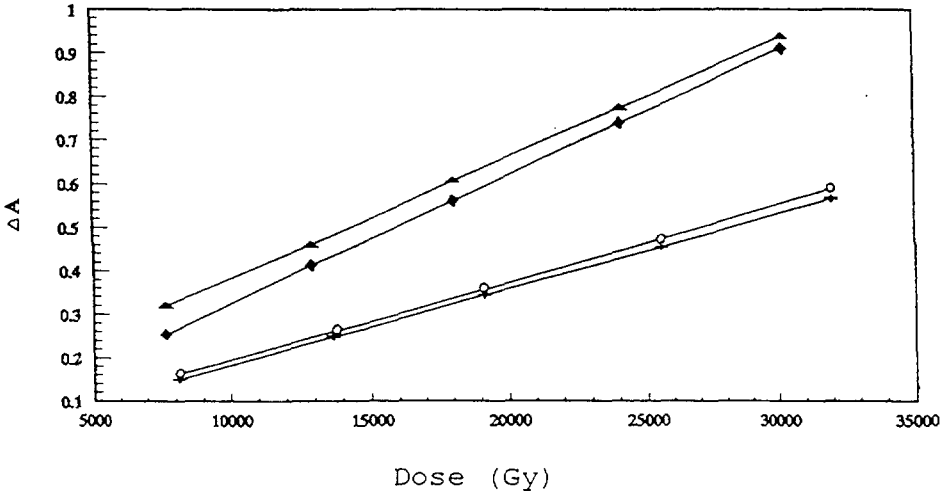

FIG. 1. Dose response curves of coin-shaped and rod-shaped potassium (silver) dichromate and ceric-cerous sulfate dosimeters

▲ – coin-shape ceric-cerous sulfate dosimeter; ♦ – rod-shape ceric-cerous sulfate dosimeter
o – rod-shape dichromate dosimeter + – coin-shape dichromate dosimeter

agreements were better than ±5% over the dose range of 10~50 kGy. Thus, we may conclude that the G values for the two dosimetry systems is independent of the dose rate under above radiation conditions. The overall uncertainties of these two liquid chemical dosimetry systems were 4.8 % at 95 % confidence level.

3. ALANINE-ESR DOSIMETRY SYSTEM

It is well known that the alanine-ESR dosimetry system has been successfully applied as a reliable high-dose transfer dosimetry, which is based on the linear relationship between the stable free radicals in irradiated DL- or L-α-alanine measured by electron spin resonance spectroscopy and absorbed dose. It has been judged to be the most suitable dosimetry system for IDAS, with its high precision, near tissue equivalency, broad useful dose range, insensitive to ambient environment, long-term stability of free radicals and nondestructive readout approach. Since 1985, some laboratories in China have studied and set up alanine-ESR dosimetry system. However, few of them have applied it for practical use with electron beam irradiation. Moreover, all of these alanine dosimeters were made in small batches, which were relatively difficult to reproduce in large batches. As there was no transfer dosimeter established for electron beams till 1996, RCCIAE started to develop a reliable and mass-producible alanine/PE dosimeter in order to meet the requirements of standardization of dosimetry for electron beam irradiation.

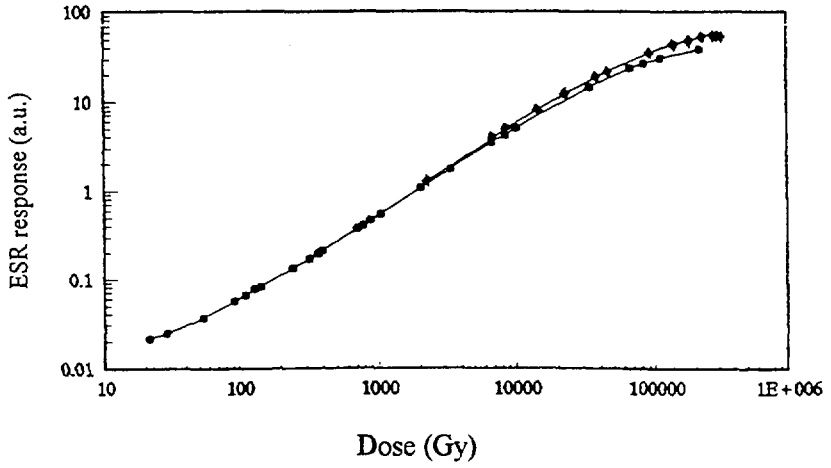

FIG. 2. Dose response curve of the alanine/PE thin film dosimeter
♦ – for 12-MeV electron beams; • – for ^{60}Co gamma rays

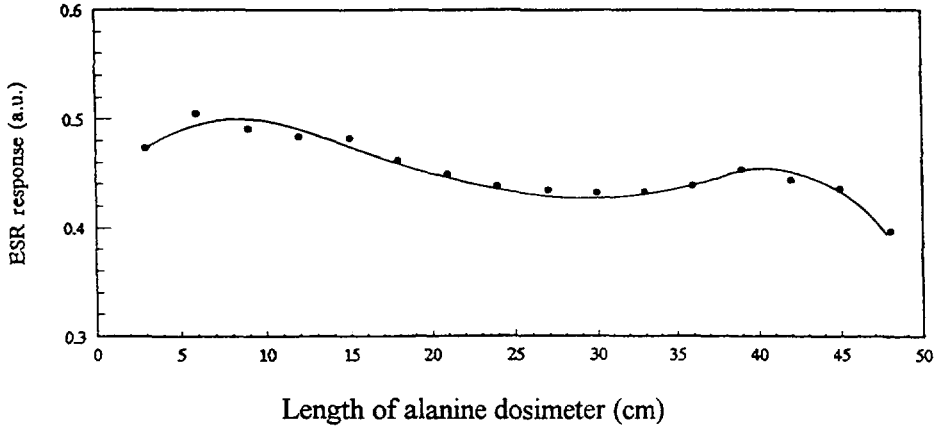

FIG. 3. Field distribution (perpendicular to conveyer motion) curve for 12 MeV electron beams with the alanine/PE thin film dosimeter

The alanine/PE dosimeter developed in RCCIAE was produced by extrusion of a mixture of 66.7 wt% ground polycrystalline DL--alanine with 33.3 wt% low-density polyethylene as binder. The mixture was extruded at 160~165 by Bravender Plastogragh into a strip with 30 mm in width and about 200 μm in thickness, which was then cut into 30 mm in length, 7.5 mm in width as one dosimeter. Before cutting, the thickness of the strip was carefully measured by HEIBENHAIN Counter (VRZ-405, HEIBENHAIN). The lateral and vertical common differences of the thickness were less than ±15 μm and ±3 μm, respectively. The density of the dosimeter was about 1.11 $g \cdot cm^{-3}$. The analysis was performed at NIM at 25using ESR spectroscopy (RE-1X, JEOL). Figure 2 shows the dose response curves for gamma rays and electron beams, in which the good linear dose range is $10^2 \sim 10^4$ Gy. Figure 3 shows the field distribution *(perpendicular to conveyer motion)* for 12 MeV electron beams. The repeatability of the dosimeter was less than 0.7 % at 68 % confidence level. Further research of other dosimetric characteristics is in process.

4. RADIOCHROMIC DOSIMETRY SYSTEM

In radiation processing with electron beams, the reproducibility of absorbed dose in the product depends not only on variation of beam current and conveyor speed, but also on variation of other accelerator parameters such as electron energy, etc. Though some film dosimeters, FWT-60 (Far West Technology, 50 μm) and GafChromic D-200 (Gaf Chemicals Corporation, 120 μm), are currently being used, they are relatively sensitive to UV-light, temperature and humidity, and relatively expensive, which make them difficult to apply for routine quality control in China.

Compared with above dosimeters, the cellulose triacetate (CTA) film is a useful and low-cost plastic dosimeter for electron beam irradiation, which is based on linear relationship between radiation-induced optical absorption at a given wavelength and absorbed dose. To meet the requirements of routine dosimetry, RCCIAE took nearly two years to develop a self-made and mass-producible CTA thin film dosimetry system (FJL-01), which was approved by NIM in 1996 and is now being used as a routine dosimeter for electron beam irradiation.

Some chemical-physical parameters and main dosimetric properties of this film dosimeter are shown in Table I.

TABLE I. SOME BASIC PARAMETERS AND DOSIMETRIC PROPERTIES OF THE FJL-01 CTA THIN FILM DOSIMETER

Mass Composition	cellulose triacetate 85 wt% triphenylphosphate 15 wt%
Average atomic number	6.7
Commercial Dimension	200 mm (l) × 70 mm (w) × 125 μm (t)
Common Difference on Thickness	± 5 μm
Density	1.295 $g \cdot cm^{-3}$
Absorbance of unirradiated film (at 280nm)	0.185~0.205
K-value [a]	6.7 $\Delta A \cdot Gy^{-1}$ (dose rate > 10^5 $Gy \cdot s^{-1}$)
Dose range	10~300 kGy
Energy range	1~12 MeV
Overall uncertainty	≤ 8% (at 95% confidence level)

[a] Defined as an optical absorbance change per unit dose.

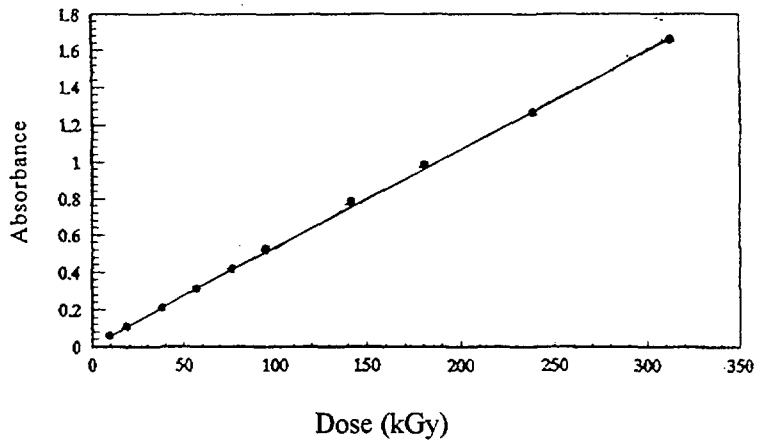

FIG. 4. Dose response curve of the FJL-01 CTA thin film dosimeter

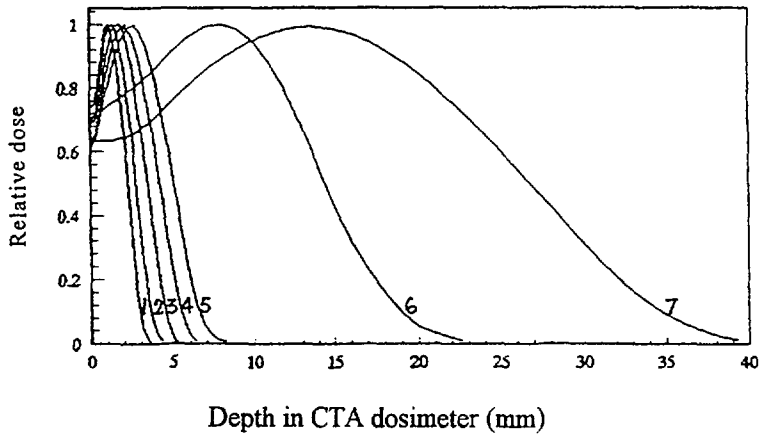

FIG. 5. Depth-dose distribution curves of different energies from 1.2 MeV to 12 MeV
1–1.2 MeV; 2–1.4 MeV; 3–1.6 MeV; 4–1.8 MeV; 5–2.0 MeV; 6–4 MeV; 7–12 MeV

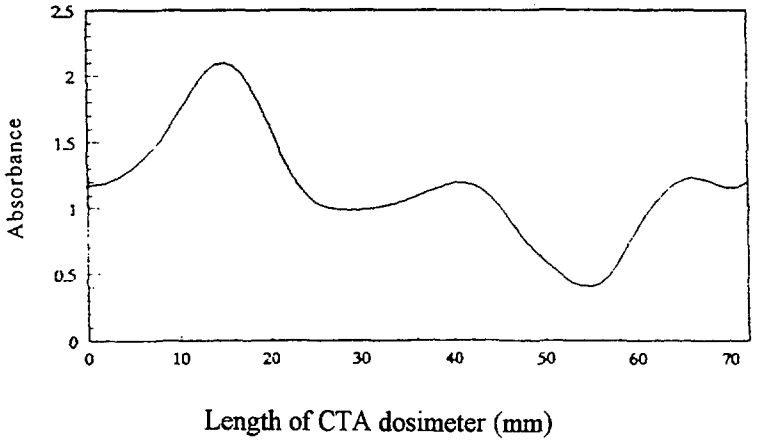

FIG. 6. Typical dose uniformity curve for dynamic irradiation of cable

The analysis was performed by spectrophotometry (Cary-3E, VARIAN). Cary-3E spectrophotometer can measure not only a single flat of 1cm×1cm dosimeter but also a strip of dosimeter with 1cm×10cm in dimension. Due to its high spatial resolution, the FJL-01 CTA dosimeter can be used to measure field distribution, depth-dose distribution and dose uniformity in products. The most probable electron beam energy and any dose values at effective points [1] can be determined from the depth-dose distribution curves. The dose response curve of the FJL-01 CTA dosimeter is shown in Fig. 4. Figures 5 and 6 show the depth-dose distribution curves for different energies, and the dose distribution for cable irradiation.

5. SUMMARY

Since 1994, RCCIAE has established several dosimetry systems of different levels, which have almost enough capability to meet the requirements for electron beam irradiation. The coin-shape potassium (silver) dichromate and ceric-cerous sulfate dosimetry systems have good linearity of dose response, with the overall uncertainty of 4.8 % (at 95 % confidence level). Based on the good agreements with the water calorimeter, the G values determined with ^{60}Co gamma rays can be directly used to measure the absorbed dose for electron beams.

The alanine/PE thin film dosimeter made in RCCIAE is mass-producible and has good uniformity and spatial resolution, which can be used to measure not only absorbed dose but also the field distribution. It is expected to play an important role in transfer dosimetry for electron beam irradiation. Our next objectives are to apply it to radiotherapy and develop another alanine dosimetry system for neutron beam irradiation.

The FJL-01 CTA thin film dosimeter is also reliable and mass-producible, which has been used as a routine dosimeter for electron beams. The combination of its high spatial resolution with continuous measurement by Cary-3E spectrometer make it extensively applicable to practical cable irradiation to provide information on dose homogeneity, which is very important and useful for industry. It can also be used to measure field distribution and depth-dose distribution, from which the most probable energy and any dose values at the effective points can be calculated. The overall uncertainty of FJL-01 CTA thin film dosimeter is 8 % (at 95 % confidence level).

REFERENCES

[1] P.H.G.SHARPE, et.al, Dose rate effects in the dichromate dosimeter, Radiat.Phys.Chem. **35** (1990), 757-761.

[2] YUNDONG CHEN, et.al, Dose measurements with liquid chemical and film dosimeters for electron beams, Radiat.Phys.Chem. **46** (1997), in print.

[3] HONGSHENG YE, et.al, Potassium dichromate dosimeter, Atomic Energy Science and Technology, **28** (1994) 284-288.

[4] GUIQIN ZHANG, et.al, A ceric-cerous sulfate dosimeter, IAE-0131 (1994) 1-8.

OXALIC ACID AS A LIQUID DOSIMETER FOR ABSORBED DOSE MEASUREMENT IN LARGE-SCALE OF SAMPLE SOLUTION

XA9949710

S. BIRAMONTRI, S. DECHBURAM, A. VITITTHEERANON,
W. WANITSUKSOMBUT, W. THONGMITR
Radiation Measurement Division,
Office of Atomic Energy for Peace,
Bangkok, Thailand

Abstract

This study shows the feasibility for applying 2.5 mM aqueous oxalic acid solution using spectrophotometric analysis method for absorbed dose measurement from 1 to 10 kGy in a large-scale of sample solution. The optimum wavelength of 220 nm was selected. The stability of the response of the dosimeter over 25 days was better than 1 % for unirradiated and ±2% for irradiated solution. The reproducibility in the same batch was within 1%. The variation of the dosimeter response between batches was also studied.

1. INTRODUCTION

Radiation application in the field of environment, such as water purification and sewage treatment or vulcalnization of natural rubber, is a growing industry and an active developmental technology [1]. In Thailand, the study on the effect of gamma radiation on microorganisms in sludge from sewage treatment plant and hospital was carried out using gamma radiation in the dose range of 2 to 5 kGy [2] and the research on the improvement of natural latex by radiation have also been studied[3]. The sewage sample in a amount of millilitre was first treated in the laboratory and then transferred to a few hundred litres for industrial application. For process validation, the absorbed dose was measured by placing a commercially available dosimeters such as PMMA or nylon thin film dosimeters inside the sample container.

Oxalic acid dosimeter was first suggested by Draganic[4]. For oxalic acid (25-600 $mM \bullet L^{-1}$) dosimetry, the radiolytic mechanism is given as follows. With oxygen present, radiation decomposes an acid molecule producing two molecules of carbon dioxide(CO_2).

$$(COOH)_2 + OH \rightarrow CO_2 + H_2O + COOH$$
$$O_2 + H \rightarrow HO_2$$
$$COOH + HO_2 \rightarrow H_2O_2 + CO_2$$
$$HO_2 + HO_2 \rightarrow H_2O_2 + O_2$$

The CO_2 is a main product of the radiolysis of oxalic acid solution. Therefore the amount of decomposed acid is determined as the concentration difference between irradiated and unirradiated samples. Draganic introduced two methods which were titration with NaOH and spectrophotometric method for determination of absorbed dose which depended on the difference in concentration of oxalic acid. He also reported the radiation yield of oxalic(G_{ox}) which was 4.9 ± 0.4. The dosimeter is quite insensitive to impurities and very stable to normal storage before and after irradiation[5]. Holm[6] reported the process for determination of absorbed dose using oxalic acid by titration with NaOH. He proposed the initial oxalic acid concentration for different dose regions. The decomposition of dosimeter dose not proceed linearly with the absorbed dose.

The aim of the present work is to apply 2.5 mM oxalic acid as a liquid chemical dosimeter for absorbed dose measurement using a spectrophotometric method in various scale of sample solution. It is also to study the effect of various parameters following the criteria for selecting suitable dosimeter[7]. The studies for optimum wavelength selection, response characteristics, pre- and post-irradiation stability, reproducibility and the variation of dosimeter response between batches were carried out. The 100 mL and 8 L of oxalic acid solution was irradiation against Fricke in the same size of sample container for validation of the process.

2. EXPERIMENTAL

The oxalic dosimeter solution was prepared using analytical grade oxalic acid dihydrate ($H_2C_2O_4.2H_2O$; MERCK grade; M = 126.07 g•mole^{-1}) and diluted to 2.5 mM with distilled water. The dosimeter solution in 5-ml glass ampoules was irradiated in the centre position of a "Gamma-Cell 220" ^{60}Co gamma irradiator with annular geometry. The oxalic acid solution was calibrated against Fricke as a reference dosimeter. The absorbed dose rate at the time of irradiation was 3.12 Gy/s. The absorption spectra and optical absorbance at specific wavelengths were measured with a double-beam Shimadzu model UV-3101 PC spectrophotometer, using a band pass setting of 1 nm. The solution was held in the object beam in quartz-glass, 10 mm path-length cuvette, with the reference beam cuvette containing purified water. The 100 mL and 8 L of oxalic acid solution were filled in cylindrical flask (dimension: ∅ 0.5 x 7.5 cm and ∅ 0.23 x 36 cm) and were irradiated against Fricke with the same scale of solution containers using Gammabeam 650 ^{60}Co gamma irradiator .

3. RESULTS

The aqueous oxalic solution was irradiated for absorbed dose of 2.8, 5.6, 8.4 and 11.2 kGy. Fig.1 shows the optical absorption spectra of unirradiated and irradiated 2.5 mM of dosimeter solution over the range of 200-300 nm. The inset shows the decrease in the absorbance, A as a function of the absorbed dose. The optimum wavelength of 220 nm was selected. The optical density of the irradiated solution decreases with absorbed dose. The dose response in terms of net absorbance, $A_{unirrated}$-$A_{irirrated}$, is plotted as a function of absorbed dose.

In a study of the stability of the aqueous oxalic solution before and after irradiation for 2 kGy at the wavelength of 220 nm is shown in Fig.2. The variation in the optical density for storage over 25 days was less than 1% for unirradiated and ± 2% for irradiated solution. The dosimeter solution in glass ampoules were irradiated at the centre of the irradiation chamber 10 times at absorbed dose of 2 kGy for reproducibility study. The standard deviation of mean response was ± 1% (1 σ).

Figure 3 shows the variation of dosimeter response between batch A and B for the absorbed dose range of 1-6 kGy.

The 100 mL of oxalic acid solution was irradiated for 3.05 kGy against Fricke at dose rate 2.66 Gy/s in the same irradiation condition. The variation in the absorbed dose was within 3 %. The variation in the absorbed dose for 8 litre of oxalic solution and Fricke was ± 5% at 1.02 kGy and 1.18 Gy/s.

4. CONCLUSION

Oxalic acid (2.5 mM), whose density is about that of water, can estimate the absorbed dose in various size of containers over the dose range of 1-10 kGy by spectrophotometric analysis at 220 nm. The dosimeter solution should be calibrated against Fricke as reference dosimeter. The dosimeter solution can be prepared using normal distilled water.

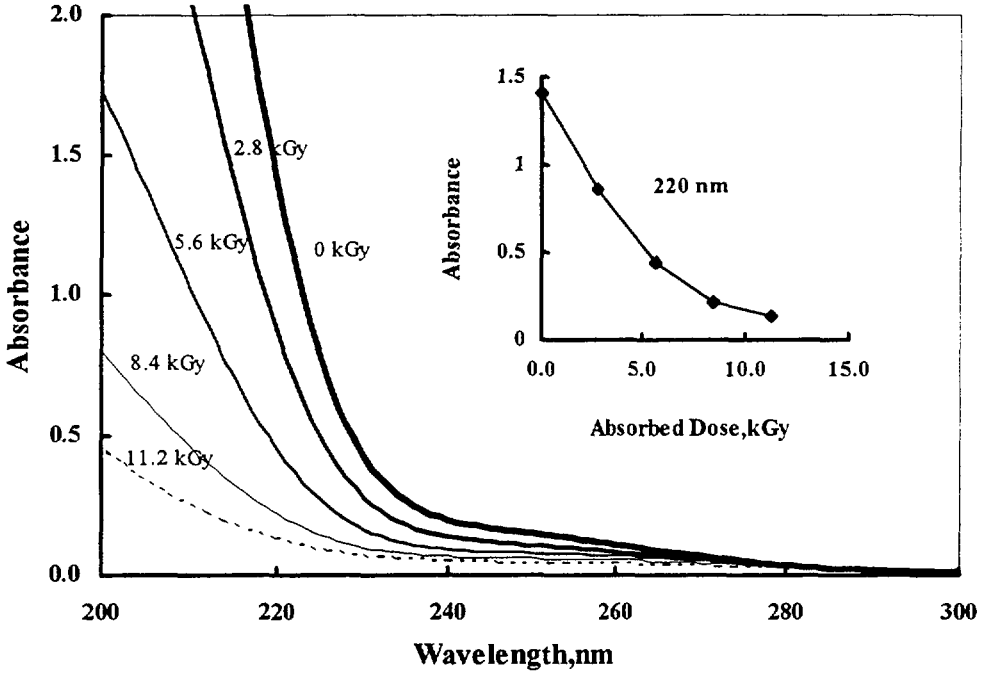

FIG. 1 Absorption spectra of unirradiated and irradiated aqueous oxalic acid; the insets show the decreases in absorbance at 220 nm

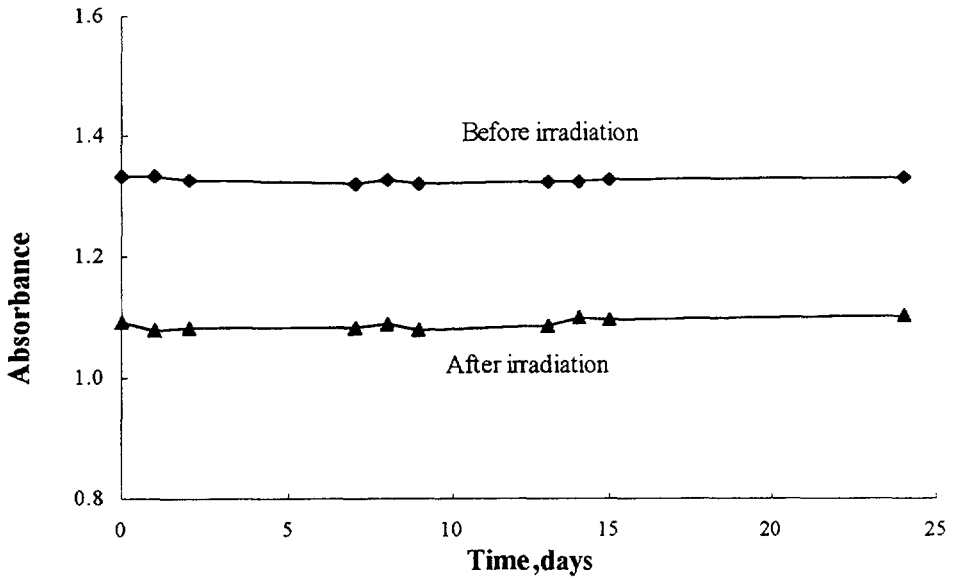

FIG.2. Stability in absorbance (λ= 220 nm) of unirradiation and irradiation 2.5 mM aqueous oxalic acid.

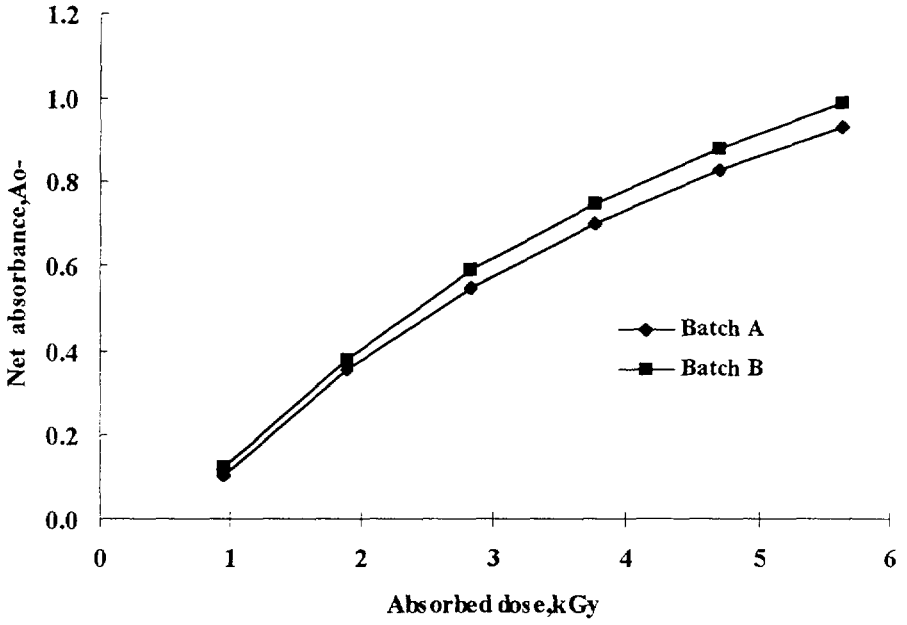

FIG. 3. Dose response curve of 2.5 mM aqueous oxalic acid batch A and batch B,measured at weavelength 220 nm

REFERENCES

[1] MCLAUGHLIN,W.L., A.W.BOYD, K.H.CHADWICK, J.C. MCDONALD and A.MILLER, Dosimetry for Radiation Processing,Taylor and Francis,London(1989).

[2] SERMKIATTIPONG,N., PONGPAT,S., "Gamma Radiation Inactivation of Pathogens in Sludge under Large-Scale Condition", Nuclear Science and Technology (Proc. Conf. Bangkok, Thailand(1996) 404-419.

[3] SIRI-UPATHUM,C., SONSUK,M., "Development of an Efficient Process for Radiation Vulcanization of Natural Rubber Latex Using Hydroperoxide with Sensitizer", Nuclear Science and Technology (Proc. Conf. Bangkok, Thailand(1996) 228-236.

[4] DRAGANIC,I., "Oxalic Acid: The Only Aqueous Dosimeter for In-Pile Use", Nucleonic. 21(1963) 33-35.

[5] CHUNG,W.H.,Techniques of Radiation Dosimetry, (MAHESH,K., AND VIJ, D.R.,Eds.), Wiley Eastern Limited(1985).

[6] HOLM,N.W.,BERRY,R.J., (Ed.), Manual on Radiation Dosimetry, Marcel Dekker, New York(1970)

[7] MCLAUGHLIN, W.L., DESROSIERS,M.F., "Dosimetry Systems for Radiation Processing", Radiat.Phys.Chem.46(1995) 1163-1174.

SIMPLE OPTICAL READOUT FOR ETHANOL-CHLOROBENZENE DOSIMETRY SYSTEM

XA9949711

B. ILIJAŠ, D. RAŽEM
Ruder Bošković Institute,
Zagreb, Croatia

Abstract

Optical readout of the ethanol-chlorobenzene (ECB) or Dvornik dosimetry system is based on the development of the coloured secondary complex of ferric thiocyanate which has a maximum absorption at 485 nm. The applicability of a rugged, hand-held, battery powered filter colorimeter operating at 480 nm has been investigated as a reader for this purpose. This simple reader performs very well within absorbance one displaying an excellent linearity of absorbance with the concentration of Cl^- ions. It is shown that by choosing the appropriate dilution factor when preparing the secondary complex solution the entire useful dose range of the dosimeter up to 2 MGy can be covered. The applicability of this reader to some other liquid chemical dosimeters is also discussed.

1. INTRODUCTION

The use of ethanolic solutions of chlorobenzene (CB) in high-dose dosimetry (ECB or Dvornik dosimeter) is based on radiolytic dechlorination of chlorobenzene and subsequent determination of hydrochloric acid formed in the irradiated solutions. The radiation-chemical yield of HCl, G(HCl), is a function of CB concentration, but at any constant CB concentration the value of G(HCl) is reproducible and independent of dose [1], dose rate [2] and incident radiation energy [3] over a wide range of these variables of interest in kGy/MGy dosimetry.

The ECB dosimetry system exhibits favorable metrologic properties with respect to both of its two fundamental aspects, radiation-chemical and analytical one. On the one hand, the radiation-chemical mechanism of the system's response to irradiation is sufficiently well understood [4], and has been characterized with respect to a number of variables, such as radiation quality [5], temperature of irradiation [6], etc. On the other hand, the ease of analytical determination of HCl in ethanol, and the availability of many analytical methods suitable for its quantitation [7] make it possible to choose a readout method for which the necessary equipment and/or sufficient experience already exist at the user's site.

Spectrophotometry has been known as one of the most versatile and sensitive analytical methods, and as such, one of the readout methods well suited for chemical dosimetry. Its application to ECB dosimetry involves the precipitation of insoluble $HgCl_2$ in the reaction between radiolytically formed Cl^- ions and the reagent $Hg(SCN)_2$, and subsequent complexation of the equivalent amount of liberated SCN^- ions with ferric ions. The ensuing red colored complex has a maximum absorption at 485 nm [8].

While spectrophotometry has not been suitable for field use until recently, recent advances in photonics, together with environmental needs and concerns have brought about a new generation of compact, hand-held filter colorimeters which could also be used as dosimetry readers.

This paper describes the use of a rugged, battery powered, hand-held filter colorimeter, operating at 480 nm, as an ECB dosimetry reader. Its performance has been checked against a Cary 2200 spectrophotometer and satisfactory characteristics have been established. The paper gives information necessary for the routine use of this reader in dosimetry practice.

2. EXPERIMENTAL

Absolute ethanol (Merck, *pro analysi*) and triply distilled water were mixed to prepare 96 vol% ethanol. It was then used for topping appropriate amounts of chlorobenzene (Fluka, *puriss.*) in volumetric flasks to obtain dosimetric solutions containing 4, 10, 20, 25 and 40 vol% of CB. The use of several formulations of dosimetric solutions is recommended for cross-checking of the internal consistency of measurements. The five formulations have been extensively used in the past and their characteristics are well known.

Commercial pharmaceutical ampoules (15 mm outer diameter) were filled with 5 mL of dosimetric solution. ECB solutions were partly deoxygenated by bubbling with nitrogen for 1 minute at about 30 mL/min immediately before flame sealing. Sealed dosimeters were stored in dark.

Dosimeters were irradiated with ^{60}Co gamma rays up to 25 kGy at dose rate of about 5 Gy/s. Irradiated dosimeters were opened and 0.1 mL of each dosimetric solution was transferred to 10 mL volumetric flasks. The reagent for developing color of the secondary complex was added to each volumetric flask and the flask was topped with technical grade 96% ethanol. The reagent consisted of 0.6 mL 5.25 mol/dm^3 $HClO_4$, 0.02 mL 0.37 mol/dm^3 $Fe(NO_3)_3$ and 0.2 mL saturated ethanolic solution of Hg $(SCN)_2$. At the same time, one blank of each dosimetric formulation was prepared in the same manner, using 0.1 mL of unirradiated dosimetric solution.

After completion of the complexation reaction and development of the colour, which takes less than half an hour, the coloured solution was divided in two parts. About 3 mL were filled into a 1-cm pathlength spectrophotometric cell, and the remaining 7 mL into a cylindrical 1-inch (25 mm) diameter borosilicate glass cell with screw cap.

The spectra of the secondary complex solutions between 750 and 300 nm were taken against the corresponding blanks with a Cary 2200 UV-VIS spectrophotometer by Varian, and absorbance at the maximum wavelength 485 nm was recorded. The colorimeter was a DR/700 model of a portable, digital, optical filter colorimeter by Hach. It uses plug-in filter modules with preprogrammed calibrations for various measurements. We used it in the absorbance mode with the 480 nm plug-in filter module and zeroed it with the appropriate blank solution.

The concentration of radiolytically formed HCl in irradiated dosimetric solutions was also determined by mercurimetric titration of Cl^- with $Hg(NO_3)_2$ in nitric acid-acidified ethanol, with diphenylcarbazone as indicator. The concentration of $Hg(NO_3)_2$ solution was checked daily by titrating standard solutions of NaCl.

3. RESULTS

One of the basic requirements expected of a chemical dosimetry system is the linearity of its response with dose. This requirement implies that the linearities of both of the two basic aspects of a chemical dosimetry system, radiation-chemical and analytical-chemical, should be fulfilled: the linearity of the radiation-chemical yield with dose, and the linearity of the response of the used analytical technique with the concentration of the analyzed radiation-chemical product.

The linearity of the radiation-chemical yield of the ethanol-chlorobenzene dosimetry system was the subject of several earlier papers [2, 7, 9]. The linearity of the spectrophotometric readout method was also established earlier [8]. The present work concerns itself with the suitability of a filter colorimeter as a readout instrument.

The results of colorimetric as well as of spectrophotometric readings of irradiated dosimeters are presented in the form of absorbance as function of irradiation dose to water for two extreme

formulations of the ECB dosimeter, 4 vol% CB and 40 vol% CB in Figs 1a and 1b. While a good linearity of the spectrophotometric response of the 4 vol% CB formulation throughout the used dose range is obtained, the colorimetric response of the same formulation deviates from the linearity above absorbance larger than one. Admittedly, the spectrophotometric response of this formulation shows a tendency of sublinearity too at 25 kGy, which may be due to the consumption of about 2% of CB at this dose, and consequent decrease of the G(HCl) value. To compensate for all non-optical effects, the ratio of the absorbances taken by the two instruments was calculated relative to spectrophotometer and shown in the same figure as function of the spectrophotometer reading. Any nonlinearity of optical origin is enhanced in this ratio, and indeed, the sublinearity is seen to set in above absorbance 1 of the colorimeter.

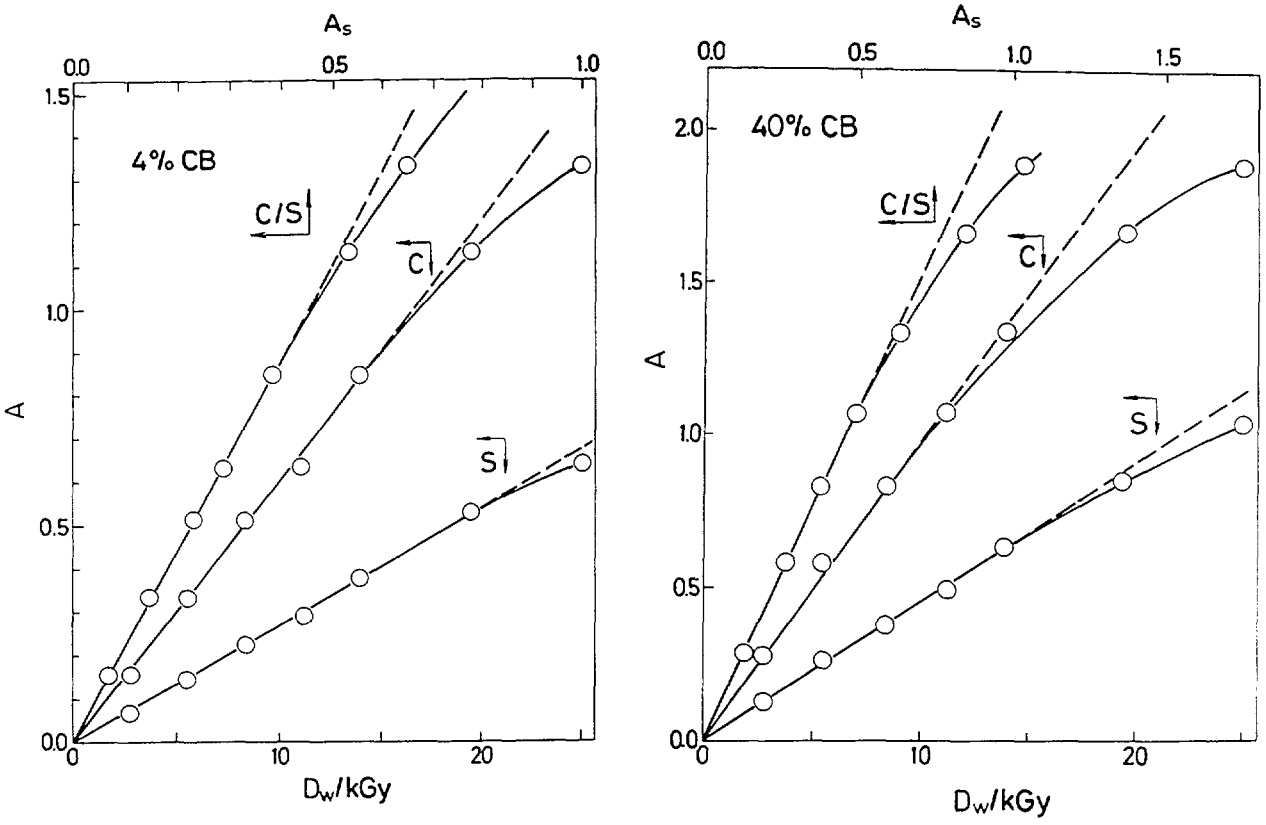

FIG. 1. Absorbance A as function of dose to water D_w as measured by a spectrophotometer (S) and a colorimeter (C). The dependence of the colorimetric absorbance on the spectrophotometrically obtained absorbance A_S is also shown (C/S). a) Formulation containing 4 vol% CB; b) formulation containing 40 vol% CB.

The same is seen in the formulation containing 40 vol% CB, and it may be reasonably assumed that this is a general phenomenon, and that it occurs at all intermediate CB formulations as well. It may also be concluded that it is not due to the decrease of the radiation chemical yield caused by the radiolytic depletion of the CB concentration, because this decrease would not amount to more than 0.3% at 25 kGy in 40 vol% CB formulation, which would have a negligible effect on $G(Cl^-)$.

Possible interference of the radiation-chemical aspect with the analytical-chemical one has been eliminated in the way Fig. 2 is presented. The absorbance scale is expanded and shown as function of the concentration of Cl^- ions independently quantitated by mercurimetric titration. A very good linearity of both, spectrophotometric and colorimetric responses is achieved within absorbance one in all formulations of the dosimetry system.

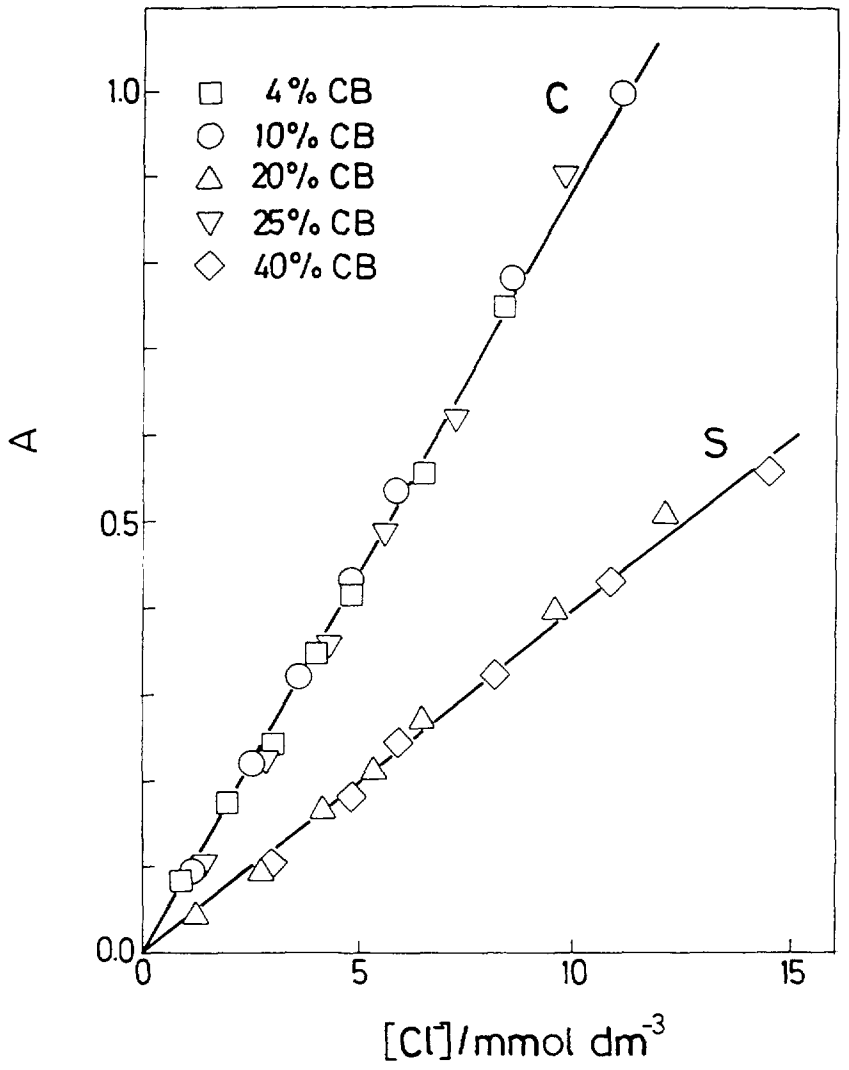

FIG. 2. Absorbance A as function of the concentration of radiolytically formed Cl^- ions as determined by a spectrophotometer (S) or a colorimeter (C) for various formulations of the ECB dosimeter.

Molar absorptivity ε of the ferric thiocyanate complex was calculated from the spectrophotometric data for each dosimeter formulation separately. No influence of the composition on ε was found, and the average value was 3800 ± 300 $dm^3mol^{-1}cm^{-1}$, which is 5% lower than the previously determined value (3990 $dm^3mol^{-1}cm^{-1}$) [8]. The conformity of the colorimetric readings to the Lambert-Beer Law permitted the effective pathlength of the cylindrical colorimetric cell to be calculated. The value 2.22 ± 0.07 cm was obtained as a ratio of the colorimetric and spectrophotometric absorbance at the same dose.

The validity of the Lambert-Beer Law of the colorimetric readout (the linearity) was examined beyond absorbance 1 by comparing the colorimetric and spectrophotometric readings up to the absorbance 2, the upper limit of the declared colorimetric range (Fig. 3). Above absorbance 1.5 the linearity rapidly deteriorates and the range above 1.3 is not recommended for dosimetry use.

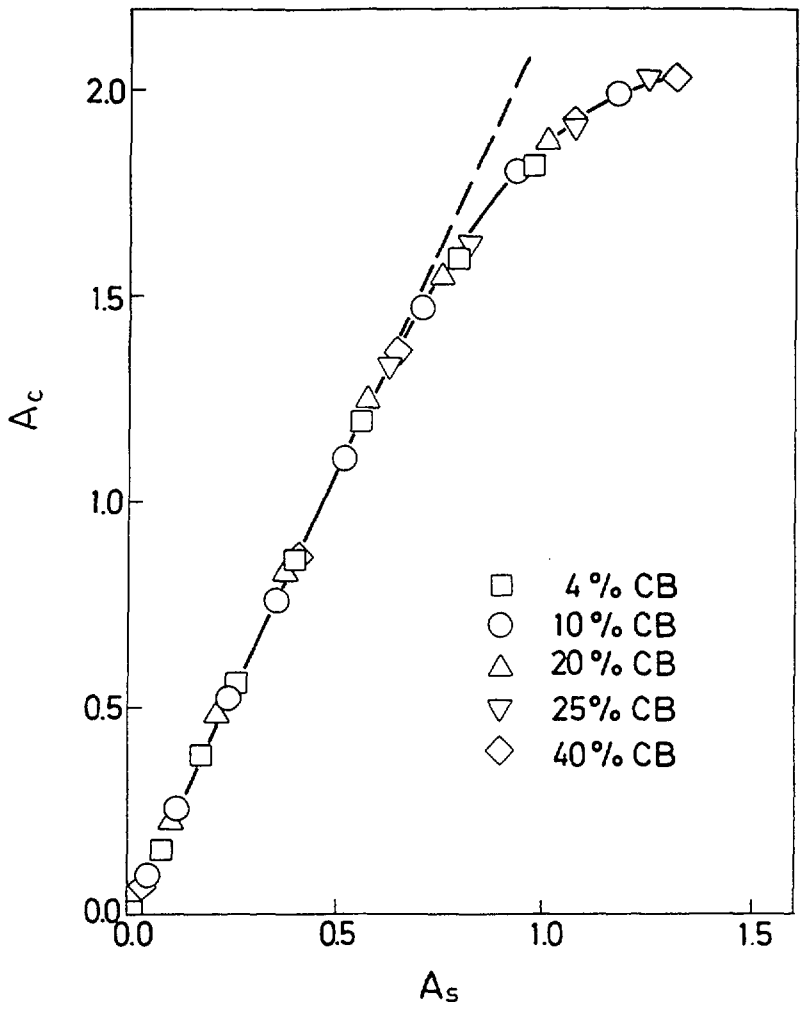

FIG. 3. Colorimetrically obtained absorbance A_C as function of the spectrophotometrically obtained absorbance A_S for the five formulations of the ECB dosimeter.

4. DISCUSSION

A great variety of physico-chemical changes inducible by irradiation, as well as a number of analytical methods available for their quantitation has led to a popular belief that almost anything can be a dosimeter. Potential new dosimetry systems are being investigated in hope that a special set of characteristics will be discovered, which might prove uniquely suitable for a particular purpose. At the same time, the scope of the well known dosimetry systems is improved by calibrating their response to an ever widening set of operating variables and applying novel readout techniques. However, technical and operational selection criteria impose restrictions upon prospective dosimetry systems, reducing the number of really useful chemical dosimeters to not more than a dozen.

It is not realistic to expect that the practicality of the use of the ECB dosimetry system could be enhanced by any modifications of the radiation-chemical aspect of the system's response to irradiation. A more productive approach to the improvement of the system's practicality would concern itself with the analytical-chemical (readout) aspects.

The oscillometric readout method of ECB dosimeters was one such improvement, which has greatly increased the practicality of the dosimetry system and has significantly contributed to its acceptance worldwide [10]. A simple optical readout method might be competitive in that respect, provided the limitations of a rugged filter colorimeter are recognized and taken into consideration.

The exponential law of light absorption is valid for monochromatic light. The optical filters used in the colorimeter have a typical bandwidth (Full Width at Half Maximum - FWHM) of 10 ± 2 nm. The light source used in the colorimeter is focused by a bulb top lens, which cannot be considered a high-precision optics. Likewise, the silicon photodiode, unlike a narrow monochromator slit in a spectrophotometer, has finite dimensions and "sees" not only the light rays which arrive perpendicularly to it across the diameter of a cylindrical cell, but also the rays traversing distances somewhat shorter than the diameter. The light striking the front and the back surfaces of the cell is partly reflected from a cylindrical surface and does not reach the detector. All these optical imperfections cause nonlinear response of the instrument, but it is remarkable that this nonlinearity becomes evident only above absorbance greater than one. This leaves sufficient space for a quite satisfactory operation.

Spectrophotometric readout of the ECB dosimetry system depends on developing the colour of the secondary complex of ferric thiocyanate. The lower limit of the dose range is given by the smallest applicable dilution factor f when adding the reagents for developing the colour. Let us assume that the smallest achievable dilution of a 5-mL dosimetric solution involves taking 4.55 mL of irradiated dosimetric solution, adding 0.3 mL of $HClO_4$, 0.01 mL of $Fe(NO_3)_3$ and 0.1 mL of $Hg(SCN)_2$ solutions, and topping it to 5 mL with a few drops of ethanol. This gives the dilution factor $5/4.55=1.10$. Let us further assume that the lowest reliable reading of the colorimeter is 3σ larger than the lowest possible reading, 0.01 absorbance units. This determines the lowest dose readings as given in Table I.

TABLE I. THE PARAMETERS OF THE COLORIMETRIC READOUT OF THE ETHANOL-CHLOROBENZENE DOSIMETRY SYSTEM

Formulation [vol% CB]	ε [$dm^3mol^{-1}cm^{-1}$]	ρ [kg/dm^3]	G [μmol/J]	Lower dose limit ($A\geq0.03$, $f=1.10$) [Gy]	Upper dose limit ($A\leq1.0$, $f=10^3$) [MGy]
4	3800	0.819	0.42	11.5	0.35
10	3800	0.839	0.52	9.1	0.27
20	3800	0.869	0.59	7.7	0.23
25	3800	0.880	0.60	7.5	0.23
40	3800	0.925	0.63	6.8	0.21

The upper dose limit is determined by the requirement that the absorbance should not exceed one, by the selection of a reasonable dilution factor, and by the operational upper limit of the dosimetry system. Giving weight to the last criterion, the operational upper limit is determined by the highest dose for which the response is known. This is beyond the linearity range of the response with dose, and amounts to about 2 MGy [1]. This in turn determines the dilution factor of 10^3, which is a reasonable value (0.1 mL of irradiated dosimetric solution diluted to 100 mL, or 0.01 mL diluted to 10 mL). Thus calculated theoretical upper limits (Table I.) may be even slightly larger than actually determined ones. In any case, the applicability of the colorimetric reader is demonstrated throughout the useful range of the ECB dosimetry system, while staying at the same time within the linearity range of the response of the instrument itself.

Let us briefly examine the applicability of the described colorimetric reader to other chemical dosimetry systems adopted as American Society for Testing and Materials (ASTM) standards [11] which are based on spectrophotometric readout. They are listed in Table II.

TABLE II. THE PARAMETERS OF THE COLORIMETRIC READOUT OF SEVERAL LIQUID CHEMICAL DOSIMETRY SYSTEMS

ASTM designation	Formulation	λ_{max} [nm]	Available filter module [nm]	G [μmol/J]	Dose range [kGy]
1026	1 mM $FeSO_4$ + 1 mM NaCl in 0.4 M H_2SO_4	304	not available	1.62	0.02 - 0.2
1025	15 mM$Ce(SO_4)_2$+15 m$MCe_2(SO_4)_3$ in 0.4 M H_2SO_4	320	not available	0.231	0.5 - 5
	0.1 $MCe(SO_4)_2$+ 0.1 $MCe_2(SO_4)_3$ in 0.4 M H_2SO_4			1.066	5 - 40
1401	0.5 mM $Ag_2Cr_2O_7$ in 0.1 M $HClO_4$	350	not available	0.17	0.2 - 2
	0.5 m M $Ag_2Cr_2O_7$+ 2 mM $K_2Cr_2O_7$ in 0.1 M $HClO_4$	440	450	0.0395	5 - 40
1540	5 mM HHEVC + 17 mM HAc in 2-MEtOH	599	610	0.025	0.01 - 1
	5 mM PRC + 51 mM HAc in 2-MEtOH	549	550	0.033	0.01 - 3
	0.1 mM NFC + 17 mM HAc in DMSO	554	550	0.0031	0.1 - 30
	5 mM PRC + 17 mM HAC + 30 mM Ph NO_2 in DMSO	554	550	0.0040	0.003 - 40
	2 mM HHEVC + 34 mM HAc + 500 ppm Ph NO_2 + + 10% PVB in 85% (v/v) n-PrOH + 15 % (v/v) TEP	605	610	0.0051	0.05 - 5
	2 mM NFC+ 68 mM HAc + 500 ppm O_2N Ph COOH + + 10% (w/w) PVB in 85% (v/v) TEP + 15% (v/v) DMSO	557	550	0.0055	0.1 - 10
	100 mM HHEVC + 68 mM HAc + 500 ppm O_2N Ph COOH + 10% (w/w) PVB in 85% (v/v) TEP + 15% (v/v) DMSO	608	610	0.28	0.005 - 0.1

HHEVC - hexa(hydroxyethyl) pararosaniline cyanide
PRC - pararosaniline cyanide
NFC - new fuchsin cyanide
HAc - acetic acid
2-MEtOH - 2-methoxyethanol
DMSO - dimethyl sulfoxide
PVB - polyvinyl butyral
TEP - triethylphosphate

Contrary to the ECB system, which requires the developing of the coloured secondary complexes prior to readout, these other dosimetry systems exhibit an inherent change of optical absorption on irradiation. This means that no additional handling of the irradiated dosimeters would be necessary, and that they would, in principle, be ready for readout after the irradiation. Of course, the effect of irradiation on the glass of the container could be a problem interfering with the reading, and might require transfering the irradiated dosimetric solutions to transparent colorimetric cells. The difference between the absorption maximum and the readout wavelength of the plug-in module must also be checked, expecially if larger than 5 nm.

REFERENCES

[1] RAZEM, D., DVORNIK, I., Application of the ethanol-chlorobenzene dosimeter to electron-beam and gamma-radiation dosimetry: II. Cobalt-60 gamma rays. *Proc. IAEA Symp. on Dosimetry in Agriculture, Industry, Biology and Medicine*, Vienna 1972, IAEA, Vienna (1973) 405-419.

[2] DVORNIK, I., RAZEM, D., BARIÆ, M., Application of the ethanol-chlorobenzene dosimeter to electron beam dosimetry: Pulsed 10 MeV electrons. *Proc. IAEA Symp. on Large Radiation Sources for Industrial Processes*, Munich, 1969, IAEA, Vienna (1969) 613-622.

[3] MILJANIÆ, S., RAZEM, D., DVORNIK, I., Energy independence of the radiation chemical yield, G(Cl^-), of ethanol-chlorobenzene dosimeter solutions for ionizing photon irradiations. *Appl. Radiat. Isot.*, 44 (1993) 711-718.

[4] RAZEM, D., DVORNIK, I., Scavenging of electrons prior to thermalization in ethanol. *J. Phys. Chem.*, 84 (1980) 3577-3581.

[5] MILJANIÆ, S., MILJANIÆ, Ð., BLAGUS, S., Response of the chlorobenzene-based dosimetry systems to protons in the energy range 3-5.5 MeV. *Radiat. Phys. Chem.*, 51 (1998) 185-189.

[6] HOANG HOA, M., RAZEM, D., Temperature effects on the ethanol-chlorobenzene dosimeter (Dvornik dosimeter). *Appl. Radiat. Isot.*, 42 (1991) 637-641.

[7] RAZEM, D., DVORNIK, I., Ethanol-chlorobenzene dosimetry for absorbed doses below 1 kGy. *Appl. Radiat. Isot.*, 38 (1987) 1019-1025.

[8] RAZEM, D., OÈIÆ, G., JAMIÈIÆ, J., DVORNIK, I., Application of the ethanol-chlorobenzene dosimeter to electron beam and gamma radiation. IV. Spectrophotometry of coloured secondary complexes. *Internat. J. Appl. Radiat. Isot.*, 32 (1981) 705-711.

[9] RAZEM, D., DVORNIK, I., Application of the ethanol-chlorobenzene dosimeter to electron-beam and gamma-radiation dosimetry: III. Tissue-equivalent dosimetry. *Proc. IAEA Symp. on Radiation Preservation of Food*, Bombay, 1972, IAEA, Vienna (1973) 537-547.

[10] STENGER, V., TORDAY, Zs., HORVATH, I., FALVI, L., PAPP, Z., Long term experience in using the ethanol chlorobenzene dosimeter system. *Proc. IAEA Symp. on High Dose Dosimetry for Radiation Processing*, Vienna, 1990, IAEA, Vienna (1991) 277-288.

[11] AMERICAN SOCIETY FOR TESTING AND MATERIALS, *Annual Book of ASTM Standards*, Vol. 12.02, ASTM, Philadelphia, PA (1998).

ON THE USE OF A BIPOLAR POWER TRANSISTOR AS ROUTINE DOSIMETER IN RADIATION PROCESSING*

P.G. FUOCHI, M. LAVALLE
Istituto FRAE – CNR,
Bologna, Italy

E. GOMBIA, R. MOSCA
Istituto MASPEC – CNR,
Parma, Italy

A.V. KOVÁCS
Institute of Isotopes,
Budapest, Hungary

A. VITANZA, A. PATTI
SGS - Thomson Microelectronics,
Catania, Italy

Abstract

The use of silicon devices as possible radiation dosimeters has been investigated in this study. A bipolar power transistor in TO-126 plastic packaging has been selected. Irradiations, with doses in the range from 50 Gy up to 25 kGy, have been performed at room temperature using different radiation sources (^{60}Co γ source, 2.5, 4 and 12 MeV electron accelerators). A physical parameter, T, related to the charge carrier lifetime, has been found to change as a function of irradiation dose. This change is radiation energy dependent. Long - term stability of the irradiated transistors has been checked by means of a reliability test ("high temperature reverse bias", HTRB) at 150 °C for 1000 h. Deep level transient spectroscopy (DLTS) measurements have been performed on the irradiated devices to identify the recombination centres introduced by the radiation treatment. The results obtained suggest that these transistors could be used as routine radiation dosimeters in a certain dose range.

1. INTRODUCTION

The use of silicon devices as possible radiation monitors has been considered since many years because of the effect of ionizing radiation on the physical and electrical properties of these devices [1]. These effects can be summarized as follows:

(1) production of a transient electric current across the p-n junction during irradiation due to diffusion of electron-hole pairs in the electric field of the depletion layer of the semiconductor;

(2) a permanent damage to the silicon crystal structure with formation of point defects, which creates generation-recombination centres that affect the charge carrier lifetime and all the related electrical parameters.

*Work performed with financial support of the National Research Council of Italy (CNR) within the Italy-Hungary (CNR-MTA) Co-operative Research Programme and within the framework of the Research Agreement No. 8054/CE of the FAO-IAEA CRP on Standardized Methods to Verify Absorbed Dose in Irradiated Fresh and Dried Fruits, Tree Nuts in Trade.

While in the first case the device can be used for real-time dose-rate measurements [2], the permanent damages in the crystal structure permit measurement of dose over a wide range in terms of radiation-induced changes in electrical characteristics [3, 4]. In this latter case such devices have been proposed for dose measurements and used in free flowing product being transported in bulk through a radiation field [5, 6]. Looking into our work done in the past years on the effects of gamma and electron irradiation on silicon power devices [7] and on the basis of the experience acquired in this field it was decided to investigate the use of some commercial power transistors for radiation dosimetry.

2. EXPERIMENTAL METHODS

2.1. Semiconductor device

A commercial bipolar transistor type BULT118 in TO-126 or SOT32 plastic packaging, manufactured by SGS-Thomson, was selected. It is a high voltage fast-switching npn power transistor which is used in electronic ballasts for fluorescent lighting and in general for medium switching power applications. It is fabricated by using a multiepitaxial mesa technology from a 70 Ω·cm CZ silicon substrate. The sensitive area is equal to 2.3 mm^2. Its mechanical data are reported in Table I.

TABLE I. SOT32 MECHANICAL DATA

DIM.	mm			DIM.	mm		
	MIN.	TYP.	MAX.		MIN.	TYP.	MAX.
A	7.4		7.8	D		15.7	
B	10.5		10.8	e		2.2	
b	0.7		0.9	e3		4.4	
b1	0.49		0.75	F		3.8	
C	2.4		2.7	G	3		3.2
c1		1.2		H			2.54

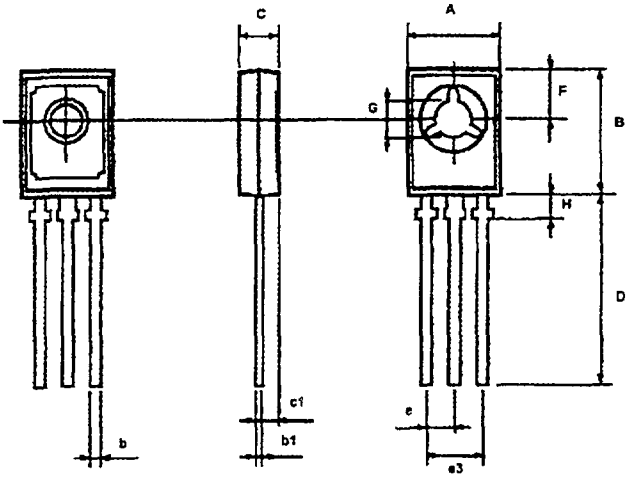

2.2. Irradiation procedures and sources

All the devices have been irradiated at room temperature using different radiation sources located in different laboratories. Gamma irradiations have been performed with the transistors enclosed in a plastic chamber with a wall thickness of 0.4 g/cm^2 which is adequate to establish electron equilibrium for ^{60}Co γ rays. The irradiation facilities used were the ^{60}Co Nordion Gammacells 220 of the FRAE Institute in Bologna and of the IAEA laboratory in Seibersdorf, having dose rates of 50 Gy/min and 2.5 and 53 Gy/min respectively and a Gammacell GC-252 with dose rate of 172.7 Gy/min of NIST, Washington. Irradiations at the Institute of Isotopes, Budapest, were done using the SSL/01 local gamma irradiator (dose rate 33 Gy/min). Electron irradiations have been carried out in Bologna, in

Budapest and in Strasbourg using pulses of electrons from an L-band 12 MeV, a Tesla Model LPR-4 MeV linear accelerators and a 2.5 MeV Van de Graaff accelerator, respectively. The machine parameters used for these irradiations are reported in Table II.

TABLE II. ACCELERATOR CHARACTERISTICS

Equipment / Characteristics	Tesla LPR-4 Linac (Magnetron) Institute of Isotopes Budapest, Hungary	L-Band Vickers Linac (Klystron) CNR – FRAE Bologna, Italy	Van de Graaff AERIAL Strasbourg, France
Max Beam Energy	4 MeV	12 MeV	2.5 MeV
Av. Beam Energy	3.8 MeV	8.2 MeV	2.2 MeV
Av. Current	20 μA	85 μA	50 μA
Pulse Duration	2.6 μs	2 μs	continuous
Repetition Rate	50 p.p.s.	50 p.p.s.	scan frequency 20 Hz

From four to six transistors for each dose, in groups of two, three, four or six, have been irradiated at the same time.

2.3. Dosimetry

The dose rate of the Gammacell in Bologna has been measured in a fixed position (i.e. at the centre of sample chamber) using the Fricke chemical dosimeter while alanine pellets, ethanol monochlorobenzene solution (ECB) and calibrated radiochromic film have been used for dose measurements in Seibersdorf, in Budapest and at NIST respectively. The dose per pulse delivered by the 12 MeV linear accelerator has been determined by means of the super Fricke chemical dosimeter and measurements have been regularly done before and after the irradiation of the devices. For the irradiation performed in Budapest with the LPR-4 Tesla electron accelerator GAFChromic films, placed close to the transistors to be irradiated, have been used for dose measurements. Calibration of this film has been done using ethanol monochlorobenzene liquid dosimeter; alanine pellets were used for dosimetry at AERIAL. The irradiation doses refer to dose in water and were in the range from 50 Gy up to 25 kGy.

2.4. Measurements of device characteristics

By knowing from previous studies [7, 8] that there is a linear correlation between the inverse charge carrier lifetime and the dose, expressed by Eq. (1)

$$1/\tau_I = 1/\tau_0 + kD \qquad (1)$$

where, τ_I is the post-irradiation lifetime,
τ_0 is the pre-irradiation lifetime,
D is the irradiation dose, and
k is the radiation damage coefficient (in general k is substrate and irradiation condition dependent),

our attention has been focused on the changes of charge carrier lifetime. For this purpose a portable instrument, whose schematic circuit diagram is shown in Fig. 1, was realized. It allows to measure on

the spot, soon after irradiation, a physical parameter T directly related to the charge carrier lifetime and defined by Eq. (2):

$$T = \tau \cdot \ln(Q_s/\tau \cdot I_b) \tag{2}$$

where, τ is the charge carrier lifetime,
Q_s is the stored charge, and
I_b is the turn-on base current.

By properly selecting the right driving conditions V_{BB}, $R_{BB(2)}$, $R_{C(2)}$, V_{CC} and I_{B1}, T can be considered a function of the lifetime only. Readout is accomplished merely by pressing a button to enable a digital display of the measured T value.

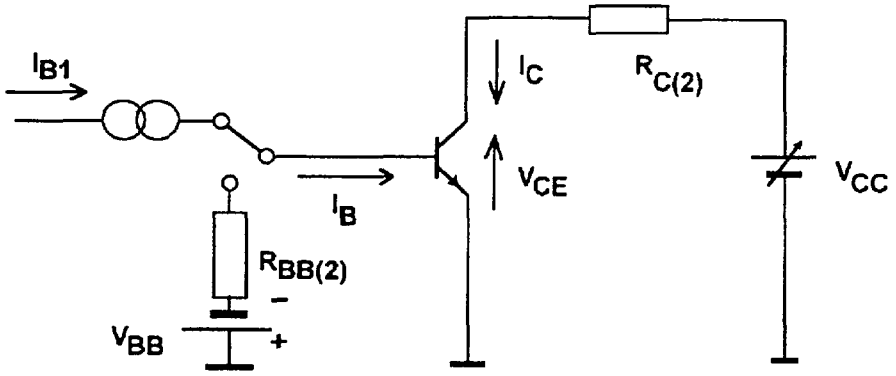

FIG. 1. Resistive load switching test circuit for measuring the parameter T. The driving conditions V_{BB}, $R_{BB(2)}$, $R_{C(2)}$, V_{CC}, I_{B1} have fixed values.

The deep levels introduced into the silicon structure of the transistor by γ or electron irradiations have been monitored by the deep level transient spectroscopy technique (DLTS) by using a commercial lock-in type spectrometer [9] and the induced defect concentrations were obtained by using a modified Zotha-Watanabe expression [10].

3. RESULTS

3.1. Irradiations

Batches of BULT118 transistors have been irradiated up to doses of 25 kGy in different laboratories and with different types of radiation sources. Measurements of the parameter T were done in Bologna. The changes of T with irradiation dose have been plotted as $\Delta(1/T) = 1/T - 1/T_0$ and are shown in Fig. 2. The response of the transistor is linear with absorbed dose up to 5 kGy, giving a linearity correlation coefficient $r^2 = 0.998$ for 12 MeV electrons, $r^2 = 0.993$ for 4 MeV electrons, $r^2 = 0.996$ for 2.5 MeV electrons and $r^2 = 0.994$ for gamma irradiations. At higher doses the response is sublinear and follows a second order polynomial fitting. To check the stability of the lifetime changes produced by irradiation, the irradiated devices, together with some blanks, were left on the shelf of a cabinet without any special precaution. They have been measured over a year period showing no significant variation of the parameter T. This is in agreement with the fact that transistors of the same type used for this study and electron irradiated, subjected to reliability tests ("high temperature reverse bias" HTRB) at 150°C for 1000 h, did not show any significant variations of the lifetime [11]. The results of these tests are reported in Fig. 3.

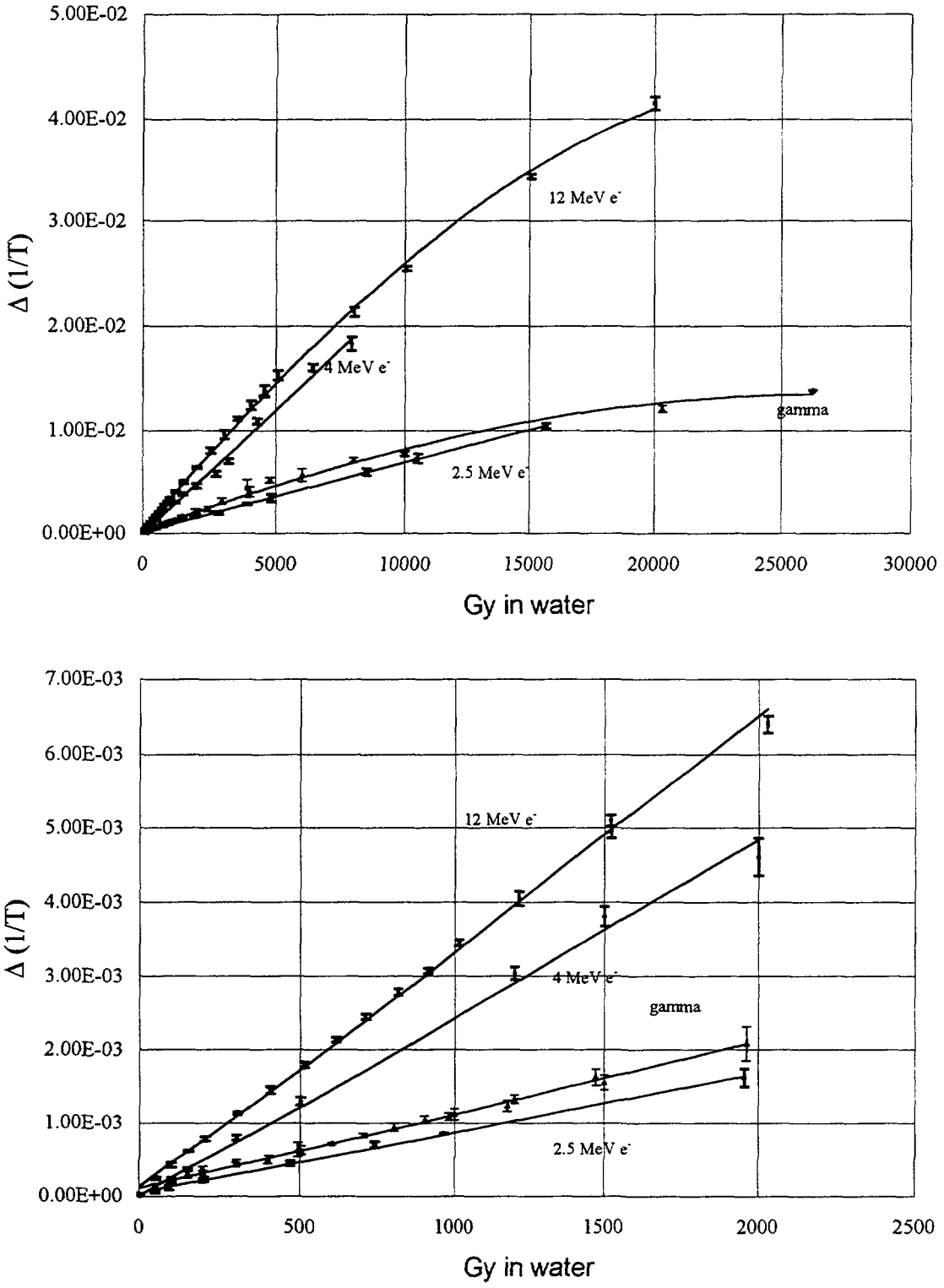

FIG. 2. Plot of $1/T - 1/T_0$ vs. dose for γ and electron irradiations performed in Bologna, Seibersdorf, Strasbourg, Budapest and Washington.

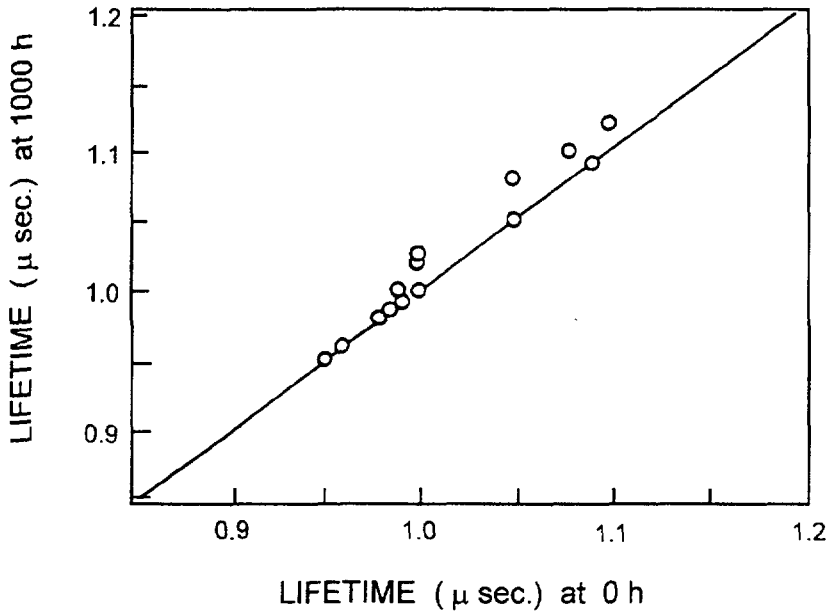

FIG. 3. Comparison of electron irradiated transistors after 1000 h annealing at 150°C and soon after irradiation.

3.2. DLTS measurements

Deep level transient spectroscopy (DLTS) measurements have been carried out on the irradiated devices in order to characterize the recombination centres, introduced by irradiation, that affect the carrier lifetime. The results of these measurements are reported in Fig. 4 and in Fig. 5. In Fig. 4 three peaks, labelled as E_1, E_2 and E_3, are clearly distinguishable in the samples irradiated with electrons. They correspond to the three main electron traps identified as the oxygen-vacancy complex (A centre), the double negative $(V\text{-}V)^{=}$ and single negative $(V\text{-}V)^{-}$ charge state of the divacancy, respectively. These three levels are all active recombination centres that can account for the changes of the lifetime, and consequently of the related electrical parameters, observed with irradiation [7]. Their thermal stability up to 150°C (the maximum working temperature of the devices), very important for safe operation of the device, is well known from previous study [12] and the results, reported in Fig. 3, are a direct consequence of that. The samples irradiated with γ rays, instead, show a clear oxygen-vacancy peak and a broad DLTS signal in the temperature range 120-300 K. This broad band is determined by the presence of a complex structure of defects in high concentration which contributes to its amplitude, thus resulting comparable with that of the related oxygen-vacancy peak, differently from what happens in the electron irradiated samples where the amplitude of the oxygen-vacancy peak is always much larger than those of the divacancy. This fact can explain the larger reduction of the lifetime obtained in the transistors with gamma rays in comparison with 2.5 MeV electron irradiation, even though the production rate of the oxygen-vacancy is lower in gamma- than in 2.5 MeV electron-irradiated samples.

4. CONCLUSIONS

The work on the characterization of these transistors as possible routine dosimeters is not yet completed. In fact the possible influence of different environmental conditions has not yet been evaluated. A large spread of lifetime values after irradiation has been observed in the low dose range (up to 150 Gy) for γ rays, 2.5 and 4 MeV electrons, nevertheless the results obtained so far, are satisfactory and promising. The bipolar transistor's advantages are its small size, low cost, ease of use, good sensitivity, possibility of immediate reuse and its ability to record dose history (dose information is

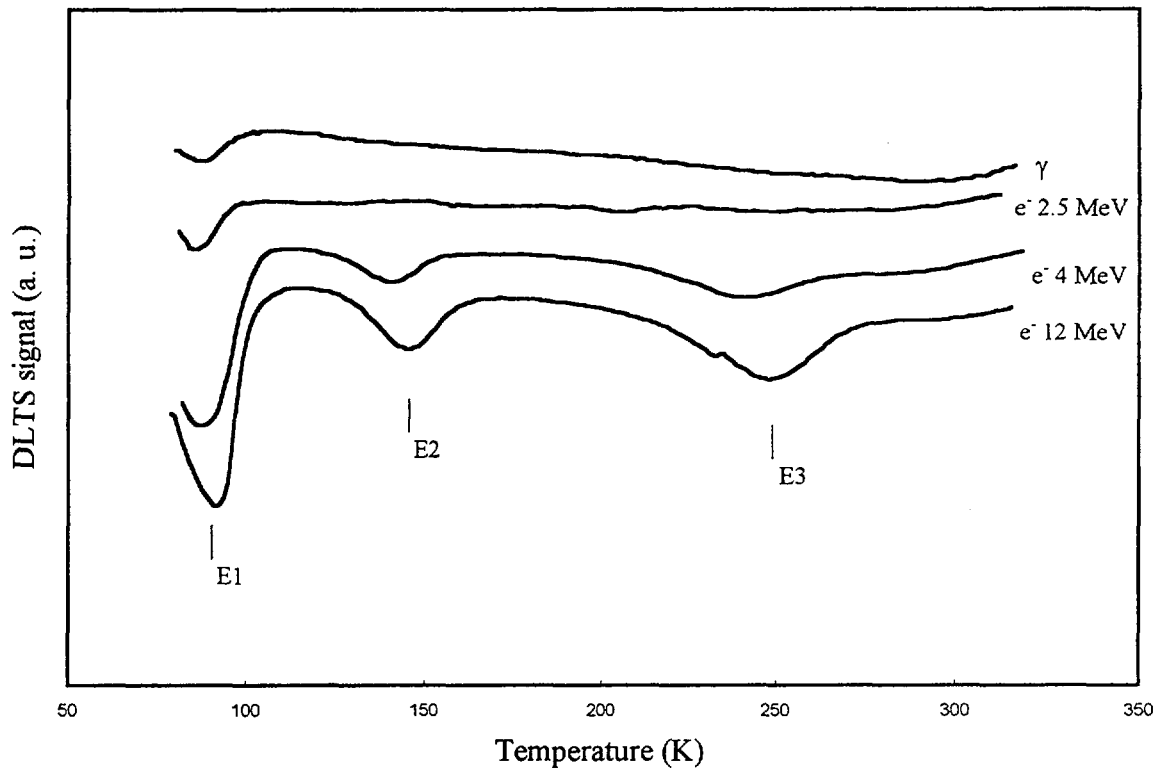

FIG. 4. DLTS spectra from transistors irradiated with γ rays, 2.5, 4 and 12 MeV electrons at a dose of 1.5 kGy. Rate window = 575 s^{-1}.

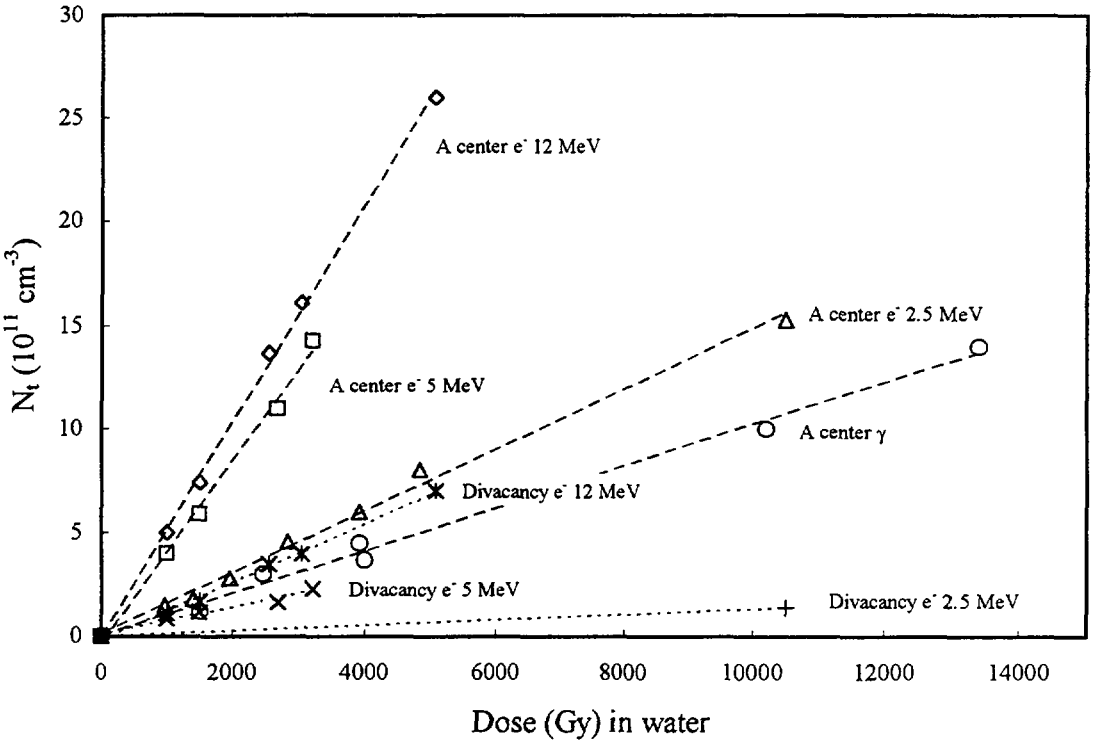

FIG. 5. Plot of concentration of A centre and divacancy vs. dose from irradiated transistors.

not lost during retrieval process). Moreover dose can be ascertained within minutes after irradiation with an inexpensive support equipment. All that brings us to conclude that such device may be a suitable dosimeter for the day-to-day monitoring of radiation process and its possible use should be taken into consideration. Particularly for 12 MeV electron irradiation the behaviour of the transistors is good; the spread of $\Delta(1/T)$ values is $\leq$ 10% for doses up to 100 Gy while it goes down to 3-4 % for the dose range 0.15-20 kGy.

The silicon devices are made from a mixture of plastic, copper and silicon, and it is difficult to evaluate their radiation absorption characteristics. The small size of the devices relative to the range of the secondary electrons makes the mass collision stopping power the most important parameter, and the ratio of mass collision stopping powers is not changing much with energy, but below 1-2 MeV the ratios differ significantly. If the devices are calibrated and used in radiation fields with significant differences in radiation energy spectra, differences in response may be expected. Anyway the results obtained by placing four sets of three transistors inside the product boxes together with ampoules containing ECB dosimeter, and irradiated with γ rays at doses from 5 kGy up to 26 kGy (Fig. 2), during a production run, do not show any significant difference in their response with respect to the transistors irradiated in gamma-cells.

ACKNOWLEDGEMENT

The authors are indebted to Dr. K. Mehta and Mr. R. Girzikowsky, Dosimetry and Medical Radiation Physics Section, IAEA, Vienna, for the γ-irradiations done in Seibersdorf, to Dr. W. McLaughlin for the γ-irradiations done at NIST, to Dr. F. Kuntz and Dr. A. Strasser, AERIAL, for carrying out irradiations of transistors with 2.5 MeV accelerator in Strasbourg and to the LINAC staff (Ing. A. Martelli, A. Monti and G. Mancini) of the FRAE Institute for their valuable technical assistance.

REFERENCES

[1] RIKNER, G., GRUSELL, E., Phys. Med. Biol. **32** (1987) 1109-1107 and references therein.
[2] For more information see: a) SCHARF, K., Health Phys. **13** (1967) 575-586; b) MULLER, A.C., "The "n" on "p" solar-cell dose-rate meter", Manual on Radiation Dosimetry (HOLM N.W., BERRY R.J., Eds), Marcel Dekker, New York (1970) 423-427; c) OSVAY, M., *et al.*, "Silicon detectors for measurement of high exposure rate gamma rays", Biomedical Dosimetry, STI/PUB/401, IAEA, Vienna (1975) 623-632.
[3] MULLER, A.C., "The "p" on "n" solar cell integrating dosimeter", Manual on Radiation Dosimetry (HOLM N.W., BERRY R.J., Eds), Marcel Dekker, New York (1970) 429-433.
[4] HARTSHORN, A., *et al.*, "Absorbed dose mapping in self-shielded irradiators using direct reading MOSFET dosimeters", (Proc. of the Health Physics Society), Annual Meeting, Boston, July 1995.
[5] GRÜNEWALD, T., RUDOLF, M., Food Irradiation Newsletter, FAO/IAEA **11** (1987) 42-47.
[6] EHLERMANN, D.A.E., "Dose distributions and methods for its determination in bulk particulate food materials", Health Impact, Identification and Dosimetry of Irradiated Foods, Report of WHO Working Group, (BÖGL, K.W., REGULLA, D.F., SUESS, M.J. Eds), ISH-Heft 125, Institut fur Strahlenhygiene des Bundesgesundheitsamt, Neuherberg (1988) 415-419.
[7] FUOCHI, P.G., Radiat. Phys. Chem. **44** (1994) 431-440.
[8] BIELLE-DASPET, D., Solid State Electron. **16** (1973) 1103-1123.
[9] MILLER, G. L., *et al.*, Ann. Rev. Mater. Sci. 7 (1977) 377-448.
[10] GHEZZI, C., *et al.*, Material Science Forum Vol. 10-12 (1986) 1213-1218.
[11] ARCORIA, G., *et al.*, Radiat. Phys. Chem. **42** (1993) 1015-1018.
[12] BARBERIS, L., *et al.*, Radiat. Phys. Chem. **26** (1985) 165-172.

DEVELOPMENT OF OSCILLOMETRIC, FLUORIMETRIC AND PHOTOMETRIC ANALYSES APPLIED TO DOSE CONTROL IN RADIATION PROCESSING

I. SLEZSÁK
Z. Bay Applied Research Foundation,
Budapest, Hungary

A. KOVÁCS
Institute of Isotopes and Surface Chemistry, Hungarian Academy of Sciences,
Budapest, Hungary

W.L. McLAUGHLIN
National Institute of Standards and Technology,
Gaithersburg, Maryland,
United States of America

S.D. MILLER
Sunna Systems Corporation,
Richland, Washington,
United States of America

Abstract

The high-frequency conductivity method (oscillometry) has been applied for absorbed dose determination by measuring irradiated dosimeter solution. In order to improve the oscillometric analysis a new digital, tuneable and programmable oscillometric reader capable of measuring absorbed doses in the range of 1 - 300 kGy has been developed recently. Fluorimetry is a rarely used method to measure high absorbed doses in radiation processing. Both organic and inorganic solid or liquid phase compounds can be applied by measuring the optically stimulated luminescence (OSL) of gamma- or electron-irradiated systems, which can be a reproducible function of absorbed dose. A novel programmable fluorimetric reader has been developed to measure the radiation-induced OSL signal of a recently developed polymeric film containing a microcrystalline dispersion of an inorganic fluor (SUNNA film). To determine absorbed dose, the irradiated dosimeter film is excited with a pulsed blue light beam at 450 nm, while the resulting Stokes-shifted emission is measured at 670 nm. After suitable calibration, the OSL signals of different dosimeter samples are measured and the absorbed dose is calculated and stored in the memory of the reader. Photometry is a widely used analytical method for absorbed dose measurements in radiation technologies, although the measurement of light reflected from the gamma- or electron-irradiated label for a suitable light source is not an accepted method so far. A hand-held reflectometric readout system has recently been developed to measure light reflected from potential dosimetric labels in the wavelength range of 400-700 nm. The instrument consists of a handset and a display unit.

1. INTRODUCTION

Quality assurance in radiation processing is achieved by carefully applying characterized dosimetry systems and procedures. In order to improve dosimetry for quality assurance of different types of radiation processes both the development of new systems as well as the improvement of the existing ones are of basic significance. In order to measure the different types of irradiated dosimeter systems, various analytical evaluation methods have been established during the past decades. Three of the existing methods, i.e. oscillometry, fluorimetry and photometry, will be discussed in the paper with respect to their technical development leading to more simple determination of absorbed dose when applying well-established dosimetry systems.

Oscillometry is an electroanalytical method of conductivity measurements, when high frequency alternating current is applied to measure or to follow changes in the composition of chemical systems [1]. Originally it has been developed to evaluate the irradiated ethanol-monochlorobenzene dosimeter solution in the dose range of 1 - 50 kGy. Recently it has been shown that the method is also applicable for the evaluation of the irradiated aqueous alanine solution in the same dose range.

Fluorimetry can be applied for dosimetry purposes due to its significant sensitivity. The method is based on the measurement of the fluorescent light; when a molecule, excited by UV or visible light, emits part of its energy in the form of light. The intensity of the fluorescent light, which is related to the concentration of the fluorescent compound e.g. formed due to ionizing radiation, can be a measure of absorbed dose [2,3].

Photometry is one of the most frequently applied analytical method in absorbed dose determination measuring in most cases the optical density of the irradiated dosimeters. The measurement of the light reflected from the irradiated dosimeter has received attention only recently due to increased interest of measuring dose of irradiated food commodities at quarantine locations. This approach requires simple, quick, easy to evaluate routine dosimeters with non-destructive analysis to be carried out on spot by regulatory inspectors e.g. at importing stations.

2. EXPERIMENTAL

The new oscillometric reader (discussed later) was tested with the ethanol-monochlorobenzene dosimeter solution, which was prepared and used as described elsewhere [1]. The solution was sealed both into 1-ml and 2-ml ampoules. Comparative measurements were done with the previous instrument, the Radelkis type analogue oscillotitrator.

The new fluorimeter was designed for the measurements of the Sunna dosimeter film, which was produced by Sunna Systems, Inc. It is an OSL dosimeter consisting of LiF as microcrystalline phosphor suspended uniformly in a polymer material. The irradiated film is excited with light at 450 nm and the emitted light is measured at around 650 nm.

The dosimeter systems used for the testing of the reflectometric instrument involved the hexahydroxyethyl-pararosanilin-cyanide containing FWT radiochromic dye film produced by Far West Company Ltd., Goleta, USA and the nitro-blue tetrazolium salt containing polymer based film produced in the Institute of Isotope and Surface Chemistry of the Chemical Research Center, Budapest, Hungary.

The dosimeters used for testing the new analytical instruments were irradiated with the pilot scale ^{60}Co gamma irradiation facility (3 PBq) of the Institute of Isotopes Co. Ltd. (Budapest, Hungary). The irradiations were performed within the source cage of the irradiator at a position where the dose rate was 18 kGy h^{-1}. The dosimeters were placed within a perspex holder designed for calibration irradiation.

3. RESULTS AND DISCUSSION

3.1. Oscillometric studies

When oscillometry is applied to measure changes in the composition of chemical systems, the ampoule containing the solution under test is placed - in case of capacitive cell - between the plates of a capacitor of an oscillator. As the main properties (for example, specific conductance and dielectric constant) of the solution change due to the change of its composition, the characteristics of the oscillator (such as plate current and voltage, grid current and voltage, frequency) also change since the resistance and/or capacitance of the circuit are altered. The main advantage of the method is that the electrodes are not in direct contact with the solution, i.e. the analysis can be carried out in sealed ampoules, which makes possible the quick, repeatable, non-destructive routine dose evaluation at any time after irradiation.

The development of the new oscillometric reader was based on the requirement of designing a digital, programmable, tuneable, microcomputer-controlled routine instrument with a built in curve fitting software, which is capable of evaluating e.g. ECB dosimeters irradiated in a wide dose range. To achieve this purpose, first the control of the working frequency of the instrument was investigated in a wide frequency range (100 kHz - 500 MHz) in order to characterise and to find the optimal measurement conditions. The resonance frequency was measured using an oscillometric capacity flow cell and a HP 4195 A impedance-meter.

The new oscillometric reader also employs a capacitive cell (like the previous oscillotitrator) when the solution under test is made part of the dielectric medium of the capacitor in the circuit. The impedance of the capacitor is dependent on the conductivity and the dielectric constant of the solution, and through measuring its change the variation of the composition of the solution - produced by irradiation - is followed. With respect to the highly sensitive part of the frequency curve of the ECB solution, the frequency of the oscillator of the new oscillometric reader was chosen as 85 MHz. Since the composition (i.e. the conductance) of the dosimeter solution varies due to irradiation, the amplitude of the tuned oscillator changes too, i.e. with increasing conductivity (increasing dose) the amplitude decreases.

The new reader contains a precise microcomputer-based signal processor, a real time clock, an alphanumeric display, EEPROMs for data storage and remote control output. By changing the ampoule holder, dosimeter solutions filled into 1-ml, 2-ml and 5-ml glass ampoules can be measured. During measurement, the oscillometric response of a given dosimeter is shown in mV units, which can be related to absorbed dose by means of a calibration function. This function is entered into the memory of the reader prior to the measurements by using a set of calibrated dosimeter ampoules, which had been irradiated previously to a set of absorbed doses covering the dose range of interest in a calibrated gamma radiation source. The calibration function (a third order polynomial curve) is then stored in the software of the reader. This function is used to evaluate the dosimeters irradiated to unknown doses after having measured their oscillometric response.

So far, the ECB dosimeter solution has been tested with the new oscillometric reader and it was found that dosimeters irradiated in the dose range of 1 - 300 kGy can be evaluated. As an example, Fig. 1 shows the calibration curve taken in the dose range of 10 - 60 kGy.

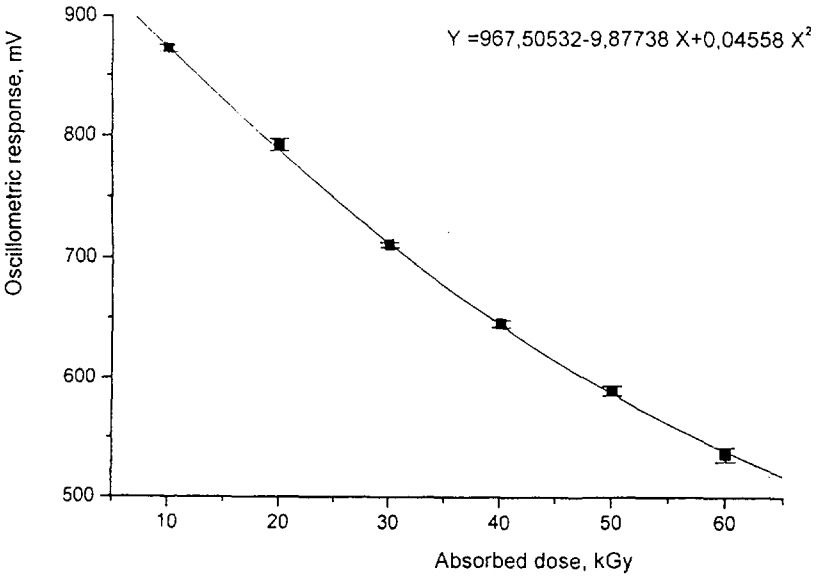

FIG. 1. Oscillometric response of the irradiated ECB dosimeters in the 10 - 60 kGy dose range.

Similar to the effect of thickness on the precision of dose evaluation for some types of dosimeters, the diameter of the ECB ampoule has to be controlled for oscillometric evaluation. The diameter dependence of the dosimeter with respect to the diameter of the calibration ampoules was also determined and the necessary correction factors established in order to achieve the required precision (±5 % at 1σ).

The introduction of the new digital, programmable oscillometric reader makes possible the quick, reliable and repeatable routine dose evaluation of the irradiated ECB and alanine dosimeter solutions.

3.2. Fluorimetric studies

Certain radiation sensitive compounds give fluorescent light (optically stimulated luminescence, OSL) after irradiation by ionizing radiation, when stimulated by UV or visible light. This phenomenon can be utilized for dosimetry purposes, when there is a suitable shift between the excitation and the emission wavelengths. This phenomenon was observed for certain organic and inorganic compounds.

The recent development of a new system, i.e. the imbedding of an inorganic fluor in a plastic matrix (the Sunna dosimeter), required the evolution of a simple, table-top fluorimeter for the evaluation and dose determination of the irradiated Sunna dosimeters. The fluorimeter type FR-2141 with a simple sample holder, precise real-time curve fitting software and a remote control function has been designed and manufactured by Sensolab Ltd. in Göd, Hungary. The 1.0 cm x 3.0 cm Sunna dosimeter can be inserted into a hinged holder of the fluorimeter to measure the OSL signal. The OSL readout of the irradiated dosimeter is achieved by exciting the fluor with a narrow light band centered at 450 nm. The emitted light (E in mV units) is measured at 670 nm. This OSL value is then related to the absorbed dose by means of the calibration function previously entered into the reader memory. Since the microcomputer-based processor and the software are very similar to the ones used in the oscillometric reader described above, the calibration and dose evaluation procedure for the irradiated Sunna dosimeters are also similar to it.

The dose response of the net OSL signal for the Sunna type dosimeters is shown in Fig. 2.

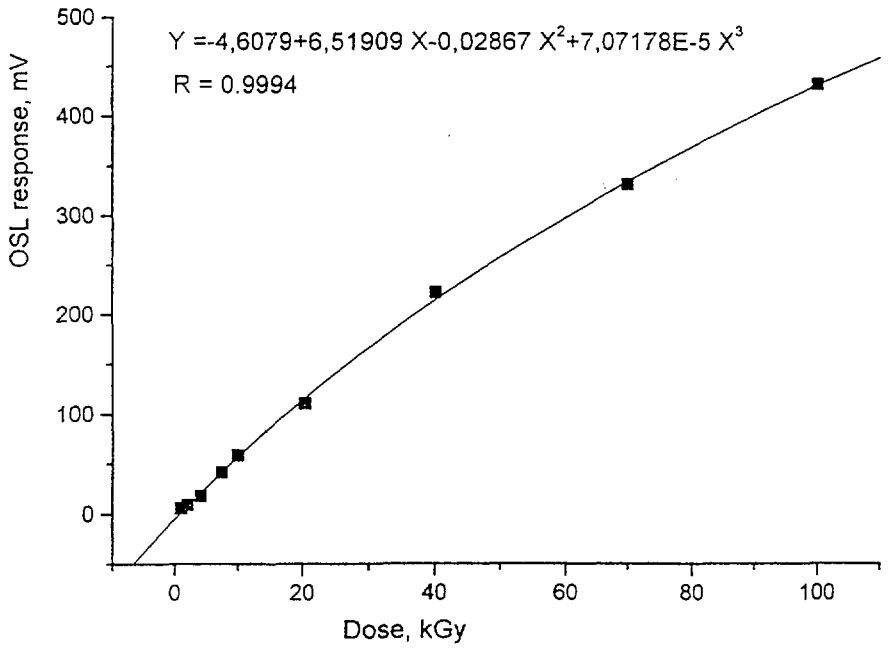

FIG. 2. Dose response of the Sunna dosimeter film in the 1 - 100 kGy dose range.

Due to the high sensitivity of the fluorimetric analytical method itself as well as that of the Sunna dosimeter and the fluorimetric reader developed recently, the irradiated dosimeters can be evaluated in the dose range of 0.005 - 100 kGy (±5 % at 1σ). However, due to the recent observations concerning the irradiation-temperature dependence of the presently available Sunna dosimeter films, the fluorimetric evaluation is suitable for doses only below 5 kGy; while at higher doses, spectrophotometric evaluation is more appropriate.

Taking into account the present development of the dosimeters and the new fluorimetric reader, the system seems to be capable for routine dose determination in various fields of radiation processing and environmental applications.

3.3. Photometric studies

To address the present need of a simple, routine reflectometric readers to evaluate irradiated dosimetric labels, our guiding principle was to develop a hand-held reflectometric instrument capable of field applications. The aim was also to develop such a system, that is capable of evaluating different types of labels (i.e. different colours) irradiated in different dose ranges.

The instrument developed for the purpose consists of two different parts, i.e. the handset and the display unit. During measurement the label is lit with a high intensity light source (laser diode or LED) and a silicon PIN photo-detector located in the handset is used to measure the intensity of the light reflected from the dosimetric label. The sensitivity of the detector is matched to the visible range. Different handsets with different light sources (red laser and yellow, green and red LEDs) are available for the different types of labels to be evaluated.

The display unit contains the intensity stability circuit for the light source, the current/voltage converter for the detector, filters and some amplifiers. The AD converter for the display unit is also located here. The instrument is battery powered and the microcontroller-based calibrating method is under development.

To test the instrument, different types of dosimeters (irradiated in the dose range of 0.1 - 30 kGy) were used. The response curve obtained with the FWT film (produced at Far West Technology, Goleta, USA) irradiated in the dose range of 1-30 kGy is shown in Fig. 3. A linear response was also observed for other films. It is important to mention that labels irradiated in the dose range below 1 kGy can also be evaluated according to our investigations.

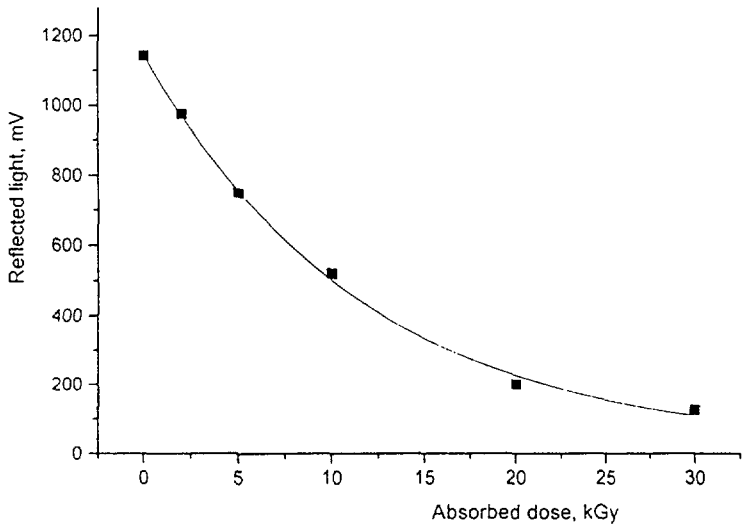

Fig. 3. Dose response of the light intensity reflected from irradiated FWT radiochromic dye film

Taking into account the present achievements and observations the system is under further test and development according to specific requirements.

REFERENCES

[1] AMERICAN SOCIETY FOR TESTING AND MATERIAL, Standard Practice for the Use of the Ethanol-Chlorobenzene Dosimeter System, ASTM Standard E 1538, Annual Book of ASTM Standards, **12.02**, ASTM, Philadelphia, USA (1993).

[2] COLLINS, A.K., MAKRIGIORGOS, G.M., SVENSSON, G.K., Coumarin Chemical Dosimeter for Radiation Therapy, Med. Phys. **21** (11), (1994), 1741-1747.

[3] REGULLA, D.F., Lithium Fluoride Dosimetry Based on Radiophotoluminescence, Health Physics, **22**, (1972), 491-496.

INFLUENCE QUANTITIES IN DOSIMETRY

(Session 4)

Chairperson

H. FARRAR IV
United States of America

Invited Paper

VARIATIONS OF INFLUENCE QUANTITIES IN INDUSTRIAL IRRADIATORS AND THEIR EFFECT ON DOSIMETRY PERFORMANCE

R.D.H. CHU
MDS Nordion,
Kanata, Ontario,
Canada

Abstract

Many environmental factors, including irradiation temperature, post-irradiation storage temperature, dose rate, relative humidity, oxygen content and the energy spectrum may affect the response of dosimetry systems used in industrial radiation processing. Although the effects of individual influence quantities have been extensively studied, the variations of these influence quantities in production irradiators and the complex relationships between the effects of different influence quantities make it difficult to assess the overall effect on the measurement uncertainty. In the development of new dosimetry systems it is important to know the effect of each influence quantity and developers of new dosimetry systems should perform studies over a wide range of irradiation conditions. Analysis parameters and manufacturing specifications should be chosen to minimize the effect of influence quantities in the environments where the dosimeters will be used. Because of possible relationships between different influence quantities, care must be taken to ensure that the response function determined in the calibration of the dosimetry system is applicable for the conditions in which the dosimeters will be used. Reference standard dosimetry systems which have been thoroughly studied and have known relationships between dose response and influence quantities should be used to verify the calibration of routine dosimetry systems under the actual conditions of use. Better understanding of the variations in influence quantities in industrial irradiators may be obtained by modeling or direct measurements and may provide improvements in the calibration of routine dosimetry systems and reduction of the overall measurement uncertainty.

1. INTRODUCTION

Industrial radiation processing performed using ^{60}Co radionuclide sources or machine sources of electrons or bremsstrahlung rely on accurate absorbed dose measurements for both establishing the required processing parameters and for confirming that the specified absorbed dose requirements are met. Accurate absorbed dose measurements are especially needed for highly regulated industries such as the sterilization of medical products and the irradiation of food. Absorbed dose measurements are required during the commissioning of an irradiation facility, following facility modifications and during the process qualification of different products. Dose mapping performed during the process qualification determines the required processing parameters to meet the specified minimum and maximum dose levels. Routine monitoring using commercial routine dosimetry systems are then performed to ensure that the process is under control and that the specified absorbed dose requirements are met.

In 1974, Chu and Antoniades [1] described differences found between readings from chemical and plastic dosimeters in irradiation plants. Calculated dose rates were given for the different irradiation positions in a typical tote box irradiator and it was suggested that these dose rate variations and the variation of other processing parameters may cause errors in the doses measured by different dosimeters. It was recommended that routine plastic dosimeters be irradiated together with chemical dosimeters in the production irradiator. Different results were found for different batches of the same

type of dosimeter, so results obtained for one batch could not automatically be assumed to be applicable for the next batch. Batch-to-batch differences were especially noticed for injection-moulded cylinders of red-dyed polymethylmethacrylate supplied as routine dosimeters. For these injection-moulded dosimeters, in-plant calibration against a reference standard dosimeter was found to be a requirement.

To ensure that the dosimetry performed provides correct absorbed dose values, the effects of external influence quantities on the response of the dosimeters should be thoroughly studied. Care should be taken to ensure that dosimeters calibrated under one set of irradiation conditions provide the correct absorbed dose value when used for measurements in the different irradiation conditions in the production irradiator.

2. INFLUENCE QUANTITIES

Influence quantities such as the irradiation temperature, storage temperature, dose rates, relative humidity, oxygen content and energy spectrum may have significant effects on the response of some commercial dosimetry systems used for industrial irradiation processing. Many studies have been performed on the effect of these influence quantities under controlled conditions [2-12]. The performance of these studies is encouraged since the data provide an indication of the possible magnitude of errors from the effects of influence quantities and may provide insight into ways to minimize these effects. However, these studies are limited in determining the actual combined effects experienced in the routine operation of industrial irradiation facilities and tests should also be conducted in the industrial irradiators where the dosimeters will be used.

The response of most reference standard and routine dosimetry systems is affected by the irradiation temperature. Many liquid chemical reference standard dosimeters, including the Fricke, ceric-cerous, and dichromate dosimeters, have small negative temperature coefficients. The alanine-EPR dosimeter supplied as a transfer standard dosimeter by several calibration laboratories has a small positive temperature coefficient. When these dosimeters are used for measurements where the irradiation temperature is not constant, the average temperature must be estimated and a temperature correction factor applied. The ethanol-chlorobenzene dosimeter is the only reference standard dosimeter which has a response which is independent of the temperature for the temperature ranges used for radiation processing [13].

The response of commercial routine dosimeters may be affected not only by the irradiation temperature but also by the post-irradiation storage temperature. The radiation-induced response, such as formation of colour centres in plastics and films used as routine dosimeters, may depend on many factors related to the production of the dosimeter material. The response may depend on variables such as the content of dye, matrix material, plasticizer, oxygen and water. Because of the effects of small differences in the manufacturing parameters, studies performed for one batch of dosimeters may not be directly applicable to other batches of the same dosimeter. The radiation-induced changes may be unstable and may continue after the completion of the irradiation. There may be either an increase or decrease in the measured response and the rate of this change may be influenced by the storage temperature..

The response of commercial plastic and film routine dosimeters may depend on the dose rate. Dose rate effects related to oxygen depletion in the dosimeter material may occur at high dose rates and may indicate differences in the response when the dosimeters are irradiated with electrons or gamma rays. At lower dose rates experienced in ^{60}Co gamma irradiators with small installed activities or in the outer passes of multipass irradiators there may be another dose rate effect related to the slow diffusion of oxygen into the dosimeter. This effect will depend on the water and oxygen content of the dosimeter and may change with the relative humidity of the environment where the dosimeters are stored or used. For many plastics and films, water and oxygen content are critical parameters and may need to be controlled. Variations in water content may result in differences in the dose response functions or

changes in dose rate dependence or post-irradiation stability. Optimization of the performance may require the conditioning of the dosimeters to known water content and use of hermetically sealed packages. Use of hermetically-sealed packages requires very tight quality control on the package integrity since pin-hole leaks can result in changes in water and oxygen content and result in differences in the dosimeter response.

Dosimeters may be sensitive to exposure to light, especially to wavelengths in the ultraviolet region, and require the use of light-tight packaging for storage and use. Some dosimeters will respond to short exposures to ultraviolet radiation and may require ultraviolet absorbing filters in all areas where the dosimeters are handled outside of their protective packages.

The response of some dosimeters may be affected by the energy spectrum of the degraded gamma photons. For dosimeters with high atomic-number components, the difference in the energy absorbed by the dosimeter and by a reference material such as water can be estimated if the energy spectrum is known [14]. Most plastic dosimeters are close to water in terms of effective atomic number, but the complexity of the radiation-induced interactions resulting in the measured response makes it difficult to assess the effect of the degraded energy spectrum.

The irradiation geometry, including the orientation of the dosimeter relative to the incident radiation and dose gradients or attenuation through the volume of the dosimeter, may also have some effect on the dosimeter response. These factors are not normally considered in studies of influence quantities but may nevertheless have a significant effect on the accuracy of the dosimeter reading.

3. INFLUENCE QUANTITIES IN INDUSTRIAL IRRADIATORS

Product processed in ^{60}Co industrial gamma irradiators usually travel around a centrally located source in a complex pattern chosen to provide a uniform dose to all parts of the product and to maximize the gamma energy absorbed. Because of this complex motion, the total dose may be delivered at widely varying dose rates. In many ^{60}Co gamma irradiators the product moves around a centrally located source in a stepwise motion. In this type of "shuffle-dwell" irradiator, the total dose received by different parts of the process load is the sum of the doses received at each irradiation position and the doses received during the transit between positions. At each irradiation position there is a wide variation in the dose rate at different parts of the product. As a result, the dose received as a function of time will vary throughout the product. Some parts of the product are exposed to high dose rates near the beginning of the irradiation time while other parts begin at lower dose rates. At the end of the irradiation cycle, all parts of the product receive approximately the same total dose but the dose as a function of time may differ, resulting in differences in the response of dosimeters located at different parts of the product volume.

Plane parallel row irradiators with vertical source racks can generally be described as source overlap or product overlap. For source overlap designs, the height of the source rack is greater than the height of the process load and product is irradiated without a vertical transfer. To obtain a uniform dose distribution over the height of the process load, source overlap irradiators usually utilize an augmented source activity distribution with higher activity per unit area in areas near the top and bottom of the source rack. The requirement for a high source rack means that the source activity is distributed over a relatively large area. Source overlap irradiators have the simplest product movement with the high dose rates occurring near the middle of the total irradiation time..

For product overlap designs, the product is irradiated in two or move levels with the source activity concentrated at the centre of the irradiation geometry to effectively use the emitted gamma radiation. This product flow pattern may result in large differences in the dose as a function of time between positions near the bottom of the product and positions near the top of the product. The desire to

optimize the radiation utilization efficiency may mean high concentrations of activity in a small area resulting in dose rates in areas adjacent to the source greater than 100 kGy/h.

The temperature rise experienced by the dosimeters used in production irradiators depends on many factors. The total dose and the specific heat of surrounding materials will result in heat input which can be estimated by calculations. However, the actual temperature rise may also be affected by the air flow past the dosimeter. This cooling depends on the design of the room ventilation and the temperature of the room air. Dosimeters located on the outer surfaces of product boxes may have different temperature versus time profiles than those located within the product. If the air entering the irradiator is not air-conditioned, the room temperature can vary between summer and winter. Some products may require irradiation at low temperatures and may require refrigeration or use of insulated totes to maintain the low temperatures during the time the product is in the irradiator.

The response of some plastic and film dosimeters is affected by the time the dosimeter remains at elevated temperatures. For irradiators with many passes, the dosimeters may receive only a small fraction of the total dose in the outer passes. If the room temperature is high, the response of the dosimeters on the product in final outer passes may be affected by time spent at these positions at elevated temperatures.

Batch versus automatic operation may also have some effect. In batch operation, processed product is removed from the irradiator and new product is introduced into the irradiator with the source lowered to the safe storage position. All process loads receive the same total dose but different process loads begin their irradiation in different positions so that dose versus time is different for different process loads. In automatic operation all process loads are irradiated in the same sequence resulting in the same dose versus time relationship.

To reduce the amount of product handling, many irradiators are designed to process the product on pallets. The irradiation of product on pallets often requires different radiation geometries, with dose contributions through the four sides of the product. Pallet irradiator designs range from a simple turntable system with continuous or step-wise rotation or a complex geometry with features like metal attenuators to improve the dose uniformity. Source geometries used for pallet irradiators include cylindrical, hexagonal or planar sources.

The design capacity for the source may vary by two orders of magnitude. Often a plant may begin with only a small fraction of the source capacity and detailed dose mapping may be performed for these conditions. There will be abrupt incremental increases in activity followed by slow steady decreases due to source decay. There may also be changes to the source geometry as the number of source capsules in the source rack increases.

Some irradiators are designed to allow product to re-enter the irradiator so that irradiations may be repeated for a number of dose increments. The product is removed when it has passed through the irradiator for sufficient increments to receive the total dose. The incremental dose feature is a useful feature assisting in the in-plant calibration of dosimeters under actual conditions of use. Dosimeters can be calibrated by placing all dosimeters in a reference position with small dose gradient at the beginning of the first increment and removing some of the dosimeters after each increment.

4. RECOMMENDATIONS FOR TESTING OF NEW DOSIMETRY SYSTEMS

Although the studies of the effects of individual influence quantities may have limited value in determining the overall effect, these studies are definitely required to understand possible sources of errors. Studies of the effects of individual influence quantities performed at irradiation facilities such as the Gammacell 220 cobalt-60 irradiator supplied by MDS Nordion provide useful data. These irradiation facilities provide well-established reproducible dose rates traceable to a national or

international standard and individual influence quantities such as the irradiation temperature can be accurately controlled.

The possible effect of influence quantities should be determined during the early stages of the development of new dosimetry systems. Although it is not possible to determine the effects of all possible factors by studies performed under conditions of constant temperature and dose rate, these initial tests can provide an initial indication of the suitability of the dosimetry system for use in industrial radiation processing These tests can also provide information for optimizing the manufacturing and analysis conditions for the reading of the dosimeters.

Any dosimeter material which may be influenced by water content should be hermetically sealed. Tests of the effect of water content can be performed by conditioning and packaging the dosimeters under conditions of approximately 20%, 55% and 80% relative humidity. Information of the response mechanism may also be obtained by packaging the dosimeters under different atmospheres.

To determine if the varying dose rates in industrial gamma irradiators may affect the dosimeter response, studies should be performed at dose rates near the minimum, maximum and average dose rates expected. Limitations in available dose rates may make this difficult to achieve at calibration facilities and require testing under the variable dose rate conditions in production irradiators. However, testing at dose rates of approximately 1, 10 and 50 kGy/h would provide a quick check to confirm that dose rate effects are small. Fractionation of the total dose over several days will also provide useful information on potential problems if processing is interrupted because of planned or unplanned shutdowns with partially irradiated product in the irradiator. Dose fractionation studies should be performed by giving samples only part of the dose during each irradiation and repeating the irradiations after dosimeters have been stored for a minimum of several hours.

Modeling of the irradiator by use of Point Kernel or Monte Carlo calculations can provide estimates of the dose rates at different irradiation positions. The Monte Carlo calculations can also be used to obtain information on the energy spectrum. Dose rate information can also be obtained by direct measurement of the dose rates. This can be achieved through static measurements, measurements by the irradiation of dosimeters passing through different fractions of the irradiation cycle or through direct real time measurements with the dose rate data transmitted during transit of a detector through the irradiator.

If the dosimetry system is to be used for electron beam irradiators, studies should be performed using an accelerator with dose rates similar to those to be used for industrial processing.

All dosimetry systems should be tested to determine the temperature response over the range of temperatures expected. Tests at 25 °C and 45 °C are recommended if the dosimetry system is to be used for radiation sterilization, and tests at -20 °C and 4 °C if the dosimetry system is to be used for refrigerated or frozen foods.

5. CALIBRATION OF DOSIMETRY SYSTEMS FOR RADIATION PROCESSING

Although the calibration laboratory may attempt to provide irradiation conditions similar to the average conditions in the production irradiator, final confirmation of the performance of the dosimetry system in industrial irradiators should be based on in-plant studies. A full in-plant calibration performed against a reference standard dosimeter is recommended for obtaining the response function for the actual conditions of use. Because of possible differences in the effect of influence quantities with different batches of the same dosimeter, and variations of the processing conditions because of source decay or additions to the source activity, in-plant calibrations should be repeated at regular intervals or whenever there are major changes.

If it is not possible to perform a complete calibration over the entire range of the dosimetry system, verification should be performed by irradiations with reference standard dosimeters over at least three dose values in the intended range of use. Another useful test to confirm the accuracy of the dosimetry system response function is to compare the response when the dosimeters are irradiated for multiple dose increments with the response when the dose is given in a single irradiation. This can be easily performed with batch gamma irradiators or with gamma irradiators with an incremental dose feature. This test can also be easily performed with electron beam accelerators.

6. CONCLUSIONS

Radiation processing dosimetry presents many challenges because of possible effects caused by influence quantities. However, by understanding the conditions in which dosimeters may be expected to provide accurate measurements, tests can be developed which will quickly provide information on the magnitude of some of these effects.

Because of interactions between the effects of different influence quantities, it may not be possible to make corrections for the combined effects of different influence quantities. In-plant calibration performed by irradiations in production irradiators with reference standard dosimeters will provide calibrations minimizing the contribution of the influence quantity on the overall uncertainty. The comparison of dose response for multiple dose increments with that for single irradiations also provide useful information.

REFERENCES

[1] CHU, R., ANTONIADES, M.T., "The use of ceric sulfate and Perspex dosimeters for the calibration of irradiation facilities", Radiosterilization of Medical Products 1974 (Proc. Symp. Bombay, 1974), IAEA STI/PUB/157, IAEA, Vienna (1975) 83-99.

[2] OLEJNIK, T.A., "Red 4034 Perspex dosimeters in industrial radiation sterilization process control", Radiat. Phys. Chem. **14** (1979) 431-447.

[3] LEVINE, H., MCLAUGHLIN, W.L., MILLER, A., "Temperature and humidity effects on the gamma-ray response and stability of plastic and dyed plastic dosimeters", Radiat. Phys. Chem. **14** (1979) 551-574.

[4] BARRETT, J.H., SHARPE, P.H.G., STUART, I.P., An Investigation, Over the Range of Conditions Occurring in Radiation Processing Plants of the Performance of Routine Dosemeters of the Type Based on Polymethylmethacrylate, Part 1, NPL Report RS49, NPL. Teddington, UK (1980).

[5] GEHRINGER, P., ESCHWEILER, H., PROKSCH, E., "Dose-rate and humidity effects on the gamma radiation responses of nylon-base radiochromic film dosimeters", Int. J. Appl. Radiat. Isotopes, **31** (1980) 595-605.

[6] MILLER, A., MCLAUGHLIN, W.L., "Evaluation of radiochromic dye films and other plastic dose meters under radiation processing conditions", High Dose Measurements in Industrial Radiation Processing, Tech. Rep.Series 205, IAEA, Vienna (1981) 119-138.

[7] MCLAUGHLIN, W.L., HUMPHREYS, J.C., RADAK, B.B., MILLER, A., OLEJNIK, T.A., "The gamma-ray response of radiochromic dye films at different absorbed dose rates", Radiat. Phys. Chem. **18** (1981) 987-999.

[8] BARRET, J.H., "Dosimetry with dyed and undyed acrylic plastic", Int. J. Appl. Radiat. Isotopes. **33** (1982) 1177-1182.

[9] MCLAUGHLIN, W.L., CHEN, W., JIA, H., HUMPHREYS, J.C., "Response of radiochromic film dosimeters to gamma rays in different atmospheres", Radiat. Phys. Chem., **25** (1985) 793-805.

[10] WHITTAKER, B., WATTS, M., MELLOR, S., HENEGHAN, M., "A study of some parameters affecting the radiation response and post-irradiation stability of Red 4034 Perspex dosimeters", High-Dose Dosimetry, (Proc. Symp. Vienna 1984), IAEA STI/PUB/671, IAEA, Vienna (1985) 293-305.

[11] MCLAUGHLIN, W.L., HUMPHREYS, J.C., BA, W.-Z., KHAN, H.M., AL-SHEIKHLY, M., CHAPPAS, W.J., "Temperature dependence of radiochromic film dosimeters", High Dose Dosimetry for Radiation Processing, (Proc. Symp. Vienna, 1990) IAEA STI/PUB/846, IAEA, Vienna (1991) 305-316.

[12] AL-SHEIKHLY, M., CHAPPAS, W.J., MCLAUGHLIN, W.L., HUMPHREYS, J.C., "Effects of absorbed dose rate, irradiation temperature and post-irradiation temperature on the gamma ray response of red Perspex dosimeters", High Dose Dosimetry for Radiation Processing, (Proc. Symp. Vienna, 1990) IAEA STI/PUB/846, IAEA, Vienna (1991) 419-434.

[13] STENGER, V., TORDAY, Zs., HORVÁTH, I., FALVI, L., PAPP, Z., "Long term experience in using the ethanol chlorobenzene dosimeter system", High Dose Dosimetry for Radiation Processing, (Proc. Symp. Vienna, 1990) IAEA STI/PUB/846, IAEA, Vienna (1991) 277-288.

[14] MILLER, A., "Calculation of energy dependence of some commonly used dosimeters", High-Dose Dosimetry, (Proc. Symp. Vienna 1984), IAEA STI/PUB/671, IAEA, Vienna (1985) 425-436.

THE INFLUENCE OF DOSE RATE, IRRADIATION TEMPERATURE AND POST-IRRADIATION STORAGE CONDITIONS ON THE RADIATION RESPONSE OF HARWELL AMBER 3042 PMMA DOSIMETERS

M.F. WATTS
Harwell Dosimeters Limited,
Harwell, Didcot, Oxfordshire,
United Kingdom

Abstract

The response of routine dosimeters is not independent of radiation dose rate, and environmental conditions such as humidity and temperature. In Harwell Amber 3042 dosimeters these influences are minimised by careful conditioning, and the use of special packaging material to maintain humidity. This paper describes studies carried out on the influences of irradiation dose rate and temperature, on two batches of dosimeters. Firstly, this paper gives gamma irradiation response data for dose rates of 6.1, 1.3 and 0.5 $Gy \cdot s^{-1}$ with irradiation temperatures of 20, 30, 40 and 50 °C. Dosimeters were irradiated, to doses of 3, 5, 7, 10 and 15 kGy. Secondly, this paper considers irradiation plus post irradiation storage temperatures, at a fixed dose rate of 1.5 $Gy \cdot s^{-1}$. Dosimeters were irradiated, to doses of 10 and 20 kGy; at temperatures of 30, 40 and 50 °C. The dosimeters were stored at these temperatures for 1, 24 and 48 hours before measurement. Results at both of the recommended measurement wavelengths, 603nm and 651nm, are presented. The choice of wavelength is discussed, in order to aid the optimum choice for the conditions prevailing.

1. INTRODUCTION

Several papers have been published about dose rate and temperature effects on Harwell Red 4034 dosimeters, but there have been few corresponding reports relating to Harwell Amber 3042. Glover et al reported some dose rate studies in 1993 [1], and in 1996 Biramontri et al reported extensive studies of the influence of low irradiation temperatures on four types of PMMA dosimeter, including Amber 3042 [2].

Currently there is much interest in the use of Harwell Amber dosimeters, due to developments in the medical product sterilization industry. However, the conditions of use, in terms of dose rate and irradiation temperature, may vary considerably from those used to calibrate the dosimeters under standards laboratory conditions. The previous papers [1,2] have reported on either temperature or dose rate parameters. This paper is a combined study of both parameters. In addition dosimeters may be stored, after irradiation, at temperatures outside the normal recommended range of 20±5 °C. Higher temperatures are due to heating within the irradiation plant, as well as abnormal ambient levels before and after irradiation.

2. EXPERIMENTAL

Following irradiation all dosimeters were measured optically at the recommended measuring wavelengths of 603 nm and 651 nm. Absorbance readings used a Pye Unicam 8800 spectrophotometer. Thickness measurements were made with a digital micrometer. The resulting specific absorbance values of k were combined, to give the mean k_m for each set of four dosimeters.

2.1 Dose rate and irradiation temperature studies

The dose rate and irradiation studies used the Harwell variable irradiation assembly. The dosimeters were irradiated in sets of four, in a copper jacket with a polythene liner. This jacket was maintained at a constant temperature by circulating liquid, provided by a thermostatic bath. This assembly has adjustable ^{60}Co source tube positions, providing a range of known dose rates.

Tables I to IV show the values of k_m obtained at each of the three dose rate positions, at temperatures of 20, 30, 40 and 50 °C. Results for both batches of dosimeters at each measurement wavelength are given. The table also gives the ratios of k_m for the high and low dose rates, to the middle value of 1.3 $Gy \cdot s^{-1}$. This gives an indication of the likely deviation from a typical calibration condition. The tables can be manipulated to give the values of k_m for temperatures of 20, 30, 40 and 50 °C at each dose and dose rate.

The trends of specific absorbance (k_m), normalised to 20 °C and a dose rate of 1.3 $Gy.s^{-1}$, over the dose range 3 to 15 kGy are summarised in Fig. 1. The four graphs show the normalised response at 20, 30, 40 and 50 °C for Harwell Amber dosimeters batch F, at a wavelength of 651 nm.

2.2 Irradiation temperatures and post irradiation studies

The irradiation temperature and post irradiation storage studies used the Harwell calibration irradiation assembly [3]. The dosimeters were irradiated in sets of four, with a dose rate of 1.5 $Gy \cdot s^{-1}$. The five irradiation positions and the storage bath in the lead sample shield, were both thermostatically controlled. This arrangement allowed for temperature control both during and after irradiation. The dosimeters were resealed after each measurement and returned to controlled temperature storage.

TABLE I. THE INFLUENCE OF DOSE RATE ON BATCH D, 651 nm

Values of k_m, cm^{-1} for the dose rates shown						
Temperature °C	Dose kGy	Position 1 6.1 $Gy \cdot s^{-1}$	Ratio 6.1/1.3	Position 3 1.3 $Gy \cdot s^{-1}$	Ratio 0.5/1.3	Position 5 0.5 $Gy \cdot s^{-1}$
20	3	0.830	0.966	0.859	1.009	0.867
20	5	1.303	0.962	1.355	0.983	1.322
20	7	1.745	0.984	1.773	0.998	1.769
20	10	2.323	0.976	2.381	0.989	2.354
20	15	3.061	0.959	3,.192	1.012	3.230
30	3	0.835	0.988	0.845	1.030	0.870
30	5	1.294	0.990	1.307	1.008	1.318
30	7	1.722	1.005	1.714	1.023	1.753
30	10	2.258	0.976	2.313	1.008	2.332
30	15	3.055	0.978	3.124	1.015	3.172
40	3	0.829	0.970	0.855	0.999	0.854
40	5	1.275	0.984	1.296	1.021	1.323
40	7	1.660	0.967	1.716	1.014	1.740
40	10	2.210	0.967	2.286	1.012	2.314
40	15	2.976	0.974	3.057	1.027	3.140
50	3	0.821	0.943	0.871	1.045	0.910
50	5	1.249	0.953	1.310	1.033	1.353
50	7	1.609	0.937	1.717	1.030	1.768
50	10	2.151	0.956	2.251	1.024	2.305
50	15	2.906	0.952	3.052	1.019	3.109

TABLE II. THE INFLUENCE OF DOSE RATE ON BATCH D, 603 nm

Values of k_m, cm^{-1} for the dose rates shown						
Temperature °C	Dose kGy	Position 1 6.1 $Gy \cdot s^{-1}$	Ratio 6.1/1.3	Position 3 1.3 $Gy \cdot s^{-1}$	Ratio 0.5/1.3	Position 5 0.5 $Gy \cdot s^{-1}$
20	3	1.447	0.975	1.484	1.009	1.498
20	5	2.270	0.971	2.339	0.979	2.290
20	7	3.041	0.968	3.141	0.995	3.125
20	10	4.062	0.992	4.094	1.017	4.164
20	15	5.336	0.976	5.467	1.031	5.634
30	3	1.465	0.992	1.477	1.034	1.527
30	5	2.268	0.981	2.312	1.031	2.384
30	7	3.061	1.008	3.038	1.057	3.210
30	10	4.028	0.972	4.144	1.033	4.280
30	15	5.385	0.969	5.556	1.039	5.773
40	3	1.496	0.949	1.577	1.046	1.650
40	5	2.307	0.945	2.440	1.075	2.624
40	7	2.970	0.916	3.241	1.067	3.457
40	10	4.037	0.931	4.334	1.061	4.598
40	15	5.413	0.934	5.797	1.050	6.088
50	3	1.612	0.868	1.857	1.109	2.060
50	5	2.489	0.879	2.832	1.059	2.998
50	7	3.326	0.905	3.677	1.063	3.907
50	10	4.281	0.907	4.719	1.048	4.945
50	15	5.663	0.920	6.155	1.034	6.366

TABLE III. THE INFLUENCE OF DOSE RATE ON BATCH F, 651 nm

Values of k_m, cm^{-1} for the dose rates shown						
Temperature °C	Dose kGy	Position 1 6.1 $Gy \cdot s^{-1}$	Ratio 6.1/1.3	Position 3 1.3 $Gy \cdot s^{-1}$	Ratio 0.5/1.3	Position 5 0.5 $Gy \cdot s^{-1}$
20	3	0.774	0.924	0.838	1.033	0.866
20	5	1.354	0.946	1.432	1.008	1.444
20	7	1.905	0.960	1.985	1.003	1.991
20	10	2.621	0.967	2.710	1.012	2.742
20	15	3.641	0.975	3.736	1.011	3.776
30	3	0.802	0.942	0.851	1.039	0.884
30	5	1.372	0.961	1.428	1.018	1.454
30	7	1.908	0.972	1.962	1.016	1.994
30	10	2.629	0.977	2.690	1.013	2.725
30	15	3.659	0.978	3.743	1.011	3.783
40	3	0.830	0.951	0.873	1.022	0.892
40	5	1.396	0.969	1.440	1.019	1.467
40	7	1.885	0.963	1.958	1.002	1.962
40	10	2.617	0.982	2.664	1.012	2.697
40	15	3.624	0.979	3.702	1.006	3.723
50	3	0.853	0.966	0.883	1.007	0.889
50	5	1.381	0.970	1.423	0.999	1.422
50	7	1.870	0.967	1.934	1.003	1.939
50	10	2.566	0.984	2.608	1.020	2.659
50	15	3.550	0.969	3.664	1.008	3.694

TABLE IV. THE INFLUENCE OF DOSE RATE ON BATCH F, 603 nm

Values of k_m, cm^{-1} for the dose rates shown						
Temperature °C	Dose kGy	Position 1 6.1 $Gy \cdot s^{-1}$	Ratio 6.1/1.3	Position 3 1.3 $Gy \cdot s^{-1}$	Ratio 0.5/1.3	Position 5 0.5 $Gy \cdot s^{-1}$
20	3	1.259	0.933	1.350	1.034	1.396
20	5	2.181	0.947	2.303	1.003	2.310
20	7	3.061	0.957	3.199	1.003	3.208
20	10	4.205	0.974	4.319	1.020	4.407
20	15	5.813	0.982	5.921	1.021	6.048
30	3	1.300	0.944	1.377	1.039	1.431
30	5	2.206	0.961	2.296	1.025	2.353
30	7	3.076	0.975	3.155	1.025	3.235
30	10	4.230	0.975	4.338	1.021	4.427
30	15	5.859	0.973	6.022	1.018	6.128
40	3	1.349	0.947	1.425	1.024	1.459
40	5	2.261	0.963	2.348	1.030	2.418
40	7	3.029	0.944	3.208	1.013	3.249
40	10	4.236	0.968	4.378	1.028	4.501
40	15	5.858	0.962	6.092	1.025	6.244
50	3	1.402	0.951	1.475	1.033	1.524
50	5	2.281	0.944	2.416	1.022	2.470
50	7	3.126	0.946	3.303	1.029	3.400
50	10	4.261	0.950	4.485	1.048	4.702
50	15	5.911	0.934	6.326	1.036	6.553

Table V shows values of k_m measured at increasing temperature, for 1, 24 and 48 hours storage time. The ratio of k_m with respect to 30 °C is also given. For practical reasons the first measurement was made 1 hour after irradiation, and this storage time was assumed to be of little significance.

Table VI gives values of k_m for 1, 24 and 48 hours storage time in relation to temperature. The table also shows the ratio to 1 hour for comparison purposes. Post irradiation storage at elevated temperatures can give much larger changes in response, and should be avoided wherever possible, or corrections made.

3. DISCUSSION

The measurement uncertainty of Harwell Amber dosimeters is quoted as ± 2.5% when applied to specific absorbance values. Therefore, ratios from 0.975 to 1.025 do not indicate significant differences.

3.1 Dose rate and irradiation temperature studies

The results in general terms show the 651 nm wavelength is less affected, by either irradiation dose rate or temperature.

Dose rate effects are smallest at 0.5 $Gy \cdot s^{-1}$ and a measurement wavelength of 651 nm, relative to the medium dose rate of 1.3 $Gy \cdot s^{-1}$; which is in common use for calibrations. This applies to the temperatures from 20 to 50 °C and is true for both batches tested, where the effect was generally less than 3 %. Larger dose rate effects were observed, generally in the region of 3 to 4 % with temperatures of 20 to 40 °C, at the higher dose rate (6.1 $Gy \cdot s^{-1}$); again using a measurement wavelength of 651 nm.

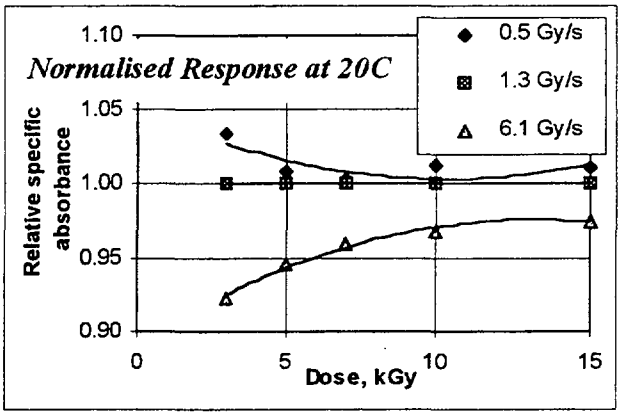

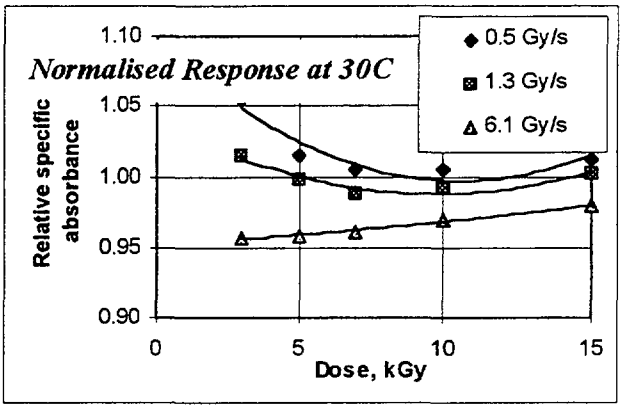

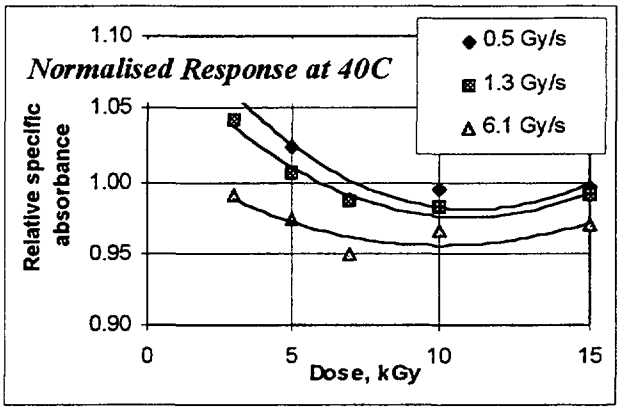

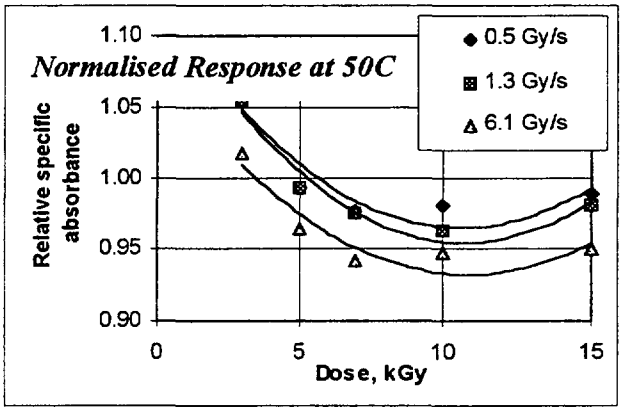

FIG.1 Harwell Amber Dosimeters, batch F_1 Change in the mean specific absorbance with dose rate. Specific absorbance measured at 651 nm, and normalised to the response at 20 ℃ and 1.3 Gy/s

TABLE V. THE INFLUENCE OF IRRADIATION AND STORAGE TEMPERATURE

Batch	Wavelength nm	Storage Time Hours	Irrad/Storage 30°C	Irrad/Storage 40°C	Ratio 40/30	Irrad/Storage 50°C	Ratio 50/30
Irradiation dose 10 kGy, values of k_m, cm^{-1} for the temperatures shown							
D	603	1	4.075	4.321	1.060	4.637	1.138
D	603	24	4.502	4.620	1.026	4.632	1.029
D	603	48	4.549	4.509	0.991	4.515	0.993
D	651	1	2.257	2.168	0.961	2.145	0.950
D	651	24	2.232	2.084	0.934	1.973	0.884
D	651	48	2.206	2.000	0.907	1.937	0.878
F	603	1	4.229	4.347	1.028	4.465	1.056
F	603	24	4.407	4.600	1.044	4.590	1.042
F	603	48	4.427	4.546	1.027	4.258	0.962
F	651	1	2.619	2.597	0.992	2.529	0.966
F	651	24	2.601	2.519	0.968	2.266	0.871
F	651	48	2.569	2.416	0.940	2.023	0.787
Irradiation dose 20 kGy, values of k_m, cm^{-1} for the temperatures shown							
D	603	1	6.588	6.773	1.028	7.099	1.078
D	603	24	6.722	6.667	0.992	6.726	1.001
D	603	48	6.696	6.529	0.975	6.211	0.928
D	651	1	3.663	3.559	0.972	3.567	0.974
D	651	24	3.519	3.260	0.926	3.204	0.910
D	651	48	3.441	3.139	0.912	2.942	0.855
F	603	1	7.276	7.411	1.019	7.589	1.043
F	603	24	7.388	7.297	0.988	6.631	0.898
F	603	48	7.334	7.111	0.970	5.621	0.766
F	651	1	4.502	4.443	0.987	4.325	0.961
F	651	24	4.416	4.112	0.931	3.416	0.774
F	651	48	4.316	3.867	0.896	2.785	0.645

Figure 1 summarises these trends, normalised to 20 °C and 1.3 $Gy.s^{-1}$, for Harwell Amber batch F at a measurement wavelength of 651 nm.

Temperature effects were small, less than 3 % at most dose levels, for Amber batch F at irradiation temperatures 40 °C and below, when measured at 651 nm. Larger temperature effects were observed for Amber D at the 603 nm wavelength. With increasing temperature, usually, measurements at the 603 nm wavelength result in a positive change but the use of 651 nm results in a negative change. For example the ratio 50/20 °C is greater than 1.0 for 603 nm wavelength measurements. This is true for batches D and F. The reverse is also generally true, that this ratio is less than 1.0 at 651 nm. The ratio 50/20 °C is usually smaller in magnitude for the 651 nm wavelength.

3.2 Irradiation temperatures and post irradiation studies

Irradiation temperature effects were relatively small, with less than 3 % change in response, for Amber F between 30 and 40 °C at both dose levels. The results for Amber D were less favourable.
Post irradiation storage at elevated temperatures can give much larger changes in response, and should be avoided wherever possible, or corrections made.

TABLE VI. THE INFLUENCE OF POST IRRADIATION STORAGE TIME

Batch	Wavelength nm	Irrad/Storage Temperature	Storage Time 1 Hour	Storage Time 24 Hours	Ratio 24h/1h	Storage Time 48 Hours	Ratio 48h/1r
Irradiation dose 10 kGy, values of k_m, cm^{-1} for the storage times shown							
D	603	30	4.075	4.502	1.105	4.549	1.116
D	651	30	2.257	2.232	0.989	2.206	0.977
F	603	30	4.229	4.407	1.042	4.427	1.047
F	651	30	2.619	2.601	0.993	2.569	0.981
D	603	40	4.321	4.620	1.069	4.509	1.044
D	651	40	2.168	2.084	0.961	2.000	0.923
F	603	40	4.347	4.600	1.058	4.546	1.046
F	651	40	2.597	2.519	0.970	2.416	0.930
D	603	50	4.637	4.632	0.999	4.515	0.974
D	651	50	2.145	1.973	0.920	1.937	0.903
F	603	50	4.465	4.590	1.028	4.258	0.954
F	651	50	2.529	2.266	0.896	2.023	0.800
Irradiation dose 20 kGy, values of k_m, cm^{-1} for the storage times shown							
D	603	30	6.588	6.722	1.020	6.696	1.016
D	651	30	3.663	3.519	0.961	3.441	0.939
F	603	30	7.276	7.388	1.015	7.334	1.008
F	651	30	4.502	4.416	0.981	4.316	0.959
D	603	40	6.773	6.667	0.984	6.529	0.964
D	651	40	3.559	3.260	0.916	3.139	0.882
F	603	40	7.411	7.297	0.985	7.111	0.960
F	651	40	4.443	4.112	0.926	3.867	0.870
D	603	50	7.099	6.726	0.947	6.211	0.875
D	651	50	3.567	3.204	0.898	2.942	0.825
F	603	50	7.589	6.631	0.874	5.621	0.741
F	651	50	4.325	3.416	0.790	2.785	0.644

4. CONCLUSIONS

Harwell Amber dosimeters are affected by irradiation dose rate. However, with respect to 1.3 $Gy \cdot s^{-1}$ the effects are small and insignificant at the lower dose rate of 0.5 $Gy \cdot s^{-1}$. Given the lower dose range of these dosimeters, they may be used under conditions where dose rates are also lower.

Therefore, the relative insensitivity to low dose rate may be an advantage. Irradiation temperature also affects specific absorbance. Where irradiation temperatures significantly in excess of the calibration value are encountered, a combination of measurements at both the 603 nm and 651 nm wavelengths may give a more precise answer. This can be useful where the exact temperature conditions are unknown.

Post irradiation storage at elevated temperature is a very significant source of error. Prolonged storage for 24 or 48 hours will lead to an under or over estimate of apparent dose, unless the calibration regime makes due allowances. Again in many cases, and where irradiation conditions are unknown, a combination of both wavelength results may give a more precise answer.

These studies reinforce the recommendation that routine dosimeters should be calibrated as close to the conditions of use as possible [1].

REFERENCES

[1] GLOVER, K.M., PLESTED, M.E., WATTS, M.F., and WHITTAKER, B., "A Study of Some Parameters relevant to the Response of Harwell PMMA Dosimeters to Gamma and Electron Irradiation", *Radiat. Phys. Chem.*, **42**, 4-6, pp. 739 -742, 1993.

[2] BIRAMONTRI, S., HANEDA, N., TACHIBANA, H., and KOJIMA, T., "Effect of Low Irradiation Temperature on the Gamma-Ray Response of Dyed and Undyed PMMA Dosimeters", *Radiat. Phys. Chem.*, **48**, 1, pp. 105-109, 1996.

[3] WHITTAKER, B., WATTS, M.F., "The Influence of Ambient Temperature and Time on the Response of Harwell Red PMMA Dosimeters", These proceedings, paper number IAEA-SM-356/51, Vienna 1998.

THE INFLUENCE OF DOSE RATE, IRRADIATION TEMPERATURE AND POST-IRRADIATION STORAGE CONDITIONS ON THE RADIATION RESPONSE OF HARWELL GAMMACHROME YR® PMMA DOSIMETERS

M.F. WATTS
Harwell Dosimeters Limited,
Harwell, Didcot, Oxfordshire,
United Kingdom

Abstract

Routine dosimeters are often influenced by changing dose rates, and also environmental conditions such as humidity and temperature. In Harwell Gammachrome YR® dosimeters these influences are minimised by a carefully controlled conditioning process, and the use of special packaging material to maintain these conditions. This paper describes studies carried out on the influences of irradiation dose rate and temperature on two batches of dosimeters. Firstly, this paper gives gamma irradiation response data for dose rates of 5.5, 1.1 and 0.5 $Gy \cdot s^{-1}$ with irradiation temperatures of -20, 0, 10, 20 and 35 °C. Dosimeters were irradiated to doses of 0.1, 0.5, 1, 2 and 3 kGy. Secondly, this paper considers both, irradiation and post-irradiation storage temperatures, at a fixed dose rate of 1.4 $Gy \cdot s^{-1}$. Dosimeters were irradiated to doses of 0.1 and 3 kGy; at temperatures of 30, 40 or 50°C. The dosimeters were stored at these temperatures for 2, 24 and 48 hours before measurement.

1. INTRODUCTION

Dose rate and temperature during irradiation under plant conditions may vary considerably from those used to calibrate dosimeters. In addition, PMMA dosimeters may be stored after irradiation at temperatures outside the normal recommended range of 20 ± 5°C. Gammachrome YR® dosimeters were developed specifically for in-plant measurement of absorbed dose in the range 0.1 to 3 kGy [1]. Glover *et al.* [2] reported mainly on irradiation dose rate and temperature parameters for Harwell Red and to a lessor extent Harwell Amber dosimeters. Sohrabpour *et al.* [3] and Biramontri *et al.* [4] reported on the temperature characteristics of dosimeters including Gammachrome YR®. Fairand [5] reported trials of Gammachrome YR® dosimeters in an industrial facility. To minimise the possible influence of factors such as dose rate and temperature, the Gammachrome YR® dosimeters were calibrated in the industrial irradiator using alanine reference dosimeters to determine the calibration doses given.

2. EXPERIMENTAL

All dosimeters were measured at the recommended measuring wavelength of 530nm, a minimum of 2 hours after irradiation to allow full colour development. Absorbance readings used a computer controlled Unicam 8755 spectrophotometer. Thickness measurements were made with a digital micrometer, and fed directly to the controlling computer. The resulting specific absorbance values of k were combined to give the mean k_m for each set of four dosimeters.

2.1 Dose rate and irradiation temperature studies

The dose rate and irradiation temperature studies used the Harwell variable Co-60 irradiation assembly. The dosimeters were irradiated in sets of four, in a copper jacket with a polythene liner. This jacket was maintained at a constant temperature by circulating liquid, chosen according to the temperature required, and provided by a thermostatic bath. To ensure that the dosimeters reached the

low temperatures used in this study, liquid was added to the polythene liner to maintain good thermal contact. All temperatures were measured with a thermocouple directly between the dosimeters. This irradiation assembly has adjustable Co-60 source tube positions providing a range of known dose rates.

Tables I and II show the values of k_m obtained at each of the three dose rate positions, with temperatures of -20, 0, 10, 20 and 35 °C. Results are given for both batches 4 and 5. The values of k_m, shown *in italics*, were adjusted to allow for the transit dose of the Co-60 sources. The table also gives the ratios of the high and low dose rates to the middle value of 1.1 $Gy \cdot s^{-1}$. This gives an indication of the likely deviation from a typical calibration condition. Tables I and II can be manipulated to give the values of k_m for temperatures of -20, 0, 10, 20 and 35 °C at each dose and dose rate.

The trends are shown in Figs 1 and 2 with representative graphs for batches 4 and 5. The graphs, for each dose rate, show the 0.1, 1 and 3 kGy dose levels. The whole range of Gammachrome YR® dosimeters is represented.

TABLE I. THE INFLUENCE OF DOSE RATE ON BATCH 4

Temp. °C	Dose kGy	Position 1 5.5 $Gy \cdot s^{-1}$	Ratio 5.5/1.1	Position 3 1.1 $Gy \cdot s^{-1}$	Ratio 0.5/1.1	Position 5 0.5 $Gy \cdot s^{-1}$
-20	0.1	*0.183* [a,b]	1.028	*0.178* [a,b]	0.999	*0.178* [a,b]
-20	0.5	0.506	1.017	0.498	1.001	0.499
-20	1	0.846	1.007	0.841	0.988	0.831
-20	2	1.297	1.014	1.279	0.973	1.245
-20	3	1.613	1.006	1.603	0.997	1.599
0	0.1	*0.177*	0.998	*0.178*	1.002	*0.178*
0	0.5	0.499	1.019	0.490	0.985	0.482
0	1	0.829	1.042	0.795	0.972	0.773
0	2	1.196	1.014	1.179	0.979	1.154
0	3	1.534	0.975	1.574	0.952	1.498
10	0.1	*0.184*	1.041	*0.177*	0.987	*0.174*
10	0.5	0.494	1.011	0.489	1.008	0.493
10	1	0.804	1.066	0.754	0.980	0.739
10	2	1.193	1.041	1.147	0.993	1.139
10	3	1.520	1.024	1.484	0.980	1.455
20	0.1	*0.177*	0.999	*0.177*	1.012	*0.179*
20	0.5	0.484	1.010	0.479	0.973	0.466
20	1	0.747	1.070	0.698	0.965	0.674
20	2	1.111	1.018	1.091	0.982	1.071
20	3	1.437	1.014	1.417	0.988	1.400
35	0.1	*0.180*	0.992	*0.181*	0.986	*0.178*
35	0.5	0.467	1.069	0.437	0.973	0.425
35	1	0.697	1.068	0.652	0.950	0.620
35	2	1.045	1.015	1.030	0.974	1.003
35	3	1.372	1.000	1.373	0.977	1.342

[a] Values of k_m, mm^{-1} for the dose rates shown

[b] 0.1 kGy specific absorbance results (*shown in italics*) are calculated

TABLE II. THE INFLUENCE OF DOSE RATE ON BATCH 5

Temp. °C	Dose kGy	Position 1 5.5 Gy·s^{-1}	Ratio 5.5/1.1	Position 3 1.1 Gy·s^{-1}	Ratio 0.5/1.1	Position 5 0.5 Gy·s^{-1}
-20	0.1	*0.172* [a,b]	0.983	*0.175* [a,b]	0.971	*0.170* [a,b]
-20	0.5	0.507	1.022	0.497	1.008	0.500
-20	1	0.852	1.014	0.840	1.014	0.852
-20	2	1.345	1.016	1.324	0.984	1.302
-20	3	1.692	1.010	1.675	0.993	1.664
0	0.1	*0.170*	0.971	*0.175*	0.952	*0.167*
0	0.5	0.489	0.986	0.496	0.986	0.489
0	1	0.867	1.057	0.820	0.977	0.801
0	2	1.232	0.996	1.237	0.956	1.183
0	3	1.594	1.036	1.538	1.017	1.564
10	0.1	*0.177*	1.051	*0.169*	1.002	*0.169*
10	0.5	0.495	0.986	0.502	0.973	0.489
10	1	0.817	1.056	0.774	0.964	0.746
10	2	1.252	1.042	1.202	0.983	1.182
10	3	1.577	1.020	1.545	0.982	1.517
20	0.1	*0.175*	1.025	*0.170*	1.004	*0.171*
20	0.5	0.500	1.020	0.491	0.981	0.481
20	1	0.788	1.096	0.718	0.990	0.711
20	2	1.140	1.017	1.121	0.991	1.111
20	3	1.508	1.018	1.482	0.966	1.431
35	0.1	*0.173*	0.977	*0.177*	0.951	*0.169*
35	0.5	0.484	1.080	0.448	0.939	0.421
35	1	0.726	1.077	0.674	0.976	0.658
35	2	1.116	1.048	1.065	0.993	1.058
35	3	1.425	1.003	1.421	0.968	1.375

[a] Values of k_m , mm^{-1} for the dose rates shown
[b] 0.1 kGy specific absorbance results (*shown in italics*) are calculated

2.2 Irradiation temperature and post irradiation storage

The irradiation temperature and post-irradiation storage studies used the Harwell calibration irradiation assembly [6]. The dosimeters were irradiated in sets of four with a dose rate of 1.4 Gy·s^{-1}. The five irradiation positions and the storage bath in the lead sample shield were both thermostatically controlled. This arrangement, allowed for temperature control both during and after irradiation. The dosimeters were resealed after measurement and returned to temperature controlled storage.

The sensitivity of Gammachrome YR® dosimeters generally decreased with increasing temperature, as found above. However, over the 30 to 50 °C range the effect was larger at the 0.1 kGy than the 3 kGy dose level, not as expected. The apparent inconsistency may be due to the storage for 2 hours at elevated temperatures before measurement.

Table III shows values of k_m measured at increasing temperature, for 2, 24 and 48 hours storage time. The ratio of k_m with respect to 30°C is also given for comparison purposes. Gammachrome YR® dosimeters need 2 hours at room temperature before measurement, to allow full colour development.

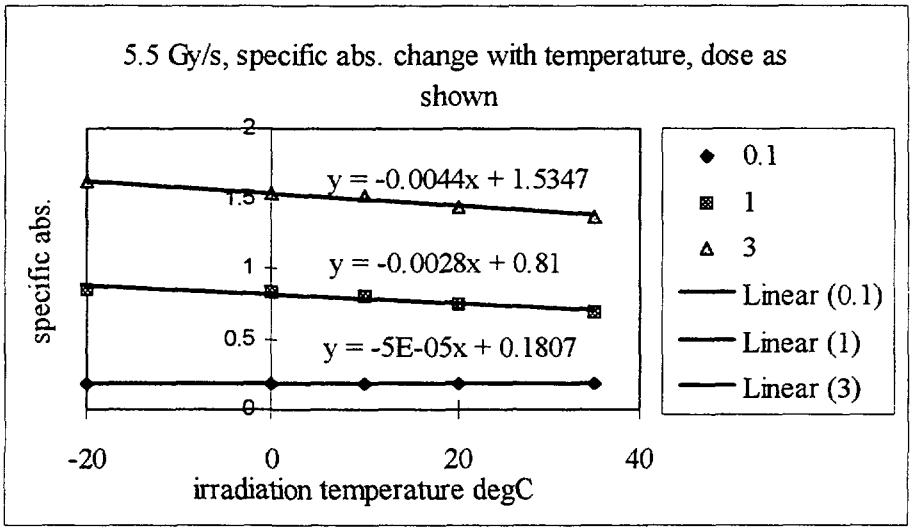

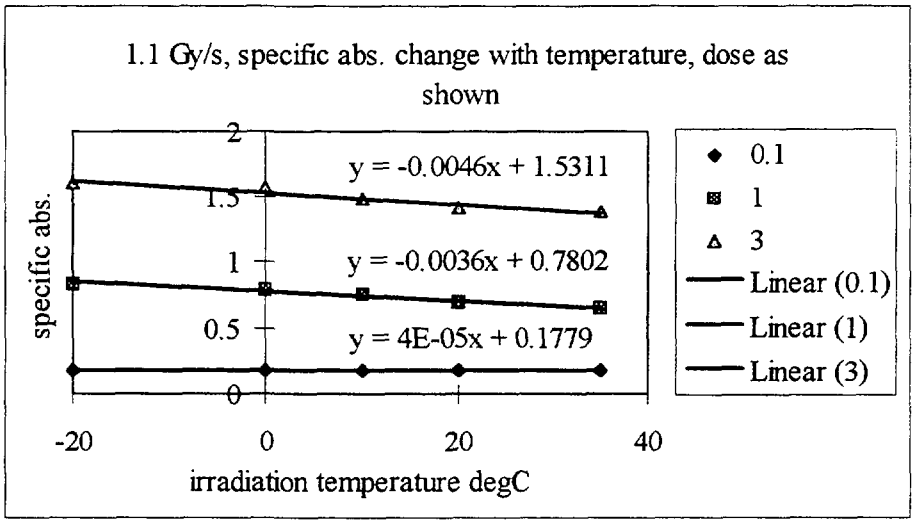

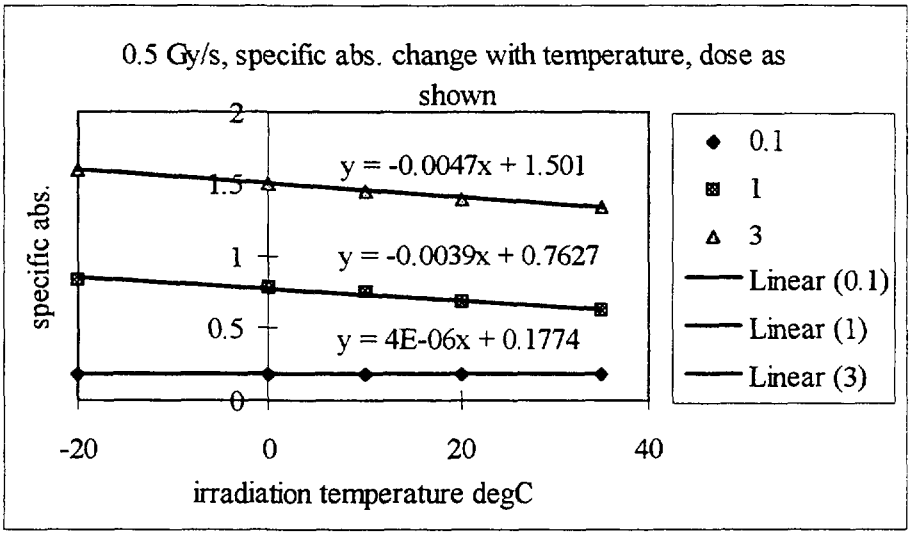

FIG. 1. Gammachrome YR® batch 4 change in k_m with increasing irradiation temperature

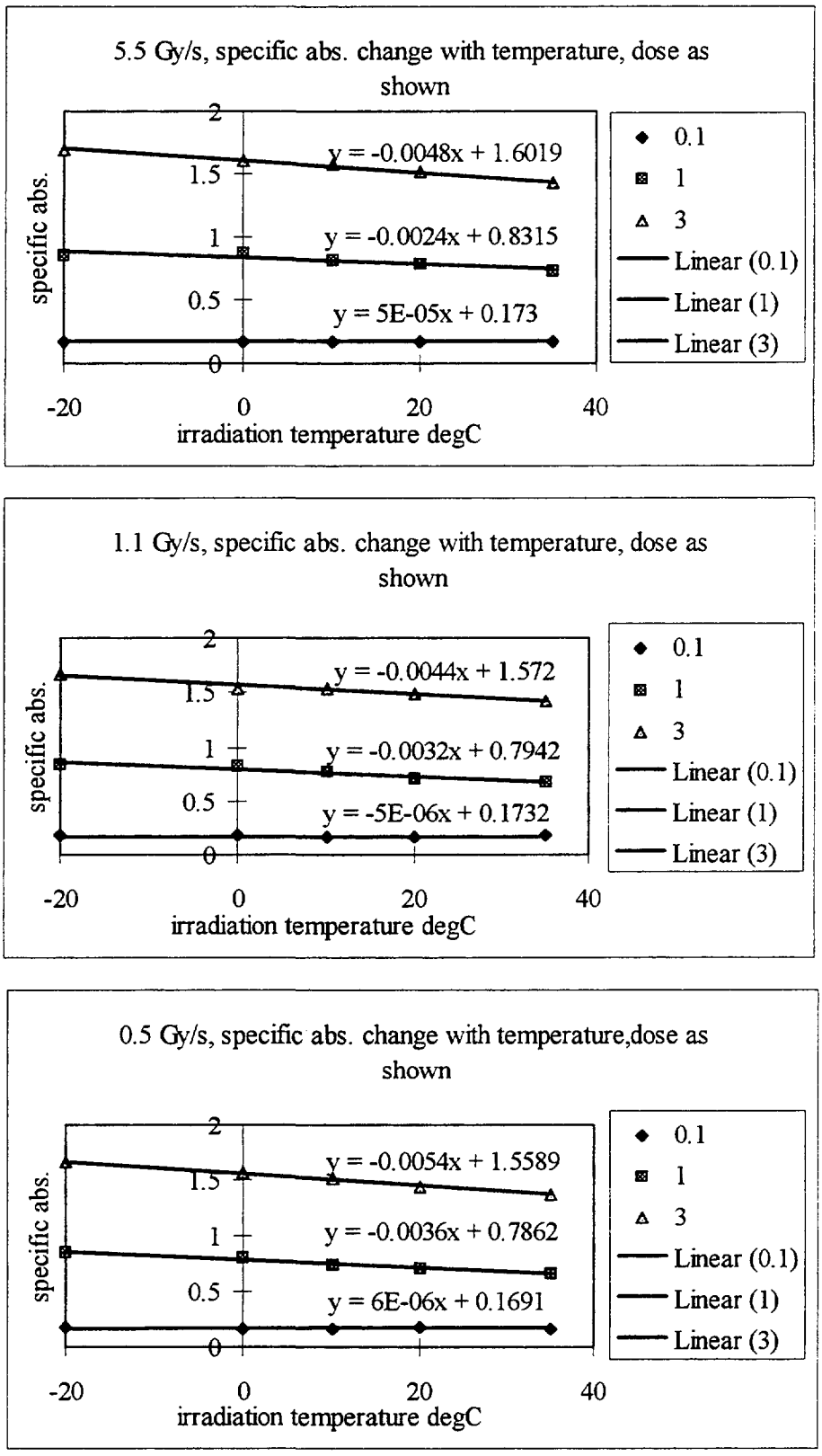

FIG. 2. Gammachrome YR® batch 5 change in k_m with increasing irradiation temperature.

TABLE III. THE INFLUENCE OF IRRADIATION AND STORAGE TEMPERATURE

Batch	Storage Time Hours	Irrad/Storage 30°C	Irrad/Storage 40°C	Ratio 40/30	Irrad/Storage 50°C	Ratio 50/30
Irradiation dose 0.1 kGy, values of k_m, mm^{-1} for the temperatures shown						
4	2	0.180	0.178	0.987	0.168	0.930
4	24	0.166	0.156	0.943	0.144	0.871
4	48	0.156	0.148	0.947	0.136	0.869
5	2	0.168	0.166	0.987	0.152	0.908
5	24	0.152	0.145	0.954	0.132	0.871
5	48	0.144	0.138	0.958	0.126	0.878
Irradiation dose 3 kGy						
4	2	1.352	1.356	1.003	1.358	1.005
4	24	1.329	1.357	1.021	1.365	1.027
4	48	1.279	1.276	0.998	1.324	1.036
5	2	1.396	1.322	0.947	1.387	0.993
5	24	1.340	1.296	0.967	1.423	1.062
5	48	1.278	1.207	0.944	1.405	1.099

TABLE IV. THE INFLUENCE OF POST IRRADIATION STORAGE

Batch	Irrad/Storage Temperature	Storage Time 2 Hours	Storage Time 24 Hours	Ratio 24h/2h	Storage Time 48 Hours	Ratio 48h/2h
Irradiation dose 0.1 kGy, values of k_m, mm^{-1} for the storage times shown						
4	30	0.180	0.166	0.918	0.156	0.867
5	30	0.168	0.152	0.903	0.144	0.857
4	40	0.178	0.156	0.877	0.148	0.832
5	40	0.166	0.145	0.873	0.138	0.833
4	50	0.168	0.144	0.860	0.136	0.810
5	50	0.152	0.132	0.867	0.126	0.830
Irradiation dose 3 kGy, values of k_m, mm^{-1} for the storage times shown						
4	30	1.352	1.329	0.983	1.279	0.946
5	30	1.396	1.340	0.960	1.278	0.916
4	40	1.356	1.357	1.000	1.276	0.941
5	40	1.322	1.296	0.980	1.207	0.913
4	50	1.358	1.365	1.005	1.324	0.975
5	50	1.387	1.423	1.026	1.405	1.013

The 2 hours storage time at elevated temperature was assumed to be of little significance. However, as noted above, this may not be an entirely legitimate assumption.

Table IV gives values of k_m for 2, 24 and 48 hours storage time in relation to temperature. The table also shows the ratio to 2 hours for comparison purposes.

3. DISCUSSION

The measurement uncertainty of Harwell Gammachrome YR® dosimeters is quoted as ±3% when applied to specific absorbance values. Therefore, ratios from 0.97 to 1.03 do not indicate significant differences.

3.1 Dose rate and irradiation temperature studies

The effect of dose rate on Gammachrome YR® dosimeters is small as shown in Table I, less than ±3% over the range tested, at -20 °C. This increases at higher temperatures. The dosimeters were generally more sensitive at higher dose rates.

The effect of irradiation temperature was interesting with both batches exhibiting very similar trends, see Figs 1 and 2. The response of the dosimeters at the lowest dose levels, such as 0.1 kGy, was not temperature dependent over the range tested. At higher dose levels of 1 kGy and above, they showed a marked linear trend with negative temperature coefficients ranging from -0.2 to -0.5% per °C. Biramontri et al [4] reported a similar temperature coefficient above -78°C, of -0.3% per °C for Gammachrome YR® batch 3 at a dose of 2 kGy. The dosimeter shows the highest sensitivity, over the dose range covered, at -20°C. This is a useful property for the irradiation of food at low temperatures.

3.2 Irradiation temperature and post irradiation storage

Post-irradiation storage of dosimeters at elevated temperatures results in a decrease in the specific absorbance, or post irradiation fading, with time. This is much greater at the 0.1 kGy dose level, than at 3 kGy as shown in Table II. Post-irradiation storage at elevated temperatures was the dominant factor affecting the measured response and should be avoided or corrections made.

4. CONCLUSIONS

Harwell Gammachrome YR® dosimeters are affected by irradiation dose rate, but the results are not significant at -20°C over the range tested. Significant dose rate effects occur at 0 °C and above. The response to temperature over the range -20 to 35 °C showed a linear temperature coefficient between -0.2 and -0.5% per °C, for doses of 1 kGy and above. The dosimeter is more sensitive at -20°C, a useful property for the irradiation of food at low temperatures.

Post irradiation storage at elevated temperature is a very significant source of error. Prolonged storage for 24 or 48 hours will lead to an under estimate of the apparent dose, unless the calibration regime makes due allowances.

These studies reinforce the recommendation that routine dosimeters should be calibrated as close to the conditions of use as possible [2].

REFERENCES

[1] WHITTAKER, B., "A new PMMA dosimeter for low doses and temperatures", Radiat. Phys. Chem. **35**, 4-6, 699, 1990.

[2] GLOVER, K.M., PLESTED, M.E., WATTS, M.F., and WHITTAKER, B., "A study of some parameters relevant to the response of Harwell PMMA Dosimeters to gamma and electron irradiation", *Radiat. Phys. Chem.* **42**, 4-6, pp. 739 -742, 1993.

[3] SOHRABPOUR, M., KAZEMI, A.A., MOUSAVI, H., and SOLATI, K., "Temperature response of a number of plastic dosimeters for radiation processing", *Radiat. Phys. Chem.*, **42**, 783, 1993.

[4] BIRAMONTRI, S., HANEDA, N., TACHIBANA, H., and KOJIMA, T., "Effect of low irradiation temperature on the gamma-ray response of dyed and undyed PMMA dosimeters", *Radiat. Phys. Chem.*, **48**, 1, pp. 105-109, 1996.

[5] FAIRAND, B., "Calibration of a polymethylmethacrylate routine dosimetry system", *Radiat. Phys. Chem.*, **52**, 1, pp. 523-536, 1998.

[6] WHITTAKER, B., WATTS, M.F., "The influence of ambient temperature and time on the radiation response of Harwell Red 4034 PMMA dosimeters", IEAE-SM-356/51, 1998.

ESR/ALANINE DOSIMETRY: STUDY OF THE KINETICS OF FREE RADICAL FORMATION — EVALUATION OF ITS CONTRIBUTION TO THE EVOLUTION OF THE SIGNAL AFTER IRRADIATION*

J.M. DOLO, V. FEAUGAS, L. HOURDIN
Département des applications et de la métrologie des rayonnements ionisants,
Laboratoire de mesure des rayonnements ionisants,
CEA Centre d'études de Saclay,
Gif-sur-Yvette, France

Abstract

$CH_3\dot{C}HCOOH$ is commonly accepted as the free radical responsible for the ESR signal detected in alanine after irradiation. The aim of this study is to find out the number of transient species leading to this radical and their kinetics of reaction. To do so, we follow the evolution of the ESR/alanine spectrum shape and correlate the response estimated from the central peak height to the absorbed dose. We use the theory of transformation systems. The first step is to make hypothesis on the number of equivalence classes and their content. From these hypotheses, we model the kinetics of free radical concentrations and check their fitting with experiment. We present comments on these different models, and their consequences on the evolution of the ESR signal on the first days after irradiation. The two successive reaction mechanisms (creation of free radicals and recombination reaction) are compared with the results obtained from a multiparametric study (experimental design) of combined effects (temperature and humidity before and after irradiation) which influence the reaction kinetics.

1. INTRODUCTION

Since the twenty last years, ESR/alanine dosimetry has been the subject of many papers which analyse different aspects of this technique and generally make the assumption that only the ESR signal of a stable free radical is observed. Many works about the irradiation of alanine have been carried out now since several years. Some deal with the fundamental reactions of radical formation in alanine.

The mechanism of radical formation in a powder is not well determined. The first step is to know correctly the crystal structure of L-α-alanine. The formula is $CH_3CH(NH_3)^+CO_2^-$ (zwitterion). After irradiation, the stable observed species by ESR is a radical anion formed by deamination. Its formula is $(CH_3)^{\cdot}CHCO_2^-$. It is trapped in the crystal lattice. A complete description of the radical reactions is based on the knowledge of the crystal structure and on the mechanisms observed in single crystals [1-3] or by spin trapping studies [4-5]. The mechanisms are similar in the two cases, and we can suppose in the first approach that in alanine powder, we have a great number of micro-crystals, so the reaction should not be different. But we must take into account that the specific area is very large and that the reaction at the surface and the influence of the neighbouring crystals for hydrogen bonds may modify the kinetic or the basic scheme.

The first consistent description of the different steps of the reaction mechanism has been proposed by Minegishi *et al.* [6] and more precisely developed by Shields *et al.* [7] :

* Work partially supported by IAEA research agreement No. 8581.

$CH_3HC(NH_3)^+CO_2^- (+ h\nu) \rightarrow [CH_3HC(NH_3)^+CO_2^-]^+ + e^-$ (1)

$(CH_3HC(NH_3)^+CO_2^-)^+ + e^- \rightarrow CH_3CH(NH_3)^+C^{\cdot}O^-O^-$ (2)

$CH_3HC(NH_3)^+C^{\cdot}O^-O^- + H^+ \rightarrow CH_3HC(NH_3)^+C^{\cdot}O^-OH$ (3)

$CH_3HC(NH_3)^+C^{\cdot}O^-OH + CH_3HC(NH_3)^+CO_2^- \rightarrow CH_3HC(NH_3)^+CO_2^- + CH_3H^{\cdot}CCOOH + NH_3$ (4)

$CH_3HC(NH_3)^+C^{\cdot}OO^-H \rightarrow NH_3 + CH_3HC^{\cdot}COOH$ (5)

The two last reactions (4) and (5), which are intermolecular and intramolecular, respectively can exist at higher temperature than 77 K, but are poorly understood.

Some authors [1, 2] describe the stable free radical in the single crystal as a planar species which can present three kinds of hydrogen bonds (two in the same plane and the third out of it) with neighbouring amino-protons. Those bonds are not equivalent for the radical formation process. It is well known that by ionising radiation, an electron is ejected and trapped by molecules to form the radical anion. The anion is trapped as a protonated radical, and protonation is replaced by a hydrogen bridge. This proton located out of the plane is selectively transferred to the anion. The authors mention that the three hydrogen exchange reactions may occur at room temperature.

2. EXPERIMENTAL

2.1. Materials

A Bruker spectrometer (EMX model) with a cavity model 4108 TMH is used for the measurements.

2.2. Sample preparation

L-α-alanine powder (Merck) is sieved without crushing to a granulometry between 150 and 180 µm. The sample mass is about 100 mg and samples are directly irradiated in a quartz "Suprasil" tube in air. The environmental conditions are ambient temperature and relative humidity close to 0 %. The powder is stored in a desiccator then transferred in a tube sealed with paraffin.

2.3. Protocol for irradiation and measurements

A Philips X rays tube type MCN 321 was used. It delivers photons with an average energy of 200 keV after filtration with 3 mm of aluminium. The experimental conditions of irradiations are 300 kV and 30 mA. Irradiation is performed at room temperature.

Two experiments were carried out, consisting of successive and cumulative irradiation steps, each irradiation being immediately followed by the ESR measurement. Due to technical constraints the successive steps were not equal in time, and therefore in dose. In the first experiment, the irradiation times were at first one 5-minute step, followed by 12 steps of 10 minutes each. The dose rate was about 32.2 Gy/min, the total dose was around 4100 Gy. In the second experiment, the irradiation times were respectively : 2-2-2-3-3-3-5-5-5-5-10-10 minutes. With the same dose rate, the total dose is around 1800 Gy.

2.4. Analytical procedures for post - irradiation measurements

Each ESR measurement is performed as soon as possible after the end of each irradiation step (within a few minutes). The small signal coming from the irradiated quartz is insignificant for the measurements of the alanine signal. After irradiation, the sample remains in the cavity of the

spectrometer at room temperature and is measured at regular time steps. In the first experiment, the measurements were performed for 8 days, the second for 25 days. The parameters used for the measurements were: frequency around 9.8 GHz, microwave power 1.3 mW, amplitude modulation 2.5 G, and sweep width of 160 or 20 G. All the results have been normalised for comparison purposes.

3. RESULTS

In Fig. 1, we observe a curve close to a sigmoid. Figure 2 presents the evolution of the signal after irradiation for the first experiment. During the next 8 days it increases slowly. After irradiation, the signal continues to increase more than 2 % during the first 144 hours. Figure 3 presents the evolution of the signal after irradiation for the second experiment. The signal increases also after irradiation. For comparison purposes, Fig. 4 presents the first part of the curve corresponding to the first 200 hours, which concerns only the first increase (~ 1 %) and stabilisation of the signal. In the two experiments, many experimental points are affected by the thermal sensitivity of ESR spectrometer diodes as shown by the observed cyclic variations due to the ambient temperature control system. These artefacts have been identified and these points have been suppressed before using the data for modelling.

For the analysis of those curves, an assumption can be made on species which are involved, and on the mechanism of reactions. The corresponding kinetic equations and curves can then be compared to experimental data. Concerning the observed increase of the signal after irradiation, it may be assumed that there several species that are not seen in our experiment and which would be transient species. The scheme of reactions would be :

$$A(+h\nu) \rightarrow \cdots \rightarrow B \rightarrow R^{\bullet} \qquad (6)$$

where, A is the alanine molecule,

B is a transient species. This species has not been observed by ESR measurements at room temperature in our experiments,

$R^{\bullet}$ is the radical measured by ESR. It is often called secondary radical. The last reaction continues after irradiation.

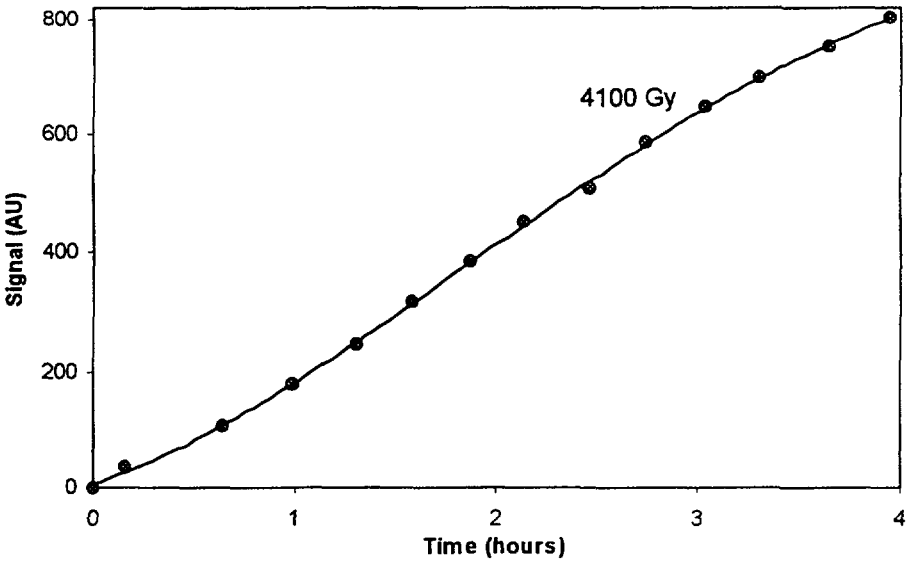

FIG. 1. ESR Signal versus elapsed time during successive irradiation.

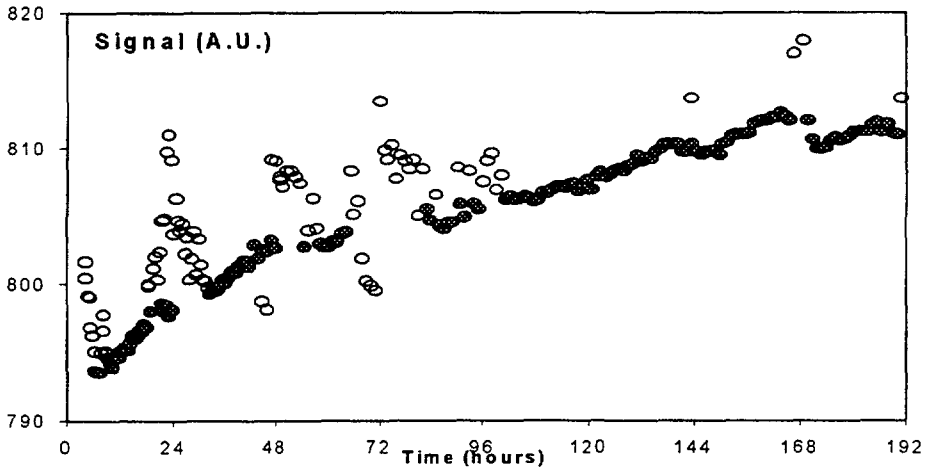

FIG.2. Signal versus time after irradiation (4100 Gy - 192 h) (solid points are data used for calculations.)

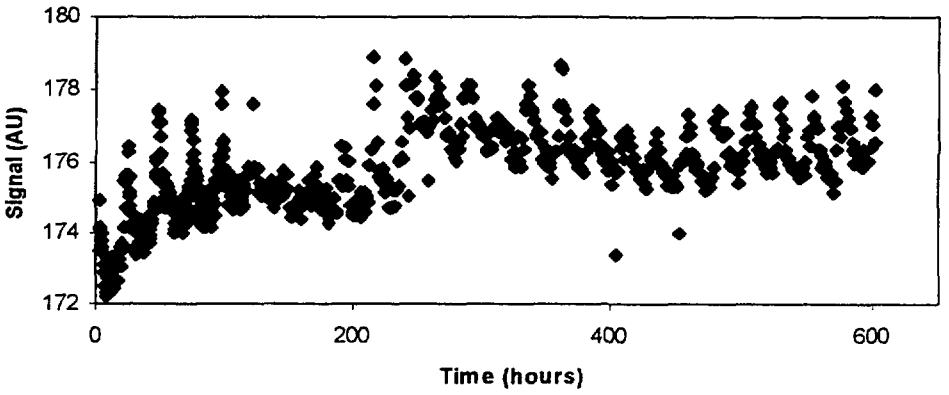

FIG.3. Signal versus time after irradiation (1800 Gy - 600 h)

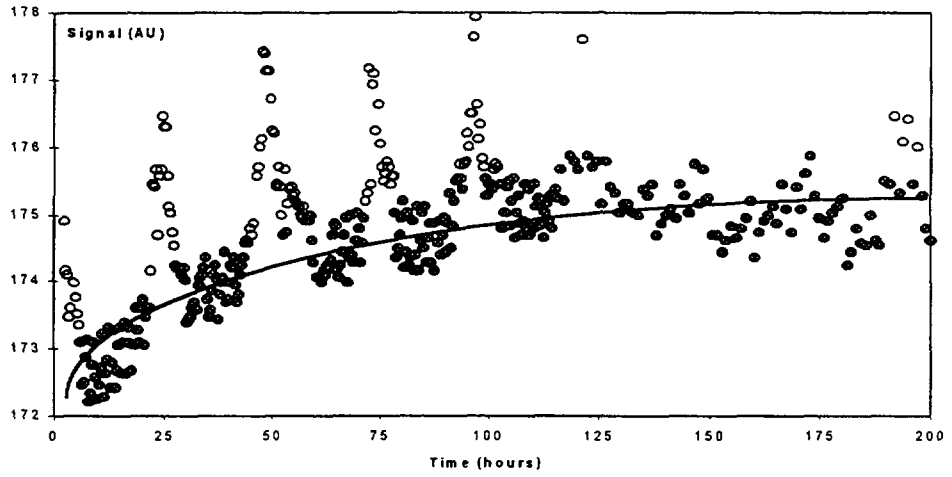

FIG.4. Signal versus time after irradiation (1800 Gy - 200 h) (solid points are data used for calculations.)

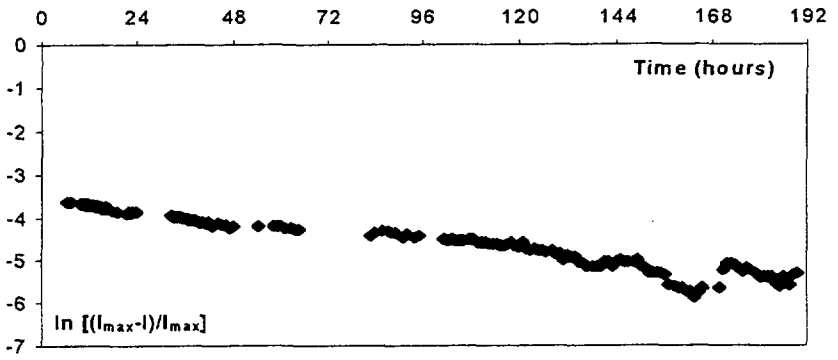

FIG. 5. ln [(I_{max}-I)/I_{max})] versus time after irradiation (4100 Gy - 192 h)

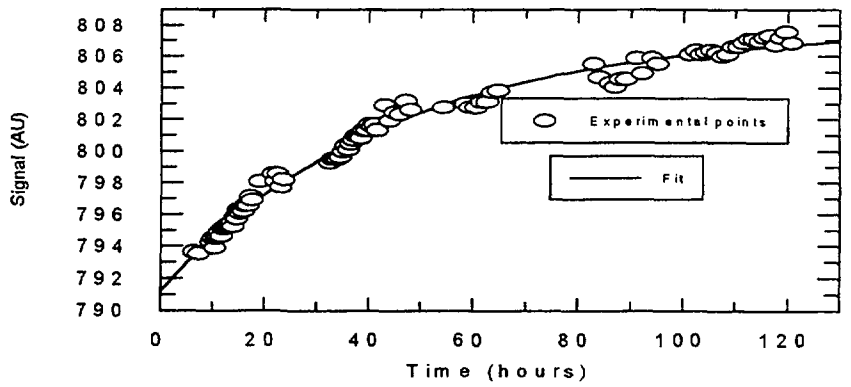

FIG. 6. Comparison with fitted values - Signal versus time after irradiation (4100 Gy - 120 h)

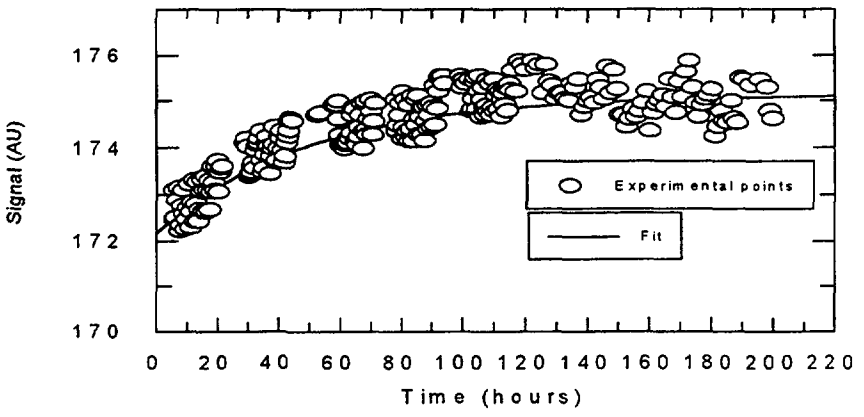

FIG. 7. Comparison with fitted values - Signal versus time after irradiation (1800 Gy - 200 h)

From a technical point of view and taking into account the two last proposed reactions of deamination (4) and (5), a first order reaction is proposed as in Eq. (7) :

$$- d[B] /[B] = k . dt \qquad (7)$$

which gives by integration :

$$ln [(I_{max}-I)/I_{max})] = - k . t \qquad (8)$$

where, k is the apparent rate constant,
I is the value of the ESR signal at t of the R secondary radical corresponding to the disappearing of the B transient species,
I_{max} is the maximum value of the normalised signal representing the R secondary radical.

A straight line can be drawn up to 120 hours and 200 hours respectively for the first and the second experiment. So, only these experimental points are used for calculation. If R_0, number of radicals existing at the end of irradiation, is taken as the initial condition, the equation can be written as :

$$R = \Delta R_b . (1 - e^{-kt}) + R_0 \qquad (9)$$

where, ΔR_b represents the increasing of the signal corresponding to the disappearance of the transient species,
$(\Delta R_b + R_0)$ represents the limit value of the signal.

The rate constants, calculated from experimental data by using equation (9), leads approximately to the same value of $2x10^{-2}$ h^{-1}.

4. DISCUSSION

These results suggest three conclusions. First, as it was shown in Refs [1-3] for a single crystal, a transient species also exists in powder. Because the signal increases after irradiation, at least one intermediate species and one reaction are likely. In the first approximation, the reaction mechanism can be considered identical to that in the single crystal. The transformation to the final stable radical takes place during and after irradiation. This mechanism is relatively slow and clearly observable at room temperature.

Two other works suggest a mechanism of formation of the final free radical. The study which has been performed by Sinclair and Hanna [8] at low temperature and on a single crystal of L-alanine suggests that the primary radiation effect is the ejection of an oxygen electron. This fact is characterised by an unpaired electron localised on the carboxyl group. This is confirmed by the work of Gottschall and Tolbert [9] on metal chelates of alanine. Sinclair and Hanna mentioned several steps for the radical reaction : the ejection of an electron leads to the formation of a positive ion (1) and a negative ion (2). This negative ion is transformed in unstable free radicals which will give, by direct deamination, the final stable radical. They suggested that the mechanism of decarboxylation of the positive ion is possible at low temperature creating an ethyl ammonium radical. Zagorski [10] suggested that the intermediate species, that he observed by absorption of light, is due to one or several precursors of the more stable ESR detected species before deamination and decarboxylation. This intermediate species has been studied by pulsed radiolysis [11]. He studied the kinetics of formation and the decay of this intermediate species in a mono-crystal of L-α-alanine.

Those approaches tend towards the same scheme: a simplification of the mechanism in two steps and at least one transient species. The first reaction has a very high rate constant, and thus the correspondent species is only observable at low temperature.

Pilbrow *et al.* [12] put in evidence that, in irradiated alanine powder, two different free radicals might exist; but the irradiation conditions are not well defined. Makino *et al.* [5] have studied irradiation of alanine in aqueous phases. They mentioned two parent radicals. The first radical ($^{\cdot}CH(CH_3)COO^-$) is formed by deamination reaction caused by the attack of an aqueous electron, the second ($^{\cdot}CH_2CH(NH_3^+)COO^-$) by hydrogen abstraction reaction from the methyl group. For this last one, the observed spectrum is presented as the overlap of two forms: zwitterion and anion with a low interchange. We assume that the kinetics are generally faster in aqueous than in solid phase and that the previously described reactions are probably similar in powder form with slower kinetics.

Several researchers have studied the evolution of the ESR signal after irradiation [13-15]. They used in each case their own alanine pellets, that makes the comparisons with these works difficult. These studies mention the influence of some parameters, such as temperature and humidity, without detailed operative conditions. They could be included in a kinetic modelling. From the results presented in Refs [14, 15], we can suppose that the apparent signal evolution is the results of the competition between the increase due to the last reaction of formation of the observed radical and its disappearing by recombination or destruction in presence of water. In a previous work [16], we have shown using an experimental design that the results may be altogether very different and consistent depending on the experimental conditions used.

Presently, no explanation can be proposed for the second increase of signal and why it happens at different times. We need further investigations to prove its existence and formulate available hypothesis of several mechanisms with different ways leading to the same observed radical. With the lack of evident reaction mechanisms, the compatibility between the experimental data and the fits performed with a simple set of kinetic equations was tested and found consistent.

Acknowledgements - Support from French 'Bureau National de Métrologie' (BNM) is gratefully acknowledged.

REFERENCES

[1] IWASAKI M., MUTO H., ENDOR studies of the superfine couplings of hydrogen-bonded protons. IV. Carboxyl radical anions in irradiated glycine and alpha-amino isobutyric acid, J; Chem. Phys., **61**, n°12, (1974) 5315-5320

[2] KURODA S., MIYAGAWA I., ENDOR study of an irradiated crystal of L-alanine : Environment of the stable $CH_3C^{\cdot}HCO_2^-$ radical, J. Chem. Phys., **76**, n° 8, (1982) 3933-3944

[3] MATSUKI K., MIYAGAWA I., ENDOR study of an irradiated crystal of L-alanine : Environment of the unstable $CH_3C^{\cdot}HCO_2^-$ radical, J. Chem. Phys., **76**, n° 8, (1982) 3945-3952

[4] RIESZ P. and RUSTGI S., Aqueous radiation chemistry of protein and nucleic acid constituents : ESR and spin trapping studies, Radiat. Phys. Chem., **13**, (1979) 21-40

[5] MAKINO K., MORIYA F. and HATANO H., Application of the spin trap HPLC-ESR Method to radiation chemistry of amino acids in aqueous solutions, Radiat. Phys. Chem., **23**, n°1-2, (1984) 217-228

[6] MINEGISHI A., SHINOZAKI Y., and MESHITSUKA G., Radiolysis of solid L-a-alanine, Bull. Chem. Soc. Jap., **40**, n° 5, (1967) 1271-1272

[7] SHIELDS H., HAMRICK Jr. P.J., SMITH C. HAVEN Y., Kinetics of low temperature of radicals in l-alanine and alpha-amino isobutyric acid, J. Chem. Phys., **58**, n° 8, (1973) 3420-3423

[8] SINCLAIR J.W.,HANNA M.W., Electron paramagnetic resonance study of L-alanine irradiated at low temperatures, J. Phys. Chem.,**72**, n° 1, (1967) 84-88

[9] GOTTSCHALL W.C. Jr, TOLBERT B.M., The solid state radiation chemistry of selected transition metal chelates of glycine and alanine, J. Phys. Chem., **72**, n° 3, (1968) 922-925

[10] ZAGORSKI Z.P., TOMASINSKI, Transient optical absorption spectra in pulse irradiated solid amino acids, J. Radioanal. Nucl. Chem., letters,**146**, n° 3, (1990) 197-204

[11] ZAGORSKI Z.P., SEHESTED K., Transients and stable radical from the deamination of α-alanine, J. Radioanal. and Nucl. Chem., **232**, n° 1-2, (1998) 139-141
[12] PILBROW J.R., HUTTON D.R., ZHONG Y.C. NOBLE C.J. and SONG R., Pulsed EPR investigation of hyperfine structure in gamma irradiated alanine, Appl. Radiat. Isot., **47**, n°11/12, (1996) 1257-1261
[13] REGULLA D.F., DEFFNER U., Dosimetry by ESR spectroscopy of alanine, Appl. Radiat. Isot.; **33**, (1982) 1101-1114
[14] ARBER J.M., SHARPE P.H.G., Fading characteristics of irradiated pellets: the importance of pre-irradiation conditioning, Apll. Radiat. Isot., **44**, n°1-2, (1989) 19-22
[15] NAGY V.Y., DESROSIERS M.F., Complex time dependence of the EPR signal of irradiated L-α-alanine, Appl. Radiat. Isot., **47**, n°8, (1996) 789-793
[16] DOLO J.M., PICHOT E., FEAUGAS V., Evaluation of some parameters which influence the ESR measurements for the fading study of alanine dosimeters, Appl. Mag. Res., **15/2**, (1998) 269-277

THE INFLUENCE OF AMBIENT TEMPERATURE AND TIME ON THE RADIATION RESPONSE OF HARWELL RED 4034 PMMA DOSIMETERS

B. WHITTAKER
Wantage, Oxfordshire

M.F. WATTS
Harwell Dosimeters Ltd,
Harwell, Didcot, Oxfordshire

United Kingdom

XA9949718

Abstract

Previously we have reported the short term effects, if significant, of different dose rates and different irradiation temperatures on the radiation response characteristics of four different batches of Harwell Red 4034 PMMA dosimeters. Using dosimeters randomly selected from these same four batches we have extended the earlier work by investigating the effects of elevated temperatures, up to 50 °C imposed both **during** and **after** irradiation. Dosimeters were irradiated to known doses of 15 and 25 kGy at a dose rate of 1.5 Gy. s^{-1}, and fixed temperatures of 30, 40 or 50 °C, then held at these temperatures for periods of 1, 24 and 48 hours prior to measurement. The data produced in these studies were compared with original Harwell 15 and 25 kGy calibration data for these batches, based on calibration irradiations carried out at temperatures of 20 to 25 °C. In agreement with previous studies, the short-term (1 hour) effects of elevated temperatures were small and only marginally significant, ±3 % maximum, at 30 and 40 °C, but in some cases larger, depending on batch, up to + 9 % at 50 °C. At 30 °C the long-term (24 and 48 hour) effects were insignificant, within ±2%, but significant, up to +34%, at the higher temperatures, indicating the need for a special calibration protocol under these adverse temperature / time conditions.

1. INTRODUCTION

Harwell Red 4034 PMMA[1] dosimeters have been extensively used for routine monitoring of doses delivered in industrial ^{60}Co gamma irradiation facilities since the early 1960s. In the original development work this type of PMMA dosimeter was found to be insensitive to irradiation temperature over the range of 0 to 30 °C, effectively covering the range of temperatures encountered in the UK industrial irradiators at that time. However, it was also shown that the dosimeters were susceptible to heat, both during and after irradiation [1]. The dosimeter calibration method then established, now referred to as the 'classical method', depended simply on irradiation of dosimeter sets to known doses at normal (UK) ambient laboratory temperatures, 20 to 25 °C in a suitable ^{60}Co gamma calibration facility. After irradiation the dosimeters were kept away from sources of heat, then subsequently measured in order to establish the dosimeter response versus dose function. This method is still used by the manufacturers, Harwell Dosimeters Ltd. in the calibration and characterisation tests applied to each batch of dosimeters prior to sale, although, during calibration the dosimeters are now held at a controlled temperature, 25 ±2 °C. In addition, the radiation response of each batch is tested by means of an inter-laboratory comparison protocol involving HDL and the UK National Physical Laboratory [2].

The development and world-wide expansion of radiation processing since the 1960's has effectively placed greater demands on routine dosimetry systems, because these systems are now required to perform well in a wide range of climatic conditions, in many different kinds and sizes of

[1] The dosimeter material was originally called Red 400. The code Red 4034 defines the exact dye formulation and dye concentrations required in the dosimetry application.

processing facility. Temperature, in particular has become more important, because of irradiator location and/or because of significant radiation heating in those industrial irradiators that contain large source loadings. Cobalt-60 sources have an energy output of 15 kW per installed megacurie (3.7×10^{16} Bq) [3]. A large proportion of this energy degrades to heat, the effect of which is only partly removed by the installed ventilation system. Information on temperatures in commercial irradiators is sparse, however in 1988 Shaffer and Garcia reported temperature conditions up to 45 °C in one facility [4], and in 1990 Al-Sheikhly et al. reported up to 43 °C in the centre of product boxes in a 7.4×10^{16} Bq facility [7]. We are aware of even higher temperatures. Depending on facility design and operating procedures, irradiated dosimeters may remain at elevated temperatures for several hours or days before collection and final measurement. Therefore, the temperature / time conditions met in practice can be quite different to those used in the classical calibration method.

Full awareness of irradiation temperature and post-irradiation temperature as influence factors that can affect the performance of commonly used routine high-dose dosimeters such as Red 4034 PMMA in the field dates back to a paper published in 1975 by Miller *et.al.*[5]. We reviewed the subject and published information on the performance of Red 4034 PMMA with regard to batch, water concentration, dose rate, irradiation temperature and elapsed time before measurement in 1984 [6]. Al-Sheikhly *et.al.* reported extensive irradiation temperature and post-irradiation temperature studies with Red 4034 batch AW dosimeters in 1990, showing that a calibration made at 22 °C may not apply at elevated temperatures (40 °C and above), and if used, could result in overestimates of delivered dose [7]. More recently, we extended our dose-rate / irradiation temperature studies and in 1993 reported the short-term effects of different dose rates (0.5 to 6.5 Gy/s) and different irradiation temperatures (20 to 50 °C) on the radiation response of four different batches of Harwell Red 4034 dosimeters, batches AA, BP, BV and BW [8]. At that time Sohrabpour *et al.* also reported the temperature response of five kinds of plastic dosimeters, including Harwell Red 4034 [9]. Although both of these reports [8,9] indicated very significant changes in the response of Red 4034 at irradiation temperatures above 40 °C, the effects of elevated temperature **after** irradiation were not reported at that time. In 1996 Biramontri *et al.*[10] reported the effects of **low** irradiation temperatures, down to -196 °C on four types of PMMA dosimeter, including Harwell Red 4034.

2. EXPERIMENTAL

Using dosimeters from the same four batches used in the earlier work [8], we have now extended the temperature influence study by examining the effects of elevated temperature both **during** and **after** irradiation. The dosimeters were irradiated in sets of four at a fixed dose rate of close to 1.5 Gy/s in the previously described ^{60}Co calibration facility [2]. In order to provide fixed temperatures of 30, 40 and 50 °C both the irradiation volume and the lead shield used to collect the irradiated dosimeters were thermostatically-controlled (see Fig. 1). The dose rates in the five irradiation canisters were previously measured using dichromate reference dosimeters provided and measured by the UK National Physical Laboratory. Dosimeters were kept in their sealed sachets at the fixed temperatures for 1, 24 and 48 hours prior to measurement, to simulate the kind of measurement delays that occur in practical use. To minimise the number of dosimeters used and measurements made to manageable proportions, i.e. 288 dosimeters and corresponding measurements, responses at 15 kGy and 25 kGy doses only were examined, representing typical doses used in the industrial applications of this type of dosimeter.

After irradiation, the dosimeters were either removed from the irradiation cell for early measurement (1 hour data), or placed in thermostatically controlled container (24 and 48 hour data).The dosimeters were measured in the normal manner, using a Pye-Unicam PU8800 spectrophotometer and Moore and Wright digital thickness gauge to obtain values of specific optical absorbance, k, at 640 nm wavelength. The resulting data were reduced to average values of k, k_m for each set of four dosimeters. These averages are shown in Table I. The respective values of k_m and their associated standard deviations determined during normal calibration at 20-25 °C are shown in Table II. To present the Table I data in terms of the effect of irradiation and post-irradiation temperature on measured specific

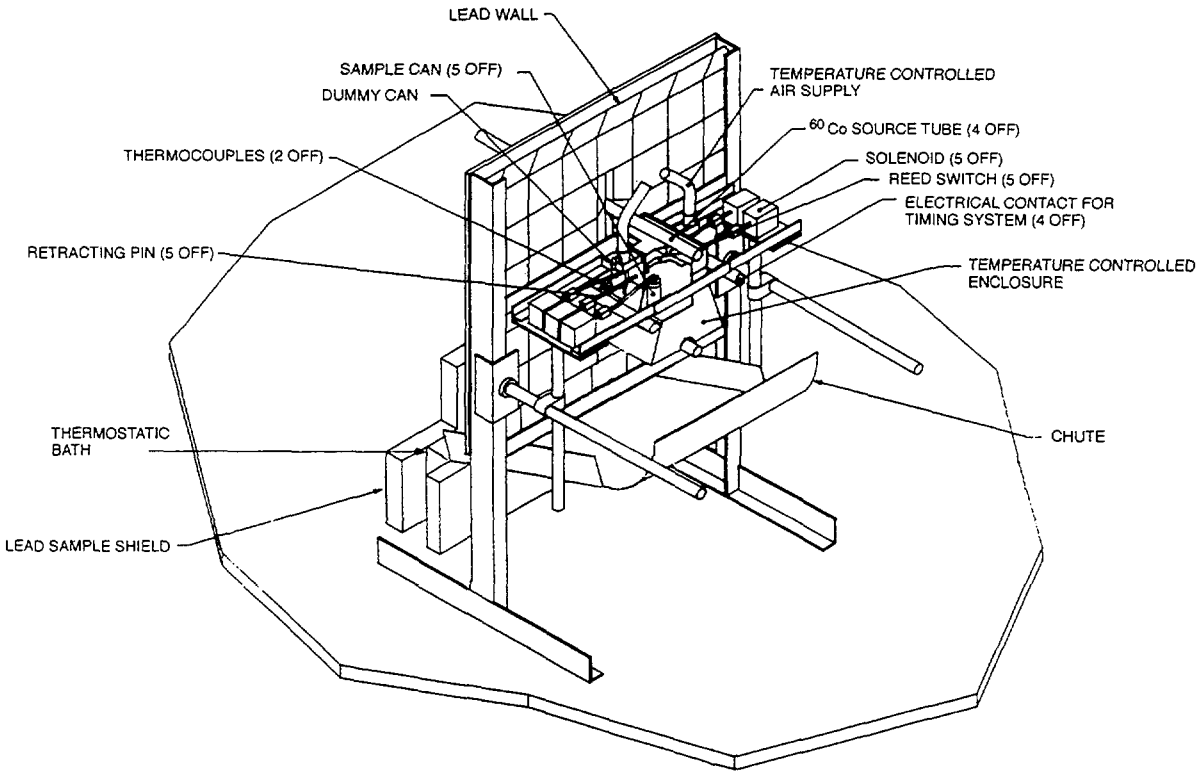

FIG.1. Harwell irradiation assembly

absorbance, the k_m values were normalised by dividing by the respective normal calibration values from Table II. The resulting ratios (r) were rounded to two decimal places, then converted to percentage deviations (d, where d = 100.r-100). These deviations are presented in Table III.

3. DISCUSSION

Dependant on a number of considerations, for example the time elapsed between the original determinations of k_m during classic batch calibrations and the temperature studies, a period of up to two years, we judge that a significance level of 3% is appropriate, i.e. any percentages outside ±3% in Table III are considered significant. Thus, of the 72 values presented, 36 values indicate significant temperature and temperature / time effects, including in some cases, indications of large increases in k_m versus dose response up to a maximum of 34 % in the case of batches BV and BW irradiated and stored for 48 hours at 50 °C. The one-hour values are consistent with our earlier report [8].

The results clearly indicate that in the calibrations made using a calibration facility operating at 20-25 °C cannot be expected to apply at 40 °C if circumstances dictate that the dosimeters are held at this temperatures for more than one hour after irradiation. At 50 °C the temperature influences are considerably larger and the classic calibration cannot be expected to apply under any circumstances.

In all cases, the effects found were positive, i.e. the values of k_m were higher than measured in the original calibrations. Therefore if these calibrations were used to interpret data obtained from elevated temperature irradiations, doses would be **overestimated** (see Ref. [7]). It should be said, also that because of the non-linearity of the k versus dose relationship, these overestimates would in fact be greater than Table III suggests. Non-linearity factors (NLFs) [11, 12] should be applied to convert the increases in k to dose overestimates. For example, for batch BV dosimeters irradiated to 25 kGy at 50 °C, then held at this temperature for 24 hours, an increase in k_m of 17 % is reported (Table III), and using a NLF of 1.7 applicable to Red 4034 at 25 kGy [11], this converts to a dose overestimate of 1.7x17 = 29 %.

TABLE I. MEAN SPECIFIC ABSORBANCE DATA, k_m, cm^{-1}

Batch	Dose, kGy	Temperature	Elapsed Time, h 1	24	48
AA	15	30	1.506	1.518	1.520
AA	15	40	1.527	1.564	1.597
AA	15	50	1.534	1.737	1.888
AA	25	30	2.093	2.104	2.111
AA	25	40	2.141	2.213	2.282
AA	25	50	2.220	2.394	2.390
BP	15	30	1.608	1.622	1.637
BP	15	40	1.598	1.692	1.778
BP	15	50	1.675	2.023	2.157
BP	25	30	2.248	2.263	2.295
BP	25	40	2.298	2.445	2.541
BP	25	50	2.427	2.597	2.539
BV	15	30	1.670	1.697	1.717
BV	15	40	1.687	1.786	1.864
BV	15	50	1.752	2.098	2.261
BV	25	30	2.361	2.385	2.408
BV	25	40	2.421	2.586	2.681
BV	25	50	2.578	2.771	2.724
BW	15	30	1.576	1.598	1.614
BW	15	40	1.567	1.658	1.739
BW	15	50	1.640	1.995	2.130
BW	25	30	2.214	2.238	2.266
BW	25	40	2.276	2.413	2.505
BW	25	50	2.381	2.566	2.518

TABLE II. NORMAL CALIBRATION DATA

Batch	Dose, kGy	Mean Specific Absorbance	Standard Deviation
AA	15	1.494	0.019
AA	25	2.070	0.013
BP	15	1.646	0.021
BP	25	2.281	0.018
BV	15	1.700	0.005
BV	25	2.365	0.006
BW	15	1.586	0.010
BW	25	2.229	0.006

Clearly, if Red 4034 dosimeters are to be used under adverse temperature / time conditions they should first be calibrated for actual **conditions of use.** There are two basic methods for this :

1. In a calibration irradiator capable of irradiating and maintaining the dosimeters at some temperature close to the average temperature they will encounter in practise.

2. In the actual industrial irradiator, using reference dosimeters such as dichromate or alanine to determine the calibration doses given.

TABLE III. PERCENTAGE DEVIATIONS

Batch	Dose, kGy	Temperature	Elapsed Time, h 1	24	48
AA	15	30	1	2	2
AA	15	40	2	5	7
AA	15	50	3	16	26
AA	25	30	1	2	2
AA	25	40	3	7	10
AA	25	50	7	16	15
BP	15	30	-2	-1	-1
BP	15	40	-3	3	8
BP	15	50	2	23	31
BP	25	30	-1	-1	1
BP	25	40	1	7	11
BP	25	50	6	14	11
BV	15	30	-2	0	1
BV	15	40	-1	5	10
BV	15	50	3	23	33
BV	25	30	0	1	2
BV	25	40	2	9	13
BV	25	50	9	17	15
BW	15	30	-1	1	2
BW	15	40	-1	5	10
BW	15	50	3	26	34
BW	25	30	-1	0	2
BW	25	40	2	8	12
BW	25	50	7	15	13

Both of these methods are presently advocated in an ASTM standard [13]. Method 2 is generally thought to be the better of the two because the conditions applied must normally be very similar to conditions of use. There may be practical difficulties, for example in achieving a wide enough calibration dose range without interrupting commercial productivity, and in correcting reference dosimeters for temperature / time effects, but the potential advantages of method 2 appear to outweigh the surmountable difficulties. If the method is used, it is important to choose reference dosimeters that have minimal and well-known temperature sensitivity, as the actual temperature / time conditions may not be accurately known. Some well - known reference dosimeters are reported to have temperature coefficients of the order of 0.2% / °C [3]. In this case temperature uncertainties of ±5 °C would not significantly affect the accuracy of the resulting routine dosimeter response curve, and uncertainties up to ±10 °C (±2% in dose uncertainty) may even be tolerable.

Temperature effects are not peculiar to Red 4034 dosimeters, and all known kinds of polymer-based routine dosimeter appear to be affected to some degree [3]. This being so, **conditions of use** calibration methodology is presently under consideration in the revision of a **generic** ASTM standard, last published in 1994 [14].

4. CONCLUSIONS

The k versus dose response of Harwell Red 4034 PMMA dosimeters is sensitive to both irradiation- and post irradiation- temperature. At 40 °C the effect is insignificant shortly after irradiation

(1 hour), but if dosimeters are maintained at that temperature, further colour development results in a considerable increases in k, up to +13 % for irradiated dosimeters kept at 40 °C for 48 hours. At 50 °C the enhancement in k can be very significant (up to 9 % in these experiments) even in the short term (1 hour), and again, post-irradiation storage at this temperature results in further increases in k.

In practice the classic k versus dose calibration, normally carried out in ambient temperatures of the order of 25 °C cannot be expected to apply under these adverse temperature / time conditions, and the routine use of such a calibration could result in serious overestimation of delivered dose.

In these circumstances, Red 4034 dosimeters require calibration in temperature / time conditions that closely simulate the conditions met in the production facility. These conditions are best achieved in the actual production irradiator, using reference dosimeters with low temperature sensitivity to measure the calibration doses given.

REFERENCES

[1] WHITTAKER, B., "Radiation dosimetry technique using commercial red Perspex", Harwell report AERE- R 3360 (unclassified), 1964.

[2] GLOVER, K. M. et al., "Calibration and Intercomparison of Red 4034 Perspex Dosimeters", IAEA conference: High Dose Dosimetry, paper number IAEA-SM-272/6,1984, IAEA publication High Dose Dosimetry, STI/PUB/671, pp 373 - 395, Vienna 1985.

[3] McLAUGHLIN, W.L. et al., Dosimetry for Radiation Processing, Taylor and Francis, 1989, ISBN 0-85066-740-2.

[4]SHAFFER, H. L. and GARCIA, R.D., "Practical application of dosimetry systems utilised in radiation processing of medical devices", *Radiat. Phys. Chem.*, **31**, 4-6, pp. 497 - 504, 1988.

[5] MILLER, A. et al., "Some limitations in the use of plastic and dyed plastic dosimeters", *Int. J. Appl. Radiat. Isot.*, **26,** 611, 1975.

[6] WHITTAKER, B et. al., "Some parameters affecting the radiation response and post - irradiation stability of Red 4034 Perspex dosimeters", IAEA conference : High Dose Dosimetry, paper number IAEA-SM-272/5,1984, IAEA publication High Dose Dosimetry, STI/PUB/671, pp 293 - 305, Vienna 1985.

[7] Al-SHEIKHLY, M et. al., "Effects of absorbed dose rate, irradiation temperature and post-irradiation temperature on the gamma ray response of red Perspex dosimeters", IAEA conference : High Dose Dosimetry, paper number IAEA-SM-314/37, pp. 419 - 434, 1990.

[8] GLOVER, K. M. et. al., "A study of some parameters relevant to the response of Harwell PMMA dosimeters to gamma and electron irradiation", *Radiat. Phys. Chem.*, **42,** 4 - 6, pp. 739 - 742, 1993.

[9] SOHRABPOUR, M. et. al., "Temperature response of a number of plastic dosimeters for radiation processing", *Radiat. Phys. Chem.*, **42,** 4 - 6, pp. 783 - 787, 1993.

[10] BIRAMONTRI, S. et. al., "Effect of low irradiation temperature on the gamma- ray response of dyed and undyed PMMA dosimeters", *Radiat. Phys. Chem.*, **48,** 1, pp. 105 - 109, 1996.

[11] WHITTAKER, B., " Uncertainties in absorbed dose as measured using PMMA dosimeters", *Radiat. Phys. Chem.*, **42,** 4 - 6, pp. 841 - 844, 1993.

[12] WHITTAKER, B. et. al., " Extending the dose range of the red 4034 PMMA dosimeter", *Radiat. Phys. Chem.*, **49,** 4, pp. 505 - 508, 1997.

[13] Standard Practice for Use of a Polymethylmethacrylate Dosimetry System, ASTM standard E 1276 - 96, published in Annual Book of ASTM Standards, volume 12.02, 1997, ASTM, West Conshohocken, PA 19428, USA.

[14] Standard Guide for Selection and Calibration of Dosimetry Systems for Radiation Processing, ASTM standard E 1261 - 94, published in Annual Book of ASTM Standards, volume 12.02, 1997, ASTM, West Conshohocken, PA 19428, USA.

EFFECT OF LOW IRRADIATION TEMPERATURES ON THE GAMMA-RAY RESPONSE OF THE GAD 1, 2, 4 AND 6 DOSIMETRY SYSTEMS*

M. IVANOVA, M. NIKOLOVA
Elgatech Ltd

I. PETKOV, N. SERDOVA
Department of Organic Chemistry,
Faculty of Chemistry,
Kliment Ohridski University

Sofia, Bulgaria

Abstract

The response of four types of the GAD radiochromic film dosimeters at low irradiation temperatures was investigated within the dose interval of 0.05-10 kGy. The optical density was measured 24 hours after the irradiation. The low temperature interval was from -18 °C to 0 °C and the results are compared to those obtained at 20-25 °C. A quantitative estimation is made of the effect of the temperature on the dose determined with these dosimeters. It is established that the GAD dosimetry systems can be used to measure doses at temperatures below 0 °C, but with a calibration curve constructed specifically for the low temperature interval.

1. INTRODUCTION

The present investigation is a part of a project aimed at the technological development of the dosimetry systems for the control of radiation processing of frozen food products. The GAD radiochromic film dosimeters are routine dosimeters used at normal room temperatures in the practice of the UGO-100 gamma-plant in Sofia. With the adoption of the technologies for the radiation decontamination of frozen food products, two questions had to be answered:

- whether the characteristic for the GAD dosimeters, simple relation between the absorbed dose and the measured parameter (the optical density) at room temperatures, is preserved at temperatures below 0 °C;
- whether there exist quantitative differences in the response of the dosimeters at temperatures below and above 0 °C and whether the calibration curves obtained for room temperatures could be used at low irradiation temperatures as well.

2. EXPERIMENTAL

2.1. GAD dosimeters characteristics

The GAD dosimeters are cast PVC films, yellow in colour, containing azodyes. There are four types of GAD radiochromic film dosimeters:

- GAD 1 - 0.100 mm thick, with 4-methoxy-4'-dimethylazobenzene in concentration 0.25 wt%, useful dose interval 0.05 - 2 kGy, colour changes through orange to red with irradiation;
- GAD 2 - 0.100 mm thick, with 4-dimethylaminoazobenzene in concentration 0.25 wt%, useful dose interval 0.05 - 2 kGy, colour changes through brown to violet with irradiation;
- GAD 4 - 0.055 mm thick, with 4-methoxy-4'-dimethylaminoazobenzene in concentration 0.5 wt%, useful dose interval 0.5 - 5 kGy, colour changes through orange to red with irradiation;

* Work partially supported by IAEA research contract No. 8528.

- GAD 6 - 0.025 mm thick, with 4-methoxy-4'-dimethylaminoazobenzene in concentration 1 wt%, useful dose interval 1 - 10 kGy, colour changes through orange to red with irradiation.

The dosimeters are stored at room temperature in light-proof paper packages before and after irradiation.

2.2. Optical measurements

The parameter of the dosimeters under evaluation is optical density measured 24 hours after the irradiation on a spectrophotometer Specord UV-Vis at λ=555 nm with accuracy of 1%.

2.3. Calibration

The investigation of the stability of the dosimeter response with time has shown that the GAD dosimeters can be supplied with two calibration curves, constructed 1 hour and 24 hours after irradiation. In the present investigation, calibration of each batch was done 24 hours after irradiation.

The irradiation was done in a laboratory gamma-installation "Issledovatel", with the volume of the irradiation chamber of 4 L. The position of the dosimeters (three for each dose) in the chamber was fixed by a specially constructed device. The dose rate in this position is determined by chlorobenzene dosimetry and by alanine dosimeters supplied by the IDAS of the IAEA. On May 15 1997, the measured dose rate was 1.66±0.07 kGy/h.

The uncertainty of the calibration at room temperatures (20 - 25 °C) is about to 5 %, while the overall uncertainty of the measurement with the dosimetry systems is 10 % at 0.95 confidence level.

2.4. Irradiation

In order to keep the irradiation temperature comparatively constant, especially below 0 °C, a thermos flask was used with double walls filled with alcohol and hermetically closed. The temperature of alcohol was fixed before pouring it into the flask - by heating or cooling. The alcohol temperature during irradiation was monitored by a digital thermometer connected to a thermocouple immersed into alcohol. Its accuracy was ±0.1°C. A series of preliminary experiments were carried out in order to follow the change of the temperature in the chamber with time. It was established that the temperature rise was about 1°C per hour in the low temperatures interval. For irradiation at room temperature, the rise was insignificant. A procedure was established to replace alcohol, after an increase of 2 °C, with a new portion with the appropriate temperature. This had to be done for doses above 2 kGy.

The dosimeters were placed in a glass vessel with a volume equal to that of the calibration volume of the device and with a fixed position in the thermos flask. The vertical deviation was less than ±2%. The films in their packages were placed into the vessel and then the latter was immersed into alcohol. Three dosimeters were used for each irradiation. Several batches from each type of GAD dosimeters were checked.

Figures 1 to 4 present the calibration curves of two batches for each of the four types of dosimetry systems, constructed 24 hours after the irradiation at room temperature.

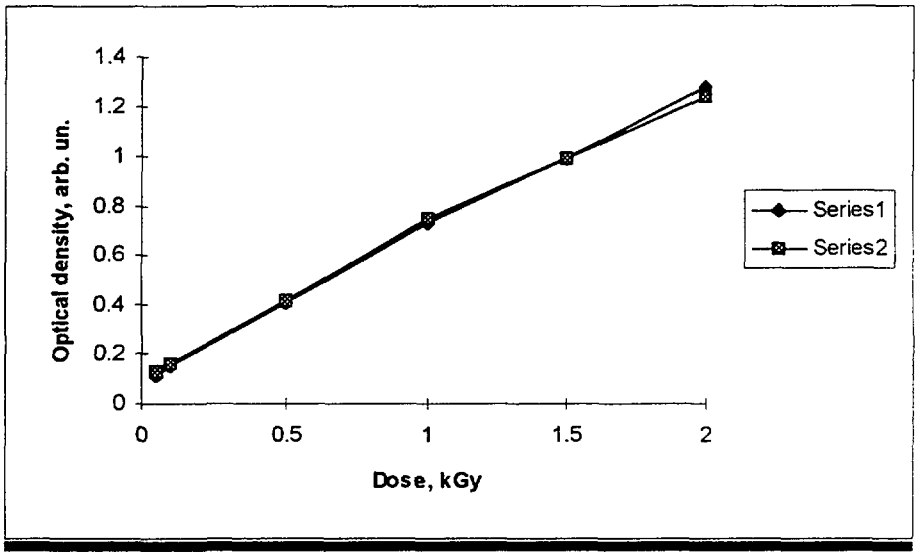

FIG.1. Calibration curves of GAD 1, batch No. 15 (series 1) and 17 (series 2)

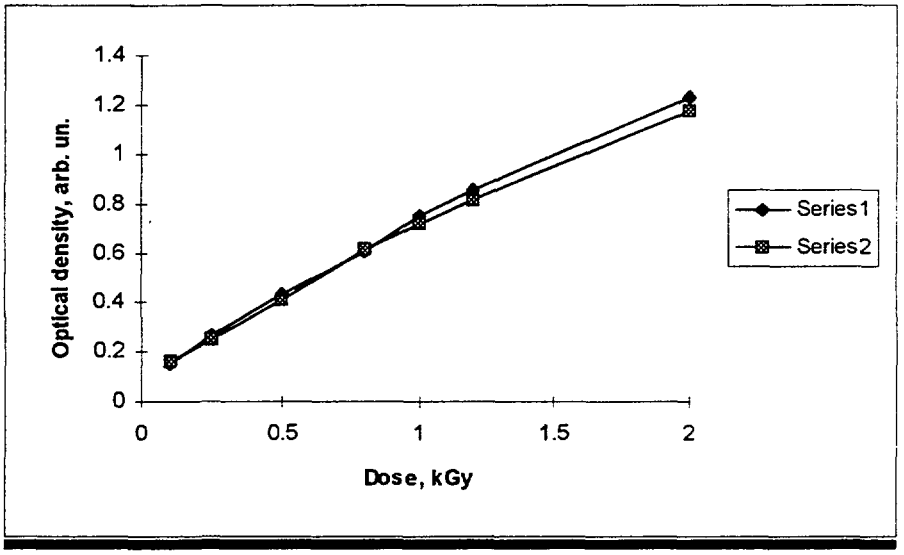

FIG.2. Calibration curves of GAD 2, batch No. 18 (series 1) and 20 (series 2)

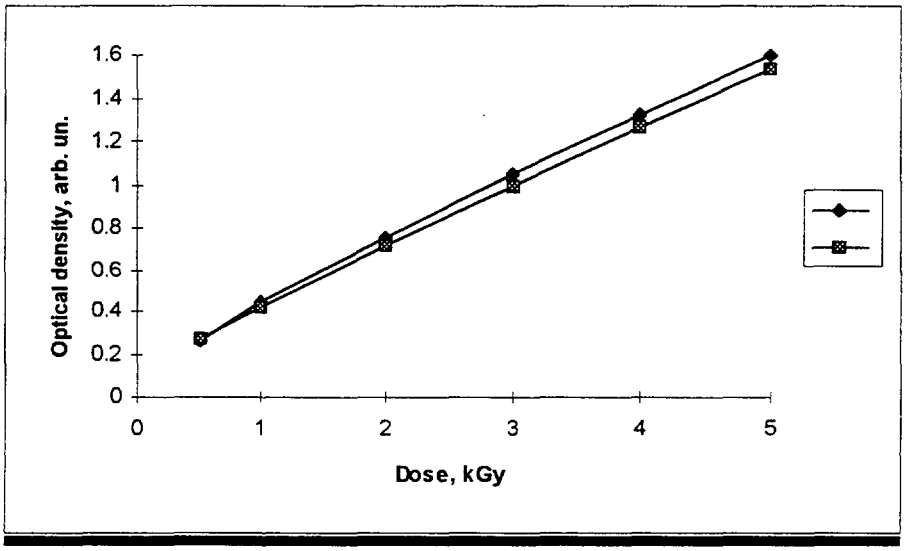

FIG.3. Calibration curves of GAD 4, batch No. 9 (series 1) and 21 (series 2)

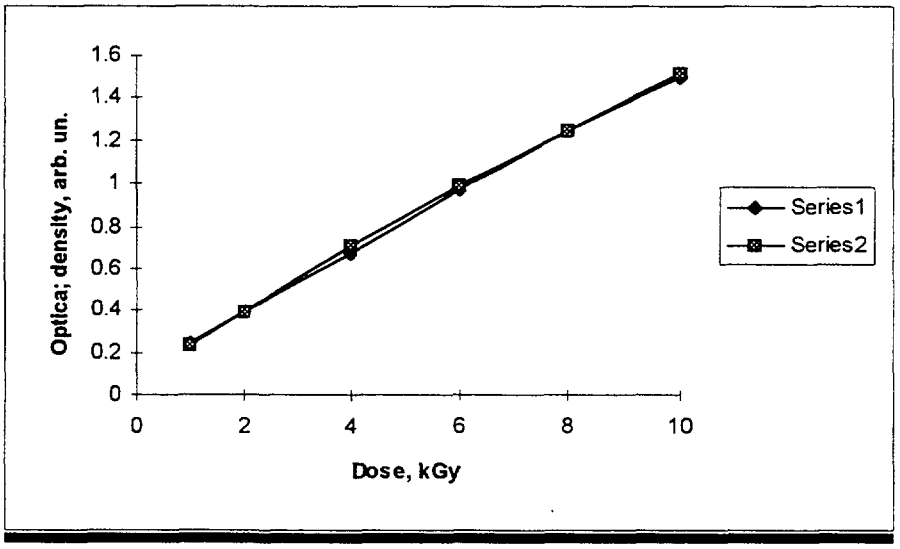

FIG. 4. Calibration curves of GAD 6, batch No. 24 (series 1) and 12 (series 2)

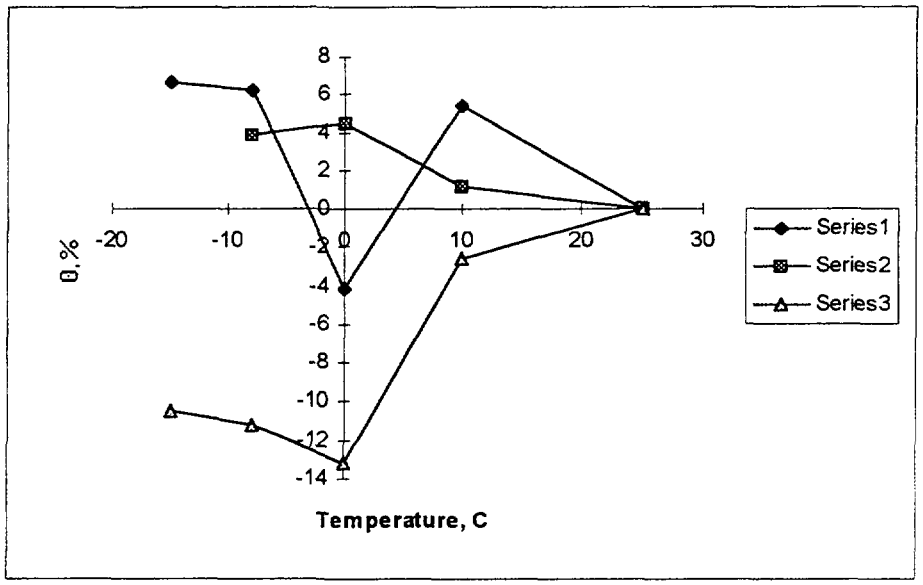

FIG. 5 Quantitative parameter θ vs temperature of irradiation for GAD 1 series 1 - 0.45 kGy, series 2 - 1 kGy, series 3 - 2 kGy

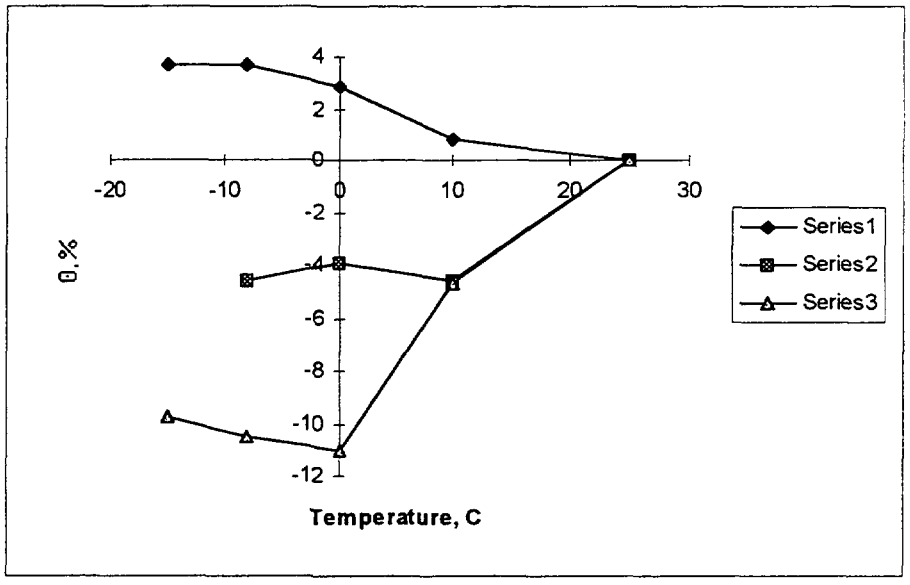

FIG 6. Quantitative parameter θ vs temperature of irradiation for GAD 2 series 1 - 0.45 kGy, series 2 - 1 kGy, series 3 - 2 kGy

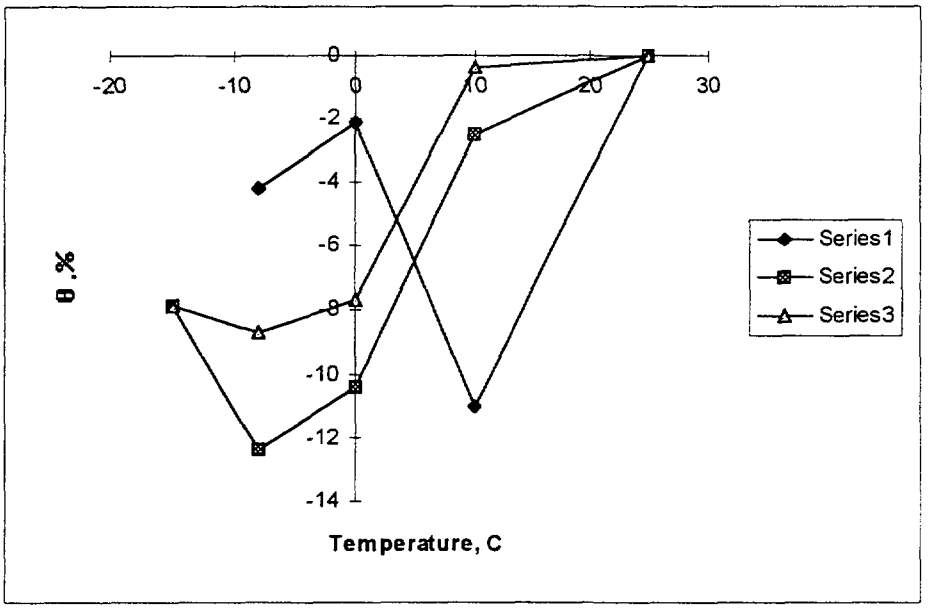

FIG. 7. Quantitative parameter θ vs temperature of irradiation for GAD 4 series 1 - 1 kGy, series 2 - 2 kGy, series 3 - 5 kGy

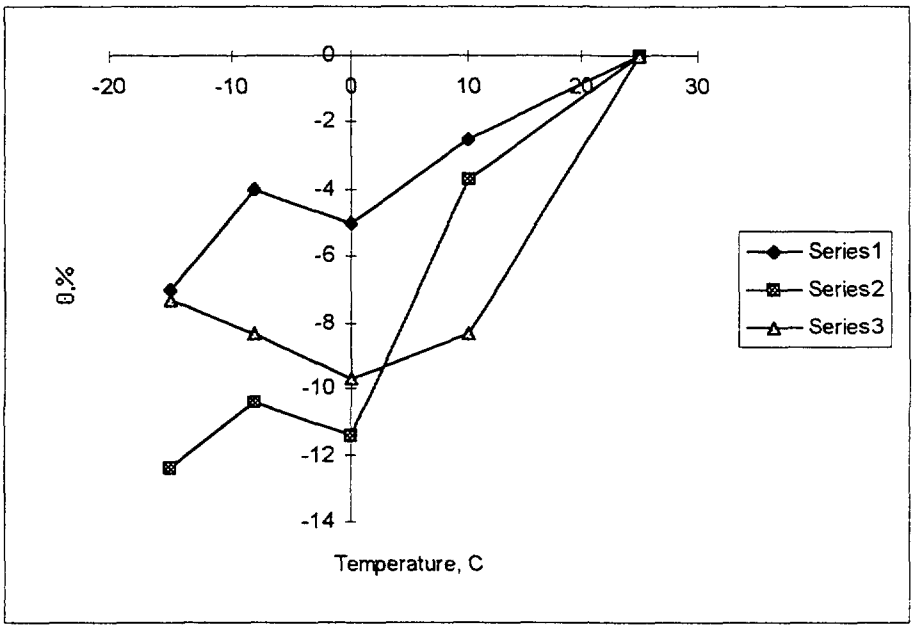

FIG. 8. Quantitative parameter θ vs temperature of irradiation for GAD 6 series 1 - 2 kGy, series 2 - 5 kGy, series 3 - 7.5 kGy

3. RESULTS AND DISCUSSION

To make the quantitative estimation of the effect of the irradiation temperature on the dose measurements, the deviation θ was calculated for each irradiation for the corresponding temperature as in Eq. (1):

$$\theta\ (\%) = (\ D(T) - D(25°C)\ )/\ D(25°C) \qquad (1)$$

where, D(T) - the dose absorbed at temperature T and calculated from the calibration curve for 25 °C,
D(25 °C) - the dose absorbed at 25 °C and calculated from the calibration curve for 25 °C.

This parameter represents the error introduced in the measured dose value at various irradiation temperatures by the use of the calibration relationship determined at the room temperature (20-25 °C). Figures 5 to 8 illustrate the values of θ for the four types of dosimeters.

The sources of uncertainty for the experiments, including the characteristics of the used dosimeter batches, were investigated, and it was established that all the factors affecting the experiments at temperatures 20-25 °C lead to a maximum uncertainty of 7%. Thus, any value of the deviation θ above 7% could be attributed to the effect of the irradiation temperature.

It can be observed for GAD 1 (batch No 39) and GAD 2 (batch No 41) that all the deviations are below 7 % on the first and second dose levels (doses below 1 kGy). While for the third dose level, the deviations at low temperatures vary from about -10 to -14 %. Similar results have been obtained for the other investigated batches and they are not shown here.

The results for GAD 4 (batch No 36) and GAD 6 (batch No 31) are some what similar to those for GAD 1 and 2 for temperatures below 0 °C – below 1 kGy (the first dose level), the quantitative parameter θ is less than 7 %, while for higher doses its values are -8 to -12.4 % . For temperatures above 0 °C, the values of θ vary from -2.1 to -11 % for GAD 4 while for GAD 6 they remain below 7 % on the first dose level. For higher doses, θ continuously decreases with the increase of the temperature from its values at 0 °C . The other investigated batches showed a similar tendency in the behaviour of θ.

4. CONCLUSIONS

The results from the investigation of the effect of the irradiation temperature on the response of the dosimeters and on the dose measured with the dosimetry systems lead to the following conclusions:

- the four types of GAD dosimeters can be used for dosimetric measurements at temperatures below 0 °C;
- a dependence of the response of the dosimeters on the irradiation temperature has been established. It varies with the dose interval and with the batch;
- the calculation of the dose absorbed at temperatures below 0 °C using the calibration curve for 20-25 °C leads to considerable deviations from the true values;
- the introduction of a temperature coefficient is not recommended, since the temperature effect depends on the dose and on the temperature interval;
- calibration of the dosimeters under the conditions of their possible application is recommended ;
- the behaviour of the quantitative parameter θ suggests the possibility of constructing a single calibration curve that is valid for the entire interval of temperatures from -18 to 0 °C

ACKNOWLEDGEMENTS

The authors would like to thank Mr. Kishor Mehta for the most helpful discussions. They also greatly appreciate the financial support by the IAEA Project No. 8528.

EFFECT OF THE IRRADIATION TEMPERATURE AND RELATIVE HUMIDITY ON PVG DOSIFILM*

Haishun JIA, Wenxiu CHEN, Yuxin SHEN
Department of Chemistry,
Beijing Normal University,
Beijing, China

Abstract

The effect of environmental factors, such as irradiation temperature and relative humidity, on the PVG dosifilm irradiated by EB was tested. Experiments show that the temperature coefficient of irradiated PVG dosifilm was 0.008 $°C^{-1}$ from 20 °C to 55 °C, and the humidity coefficient was 0.006 per r.h. (%) from r.h.0% to 76 %. The PVG dosifilm can be used as a routine dosimeter for dose measurement for low-energy EB processing. The absorbed dose values for various irradiation temperature and humidity can be corrected based on experimental data.

1. INTRODUCTION

The environmental factors affected the measurement accuracy of the dosifilm, which was used for quality control of irradiation processing. For example, the relative humidity below r.h. 20 % has less effect on the response of undyed PMMA dosimeter, but the response decreased significantly above r.h. 80 % [1, 2, 3]. During irradiation temperature below 30 °C, the response of the PMMA dosimeter seemed independent of temperature, however, above 30 °C, the response decreased[4]. For other dosifilms, such as CTA, radiochromic dosifilm, alanine dosimeter, the dose response was also affected by irradiation environment [5-9]. For these reasons, the effects of temperature and relative humidity during irradiation on PVG dosifilm were investigated.

2. EXPERIMENTAL

A water jacket for sample irradiation, with recycle water from a thermostat for keeping a given constant temperature during irradiation, was used to examine the effect of irradiation temperature (see Fig. 1). The temperature values were read out from both thermometers (1 and 2) which were put in the inlet and outlet of water jacket, respectively. In front of the dosifilm, the thickness of the wall material (plastic) of the water jacket plus the thickness of the water layer was 10 mm. The temperature difference between both thermometers for each given temperature was less than 0.5 °C during irradiation.

Several plastic vials with various relative humidity for PVG dosifilms irradiation were prepared as Fig.2. The relative humidity was 0 %, 33.6 %, 54.9 % or 75.7 % in each vial. Three PVG dosifilms were placed in each vial with a given relative humidity at least one day before irradiation.

Irradiations were performed by LINAC model BF-5 with electron energy of 4 MeV (±5%), and the current intensity of 100 μA. Dose was calibrated by calorimeter and dichromate dosimeters.

Absorbance on PVG dosifilms was measured by DMS-300 spectrophotometer, Varian Ltd. USA at least one day after irradiation.

---

*Present work supported by research contract 8580/RB, IAEA.

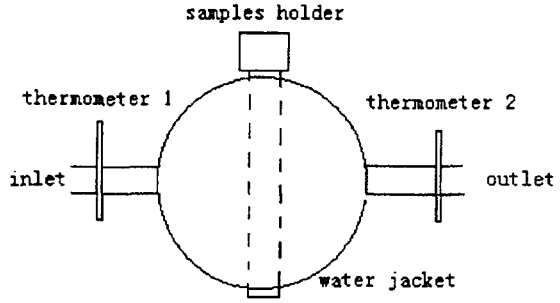

FIG. 1. Temperature controllable water jacket with thermometers and recycle water from thermostat.

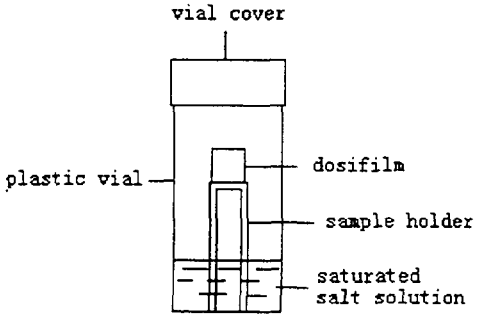

FIG.2. Plastic vial for PVG dosifilm irradiation with a given relative humidity at various doses.

3.RESULTS AND DISCUSSION

3.1. Temperature effect on EB irradiated PVG dosifilm

PVG dosifilms were irradiated with dose from 1 kGy to 55 kGy at a given temperature in the water jacket. Absorbed dose was calibrated by dichromate dosimeter and calorimeter. As shown in Fig.3, the relationship between the absorbed dose and the specific net absorbance ($\Delta A/Thickness\ (mm^{-1})$) depends on the irradiation temperature. At 20 °C (curve with symbol ■), this relationship can be expressed as shown in Eq. (1):

$$\Delta A/Thickness_{(20°C)}\ (mm^{-1}) = 0.49 + 0.79 \bullet D - 0.002 \bullet D^2 \quad (1)$$

where, D is the absorbed dose (kGy).

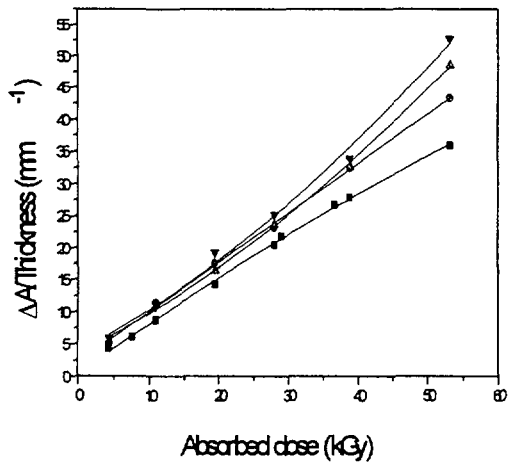

FIG 3. ΔA/Thickness (mm^{-1}) vs. absorbed dose at different irradiation temperature. ■:20 ℃, ●:35 ℃, ▲:45 ℃, ▼: 55 ℃.

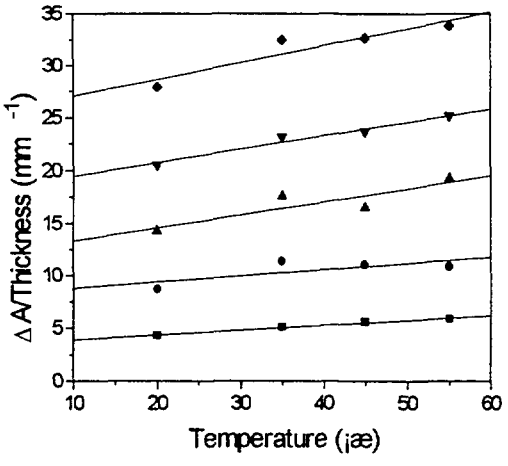

FIG. 4. ΔA/Thickness (mm^{-1}) vs. irradiation temperature at various absorbed dose. ■:4.3 kGy, ●:11 kGy, ▲:19.5 kGy, ▼: 29 kGy ◆:39kGy

TABLE I. THE EXPERIMENTAL VALUE ΔA/Thickness $_{(t°C)}$ (mm^{-1}) OF PVG DOSIFILM AND CALCULATION VALUE BY EQUATION (2) AT VARIOUS TEMPERATURES.

Irradiation	10.9 kGy		19.4 kGy		28 kGy		39 kGy	
temperature °C	ΔA/Thickness (mm^{-1})		ΔA/Thickness (mm^{-1})		ΔA/Thickness (mm^{-1})		ΔA/Thickness (mm^{-1})	
	[1]Exp.	[2]Cal.	[1]Exp.	[2]Cal.	[1]Exp.	[2]Cal.	[1]Exp.	[2]Cal.
20	8.75	[3]8.82	14.26	[3]14.92	20.54	[3]20.83	27.92	[3]27.42
35	11.4	10.06	17.6	16.4	23.2	23.62	32.5	32.11
45	11.1	10.94	16.5	17.82	23.7	25.67	32.7	34.9
55	10.9	11.81	19.3	19.25	25.2	27.73	33.9	37.69

[1]Exp. = experimental values, [2]Cal. = the values calculated by Eq. (2),

[3]data = the values calculated by Eq. (1).

This indicates that the relation of ΔA/Thickness (mm^{-1}) vs. absorbed dose is sublinear. Curves with symbol ●*(35°C)*, ▲*(45°C)*, and ▼*(55°C)* in Fig. 3 showed that at the same dose the specific net absorbance of the irradiated PVG dosifilm increased with the increasing irradiation temperature. The specific net absorbance of the PVG dosifilm vs. irradiation temperature for various doses are shown as Fig. 4. Experiments showed that the temperature coefficient of the PVG dosifilm from 20 °C to 55 °C *was approximately +0.008* $°C^{-1}$. *The value of* ΔA/Thickness (mm^{-1}) at any temperature can be expressed by Eq. (2):

$$\Delta A/Thickness_{(t°C)}\ (mm^{-1}) = \Delta A/Thickness_{(20°C)}\ (mm^{-1})\ [1 + (t\ °C - 20) \times 0.008] \qquad (2)$$

where, $\Delta A/Thickness_{(t°C)}$ (mm^{-1}) is the specific net absorbance at t°C irradiation temperature.

The comparison of the experimental values and the calculated values of ΔA/Thickness $_{(t°C)}$ (mm^{-1}) on PVG dosifilm from Eq. (2) and Eq. (1) are listed as Table I. At 20°C, the deviation between [1]Exp and [3]data was around ± 2%. It was determined from the experimental uncertainties i.e. it was the deviation from the regression Eq. (1). Also, the deviation between [1]Exp with [2]Cal values was around ±5 %. This was determined by the experimental and temperature corrections. This value is less than 10 %, i.e. less than the uncertainty of the routine dosimetry. So this [2]Cal. value of ΔA/Thickness $_{(t°C)}$ (mm^{-1}) was adequate for conversion into dose value by Eqs (2) and (1).

3.2. Relative humidity effect on EB irradiated PVG dosifilm

The relationships of ΔA/Thickness (mm^{-1}) vs. dose for various relative humidities are shown in Fig. 5. It indicates that, at the same dose, ΔA/Thickness (mm^{-1}) value increases with relative humidity from r.h.0% to 76%; the humidity coefficient is calculated to be 0.006 per r.h.(%). The change of ΔA/Thickness (mm^{-1}) value for various doses from r.h. 0 % to 33.6 % is less than 4%; therefore, the effect of relative humidity on the irradiated PVG dosifilm can be neglected below r.h.33.6% and below 25 kGy. However, at higher relative humidity the effect cannot be neglected, i.e. the response of the dosifilm must be corrected by the coefficient 0.006. If the dosifilm is kept in a dry container with lower relative humidity before and after irradiation, and irradiated in a sealed package, the correction for relative humidity can be neglected.

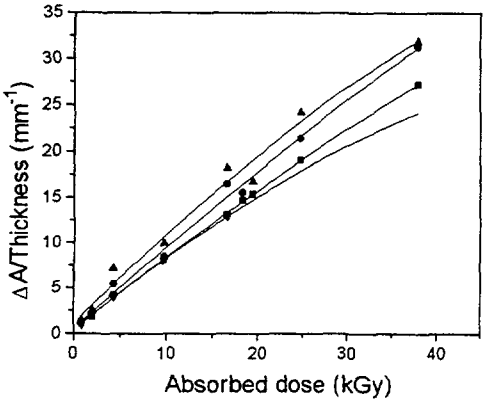

FIG. 5. Specific net absorbance vs. absorbed dose at various relative humidity. ▼: r.h. 0%, ■: r.h. 33.6%, ●: r.h. 54.9%, ▲: r.h. 75.7%.

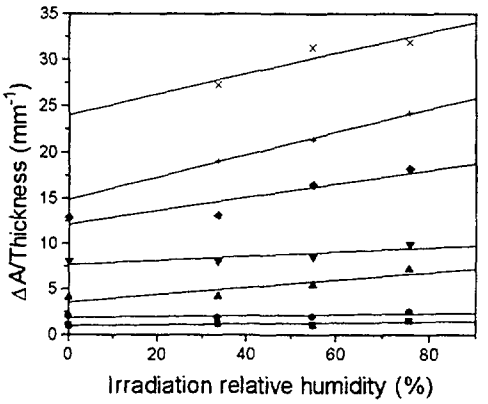

FIG. 6. Specific net absorbance vs. relative humidity at various absorbed dose.
■:0.8kGy, ●:2kGy, ▲:4kGy, ▼: 10kGy, ◆:17kGy, ✚: 25kGy, ✖:38kGy.

4. CONCLUSION

The influence on the specific net absorbance value for various irradiation temperature or humidity conditions was determined on the EB irradiated PVG dosifilm. At 20 °C, the absorbed dose can be calculated from the specific net absorbance of the irradiated PVG dosifilm by Eq. (1) up to 150 kGy. For other temperatures, the $\Delta A/Thickness_{(20°C)}$ can be calculated from $\Delta A/Thickness_{(t°C)}$ by Eq. (2) using experimental temperature coefficient 0.008 $°C^{-1}$. The relative humidity effect on the irradiated PVG dosifilm can be neglected below r.h.30%, but the correction is necessary at higher relative humidity values by the coefficient 0.006.

Experiments showed that the PVG dosifilm can be used as a routine dosimeter for electron beam irradiation processing.

REFERENCES

[1] BARRETT J. H., SHARPE P. H. G., STUART I. P., "An investigation over the range of conditions occurring in radiation processing plants, of the performance of routine dosimetry of the type based on polymethylmethacrylate",*Part 1 NPL Report RS 49* (1980). UK

[2] BARRETT J. H., SHARPE P. H. G., STUART I. P., "An investigation over the range of conditions occurring in radiation processing plants, of the performance of routine dosimetry of the type based on polymethylmethacrylate",*Part2, NPL Report RS 52*(1981)

[3] CHADWICK K. H., "The effect of humidity on the response of HX dosimetry Perspex to radiation"' *Research in radiation Processing Dosimetry, IAEA Tech. Doc.* (1985) 321, *Report of Coordination Meeting,* Munich, 1983 (Vienna, IAEA)

[4] MILLER A., McLAUGHLIN W. L., "Evaluation of radiochromic dye films and other plastic dose meters under radiation processing conditions", *In High-Dose Measurements in Industrial Radiation Processing. Tech. Report Ser. No. 205*, IAEA, Pub. STI/DOC/10/205, 219 p.119 IAEA (1981).

[5] LEVINE H., McLAUGHLIN W. L. MILLER A., "Temperature and humidity effect on the gamma-ray response and stability of plastic and dyed plastic dosimeters", *In Advances in Radiation Processing Vol.11, Transaction of 2nd International Meeting.* Miami 1978, edited by Silverman J., *Radiat. Phys. Chem., 14,551* (1979)

[6] TANAKA R., MITOMO S. TAMURA N., "Calculation of longitudinal dose non-uniformity with simultaneous product movement and beam scanning in industrial electron irradiation" *Int J. Appl. Radiat. Isotopes 35,875* (1984)

[7] SHAFFER H. L., GARCIA R. D., "Practical application of dosimetry systems utilized in radiation processing of medical devices", *In progress in Radiation Processing. Vol.II, Proceedings of 6th International Meeting*, Ottawa 1987, edited by Fraser F. M., *Radiat. Phys. Chem. 31,497* (1988)

[8] HASAN M. KHAN, LIAN S. WAHLD, "Effects Temperature and Humidity during Irradiation on the Response of a Film dosifilm", *Proceedings of the 9th International Meeting on Radiation Processing, Part 2*, 11-16 Sept. 1994, Istanbul, Turkey. *Radiat. Phys. Chem. 46(4-6) p.1207* (1995)

[9] McLAUGHLIN W. L., PUHL J. M., MILLER A., "Temperature and Relative Humidity Dependence of Radiochromic Film Dosimeter Response to Gamma and Electron Radiation" *Proceedings of the 9th International Meeting on Radiation Processing, Part 2*, 11-16 Sept. 1994, Istanbul, Turkey. *Radiat. Phys. Chem. 46(4-6) p.1227* (1995)

DEPENDENCE OF THE DOSE FIELD MEASUREMENT RESULTS ON DOSIMETRIC FILMS ORIENTATION FOR PRODUCTS IRRADIATED BY ELECTRON BEAM

XA9949721

L.P. ROGINETS, G.M. SAPOSHNIKOVA, S.A. TIMOFEEV, J.A. KHARITONJUK
Radiation Physics and Chemistry Problems Institute,
National Academy of Sciences,
Minsk-Sosny, Belarus

Abstract

The dosimetric films or tapes, for example standard sample of a dosimeter SO PD(F) 5/150 (Russia), are often used when dose fields are measured in a product irradiated by accelerator electron beams. The orientation of these films with respect to the beam direction may be fairly arbitrary. This is a source of a serious errors in the dose field measurement results, if that orientation is not taken into account. The error consists in an underestimate of the dose value up to 30-40 %. The error is maximum for an unscattered beam (near the boundary of target) and for the angle between the film plane and the beam direction smaller than 20-30° . Besides that, a mean square-root error in these cases is about a factor of 1.5 larger.

1. INTRODUCTION

Measurements of the dose fields in products irradiated by an accelerator electron beam are needed for the correct selection of the conveyor velocity, current and energy of beam, scanning length, size of a box and mode of product loading inside the box. Such measurements often are fulfilled with using the dosimetric films or tapes; in these cases their orientation are generally fairly arbitrary.

Some results obtained in practice force us to pay attention and to study the effect of film orientation on the obtained results. Since we do not have analogous information from literature or other sources we conducted several experiments to study this effect.

2. DESCRIPTION OF MEASUREMENTS AND ITS RESULTS

Investigations were carried out with the electron beam of linear accelerator UELV-10-10 with energy of 6.3 MeV. We used the standard dosimeter films fenazin SO PD(F) 5/150, produced and attested in NIIFTRI, Russia, with thickness of 0.060-0.065 mm. The value of dose is determined by the measurement of the optical density with a spectrophotometer SF-26 at a wavelength of 512 nm. First, the measurements of the dependence of the registered dose on the angle between the beam direction and the film plane were done in air. The measured dose was nearly constant between the angles 30 and 90°, but decreased quickly up to a factor of 1.4 as the angle decreased from 30° to 0° (see Fig. 1).

All further experiments were carried out with the dosimetric films oriented either parallel (II) or perpendicular (⊥) to the beam direction, and for various depths in different materials. The results of the measurements for a large block of light homogeneous foampolystyrol with a density 0.028 g/cm^3 and thickness 25 cm are presented in Fig. 2. At short distances from the boundary, the difference between the measured dose values may reach 100 %. The small rise in the dose value for both the (⊥ and II) dosimeters at distances of 20-25 cm is explained apparently by the backscattering from the aluminium tray of the conveyor system. It is important to note, that the precision of the measurements for II-films is worse than that for ⊥-films (see Fig. 3), and it increases as the distance is decreased.

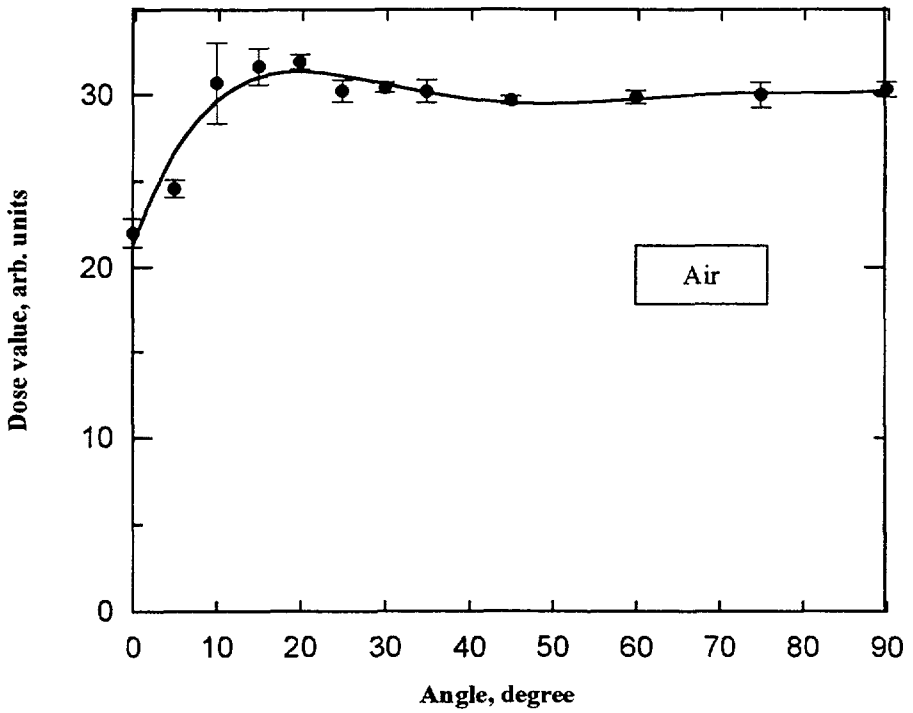

Fig. 1. Measured absorbed dose value versus angle between the dosimetric film plane and electron beam direction in air.

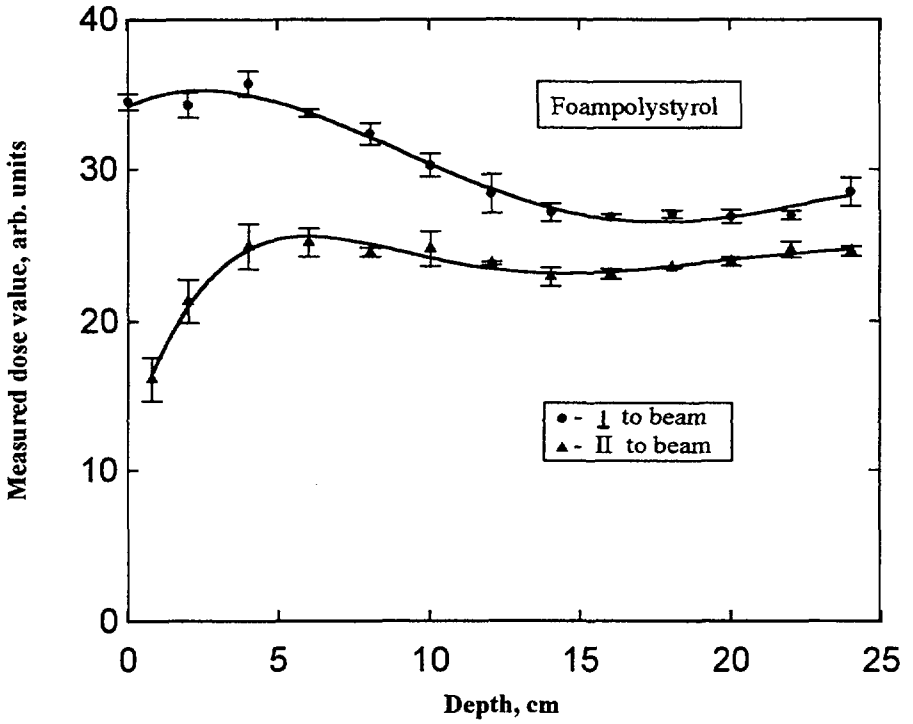

Fig. 2. Dependence of measured dose values on distances in foampolystyrol for two different dosimetric film orientations.

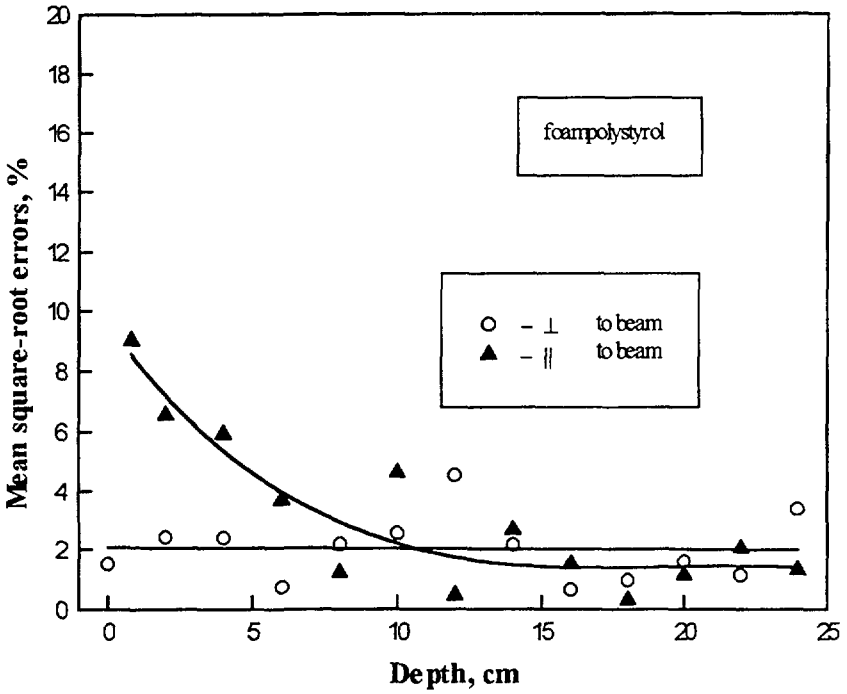

Fig. 3. Errors of dose value measurements versus distances in foampolystyrol for two different dosimetric films orientations.

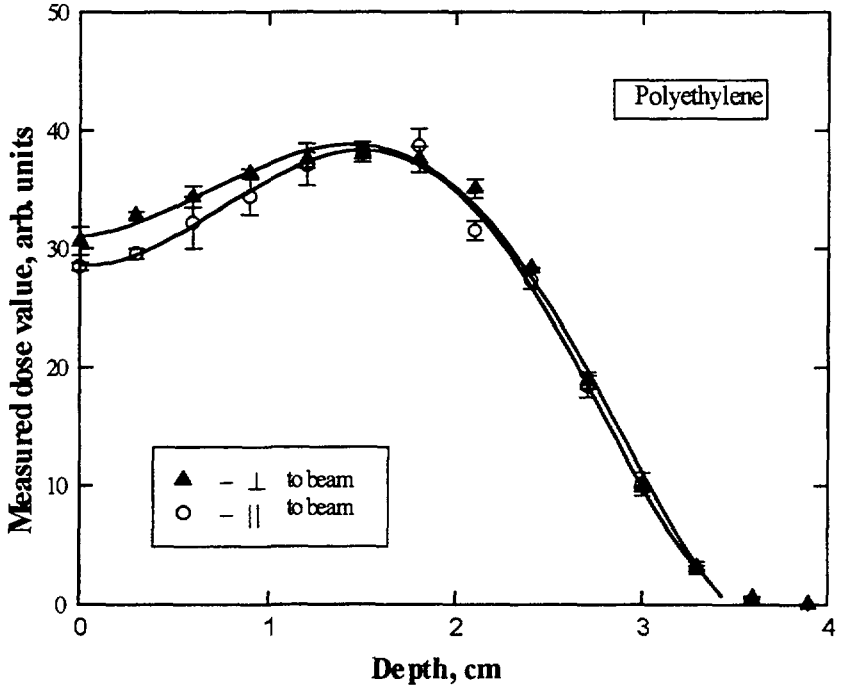

Fig. 4. Dependence of the measured dose values from distances in polyethylene for two different dosimetric films orientations.

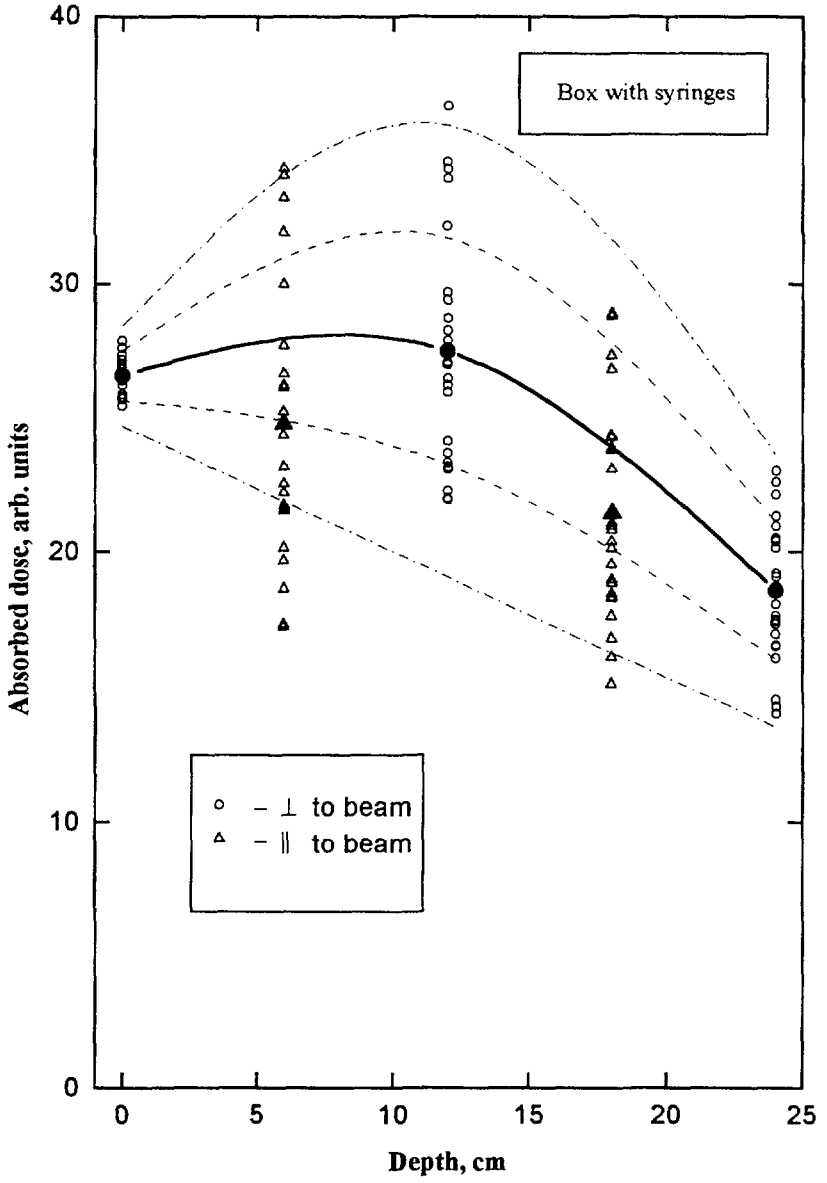

Fig. 5. The dose fields measured in a box with syringes with the dosimetric films with two different orientation. The lines represent measurements with the dosimeters oriented perpendicular to the beam; dash lines represent distribution width ($\pm\sigma$, $\pm 2\sigma$). The solid circles and triangles are mean values of the measured dose distributions.

Analogous measurements were made for a more dense medium, such as polyethylene with density 0.95 g/cm^3 (see Fig. 4). That tendency is observed here as well. The dosimetric films, mounted parallel to the beam direction, in all measurement cases of unscattered beam, have not only smaller dose value, but have a worse precision, up to 20-50 %.

In Fig. 5, one can see the distortion that may be introduced into the dose field measurement results if the dosimetric films with different orientation are used. For example, consider a box 37x37x23 cm^3 with disposable syringes (400 pieces x 5 ml), organized in two storey (2 x 200 pieces) at vertical position. The dosimetric films were placed in a plane matrix 5 x 5 covering the box completely. Five matrix were placed at equal distances and oriented perpendicular to the electron beam; the film

themselves were mounted perpendicular to the beam at the top, middle and the bottom of a box, and along the electron beam direction in rest of the two planes. The mean dose value, measured by the films oriented parallel to beam, obviously is smaller compared to that measured by films oriented perpendicular to beam. They also exhibit a more wide distribution of individual values. Using all the measured data independent of the film orientation and without critical approach will lead to the incorrect results and incorrect choice of irradiation mode of operation.

3. CONCLUSION

Use of the dosimetric films, such as SO PD(F) 5/150, may lead to error in the measured results if the film orientation with respect to the electron beam is not taken into account. Dosimetric films mounted parallel to the beam will register smaller dose values than the films oriented perpendicular to the beam. That difference is larger in light media. The precision is worse for the films parallel to the electron beam axis.

To avoid or to minimize the error connected with the film orientation, it is necessary to use the films under conditions that are close to those during their calibration. It is obvious that the effect is connected with the dosimetric film geometry, however, it is advisable to conduct analogous investigations with other types of dosimeter, having similar geometry (films, tapes or plates). It is interesting also to extend the measurements to other electron energies.

MEDICAL AND OTHER APPLICATIONS

(Session 5)

Chairperson

T. KOJIMA
Japan

Invited Paper

XA9949722

EPR DOSIMETRY—PRESENT AND FUTURE

D.F. REGULLA
GSF—National Research Centre for Environment and Health,
Institute of Radiation Protection,
Neuherberg, Germany

Abstract

In the past, IAEA has played a central role in stipulating research and development in EPR high-dose standardisation as well as co-ordinating and organising international dose intercomparison programs, within the Member States of the United Nations from the mid-seventies till today. The future tasks of EPR dosimetry seem to tend towards different subjects such as biomarkers, biological radiation effects, post-accident dose reconstruction in the environment, and retrospective human dosimetry. The latter may be considered a promising tool for epidemiology on the way to re-define radiation risk of man for chronicle radiation exposures, based on e.g. South Ural civil population and radiation workers. There are on-going international activities in the field of standardising high-level dosimetry by the American Standards on Testing and Materials (ASTM), and the International Organisation of Standards (ISO) as well as those of the International Commission on Radiation Units and Measurements (ICRU) considering the establishment of relevant recommendations concerning industrial radiation processing, but also human dose reconstruction.

1. INTRODUCTION

High-level application of ionising radiation from 10^3 to 10^6 Gy was described in the early seventies. The growing field of industrial radiation processing, under the aspects of safety and economy, was soon recognised to require a reliable and accurate dosimetry [1]. There were dosimetry techniques available at that time, but traceability to primary standards, access to national calibration services or availability of international recommendations on standardisation of high dose dosimetry were missing.

It was in 1977 that the Agency took initiative and invited international experts to discuss new methods of dosimetry and standardisation in radiation processing at the occasion of a Consultants' Meeting on High-Dose Standardisation and Intercomparison for Industrial Radiation Processing [2]. Decision was taken to accept a proposal of the author and implement a "new" technique based on radiation induced generation of radicals in an amino acid, i.e. alanine [3]. Electron paramagnetic resonance (EPR) spectrometry was chosen for quantification of the radical concentration. Within the subsequent IAEA co-ordinated research programme, EPR became a scientific tool for dosimetric application in routine and metrology [4,5]. Later, the Agency established the International Dose Assurance Service (IDAS) to the member states of IAEA using the meanwhile standardised alanine/EPR technique. IDAS was operated jointly between IAEA and GSF [6]. Since 1991 the Agency continues to offer IDAS successfully as an exclusive service supplier [7,8].

This paper does not deal with archaeological and geological dating [9,10] nor with EPR imaging [11]. It should however be noted that it is particularly the task of geological dating for human sciences that stipulated great interest and initial progress in EPR dosimetry [12].

2. PRESENT STATUS

2.1.The Alanine/EPR system

Alanine/EPR dosimetry uses organic crystalline amino acids (e.g. alanine, CH_3-$CHNH_2$-COOH) as a sample material [3]. This method is applicable to dosimetry of different types of radiation as well as, within limits, to dosimetry in mixed radiation fields, e.g. x and gamma rays, beta radiation, accelerator electrons, protons [13], neutrons [14], and ions [15-18].

The free radicals in crystalline biomolecules are relatively stable interim products in a chain of events, that similar to tissue, start with the absorption of radiation energy. Since free radicals take key positions in the chain of events which lead to biological damage in cell structures, the quantification of free radicals in alanine can even be used for a biologically relevant dosimetry.

Accurate EPR dosimetry requires the availability of an appropriate "system" as well as qualified personnel with know-how, experience and care. The essential system components are: Alanine detectors of a high purity production and metrological quality, a high performance EPR spectrometer and an air-conditioned laboratory, calibration facilities in the respective dose range, as well as dosimeters of secondary standard or reference quality level, whose calibration is traceable to the primary standards of national laboratories (Fricke dosimetry, calorimetry, ionisation chamber dosimetry). Essential dosimetric properties for GSF alanine/EPR dosimetry system are compiled in Table I.

2.2. Radiation processing: Reference and transfer dosimetry

Meanwhile a number of acknowledged national laboratories world-wide started to use the alanine/EPR technique for quality control programs in radiation processing. The alanine/EPR technique has been introduced for quality control also in therapy [19] using the alanine/EPR technique similar to the IDAS programme [21,22]. Future applications will probably be based on a new EU Medical Devices Directive [20].

TABLE I. CHEMICAL, PHYSICAL AND DOSIMETRIC PROPERTIES OF GSF ALANINE/EPR DOSIMETRY SYSTEM

Composition	Alanine CH_3-$CHNH_2$-COOH (85 %) and paraffin (15 %)
Effective atomic number	$Z_{eff} \cong 7.2$ (tissue: $Z_{eff} \cong 7.4$)
Specific gravity	$\cong 1.15$ g/cm^3
Dimensions	4.9 mm in diameter × 10 mm length
Measuring quantity, D_w	Absorbed dose to water; otherwise on request
Measuring range	0.5 Gy < D_w < $5 \cdot 10^5$ Gy
Detection threshold	0.05 Gy
Dose rate dependence	Not detectable till to 10^{11} Gy·h^{-1}
Energy dependence	Approx. independent, for $E_{ph} \geq 100$ keV and $E_e \geq 1$ MeV
Irradiation temperature, θ	Negligible or correctable in the range -90°C < θ < +70°C ($k_\theta = 0.0018$ °C^{-1} for D ≤ 40 kGy)
Fading (signal loss) within 2 years	< 1 % at 22°C and <70 % r.h.
Interspecimen scattering	1 s.d. ≤ ± 0.5 %, within a batch
Interbatch scattering	≤ 1 %
Precision	u ≤ ± 1.5 % at 95 % confidence level, approved by a national laboratory intercomparison protocol
Electron/photon ratio of response	1.0, for $E_e > 1$ MeV
Neutron/photon ratio of response	about 0.6, for $E_n > 0.1$ MeV

2.3. Therapy-level dosimetry

The properties of alanine/EPR dosimetry have always been studied with an eye focusing on radiation therapy [23]. The advantages of alanine/EPR dosimetry in this field are evident, e.g. the dynamic dose range, the archival character of dose information based on a non-destructive readout that allows for repeated EPR measurements and sample storage, and the tissue equivalency of detector samples. The latter property makes the method applicable also in high-energy radiation dosimetry without the impact of perturbation and displacement effects as known from ionisation chamber dosimetry. A mathematical method based on Fast Fourier Transform has meanwhile been developed capable to filter simultaneously background and noise in the frequency domain of EPR spectra [24]; it provides significantly higher resolved alanine/EPR signals, and this down to about 50 mGy.

It was again the Agency which at an early stage had organised an alanine/EPR intercomparison in the therapy-level range [25]. Also, it recently convened a consultants' meeting to review the current status of use of alanine for therapy [26]. Complementary investigations are reported on the use of alanine EPR dosimetry in proton therapy [27,28].

2.4. Identification of irradiated food

For a long period of time there was a lack of appropriate identification methods of irradiated foodstuffs, however the situation has changed during the past decade [29]. A variety of methods has become available to evaluate on the status of radiation processing, or even roughly estimate the dose level, valid for irradiated spices and spice products, herbs, dried vegetables, some kind of fruits, coffee beans, different meats and meat products as well as fish, shell-fish, shrimps, etc. [30]. EPR spectroscopy is applicable to the identification of irradiated foods, for discrimination against unirradiated foods or exclusion of two- or more-fold food irradiations [31-36]. Some food allows an EPR dose assessment within ≤ 5 % [37]. For a relevant Food Control Dosimetry Network based on EPR, standard EPR spectra from the above foods should be available to be transferred for calibration and measurement, between laboratories and authorities involved by internet.

2.5. Ultra high-level dosimetry

Since material fatigue of radiation sensitive components is an imported factor in nuclear fuel safety, it should carefully be checked before the components are implemented in the facility construction, and be under continued control during operation. Dose control by an appropriate dosimetry technique is inevitable for this task. For quantification of doses up to 10^8 Gy and above, EPR spectroscopy based on crystalline detectors was developed for irradiation temperatures of up to several hundred degrees Celsius [38,39] and verified by Monte Carlo based simulation of the radiation transport [40].

2.6. Standards and recommendations

Principles, procedures and quantities used in the alanine/EPR technology are described in an ASTM standard [41] which is now also a recognised ISO standard [42]. ICRU is presently considering to establish a task group on "Dosimetry in Industrial Uses of Ionising Radiation" [43,44]. An ICRU recommendation in this field would be of great interest and need, for public acceptance, benefit and health as far as dosimetry is concerned for radiation preserved food, sterilised pharmaceuticals, and medical and health care products [29]. IAEA and other international and national bodies, e.g. WHO, FAO, CEC and FDA, should be invited to contribute to the recommendation with their great expertise and the available technical documents, particularly in the field of EPR dosimetry.

2.7. EPR spectrometry

Alanine/EPR dosimetry uses sophisticated research EPR spectrometers in the X band microwaves. The state of the art of this equipment, in course of time, and its future potential are described by Ettinger [45], Pilbrow [46] and Ikeya [47]. Routine dosimetry makes use of meanwhile available

table-top EPR spectrometers with permanent magnets. Interesting parametric improvement of equipment as well as procedures has recently been proposed [48,49]. A pitch-activated alanine detector type [50] or the use of an in-cavity Mn^{++} standard [51] offer approaches to introduce individual calibration factors for alanine samples. The use of a continuously rotating goniometer reduces the effect of response anisotropy and results into reduced detection limits [52]. Large-scale alanine dosimetry services in national or international quality control may profit from automatic sample changing devices by robot [53] or magazine type mechanisms [54]. Future *in situ* oriented biophysical dosimetry will make use of EPR spectroscopy applying different microwave bands and magnetic field strengths [55,56].

3. FUTURE TASKS

EPR spectroscopy started playing a role in tooth dosimetry in the late seventies addressed to victims of Hiroshima and Nagasaki. Since scientists started in the nineties to work on dose histories of individuals from the early nuclear production plants of the former Soviet Union, remarkable progress has been achieved in extending the lower detection limit for this material.

3.1. Biophysical dosimetry

So far, the most known biological dosimetry technique is based on chromosome analysis in peripheral human lymphocytes serving in cases of acute exposures, dose estimates above 100 mGy, and a number of victims for evaluation [57]. Further improvement is expected from the so-called fluorescence in situ hybridisation (FISH) method based on translocations [58,59].

Today the biophysical EPR dosimetry using tooth (and bone) samples from exposed victims may represent a potential completion of the biological dosimetry for reasons of accuracy, reliability, dose individuality and procedural simplification [60,61]. EPR dosimetry is based on radiation induced radicals in hydroxyapatite, which is the mineral phase of teeth and bones. The most stable radical known is CO_2^- [62], whose life time has been reported to be 10^7 years (at 25°C) [63]. At present, doses from about 50 mGy to above 100 Gy can be evaluated, which is the relevant range of potential accidental doses [64,65], including photon and electron radiation as well as potentially α-particles and ions [66].

3.2. Environmental dose reconstruction and accident dosimetry

Management of dose assessment from objects of man's environment can profit from the free radical generation in and EPR spectroscopy of many deserted objects [67], e.g. sugar [68], pharmaceuticals [69], egg shells [70,71], cellulose [72] and pot-scale [73]. In future, also the mineral phase of soil and bricks [74,75], building materials [76] and appropriate tissues of animals [77] will be considered more intensively. Subsequently, accidental doses of individuals can be derived from the material doses to the human environment by computational conversion if not directly assessed from teeth and bone samples [78-80]. Recently doses were evaluated using EPR methodology to individuals exposed to radioactive sources or radioactive scrap metal in public areas or in possession of private persons [81].

3.3. Retrospective dosimetry

Biophysical EPR dosimetry is on the way to become a tool of increasing interest for retrospective dosimetry, i.e. evaluation of individual exposures that occurred years or decades and more ago [82]. It was first described by Ikeya et al. for the atomic bomb survivors of Hiroshima and Nagasaki [83], later for victims of the Chernobyl accident [84,85], nuclear workers of the PO Mayak [64], and residents of the Techa river valley, the latter both in the Southern Ural region [86]. A valuable survey is given in [87]. ICRU has meanwhile established a working group in the field of retrospective dosimetry; the IAEA also has established a co-ordinated research project in the same field.

3.4. Uncertainties in retrospective dosimetry

Individual and environmental retrospective dosimetry may serve, e.g. for verification of dose records as a basis for epidemiological studies. Comparisons with risk data from Hiroshima and Nagasaki require careful consideration of uncertainties. The uncertainties cover, e.g., the EPR spectrometer, sampling, sample treatment and evaluation procedures, the impact of influence parameters (e.g. ultraviolet light, diagnostic x-rays; etc.), calibration, and the statistical treatment of data [88,89]. Future research tasks in this domain should focus unbiased scientific attention to identify component uncertainties and evaluate overall uncertainties [90-93].

4. PERSPECTIVES

4.1. Emergency network for dosimetry

The capability of EPR to contribute to emergency response dosimetry was recently under consideration [94] demonstrating a rapid analysis method for screening deciduous teeth of children in the days and weeks following a radiation accident [95]. Such a response could conceivably aid in medical and social decision making.

Also of importance are the savings of time and manpower and the increase in reliability which could be achieved in dose reconstruction if identification and collection of biological and environmental dosimetry materials were promptly undertaken. The complexity of reconstructing doses from a population years after an accident would be greatly reduced if consideration were given to the task immediately following an accident [96]. Protocols for such response are currently not available [97].

4.2. Basis for juridical consequences

EPR based dose reconstruction will compete and equally complement the established biological dosimetry in the future, particularly in accidental or emergency dosimetry cases. Contrary to biological methods, the biophysical methods will allow to evaluate doses reliably for all those exposures of humans which occurred decades and more ago. The achievements to be expected represent new perspectives for labour inspection authorities in cases of radiation accidents at work and for the juridical consequences in cases of prosecution or legitimate claims for compensation.

4.3. Epidemiology and redefinition of radiation risk

Interest in the new perspectives of EPR dosimetry will hold particularly also for retrospective dosimetry of individuals with long-term exposures where the traditional biological methods may be of limited use only, e.g. for the determination of exposures of radiation workers from nuclear centres starting in the forties. Individual retrospective dosimetry based on tooth tissues and bones, also for the verification of corresponding film dosimetry records, may help us together with available health records of those radiation workers, to redefine radiation risk for - contrary to the acute exposure in Hiroshima and Nagasaki - chronicle exposure of man. First evaluations showed a reduced risk for leukaemia [98].

4.4. *In vivo* and space dosimetry

On the horizon we may, in not a too far future, discover new techniques of EPR or magnetic resonance (MR) spectrometry for human *in vivo* dose evaluation [99] and local dose imaging after accidents, e.g. *non invasive* dosimetry from teeth, skeleton, cell membranes and other tissues capable to produce and store radiolysis products detectable with EPR spectrometry. This might probably lead to a presently still visionary development of a "whole body dose scanner", equivalent to the established whole body counter. The human body appears to represent a still widely undiscovered field for dosimetry - and an exciting reservoir for radiation research also in future [100].

Such dosimetry techniques lead to the further vision of an individual biodosimetry, e.g. for space missions, providing dosimetry that can not be lost, inappropriately handled or manipulated by an individual, and a permanent record of cumulative doses due to different radiation types [101,102].

5. CONCLUDING REMARKS

Present dosimetry techniques in radiation processing, including EPR, will in future be supplemented by new, e.g. radiofluorescence type, techniques for routine and quality control programmes [103,104]. For treatment planning of products the experimental dosimetry may be supplemented by dose computations based on source-target modelling. The necessary product parameters for absorption and scatter can be transferred from a central data bank, by the world wide web [105]. Its implementation shows new perspectives to exchange information between processing plants, trade companies, and authorities, and will make the radiation processing level of a product traceable. The internet can equally serve to check the local dosimetry quality of a processing plant by a future telemetrology, whose technique and logistics has still to be developed and established [106]. The internet will facilitate the exchange of dosimetry results, calibration and traceability certificates as well as of acceptance passports for products - to be verified by EPR dosimetry.

By contrast, the importance of EPR for biophysical dosimetry promises to expand in future. Unification and standardisation will allow individual dose reconstruction in emergency cases which tool was not available earlier [81, 107-115]. Apart from the mineral tooth enamel, it is the metabolic dentine which can probably provide additional EPR information on e.g. bone seekers. Also this potential will continue to keep scientific interest focused on EPR biophysical dosimetry in future [116,117].

The present duties of the world-wide SSDL network for radiation protection and radiation application in medicine could in principle be considered a basis for expansion to biophysical - accident and retrospective - dosimetry and a first step towards a concept of a world-wide operating "Integrated Retrospective Dosimetry Network" [94,118]. It could provide permanent assistance and expertise in biophysical dosimetry, probably in co-operation with other national or regional laboratories, that can offer biological dosimetry, whole body counting and bioassays, as well as thermally and optically stimulated luminescence dosimetry techniques for objects taken from an incidental environment (Fig. 1).

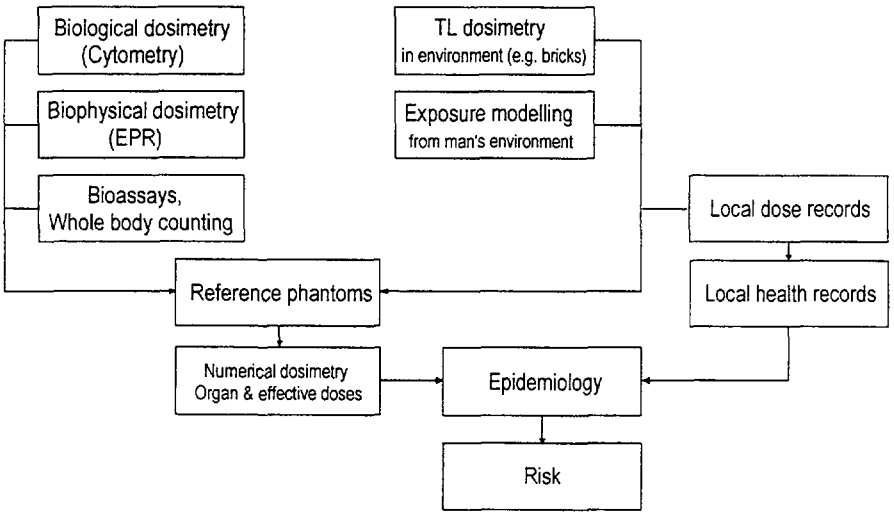

FIG. 1. Implementation of EPR biophysical dosimetry into a still visionary integrated retrospective dosimetry network, for further discussion [94,118].

REFERENCES

Part of the references refer to manuscripts presented at the recent "International Conference on Biodosimetry and 5th International Symposium on ESR Dosimetry and Applications", Obninsk/Moscow, Russia, 22-26 June 1998"; they are under process of peer-reviewing, and planned to be published in the International Journal of Applied Radiation and Isot. in 1999. Extended abstracts are available from the Conference Book of Abstracts (Prof. A. Tsyb, or Dr. Y. Skoropad, Medical Radiological Research Center of Russian Academy of Medical Sciences, Obninsk, email address: mrrc@obninsk.ru). A condensed review on the development and achievements of EPR dosimetry and applications in the past two decades can be found in: "ESR Dosimetry and Applications", Appl. Radiat. Isot. **40** (1989) 829-1246; **44** (1993) 1-468; and **47** (1996) 1151-1687, as well as in: "Retrospective Dosimetry - Physical and Biological Aspects", Radiat. Prot. Dosim. **77** (1998) 1-138.

[1] WORLD HEALTH ORGANIZATION, Wholesomeness of Irradiated Food, Report on a Joint FAO/IAEA/WHO Expert Committee 1980, WHO Technical Reports Series 659, Geneva (1981).

[2] High-dose Standardization and Intercomparison for Industrial Radiation Processing, Report of a Consultants' Meeting, IAEA, Vienna (1977).

[3] REGULLA, D.F., DEFFNER, U., Dosimetry by EPR spectroscopy of alanine. Appl. Radiat. Isot. **33** (1982) 1101-1114.

[4] SCHARMANN, A., ESR - A scientific tool for applications. Appl. Radiat. Isot. **40** (1989) 829-834.

[5] McLAUGHLIN, W.L., Radiation processing dosimetry - past, present and future, these Proceedings.

[6] NAM, W.J., REGULLA, D.F., The significance of the International Dose Assurance Service for radiation processing. Appl. Radiat. Isot. **40** (1989) 953-956.

[7] METHA, K., "Report of the Second Research Co-ordination Meeting (RCM) for the Co-ordinated Research Project (CRP E2 40 06) on Characterisation and Evaluation of High-dose Dosimetry Techniques for Quality Assurance in Radiation Processing", SSDL Newsletter No. 39, IAEA, Vienna (1998) 19-31.

[8] METHA, K., High-dose dosimetry programme of the Agency, these Proceedings.

[9] GRÜN, R., Present status of ESR-dating. Appl. Radiat. Isot. **40** (1989) 1045-1055.

[10] SKINNER, A., The maturing of a technique: Is ESR still an "experimental" technique? Appl. Radiat. Isot. (in press, 1999).

[11] EATON, G.R., EATON, S.S., MALTEMPO, M.M., Three approaches to spectral-spatial EPR imaging. Appl. Radiat. Isot. **40** (1989) 1227-1231.

[12] IKEYA, M. (Ed.), "EPR Dating and Dosimetry", Ionics Publications Co, Ltd., Japan (1985) 1-538.

[13] ONORI, S., D'ERRICO, F., DE ANGELIS, C., EGGER, E., FATTIBENE, P., JANOVSKY, I., Proton response of alanine based pellets and films. Appl. Radiat. Isot. **47** (1996) 1201-1204.

[14] SCHRAUBE, H., WEITZENEGGER, A., WIESER, A., REGULLA, D.F., Fast neutron response of alanine probes. Appl. Radiat. Isot. **40** (1989) 941-944.

[15] HÜTTERMANN, J., SCHAEFER, A., Heavy-ion-induced free radical formation in solid DNA-constituents: Quantitative and structural aspects. Appl. Radiat. Isot. **40** (1989) 915-921.

[16] WALIGORSKI, M.P.R., DANIALY, G., KIM SUN LOH, KATZ, R., The response of the alanine detector after charged-particle and neutron irradiation. Appl. Radiat. Isot. **40** (1989) 923-933.

[17] HITOSHI KOIZUMI, TSUNEKI ICHIKAWA, HIROSHI YOSHIDA, Radiation chemistry in alanine irradiated with γ-rays and ion beams. Appl. Radiat. Isot. **47** (1996) 1205-1210.

[18] CIESIELSKI, B., STUGLIK, Z., WIELOPOLSKI, L., ZVARA, I., The effect of high LET radiation on the dynamics of microwave power saturation of EPR signal in alanine. Appl. Radiat. Isot. (in press, 1999).

[19] BARTOLOTTA, A., INDOVINA,F.L., ONORI, S., ROSATI, A., Dosimetry for cobalt-60 gamma rays with alanine. Radiat. Prot. Dosim. 9 (1984) 277-281.

[20] GAO JUNCHENG, The NIM alanine-ESR dosimetric system for industrial radiation processing. Appl. Radiat. Isot. **47** (1996) 1161-1164.

[21] REGULLA, D.F., BARTOLOTTA, A., DEFFNER, U., ONORI, S., PANTOLONI, M., WIESER, A., Calibration network based on alanine/EPR dosimetry. Appl. Radiat. Isot. **44** (1993) 23-31.

[22] COUNCIL DIRECTIVE ON MEDICAL DEVICES, 93/42/EEC, Official Journal of the European Communities No. L 169, 14 June 1993.

[23] CHU, S., WIESER, A., FEIST, H., REGULLA, D.F., EPR Alanine dosimetry of high-energy electrons in radiotherapy. Appl. Radiat. Isot. **40** (1989) 993-996.

[24] RUCKERBAUER, F., SPRUNCK, M., REGULLA, D.F., Numerical signal treatment for optimised alanine/EPR dosimetry in the therapy-level dose range. Appl. Radiat. Isot. **47** (1996) 1263-1268.

[25] NETTE, P., ONORI, S., FATTIBENE, P., REGULLA, D.F., WIESER, A., Co-ordinated research efforts for establishing an international radiotherapy dose intercomparison service based on the alanine/EPR system. Appl. Radiat. Isot. **44** (1993) 7-11.
[26] METHA, K., GIRZIKOVSKY, R., Alanine/ESR dosimetry for radiotherapy IAEA experience. Appl. Radiat. Isot. **47** (1996) 1189-1192.
[27] GALL, K., DESROSIERS, M., BENSEN, D., SERAGO, C., Alanine EPR dosimeter response in proton therapy beams. Appl. Radiat. Isot. **47** (1996) 1197-1200.
[28] ROMANYUKHA, A.A., WIESER, A., REGULLA, D., EPR dosimetry with different biological and synthetic carbonated materials. Radiat. Prot. Dosim. **65** (1996) 389-392.
[29] BÖGL, K.W., REGULLA, D.F., SUESS, M.J. (Eds.), "Health Impact, Identification and Dosimetry of Irradiated Foods", WHO, Regional Office for Europe in co-operation with BGA-Federal Health Office, Neuherberg, Germany and GSF-National Research Centre for Environment and Health, Neuherberg, Germany. Report BGA/ISH 125, ISBN 3-89254-050-0 (1988) 155-161.
[30] BÖGL, K.W., Identification of irradiated foods - Methods, development and concepts. Appl. Radiat. Isot. **40** (1989) 1203-1210.
[31] DODD, N.J.F., SWALLOW, A.J., LEY, F.J., Use of ESR to identify irradiated food. Radiat. Phys. Chem. **26** (1985) 451-453.
[32] DODD, N.J.F., LEA, J.S., SWALLOW, A.J., ESR detection of irradiated food. Nature **334** (1988) 387.
[33] RAFFI, J. EVANS, J.C., AGNEL, J.-P., ROWLANDS, C.C., LESGARDS, C., ESR analysis of irradiated frogs' legs and fishes. Appl. Radiat. Isot. **40** (1989) 1215-1218.
[34] YORDANOV, N., GANCHEVA, V., Studies on the possibilities for extension of the period for identification of irradiated herbs by the method of EPR. Appl. Radiat. Isot. (in press, 1999).
[35] DE JESUS, E., ROSSI, A. LOPES, R., Identification and dose determination using ESR measurements in the flesh of irradiated vegetal products. Appl. Radiat. Isot. (in press, 1999).
[36] DESROSIERS, M.F., Current status of the EPR method to detect irradiated food. Appl. Radiat. Isot. **47** (1996) 1621-1628.
[37] REGULLA, D.F., GÖKSU, Y.H., VOGENAUER, A., WIESER A., Retrospective dosimetry based on egg shells. Appl. Radiat. Isot. **45** (1994) 371-373.
[38] WIESER, A., REGULLA, D.F., EPR dosimetry in the giga-rad range. Appl. Radiat. Isot. **40**, 911-914 (1989).
[39] ROTHFUCHS, T., DE LAS CUEVAS, C., DONKER, H., FEDDERSEN, H.-K., GARCIA-CELMA, A., GIES, H., GOREYCHI, M., GRAEFE, V., HEIJDRA, J., HENTE, B., JOCKWER, N., LEMEUR, R., MÖNIG, J., MÜLLER, K., PRIJ, J., REGULLA, D., SMAILOS, E., STAUPENDAHL, G., TILL, E., ZANKL, M., "The HAW-Project: Test Disposal of Highly Radioactive Radiation Sources in the Asse Salt Mine", Final Rep. GSF 6/95, GSF, Neuherberg (1995) 1-238.
[40] TILL, E., ZANKL, M., ROTHFUCHS, T., REGULLA, D., Calculation of the radiation transport in rock salt using Monte Carlo methods. Nucl. Instrum. Meth. **B 111**, 95-103 (1996).
[41] AMERICAN STANDARDS FOR TECHNIQUES AND MATERIALS, Standard practice for use of the alanine/EPR dosimetry system, ASTM Standard E1607-94 (1998).
[42] INTERNATIONAL ORGANISATION OF STANDARDS, ISO/TC85/WG3, AFNOR, Paris and ISO, Geneva.
[43] NEY, W.R., The 1997 meeting of the ICRU, ICRU News Letters **2** (1997) 14-15.
[44] NEY, W.R., Plans for the 1998 meeting of the ICRU, ICRU News Letters **1** (1998) 17.
[45] ETTINGER, K.V., NAM, J.W., McLAUGHLIN, W.L., CHADWICK, K.H., "Progress in high-dose dosimetry", Biomedical Dosimetry - Physical Aspects, Instrumentation, Calibration, IAEA, Vienna (1981) 405-432.
[46] PILBROW, J.R., ESR fundamentals. Appl. Radiat. Isot. **47** (1996) 1465-1470.
[47] IKEYA, M., New applications of electron spin resonance - Dating, Dosimetry and Microscopy. World Scientific Publishing Co. Pte. Ltd., Singapore (1993).
[48] BUGAY, A., KOLESNIK, S., Gaponenko, H., Alanine EPR dosimetry of therapeutic irradiators, these Proceedings.
[49] BUGAY, A., KOLESNIK, S., TESLENKO, V., METHA, K., NAGY, V., DESROSIER, M., Temperature stabilisation of alanine dosimeters used for food processing and sterilization. Appl. Radiat. Isot. (in press, 1999).
[50] YORDONOV, N., New generation of self-calibrated SS/EPR dosimeters - Alanine/EPR dosimeters, these Proceedings.
[51] HASKELL, E.H., HAYES, R.B., KENNER, G.H., A high sensitive EPR technique for alanine dosimetry. Radiat. Prot. Dosim. 77 (1998) 43-49.
[52] HASKELL, E.H., HAYES, R.B., KENNER, G.H., Improved accuracy of EPR dosimetry using a constant rotation goniometer. Radiation Measurement **27** (1997) 325-329.

[53] SOLLIER, T.J.L., MOSSE, D.C., CHARTIER, M.M.T., JOLI, J.E., The LMRI ESR/alanine dosimetry system: Description and performance. Appl. Radiat. Isot. **40** (1989) 961-965.
[54] SHARPE, P., SEPHTON, J., An automated system for measurement of alanine/EPR dosimeters. Appl. Radiat. Isot. (in press, 1999).
[55] MAILER, D., SCHMALBEIN, D., A dedicated EPR analyser for dosimetry. Appl. Radiat. Isot. **44** (1993) 345-350.
[56] HOLE, E., SAGSTUEN, E. HAUGEDAL, S., NELSON, W., The nature of the major alanine and ENDOR studies of solid L-alanine X-irradiated at 295 K. Appl. Radiat. Isot. (in press, 1999).
[57] BAUCHINGER, M., SCHMID, E., BRASELMANN, H, WILLICH, N., CLEMM, CH., Time-effect relationship of chromosome aberrations in peripheral lymphocytes after radiation therapy for seminoma. Mutation Research **211** (1989) 265-272.
[58] SCHMID E., ZITZELSBERGER H., BRASELMANN H., GRAY J.W., BAUCHINGER M., Radiation-induced chromosome aberrations analysed by fluorescence in situ hybridisation with a triple combination of composite whole chromosome-specific DNA probes. Radiat. Biol. **62** (1992) 673-678.
[59] LLOYD, D.C., New development in chromosomal analysis for biological dosimetry. Radiat. Prot. Dosim. 77 (1998) 33-36.
[60] WIESER, A., GÖKSU-ÖGELMAN, H.Y., REGULLA, D.F., VOGENAUER, A., Dose rate assessment in tooth enamel. Quat. Sci. Rev. 7 (1988) 491-495.
[61] DESROSIERS, M.F., EPR bone dosimetry: a new approach to spectral deconvolution problems. Appl. Radiat. Isot. **44** (1993) 81-83.
[62] CALLENS, F.J., VERBEECK, R.M.H., MATTHYS, P.F.A., MARTENS, L.C., BOESMAN, E.R., The contribution of CO_3^{3-} and CO_3^{2-} to the EPR spectrum near g = 2 of powdered human tooth enamel. Calcif. Tissue Int. **41** (1987) 124-129.
[63] SCHWARCZ, H.P., EPR study of tooth enamel. Nucl. Tracks **10** (1985) 865-867.
[64] ROMANYUKHA, A.A., REGULLA, D., VASILENKO, E., WIESER, A., South Ural nuclear workers: Comparison of individual doses from retrospective EPR dosimetry and operational personal monitoring. Appl. Radiat. Isot. **45** (1994) 1195-1199.
[65] ROMANYUKHA, A.A., DEGTEVA, M.O., WIESER, A., SEREZHENKOV, V.A., KOZHEUROV, V.P., VOROBIOVA, M.I., VASILENKO, E.K., KLESHCHENKO, E.D., IGNATIEV, E.A., KOSHTA, A.A., SHISHKINA, E.A., KHOKHRYAKOV, V.F., Pilot study of the Ural region with EPR tooth dosimetry. Proc. International Workshop on Chronicle Exposure. Risk of Long-term Effects. Chelyabinsk (1995).
[66] STULIK, Z., MICHALIK, J., STACHOWICZ, W., OSTROWSKI, K., ZVARA, I., DZIEDZIC-GOCLAWSK,A A., Bone powder exposed to the action of ^{12}C and ^{25}Mg ion beams as investigated by electron paramagnetic resonance spectroscopy. Appl. Radiat. Isot. **45** (1994) 1181-1187.
[67] HASKELL, E.H., Retrospective Accident Dosimetry using Environmental Materials. Radiat. Prot. Dosim. **47** (1993) 297-303.
[68] NAKAJIMA, T., Sugar as an emergency population dosimeter for radiation accidents. Health Phys. **55** (1988) 951-955.
[69] REGULLA D.F., DEFFNER U., Dose estimation by EPR spectroscopy at a fatal radiation accident. Appl. Radiat. Isot. **40** (1989) 1039-1044.
[70] ODUWOLE A.D., SALES K.D. AND DENNISON K.J., Some EPR observations on bone, tooth enamel and egg shell. Appl. Radiat. Isot. **44** (1993) 261-266.
[71] REGULLA, D.F., GÖKSU, Y.H., VOGENAUER, A., WIESER A., Retrospective dosimetry based on egg shells. Appl. Radiat. Isot. **45** (1994) 371-373.
[72] WIESER A., REGULLA D.F., "Cellulose for high-level dosimetry", High Dose Dosimetry for Radiation Processing, IAEA, Vienna (1991) 203-212.
[73] WIESER A., GÖKSU H.Y., REGULLA D.F. AND VOGENAUER A., Limits of retrospective accident dosimetry by EPR and TL with natural materials. Radiat. Meas. **23** (1994) 509-514.
[74] PIVOVAROV, S., SEREDAVINA, T., RUKHIN, A., ESR of environmental objects at Semipalatinsk Nuclear Test Site. Appl. Radiat. Isot. (in press, 1999).
[75] OKA, T., IKEYA, M., ESR dosimetry using quartz grains in bricks. Appl. Radiat. Isot. (in press, 1999).
[76] GINSBOURG, S.F., BABUSHKINA; T.A., BASOVA, L.B., KLIMOVA, T.P., ESR spectroscopy of building materials as a dosimetry technique. Appl. Radiat. Isot. 77 (1996) 1381-1383.
[77] NASIROV, R., MOULUKOV, R., The γ-irradiation dose measurement for animals of West Kazakhstan. Appl. Radiat. Isot. (in press, 1999).
[78] SKVORTZOV, V., IVANNIKOV, A., WIESER, A., BOUGAI, A., BRIK, A., CHUMAK, V., STEPANENKO, V., RADCHUK, V., REPIN, V., KIRILOV, V., "Retrospective individual dosimetry using EPR of tooth enamel", The Radiological Consequences of the Chernobyl Accident, EUR 16544 (KARAOGLOU, A., DESMET, G., KELLY, G.N., MENZEL, H.G., Eds.), Brussels (1996) 949-955.

[79] WIESER, A., CHUMAK, V., BAILIFF, I., BARAN, N., BOUGAI, A., BRIK, A., DUBROVSKY, S., FININ, V., HASKELL, E., HAYES, R., IVANNIKOV, A., KENNER, G., KIRILLOV, V., KOLESNIK, S., LIIDJA, G., LIPPMAA, E., MAKSIMENKO, V., MATYASH, M., MEIJER, A., MINENKO, V., PASALSKAYA, L., PAST, J., PAVLENKO, J., PUSKAR, J., RADCHUK, V., SCHERBINA, O., SHOLOM, S., SKVORTSOV, V., STEPANENKO, V., VAHER, U., "International intercomparison of dose measurements using EPR spectrometry of tooth enamel", The radiological consequences of the Chernobyl accident, EUR 16544 (KARAOGLOU, A., DESMET, G., KELLY, G.N., MENZEL, H.G., Eds.), Brussels (1996) 957-964.

[80] WU, K., GUO, L., CONG, J.B., SUN, C.P., HU, J.M., ZHOU, Z.S., WANG, S., ZHANG, Y., ZHANG, X., SHI, Y.M., Researches and applications of ESR dosimetry for radiation accident dose assessment. Radiat. Prot. Dosim. 77 (1998) 65-67.

[81] HÜTT, G., BRODSKI, L., POLYAKOV, V., Gamma-dose assessment after radiation accident in Kiisa (Estonia): Preliminary results. Appl. Radiat. Isot. **47** (1996) 1329-1334.

[82] GRIFFITH, R.V., Retrospective dosimetry needs from an IAEA perspective. Radiat. Prot. Dosim. 77 (1998) 3-9.

[83] IKEYA, M., MIYAJIMA, J., OKAJIMA, S., EPR Dosimetry for atomic bomb survivors using shell buttons and tooth enamel. Jap. J. Appl. Phys. **23** (1984) L697-L699.

[84] ISHII, H., IKEYA, M, OKANO, M., EPR dosimetry of teeth of residents close to Chernobyl reactor accident. Nucl. Sci. Technol. **27** (1990) 1153-1155.

[85] SEREZHENKOV, V.A., DOMRACHEVA, E.V., KLEVEZAL, G.A., KULIKOV, S.M., KUZNETSOV, S.A., MORDVINCEV, P.I., SUKHOVSKAYA, L.I., SCHKLOVSKY-KORDI, VANIN, A.F., VOEVODSKAYA, N.V., VOROBIEV, A.I., Radiation dosimetry for residents of the Chernobyl region: A comparison of cytogenetic and electron spin resonance methods. Radiat. Prot. Dosim. **42** (1992) 33-36.

[86] WIESER, A., ROMANYUKHA A.A., KOZHEUROV, V.P., DEGTEVA, M.O., Retrospective EPR dosimetry with teeth of Techa river residents. Intern. Workshop on the Scientific Bases for Decision Making after a Radioactive Contamination of an Urban Environment, Rio de Janeiro and Goiânia, Brazil, 29 August - 2 September (1994).

[87] ROMANYUKHA, A.A., IGNATIEV, E.A., DEGTEVA, M.O., KOZHEUROV, V.P., WIESER, A., JACOB, P., Radiation doses from Ural region. Nature **381** (1996) 199-200.

[88] NAGY, V., Accuracy problems in EPR dosimetry. Appl. Radiat. Isot. (in press, 1999).

[89] HAYES, R.B., HASKELL, E.H., KENNER, G.H., A mathematical approach to optimal selection of dose values in the additive dose method of EPR dosimetry. Radiat. Meas. **27** (1997) 315-323.

[90] SKVORTSOV, V.G., IVANNIKOV, A.I., EICHHOFF, U., Assessment of individually accumulated irradiation doses using EPR spectroscopy of tooth enamel. Molec. Struct. **347** (1995) 321-329.

[91] TERMINE, J.D., EANES, E.D., GREENFIELD, D.J., VYLAN, M.U., HARPER, R.A., Hydrazine-deproteinated bone mineral. Calcif. Tissue Res. **12** (1972) 73-90.

[92] IGNATIEV, E.A., ROMANYUKHA, A.A., KOSHTA, A.A., WIESER, A., A selective saturation method for EPR dosimetry with tooth enamel. Appl. Radiat. Isot. **47** (1996) 333-337.

[93] HASKELL, E., KENNER, G., HAYES, R., SHOLOM, S., CHUMAK,V., An EPR intercomparison using teeth irradiated prior to crushing. Radiat. Meas. **27** (1997) 419-424.

[94] REGULLA, D.F., An integrated approach to retrospective dosimetry. IAEA Research Co-ordinated Meeting on the Use of Natural Materials for Solid State Dosimetry in Accident Zones and the Environment, Salt Lake City, Utah, USA, 25-29 January 1993.

[95] HASKELL, E.H., HAYES, R.B., KENNER, G.H., An EPR dosimetry method for rapid scanning of deciduous teeth following a radiation accident. Health Phys. (in press, 1999).

[96] OLIVEIRA, A.R., VALVERDE, N.J.L., BRANDAO-MELLO, C.E., ALMEIDA, C.E.V., Revisiting the Goiania accident: Medical and dosimetric experiences. Radiat. Prot. Dosim. 77 (1998) 107-111.

[97] DESROSIERS, M., ROMANYUKHA, A.A., "Technical aspects of the electron paramagnetic resonance method for tooth enamel dosimetry", Biomarkers - Medical and Workplace Applications (MENDELSOHN, M.L., MOHR, L.C., PEETERS, J.P., Eds.), Joseph Henty Press, Washington, D.C. (1998) 53-64.

[98] KOSHURNIKOVA, N.A., BULDAKOV, L.A., BYSOGOLOV, G.D., BOLOTNIKOVA, M.G., KOMLEVA, N.S., PETERNIKOVA, V.S., Mortality from malignancies of the hematopoietic and lymphatic tissues among personnel of the first nuclear plant in USSR, Sc. Tot. Environm. **142** (1994) 19-23.

[99] MÄDER, K., GALLEZ, B., SWARTZ, H.M., *In vivo* EPR: An effective new tool for studying pathophysiology, physiolgy and pharmacology. Appl. Radiat. Isot. **47** (1996) 1663-1667.

[100] SWARTZ, H.M., private communications.

[101] HASKELL, E.H., HAYES, R.B., KENNER, G.H., SHOLOM, S.V., CHUMAK, V.I., Electron paramagnetic resonance techniques and space biodosimetry. Radiat. Res. **148** (1997) S51-S59.

[102] IKEYA, M., From earth to space: ESR dosimetry moves towards the 21st century. Appl. Radiat. Isot. **44** (1993) 1-5.
[103] REGULLA, D., Lithium fluoride dosimetry based on radiophotoluminescence. Health Phys. **22** (1972) 491-496.
[104] KOVÁCS, A., BARANYAL, M., WOJNÁRROVITS, L., SLEZSÀK, I., McLAUGHLIN, W.L., MILLER, S.D., MILLER, A., A polymeric dosimeter film based on optically-stimulated luminescence for dose measurements below 1 kGy, these Proceedings.
[105] STENGER, V., HALMAVÁNSZKI, J., FALVI, L., FEHÉR, I.,DEMIREZEN, Ü., Dose planning, reading and controls using PC at gamma radiation processes, these Proceedings.
[106] DESROSIER, M., National Institute of Standards and Technology, Gaithersburg, D.C., personal communication, 1998.
[107] SAGSTUEN, E., THEISEN, H., HENRIKSEN, T., Dosimetry by ESR spectroscopy following a radiation accident. Health Phys. 45 (1983) 961-968.
[108] INTERNATIONAL ATOMIC ENERGY AGENCY, The Radiological Accident in Goiania, IAEA, Vienna, STI/PUB/815 (1988).
[109] INTERNATIONAL ATOMIC ENERGY AGENCY, The Radiological Accident in San Salvador, IAEA, Vienna, STI/PUB/847 (1990).
[110] INTERNATIONAL ATOMIC ENERGY AGENCY, The Radiological Accident in Soreq, IAEA, Vienna, STI/PUB/925 (1993).
[111] CHUMAK, V., LIKHTAREV, S., SHOLOM, S., MECKBACH, R., KRJUCHKOV, V., Chernobyl experience in field of retrospective dosimetry: Reconstruction of doses to the population and liquidators involved in the accident. Radiat. Prot. Dosim. 77 (1998) 91-95.
[112] IVANNIKOV, A., SKORTSOV, V., STEPANENKO, V., TSYB, A., Tooth enamel EPR dosimetry: Progress and limitation. Appl. Radiat. Isot. (in press, 1999).
[113] ROMANYUKHA, A.A., REGULLA, D., VASILENKE, E.K., WIESER, A., DROZHKO, E.G., LYZLOV, A.F., KOSHURNIKOVA, N.A., SHILNIKOVA, N.S., PANFILOV, A.P., Verification of occupational doses at the first nuclear plant in the former Soviet Union. Appl. Radiat. Isot. **47** (1996) 1277-1280.
[114] KEIRIM-MARKUS, I., KLESCHENKO, E., About adequacy of personal dosimetry data obtained by EPR signal of teeth enamel. Appl. Radiat. Isot. (in press, 1999).
[115] BOCHVAR, I., KEIRIM-MARKUS, I., KLESCHENKO, E., KUSHNEREVA, K., LEVOCHKIN, F., New possibilities of the method of EPR dosimetry by teeth tissues. Appl. Radiat. Isot. (in press, 1999).
[116] WIESER, A., ROMANYUKHA, A.A., DEGTEVA, M.O., KOZHEUROV, V.P., PETZOLD, G., Tooth enamel as a natural dosimeter for bone seeking radionuclides. Appl. Radiat. Isot. **65** (1996) 413-416.
[117] IGNATIEV, E., LYUBASHEVSKII, N. SHISHKINA, E., ROMANYUKHA, A., EPR dose reconstruction for bone seeking ^{90}Sr. Appl. Radiat. Isot. (in press, 1999).
[118] ROMANYUKHA, A.A., REGULLA, D.F., Aspects of retrospective dosimetry. Appl. Radiat. Isot. **47** (1996) 1293-1297.

ALANINE DOSIMETRY AT NPL — THE DEVELOPMENT OF A MAILED REFERENCE DOSIMETRY SERVICE AT RADIOTHERAPY DOSE LEVELS

P.H.G. SHARPE, J.P. SEPHTON
Centre for Ionising Radiation Metrology,
National Physical Laboratory,
Teddington, United Kingdom

XA9949723

Abstract

In this paper we describe the work that has been carried out at National Physical Laboratory (NPL) to develop a mailed alanine reference dosimetry service for radiotherapy dose levels. The service is based on alanine / paraffin wax dosimeters produced at NPL. Using a data analysis technique based on spectrum fitting, it has been possible to achieve a precision of dose measurement better than ±0.05 Gy (1σ). A phantom set has been developed for use in high energy photon beams, which enables simultaneous irradiation of alanine dosimeters and ionisation chambers in a well defined geometry. Studies in photon beams of energies between ^{60}Co and 20 MeV have shown no significant energy dependence (<1%) for alanine relative to dose determination using a graphite calorimeter. Work is underway to extend the service to electron beams, and preliminary results are presented on the direct calibration of alanine in electron beams using a graphite calorimeter.

1. INTRODUCTION

The potential of alanine as a dosimeter for radiotherapy applications has been appreciated for many years, but it is only recently that developments in instrumental and analytical techniques have enabled reliable measurements to be made at doses between 1 and 10 Gy. Alanine dosimeters are

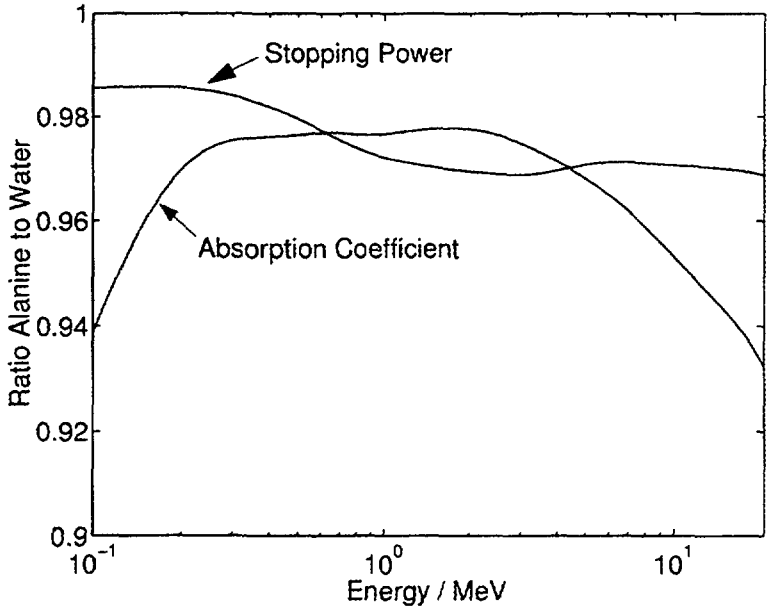

FIG. 1. Ratio of alanine mass energy absorption coefficients and mass collision stopping powers to those of water, as a function of energy.

intrinsically close to water both in terms of density and radiation absorption properties. Figure 1 shows the ratio of mass collision stopping powers and mass energy absorption coefficients for alanine and water. Mass collision stopping power ratios vary only slowly with energy, changing by approximately 2% over the energy range 0.1 to 20 MeV, shown in Fig. 1. Mass energy absorption coefficient ratios show more variation with energy, and the ratio alanine to water falls rapidly below 0.1 MeV. Nevertheless, in the region between 0.2 and 10 MeV, variation is relatively small, and the ratios themselves are close to the ratios of stopping powers. This suggests that the alanine dosimeter should show only small energy dependence in the high energy photon region used for radiotherapy. It should be noted that the variation in response of alanine with energy will also be influenced by variation in the radiation chemical yield, and this can only be determined by experiment.

NPL has operated an alanine mailed reference dosimetry service in the 0.1 to 70 kGy region since 1991, and the work described in this paper represents the extension of that service to the radiotherapy dose region.

2. DOSIMETERS

Alanine dosimetry at NPL is based around NPL produced pellets comprising, by weight, 90% L-α-alanine and 10% high melting point paraffin wax (m.p. 98°C). The pellets are 5 mm diameter and approximately 2.5 mm thick. The average mass varies slightly from batch to batch, but is nominally 55 mg. Pellets are selected to be within a ±2 mg band. Each pellet is weighed immediately prior to measurement, and the EPR signal normalised for mass by simple division. The production process has been described earlier [1], and does not introduce any detectable alanine radical signal (see later). In order to reduce post-irradiation fading, dosimeters are conditioned at 55% relative humidity for 10 weeks prior to use. An NPL alanine dosimeter consists of four pellets enclosed in either a polyacetal or polystyrene holder. Two types of holder are used: a cylinder of outer diameter 12 mm and height of 17 mm, in which the pellets are stacked on top of each other, and a disc of diameter 25 mm and thickness 6 mm, in which the pellets lie side by side. The cylindrical holder can be made water tight for use in a water phantom. The four pellets in a dosimeter are measured separately. Above 10 Gy individual pellet doses are calculated, but below 10 Gy it is necessary to sum the signals from individual pellets to achieve the required precision. All data described in this paper are based on summed signals from four pellets.

3. SPECTROMETER PARAMETERS

Microwave power, modulation amplitude and spectral acquisition time can all be increased in an attempt to detect smaller signals, and hence measure lower doses. None of these is without penalty, and a compromise has to be made in order to record relatively undistorted spectra in a reasonable time. The use of excessive microwave power or modulation amplitude can also lead to machine instability. Details of the spectrometer and measurement parameters used at NPL are given below:

Spectrometer - Bruker ESP 300, X-band with 9" magnet;
Cavity - standard Bruker st4102 rectangular cavity;
Microwave power - 6 mW;
Modulation amplitude - 0.6 mT;
Field sweep - 20 mT;
Acquisition time - 120 s (6 x 20 s scan with 90° rotation of pellet between 3rd and 4th scan).

Reproducible positioning of the sample and associated holder within the EPR cavity is essential for high accuracy at any dose. Experience at NPL indicates that this becomes more critical at low doses, where spectrometer baseline distortions are comparable in amplitude to the radical signal being measured. To ensure reproducible positioning a sample holder has been designed based on two concentric quartz tubes. This holder also allows automatic rotation of the pellet through 90°, in order to

average out anisotropic effects. This holder has been described in detail previously [2], but for completeness, is shown schematically in Fig 2. An automatic pellet loading system based around this holder has also been developed [3].

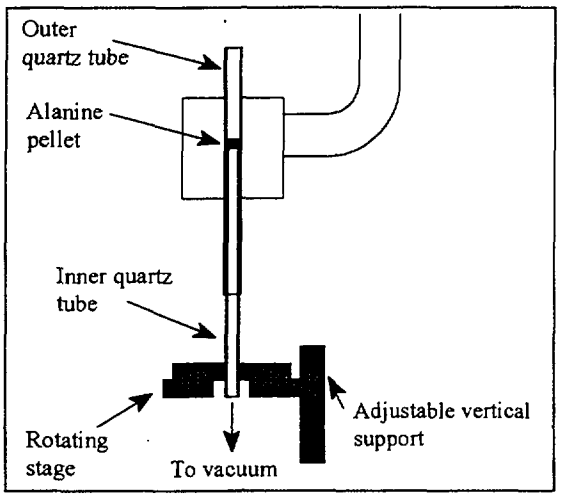

FIG. 2. Schematic diagram of system for holding alanine pellets in EPR cavity.

4. DATA ANALYSIS

The most common method of analysis of alanine/EPR dosimeters is the measurement of the peak-to-peak height of the central feature of the radiation induced radical spectrum. This works well at doses above approximately 10 Gy, and has been shown to be superior to supposedly more sophisticated methods, such as double integration [4]. Below 10 Gy, the measured EPR spectrum becomes increasingly affected by both high frequency noise, and low frequency baseline distortion. The high frequency noise component can be removed by filtering, but the low frequency distortion is more problematic. Baseline distortion can arise from several sources, including, the cavity, the holder used to position the alanine, and the alanine sample itself. Much of this distortion can be removed by subtracting the average spectrum of unirradiated pellets from the spectrum of an irradiated one. There remains, however, a significant component that varies from pellet to pellet and cannot be removed by simple subtraction. In order to take account of this, we have developed a procedure based on Least Squares techniques, which allows estimation of the amount of the "known alanine radical spectrum" that is present in the distorted measured signal. The "known alanine radical spectrum" is determined by measuring the spectrum of a pellet irradiated to 100 Gy. All spectrometer parameters, except signal channel gain, are the same as those used for measurements below 10 Gy. The procedure used has been described previously [2], and is illustrated in Fig. 3, where a measured 5 Gy spectrum a) is shown split into its component parts. Spectrum b) is the average baseline spectrum obtained by measuring a number of unirradiated pellets, and c) is the computed "dosimeter dependent" part of the spectrum, which is approximated by a fourth order polynomial function. Spectrum d) shows the amount of the underlying "known alanine radical spectrum" that is present in the measured signal.

5. ACHIEVABLE ACCURACY AND PRECISION

Using the data analysis procedure described above, the relationship between the amount of the "known alanine radical spectrum" and absorbed dose is found to be linear over the range 1 to 10 Gy, with no significant "zero dose" intercept. Measurement precision, as determined by the residual standard deviation about the line, is better than ±0.05 Gy (1σ). This translates into a minimum usable dose of 5 Gy for a reference dosimetry service, assuming a realistic requirement of 1% (1σ) for the precision of a single measurement.

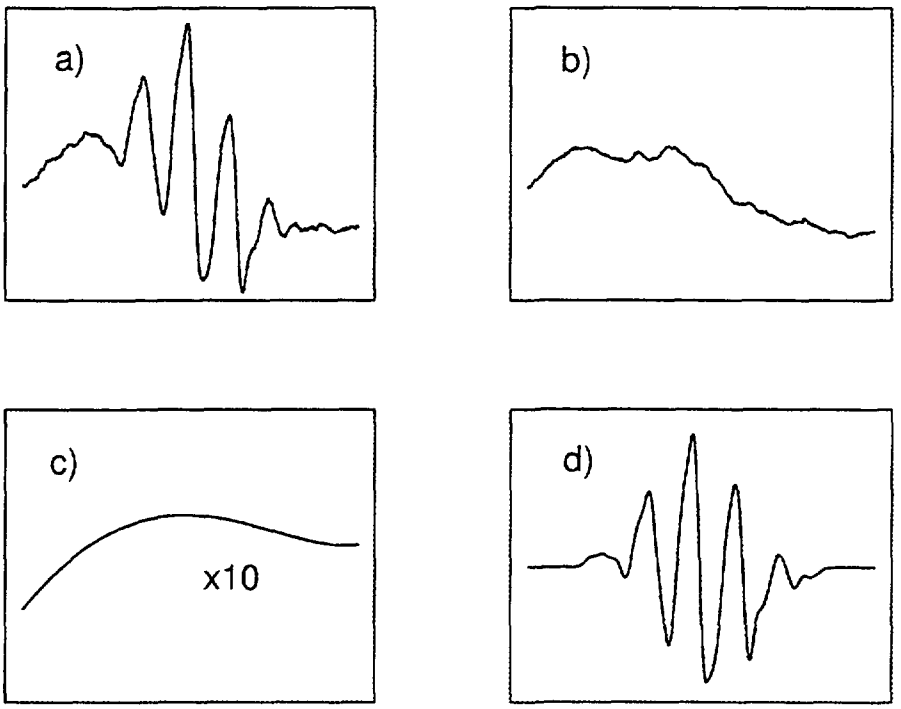

FIG. 3. Analysis of EPR spectrum in terms of its component parts: a) Measured EPR spectrum of alanine dosimeter irradiated to 5 Gy. b) Average baseline of unirradiated dosimeters. c) Calculated polynomial correction for individual dosimeter baseline. d) Calculated component of known alanine radical spectrum. The y-scale of plot c) is expanded 10 times relative to that of the other plots.

Overall accuracy depends on a number of factors, including, the calibration standard being used and the accuracy of correction for factors such as energy dependence, irradiation temperature and post-irradiation fading. In radiotherapy applications, temperature can generally be monitored and controlled within quite tight limits, and uncertainties due to irradiation temperature effects are therefore usually negligible. Similarly, fading is not usually a significant problem, and can be monitored by the use of irradiated control dosimeters, which accompany the service dosimeters during transport. The rate of fade of NPL dosimeters stored at 55% R.H. has been measured to be approximately 4% over a 17 month period. NPL alanine dosimeters are calibrated in terms of absorbed dose to water using Co-60 radiation, in a field whose dose rate is directly traceable to the NPL primary standard graphite micro-calorimeter. The overall uncertainty associated with this calibration is estimated to be ±2% (2σ). Uncertainties arising from the energy dependence of the alanine dosimeter are discussed below.

6. PHANTOM

In radiotherapy calibration applications, it is essential that alanine dosimeters are irradiated under well defined conditions, and in such a way that their dose reading can be easily related to the dose reading of other systems, such as ionisation chambers. In order to achieve this with a mailed service, a polymethylmethacrylate (PMMA) phantom plate has been designed for photon irradiations, which

enables alanine dosimeters in cylindrical holders (12 mm diameter, 17 mm length) to be irradiated alongside thimble ionisation chambers (either NE 2561 or NE 2571). The alanine and ionisation chamber inserts are interchangeable, allowing the two to be exchanged half-way through an irradiation, in order to eliminate the effect of field asymmetry. To achieve the standard measurement depths of 5 or 7 cm, additional, locally provided, phantom material is placed in front of and behind the 2 cm thick PMMA plate. The PMMA plate is shown in Fig. 4.

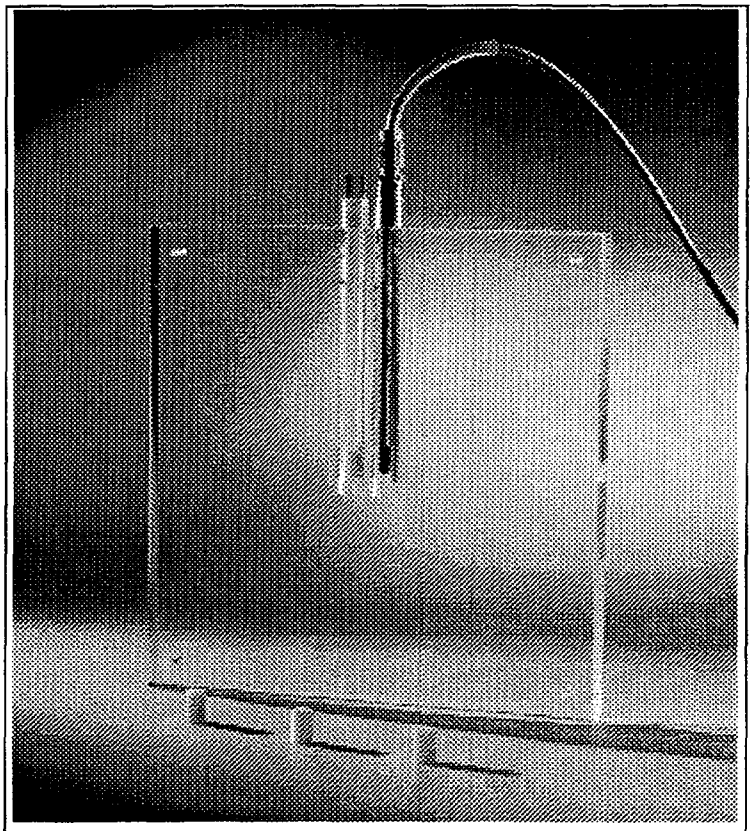

FIG. 4. Phantom plate showing interchangeable locations of ionisation chamber and alanine dosimeter.

7. PHOTON ENERGY DEPENDENCE

One of the most important potential applications for alanine at therapy level is as a reference dosimetry service for quality assurance and audit purposes. In order to minimise systematic errors, the response of dosimeters used for such applications should ideally have very little dependence on radiation type and quality. Figure 5 shows a plot of the relative response of NPL alanine dosimeters irradiated over a range of photon energies. Radiation quality is given in terms of Tissue Phantom Ratio (TPR^{20}_{10}), a measure of the effective energy of the photon beam. The range plotted corresponds to photons from Co-60 and those generated between 4 and 20 MeV. The basis of dose determination at each quality was the NPL graphite micro-calorimeter, the conversion to absorbed dose to water being made using the photon fluence scaling theorem [5]. As can be seen, there is no significant energy dependence over this energy range, all experimental points lying within a 1% band. Also shown in Fig. 5, for comparison, is the relative response of a NE 2561 ionisation chamber.

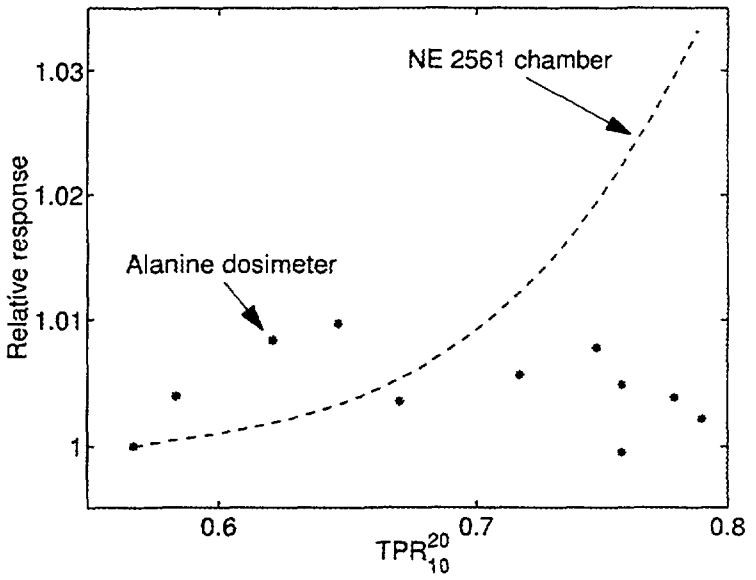

FIG. 5. Relative response of alanine dosimeters and ionisation chambers in high energy photon beams.

8. ELECTRON RESULTS

Work is currently underway at NPL to extend the therapy level alanine service to high energy electron beams. In order to provide a direct calibration of alanine in electron beams, a replica of the primary standard electron beam calorimeter has been constructed. This replica has cut-outs which allow four alanine pellets to be embedded directly in the calorimeter core. Three energies have been studied, nominally 6, 10 and 16 MeV. The absorbed dose to alanine was derived by multiplying the absorbed dose to graphite in the calorimeter core by the mean alanine to graphite stopping power ratio, calculated for the known spectrum of the NPL beam. As discussed above, alanine dosimeters are normally used with an absorbed dose to water calibration derived from the primary standard graphite micro-calorimeter in a Co-60 beam. This can be converted into an absorbed dose to alanine calibration using cavity theory, and compared directly with the electron beam derived calibration. Data analysis is not yet complete, but provisional results for the 10 MeV irradiations show agreement between the electron beam and Co-60 calibrations within 0.6%, (derived from 19 individual measurements, with a scatter of 0.6% (1σ)). This agreement is well within the uncertainties of the comparison, and demonstrates the equivalence of alanine response in Co-60 and high energy electron beams.

9. CONCLUSION

A mailed reference dosimetry system for high energy radiotherapy photon beams has been developed based on alanine/paraffin wax dosimeters. A limiting measurement precision of ±0.05 Gy has been shown to be consistently achievable using a Bruker ESP 300 spectrometer and standard rectangular cavity, provided steps are taken to ensure precise sample positioning. A data analysis procedure based on spectrum fitting has been developed to correct for dosimeter dependent baseline distortions. A phantom plate and adapter set has been designed to enable simultaneous irradiation of alanine dosimeters and ionisation chambers. No significant energy dependence (<1%) has been observed in photon beams from Co-60, or generated between 4 and 20 MeV. Provisional results from a 10 MeV electron beam also indicate no significant difference in response compared to Co-60.

REFERENCES

[1] ARBER, J.M., SHARPE, P.H.G., "Fading characteristics of irradiated alanine pellets: the importance of pre-irradiation conditioning", Appl. Radiat. Isot., **44**, (1993) 19-22

[2] SHARPE, P.H.G., et al., "Progress towards an alanine/ESR therapy level reference dosimetry service at NPL", Appl. Radiat. Isot., **47**, (1996) 1171-1175

[3] SHARPE, P., SEPHTON, J., "An automated system for the measurement of alanine / EPR dosimeters", 5th International Symposium on ESR Dosimetry and Applications, (Proc. Conf. Moscow, 1998)

[4] AHLERS, F.J., SCHNEIDER, C.C.J., "Alanine ESR dosimetry: an assessment of peak-to-peak evaluation", Radiat. Prot. Dosim., **37**, (1991) 117

[5] BURNS, J.E., "Absorbed-dose calibrations in high-energy photon beams at the National Physical Laboratory: conversion procedure", Phys. Med. Biol., **39**, (1994) 1555-1575

ALANINE EPR DOSIMETRY OF THERAPEUTIC IRRADIATORS

O. BUGAY, V. BARTCHUK, S. KOLESNIK, M. MAZIN
Institute of Semiconductor Physics

H. GAPONENKO
Kiev City Oncology Centre,

Kiev, Ukraine

Abstract

The high-dose alanine EPR dosimetry is a very precise method in the dose range 1-100 kGy. The system is used generally as the standard high-dose transfer dosimetry in many laboratories. This is comparatively expensive technique so it is important to use it as a more universal dosimetry system also in the middle and low dose ranges. The problems of the middle-dose alanine dosimetry are discussed and the solution of several problems is proposed. The alanine EPR dosimetry has been applied to the dose measurements of medical irradiators in the Kiev City Oncology Center.

1. INTRODUCTION

In the Ukraine, the sources of ionizing radiation are widely used for the cancer radiotherapy in a number of hospitals. These medical irradiators were fabricated 20 to 30 years ago and need careful checking and calibration. Dosimetry devices are also very old and need calibration. Also, there is no standard transfer TLD dosimetry system for the checking of medical irradiators. Now, there are no means for purchasing of new dosimetry equipment and even for the regular calibration of the old devices.

In the laboratory of EPR dosimetry of the Institute of Semiconductor Physics, the standard high dose transfer alanine EPR dosimetry system based at the old Varian E12 spectrometer was developed. We have decided to develop the middle-dose transfer alanine EPR dosimetry system and use it for dose measurements of medical irradiators in Ukrainian hospitals.

The high-dose alanine EPR dosimetry is a very precise method and in the dose range 1-100 kGy the uncertainty of dose measurements can be as low as 2 %. Because of this in early 1980s it was selected as the standard transfer dosimetry system for the International Dose Assurance Service (IDAS) of the International Atomic Energy Agency (IAEA) [1].

In the middle and small dose range the uncertainty of the standard alanine EPR dosimetry can be much more than 2% due to many factors:

- background EPR spectra of the cavity, sample holder and alanine tablet;
- alanine tablet EPR anisotropy;
- intra-batch variability of tablets;
- sensitivity of the EPR response to the humidity level of the tablet during the storage and measurements;
- instability of the EPR spectrometer parameters due to instability of electronic units;
- instability of the EPR spectrometer output due to the variability of the room humidity and the temperature of microwave cavity;
- random noise of electronic circuits.

For the correct dosimetry of medical irradiators in the dose range 1-10 Gy it is desirable to decrease uncertainties of all components of the alanine EPR dosimetry system. We have proposed the technical solution of the above mentioned problems. Presently we are developing the middle-dose alanine EPR dosimetry system of high accuracy. Some components of the system have been manufactured, but others are not yet ready. The system is described and discussed in the next section.

For dose measurements of the medical irradiators in Kiev City Oncology Center the routine high-dose alanine EPR technique was used.

2. MIDDLE-DOSE ALANINE EPR DOSIMETRY SYSTEM

2.1. Alanine dosimeter technology

Alanine tablets produced by BRUKER Analytische Messtechnik GMBH and tablets produced in our laboratory were used for EPR dosimetry. Bruker tablets were EMS 914-1005 type. These have cylindrical form with 4.9 mm diameter and 5 mm height. They have been prepared from the mixture of the alanine powder(80%) and polyethylene(20%) as a binder. The weight of tablet is 87 mg ± 2%. But the variation of the alanine content may be more than 2% due to the heterogeneity of the mixture. Thus, the intra-batch variability for such tablets is due to (1) variation of the tablet mass and (2) variation of alanine content in the tablet.

We have developed the technology of tablet preparation using pure alanine without a binder. This technology allows to eliminate the uncertainty due to the alanine content variation and to measure precisely the alanine mass of each tablet. We have used the chromatographically pure L-α-alanine of "REANAL", Budapest. The "Sigma" L-α-alanine also was used. Our tablets are quite firm. The size is 4.9 mm diameter and 5 mm height, and the weight is 100 ± 3 mg. For the precise alanine EPR low-dose measurements the individual weight of each tablet must be measured. We have used electronic balance with uncertainty of 0.1mg. Alanine tablets are anisotropic. The EPR intensity of an irradiated tablet changes by about 0.5 % when the tablet is rotated in the microwave cavity.

2.2. EPR techniques

Varian E12 X-band spectrometer has been modernized for EPR dosimetry. Magnetic field sweep system and microwave cavity were improved. We have also found a significant drift of the Varian magnetic field modulation unit. The system for the stabilization of the magnetic field modulation has been manufactured. The optimized parameters used were: 9.3 GHz microwave frequency, 2 mW microwave power, 100 kHz magnetic field modulation frequency, 1 mT modulation amplitude, 2,5...10 mT scan width, 60 s time of one sweep, 16...64 number of sweeps, 4 ms time constant.

2.2.1. Magnetic field sweep system.

A digital control of the magnetic field sweep unit has been designed. Due to the digital control of the microwave frequency and a nuclear magnetic resonance magnetometer, the EPR spectrum is presented in units of g-factor. The new control unit allows changing the sweep speed in some sections of the sweep range. Critical sections of the EPR spectrum can be scanned with a slower speed for more effective averaging of the electronic noise or for correct registration of narrow EPR lines of a reference sample with Mn^{2+} impurity or Varian pitch. The system thus allows using the time of a sweep more effectively.

2.2.2. Microwave cavity.

We have used two cavities. Varian E-233 Cylindrical Rotating Cavity with the quality factor 20 000 has been used for low dose measurements. Reference sample MgO with $Mn(2^+)$ impurity was placed at the bottom of the cavity. Varian E-231/E-232 dual sample cavity with quality factor 7000 has been used for high dose measurements. In this case, the Varian 'Strong Pitch' can be used as a reference sample. All measurements of alanine EPR intensities were normalized to the intensity of the reference samples.

Cavity stabilization. The stability of the alanine EPR intensity depends on the variation of the cavity quality factor and the temperature of the cavity. The quality factor and tuning of a microwave bridge depend on the room humidity and the cavity temperature. The temperature of the microwave cavity changes due to the magnetic field modulation and the ambient variation during a day. Also, the humidity of air depends on the weather. We have manufactured a system for the humidity and temperature control of the cavity. The microwave cavity is isolated from the temperature variation in the room with foam plastic bandage. The volume of the cavity is filled with the flow of dry nitrogen gas with controlled temperature. The temperature of the cavity is maintained at 28 °C.

2.2.3. Sample rotation system.

An axial rotation of a sample was proposed to minimise the effect of anisotropy of the alanine samples [2] by scanning the samples through the angular range using a goniometer system [3,4]. The use of a goniometer allows also to subtract background spectra of empty cavity, sample tube and alanine tablet in a correct way. The shortcoming of the system proposed in Refs [3,4] is the necessity of precise manual adjustment of the system after each change of a sample. The change of the samples is a complicated procedure. We have designed an automatic system for sample rotation with a worm-gear. The large gear is placed at the sample tube, which is open and allows changing samples using an air lift. The system does not need manual adjustment after a sample changing. The step motor is used for the sample tube rotation. After each step of rotation the EPR spectrum is stored and normalized to the intensity of the reference EPR sample. The system allows averaging the EPR spectrum over the anisotropy of a sample.

2.2.4. Humidity control of alanine tablets

The humidity of the alanine tablets essentially influences the accuracy of alanine EPR dosimetry [5]. The humidity of the tablets changes along the cycle: tablet preparation - storage - irradiation - transportation - storage - measurements. To exclude the influence of the humidity variations, we propose to design a closed space system for tablet storage, processing and measurements. The base of the system is near the microwave cavity and the inner parts of electromagnet. This space is filled with dry nitrogen gas continually. After preparation, tablets are stored here. All stages of tablet processing would be performed in this space. For irradiation, the tablets will be placed in hermetic capsules inside this space. After irradiation, the tablets will be returned to the space and will be transferred from the capsule to the sample holder for the EPR measurements. Microwave cavity is constantly in this space. The system is not completed yet.

2.3. EPR spectrum processing

In the middle-dose range the important point of spectrum processing is a correct subtraction of a background spectrum. The best way is to obtain the correct (i.e. reproducible) individual background spectrum of each tablet. Due to the angular dependence the correct EPR background spectrum of a tablet and a sample holder is the average of number of spectra measured at different angles of the sample holder. The spectrum at each angle is normalized to the intensity of the reference sample. The goniometer system described in 2.2 was used for this process. The spectrum

of the irradiated tablet is also averaged over all the angles. For the dosimetry, the difference of these two averaged spectra was used.

2.4. Reference samples

As reference samples we have used:

(1) Bruker tablets, irradiated at the primary standard of the National Physical Laboratory, UK. We have 5 sets of tablets with absorbed doses 0.5, 1.0, 3.0, 10.0 and 30.0 kGy. For middle-dose EPR dosimetry, we have also used the set with an absorbed dose at 500 Gy and assumed the linear approximation.
(2) Set of 5 Bruker tablets irradiated at the primary standard of the National Institute of Standards and Technology, USA. The irradiation dose was 30 Gy.
(3) Set of 5 AWM (Albrecht Wieser Messtechnik) tablets irradiated at the primary standard of the National Institute of Standards and Technology, USA. The irradiation dose was 30 Gy.

3. DOSIMETRY OF THERAPEUTIC IRRADIATORS

The ASTM standard practice [8] was used for high-dose range (> 100 Gy). For middle-dose range (< 100 Gy), the amplitude of the observable random noise must also be taken into account. To obtain the correct EPR intensity, the short-term noise must be averaged using the computer code. The background spectra of the empty cavity, sample holder and alanine tablets before irradiation must also be taken into account as discussed in 2.3. All measurements were performed in the Kiev City Oncology Center.

3.1. Gamma irradiator

Gamma irradiator ROCUS-AM (manufactured in Russia) - The calibration in the center of the irradiation area and the estimation of the dose distribution over that irradiation area (10 x 10 cm^2) at the distance of 75 cm from the source has been made. For measurements the plexiglas matrix of 22 x 22cm^2 was manufactured. The matrix has 11x11 cells of 5 mm diameter for alanine tablets with steps of 1cm. In addition, 5 cells in each of N,S,E and W directions outside the main irradiation area, were provided. In total, 141 alanine tablets were used for dose mapping with the results: (a) pre-determined dose was 200 Gy; (b) the alanine EPR dose was 220 Gy in the center of the irradiation area, and (c) the total uncertainty was 5 %.

3.2. X-ray irradiators.

The alanine tablets were placed in the cells of the plexiglass plate at the distance of 40 cm from the tubus. Results are presented in Table I.

TABLE I. RESULTS OF ALANINE EPR DOSIMETRY OF X-RAY IRRADIATORS

Type of irradiator	Tube voltage, (kV)	X-ray energy, (keV)	Pre-determined dose, (Gy)	EPR dose, (Gy)
RUM 17	180	90	5.0	5.9 ± 0.3
RUM-17	230	110	5.0	6.2 ± 0.3
RUM-7	60	32	5.0	4.5 ± 0.4

3.3. Electron beam irradiator

Electron irradiator "MICROTRON-M" (manufactured in Russia) - Alanine tablets were placed in the cells of the plexiglass plate at the distance of 100 cm. The electron beam energy was 8

MeV. The pre-determined dose was 10 Gy. The alanine EPR dose was 9.6 Gy (1σ=5%). The dose distribution at a deeper plane inside the standard phantom was also measured for electron energy of 8 and 15 MeV.

3.4. Bremsstrahlung radiation of the "MICROTRON - M".

The energy of the bremsstrahlung radiation was 20 MeV. The distance to the dosimeters was 100 cm. Alanine tablets were placed in the cells of the plexiglass plate. Time of irradiation was 150 s. The pre-determined dose was 10 Gy. The alanine EPR dose was 5.7 Gy (1σ = 5%).

3.5. Uncertainties

The uncertainty of the EPR intensity measurement is:
- 1 % for large EPR signals ($I_{EPR} >> I_{NOISE}$, dose range > 100 Gy);
- 3 % for small EPR signals (I_{NOISE} is about 3 % of I_{EPR}, dose range about 10 Gy).

Total uncertainty of the alanine EPR dose measurements is:
- 3 % for dose > 100Gy; and
- 5 % for dose 10 Gy.

4. DISCUSSION

The principal concerns of the alanine EPR dosimetry which can significantly increase the total uncertainty of the dose measurements at high and middle doses are: the EPR spectropmeter stability, the intra-batch variability of the tablets, the tablet anisotropy, the background EPR spectrum, the long term stability and reproduceability of the EPR measurements, the random electronic noise of the spectrometer, and the tablet humidity variation during the work cycle.

Here we have proposed and discussed the solution for some of the problems. The problem of the total humidity control is not yet resolved. We hope to solve this problem soon. After this, the total uncertainty of the middle-dose alanine EPR dosimetry will decrease to the level that will allow the use of this system as the transfer dosimetry system in the middle-dose range.

The application of the alanine EPR dosimetry for the routine measurements at the medical therapeutic irradiators in the Kiev City Oncology Center has proved to be useful for the local dosimetry service.

REFERENCES

[1] MEHTA, KISHOR, High-dose standardization service of the IAEA, Appl. Radiat. Isiot., **47**, No 11/12, (1996) 1155-1159.

[2] MEHTA, KISHOR and GIRZIKOWSKI, R., Alanine-ESR Dosimetry for Radiotherapy.IAEA Experience, Appl. Radiat. Isot., **47**, No 11/12 (1996) 1189-1192.

[3] HASKELL, E.H., et al., Improved Accuracy of EPR Dosimetry Using a Constant Rotating Goniometer, Radiat. Meas., **27** (1997) 325-329.

[4] HASKELL, E.H., et al., A high sensitivity EPR technique for alanine dosimetry, Radiation Protection Dosimetry , **77**, No 1/2 (1998) 43-49.

[5] DESROSIERS, M., et al., Alanine dosimetry at the NIST, International Conference on Biodosimetry and 5TH International Symposium on ESR Dosimetry and Applications, Moscow/Obninsk, Russia, June 22-26 (1998) Final Programme and Book of Abstracts, 149.

[6] JANOVSKY, I., et al., Progress in Alanine Film/ESR Dosimetry, High-Dose Dosimetry for Radiation Processing (Proc. Int. Symp. High-Dose Dosimetry for Radiation Processing, Vienna, November 5-9 (1990) 173-187, IAEA-SM-314/47; ISBN 92-0-010291-3 (1990).
[7] M.K.H SCHNEIDER, M.K.H., et al., Dosimetry of Electron and Gamma Radiation with Alanine/ESR Spectroscopy, High-Dose Dosimetry (Proc. Int. Symp. High-Dose Dosimetry Organized by Int. Atomic Energy Agency and Held in Vienna, October 8-12, 1984, IAEA, Vienna,. 237-244, IAEA-SM-272/12; ISBN 92-0-010085-6 (1984).
[8] ASTM, Annual Book of Standards, E 1607-94, Practice for use of the Alanine-EPR Dosimetry System, **12.02**, 846-851, ASTM, Philadelphia, Pa (1995).

DOSIMETRY SYSTEMS FOR 5–20 MeV/amu HEAVY CHARGED PARTICLE BEAMS

T. KOJIMA, H. SUNAGA, H. TAKIZAWA, H. TACHIBANA
Japan Atomic Energy Research Institute,
Takasaki, Japan

Abstract

The measurement systems consisting of a Faraday cup, a total-absorption calorimeter and film dosimeters have been developed for dosimetry for heavy charged particle (ion) beams with kinetic energy per nucleon of about 5–20 MeV/amu which are provided by the TIARA AVF cyclotron. The uncertainty in the fluence measurement using a Faraday cup was estimated to be ±2%(1σ) by comparison of the measured values and the calculated values based on the energy fluence obtained using a total-absorption calorimeter and the nominal incident particle energy derived from the accelerator parameters. Several film dosimeters, well-characterized for low LET radiations, were irradiated by ion beams on the basis of this real-time beam monitoring and their dose responses were compared with those for low LET radiations. The results show that the dose response has a tendency to decrease with LET for radiochromic dye film FWT-60 and alanine film dosimeters. Combining uncertainty components for fluence measurement (±2%) and film dosimetry (±4%), the overall uncertainty in ion beam dosimetry is better than ±5%(1σ), which meets the requirements of material science and biological research.

1. INTRODUCTION

Various heavy charged particle beams (e.g., $^{1}H^{+}$ ions with maximum energy of 90 MeV), provided by the AVF cyclotron of Takasaki Ion Accelerators for Advanced Radiation Application (TIARA), are being applied extensively for material science and biological studies, because of a wide range of linear energy transfer (LET) giving different radiation effectiveness and relatively deep penetration [1]. Practical absorbed dose measurement is required, parallel to theoretical dose calculation, for accurate interpretation or comparison of the radiation effects in interested materials induced by different radiation qualities considering inhomogeneity of energy deposition in materials.

Dosimetry for such research work using ion beams should cover the dose range of 0.01 to 200 kGy with an accuracy of about ±5% (1σ). The thin film dosimeters of about 10 to 200 μm in effective thickness, for instance, alanine-PE film and radiochromic dye film (FWT-60) dosimeters, have been well-characterized for low LET radiations of ^{60}Co γ-rays and 1-10 MeV electrons so far [2, 3]. These dosimeters are promising also for ion beams as easy-handling dosimeters, when LET dependence of their dose response characteristics is known.

Reliability check of the real-time beam monitoring technique, e.g. a Faraday cup, is also indispensable for such dose response characteristics studies. From this point of view, dosimetry technique for ion beams has been developed through a two-step procedure: uncertainty estimation of Faraday cup measurements by simultaneous use with a calorimeter, and study on LET dependence of dose response characteristics of film dosimeters based on this reliable real-time beam monitoring. Figure 1 shows the schematic diagram of combination of dosimetry systems simultaneously used for ion beams, to develop a common measure in interpretation or comparison of radiation effects in materials and biological substances.

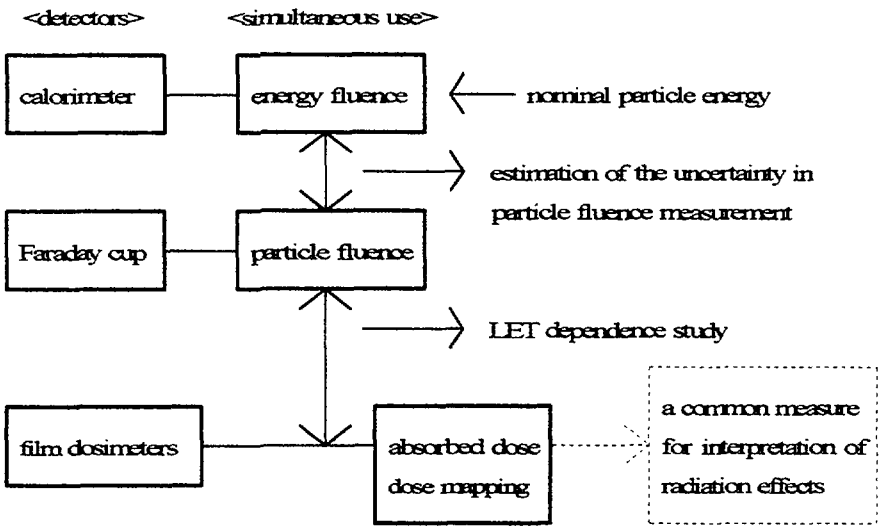

FIG.1. The schematic diagram of combination of dosimetry systems for ion beams

2. SIMULTANEOUS USE OF A TOTAL-ABSORPTION CALORIMETER FOR ESTIMATION OF UNCERTAINTY IN FARADAY CUP MEASUREMENT

2.1. The procedure for estimation of uncertainty in Faraday cup measurement

Fluence measurements were applied to 5-20 MeV/amu ion beams using a Faraday cup consisting of 130-mm long aluminum cup with 30-mm thick graphite absorber at the bottom and 30-mm long cylindrical suppression electrode (-100V) at the entrance of the cup. A total absorption calorimeter with aluminum absorbers of different thickness appropriate to penetration range of the beams under study was designed for simultaneous use with a Faraday cup in a uniform fluence irradiation field through a pair of circular aperture windows of the same size. The Faraday cup and a calorimeter were placed in the scanned-beam irradiation area (100×100 mm^2) under vacuum (about 2×10^{-4} Pa) at the LD-1 port of the TIARA AVF cyclotron, as shown in Fig.2. The experimental procedure is described in detail elsewhere [4].

The uncertainty in the Faraday cup measurements was evaluated through the comparison of the measured particle fluence values and the estimated ones derived from the calorimetry measurements on the basis of the nominal particle energy determined by the cyclotron acceleration parameters.

The particle fluence Φ_m(cm^{-2}) experimentally measured is defined by the equation:

$$\Phi_m = \frac{dN}{d_a} = \frac{Q}{Ze}$$

where, dN is the number of particles entering cross sectional area d_a(area of the circular aperture in this study, 7.07cm^2), Q is the integrated charge in coulomb in d_a collected by the Faraday cup, Z is the number of charge carried per particle, and e is electronic charge in coulomb.

The energy fluence F(J/cm^2) received by the calorimeter absorber (w = mass of the absorber (kg) corresponding to the effective irradiation area) is given by the following equation when the temperature increase of the absorber is ΔT(°C) :

$$F = \frac{\Delta T\, w\, C(T)\times10^{-3}}{7.07}$$

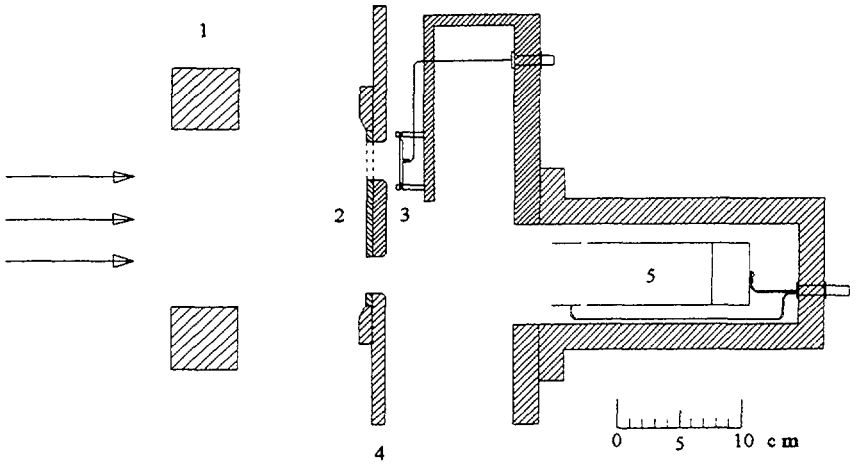

Fig.2. Set-up of the simultaneous use of a total-absorption calorimeter(3) and a Faraday cup(5) which are exposed to the scanned ion beams preliminarily defined to be 100×100mm² by the slit(1) through a pair of circular aperture windows in the same size of 30-mm diameter(4). When the film dosimeters are irradiated based on the Faraday cup measurement, the aperture window to the calorimeter is covered completely by the 5-mm thick aluminum plate as the film mount(2).

TABLE I. UNCERTAINTY IN FLUENCE MEASUREMENT

Ion beams	Energy (MeV)	Range of measured charge(nC)	Fluence measured/estimated[a]	Coefficient of variation(%)[b]	Ref.
$^{1}H^{+}$	20	780-1900	1.056	±0.8	[4]
$^{4}He^{2+}$	20	390-540	1.073	±3.0	[4]
		26-27	1.015	±2.1	this work
	50	360-550	0.993	±1.3	[4]
$^{12}C^{5+}$	220	160-300	0.991	±1.4	[4]
$^{16}O^{6+}$	160	150-200	1.040	±4.0	[4]
		16- 60	1.044	±0.7	this work
$^{20}Ne^{8+}$	260	5- 19	1.014	±2.7	this work
	350	110-140	0.997	±4.7	[4]
		5-7	1.000	±0.5	this work
$^{40}Ar^{11+}$	330	200	1.043	±0.3	[4]
		10-15	0.996	±2.0	this work
$^{48}Kr^{20+}$	520	40	1.001	±1.8	[4]
		5-10	1.001	±2.4	this work

[a] The ratio of measured fluence across the irradiation area of 30mm diameter aperture (7.07cm²) to that estimated based on nominal particle energy imparted over the same area as measured by calorimetry.
[b] Coefficients of variation at a 68% confidence level as estimated from at least three repeated measurements.

where, C(T) is the specific heat capacity of aluminum for temperature range 10-40 °C expressed as C(T)= 0.8612+0.00126T (J/kg °C) and T is the average temperature of the absorber before and after irradiation (°C).

Under simultaneous irradiation of two measurement systems, the fluence values Φ_m were obtained experimentally in terms of integrated charge in the 7.07 cm² area collected by the Faraday cup

taking into account of the charge state of the incident ions (q). On the other hand, estimated fluence values Φ_e were calculated from the calorimetry results and the nominal particle energy (E_n) in MeV which is derived from the cyclotron acceleration parameters using the following equation:

$$\Phi_e = \frac{\Delta T \, w \, C(T) \, q}{E_n \times 1.602 \times 10^{-19}}$$

The measured fluence value Φ_m was compared with the estimated fluence value Φ_e for uncertainty evaluation.

2.2. Results and discussion on uncertainty in Faraday cup measurement

For the ion beams in the range of kinetic energy per nucleon of 5-20 MeV/amu, Table I lists the range of charge measured by the Faraday cup, the ratio of the measured fluence Φ_m to the estimated fluence Φ_e using the above equations, and the scattering of the measured values in the terms of coefficient of variation. The previous result [4] are also included in the table. The average value of the ratio Φ_m / Φ_e is 1.02, and the average precision among at least three measurements is better than ±2% at a 68% confidence level for an integrated charge above 5 nC/cm^2, which are often used for material science. Some measurements were tested also for lower fluence range (at a few nC/cm^2 level), which are useful beam currents for biological studies, by improvements in the correction of the dark current at picoampere level and minimization of the heat-loss for calorimetry of temperature difference of <0.5 °C. As shown in Table I, similar results were obtained also for lower fluence measurement after these improvements. These results lead us to expect that this system is useful to measure wide fluence range of 5-20 MeV/amu ion beams.

3. DOSE RESPONSE CHARACTERISTICS OF FILM DOSIMETERS FOR ION BEAMS

On the basis of the Faraday cup measurement as beam monitoring, dose response characteristics of several thin film dosimeters, e.g. alanine-PE (thickness:223 μm) and radiochromic dye film FWT-60 (thickness:50μm), were preliminarily studied for ion beams with a kinetic energy of 5-20 MeV/amu which have enough energy to pass through the films except for $^{48}Kr^{20+}$ ions. The doses given to the dosimeters were those in their linear dose response range when irradiated by low LET radiation, for example, 1-10 kGy for alanine-PE and radiochromic dye film FWT-60. Average LET values were calculated using OSCAR code [5] based on the data of Ziegler *et al.* [6], taking into account the change of LET values in the dosimeter materials. Dose responses were calculated in terms of relative ESR signal amplitude per unit mass and unit dose for alanine-PE or net absorbance at 600 nm per unit thickness and unit dose for FWT-60 in the dose range of 2-8 kGy, and normalized to those for the low LET radiations. Such relative effectiveness of dose response for both dosimeters decreases with the increase in the averaged LET value of the incident particle beam for mass collision stopping power greater than about 100 MeV•cm^2/g, as shown in Figs 3 and 4. These tendencies are in agreement with those reported by Hansen *et al.* [7, 8] taking account of the difference in averaging of the mass collision stopping power value changing in the dosimeter, although they used alanine pellets (4.5 mm in diameter, 2 mm in thickness) molded with 5% polyvidone instead of alanine-PE films. The scattering range of the dose responses for one data point is about ±4%, for our results.

4. SUMMARY

Uncertainty in Faraday cup measurement was estimated to be ±2%(1σ) for a wide fluence range of ion beams with the kinetic energy of 5-20 MeV/amu. On the basis of this beam monitoring, the coefficients of the LET dependence of the film dosimeter dose responses were preliminary evaluated with precision of about ±4%. Combining these results, overall uncertainty better than ±5% is ultimately achievable for ion beams, that is sufficient for radiation effects studies in materials and biological substances.

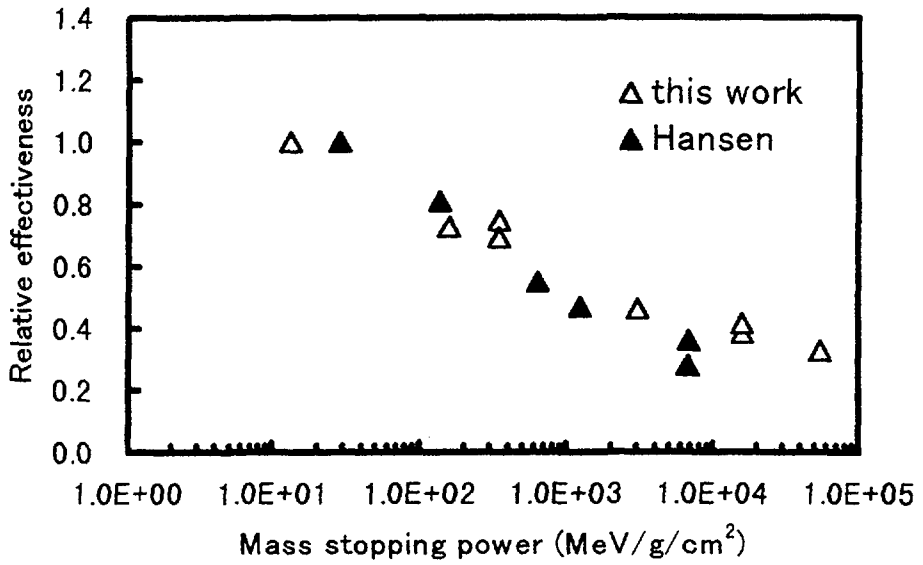

FIG.3. The dependence of dose response of FWT-60 for different radiation qualities. Data of Hansen is cited from Ref.[7].

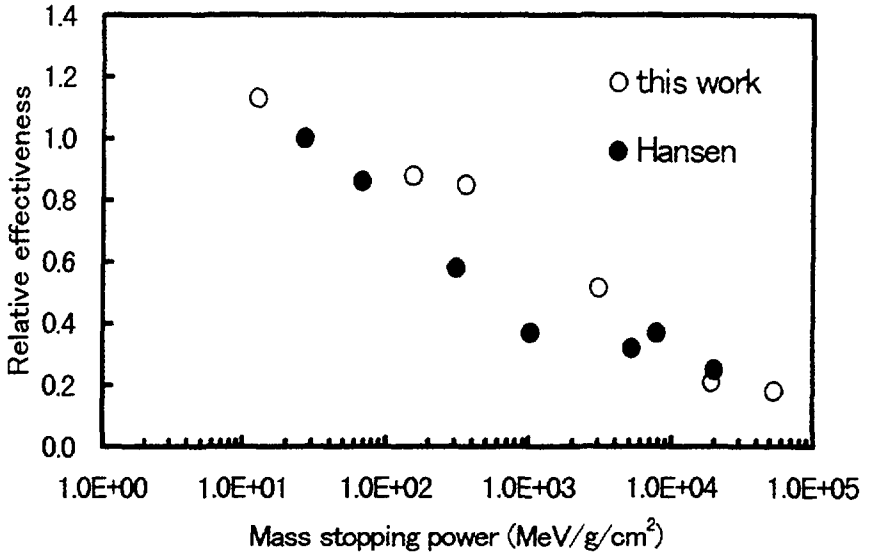

FIG.4. The dependence of dose response of alanine dosimeters for different radiation qualities. Alanine-PE film (8×30 mm, 223 μm) was used in this work while Hansen used pellets (4.5 mm in diameter and 2 mm in thickness) molded with 5% polyvidone[8].

Film dosimeters, for instance alanine-PE and radiochromic film FWT-60, show decrease in the effectiveness of the dose response, relative to that for low LET radiations, with increase in the mass collision stopping power of the incident ions. The tendency of both, alanine-PE and FWT-60 films, mostly agrees with the previous report of Hansen *et al.* Similar studies using other film dosimeters, e.g. cellulose triacetate film and GafChromic film, and their applicability to lateral or depth dose profile measurement are in progress, parallel with the improvement of the dose interpretation considering the LET dependence and reaction mechanism taking into account the track structure [9].

These approaches are expected to contribute towards establishing reliable dosimetry for heavy charged particle beams on the basis of well-established gamma-ray reference dosimetry [10].

REFERENCES

[1] TIARA Annual Report 1996, JAERI-Review 97-015, JAERI, Ibaraki(1997)

[2] McLAUGHLIN, W.L., et al., "Dosimetry for Radiation Processing", Taylor and Francis, London (1989) 167-169

[3] KOJIMA, T. et al., "Thin film alanine-polyethylene dosimeter", Appl.Radiat.Isot., **44** (1993) 41-45

[4] KOJIMA, T. et al., "Fluence measurements applied to 5-20 MeV/amu ion beam dosimetry by simultaneous use of a total absorption calorimeter and a Faraday cup", Radiat. Phys. Chem., **53** (1998) 115-121

[5] HATA, K. and BABA, H., "OSCAR, a code for the calculation of the yield of radioisotopes produced by charged particle-induced nuclear reactions", JAERI M 88-184, JAERI, Ibaraki (1988)

[6] Ziegler, S.M. et al., "The stopping powers and range of ions in solids", Vol.1, Pergamon press, Oxford(1985)

[7] HANSEN J.W. and OLSEN K.J., " Experimental and calculated response of radiochromic dye film dosimeter to high-LET radiations", Radiat.Res., **97** (1984) 1-15

[8] HANSEN et al., "The alanine radiation detector for high and low LET dosimetry", Radiat. Prot.Dosim., **19** (1987) 43-47

[9] KOIZUMI, H. et al., "Radical formation in the radiolysis of solid alanine by heavy ions", Nucl.Instrum.Methods Phys.Res., **B 117** (1996) 431-435.

[10] KOJIMA, T. et al., "Uncertainty estimation in ^{60}Co gamma-ray dosimetry at JAERI involving a two-way dose intercomparison study with NPL in the dose range 1-50 kGy", accepted and to be published in Radiat.Phys.Chem.(1999)

DEVELOPMENT OF A PORTABLE GRAPHITE CALORIMETER FOR PHOTONS AND ELECTRONS

XA9949726

M.R. McEWEN, S. DUANE
Centre for Ionising Radiation Metrology,
National Physical Laboratory,
Teddington, Middlesex,
United Kingdom

Abstract

The aim of this project is to develop a calorimeter for use in both electron and photon beams. The calorimeter should be more robust than the present NPL primary standard X-ray calorimeter and is designed to be sufficiently portable to enable measurements at clinical accelerators away from NPL. Although intended for therapy-level dosimetry, the new calorimeter can also be used for high-dose measurements at industrial facilities. The system consists of a front end (the calorimeter itself), means for thermal isolation and temperature control, and a measurement system based on thermistors in a DC Wheatstone bridge. The early part of the project focused on the development of a temperature control system sensitive enough to allow measurements of temperature rises of the order of 1 mK. The control system responds to the calorimeter, phantom and air temperatures and maintains the temperature of the calorimeter to within ± 0.2mK over several hours. Initial operation at NPL in 6, 10 and 16 MV X-ray beams show that the system is capable of measurements of 1 Gy at 2 Gy/min with a random uncertainty of ± 0.5% (1 standard deviation).

1. INTRODUCTION

Graphite calorimeters have been under development at NPL for many years. There are separate primary standard graphite calorimeters for high energy photon and electron beams. The photon calorimeter [1] is based on the design by Domen and Lamperti [2] and is a complex device able to measure dose rates down to 1 Gy/min. The electron beam calorimeter was first developed for high dose applications in radiation processing and sterilization [3] but has been enhanced to operate at radiotherapy dose rates as low as 5 Gy/min [4]. Graphite has obvious advantages as the material to use for a calorimeter in that it is a solid with a high thermal conductivity and zero heat defect (i.e. all the energy deposited by the radiation is expressed as heat). However, its major limitation is that it is not the material of interest. In the majority of dosimetry applications absorbed dose to water is the quantity required and therefore, corrections are required to convert from absorbed dose to graphite to absorbed dose to water. A water calorimeter would give the desired quantity directly, but water calorimeters tend to be very complex devices and the radiochemical reactions in water lead to a heat defect which makes it difficult to obtain an accurate value of the absorbed dose. Water calorimeters are under development at a number of institutions worldwide - including NPL - and their use is generally restricted to radiotherapy dose levels.

Since the two graphite calorimeters at NPL are of very different designs, it is not possible to define either one as the primary standard for both radiation types. The photon calorimeter can operate in high energy photons from Co-60 to 20 MV but is restricted to electron energies above 12 MeV. The electron calorimeter's simplicity of design means that it cannot operate at the limited dose rates available for high energy photons. It would be preferable to have a single calorimeter for both electron and photon beams for a range of dose rates - from therapy levels up to industrial levels.

NPL offers a number of dosimeter calibration services for high energy photon and electron beams at therapy and industrial dose rates. One area of concern for all these services is the validity of the transfer of the calibration from NPL to other radiation facilities. It is assumed that the secondary dosimeters calibrated, whether they be ion chambers or chemical dosimeters, behave in the same way in two radiation beams defined by some beam quality. It is difficult to test this assumption since it has not

be generally possible to operate primary standard calorimeters away from NPL. It is a desirable objective to be able to operate a calorimeter in the user's own radiation field. This would enable one to check the transfer of calibrations and investigate beam quality issues. This is primarily a concern at radiotherapy dose levels where the uncertainty associated with a calibrations has to be much smaller, but it would also be beneficial to have a calorimeter that could be taken from one industrial facility to another. This paper will deal primarily with calorimetry at radiotherapy levels since this is the most demanding application.

2. DESIGN

2.1. Design requirements

The design requirements of this new calorimeter can be stated quite simply:

(1) A single calorimeter to operate in high energy photon and electron beams (gammas: Co-60 to 20 MV, and electrons: 3 MeV to 25 MeV) at dose rates from 1 Gy/min to 10 kGy/min.
(2) A simple and robust design, easy to maintain.
(3) Portable, to allow measurements at other radiation facilities, primarily in the UK but also in other countries.

There are two main problems with therapy-level calorimetry - measuring the radiation-induced temperature rise, and preventing environmental changes from swamping the measurement. The radiation-induced temperature rise in a material is related to the absorbed dose via the specific heat; a dose of 1 Gy (a typical dose at radiotherapy levels) to graphite leads to a temperature rise of 1.4 mK. To be useful, the calorimeter must be able to measure this dose with an uncertainty better than ± 0.5%, which is equivalent to ± 7μK. To resolve temperatures to this level at room temperature is a severe problem requiring state-of-the art equipment. The second problem is that of temperature control. To be able to measure the radiation-induced temperature rise in the calorimeter, environmental effects must be kept to a minimum. The radiation-induced temperature rise is obtained by extrapolating the pre-and post-irradiation temperature traces to the mid-point of the irradiation. Changes in these traces due to environmental effects would result in an error in the extrapolation. Ideally the pre- and post-heat temperatures should be constant, but a linear drift in one direction does not have an effect on the extrapolation. However, any non-linear behaviour in the drift would significantly affect the derivation of absorbed dose. This therefore implies that the room where the calorimeter is used must have very stable air conditioning, or the calorimeter must have built-in temperature control. The NPL linac benefits from a very stable air conditioning system which keeps the temperature of the irradiation room within ± 0.1 °C, allowing operation of the electron beam calorimeter down to 5 Gy/min with only minimal expanded polystyrene insulation. However, such air conditioning is not generally available in other radiation facilities and therefore the only option is to design a calorimeter with built-in temperature control. Such a control system would have to cope with a wide range of temperatures and rapid temperature changes. For example, a linac exposure room in a radiotherapy clinic has a maze entry but no doors, and therefore a calorimeter in such a room could experience a combination of effects due to draughts and heat sources (e.g. the linac itself). The situation in industrial facilities is likely to be even more severe, although the measured temperature rise due to the radiation is much larger.

2.2. Calorimeter design

After some consideration it was decided to base the new calorimeter on the present electron beam primary standard calorimeter. Such a device would need further enhancements to allow operation at 1 Gy/min and in more hostile environments than those found at NPL. Graphite was the material of choice since there was already much experience of using graphite calorimeters at NPL. The only other choices are water or some water-equivalent plastic. Water is just not practicable for a portable calorimeter and little work has been done on plastics, except for polystyrene. Although the conversion from graphite to water adds an additional uncertainty, it was not felt to be a significant problem. The basic elements of the calorimeter are shown schematically in Fig. 1. The main calorimeter body is a graphite core and a graphite

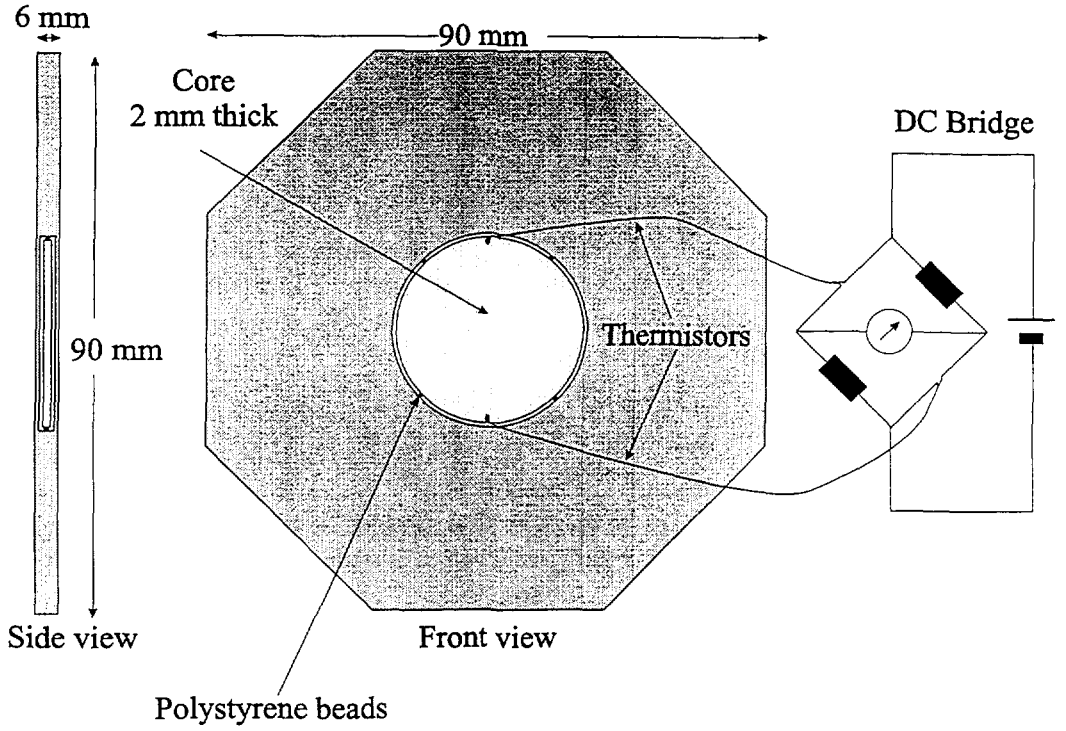

FIG. 1. Schematic diagram of calorimeter. For clarity the second bridge and associated thermistors are omitted.

surround. The core is a disc 20 mm in diameter and 2 mm thick, with holes drilled radially into the disc to accommodate four 22 kΩ bead thermistors of diameter 0.5 mm and length 3 mm. The graphite surround is an octagon 90 × 90 mm in cross section and 6 mm in thickness. The core is thermally isolated from the surround by a nominal 1 mm air gap at all faces and is supported by small expanded polystyrene beads. The octagon is a convenient approximation to the nominal 90 mm diameter circular field of the NPL linac at a SSD of 1 m. The thickness of the calorimeter core is chosen so that it can be used in the lowest electron energy available from the NPL linac - 3 MeV. The diameter of the core is such that any correction for radial beam uniformity is small.

Graphite plates are added in front of the calorimeter body to position the core at the desired measurement depth and also added to the rear to provide backscatter. The thickness of this backing depends on the radiation type, the incident beam energy and on the measurement depth and is chosen so that the temperature rise in the backing is as close as possible to that in the core. One of the major problems with electron dosimetry is the rapid fall-off of the depth-dose curve. If one used a traditional "thick" phantom, such as employed in the photon primary standard calorimeter, there would be significant heat transfer from the core to the graphite surround (especially without the benefit of a vacuum system) making extrapolations difficult. The entire calorimeter assembly is enclosed in 25 mm of expanded polystyrene to provide a first level of thermal isolation.

The thermistors that measure the temperature rise in the graphite core are included in opposing arms of two simple DC Wheatstone bridges constructed from precision resistors with a very low temperature coefficient (<1 ppm/°C). Two commercial 6½-digit voltmeters (DVMs) read the out-of-balance voltages from the bridges simultaneously and are operated under IEEE-488 computer control. The power supply for the bridge is a precision voltage supply (Vsup equivalent to 1.4 V) constructed at NPL [5]. The aim of these enhancements to the basic electron calorimeter design was to increase the signal to noise ratio. Two bridges gives an immediate improvement. By using thermistors in opposing arms of the bridge one can cancel out some of the induced noise, which theory suggests should be better than single thermistors in individual bridges. Shielded, twisted pair cable is used throughout to keep noise

pickup to a minimum - a linear accelerator is a very electrically noisy environment and therefore every precaution must be taken to minimise the effects of noise. A larger value of the bridge power supply can also be used to increase the signal-to-noise ratio, although it also increases the power dissipated in the thermistors and raises the question of non-linear effects due to thermistor self-heating. Calculations have indicated that a value of up to 2V can be used safely.

The bridge out-of-balance voltage is calibrated directly against the absolute core temperature using a commercial platinum resistance thermometer (PRT). The thermistors used in the calorimeter have been found to be very stable requiring re-calibration only every two years. The effect of accumulated dose on the response of the thermistor type used here has been measured at NPL [6]. No change was measured at the ±0.1% level for doses in excess of 1MGy.

As stated earlier, the absorbed dose to the graphite core D_g is derived directly from the absolute temperature rise ΔT_g and the specific heat capacity c_g of the core ($D_g = c_g \times \Delta T_g$). Extensive measurements have been carried out at NPL to measure the specific heat capacity of the graphite core over the temperature range 18-32 °C. Williams [7] looked at several samples of graphite and found no significant difference in the specific heat capacity. He also irradiated a sample up to a dose of 3 MGy and re-measured the specific heat capacity. Again, there was no significant difference in the result. The result also agreed with previous measurements of the specific heat capacity made at NPL using the method of differential scanning calorimetry [8], but with a much reduced uncertainty.

The most significant drawback of this design is the isolation of the core from the surround. By using only a 1 mm air gap , rather than a vacuum gap as in the photon primary standard calorimeter, one increases the heat transfer from the core to the surround. If the time constant associated with this transfer is too small then what is measured is the bulk temperature rise rather than the core temperature rise.

2.3. Temperature control system

The temperature control system is shown schematically in Fig. 2. It consists of a large graphite body (total mass 14 kg) which surrounds the calorimeter on five sides. It is not possible to put material in front of the calorimeter since that would affect the measurement depth and prevent operation at the lowest electron energies. Embedded within the graphite body are electrical heater elements which elevate the body temperature to approximately 30 °C. By operating at an elevated temperature one can use the environment as the cooling circuit rather than employing Peltier heat engines. The entire body is surrounded by 25 mm of expanded polystyrene, with an extra 50 mm at the front to reduce the heat transfer from the environment to the calorimeter. This polystyrene is enclosed in a hard plastic case, open at the front, which is electrically screened to reduce noise pickup. The current to the heater elements is provided by a computer-controlled power supply. Three temperatures are sensed - the calorimeter surround, graphite body, and outside air. An algorithm running on the controlling PC adjusts the heater current according to the temperatures of the air, body and core in order to keep the calorimeter temperature constant. An alternative to this system would be to place the calorimeter inside an air-conditioned box. However, to obtain the same stability as the graphite body arrangement one would need a large volume of air which would make transport more difficult. The overall dimensions of the body controller are 40 × 40 × 40 cm which makes it relatively easy to transport. It should be noted that there are no heater elements in the calorimeter itself and that the body is outside the field size of the NPL beam (except behind the calorimeter). This design is therefore best suited to a scattered, rather than swept, beam.

The temperature sensing thermistors used for the control system are separate from those used to determine the absorbed dose. The sensor for the calorimeter surround is a single glass bead thermistor in a DC bridge. The graphite body uses nine thermistors in a series/parallel arrangement in a single arm of a DC bridge. This arrangement behaves like a single thermistor but gives the mean temperature over the whole of the graphite body. Similarly, the air is sensed using four thermistors in a series/parallel arrangement to give the mean air temperature over four sides of the outer case. These air sensors are mounted on thin graphite plates to reduce any self-heating effect and give a more reliable response. The

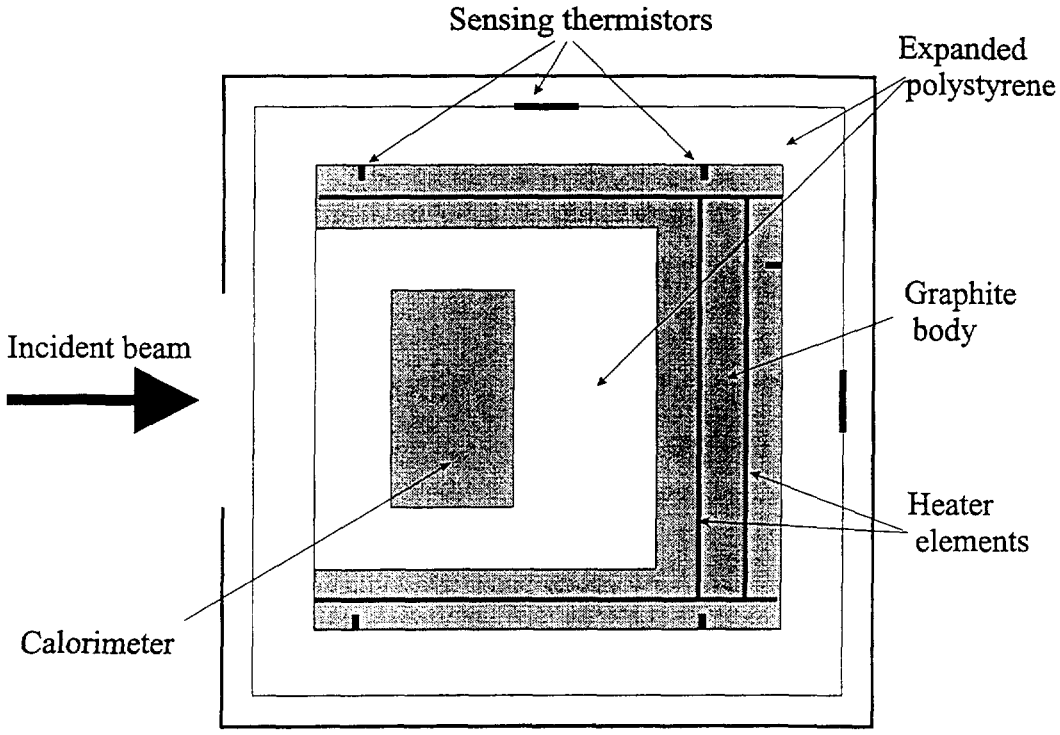

FIG. 2. Schematic diagram of the body design - side view.

major assumption in this approach is that the three-dimensional system approximates to a one-dimensional system defined by the three temperatures - calorimeter surround, mean body, and mean air. Such an assumption is a reasonable starting point and makes it easier to construct a control algorithm. The three temperature sensors are calibrated in terms of absolute temperature against a PRT in the same way as the thermistors used to measure the absorbed dose.

A significant amount of work has been put into developing the control algorithm. This is superior to a standard PID (proportional-integral-differential) algorithm in that it anticipates the effect of variations in the air temperature on the calorimeter core and adjusts the body temperature to compensate. The control system is somewhat asymmetric in that heat can be put much more quickly into the body through the electrical heating than it is lost through conduction to the air. Effort has been made to derive, by measurement, the heat transfer coefficients for the three components - air:body, air:core and body:core. The aim was not to derive a full thermal model of system but to use a simplified model based on one dimensional heat transfer. The algorithm also has to rapidly stabilize the calorimeter. If one is to make measurements in the field then one cannot wait several days for the calorimeter to be ready for use. Separate PCs are used to control the calorimeter temperature and measure the absorbed dose - although this involves more equipment it simplifies the software.

3. TESTING

There are three aspects to the testing of this calorimeter - testing the temperature control algorithm, investigating the performance of the calorimeter and any systematic effects, and validation of the calorimeter against the present primary standards at NPL. Only when this has been completed can the final test of use in the field be carried out. The calorimeter was tested in 6, 10 and 16 MV photons and 16 MeV electrons using the NPL linear accelerator. The NPL linac is a travelling-wave, two-section research accelerator allowing manual control of all the important operating parameters (pulse current, prf, pulse width etc) at any electron energy in the range 3-20 MeV. A tungsten target (for X-rays) or an aluminium scatter plate (for electrons) is placed at the end of the accelerator flight tube. For the photon measurements a SSD (source-surface distance) of 1 m and field size of 9 cm diameter was used; for the

electron measurements a SSD of 2 m and a field size of 15 cm × 15 cm was used. The dose rate in photons was varied between 2 and 5 Gy/min while in electrons a higher dose rate between 10 and 20 Gy/min was used. By operating at higher dose rates one can give the required dose (typically 1 Gy) in a much shorter time and therefore one can investigate more thoroughly the transfer of heat between the calorimeter core and its immediate surround. It is obviously easier to obtain the higher dose rates in electrons. A transmission monitor ion chamber is used to correct for current variations in the linac output. This monitor is of an NPL design - aluminium electrodes are evaporated onto 25 μm polyimide foils - putting a minimal amount of material in the beam.

4. RESULTS

The performance of the temperature control algorithm is shown in Figs 3 and 4. A typical calorimeter run is shown in Fig. 5.

5. DISCUSSION

Figure 3 shows what the various temperature sensors measure when the control program is started. Initially the calorimeter is at room temperature with all three sensors reading the same temperature. As stated earlier, rapid stabilization of the calorimeter at its operating temperature is a primary requirement of the algorithm, and this is achieved by rapidly heating the body above its operating temperature and then, at the appropriate moment, switching the electrical heating off. This makes the calorimeter temperature drift up to the desired operating temperature and, just before its temperature would start to fall again, the body is turned on again to maintain constant temperatures. The user is able to set the required temperature of the calorimeter and the control program adjusts the body temperature to suit, depending on the air temperature. As can be seen the air sensor also indicates an increase in temperature. This is because the air sensors are placed on the outside of the case of the body and respond to heat conducting through the polystyrene insulation. Although this means that the air sensors do not measure the true air temperature, it does not significantly affect the performance of the control program. Stabilization of the calorimeter is achieved within eight hours.

Figure 4 shows the stability of the calorimeter at a later time when stabilization has been achieved. By varying the body temperature in response to air temperature variations, the calorimeter temperature is maintained to ± 0.2 mK over several hours. As one can see, there is a slight systematic residual in the calorimeter temperature (at the 0.1 m K level) indicating that the control algorithm is not fully correcting for air variations. Although the long term stability is impressive, one is really interested in the stability of the system over the length of a calorimeter run - typically five minutes. Slow changes in temperature are acceptable since these produce linear drifts in the calorimeter trace and these are typical of the NPL environment. It is not so certain that other radiation facilities are so benign. One of the concerns in developing the algorithm was whether the parameters determined in the model were 'universal' or situation specific. Ideally the control program would perform the same in any radiation facility, but further work is required to see whether this is true. Work is currently underway at NPL to gain a deeper understanding of the physical processes involved in the calorimeter system which should yield a more robust and reliable control algorithm.

Figure 5 shows a typical calorimeter run in a 16 MV photon beam at a dose rate of 5 Gy/min. The irradiation time was kept to a minimum so that any heat transfer between core and surround in the calorimeter would be clearly shown. If one had complete isolation of the core from the surround then the post-heat trace would have exactly the same gradient as the pre-heat trace, but this is obviously not the case here. Curvature in the post-heat trace indicates significant heat transfer from core to surround. The extrapolations will correct for this heat loss but the uncertainty is increased due to the non-linear behaviour. This effect can be minimised by using short irradiation times but one is constrained by the signal-to-noise ratio which, at present, limits the minimum measurable dose to about 0.5 Gy. The typical standard deviation in the calorimeter/monitor ratio for ten calorimeter runs is 0.5%. This is the random

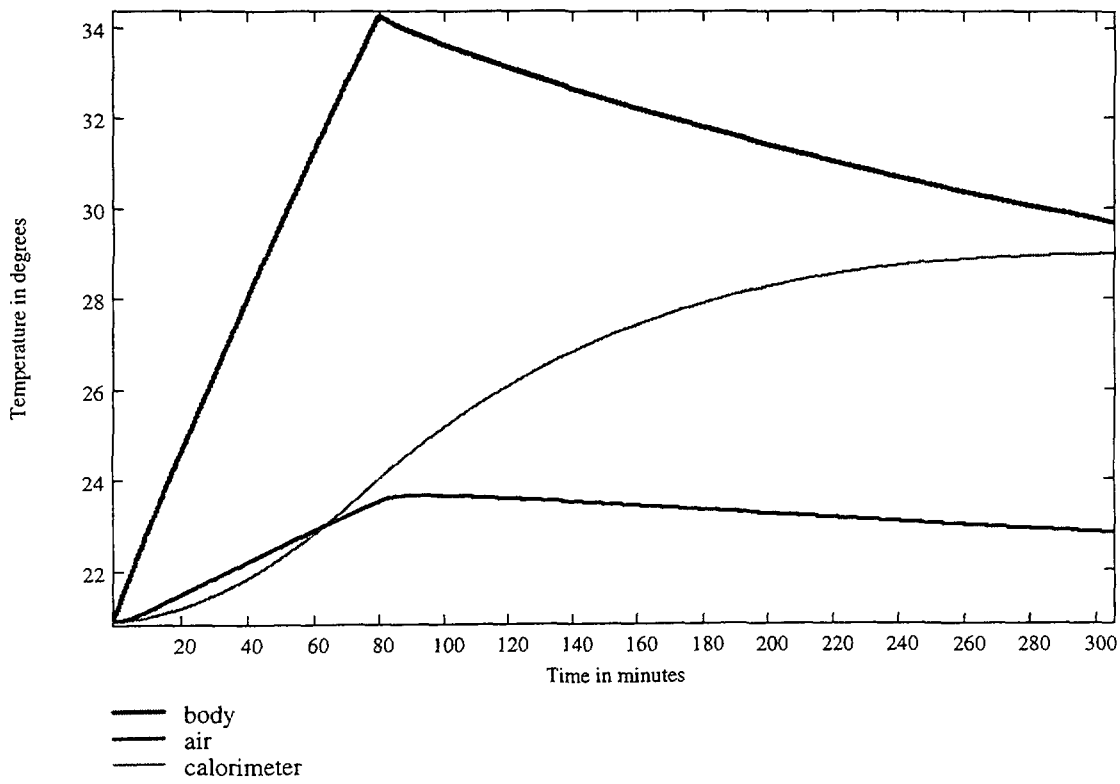

FIG. 3. Performance of temperature control system from switch on

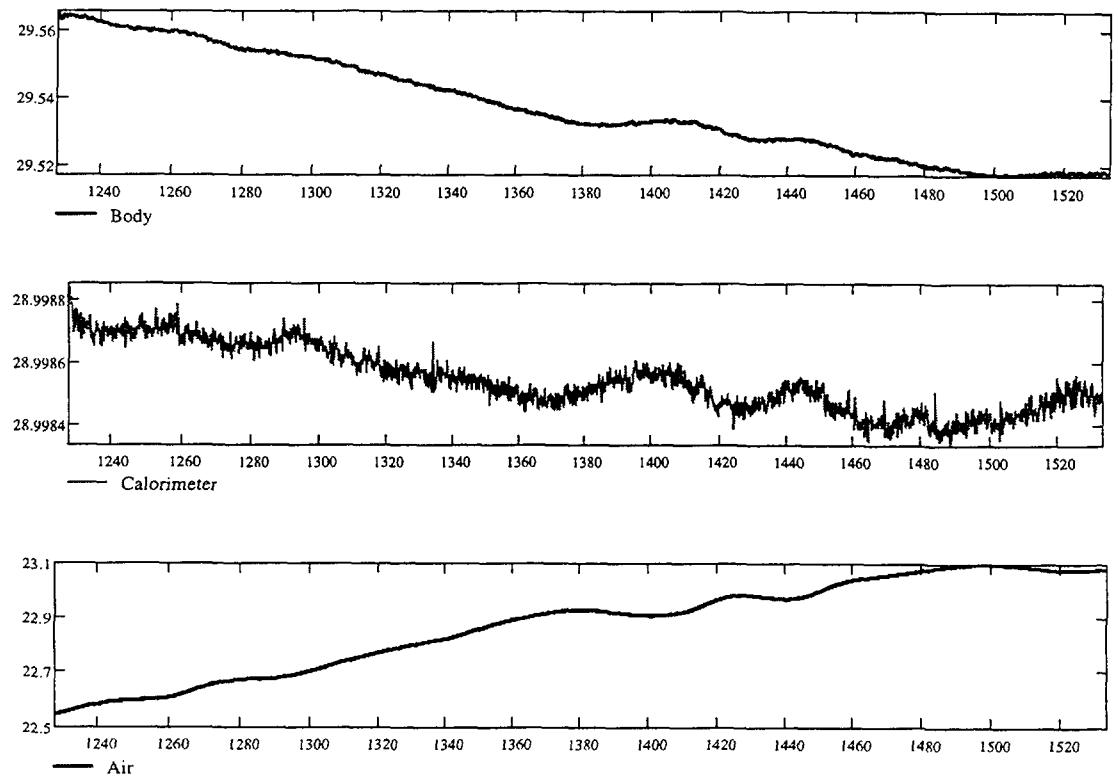

FIG. 4. Stability of temperature control system. X axes - time (min), Y axes - temp (°C)

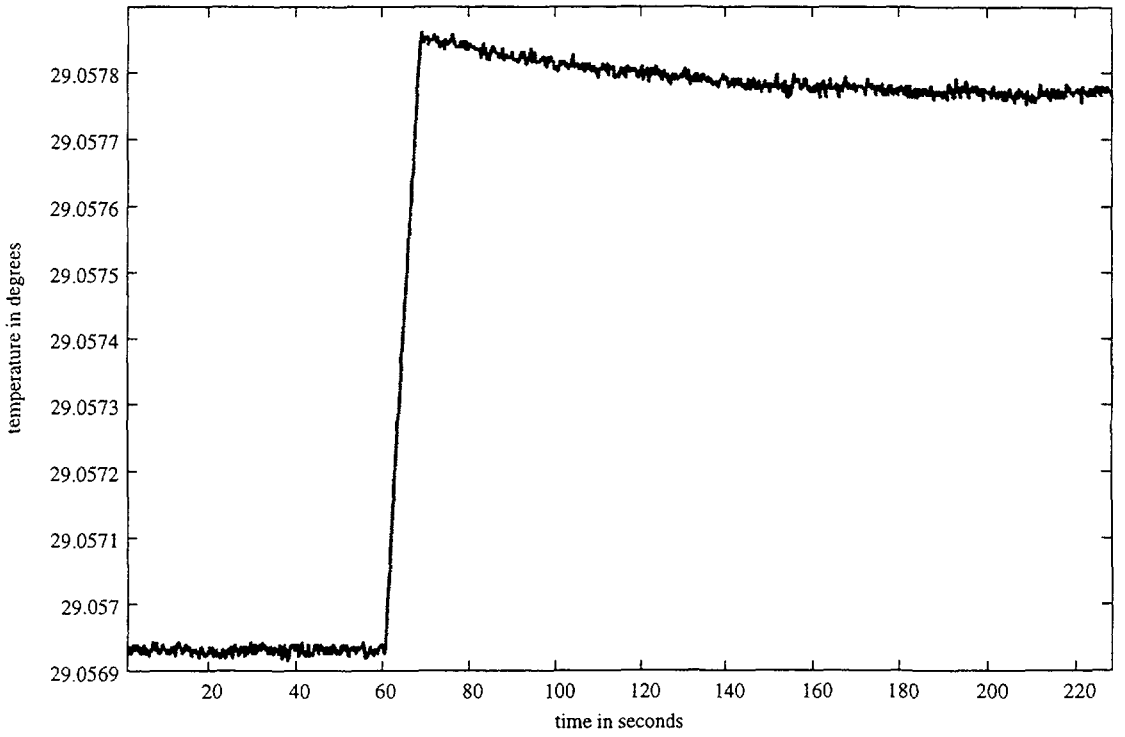

FIG. 5. Typical calorimeter run at NPL in a 16 MV photon beam at a dose rate of ~ 5 Gy/min

uncertainty and is due to a combination of effects including noise, extrapolations and drifts in linac output, and is slightly larger than one would like. It is hoped to further improve the signal-to-noise, which should reduce this uncertainty.

5. CONCLUSION

Initial testing of the calorimeter has confirmed the suitability of the design. Radiotherapy dose rates can be measured with an uncertainty close to that of the present primary standards. The system is portable, opening up the possibility of making direct measurements in user radiation facilities - particularly radiotherapy clinics. Further work is required to improve the temperature control algorithm by modelling of the heat transfer processes in three dimensions. It is hoped to extend this work to model the heat transfer during irradiation and so derive a correction for the heat transfer from core to surround in the calorimeter.

Before the calorimeter can be used outside NPL it must be validated against the present primary standard calorimeters together with a full investigation of any systematic effects. It should be noted that this calorimeter is not intended to replace the present primary standards, but as a transfer instrument between NPL and other radiation users. Once this work is complete it is hoped to carry out measurements in UK radiotherapy clinics, as well as other radiation facilities. This will give a direct determination of absorbed dose where it is required, check the validity of dosimeter calibrations provided at NPL, and allow investigation of issues such as beam quality definition.

ACKNOWLEDGEMENTS

The authors would like to acknowledge the financial support of the National Measurement Policy Unit of the UK Department of Trade and Industry.

REFERENCES

[1] DUSAUTOY, A.R., The UK primary standard calorimeter for photon beam absorbed dose measurement, Phys. Med. Biol.**41** (1996) p137

[2] DOMEN, S.R., LAMPERTI, P.J., J. Res. Natl. Bur. Stand**78** (1974) p595

[3] BURNS, D.T., et al., An NPL absorbed dose calibration service for electron beam radiotherapy, (Proc. Int. Symp. on Measurement Assurance in Dosimetry, 1993) IAEA-SM-330/34 (FLITTON, S.P., Ed.), IAEA, Vienna (1994) p61

[4] MCEWEN, M.R., et al., The calibration of therapy level electron beam ionisation chambers in terms of absorbed dose to water, Phys. Med. Biol**43** (1998) 2503-2519

[5] SANDERS, R.P., THOMAS, C.G., A precision voltage supply for the NPL primary standard electron beam calorimeter, NPL Report RSA(EXT)24 National Physical Laboratory, Teddington (1991)

[6] MCEWEN, M.R. et al., The use of thermistors in the NPL electron beam calorimeter, NPL Report RSA(EXT)41, National Physical Laboratory, Teddington (1993)

[7] WILLIAMS, A.J., et al., Measurement of the specific heat capacity of the electron beam graphite calorimeter, NPL Report RSA(EXT)40, National Physical Laboratory, Teddington (1993)

[8] RICHARDSON, M.J., Compendium of thermophysical property measurement methods Vol 1; Survey of measurement techniques (MAGLIC, CEZAIRLIYAN and PELETSKY, Ed.) Plenum Press, New York (1984)

ABSOLUTE AND SECONDARY DOSIMETRY AT THE CYCLOTRON ION BEAM RADIATION EXPERIMENTS*

Z. STUGLIK
Laboratory for Measurement of Technological Doses,
Institute of Nuclear Chemistry and Technology,
Warsaw, Poland

Abstract

One of the characteristic features of ion beam radiation experiments is that the absolute methods of dosimetry are more convenient than secondary ones. In this paper the absolute method used in the course of the radiation experiments performed on the U-400 Dubna cyclotron is presented in detail. Some remarks dealing with the secondary methods are also given.

1. INTRODUCTION

The principle of resonant particle acceleration in a static magnetic field was discovered by Ernest O. Lawrence in 1930 and only two years after the first cyclotron was built at Berkeley. From that time, the technology of particle acceleration has undergone big development giving such constructions as synchrotrons and storage rings both capable to accelerate particles up to TeV. Nevertheless, the cyclotrons still hold an important position. They give an intensive and good quality beams of different ions with energy in the range 1-100 MeV/amu. Compact size, reasonable cost of installation and limited power consumption are positive economical factors of these devices. Actually, more than 200 cyclotrons are in operation over the world. From many years the number of facilities dedicated to applied studies has increased faster than that for the pure physics. Cyclotrons are used in atomic and nuclear physics, material science, biology and medicine. Chemical studies have been done rather seldom. It results not only from still high cost and hard access to the ion beams but also from experimental difficulties, among them – dosimetry. The secondary methods, useful and commonly used in low-LET experiments lose their versatile character in high-LET area. It is connected mainly with LET-dependence of the G-values. As a consequence, "the dosimetric answers" to the same dose are different not only for different ions with the same energy, but also for the identical ions with different energies. The secondary dosimeters may be eventually applied in the experiments using one kind of ions with the same energy. Of course, they should be carefully calibrated with an absolute dosimeter before using them. In such situation, the advantages in using secondary dosimeters are rather low and the absolute methods (despite their time-consuming and complicated character) are recommended for high-LET ion beam radiation experiments.

The absolute methods could be divided in two classes:

a) calorimetric methods,

b) methods based on energy and fluence measurements.

The range of the ions in matter - the third quantity necessary for dose evaluation – can be taken from physical tables [1,2] or calculated by means of computer programs [3,4].

The calorimetric methods can be used only for the light particles with relatively long ranges. However, their applicability is rather doubtful for intermediate energy heavy ions with the ranges of about 10 mg/cm^2 (~ 0.1 mm in water). The next shortcoming is that they cannot be used as on-line methods. The cyclotron ion beams are rarely so stable as electron ones and to achieve reasonable accuracy of the experiments, the ion beam fluences has to be measured directly during the irradiation.

*The work partially supported by the State Committee for Scientific Research, Poland, under contract 2 2446 91 02

The methods based on energy and fluence measurements have fewer disadvantages than calorimetry and are commonly used in the cyclotron experiments. One of such methods - used in the course of the radiation experiments at Dubna facility - will be presented below.

2. EXPERIMENTAL CONDITIONS

2.1. U-400 cyclotron and the ion beams used at the chemical radiation experiments

Four-meter U-400 isochronous cyclotron has operated at Flerov Laboratory of Nuclear Reactions, JINR, Dubna, Russia from 1978. During our experiments (1990 – 96) it was equipped with PIG ion source and capable of accelerating ions from Li to Xe with a mass-to-charge ratio from 5 to 12. The maximum energy per nucleon ranged from 18 MeV for lighter ions to 3.8 MeV for ^{129}Xe.[1] The ions were extracted via charge exchange in thin (40-200μg/cm^2) graphite foils. The intensities of external beams were in the range of 10^{13} particles per second (pps) for the light ions and 10^9 pps for the heaviest one. The energy of the ions produced by the U-400 cyclotron depended on the "extraction mode" and could be changed by step of 30-40%. At a fixed extraction mode, the energy could be changed smoothly within ±5% around the value corresponding to the maximum intensity for each charge. The U-400 ion beams had a time structure: there was a train of 1.5 ms pulses separated by 5.1 ms intervals, and each such pulse consisted of a number of much shorter pulses with a duty factor of 10 and a frequency equal to that of the accelerating RF voltage (5-12 MHz). As a consequence, the instantaneous dose rate is ~40 times higher than the average value obtained as a dose divided by time of irradiation. For more experimental details see [6,7].

TABLE I. PHYSICAL PARAMETERS OF THE IONS USED IN THE RADIATION EXPERIMENTS

cyclotron chamber	extracted beams	energy in vacuum, E_0 (MeV)	specific energy in vacuum (MeV/amu)	energy on the surface of the sample, E_S (MeV)	specific energy on the surface (MeV/amu)	range in air [a] for $E = E_S$ (mm)	range in water [a] for $E = E_S$ (μm)
$^{11}B^{2+}$	$^{11}B^{4+}$	113	10.3	102	9.3	460	462
$^{12}C^{2+}$	$^{12}C^{6+}$	133	11.1	122	10.2	410	433
$^{18}O^{2+}$	$^{18}O^{8+}$	118	6.5	79	4.4	112	108
$^{22}Ne^{3+}$	$^{22}Ne^{9+}$	182	8.3	131	5.9	141	147
$^{24}Mg^{3+}$	$^{24}Mg^{11+}$	186	7.7	138	5.7	106	110
$^{40}Ca^{5+}$	$^{40}Ca^{18+}$	299	7.5	177	4.4	62	64
$^{52}Cr^{6+}$	$^{52}Cr^{21+}$	326	6.3	168	3.2	47	48
$^{56}Fe^{6+}$	$^{56}Fe^{22+}$	317	5.7	108	1.9	29	30
$^{59}Co^{7+}$	$^{59}Co^{25+}$	397	6.7	203	3.4	50	51

[a] The ranges were calculated by means of TRIM programme [3]

In the radiation chemical experiments we used defocused external ion beams which characteristics are shown in Table I. The flux was commonly attenuated to 10^8 - 10^9 pps and the fluence was usually in the range 10^9 - 10^{11} ions/cm^2. As it is seen from Table I the ranges of the ions are directly proportional to the specific energies and inversely proportional to masses. The first dependence is much stronger than the second one. The ranges in water varied from some hundreds of micrometers for the lightest ions to some tens of micrometers for the heaviest one. The arrangement of the experiment has been fitted to the ion beam characteristics, especially penetration.

[1] Some years ago it was updated (ECR source, axial injection system) and its current possibilities are much higher [5].

2.2. KHIPTI facility and irradiation conditions

The chemical laboratory KHIPTI (Russian abbreviation of the name Chemical Investigation on Heavy Ion Beams) has been dedicated mainly to radiochemical studies of super-heavy elements but also to high-LET radiation experiments. The laboratory is situated at the basement near the vertical channel of cyclotron (Fig.1). The beam extracted from U-400 chamber passes through ~8-meter long horizontal beam-pipe and then is turned 90° down by a magnet into the vertical ~10-meter part of the channel. Above mentioned magnet, two pair of magnetic lenses, a pair of steering magnets and three diagnostic loops allow to focus and guide the beam. The third diagnostic loop, situated just in chemical room was equipped with the shutter (to cut-off the ion beam if necessary), a Faraday cup (for fluence measurements), a BeO-luminofor (for visual beam profile control) and a scattering foil (0.2 μm Au) for energy measurement. The last one was driven by an electric drive, the other one pneumatically. The accelerated ions were extracted into atmosphere through thin (~ 10-μm Al or 4-μm Ti) vacuum windows. Due to the small thickness of the exit windows and rather low ion fluxes no cooling system was necessary.

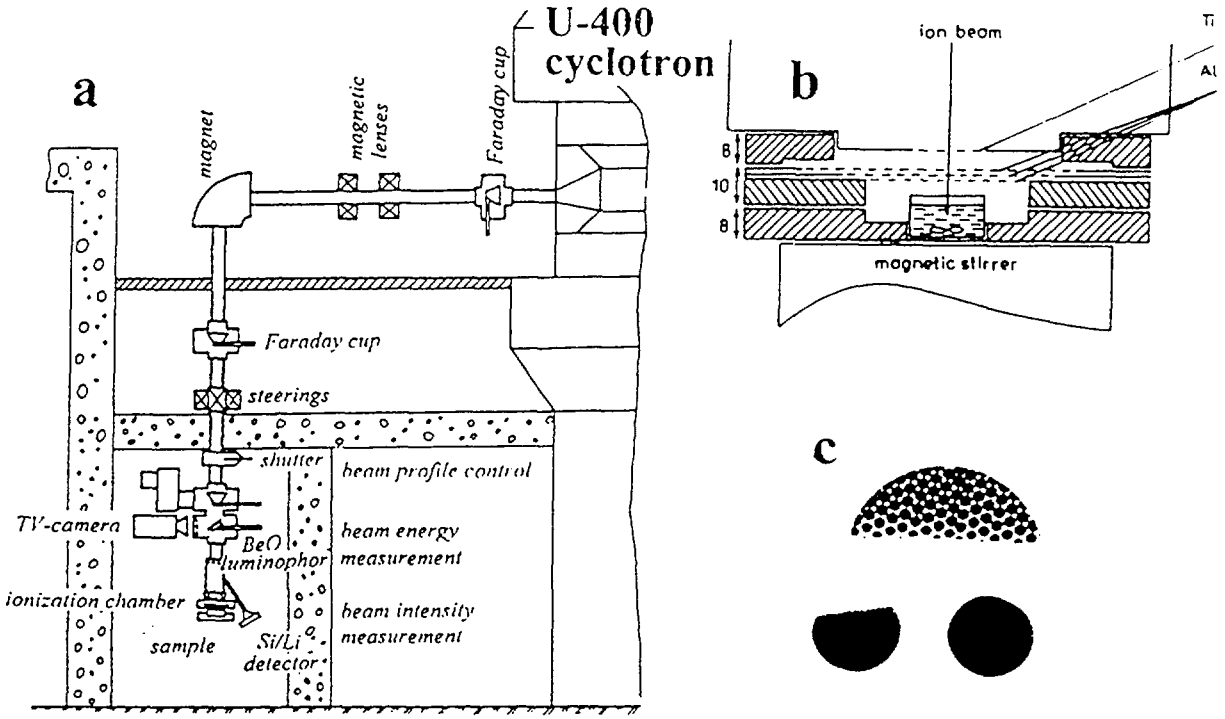

FIG.1. a) KHIPTI facility for radiochemical and radiation experiments,
b) an arrangement for the chemical ion-beam radiation experiments,
c) PVC foils used as a beam profile indicators at the time of ion beam tracing.

Unlike many other works, the samples were bombarded with the ion beams perpendicular to the air/sample surface. Such geometry has been very convenient for powder and liquid samples.

The irradiation set-up is shown on the Fig.1b. It consists of polystyrene support, thin ionization chamber, the vessel and the vessel's holder. All the elements are carefully aligned and fastened to the end of the pipe. The magnetic stirrer allows to stir liquids, if necessary.

The samples were irradiated in two positions. For the light ions, the distance between the exit window and the sample was 30-60 mm, while it was reduced to 14 mm for the heavy ones. In the last case the vessel with the sample was placed in a cavity made in the jacket of the ionization chamber. The diameter of the vacuum window was much smaller than that of the ionization chamber electrodes and also 2 mm smaller than the diameter of irradiation vessel. At such arrangement all the ions going through the exit window were registered by the ionization chamber before they were stopped in the sample.

3. ABSOLUTE DOSE MEASUREMENTS

In the intermediate energy region (few MeV/nucleon) the radiative losses are negligible and, as a rule, the ions are stopped in the samples. In such conditions the overall energy imparted to the sample, energy input, E_{in}, can be calculated according to Eq. (1)

$$E_{in} = E_s \, S \, \Phi \qquad (1)$$

where, E_s : is the ion energy at the surface (eV),
S : is the beam spot (cm^2), and
Φ : is the fluence (cm^{-2}).

and the mean dose, D_{av}, according to Eq. (2)

$$D_{av} = E_s \, \Phi \, (r)^{-1} \, (\rho)^{-1} \qquad (2)$$

where, r : is the range of the ion (cm), and
ρ : is the density of the sample (g cm^{-3}).

So, to determine the mean dose we had to measure fluence and energy on the surface of the sample. Ranges and densities were taken from literature.

3.1. Energy measurement

According to the technical properties of U-400 cyclotron, the particle energy corresponding to the maximum intensity of the ion beams is strictly defined (for the set parameters) and the half width of the peak is about of 1% of the energy value. However, there are some sources of uncertainty, also. First of all the tuning parameters allow to change the energy (at the same mode) within the range ±5%. Further, ion beam extraction performed via charge exchange in stripping foils results in 2 or 3 ion beams with a little different (2–5 MeV) energies and different charges. Theoretically it is possible to calculate energy in vacuum, E_o, but it is better to measure it. An additional benefit from energy measurements is an assurance that we are really working on the selected ion.[2]

The simple and attractive idea of energy control by the measurement of the magnetic field inside the bending magnet had to be rejected because of technical reasons. Instead, a semiconductor detector (situated in the arm of the vacuum pipe) has been used. It measured the energy of the ions scattered in the Au-foil. The signals produced in the detector were pre-amplified and sent across the biological shielding to an amplifier, a multi-channel analyzer and computer. The detectors (Si surface-barrier or Si/Li) were calibrated by α-particles from ^{212}Bi (E_α = 6.090 MeV, $t_{1/2}$ = 60.6 min) and ^{212}Po (E_α = 8.78 MeV, $t_{1/2}$ = 0.3 ms). The source was prepared just before the experiment. Scattering angle and energy losses were taken into account when evaluating the ion energy in the beam pipe.

[2] The ions with the same rigidity are accelerated together and may be difficult to judge between for instance $^{16}O^{2+}$ and $^{24}Mg^{3+}$ without the energy measurement.

The energy on the surface of the sample, E_s, was calculated as E_o minus energy losses in the target system. The losses were calculated on the base of stopping power data taken from Refs [1, 2] or computer programs [3, 4]. As it is seen from Table I the energy losses for the ions depend very much on the specific energy and on the mass of the ion. For nearly the same target system (Ti exit window, air, electrodes of ionization chamber, thin layer of air) energy losses changed from 11 MeV for 113 MeV ^{11}B up to more than 200 MeV for 397 MeV ^{59}Co. Thus, the overall accuracy of E_s determination was different for different ions. Two factors, the accuracy of the stopping power data and the decrease of energy on the way from vacuum to the sample, had to be taken into account.

For the light ions, all sources of the stopping power data gave practically the same results. This and the small energy loss on the way to the sample led us to the conclusion that the energy of the light ions on the surface of the sample can be determined with the accuracy ±2 to 3 %. For heavy ions, the situation was worse. The discrepancies between the stopping power data (especially for air) reached 8-10% and the energy losses in the targets reached 50%. In such conditions the overall accuracy of the energy measurements was estimated to be ±5 to 10 %.

3.2. Fluence measurement

There are several of methods of fluence measurements. For low fluences ($<10^8$ ions per cm^2) and not very high fluxes ($<10^8$ pps) it is possible to use solid state track detectors, SSTD. For lower fluxes (10^6 pps or less) one can use thin ionization chambers working in the particle counting regime. For fluxes higher than 10^8 pps and fluences higher than 10^9 ions per cm^2 (ordinary conditions for chemical experiments) one can choose between the ion beam current collection [8-10] and fluence measurement with ionization chamber working in current registration regime.

The ion beam current collection method is more difficult than in the case of electron beams. It is because a charge of the ion changes from the initial value (vacuum conditions) up to zero. Nevertheless, this method was successfully used in many experiments [8-10]. Generally, it is more applicable to cyclotrons with electrostatic beam extraction system because only in such conditions the initial charge of the extracted ions is sufficiently known.

In our facility the fluence was measured by means of an air ionization chamber working in the current registration regime. The number of the ion pairs was proportional to the number of projectiles and their energy losses and inversely proportional to energy of ion pair formation in air, w_{air}. The chamber consisted of three parallel flat electrodes made of 5.6 μm thick Al-foil with a 0.48 mm air space, f, between them. A collar support sealed the electrodes and fixed the distance between them. The diameter of the smallest electrode was 6 mm larger than the diameter of the largest circular vacuum window. The chamber worked at ambient pressure. The potential of the outer electrodes with respect to the inner, collecting one was +250V, giving electric field strength of about 2.7 kV/cm. Such conditions ensured the full charge collection. The charge from the collecting electrode was measured using digital electrometer (P-100, P-Firm, Poland) with the accuracy of 0.5%.

The number of ions that passed through the ionization chamber and stopped in the sample was calculated from Eq. (3)

$$\Phi = w_{air}\, Q\, (\Delta E)^{-1}\, (S)^{-1}\, (e^-)^{-1} \qquad (3)$$

where, Φ : is the fluence (cm^{-2}),
Q : is the charge collected from signal electrode (C),
ΔE : is the energy deposited between the electrodes of ionization chamber (eV),
S : is the beam spot (cm^2) and
e^- : is the electron charge (C).

And, ΔE was calculated from Eq. (4)

$$\Delta E = \rho_{p,T} \; [(dE/dm)_1 + (dE/dm)_2] \; f \qquad (4)$$

where, $\rho_{p,T}$: is the pressure and temperature dependent air density (g cm^{-3}),
f : is the thickness of the air gap between two electrodes (cm),
$(dE/dm)_1$: is the mass stopping power in the first gap (eV g^{-1} cm^2) and
$(dE/dm)_2$: is the mass stopping power in the second gap (eV g^{-1} cm^2).

It should be mentioned that the accuracy of the fluence determination in this method is doubly dependent on the accuracy of the mass stopping power data: apparently (Eq. 4) and non-apparently (calculation of energy of the ions reaching the ionization chamber). According to the considerations in the section 3.2 the overall accuracy of fluence determination will be much higher for the light ions than for the heavy ones.

The second source of uncertainty is w_{air} value. It is well known for electrons [11] and sufficiently for protons [11], alpha particles [11] and carbon ions [12]. For heavy ions the experimental data are scarce and scattered. Taking into account state of affairs we decided to calibrate our ionization chamber directly on the solid state track detectors. Thin polyethylene terephtalate foils have been used as SSTD. The foils were situated at the place of the sample and irradiated with uniform, low intensity (10^7–10^8 pps) ion beam. The charge collected from ionization chamber was measured simultaneously. Then, the irradiated foils were etched in 6M NaOH and analyzed on JSM-840, JEOL electron microscope. From such experiment we could calculate the coefficient k equal to the charge generated inside the ionization chamber by one heavy ion.

$$k = Q \; (N)^{-1} \; (S)^{-1} \qquad (5)$$

where, N : is the number of tracks per cm^2 (cm^{-2}).

Using this calibration, no data about w_{air} and stopping power data were necessary for fluence determination. Additionally, the k coefficients enabled us to calculate unknown w_{air} – values of heavy ions if ΔE-values are known from elsewhere. The reasonable values of w_{air} obtained for ^{40}Ca and ^{59}Co [13] confirmed the dosimetry technique described in this work. Another confirmation of our ion beam dosimetry system was presented in [14]. Dose and energy dependence of the integral yield of Fe^{3+} formation in Fricke solution bombarded with ^{12}C ion beam was measured and compared with the data from three other laboratories. An agreement was satisfactory.

4. SECONDARY DOSIMETERS

We checked four dosimetry systems: a) Fricke dosimeter, b) ethanol solution of nitryl of malachite green, c) L-α-alanine, and d) standard bone powder. Transparent and dyed PVC foils were successfully used as a beam profile indicators at the time of tracing of the beam (Fig. 1c).

Each of the investigated dosimetry system has its own advantages and shortcomings. EPR dosimeters (with alanine or standard bone powder as dose-sensitive material) can be used successfully for the total fluences in the range 10^8-10^{10} ions per cm^2. For the higher fluences, the signal-to-dose curve saturates because of overlapping of the latent tracks and the radiation destruction of previously created radicals [15]. The interesting feature of alanine is its sensibility to the LET of ionizing radiation. It reveals in the characteristic changes of the shape of EPR signal, especially on the borders [16] but also in power saturation characteristics of the central line [17].

On the base of literature data [8-10] and our own experience we consider that Fricke dosimeter can be useful for high-LET dosimetry. NaCl supplement is necessary. Without it, the contamination of

Fricke solution with organics will give a substantial increase in $G(Fe^{3+})$ values in stirred solutions but a decrease or only slight increase in non-stirred ones [18].

Ethanol solutions of malachite green can be used without stirring (which is very convenient) and for high doses. Additionally, they immediately deliver an initial information about the dose from the colour of irradiated sample. The main disadvantages of this dosimeter are sensitivity to UV light and volatility of solvent.

REFERENCES

[1] NORTHCLIFFE L.C., SCHILLING R.F. Range and stopping-power tables for heavy ions. Nucl. Data Tables **A7** (1970) 233-436.

[2] HUBERT F., et al., Range and Stopping power tables for 2.5 – 500 MeV /nucleon heavy ions in solids. Atom Data Nucl.Data Tables **46** (1990) 1–213.

[3] ZIEGLER J.F., BIERSACK, TRIM-90 programme "The Stopping and Range of Ions in Matter"

[4] HENNINGER J., HORLBECK B., STOPPOW/82 – the programme of calculation of stopping powers and ranges of heavy ions with energy from 1 keV to 10GeV/amu. JINR report 10-83-366 (in Russian) (1983).

[5] OGANESSIAN Yu.Ts, et al., Axial injection system for the U-400 cyclotron with the ECR-4M ion source. " JINR, Flerov LNR, scientific reports 1995–1996", (PUSTYLNIK B.I. ed.) Dubna (1997) pp. 270 – 276.

[6] GIKAL B.N., GULBEKYAN G.G., Extracted beams from U-400 cyclotron. JINR report B1-90-453, Dubna, (1990).

[7] STUGLIK Z. et al. The facility for liquid-phase radiation experiments on heavy ion beams. Radiat.Phys.Chem., **43** (1994) 463-469.

[8] SCHULER R.H., ALLEN O.A., Absolute measurement of cyclotron beam currents for radiation-chemical studies.Rev.Sci.Instr., **26** (1955) 1128–1130.

[9] MATSUI M. et al., Radiation chemical studies with cyclotron beams, (I) Fricke solution, J.Nucl.Sci.& Technol., 7 (1970) 97-104.

[10] LaVERNE J.A., SCHULER R.H., Radiation chemical studies with heavy ions: oxidation of ferrous ion in the Fricke dosimeter, J.Phys.Chem. **91** (1987) 5770-5776.

[11] ICRU-report No **31**, Average energy required to produce an ion pair, Washington, (1979).

[12] KANAI T. et al. Dosimetry and measured differential W values of air for heavy ions. Rad.Res. **135** (1993) 293-301.

[13] STUGLIK Z., APEL P.Yu., An attempt of experimental determination of differential energy of ion pair formation in air bombarded with 240 MeV ^{40}Ca ions, 300MeV ^{59}Co ions and 200 MeV ^{56}Fe ions, Proc.of VI International School-Seminar on Heavy Ion Physics (1997, Dubna) (in press).

[14] STUGLIK Z., Radiation facility at the JINR U-400 cyclotron checked by Fricke dosimeter measurements, Polish J.Med. Phys.&Eng. **1**(1995) 103-111.

[15] STUGLIK Z., SADLO J., Latent tracks generated in micro-crystalline L-α-alanine and standard bone powder by ^{59}Co ion beams as investigated by EPR-method. Radiat. Meas. **25** (1995) 95-98.

[16] STUGLIK Z., SADLO J., A response of L-α-alanine and standard bone powder on 3.4 MeV/amu ^{59}Co ion beams, Appl.Radiat.Isot. **47** (1996) 1219-1222.

[17] CIESIELSKI B. et al., The effect of high LET on EPR signal induced in alanine, Radiat. Res., **150** (1998) 469-474.

[18] STUGLIK Z., On the 'oxygen in heavy ion track' hypothesis, Radiat.Res. **143** (1995) 343-348.

XA9949728

SOME PECULIARITIES AND COMPLICATIONS IN HIGH-DOSE ESR-DOSIMETRY

S.P. PIVOVAROV, A.B. RUKHIN, L.A. VASILEVSKAYA, T.A. SEREDAVINA,
R. ZHAKPAROV, A. BAKHTIGEREEVA
Institute of Nuclear Physics,
National Nuclear Centre,
Almaty, Kazakhstan

Abstract

A number of experimental data reveal that ESR-dosimetry used for high doses sometimes fails as a result of radiation defect interactions at high radiation temperatures or after preliminary annealing stages, etc. Such interactions lead to non-linearities in the defect accumulation in a sample matrix vs. irradiation dose. The ways of accurate consideration of such effects by means of two phenomenological models are discussed.

1. INTRODUCTION

The ESR-dosimetry methods are very popular up to date, as they allow to determine, with a high accuracy and reproducibility, the integral radiation dose received by a particular person or some objects. Obvious advantages of the ESR-dosimetry are that it provides an opportunity to repeat measurements and to control the results obtained at various laboratories, because, when recording an ESR signal, the information contained in a sample is not lost and is conserved, practically, for a long time.

The advantages of the method are the results of it's physical essence: the magnetic resonance spectrum recorded without any lattice distortions (a working quantum $h\nu=\mu H<<kT$) serves for recording the number of radiation defects, used, in turn, for determining the radiation defect yield constant and, further, for calculating the dose absorbed by the sample.

Then it follows immediately that for correct application of the ESR-dosimetry methods, at least, two conditions are required. First, radiation defects in the sample used as a detector must be rather stable in order to have chance to neglect or to take into account accurately the influence of the recombination processes and other pathways of disappearance/transformation of paramagnetic centres (PMC). Secondly, one must know exactly the relationship governing radiation defects accumulation in a specific sample under some specified irradiation conditions. It is strongly desirable that this relationship is monotonous, i.e. it gives unambiguous predictions. Besides, stability of the defects relaxation characteristics is required, as variation in the magnetic relaxation time can result noticeably in the change of the spectrometer sensitivity.

2. RESULTS AND DISCUSSION

In practice, these conditions are satisfied quite well. The stability of the radiation defects and its relaxation characteristics are provided by an appropriate choice of the working sample material (for example, tooth enamel, crystal alanine, etc.). The relationship for radiation defect accumulation is determined by means of extra irradiations, and it can be considered as linear with the accuracy being sufficient in practice.

The situation, however, becomes more complicated if the conditions for defects interactions exit. Such conditions are present: at high radiation doses, at raised temperatures or mechanical pressure in a matrix during irradiation or at large dose rates when radiation heating of a sample is possible. In these cases, accurate determination of dose becomes more difficult; moreover, as it will be shown below, some ambiguities can arise.

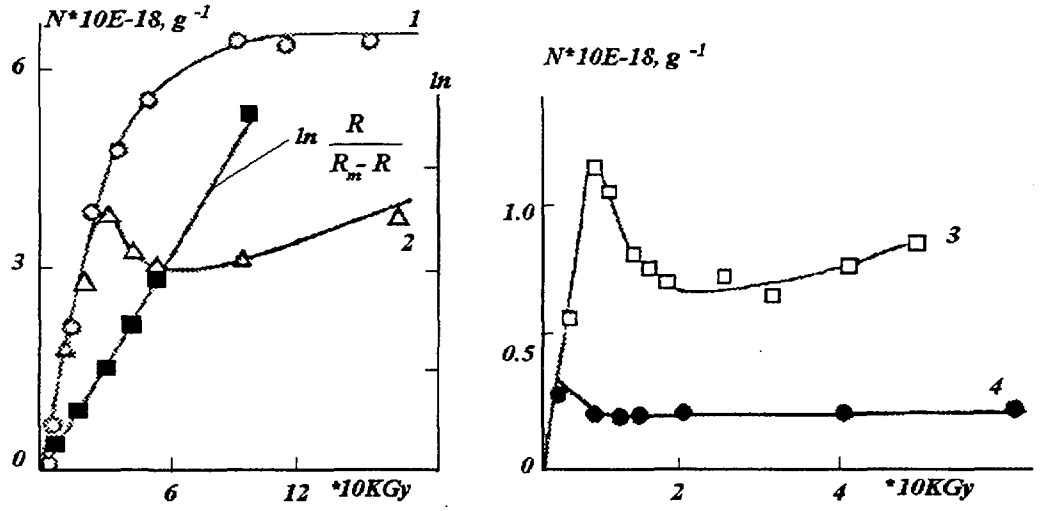

FIG. 1. Accumulation curves for free radicals in PMMA. 1) - at normal conditions (273 K); 2) , 3), 4) - at 305, 335, 381 K, respectively

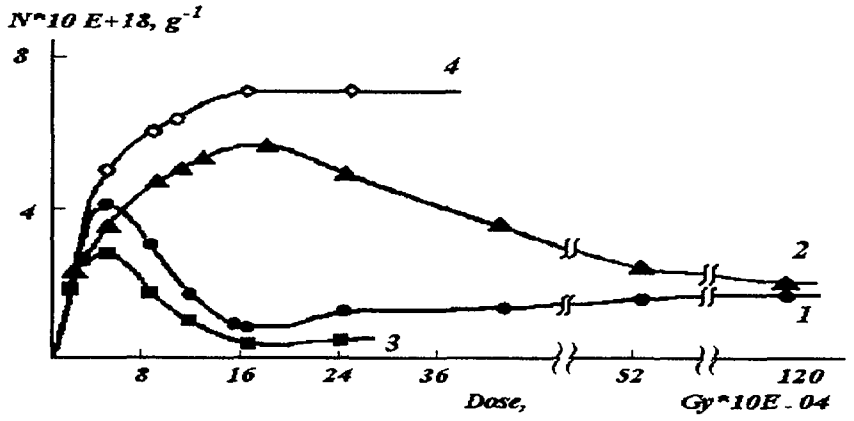

FIG.2. Accumulation curves for free radicals in PMMA. 1) - normal conditions; 2) - compressed (10 GPa); 3) - tensioned (25 MPa); 4) - low temperature, atmospheric pressure.

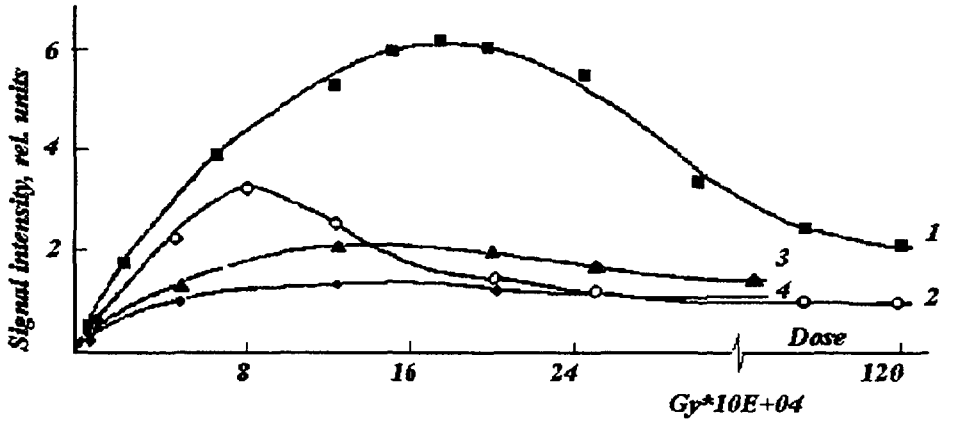

FIG. 3. Accumulation curves for free radicals in PMMA. 1) - initial irradiation at compression (10 GPa); 2) - initial irradiation at normal conditions; 3) - secondary irradiated under pressure after annealing; 4) - annealed and secondary irradiated without compression.

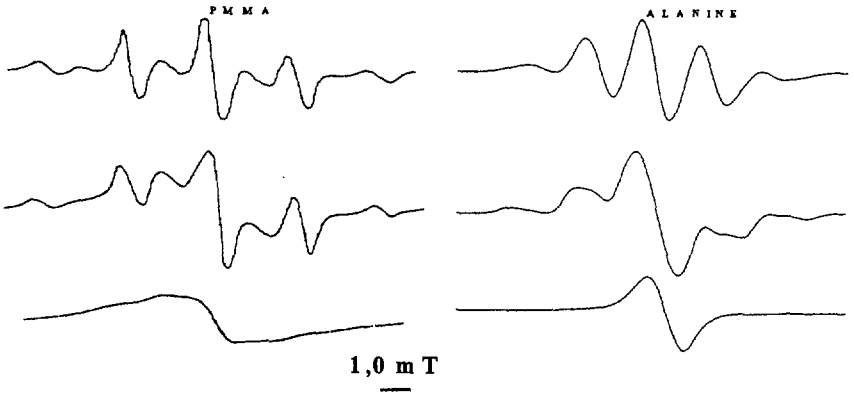

Fig. 4. The shapes of ESR signals in irradiated PMMA (left side) and α–alanine (right side) for low doses (top), intermediate doses or raised irradiation temperatures (middle), and very high doses or after annealing (bottom)

Another reason for troubles is a "radiation history" of a sample. Experiments have shown, that, as a rule, in dielectrics and in semiconductors the radiation yield constant strongly depends on whether the sample is irradiated for the first time, or it was earlier irradiated, annealed and then again irradiated. In the latter case in the course of repeated irradiations in many substances other types of defects, in addition to primary ones, are generated, therefore the relationship of PMC accumulation as well as its relaxation characteristics may change.

These concepts are exemplified below.

In Fig. 1, the curves of accumulation of radiation defects (in this case, radicals) in polymethylmethacrilate (PMMA) with irradiation dose are displayed for various irradiation temperatures [1].

As the sample temperature increases at various stages of irradiation, the accumulation curve shape varies significantly: it is transformed from an usual curve with saturation to a non-monotonic curve with extrema, thus for large doses an ambiguity occurs. Similar situation is observed [2] during irradiation of a sample at mechanical stresses (see Fig. 2). The compressing stress increases the maximum concentration of radicals and shifts the extremum to higher doses, while the tension causes an opposite effect. Like in the first case, these effects manifest only at rather high doses, whereas the specified peculiarities are, practically, non-distinguishable at small doses .

The "radiation history" of a sample plays an important role also. In Fig. 3 the accumulation curves of radiation defects in PMMA are shown for varied radiation conditions and "radiation history". One can observe a significant effect of preceding irradiation, annealing and mechanical pressure. The "radiation history" of a sample strongly influences also the amount of radiation defects that are stabilized in it.

PMMA is a more "soft" system, than alanine, which is the reasons why it is chosen as a main working sample for ESR-dosimetry; however, the same effects are observed in alanine too (see Fig. 4). Analogy with PMMA is evident, i.e. the transformation of the ESR spectrum that implies occurrence of other radicals, and the change in the PMC accumulation relationship as the radiation dose increases are observed.

In both cases, transformation of the PMC structure takes place: at the start of the radiation an alkyl type of radical stabilizes, and then an allyle one occurs. On the last steps, polyene radicals may appear [3].

For interpretation of these data and quantitative description of observable effects we have developed two phenomenological models, which take into account other types of defects that occur as the radiation dose increases (in this case allyle radicals are generated instead of alkyl ones). This can be a result of the interactions between the accumulated defects and the radiation field occuring as the dose increases.

This problem of the influence of the radiation field on the defects accumulation has been studied quite well. In numerous works (see references in [4]) it was shown that the interaction with a radiation field results in (beginning with a certain value of the dose) decreasing the number of stabilized defects and in saturating the accumulation curve. As a result, the *a priori* relationship of radiation defect accumulation

$$\frac{dN}{dD} = KD \tag{1}$$

changes to:

$$\frac{dN}{dD} = KD - K_1 N \tag{2}$$

where, N is the number of stabilized defects in a matrix, D is the irradiation dose, K is determined via the dose rate and the radiation yield of the defects, the constant K_1 takes into account the disappearance of the defects as a result of the radiation field influence.

In Ref. [4], it is stressed that Eq. (2) describes rather a large amount of observed experimental data (provided the recombination processes are negligible, otherwise it is necessary to introduce one more term K_2N^2). This relationship represents a standard curve with saturation, like the curve 1 in Fig. 1. However, other experimental data presented above point to the fact that the situation can be much more complicated if the accumulation curve becomes non-monotonic, that is related to simultaneous formation of another type of defects.

The mechanism of "secondary" radical production can be caused by the heat of recombination of the initial radicals as a result of the radiation field influence. The recombination energy release causes local heating in the matrix and changes it's composition, therefore "secondary" radicals can appear there.

These processes can be taken into account by the set of two equations for the "primary" defects N_1 and the "secondary" ones N_2 [5]:

$$\begin{cases} \dfrac{dN_1}{dD} = 1 - C_1 N_1 N_2 - C_2 N_1 \\ \dfrac{dN_2}{dD} = C_3 N_1 N_2 - C_4 N_2 + C_5 \end{cases} \tag{3}$$

Here the factors C_2 and C_4 are similar to the constants K_1 in Eq. (2), C_1 and C_3 take into account the formation of the N_2 defects at the expense of the annihilation of the N_1 defects and C_5 is related to the mechanism of direct generation of the defects N_2 by radiation.

a)

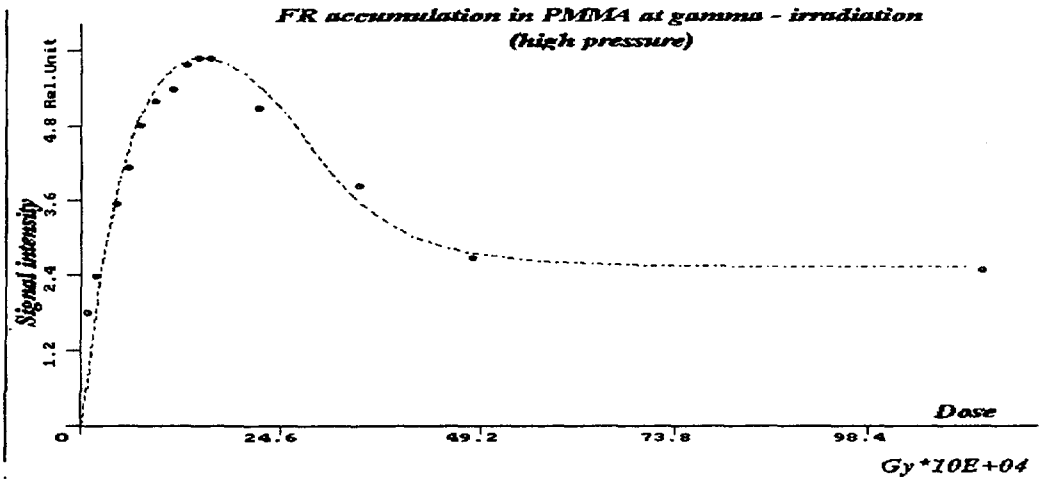

b)

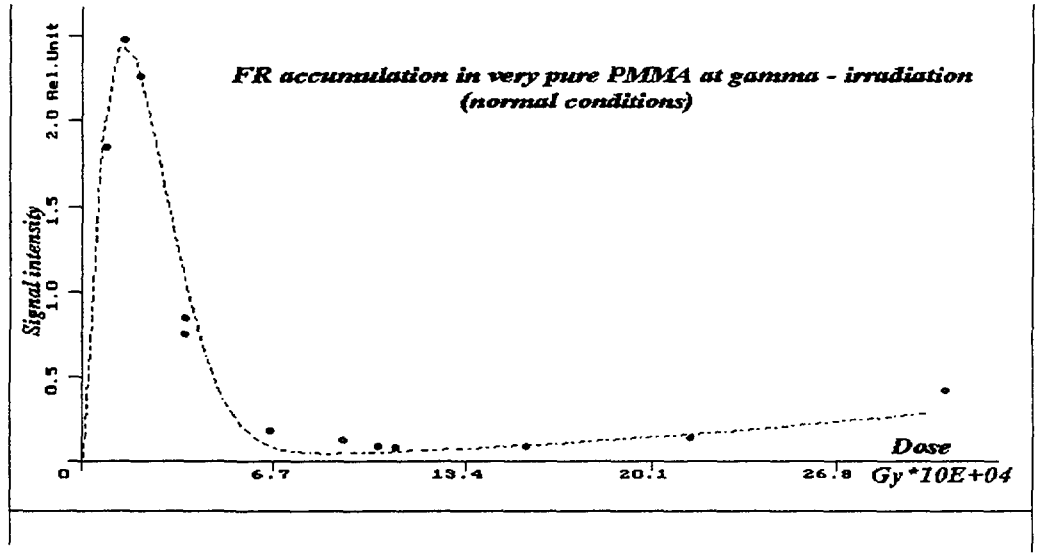

FIG. 5. Fitting to the experimental accumulation curve in the frame of the models: points represent experimental data, line represents the model; a - model (3), and b - model (4)

The other approach, close to this one, is related to the introduction of a "damaged volume" concept. According to this model, the primary defects can be produced only in an initial intact matrix. As a result of its interaction with the radiation field, however, they disappear in a matrix and a "damaged volume" is formed locally, i.e. it's structure changes. The secondary defects can be produced only within this "damaged volume", thus they can also interact later with the radiation field. Occurrence of the "damaged volume " is determined simply by the Poisson's distribution:

$$\begin{cases} \dfrac{dN_1}{dD} = exp(-C_1 D) - C_2 N_1 D \\ \dfrac{dN_2}{dD} = \left[1 - exp(-C_3 D)\right] - C_4 N_2 D \end{cases} \qquad (4)$$

The conformity of the models described by Eqs (3) and (4) to the experimental data is illustrated by Figs 5a and 5b.

3. CONCLUSION

The data presented here (its number could be increased) show that it seems to be reasonable, in view of ESR-dosimetry, to separate, at least, three stages of radiation damage in solids:

- the initial stage (small doses), when the defect concentration is low, they, practically, don't interact between each other, and the relationship of defects accumulation versus the dose is close to linear;
- the intermediate stage, when interaction between defects occurs, as a result, the relationship of accumulation noticeably differs from the linear one, and a non-monotonic character can occur;
- the high-dose stage, when the significant damaged volume has been accumulated (paramagnetic defects can be even annealed and, from the point of view of ESR, the sample may be represented as unirradiated or as irradiated by a small dose) and all peculiarities of the second stage manifest itself more prominently.

For various substances and various conditions of irradiation, the effects of the second and the third stages manifest themselves at different values of irradiation dose. For example, for PMMA the second stage is obviously observed already at 5 kGy as the irradiation temperature increases, and in α-alanine the relationship of accumulation is close to linear up to 100 kGy; nevertheless, the same effects occur.

Apparently, the marked peculiarities are characteristic of all solids, e.g., in Refs [5, 6] data about "radiation memory" of metals and alloys even after deep annealing up to the melting condition are presented.

Thus, for correct application of ESR- dosimetry methods it is necessary either to ensure the conditions of the first stage, or to take into account potential nonlinearities arising, for example, on the basis of the model like (3) or (4); otherwise very significant errors can appear.

REFERENCES

[1] S.P. PIVOVAROV, A.I. POLYAKOV, YU.A. RYABIKIN et al., Investigation of the Accumulation Kinetics of free Radicals under Irradiation if Some PMMA Copolymers in the 270 -400 K temperature range. Radiation Effects, **59** (1982) 179-182.

[2] S.P. PIVOVAROV, A.M. ATAGULOV, L.A. VASILEVSKAYA, Influence of Compressed and Tension Stresses on Accumulation of Free Radicals in PMMA (Proc. 9th Spec. Colloq. AMPERE, Prague, 1989) 34-35.

[3] S.R. RAFICOV, SH. SH. IBRAGIMOV, S.P. PIVOVAROV et al., On Mechanism of Radiation Damaging of PMMA. Chimia Vysokich Energii. **15** (1981, ' 4) 333- 337.

[4] S.J. PSHEJETSKII et al. ESR of Free Radicals in Radiation Chemistry, Moscow, Chimia (1972) 480 pp.

[5] A.M. ATAGULOV, L.A. VASILEVSKAYA, S.P. PIVOVAROV, A.B. RUKHIN, Model of the Radicals Accumulation in PMMA. Pisma JTF, **18** (1992, ' 21) 51- 56.

[6] SH.SH. IBRAGIMOV, V.D. MELIKHOV, S.P. SENSHIN et al., Display of Radiation Memory Effects in Quadrupole Interaction of the Neutron Irradiated Aluminium, Phys. Lett., **32** (1985) 217-219.

[7] V.D. MELIKHOV, M.K. SKAKOV. Radiation- Stimulated Proccesses of Intermetallides, Alma-Ata, Hylim (1996) 326 pp.

PROCESS VALIDATION

(Session 6)

Chairperson

D.A.E. EHLERMANN
Germany

XA9949729

Invited Paper

PROCESS VALIDATION FOR RADIATION PROCESSING

A. MILLER
Risø High Dose Reference Laboratory,
Risø National Laboratory,
Roskilde, Denmark

Abstract

Process validation concerns the establishment of the irradiation conditions that will lead to the desired changes of the irradiated product. Process validation therefore establishes the link between absorbed dose and the characteristics of the product, such as degree of crosslinking in a polyethylene tube, prolongation of shell life of a food product, or degree of sterility of the medical device. Detailed international standards are written for the documentation of radiation sterilization, such as EN 552 [1] and ISO 11137 [2], and the steps of process validation that are described in these standards are discussed in this paper. They include material testing for the documentation of the correct functioning of the product, microbiological testing for selection of the minimum required dose and dose mapping for documentation of attainment of the required dose in all parts of the product. The process validation must be maintained by reviews and repeated measurements as necessary. This paper presents recommendations and guidance for the execution of these components of process validation.

1. INTRODUCTION

Process validation is an exercise that is aimed at obtaining documented evidence that the radiation process leads to an acceptable product. Documentation requirements for the radiation sterilization process are provided in the two sterilization standards EN 552 [1] and ISO 11137 [2]. They describe process validation a little differently, but the goal is the same. The minimum dose that is required for the sterilization process must be established and documented, the maximum dose that the product can tolerate must likewise be documented, and irradiation parameters must be established that ensure that the product is irradiated within these doses. The maximum dose is determined from the testing of the material and product – sometimes published data may be used as a part of the documentation. The minimum dose is based on microbiological experimentation to find the dose that will give the required degree of sterility assurance level (SAL). In order to make meaningful dose measurements, it is necessary to understand how the dose measurements are used – to understand the relationship between the product characteristics and the absorbed dose. The aim of this paper is to give the reader a backgeound for understanding these relationships.

These considerations concern radiation sterilization, but similar considerations can be made for e.g. food irradiation or crosslinking of plastics. A required minimum dose and a tolerable maximum dose must be established, and it must be documented that the absorbed dose stays within these limits.

2. MAXIMUM DOSE

It is difficult to give exact information about radiation tolerance of various polymers, because the property in question is often very product-specific. Guidance in selecting polymers for a specific use may be found in ISO 11137, appendix A [2].

Polymeric materials are influenced by radiation through two main processes, crosslinking and chain scission [3,4]. Which type of process that dominates in a specific polymer type depends on its molecular characteristics. In polyethylene, for example, with its carbon backbone with only hydrogen substitutions, crosslinking predominates, although influences of the bulk properties are typically seen only at doses higher than the doses used for sterilization. The properties are changed only little at room temperature, but at higher temperatures it becomes obvious that the polymer has turned from a thermoplastic to a thermoset polymer, and therefore the crosslinked polyethylene product keeps its shape at elevated temperatures – above the crystallite melting temperature.

In polypropylene, on the other hand, where every other hydrogen is replaced by a methyl group, chain scission is the dominating reaction. The chain scissions in polypropylene can be observed as changes in molecular weight distribution as shown in Fig. 1, where samples have been irradiated with one and five times 17 kGy with electron and gamma radiation, respectively. The decreasing signal for the higher doses is caused by the measurement technique that is most sensitive for high molecular weight molecules.

The chain scission may, however, not happen immediately, but only after some time. Radiation induced free radicals – often peroxy radicals – created in the crystalline regions need time to migrate to locations where they may react with the polymer and create a scission. Therefore measurements of mechanical properties carried out shortly after irradiation do not necessarily give a useful answer. The properties have to be documented over a long time, typically months. The presence of free radicals is an indication of the possibility for late chemical reactions, and the concentration of the radicals can be measured by EPR spectrometry as shown in Fig. 2. EPR is a very sensitive technique, and the measurement of the free radicals can be used to follow in time the decay of the free radical concentration.

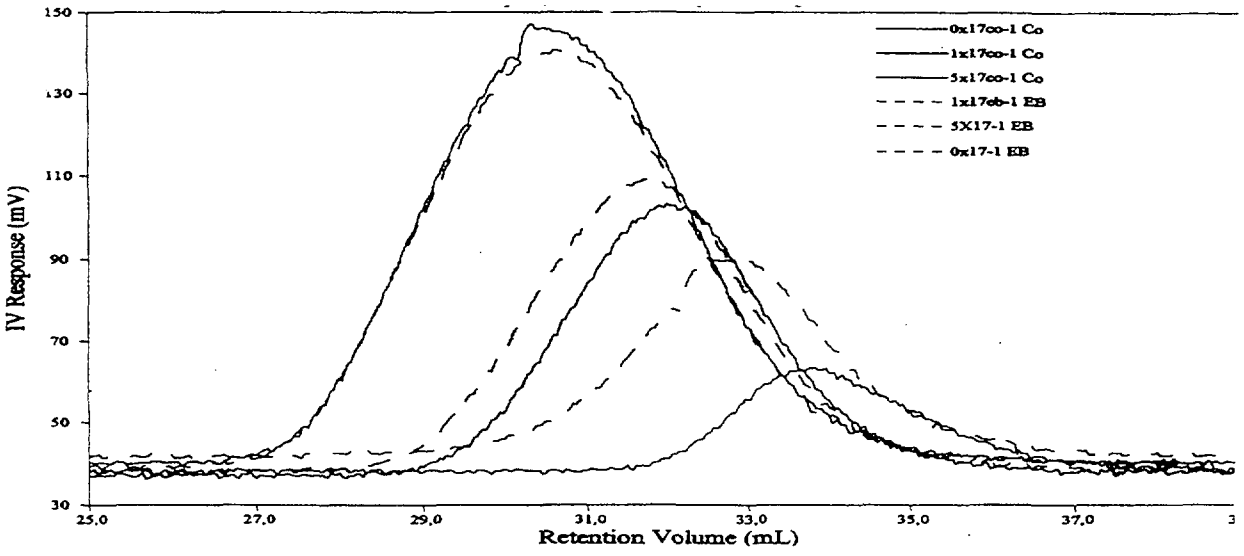

FIG. 1. The molecular weight distributions of irradiated polypropylene films irradiated by electron and gamma radiation (higher retention volume → lower molecular weight).
Full lines: gamma. Dashed lines: electrons.

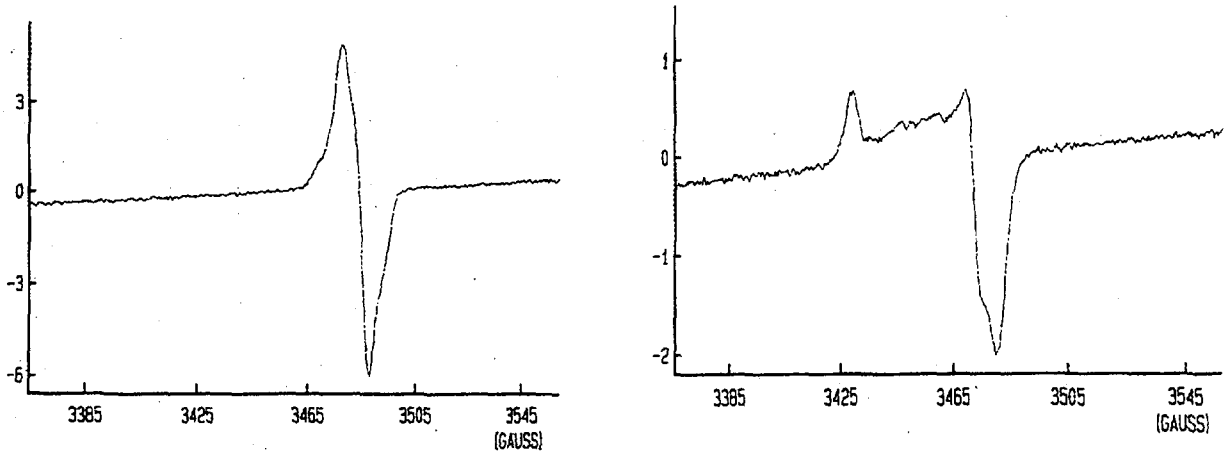

FIG. 2. EPR spectra of free radicals in polypropylene (left) and polycarbonate (right) created by radiation. Both materials were irradiated at a 10-MeV electron accelerator to approximately 50 kGy.

The efficiency of the radiation-induced changes depends to some extent on the dose rate. The free radicals created by the electrons – primary as well as well secondary – may react with other free radicals if the concentration is high as in the case of electron irradiation, thereby reducing the possibility of the free radicals to react with the polymer molecules or to create peroxy radicals that in turn react with the polymer molecules. The duration of the electron irradiation is usually less than a minute and that creates another effect: The oxygen dissolved in the polymer is consumed within a fraction of the total dose, and the remaining irradiation is effectively carried out under oxygen-free conditions thereby reducing the number of radiation induced reactions. The duration of gamma irradiation, on the other hand, is often several hours, and oxygen may diffuse into the polymer. Electron irradiation therefore often produce less changes compared to gamma irradiation at the same dose, and this effect is most visible at the surface of the product [5].

It is the physical, chemical and mechanical properties of the medical device that are of importance for its approval, and these properties, that may be affected by radiation must be tested and documented before the device can be released for use. It is important that the testing is carried out at least at the maximum dose that the product will experience during radiation sterilization, and it is important to realize that it is not possible to irradiate a product to only one dose level. In practice it will be exposed to a range of doses, and at an early stage in the development of a device it may not be possible to know the maximum dose. In stead, testing should be done at a range of doses e.g. 25, 50 and 75 kGy, so that a relationship between dose and the relevant property can be established and used for determination of the allowable *maximum dose*.

3. MINIMUM DOSE

In Europe, before the implementation of the Medical Device Directive, it was an accepted practice to irradiate for sterilization with an absorbed dose of 25 kGy, and the National Health Authorities, that were responsible for the approval of the medical devices accepted that the device was sterile if it could be documented that the device was produced under good manufacturing conditions and that the initial microbiological contamination - the bioburden - was low.

In a parenthesis it might be mentioned that in Scandinavia special rules were in force. The dose required for sterilization depended both on the type of radiation and on the level of contamination, with a minimum dose of 35 kGy for electron and 32 kGy for gamma radiation.

The implementation of the Medical Device Directive means that the primary manufacturer has become responsible for producing evidence for compliance with EN 556[6], i.e. for obtaining and maintaining an SAL of 10^{-6}. An absorbed dose must be determined that can produce the required level of sterility, and that dose can be lower than 25 kGy, but it is also possible that higher doses are required. The sterilization dose is determined on the basis of microbiological documentation, and EN 552 indicates that the choice must be based on the information on the radiation resistance of the microorganisms naturally occurring on the medical device. EN 552 indicates the type of microbiological documentation that is considered acceptable. This may be either a measurement of the radiation resistance or it may be comparison with microorganisms with a known radiation resistance. The latter method is – with reference to ISO 11137 – referred to as Method 1, and it is briefly described here.

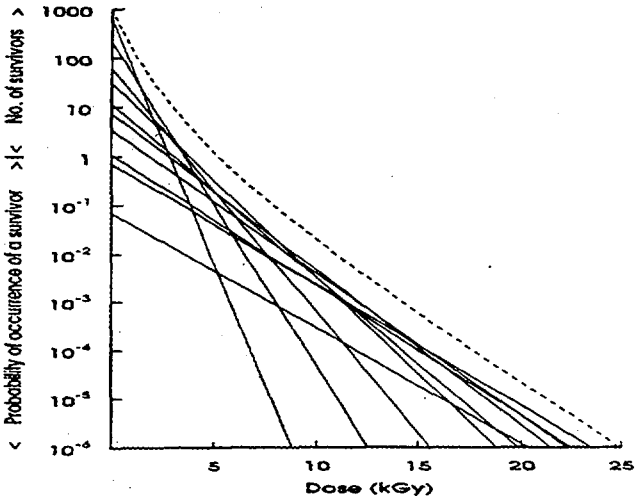

FIG. 3. The Standard Distribution of Resistances (SDR) is composed of several representative microorganisms having increasing radiation resistance. The dotted line is the combined SDR, that is used for prediction of the dose that will give SAL = 10^{-6}. In this example with an initial bioburden of N(0) = 1000, the dose for SAL = 10^{-2} is 11 kGy and the dose for SAL = 10^{-6} is 25 kGy. At lower initial bioburden values the sterilization dose will be reduced.

The main principle in Method 1 is that the radiation resistance of the microorganisms contaminating the product prior to sterilization – the bioburden – is compared with the population of microorganisms having a radiation resistance known as the Standard Distribution of Resistances (SDR). If the radiation resistance of the product bioburden is less than that of the SDR, then the SDR is used to select the dose that will produce an SAL of 10^{-6}

The procedure involves measurement of the product bioburden by testing 10 units from each of three different production batches. Based on the average of the three bioburden measurements a dose is found that will give a sterility assurance level of 10^{-2}, and 100 product units are irradiated to that small dose. These 100 units are tested for sterility, and if no more than 2 unsterile product units are found, the test is passed and the necessary dose for sterilization to SAL $\leq 10^{-6}$ is determined by extrapolation of the SDR. The SDR is represented as tables in ISO 11137. This dose is the required *minimum dose.*

Documentation that the microbiological status of the product is maintained must be produced by repeating the exercise about every three months. However, it has been suggested that under certain circumstances this frequency of verification may be reduced [7, 8].

4. DOSE MAPPING

Not all parts of a medical device will be irradiated to the same dose when it is exposed to electron or gamma radiation. Due to the local absorption and scatter of radiation a range of doses will be experienced, which for more complex product can be very difficult to predict, and which therefore have to be measured. This is done in a dose mapping exercise, where the doses in or on a medical

device are measured under actual processing conditions. This means that irradiation for the dose mapping as a rule shall be carried out at the facility, where the device is going to be sterilized, and the device shall be packaged in its final product package.

It is not possible to place dosimeters everywhere in the device, and choices have to made. Dosimeters shall be distributed throughout the device in a pattern, so that they are likely to measure the dose extremes. The information obtained during the dose mapping in facility qualification regarding maximum and minimum dose zones can be useful, and can provide guidance as to where to place the dosimeters for this exercise. Particular attention shall be given to inhomogeneous product distribution, orientation of the product relative to the direction of the radiation, voids, local differences in specific density, and interfaces. Previous experience may prove indispensable. The problems of defining the proper placement of dosimeters are most pronounced for electron irradiation, which because of a monoenergetic energy distribution and a well-defined direction of the electron beam is known to produce large dose gradients.

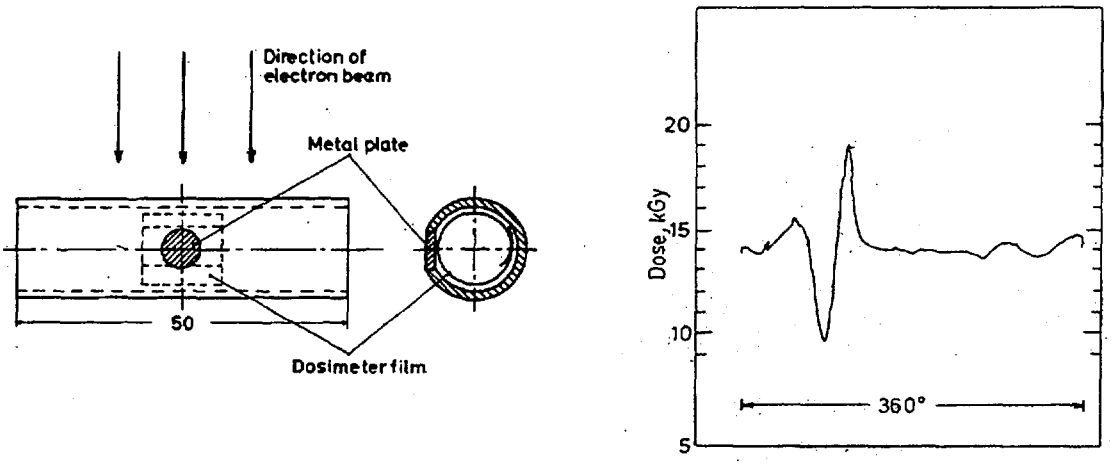

FIG. 4. The tube shown to the left was irradiated from one side with 10-MeV electrons. Dose distribution is shown to the right. 360^0 corresponds to a dosimeter length of 30 mm.

Another problem concerns the spatial resolution of the dosimeters. In particular for electron irradiation, dose gradients may occur within millimeters or even less, and the dosimeter system must be able to resolve and measure the doses at the location of these gradients, see Fig. 4.

The minimum and maximum doses and their locations are determined in this exercise, but the dose map should be carried out in more than one product box in order to determine the measurement uncertainty. A complete dose map may be carried out in – as a minimum – three product boxes, or repeated measurements (e.g. 10) of only the minimum and maximum doses can be made, if their locations have been well characterized in a one-box dose map.

Simultaneous with the measurements of the maximum and minimum doses, the parameters of the irradiation facility must be recorded and a reference dose must be measured. The reference dose is measured in a specific geometry outside the product (or often on the outside of the product box). It is a parameter that is used to monitor the output of the irradiation facility, and it is used for routine process control. A major outcome of the dose mapping exercise is to determine the relationship between the maximum and minimum doses and the reference dose.

For gamma radiation, ratios of D(max)/D(min) – the uniformity ratio – is often between 1.2 and 1.4, while this ratio is more likely to be between 1.5 and 2 for electron irradiation, and even higher

ratios are not uncommon. The allowable limit of the uniformity ratio is determined by minimum and maximum dose limits determined in Sections 2 and 3. If this limit is exceeded for the product being dose mapped, then redesign of the product or its packaging must be considered, or different irradiation parameters may be chosen that may fulfil the requirement.

A reference dose – and associated irradiation facility parameters – can now be chosen that will allow the measured minimum dose to be larger than the required minimum dose. During the normal radiation sterilization process the minimum (and maximum) dose cannot be measured, and therefore the parameters shall be chosen so that if measured, the minimum dose will be larger than the required minimum dose. Recognizing the statistical nature of dose measurement, the choice can be based upon the known measurement uncertainty, and to choose the measured minimum dose on average to be 2 standard deviations larger than the required value may seem a reasonable choice [9].

5. CONCLUSIONS

Radiation processing can be carried out within documented dose limits ensuring that products are produced with parameters that are in accordance with specifications. The procedures for providing the documentation are specific in some cases, in others not. For example the procedures for documenting the required minimum dose for sterilization are specific, but for measuring the minimum dose in a dose mapping exercise the procedures are not specific and choices will have to made. The basis for the choice must always be that no product may be irradiated outside specifications.

REFERENCES

[1] CEN (1994). EN 552, Sterilization of medical devices – Validation and routine control of sterilization by irradiation. European Committee for Standardization, Rue de Stassart 36, B-1050 Brussels, Belgium.

[2] ISO (1995). ISO 11137, Sterilization of health care products – Requirements for validation and routine control – Radiation sterilization. International Organization for Sterilization, C.P. 56, CH-1211 Genève 20, Switzerland.

[3] HARRISON, N. (1991). Radiation sterilization and food packaging. Chapter 8 in Irradiation Effects on Polymers, edited by D.W. Clegg and A.A. Collyer. Elsevier Applied Science.

[4] O'DONNELL, J.H. (1991). Chemistry of radiation degradation of polymers. Chapter 24 in Radiation Effects on Polymers. ACS symposium series 475. Edited by Roger L. Clough and Shalaby W. Shalaby. American Chemical Society, Washington DC, USA.

[5] IEC (1993). IEC 1244-1. Determination of long-term radiation ageing in polymers. Part 1: Techniques for monitoring diffusion limited oxidation. Bureau Central de la Commission Electrotechnique Internationale, 3, Rue de Varembè, Genève, Switzerland.

[6] CEN (1994, EN 556 Sterilization of medical devices –Requirements for medical devices to be labeled "Sterile". European Committee for Standardization, Rue de Stassart 36, B-1050 Brussels, Belgium.

[7] LAMBERT B.J., HANSEN J.M. (1998). ISO radiation sterilization standards. Radiat. Phys. Chem. **52,** no. 1-6, pp 11-14. Proceedings of the 10th International Meeting on Radiation Processing, 11-16 May 1997, Anaheim, CA, USA. Editors J.F. Clouser, J. Barker, A. Miller.

[8] ISO (1998), ISO CD 15843, Sterilization of health care products – Radiation sterilization – Product families, sampling plans for verification dose experiments and sterilization dose audits. International Organization for Sterilization, C.P. 56, CH-1211 Genève 20, Switzerland.

[9] MILLER A. (1998). Dosimetry requirements derived from the sterilization standards. Radiat. Phys. Chem. **52,** no. 1-6, pp 533-537. Proceedings of the 10th International Meeting on Radiation Processing, 11-16 May 1997, Anaheim, CA, USA. Editors J.F. Clouser, J. Barker, A. Miller.

DOSE FIELD SIMULATION FOR PRODUCTS IRRADIATED BY ELECTRON BEAMS: FORMULATION OF THE PROBLEM AND ITS STEP BY STEP SOLUTION WITH EGS4 COMPUTER CODE

XA9949730

I.L. RAKHNO, L.P. ROGINETS
Radiation Physics and Chemistry Problems Institute,
National Academy of Sciences,
Minsk, Belarus

Abstract

When performing radiation treatment of products using an electron beam much time and money should be spent for numerous measurements to make optimal choice of treatment mode. Direct radiation treatment simulation by means of the EGS4 computer code fails to describe such measurement results correctly. In the paper a multi-step radiation treatment planning procedure is suggested which consists in fitting the EGS4 simulation results to reference measurement results, and using the fitted electron beam parameters and other ones in subsequent computer simulations. It is shown that the fitting procedure should be performed separately for each material or product type. The procedure suggested allows to replace measurements by computer simulations and therefore reduces significantly time and money required for such measurements.

1. INTRODUCTION

At present the computer code EGS4 is one of the most popular tools for performing coupled electron-photon transport simulation [1]. For radiation treatment planning the most important consequence of such computer simulation is the calculated absorbed dose distribution. However in Figs 1 and 2 one can observe significant differences between measured and calculated dose distributions even for simple homogeneous well-studied medium like aluminium. The differences are systematic ones and reveal themselves as increased slopes (both left and right) of dose-depth curve as well as some shift of the curve maximum to deeper layers. When considering realistic heterogeneous objects like a box with syringes the problem becomes more complicated. The differences between measurement and calculation can be attributed partially to incorrect knowledge of energy distribution in the incident electron beam.

2. THE PROBLEM FORMULATION

For more correct calculation of absorbed dose distribution inside objects irradiated using electron accelerators it is very important to single out the most important parameters which influence the distribution. The knowledge can help to choose optimal radiation treatment mode. To our mind the parameters are the following:

(1) Dependence of average absorbed dose in a layer on its depth, i.e. distance from the surface (curve dose-depth)
(2) Statistical deviation from the average value for each of the layers (variance)
(3) Depth range significant in practice.

To achieve uniform object irradiation the entrance dose should approximately be equal to double exit dose. Relevant object thickness corresponds to almost total (80-90%) deposition of energy delivered to the object. Then using two-sided treatment gives rise to almost uniform irradiation.

3. THE STAGES OF THE PROBLEM SOLUTION

As far as direct radiation treatment simulation fails to describe correctly the measured dose distribution, one should perform some fitting to a reference measurement. We suggest to use the following multi-step procedure:

(1) Approximate choosing of an irradiation mode for product to be irradiated;
(2) Performing a 'reference' measurement for the same mode with fixed electron beam current, electron energy, scanning length and conveyor velocity. The measurement includes:
   - experimental determination of electron beam parameters with a standard spectrometer like a set of aluminium or polyethylene plates, and
   - experimental determination of the dose field inside treated product with a large set of thin dosimetry films which are distributed uniformly over the box volume without distorting the dose field significantly;
(3) Fitting of electron beam parameters with the modified EGS4 computer code to achieve reasonable coincidence between calculated and measured dose distributions for aluminium and/or polyethylene
(4) Calculation of dose distributions for realistically treated product for two extreme types of description, i.e. homogeneous and heterogeneous;
(5) Determination of appropriate homogenization degree and fitting of calculated average dose distribution to experimental one preserving realistic deviations from the average values at different depths;
(6) Additional calculations for another treatment modes (using fitted parameters) to achieve minimal dose non-uniformity factor. For the mode found averaged over volume absorbed dose should be calculated as well as averaged over surface absorbed dose to compare the value with a reference dose value obtained using a surface dosimeter.

4. MEASUREMENT RESULTS AND DISCUSSION

Previously we have modified the well-known EGS4 computer code [1, 2] to take into account 3D structure of irradiated objects as well as developed some tallying routines to make it more suitable for serial calculations. Since then it have been successfully used for resolving different problems [3-5]. Therefore it has been used in present work also.

Irradiation treatment has been performed using electron accelerator UELV-10-10 installed at RPCPI. Available electron energies extend up to 10 MeV with electron beam power up to 10 kW. Dosimetry studies have been performed using films SOPD(F)5/150 tested metrologically at VNIIFTRI (Mendeleevo, Russia). Absorbed dose has been determined using a spectrophotometer SF-26 comparing optical density of the films to that of the reference specimen at wavelength equal to 512 nm.

When fitting calculated distributions to measured ones some shift of maximum for the calculated curves can be achieved by a small variation in the incident electron energy (±0.5 MeV). The sharp maximum can be smeared out using a Gaussian energy distribution instead of δ-function. Absorbed dose at entrance in a treated object can be increased if one allows existence of a low energy (1-5 MeV) tail in the primary electron beam. Slope of a dose-depth curve in its right part increases with energy decreasing and is one of the most difficult values for fitting. The calculated dose-depth distributions were normalized in area to the measured ones using the thickness where the absorbed dose is equal approximately to one half of the dose at the entrance. Accelerator outlet window was supposed to be titanium plate 50 μm thick. Variations of this value did not influence the calculated dose distributions noticeably.

In Figs 1 and 2 measured absorbed dose distributions are represented for homogeneous aluminium and polyethylene slabs. They were obtained in one irradiation run at 6.9 MeV. The energy was determined from the extrapolated range in alumunium according to formulae and recommendations of ASTM. Direct simulation fails to describe measured dose distribution. Fitted dose-depth curve for

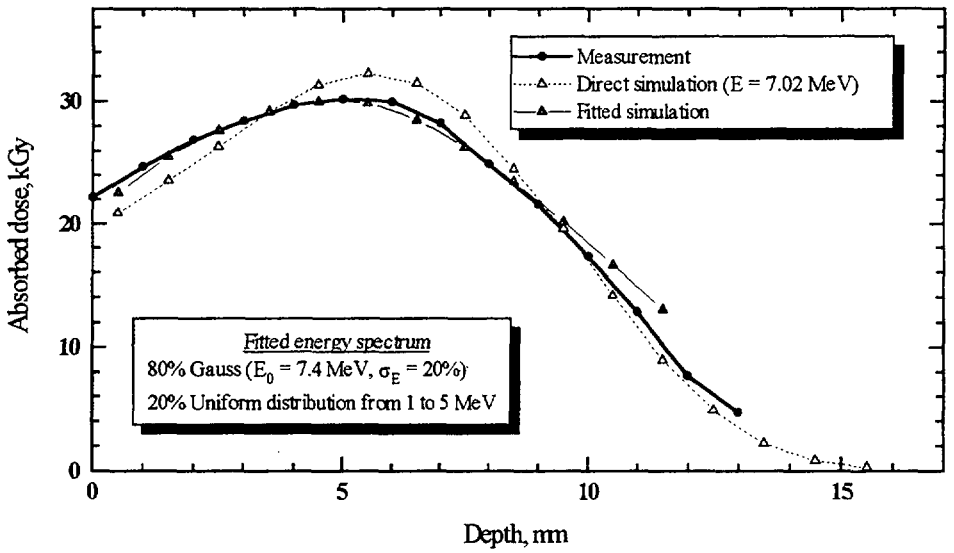

FIG.1. Measured and calculated absorbed dose distributions in an aluminium layer irradiated by an electron beam. The calculations were performed by the EGS4 computer code [1,2].

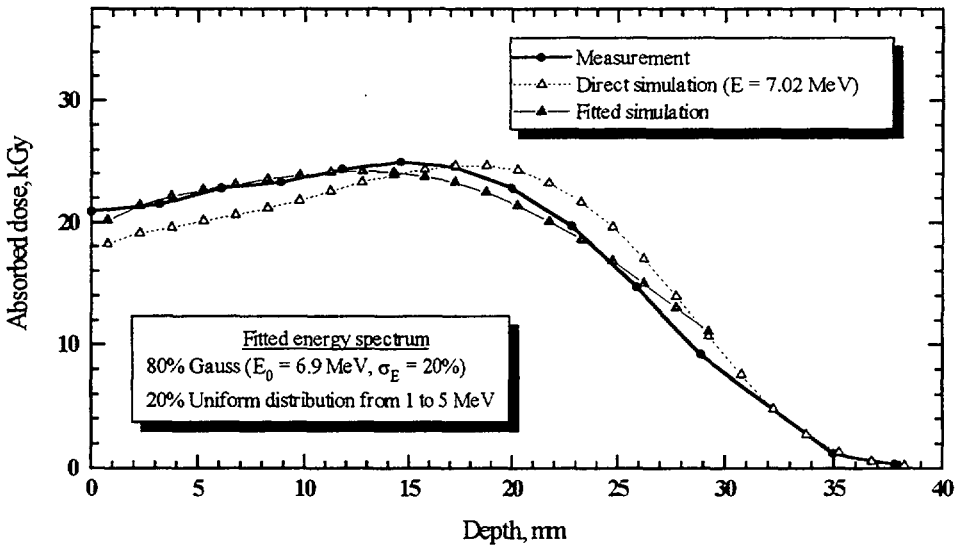

FIG.2. Measured and calculated absorbed dose distributions in a polyethylene layer irradiated by an electron beam. The calculations were performed by the EGS4 computer code [1,2].

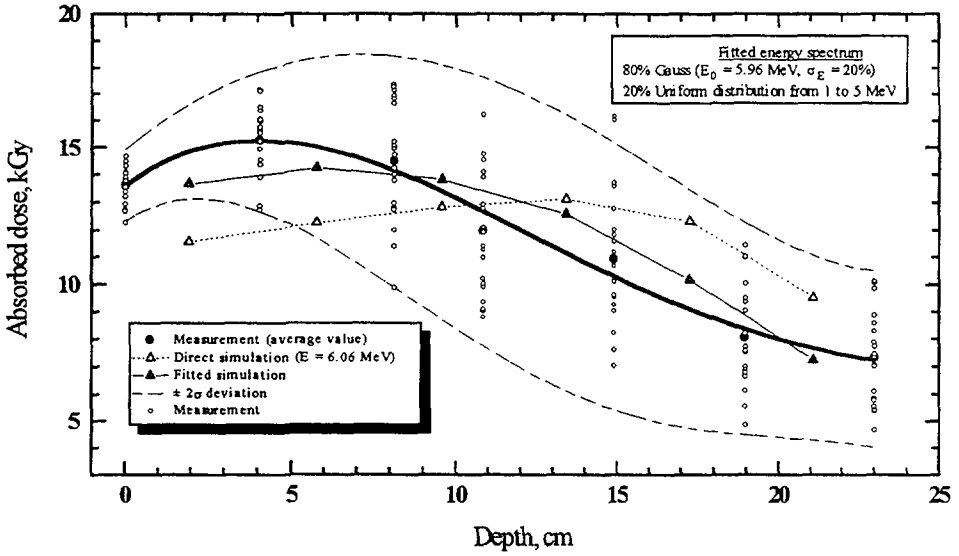

FIG.3. Measured and calculated absorbed dose distributions inside a box with 'Polmed' syringes irradiated by an electron beam. The calculations were performed by the EGS4 computer code [1,2].

aluminium did not fit measured distribution for polyethylene. Thus one should perform individual fitting for each material under investigation.

In Fig. 3 measured and calculated dose distributions for a box with syringes ('Polmed', Poland) are represented. The box (600x400x250 mm^3) contained 1400 syringes each with capacity equal to 2 ml. Inside the box 140 dosimetry films were situated at 7 different depths, i.e. 20 films at each depth. One can observe from the figure that calculated curve obtained for homogenized model of the box fits to measured one reasonably good. The calculated curve was obtained using beam parameters fitted to measurement in the case of the polyethylene slab (Fig. 2).

5. CONCLUSION

It is shown that direct radiation treatment simulation with EGS4 computer code fails to describe correctly absorbed dose distributions inside a box with realistic objects irradiated by an electron beam. The suggested procedure which consists in fitting to a reference measurement enables to describe the measured dose distributions more correctly. Therefore one can perform minimal number of measurements with less labour, time and money consumption preserving reasonably high accuracy in description of dose fields. Thus one can state that the approach can be very useful in practice. In future we shall continue the work for more detailed description of dose fields using more realistic (heterogeneous) calculation models.

REFERENCES

[1] NELSON, W.R., HIRAYAMA , H., ROGERS, The EGS4 code system, Rep. SLAC-265, Stanford Linear Accelerator Center, Stanford, CA (1985).

[2] LANTSOV, I.E., RAKHNO, I.L., ROGINETS, L.P., Modification of computer code EGS4 for simulation of electron-photon showers transport through matter, Preprint #1, Radiation Physics & Chemistry Problems Institute, Minsk, Belarus (1992).

[3] RAKHNO, I.L., LANTSOV, I.E., KORNEEV, S.V., ULANOVSKY, A.V., "Simulation of gamma spectrometers", Izvestiya AN Belarusi, fiziko-tekhnicheskaya seriya, #2 (1996) 104-108.

[4] ULANOVSKY, A.V., MINENKO, V.F., KORNEEV, S.V., "Influence of measurement geometry on the estimate of ^{131}I activity in the thyroid: Monte Carlo simulation of a detector and a phantom", Health Physics, v.72, #1 (1997) 34-41.

[5] RAKHNO, I.L., TARUTIN, I.G., "Planning of multi-positional total body irradiation for bone marrow transplantation" (Proc. 3rd Scientific Conf. «Medical Physics - 97. New technologies in radiation oncology», Obninsk, Russia, December 8-12, 1997), Medical Radiology Scientific Center, Russian Academy of Medical Sciences, Obninsk (1997) 118-119.

DOSE PLANNING, DOSIMETER READING AND CONTROLS USING PC FOR GAMMA RADIATION FACILITY

V. STENGER, J. HALMAVÁNSZKI, L. FALVI
Institute of Isotopes Company Ltd,
Budapest, Hungary

I. FEHÉR
Technical University,
Budapest, Hungary

Ü. DEMIRIZEN
Turkish Atomic Energy Authority,
Ankara, Turkey

Abstract

Mapping of relatively strong gamma radiation fields using computer modelling started already in the 60's. The Institute of Isotopes (Institute) was one of the developers and users of this technique in connection with high activity Co-60 source installation, for commissioning and dose planning. We have found this technique very useful, economical, fast, sometimes unique for the determination of the dose rate distribution for the operators and dosimetrists, and also for designers to design such gamma irradiators. Several institutions and individuals in Hungary and abroad were involved in the development work, for example, Bulgaria, ex East Germany, Singapore, Iran, Turkey, Libya and Cuba. Computer programmes were distributed during the IAEA Radiation Engineering Courses in Budapest, IAEA Course for Health Physics Inspectors in Prague, and other National and Regional Courses organised by the IAEA. The continuous activities have resulted in several small programmes to calibrate and to readout the ECB dosimeters, to design shielding, transportation containers, irradiation units and large plants. Finally, we have developed a universal modelling programme to calculate the details of the operational parameters of irradiation units. Our concept was and is that, for process control, it is equally important to know the details of the irradiation unit as to have reliable dosimetry systems.

1. HISTORICAL BACKGROUND

The first computer programme to map the dose rate distribution for our multipurpose panoramic irradiator [1] was written by Prof. Dr. P. Fejes in 1967. [2]. This programme was verified by chemical and physical dosimeters [2, 3]. This programme, called "Fline", was developed by Dr. L Naszódi in our Institute in 1973 as a first step to evaluate gamma radiation fields for different large activity source geometries [4].This programme was also verified by several physical dose-rate meters and dosimeters [5]; the results were compared at several large scale irradiators in Hungary and abroad. Pure physical calculation was made at the University of Singapore at the Physics Department to check the dose rate distribution for a line source in air. The results agreed within less than 1 %.

This programme is more useful for laboratory and pilot irradiators for dose-rate mapping of the irradiation chamber or room in air. To search for a radiation field for calibration, first we can analyse the field distribution using computer modelling either for a gammacell (a cage source) or any other panoramic irradiator. We can map the relative field in the centre of the cage or inside the volume of the cage, mm by mm, in three dimensions in few minutes; no other method is able to do this. Rate distribution in air can be mapped for a source or for a room of size 19.9 m x 19.9 m. This programme was originally written for Commodore and Apple II computers, and then later translated for AT PC computers. The calculated dose rates are accompanied by the distances tabulated in cm.

A new programme was developed by Dr. P. Hargittai at our Institute to determine radiation technological parameters including dose distribution in large irradiation unit boxes or pallets [6]. Rate reduction due to absorption in the material to be irradiated was taken into account using a water equivalent linear absorption factor. We did the same when designing large scale irradiators for radiation processes. Several other computer programmes were developed [7,8]; some of them following our example, such as in Bulgaria, Iran, Germany and Libya.

The dose planning procedure becomes easy for a trained operator or a dosimetrist with the use of the "Fline" computer code. The dose distribution in a standard carton filled with goods, or in a large container at a pilot plant can be determined within 2-5 % limits, which is the accuracy limit of the dosimeter used for process control. After each source reload, such calculations can be carried out immediately saving work and time, instead of mapping the irradiation room again with several dosimeters lasting several days or weeks.

We have continued our activity on introduction of PC for the analogue oscillotitrator reader for the Ethanol-Chlorobenzene(ECB) dosimeter. This system is in use at about 30 irradiators around the world. We have succeeded to calculate the calibration tables and curves very fast (in a few minutes) using standard ampoules exposed in a calibrated irradiation field [9]. A separate small programme is developed that can determine the dose versus the reader-scale or visa-versa, replacing the calibration and readout tables and curves. A PC controlled readout of the ECB dosimeter for the dose range of 1-200 kGy can be used. In most cases, together with the Fricke dosimeters, this is enough to cover the dose range of daily need. The Fricke system can measure the low dose range (10-400 Gy); and can also be used to calibrate the ECB system.

2. NEW COMPUTER PROGRAMMES

2.1. Calibration and readout programme

As a recent development, we have introduced a PC calibration and readout programme replacing the analogue meter for ECB. We kept the same ampoule holder used for the analogue readout meter, but a new slot, PCB card and a simple programme resulting in a multi-use PC controlled dosimeter readout. This method can read the dose from 1000 Gy to 200 kGy using two calibration ranges: 1000 Gy - 60 kGy and 50 kGy - 200 kGy. The computer stores the calibration data and the readings in the form of a dose protocol as a part of the GMP. This method has already been transferred to Yugoslavia, Cuba, Vietnam and Agroster-Hungary.

The PC controlled readout of the ECB dosimeter can be installed at any XT or AT type computer with an interface and a very simple programme. The ampoule holder connected to the computer can perform the calibration with standard ampoules exposed to known doses. Calibration data as well as the routine measured readouts of the individual dosimeters can be stored and printed in a form of a dose report as required. The system is available from the Institute, or can be adapted using the oscillator head with the ampoule holder of an existing RADELKISZ OK-301,302 Hungarian made reader.

2.1.1 Installation

The programme can be loaded using a diskette to a directory (about 50 Kbytes). For the individual dose protocols, about 2-5 Kbytes is required. Thus, about 200 protocols can be stored in 1-Mbyte space of the hard disk drive. When executing the readout programme with the "d2-exe" entry, the computer will confirm that the oscillotitrator head (ampoule holder) is present and connected to the computer. Now the system is ready for calibration and dose measurements.

2.1.2. Calibration

The following procedure is used for establishing the calibration relationship for the Ethanol-Chlorobenzene dosimetry system:

(1) Minimum of four ampoules are needed for the calibration of the selected dose range (1 unexposed and three exposed to known doses).
(2) It is recommended to wait about 15 min. to let the system warm up before use; this is displayed on the monitor.
(3) Select the "Z" (zero) option from the menu and place the unexposed ampoule into the ampoule holder when the programme requests as "PUT THE AMPOULE INTO THE AMPOULE HOLDER".
(4) Now, select the "C" (calibration) option. Also, fill in the questioner: the "NUMBER OF STANDARDS" should be 4 (see point 1 above), and the "NUMBER OF PARALLELS" is recommended to be 3. (Number of parallels means that the ampoule is rotated between each read out by hand, clock wise or otherwise; thus, the same ampoule is measured three times and the ovality of the ampoule is averaged, improving the statistics of the readout. If the zero-dose ampoule is used for calibration, the polynomial fitting curve is forced to pass through the zero dose value.).
(5) When the calibration is completed, save it under a file name for subsequent dose measurements.

2.1.3. Sample measurements

The following procedure is used for analysing the ECB dosimeters to determine the dose:

(1) Check the zero dose ampoule selecting the "Z" option; this step is essential.
(2) Select the "S" ("SAMPLE MEASUREMENT") option. Fill in the questioner on the screen.
(3) Place the ampoules in the holder, one by one, rotating them is optional. When finished, exit to DOS; the measured values are stored in the text and doc files.
(4) Any file can be printed out as a dose measurement document protocol.

The standard calibration ampoules as well as the dosimeter ampoules for daily routine dose measurements are available from our Institute.

2.1.4. Test measurements

In the menu, there is an option to measure one ampoule 100 times to determine the readout precision. The 100 readouts are made automatically and at the end of this "TEST" measurement, the value for the standard deviation is given; this may be different for the different dose ranges.

2.1.5. Files

Files "doc" are the protocol files. Files "text" are the detailed calibration curve files. Files "cal" are the files storing the data when the calibrations are made and can be selected for any measurements (see menu when selecting the calibration 0,1, 2, 3 points).

The data stored in the "text" file can be transferred to QPRO or EXCEL programmes and printed or plotted to visualise the calibration curves for the various dose ranges. The "doc" files can be edited by the Norton Commander or any other editor programmes.

2.2. Improved multipurpose programme

Our next development of the PC technique is a relative multipurpose dose setting and evaluation programme. This user-friendly programme can determine all necessary process parameters: for

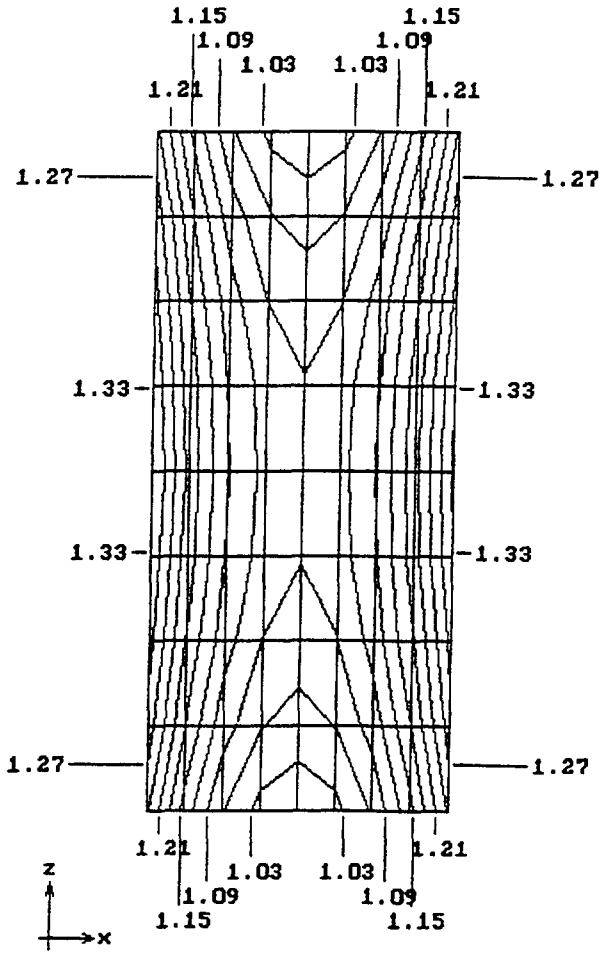

FIG. 1. Isodose distribution curves for a standard irradiation unit box central vertical sheet size 50x50x90 cm for the density 0.2 kg/dm³

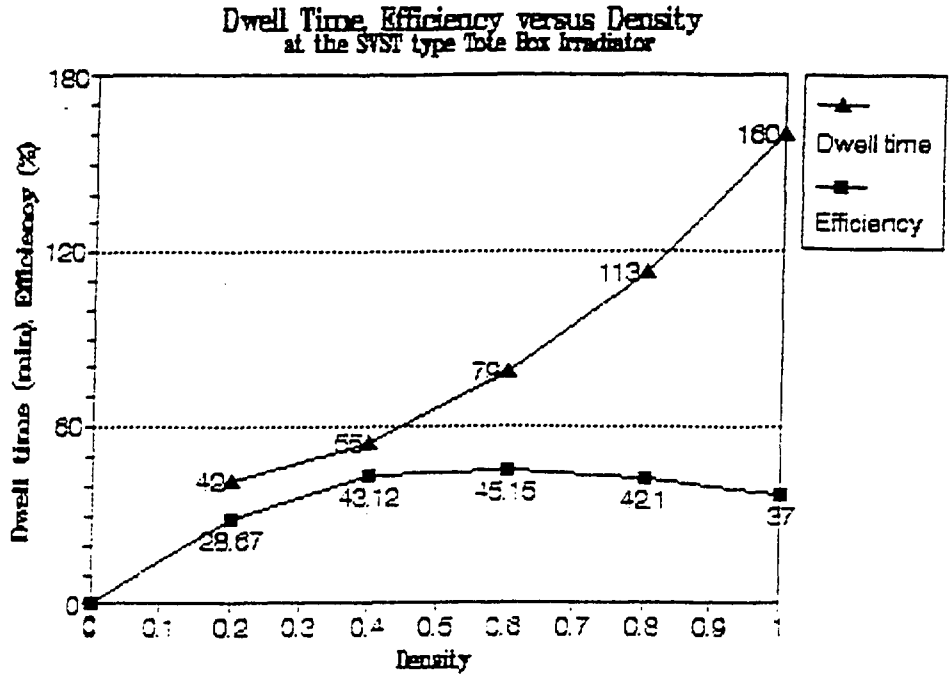

FIG. 2. Dwell time and efficiency versus density

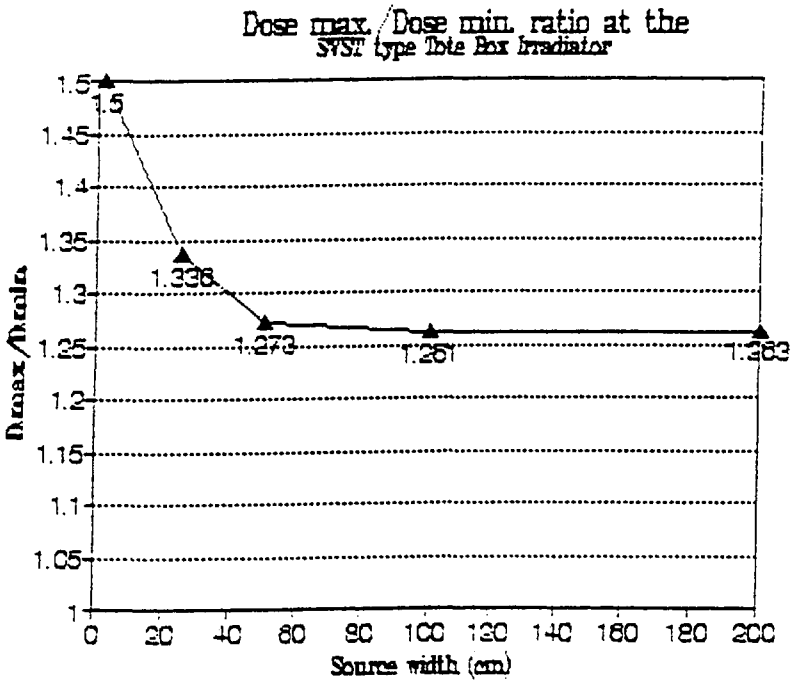

FIG. 3. Dmax/Dmin versus source width

example, minimum and maximum dose locations, isodose distribution curves (see Fig. 1), radiation efficiency and dwell time versus density (see Fig. 2), activity distribution, source size versus dose ratio (see Fig. 3), efficiency depending on the source size, and transport system layout in three dimensions versus source position affecting the output. All these calculations can be done for the density range from air to density of 1 (e.g., water) for all existing large scale process plants - from batch to single or multilayer, single or multipass up to the largest pallet transport systems including parallel source racks. The programme takes into account the source self absorption in the vertical direction and uses a linear absorption water equivalent factor concerning the different density of the product. The decay of the Co-60 is also included in the programme; if the installation activity is given the output is calculated for the present time. This programme was verified at several irradiation facilities operated in Hungary, Yugoslavia, China, Turkey, and the results were compared with the data given by the manufacturers (such as, Canadian, French, Chinese, Russian, USA and Hungarian) for nine different types of irradiators.

One unique feature of the programme is that the isodose distribution curve can be seen and printed out. When an analysis of any type of design is made the following basic features are made obvious:

- the advantages and disadvantages of the design;
- parameters influencing the outputs of the irradiation unit;
- how the positioning of the source and transport mechanism can change the efficiency;
- how the source height relative to the transport system can influence the dose distribution in the product if the source position can be changed by the time of operation;
- how the source dimension and the source loading pattern can affect the dose ratio and the radiation efficiency;
- how the product density can influence the dwell time, the dose ratio, the efficiency, the location of the minimum and maximum dose regions inside a standard carton; and
- if any reconstruction is planned, what should be modified to obtain the optimum output from the plant.

We consider that using this programme will improve the knowledge of the operators and the plant dosimetrists about the irradiation unit; they can have the details concerning the irradiation technique almost at a level of a radiation plant designer.

2.2.1. Hardware required for installation

We recommend to run the programme in a separate directory e.g. RAY-200, using a PC 486 66 MHz. A VGA-monitor is necessary to see the isodose distribution curves. HD capacity of about 1 Mbyte is needed for the programme.

2.2.2. Calculation

Data inputs, such as the source and product box characteristics, can be filled in a few minutes and stored for the next calculations. The dose calculations at 27 points inside standard cartons will take about 2-7 minutes, while the isodose calculations will take about 10 minutes. It should to stressed that this programme yields relative values only. A correction factor may be applied to fit the calculated values to the measured ones e.g. when giving the source activity in the source construction sheet.

2.2.3. Files

Once the computer set-up time is set, the decay of the source is taken into account. All files stored can be printed out using "print screen". For the isodose curves, if there is no color printer available, use "c" to get the print in black.

3. RESULTS AND CONCLUSIONS

We have developed a few simple and user-friendly computer programmes for routine daily dose planning, for calibration of readout instruments, for dose distribution controls and for analyses of the radiation technological parameters of the irradiators. These programmes may help to analyse and understand the irradiators concerning the dose planning and the required dose and dose distribution in the products. Dose records stored in the computer or on diskettes become essential part of the radiation technological parameters carried out.

We strongly believe that this PC process control focusing on process dosimetry will improve the GMP, and help the dosimetrists and the plant operators to overcome any difficulties they may have - especially at the service irradiators where the products to be irradiated changes frequently, almost daily - and it will also contribute to the process validation. We also believe that, besides the computer techniques already introduced in the plant operation control console, the PC-controlled dosimetry will play more important role in the near future.

We realise that our activity in this field was and is not unique; several other programmes were written and are available. Our new programmes are still at the introduction stage; we need some more international intercomparisons and experience. We also would like to call upon the designers and the users of the irradiation facilities to check our programmes, and then we would be able to release them for mutual benefits.

ACKNOWLEDGEMENT

We are thankful to the colleagues who contributed to the computer code development: Prof. Dr. P. Fejes, Dr. L. Naszódi, Dr. P. Hargittai, Mr. A. Szántó of Hungary, Mrs Dr. R. Chakarova of Bulgaria, Prof. Dr. B. Hao of Singapore, Mr. B. Basarir of Turkey, J.H. Schmidt of Germany, and Mr. M. Mashina of Libya.

REFERENCES

[1] Hirling, J., Stenger, V., Energ. Atomtechn. **22** (1969) 446.

[2] Fejes P., Horváth Zs., Stenger V., The calculation of the Relative Irradiation Dose Rate of a High-Power Gamma-Source by Digital Computer, Isotopenpraxis 6/3:98-103/ 1970/.

[3] Stenger, V., Unified Control Method In Dosimetry For High-Activity Irradiation Facilities In Hungary, High-Dose Measurements in Industrial Radiation Processing, IAEA Tech. Rep. Ser. No.**205** Vienna, 1981, 97.

[4] Stenger V., Földiák G., Horváth Zs., Naszódi L., Planning of Gamma-Fields: Forming and Checking Dose Rate Homogeneity in Irradiation Facilities. Proc. Radiosterilization of Medical Products and Biological Tissues, held by the IAEA at Bombay, 9.13 December 1974, IAEA Vienna, 1975, 323.

[5] Pavlicsek, I., Stenger, V., Csürös, M., Lakosi, L., Veres, Á., Izotóptechnika **13** (1971) 466.

[6] Stenger V., Hargittai, P., Kálmán B., Styevko, M. Design Principles of High-Activity Gamma-Irradiation Facilities, Radiation Physics and Chemistry 26/5/ :591-597 (1985)

[7] McLaughlin, W.L., A.W. Boyd, K.C. Chadwick, J.C. McDonald and A. Miller (1989). Dosimetry for Radiation Processing, Taylor & Francis Ltd., London

[8] Rizzo, F.X., Irradiation design calculation techniques based on centerline depth dose distributions, Int. J. Radiat. Eng. 1 6 (1971) 549-84.

[9] Stenger V. , Torday Zs. , Horváth I. , Falvi L. , Papp Z. , Long Term Experiences in Using Ethanol Chlorobenzene Dosimeter System , International Symposium on High Dose Dosimetry for Radiation Processing, IAEA Vienna, 5-9 November 1990.

GENERALIZED EMPIRICAL EQUATION FOR THE EXTRAPOLATED RANGE OF ELECTRONS IN ELEMENTAL AND COMPOUND MATERIALS

W. de LIMA, D. de C.R. POLI
Instituto de Pesquisas Energéticas e Nucleares,
São Paulo, Brazil

XA9949732

Abstract

The extrapolated range R_{ex} of electrons is useful for various purposes in research and in the application of electrons, for example, in polymer modification, electron energy determination and estimation of effects associated with deep penetration of electrons. A number of works have used empirical equations to express the extrapolated range for some elements. In this work a generalized empirical equation, very simple and accurate, in the energy region 0.3 keV - 50 MeV is proposed. The extrapolated range for elements, in organic or inorganic molecules and compound materials, can be well expressed as a function of the atomic number Z or two empirical parameters Zm for molecules and Zc for compound materials instead of Z.

1. INTRODUCTION

In electron beam applications, such as curing, polymer modification, sterilization of medical supplies or food decontamination, we need to estimate the depth dose curves in organic and compound materials to pre-set accelerator parameters in order to achieve the best dose uniformity.

An easy way to do this in current irradiation services is lacking and it seems to us that if we could find an analytical expression for this purpose, it would be dependent on the extrapolated or practical range.

Kobetich and Katz [1,2] and Tabata and Ito [3] formulated expressions for the depth dose curves for several absorbers, using the functional form of Weber's [4] extrapolated range-energy relation for aluminium. Instead of R_{ex}, Kobetich and Katz [2] have taken the characteristic thickness $R_{0.05}$ proposed by Dupouy [5], defined as the thickness at which the transmission coefficient has fallen to 5 %, but they employed the functional form by Weber [4]. On the other hand, Tabata *et al.* [3,6] used only the R_{ex} concept .

The present work uses the functional form of Weber relation (Eq. 1).

$$R_{ex} = AW[1 - B/(1 + CW)] \qquad (1)$$

where: R_{ex} : is the extrapolated range in aluminium,
W : is the monoenergetic energy of electrons, and
A, B, C are numerical constants.

We also employed the characteristic thickness concept, taking data of transmission curves for heavy elements.

2. EXPRESSIONS

2.1. Expression for R_{ex} (E, Z)

The extrapolated or practical range R_{ex} of monoenergetic electrons in the energy region 0.3 keV – 50 MeV for the elemental absorbers was found to be well expressed by Eq. (2):

$$R_{ex} = 1.41\frac{Z^{0.68}}{Z+1.8}E\left[1-\frac{0.985}{1+Z^{1.9}\cdot 10^{-5}+3.1E}\right]-Z^{0.45}E^{2.12}\cdot 10^{-4} \qquad (2)$$

where, R_{ex} : is the extrapolated or practical range (g/cm^2),
E : is the incident electron energy (MeV), and
Z : is the atomic number.

2.2. Expression for Zm

The same expression applies to organic or inorganic molecules since we express Z by a empirical parameter Zm defined by Eq. (3):

$$Zm = \frac{\sum_i N_i Z_i + 4N_H}{\sum_i N_i} \qquad (3)$$

where, N_i : is the number of atoms i in the molecule, excluded the hydrogen atoms,
Z_i : is the atomic number of atom i, and
N_H : is the number of hydrogen atoms in the molecule.

TABLE I. SOME VALUES OF Zm or Zc

Material	Composition	Zm or Zc
Air	0.755 N; 0.232 O; 0.013 Ar	Zc = 7.27
Polyethylene therephthalate	$(H_8C_{10}O_4)n$	8.85
Polyacrilonitrile	$(H_3C_3N)n$	9.25
Polycarbonate	$(H_{14}C_{16}O_3)n$	9.26
Acrylonitrite-Butadiene-Styrene - ABS	0.68 (H_3C_3N); 0.07 (H_6C_4);0.25 (H_8C_8)	9.6
Cellulose Triacetate - CTA	0.85 $(C_{12}H_{16}O_8)$; 0.15 $(C_{18}H_{15}PO_4)$	9.93
Aluminium oxide	Al_2O_3	10.0
Polybutadiene	$(H_4C_4)n$	10.0
Polystyrene	$(H_8C_8)n$	10.0
Cellulose	$(H_{10}C_6O_5)n$	10.54
Polymethylmethacrilate - PMMA	$(H_8C_5O_2)n$	11.14
A-150 Tissue Equivalent Plastic	0.064 H; 0.534 C;0.027 N; 0.030 O; 0.167 F; 0.177 Ca	Zc = 11.8
6.6 Nylon	$(H_{11}C_6NO)n$	11.9
Polyvinyl – alcohol	$(H_4C_2O)n$	12.0
Polyvinyl choride - PVC	$(C_2H_3Cl)n$	13.66
Polyethylene	$(H_4C_2)n$	14
Polypropylene	$(H_6C_3)n$	14
Ethanol	C_2H_5OH	14
Water	H_2O	16

2.3. Expression for Zc

For compound materials, Z is replaced by Zc expressed by Eq. (4):

$$Zc = \frac{\sum_i \frac{fi}{Ai} Z_i + 4 f_H}{\sum_i \frac{fi}{Ai}} \tag{4}$$

where, fi : is the fraction by weight of atom i, excluded the hydrogen atoms,
f_H : is the fraction by weight of hydrogen atoms, and
Ai : is the atomic mass of atom i.

2.4. Comments

Relations (3) and (4) for Zm or Zc are the average content of electrons per atom, excluding the hydrogen and inserting their electrons in the media, as if they were four times more effective than the electrons belonging to the other atoms.

We can not give any physical meaning of this interpretation for Zm or Zc but, as it is well known, the electron or hydrogen content affects directly the energy absorption ratio (stopping power) due to inelastic electron–electron collisions. Becker *et al.* [7] showed that commercial plastics and elastomers can be ordered according to their decreasing extrapolated range by ranking them in the increasing ratio of the number of hydrogen atoms to the number of other atoms in the molecule. Table I shows some materials ordered by Zm or Zc value and this order is the same as Becker's [7].

In the generalized empirical Eq. (2), the term $Z^{1.9}.10^{-5}$ actuates only for high Z and for electron energies below 100 keV, and it was inserted to increase the extrapolated range for heavy elements in this region of energy, because the stopping power decreases due to elastic electron-atom collisions. Then, for light elements (Z, Zm or Zc < 20) this term can be discarded.

On the other hand, the second term in Eq. (2) is a correction related to radiation energy losses (bremsstrahlung production), and can be neglected for low Z, Z_c or Z_m materials at energies below 10MeV (for Al, Z=13 and for 10MeV, this correction is less than 1%). Then, for E ≤ 10MeV and light materials, the following Eq. (5) can be used:

$$R_{ex} = 1.41 \frac{Z^{0.68}}{Z + 1.8} E \left[1 - \frac{0.985}{1 + 3.1E} \right] \tag{5}$$

TABLE II. SOURCES OF DATA

Ref.	Z / absorber	Ref.	Z / absorber
1	air–13–29–79–82	13	6-13-29-47-73-92
2	4–13–29-82-Polystyrene	14	4-13-29-47-79
8	6-13-79	15	water
9	13	16	6-13-29-48-82
10	13-47-50-79-82	17	4-6-13-29-47-79-92
11	13	18	Al_2O_3
12	4-29-47-79	19	water

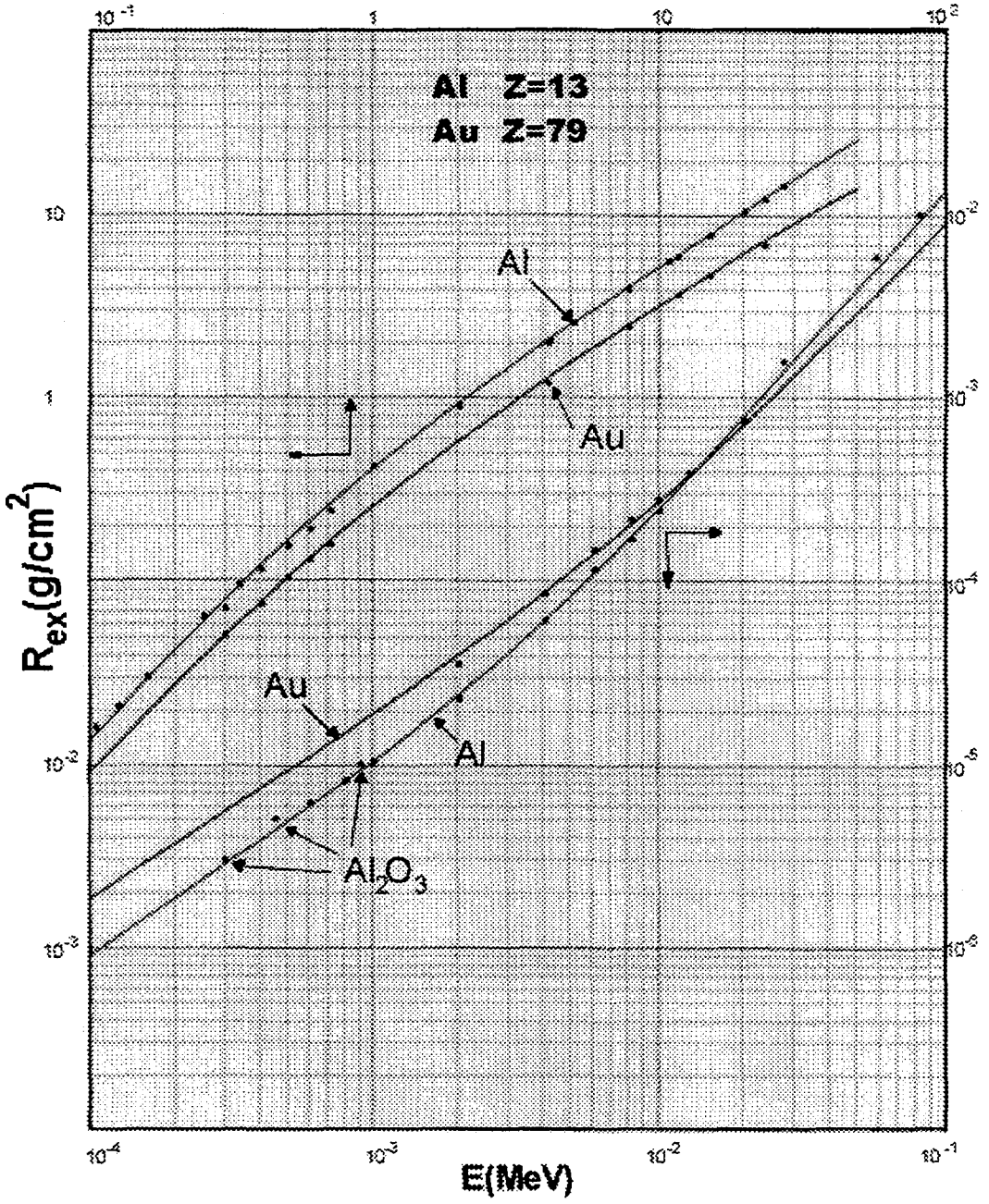

FIG. 1. $R_{ex}(E)_{Z=13}$ and $R_{ex}(E)_{Z=79}$. Lines, Eq. (2); points, experimental data.

This is Weber's Eq. (1) where the constants A, B and C are:

$$A = 1.41\frac{Z^{0.68}}{Z+1.8};\quad B = 0.985\ ;\quad \text{and}\quad C = 3.1$$

3. SOURCES OF DATA

The sources of data used are indicated in Table II. Despite the large fluctuation in the experimental data verified this does not affect so much our work for a good fitting because the simplicity of the R_{ex} expression offers the possibility of instant graphic display in the computer screen of the functions R_{ex} (Z) or R_{ex} (E).

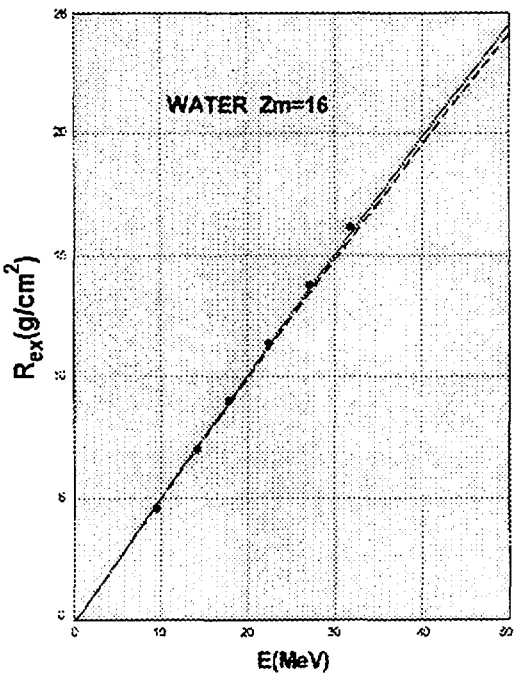

FIG. 2. $R_{ex}(E)_{water}$. Line, Eq. (2); traces, Monte Carlo analytical fit from Tabata et al [19]; points, experimental data [15].

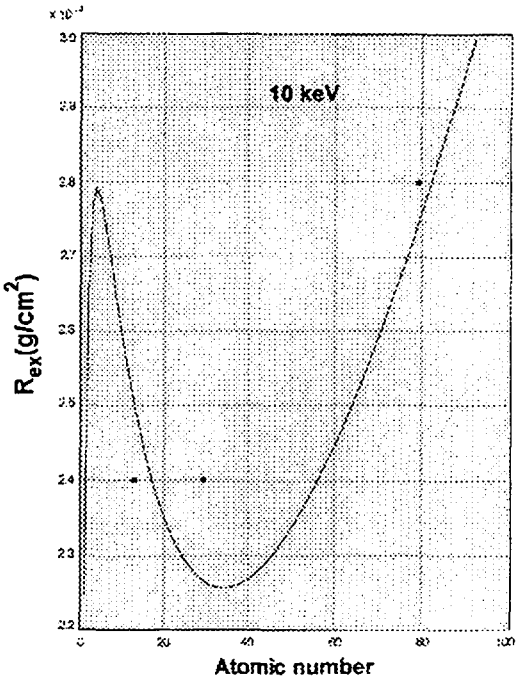

FIG. 3. $R_{ex}(Z)_{E=10keV}$. Line, Eq. (2); points, experimental data.

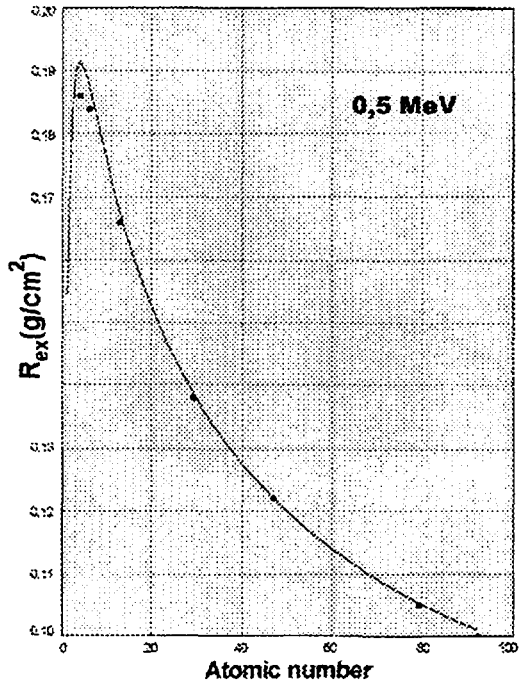

FIG. 4. $R_{ex}(Z)_{E=0.5MeV}$. Line, Eq. (2); points, experimental data.

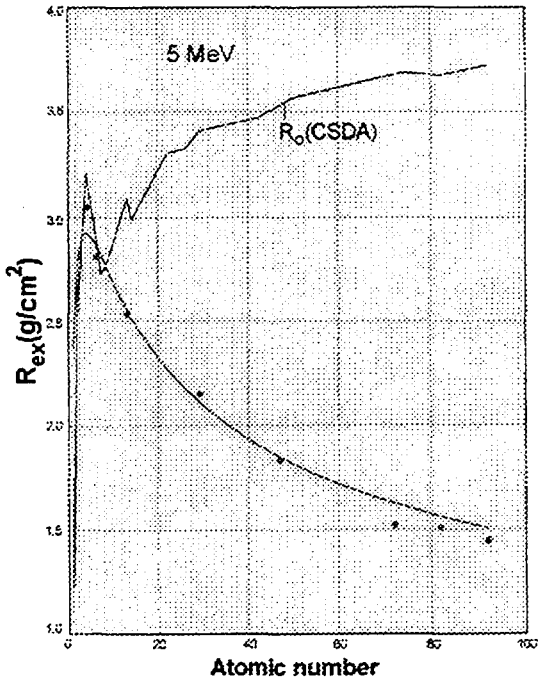

FIG. 5. $R_{ex}(Z)_{E=5MeV}$. Continuous line, Eq.(2); dashed line, r_0(csda); points, experimental data.

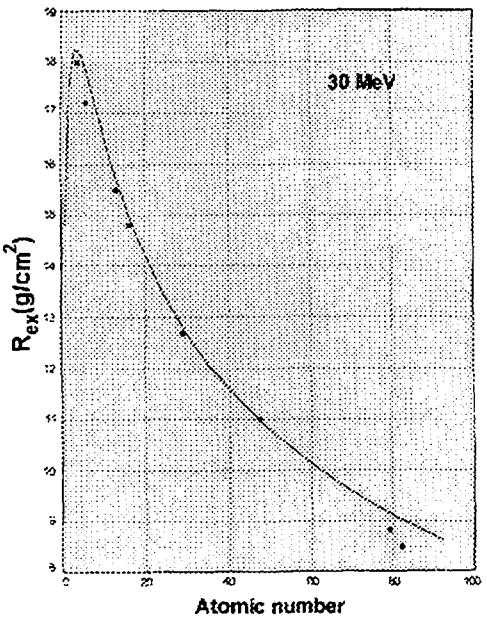

FIG. 6. $R_{ex}(Z)_{E=30MeV}$. Line, Eq. (2); points, experimental data.

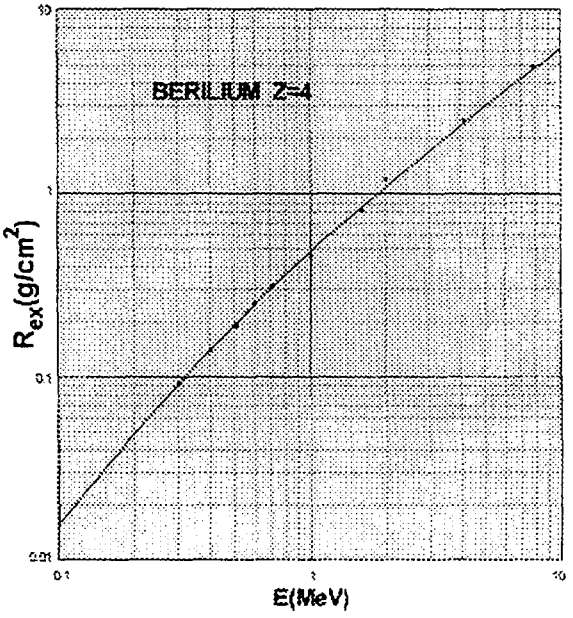

FIG. 7. $R_{ex}(E)_{Z=4}$. Line, Eq. (5), points, exper. data Refs. [2,12,14]

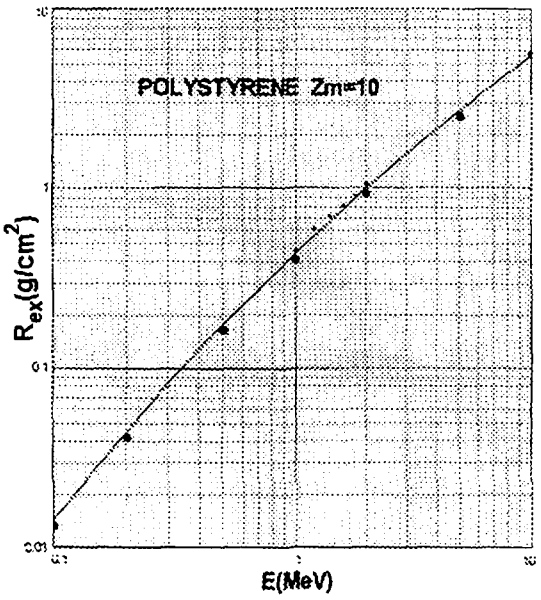

FIG. 8. $R_{ex}(E)_{Zm=10}$. Line, Eq. (5); small points, exp. data [2]; larger points, calculated by scaling law [20] between R_{ex}(water) and r_0 (csda).

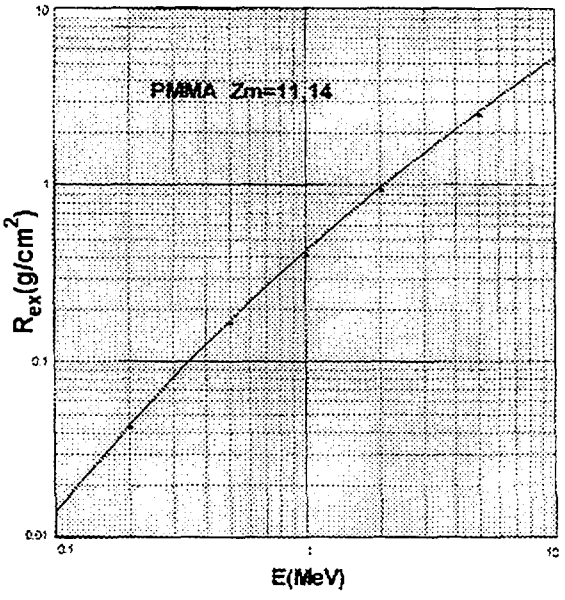

FIG. 9. $R_{ex}(E)_{Zm=11.14}$. Line, Eq.(5); points, calculated by scaling law [20] between R_{ex}(water) and r_0 (csda).

Thus we can test the relevance of one or some experimental results by their level of agreement with other absorbers data or data in other energy regions of the same absorber.

4. RESULTS AND COMMENTS

In Fig. 1 the general agreement of Eq. (2) with the available data for aluminium and gold is shown.

The relative rms deviation δ_{rms} of the generalized equation from these data in all the range is: 5.6 % for Al and 4.4 % for Au.

For aluminium, this result is similar to Tabata's equation [6] that gives 6.5 % and is a consequence of data fluctuation in some energy regions.

For gold, Tabata found 13.8 % and this difference is due to the fact that our equation fits the data better, for energies below 100 keV, without change in accuracy for distinct absorbers.

These deviations can not give more information about accuracy but for absorbers with good and enough data, like aluminium and water in the range of 0.5 – 30 MeV, the deviation is 2 % or less as it can be seen in Fig. 2 for water. In this figure, Eq. (2) was plotted against the experimental and the Monte Carlo results. We plotted the analytical fit of Tabata et al. [19] for the extrapolated range of water that gives the best accordance with present Monte Carlo codes. The agreement is very good and it seems that Eq. (2) lies closer to the experimental data.

About the general accuracy of Eq. (2), we believe that it is better than 4 % for any absorber in all the energy range. Only for H and He, the accuracy can be poorer because Eq. (2) for E=constant, $R_{ex}(Z)_{E\,=\,constant}$ has a maximum for $Z \cong 3.8$ as it can be seen in Figs 3 to 6, and we did not find experimental data for these absorbers. In figure 5, the csda range [20] was included to show the same maximum for beryllium, Z=4. We also see that Eq. (2) gives values 8 % higher for He and 100 % higher for hydrogen than the csda range r_0. As r_0 is interpreted as the mean path length, we can not have $r_0 < R_{ex}$ or the continuous-slowing down is no longer verified, for these two lightest elements.

In Fig. 3, the increase in R_{ex} for heavy elements in low energy range is shown. Figures 7, 8 and 9 show the equation (5) applied to light absorbers and energy below 10 MeV, plotted against experimental data or data estimated by a scaling law conform ICRU – 35 [20].

REFERENCES

[1] KOBETICH, E. J.; KATZ, R. Energy deposition by electron beams and δ rays. Phys. Rev. **170**(2) (1968) 391-396.

[2] KOBETICH, E.J.; KATZ, R. Electron energy dissipation. Nucl. Instr. and Meth. **71** (1969), 226-230.

[3] TABATA, T.; ITO, R. An algorithm for the energy deposition by fast electrons. Nucl. Sc. and Eng. **53** (1974) 226-239.

[4] WEBER, K. H. Eine einfache reichweite-energie-beziehung für eletronen im energiebereich von 3 keV bis 3 MeV. Nucl. Instr. and Meth. **25** (1964) 261-264.

[5] DUPOUY, G.; PERRIER, F.; VERDIER, P.; ARNAL, F. Transmission d'électrons monocinétiques à travers des feuilles métaliques minces. Comp. Rend. 260 (1965) 3655-3060. Comp. Rend. **258** (1964) 6055-6060.

[6] TABATA, T.; ITO, R. OKABE, S. Generalized semiempirical equations for the extrapolated range of electrons. Nucl. Instr. and Meth, **103** (1972) 85-91.

[7] BECKER, R.C.; BLY, J.H.; CLELAND, M.R.; FARRELL, J.P. Accelerator requirements for electron beam processing. Rad. Phys. Chem. **14** (1979) 353-375
[8] KANTER, H.; STERNGLASS, E.J. Interpretation of range measurements for kilovolt electrons in solids. Phys. Rev. **126**(2) (1962) 620-626.
[9] LANE, R.O.; ZAFFARANO, D.J. Transmission of 0-40 keV electrons by thin films with application to beta-ray spectroscopy. Phys. Rev. **94**(4) (1954) 960-964.
[10] SELIGER, H.H. Transmission of positrons and electrons. Phys. Rev. **100**(4) (1955) 1029-1037.
[11] AGU, B.N.C.; BURDETT, T.A.; MATSUKAWA, E. The transmission of electrons through aluminium foils. Proc. Phys. Soc. (London), **71** (1958) 201-206.
[12] AGU, B. N. C.; BURDETT, T. A.; MATSUKAWA, E. The transmission of electrons through metallic foils. Proc. Phys. Soc. (London), **72** (1958) 727-732.
[13] EBERT, P.J. LAUZON, A.F.; LENT, E.M. Transmissiion and backscattering of 4.0- to 12.0-MeV electrons. Phys. Rev. **183**(2) (1969) 422-430.
[14] TABATA, T.; ITO, R.; OKABE, S.; FUJITA, Y. Extrapolated and projected ranges of 4- to 24-MeV electrons in elemental materials. J. of Appl. Phys. **42**(9) (1971) 3361-3366.
[15] VAN DICK, J.; MACDONALD, J.C.F. Penetration of high energy electrons in water. Phys. Med. Biol. **17**(1) (1972) 52-55.
[16] HARDER, D.; POSCHET, G. Transmission und reichweite schneller elektronen im energiebereich 4 bis 30 MeV. Physics Letters **24B**(10) (1967) 519-521.
[17] TABATA, T.; SHINODA, K.;ANDREO, P.;CHUAN-SAN, W.;ITO, R. Analysis of Monte-Carlo depth-dose data for electron beams and four layer extension of the Edmult Code. RADTECH Asia (1993) 574-579.
[18] YOUNG, J.R. Penetration of electrons in aluminium oxide films. Phys. Rev. **103**(20) (1953) 292-293.
[19] TABATA, T.; ANDREO, P.; ITO, R. Analytic fits to Monte Carlo calculated depth-dose curves of 1- to 50-MeV electrons in water. Nucl. Instr. and Meth. In Phys. Res. **B58** (1991) 205-210.
[20] ICRU – Radiation dosimetry electron beams with energies between 1 and 50 MeV, (1984) ICRU – Rep. 35.

DOSIMETRY AS AN INTEGRAL PART OF RADIATION PROCESSING

Z.P. ZAGÓRSKI
Department of Radiation Chemistry and Technology,
Institute of Nuclear Chemistry and Technology,
Warsaw, Poland

XA9949733

Abstract

Different connections between high-dose dosimetry and radiation processing are discussed. Radiation processing cannot be performed without proper dosimetry. Accurate high dose and high dose rate dosimetry exhibits several aspects: first of all it is the preservation of the quality of the product, then fulfillment of legal aspects and last but not the least the safety of processing. Further, seldom discussed topics are as follow: dosimetric problems occurring with double-side EB irradiations, discussed in connection with the deposition of electric charge during electron beam irradiation. Although dosimetry for basic research and for medical purposes are treated here only shortly, some conclusions reached from these fields are considered in dosimetry for radiation processing. High-dose dosimetry of radiation has become a separate field, with many papers published every year, but applied dosimetric projects are usually initiated by a necessity of particular application.

1. INTRODUCTION

Dosimetry, i.e. the determination of absorbed dose in a chemically and physically defined object of particular geometry, is applied for two different purposes: in basic research, being the basis of calculation of radiation yields of products or effects, and in radiation processing of materials as a control of desired technological effect. Working in both fields requires the great responsibility: firstly, because radiation yields enable to draw important conclusions and generalizations; secondly, because it is connected with the quality of the product and the economy of processing. Whereas the choice and the performance of dosimetry in the first field of dosimetric applications is a sole responsibility of the researcher, the dosimetry in the second case is the duty of the irradiation plant management and is the subject of standards (e.g. ASTM, ISO and national organizations) and supervisions, sometimes of international scope. In the transient zone, i.e. between basic research and applications, the responsibility of the researcher in the field of dosimetry is also important. The error in determination of the radiation yield by 0.1 μmol J^{-1} and/or negligence in estimation of yields as the function of dose can turn a highly promising technology into an economic disaster.

Connections between radiation processing and dosimetry were always very close. On the one hand the radiation processing was defining problems for solution, on another the dosimetry and results obtained from measurements strongly influenced the techniques of irradiation and technologies of the processing. That is well recognised in one of the first textbooks on dosimetry [1] and in another one of the more recent books on dosimetry, in which the key word "radiation processing" has appeared in the title of the book [2].

2. DOSIMETRY IN BASIC RESEARCH

Dosimetry applied in strictly basic research will not be discussed in the present paper. However, there is a thin boundary between basic and applied research. For instance, very often the basic research reveals the existence of chain reactions. There is an extreme sensitivity of yields of chain reactions to the dose rate which has to be confirmed with proper dosimetry. For instance, reactions of oxidation running with the radiation yield of the order of hundreds per 100 eV of absorbed energy (order of 10 μmol J^{-1}) in the γ-radiation field lower their yield to a few units if high power electron beam is used [3]. The same applies to chain reactions initiated in systems where polymerization takes place.

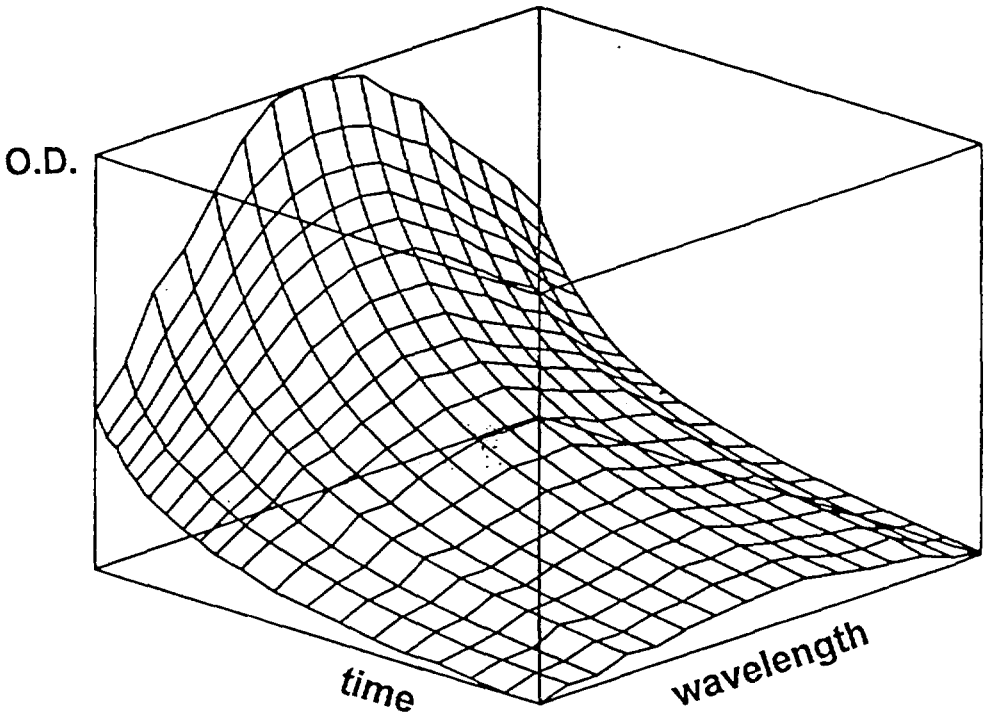

FIG. 1. 3-D diagram of spectra of $(SCN)_2^-$ decay in pulse radiolysis dosimetry. The dose is calculated from the optical density extrapolated to the zero time of beginning of the decay.

Dosimetry in pulse radiolysis experiments has been developed to the specific form taking into account high heterogeneity of the dose distribution unaccounted for in radiation processing. Nevertheless it reflects the true delivery of energy, because it averages the dose in exactly identical way, as it is in the case of experiment which follows the dosimetric measurement. The dose is measured with the same equipment as used in time-resolved measurement of concentration of a transient. The radiation-induced dosimetric reaction is also time-resolved, i.e. the determined product of reaction, (e.g. the $(SCN)_2^-$ radical anion) decays, but its concentration is extrapolated to the duration of the pulse (Fig. 1). Transient character of dosimeter is accepted in that case because it integrates the inhomogeneous dose in the same way as at experiment on unknown species. One can say that the specific dosimetry in pulse radiolysis is the integral part of this technique and it cannot be applied in other fields of radiation chemistry. Vice versa, other methods of dosimetry can hardly be applied in the pulse radiolysis.

3. DOSIMETRY FOR MEDICAL PURPOSES

The dosimetry developed for medical irradiations will not be fully considered as well. Similarly as in dosimetry used in the pulse radiolysis, medical dosimetry deals with very inhomogeneous distributions of dose, e.g. delivered by a single pulse of the straight beam of electrons. In medical applications the collimated beam of gamma radiation is used, or more frequently the straight beam of electrons, protons or heavy ions, always with the intention to concentrate the energy on a well defined spot with the minimum dose deposited around it. The approach at radiation processing is opposite to this in medical irradiations, i.e. the beam is scanned, resulting in the broad beam geometry with a characteristic depth dose curve, substantially different to that at narrow beam geometry [4]. Nevertheless, some experience with phantoms is useful for radiation chemists. All irradiations have a common basis in general radiation physical chemistry (e.g. mass absorption coefficients) which is considered in radiation processing.

4. DOSIMETRY FOR PREPARATION OF GENERAL SCHEME OF RADIATION PROCESSING

Dosimetry plays the especially important role in industrial radiation processing, in the preparation of the plan of routine irradiations, involving instructions for a producer of irradiated goods. The case of gamma irradiation is comparatively simple, as it deals with a relatively high homogeneity of dose distribution. This is the case when the unit operation of irradiation is done in large installations, where objects of irradiation are moving around the sources, collecting and averaging absorbed dose. Nevertheless, the mapping of the dose distribution should be made, considering possible irregularities if all boxes are not filled identically with the irradiated material, or the simulation of contents of boxes is not possible. The situation is even more complicated at the case of electron beam irradiations, where practically only one-step irradiation is made. Split-dose or double-side irradiations are possible only in exceptional cases. The latter technique (of double side irradiation) may improve the homogeneity of the dose, but brings the danger of a deposition of charge and a damage of irradiated objects by violent discharge, in the shape of sparks. It is discussed in separate paragraph below.

It is obvious, that the heterogeneity of dose distribution has a strong connection to the economy of processing. If higher heterogeneity can be tolerated (i.e. a larger difference between the highest and the lowest dose in the material), the cheaper is irradiation to the required average dose. The radiation resistance of the irradiated material and the radiation microbiology in the case of radiation sterilization require the defined upper and lower limits of the dose distribution. It can be shown on many examples how much may be saved of the expensive radiation energy with the proper adjustment of the maximal and minimal doses, as seen from the careful dosimetric mapping of the whole conglomerate of objects irradiated in a standard box. A complete dosimetric analysis of the dose distribution can be very expensive and requires an application of sophisticated dosimetric approaches, e.g. to solve the problem of highly increased doses in a polymer layer, which is placed close to a metallic object like a surgical needle. Such situation demands sometimes a research to be done, for particular kind of polymer, because a local overdose sometimes can be tolerated.

The margins of free choice of dose distribution are rather narrow, especially at radiation sterilization. The minimum dose delivered in particular place of the box with medical supplies must be higher than sterilization dose determined by required level of inactivation of microorganisms. On the other hand the maximal dose in the site of the highest dose must be lower than this dose allowed by the resistance of a material of the device towards radiation. The limits are set by requirements of sterility and by undesired chemical changes, induced by radiation in the material. Other limits are established by the presence of parts of the object, which exhibit energy absorption characteristics very different to the main material. These are e.g., as mentioned metallic parts like needles. The producer of devices is advised to make such parts as thin as possible.

Simple cases, e.g. uniform systems like rubber latex to be vulcanized by radiation, transported in ready-to-sell containers of the size and geometry adjusted to the energy of electrons, scanning width and conveyer construction, are very rare indeed. In this case, and in the case of any viscous liquid, especially thixotropic one which does not flow easily if not mixed, they represent cases of highest use of beam energy, where the thickness of the irradiated layer of the material is equal to the distance between the identical entrance and exit doses. In connection with latex one can notice, that pumping of liquids like that is difficult and the dosimetry in such case is extremely difficult. Due to non-uniform flow, especially close to the walls, doses received by the viscous liquid moved by pressure are different in comparison to the expected distribution of doses measured by dosimeters placed in proper places of the irradiation site. Therefore we have found the irradiation of latex on the typical conveyor best than other methods, from the point of view of both - technology and dosimetry. The application of well tried technique shows the advantage of realization of unit operation principle as the method of choice [5].

Multi-component objects of a complicated geometry, i.e. the majority of medical supplies are far from the ideal latex situation described above. Although only 10% of radiation energy is utilized in that cases, dosimetry can help to improve this value, and at the same time, also the economy.

The question arises to what extend the dosimetry of objects of composed geometry and chemical composition has to be repeated in routine irradiations. Full dosimetry, like that applied during the preparation of irradiation plan, is impossible and certainly too expensive. The management of every large irradiation plant has elaborated its own strategy in dealing with the problem. The minimum requirement are the semi-quantitative dosimetric labels, preferably with the possibility of reading the absorbed dose as the optical density with a hand-held optical DRS spectrophotometer. Traditional go-no-go labels are too primitive and not up to the state of the art.

The wide gap between the real dose distribution inside the box and the simple semi-quantitative reading from the label attached to the upper and lower surface of the box can be overcome by using electronic system of control. It consists of a continuous record of the accelerator performance, traceable to the particular box position, as well as the measurement, if possible of the power passing through the box. The latter measurement is difficult to perform with a vertical beam of electrons hitting the horizontal conveyer. There is an advantage of horizontal beam accelerators in that respect, that the dose at hanging boxes can be measured indirectly, with a detector just behind the irradiated object.

The split dose irradiation is a necessity if required doses are of the order of 100 kGy and higher, e.g. in the case of cross-linking of polyethylene. Single irradiation to that dose is technically possible but cannot be applied because of intolerable increase of temperature of the object [5]. As there is the necessity to cool down the object and letting injected electrons to dissipate, the dosimeter may be attached for every subsequent passage of the material under the electron window. There are no satisfactory dosimeters, which would integrate the dose of, e.g. 200 kGy and indicate the accumulated dose properly. Electronic control and the registration of the history of irradiation is also needed in this case of very high accumulated doses.

In many places of the present paper the difference between γ and EB irradiation is shown. Basic differences in both sources of ionization energy are projected on dosimetry. One of the basic features of electron beam processing is the congestion of isodose distributions in comparison to gamma fields,

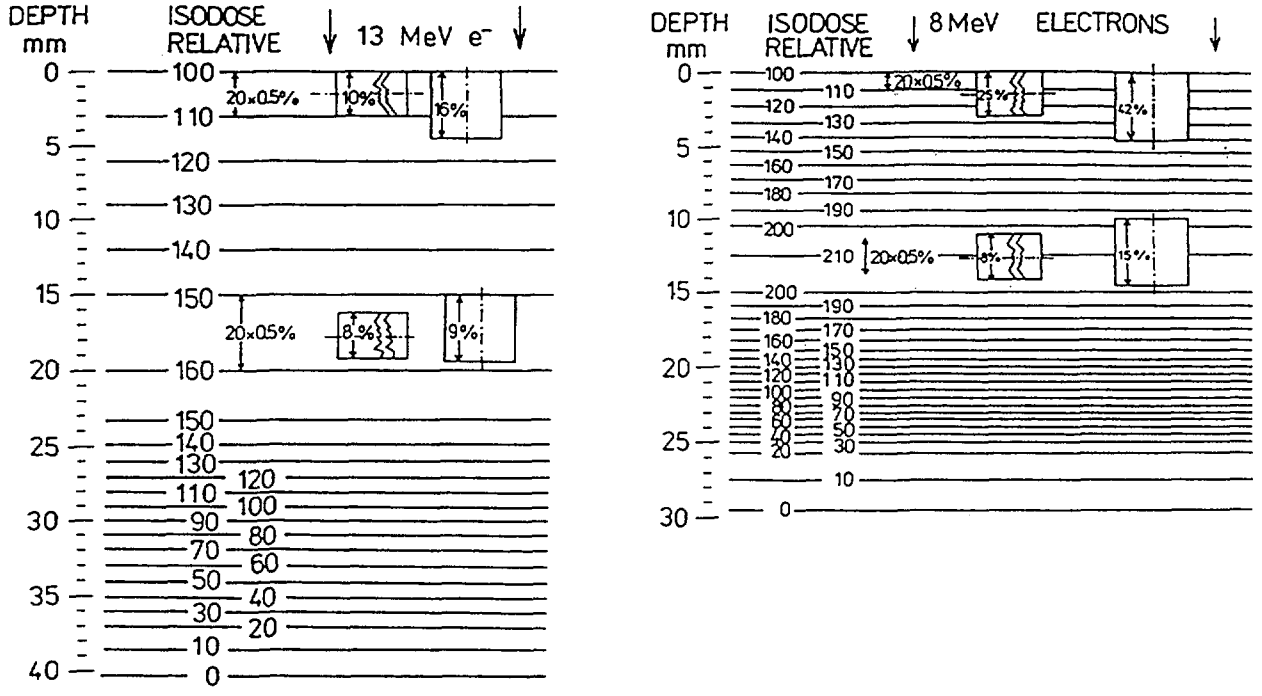

FIG. 2. Isodose layers in scanned electron beam irradiation of 13 MeV (a) and 8 MeV (b) energy. Object and dosimeter made of PCV. The surface dose (electron entrance dose) is taken as 100. Sizes of typical dosimeters are introduced with expected non-uniformities of dose distributions.

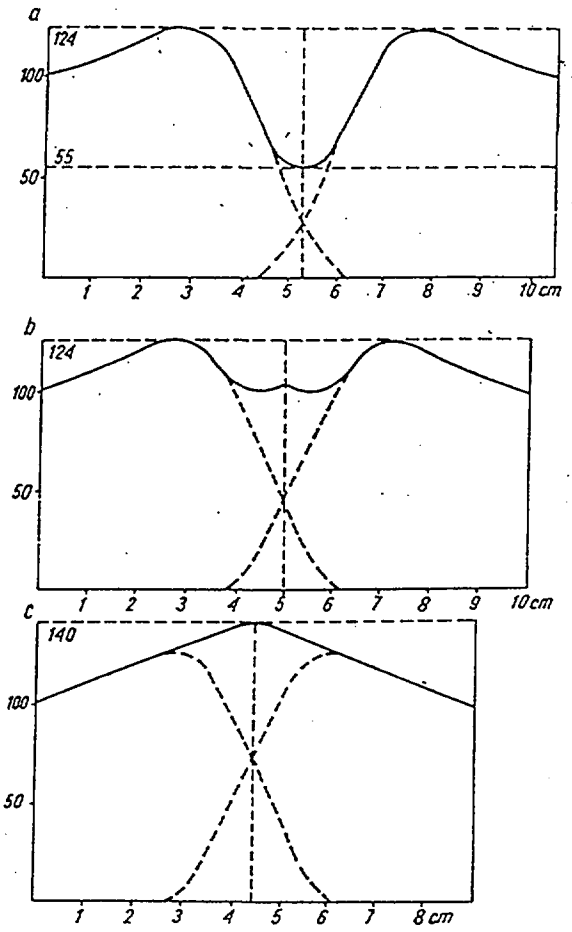

FIG. 3. Depth dose curves obtained in double sided irradiations as the function of thickness of material in the box. Entrance dose of 12-MeV electrons taken as 100%. There are three cases of thickness: a) Too high thickness of the material resulting in too low (55%) dose inside the object, b) Optimal thickness (24% overdose in relation to the minimum (entrance) dose, c) The case of too low thickness of the material (overdosage of 40% inside the object).

especially those in large cobalt-60 irradiation installations, where objects are moved across fields of very different dose rates. In the case of EB, the most convenient one step irradiation under the window passing the beam of electrons creates the dose distribution shown in Fig. 2 a and b. (Dose distribution in the shape of isodose curves is recalculated from depth dose curves describing absorption of electron beam in chosen medium, e.g. [4]). The congestion is already inconvenient at the sometimes allowed optimum of energy of 12 MeV, but is changing from bad to worse in the case of lower energies (8 MeV), not to mention such low energies as 2 MeV. The irradiated object obtains doses different in not very distant places. Geometric shapes and sizes of dosimeters which are excellent in γ-irradiation exhibit not acceptable behaviour at EB irradiation. The only solution is the application of thin layer dosimeters (see Ref. [7]).

The low range and the resulting congestion of doses has suggested the application of double side irradiations and for this purpose sophisticated mechanical constructions have been proposed, turning the boxes upside down on the conveyer, before the second run under the beam. That technique is acceptable under conditions of precise filling of boxes with the material to be irradiated. Figure 3 shows what happens if this condition is not fulfilled: substantial, easy measurable under- and over-exposures may occur. Special dosimetric control is advised in such cases, if severe errors in radiation processing have to be avoided. Application of wrong doses is not the only danger involved in double side irradiation.

For EB-radiation processing the problem of dosimetry of deposited charge arises. Deposition of electric charge in objects irradiated by electron beam is seldom taken into account. That negligence is justified when the thickness of irradiated material is limited, as usual to the „entrance dose-equal-exit-dose" treatment. Figure 4 shows the typical depth-dose curve, supplemented by the curve showing the depth distribution of deposited electrical charge. The maximum of charge is shifted towards the end of the range of penetration of electrons. Therefore the most of electrons are absorbed by the conveyor and lead to earth. The deposited charge can no longer be neglected when the object is thicker than the range of electrons in particular material. If the electrical conductivity of the material is low, the accumulated charge can reach high voltage potential, sometimes close to million of volts. It is easy to initiate the discharge, which rapidly takes the form of high intensity streams of current which creates paths of destroyed polymer. The phenomenon is used for decorative art, creating nice 'trees' in transparent polymers like PMMA [6]. In the case of radiation processing, e.g. of thick blocks of polymer the deposited charge can cause fire, which can be disastrous for the accelerator. Even without fire, the discharge destroys the material by burning holes in it. One can encounter that in techniques which are providing, sometimes with the help of sophisticated mechanical devices, the double side irradiation to improves the yield of radiation energy. There is no 'dosimetry' of the deposited charge in the sense used in the present paper. The function of dosimetry is played by theoretical preparation of the technology, considering electrical conductivities of the irradiated systems in the region of deposition of charge. After preparation of phantoms the experiment should be performed with increased doses of radiation. Careful inspection of the irradiated object for the presence of holes and/or 'trees' of discharges might convince the supervisor of production that the radiation processing in this particular case is safe for the integrity of product and the operation of irradiation is safe from the point of view of fire protection.

The deposition of electric charge has to be taken into account in the case of preparation of depth dose curves in thick phantoms (wedges, stacks etc.). If they are made of materials of poor conductivity and no charge collectors are provided, complications can occur. Phantoms well conducting the electric current i.e. all metals and polymers in which radiation induces the conductivity, like poly(vinyl chloride) presented in paper [4], are safe in that respect.

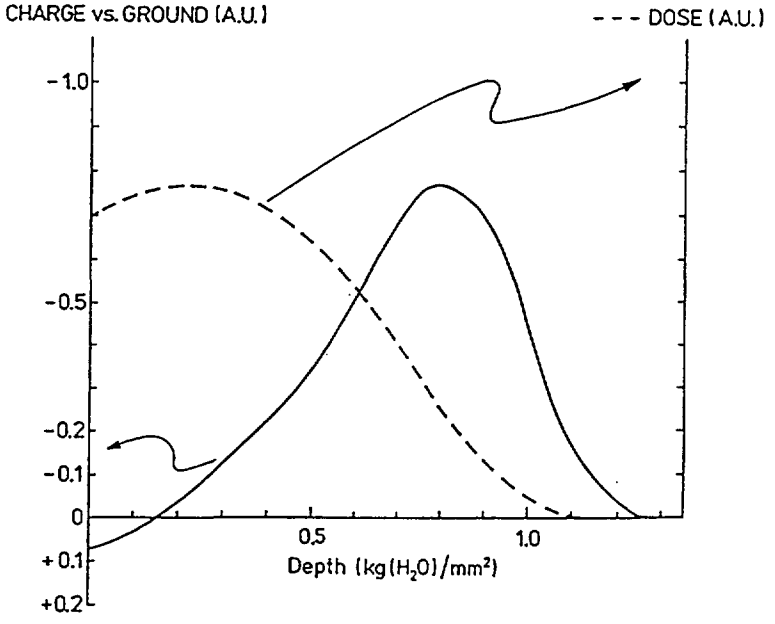

FIG. 4. Depth-dose curve, compared with the depth-charge curve for electron beam irradiation of 10 MeV energy, showing the accumulation of excess electrons at the end of the range of the beam, i.e. in the zone not used in the case of one-sided irradiation. The shift of the curve is substantial: the surface of the object is depleted of electrons.

5. SPECIAL CASES OF RADIATION PROCESSING

The question is asked sometimes if dosimetry is needed at all in the case of some exotic irradiations, far from usual radiation processing, represented, e.g. by radiation sterilization. Among seldom used applications there is a technology of perforation of thin plastic layers with a beam of heavy ions of high energy. Process of etching destroys chemically the burnt tracks. The result is a film with random holes and the product may be used for filtration of gases or liquids. In this technology the dosimetric control of the process is difficult, and the only quality assurance involves drawing attention to proper thickness of the film and its chemical quality and to keeping the parameters of heavy ion accelerator on the level previously tested as the optimal one. Computer programmes like TRIM help to determine the dose inside tracks, which often is between 10 and 100 MGy. Experimental dosimetry of heavy ion irradiations is controversial in general, because only a few percent of the absorbed energy is deposited in single ionization spurs, for which useful dosimetric methods have been developed. Most of energy is deposited in multi-ionization spurs, which represent rather the phenomenon of thermal spikes. It destroys the material completely, as it is in the case of holes and channels mentioned above. Dosimetry of energy deposited in tracks could be based on determination of debris of polymer extracted in the process of etching, but details of such method are not yet published.

6. CONCLUSIONS

Close cooperation between specialists of dosimetry and radiation processing is advised. High dose dosimetry became almost separate field in recent years. The quest for new dosimetric techniques has produced new systems, usually of no application. However, there were as well remarkable achievements in the field, probably impossible without wide front of research and new dosimetric proposals. The early confrontation with realities of large scale radiation processing may help in more efficient development of useful dosimeters. This applies in particular to high absorbed dose, high dose-rate dosimeters applied at high power electron beam irradiations. Two features of that kind of EB radiation processing have to be taken into account: the adiabatic delivery of energy, resulting in the increase of temperature of the object during irradiation and deposition of electric charge. Electron beam irradiations produce very congested isodose fields, demanding application of thin dosimeters both for the preparation of depth-dose curves and for reliable dose-mapping. Many dosimeters thick in shape, excellent for dosimetry in gamma radiation facilities, are useless at EB irradiations [7]. Dosimeters of thickness which cannot be reduced, are showing the average dose in a layer covering different doses. The dosimeter which averages the dose over unacceptable range of isodoses is of no help in detection of over- and under-irradiated regions in the object, what is the basic requirement in radiation processing for the purpose of sterilization of medical supplies.

Proper dosimetry applied to radiation processing creates a new branch of technology. Philosophy of the unit operation principle, useful in radiation processing [5] may be applied also to systematics of high dose and high dose-rate radiation dosimetry.

As the radiation processing is not supported economically by state organizations, even in former communist controlled regions with central steering, arbitrarily controlled economy [8], the proper dosimetry helps to keep the price for radiation processing in reasonable limits and promoting competition with other technologies, very often of inferior abilities as compared to radiation processing.

Dosimetry applied in radiation processing is in a constant development and revision. One can conclude that from efforts of American Society for Testing and Materials (ASTM) (recently in collaboration with ISO) in which the Subcommittee E10.01 prepares standards, e.g. E1261 'Guide for Selection and Calibration of Dosimetry Systems for Radiation Processing' (it will be published in 1999, as ISO 15556); E1707 'Guide for Estimating Uncertainties in Dosimetry for Radiation Processing' (it will be published in 1999 as ISO 15572); 'Practice for Dosimetry in a Gamma Irradiation Facility for Radiation Processing' (to be published in 1999 as ISO 15571); E1649 'Practice for Dosimetry in an

Electron Beam Facility for Radiation Processing at Energies between 300 keV and 25 MeV' (it will be published in 1999 as ISO 15569 with a revised scope); E1608-98 'Practice for Dosimetry in an X-Ray (Bremsstrahlung) Facility for Radiation Processing'. All standards refer to many related standards serving the quality of radiation processing.

REFERENCES

[1] HOLM, N.W., BERRY, R.J. (Eds), Manual on Radiation Dosimetry, Marcell Dekker Inc., New York (1970) 450 pp.

[2] McLAUGHLIN, W.L., BOYD, A.W., CHADWICK, K.H., McDONALD, J.C., MILLER, A., Dosimetry for Radiation Processing, Taylor&Francis, London (1989) 251 pp.

[3] ZAGÓRSKI, Z.P., SEHESTED, K., NIELSEN, S.O., "Pulse radiolysis of aqueous alkaline sulfite solutions" J.Phys.Chem. **75** (1971) 3510-3517.

[4] ZAGÓRSKI, Z.P. "Dependence of depth-dose curves on the energy spectrum of 5 to 13 MeV electron beams" Radiat.Phys.Chem. **22** (1983) 409-418.

[5] ZAGÓRSKI, Z.P., "The unit operation principle in effective and versatile radiation processing" Radiat.Phys.Chem. **18** (1981) 1309-1315.

[6] ZAGÓRSKI, Z.P., Chapter 13, "Thermal and electrostatic aspects of radiation processing of polymers" in A.Singh/J.Silverman (Editors), Radiation Processing of Polymers, Hanser Publishers, Munich, Vienna, New York, Barcelona (1992).

[7] ZAGÓRSKI, Z.P., RAFALSKI, A., "A thin alanine-polyethylene film dosimetry system with diffuse reflection spectrophotometric evaluation" J.Radioanal.Nucl.Chem. **196** (1995) 97-105.

[8] ZAGÓRSKI, Z.P., "Radiation processing and market economy" Radiat.Phys.Chem. **52** (1998) 607- 609.

VALIDATION OF A LABEL DOSIMETER WITH REGARD TO DOSE ASSURANCE IN CRITICAL APPLICATIONS AS QUARANTINE CONTROL*

D.A.E. EHLERMANN
Institute of Process Engineering,
Federal Research Centre for Nutrition,
Karlsruhe, Germany

Abstract

A 'label dosimeter' (dose-threshold indicator) for dose ranges of insect disinfestation became commercially available only recently. It was studied for dosimetric (metrological) properties elsewhere. The fundamental problem of its application in practice is the relation between the dose observed at a reference position and the critical minimum dose achieved in a consignment. For this reason several irradiation geometries (relations between the arrangement of the goods during irradiation and the type of the radiation source, gamma, electrons, X-rays) were studied. The observed dose distributions revealed the difficulty that for any such geometry a 'label dosimeter' with a specific but differing threshold dose-value must be utilized in order to guarantee the adherence to the required minimum dose-value. The 'label dosimeter' must be placed at a position where the minimum dose is likely to occur. In situations where the position of the minimum dose is not accessible extrapolation from the dose observed at a reference position is less reliable.

1. INTRODUCTION

The verification of absorbed dose in radiation processing is a fundamental procedure generally relying on auditing of the records at the irradiation facility. Procedures for this are well established and proven reliable and trustworthy under practical circumstances of industrial radiation processing. However, in quarantine applications special circumstances are encountered and the demand for 'label dosimeters' has been voiced. In disinfestation by ionizing radiation insects might survive still capable of movement or flight, but the purpose of the treatment, disabling proliferation of the insect in any not yet infested area is fully accomplished. Hence, once live insects are encountered during the inspection procedure availability of additional information about minimum dose applied could bolster confidence and acceptance of the respective lot.

Only recently label-indicators became available commercially which have a dedicated dosimeter function: At a given threshold dose the label changes appearance by a 'no/yes'-transition (International Speciality Products (ISP) Inc., Wayne NJ, USA), [1]). Such devices are presently manufactured for nominal dose values of 70, 125, and 300 Gy. These dosimeters were characterized for their dosimetric properties [2, 3] and found generally acceptable. Subjective and objective evaluations were applied in order to validate the possible visual judgement by inspectors and to evaluate the potential use of dedicated hand-held readers [4].

For their purposes, the radiation processing industry has already established and standardized the practice of dose mapping and process validation for each individual item accepted for treatment. This, together with records of process control measures taken, of dose measurements executed during the process, and of observations at critical control points established for the process, renders a bulk of data on random fluctuations of the process. In commercial radiation processing it is to be expected that repeating loading patterns occur regularly which can be characterized for all random fluctuations which

*Work partially supported by IAEA Research Agreement No. 7776/CF under FAO/IAEA Co-ordinated Research Programme on Standardized Methods to Verify Absorbed Dose of Irradiated Fresh and Dried Fruits and Tree Nuts in Trade.

are likely to occur and can be related to achievable dose distributions and to the measured dose at some established reference position. A study of such informations can reveal whether verification of absorbed dose administered is possible and reliable in trade. As a model, certain geometries (source-product-geometries) were studied for electron, bremsstrahlung and gamma-ray processing.

This study refers to the further validation of such labels with reference to situations to be expected under commercial circumstances. Mainly fruit will be irradiated for disinfestation. Fresh fruit trade has already established standardised transport systems including retail packages or display-units. For such systems the geometry of the arrangement of the individual items and of subunits on a collecting pallet is well defined; hence, for any given irradiation facility and its source-product geometry the pattern of dose distribution can be established. This distribution will be linked to a dose measurement at a reference in a statistically reliable manner. Finally, such reference position could be chosen on the outer surface of a product unit where a label dosimeter could reside. This particular label could undergo formal inspection and allow for a decision about accepting the respective lot.

2. MATERIALS AND METHODS

A range of types of dose distributions for geometries likely to occur under commercial practices is confined to disinfestation of fruit: On one hand it depends on shape and size of the respective fruits, on the arrangement of packing the individual fruits into a retail tray or into a transport container, on the compilation of such sub-units on a crate or palette; on the other hand it depends on type of the radiation source and its design parameters, especially the type of movement past the source. Such parameters are usually optimized during the design phase of an irradiation facility in order to achieve a relatively homogeneous dose distribution in the treated goods [5]. These design parameters together with the penetration properties of the exploited radiation type determine the expected dose patterns and the positions where minimum and maximum dose are likely to occur. Penetration properties are fixed for irradiation facilities employing radionuclide (gamma) sources. For X-ray facilities, it varies with the nominal electron energy of the generator and with the extent of absorption and filtering; standardized 5 MeV X-rays are as penetrating as cobalt-60 gamma rays. With electrons, penetration depth is physically limited and the maximum range is about 45 mm in water for 10 MeV electrons. All three kinds of sources were studied in the reported experiments.

Irradiation was done with a gamma-cell (Cobalt-60, dose rate 0.5 kGy/h) and a linear accelerator for electrons (indirect mode (microwave) 10 MeV, 10 kW, instantaneous dose rate 10^8 Gy/s, pulse duration 12 :s; bremsstrahlung (X-rays) at 5 MeV, dose rate about 10^4 Gy/s; average dose rates depending on scanning width, repetition rate and conveyor velocity). For experiments on larger scale a commercial gamma-facility was available. In order to cover the full dose range and sensitivity of available dosimetry films (GAFchromic DM-100 and FarWest FWT-60-00, sealed in paper/plastic envelopes) the target doses were chosen accordingly (eg minimum dose at 5 kGy); the results can easily be transformed to the dose range of interest (eg 250 Gy) as the geometry and, hence, the dose patterns and the relative dose distribution are not affected by setting of exposure time. Film readings were taken with a colorimeter (transmission mode, CIBA CORNING 257 or FarWest Radiachromic Reader) and filters for the appropriate wavelengths. Reference dosimetry for film calibration was done by use of Fricke dosimeter cross-checked by alanine dosimetry (International Dose Assurance Service (IDAS) of the IAEA) at accelerator and gamma-cell. In the experiments in co-operation with a contract irradiator Harwell Amber 3042 and spectrophotometer read-out were applied in addition to our own systems.

Also, in order to study a larger variety of geometries and bulk densities wheat, maize and potatoes were included as models for fresh and dried fruits as well as tree nuts; one study included apples on commercial cardboard trays stacked on standardized pallets; the main studies were executed on pistachio in commercial cardboard boxes containing 40 or 48 pouches, respectively, 125 g each.

SAS (Statistical Analysis System, Carry, USA) was applied for analysis of data and graphical presentation of results.

3. RESULTS AND DISCUSSION

A variety of experiments were conducted which are reported elsewhere in full detail (including palette dimensions and physical product characteristics) [6]. The main findings of this study were that the resulting dose distributions, regardless of the design efforts for better homogeneity, are reasonably close to normal (Gaussian) distributions. This implies that much of the irradiated energy is wasted for treatments above the minimum effective dose value. The expectation that the irradiation facilities are designed for effectiveness of radiation energy exploitation and hence asymmetric dose distributions could not be proven.

The experiments at a commercial gamma irradiation facility using maize and apples revealed only small deviations from the shape of a normal distribution (straight line in the probability net of Figs 1 and 2). As the strategies in placing dosimeters was different between the research group and the operator of the commercial facility, also the resulting distributions differ in characteristics (mean value = fine vertical line; standard deviation = slope of straight line). Consequently, also the calculated one-sided limiting dose value would be different for both dosimeter placing strategies. For the final conclusions and comparisons the data from the operator of the facility were omitted. Upon all, at this commercial facility using palettes of 2.16 m^3 volume the expected positions of minimum dose are not accessible for dosimeter placement.

In another experiment with 10-MeV electrons wheat and maize were used as substrate. Layer thickness in direction of the electron beam was 5.5 cm (corresponding to practical range of the electrons at a bulk density of 0.8 g/cm^3). The grain was filled in cardboard boxes thus simulating plug flow of the bulk material through the irradiation zone. The dose distributions for both set-ups were nearly identical (Fig. 3). Due to the known depth dose distribution of electrons and the single-sided irradiation the minimum dose would only occur underneath the cardboard boxes thus being accessible for the placement of dose indicators.

In order to achieve better homogeneity while using electron irradiation, in many applications the goods are turned between passes through the irradiation zone and the treatment is double-sided. Potatoes were used as an example (Fig. 4). Even though both the treatments, single- and double-sided, were adjusted for equal minimum dose, the mean values and standard deviations differed significantly. Double-sided irradiation allows for a narrower range (width) of the dose distribution; the position where the minimum dose is to be expected is not easily determined, in many instances it will be in the middle of the goods thus not being accessible for dosimetry.

A further experiment employed the double-sided electron irradiation of pistachio nuts in commercial size paperboard boxes holding 48 pouches of 125 g each. The resulting dose distribution (Fig. 5) is also very close to the normal distribution. A dose pattern study - reported elsewhere [6] - revealed that maximum and minimum dose values occurred inside the box; a minimum value was never observed at the surface of the boxes.

As explained above, target dose values in this study were chosen according to useable dose range of the utilized dosimetry system. These values can be easily converted to the dose range necessary in insect disinfestation. In practical application this is done by adjusting the exposure time. For a common dose value (for example, the proposed generic minimum dose of 300 Gy for the elimination of any species of fruit fly), the corresponding dose value at a specific reference position can be calculated applying appropriate safety margins and statistical probabilities. For such a single common target dose the result is a specific value of the reference dose for any occurring source-product geometry (Table I). Of course, also the confidence margin for the decision function of a given label dosimeter including its readout-system must be considered while setting this dose limit. Finally, this approach results in the requirement for a graded set of dose levels for such labels which is not yet commercially available; for example, for the reported experiments (cf Table I) at 420, 430, 490, and 940 Gy.

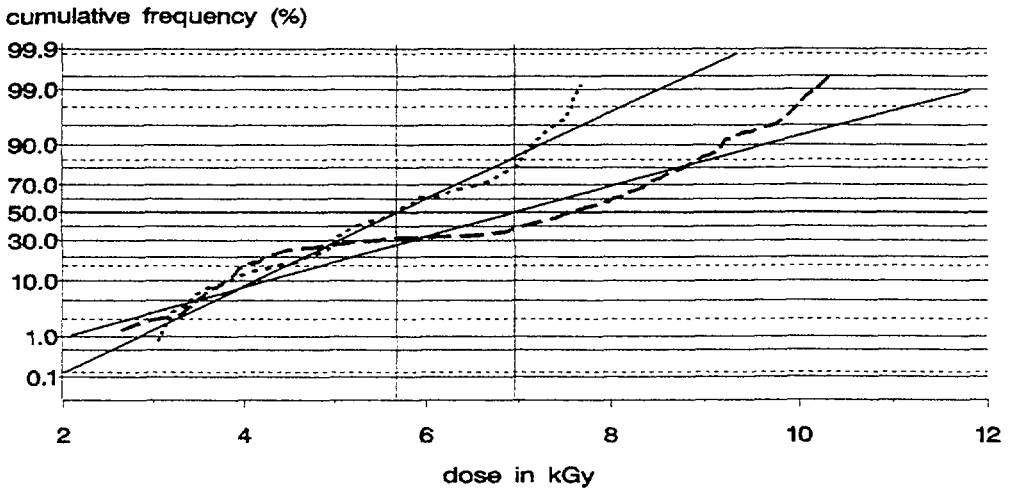

FIG. 1. Gamma-processing of maize: frequency distribution of dose determined by FRCN (dotted line) and contract irradiator (dashed line); fine vertical lines: respective mean values

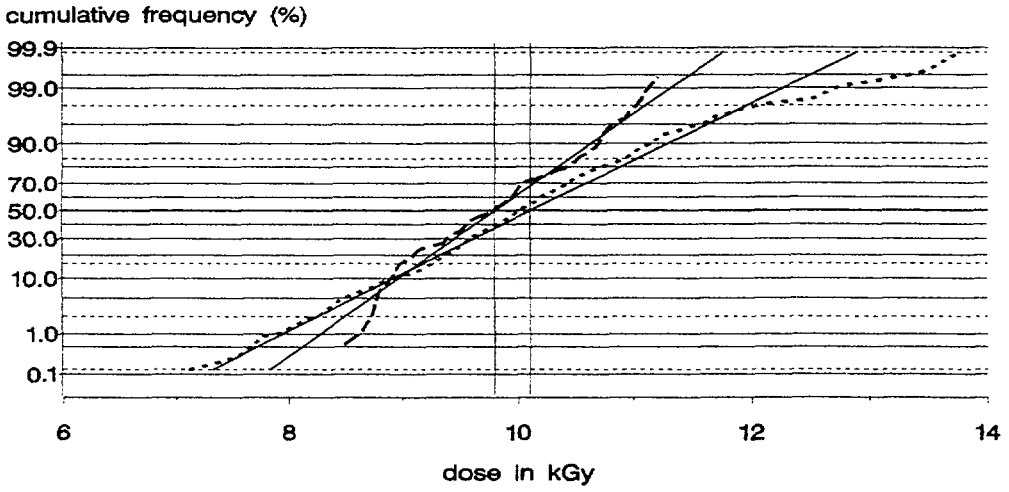

FIG. 2. Gamma-processing of apples: frequency distribution of dose determined by FRCN (dotted line) and contract irradiator (dashed line); fine vertical lines: respective mean values

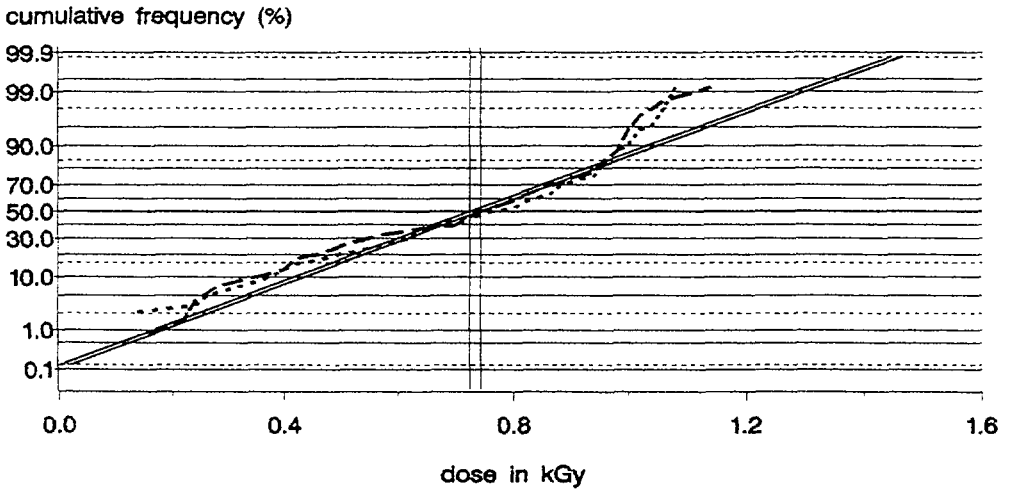

FIG. 3. Electron-processing of wheat (dashed line) and maize (dotted line): 10 MeV electrons, single-sided irradiation; fine vertical lines: respective mean values

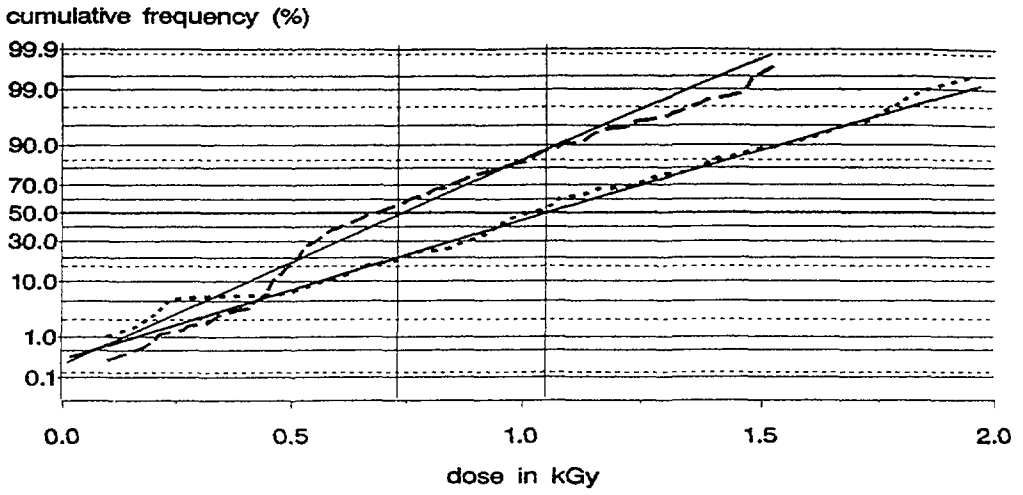

FIG. 4. Electron-processing of potatoes: 10 MeV electrons, single-sided (dotted line) and double-sided (dashed line) irradiation; fine vertical lines: respective mean values

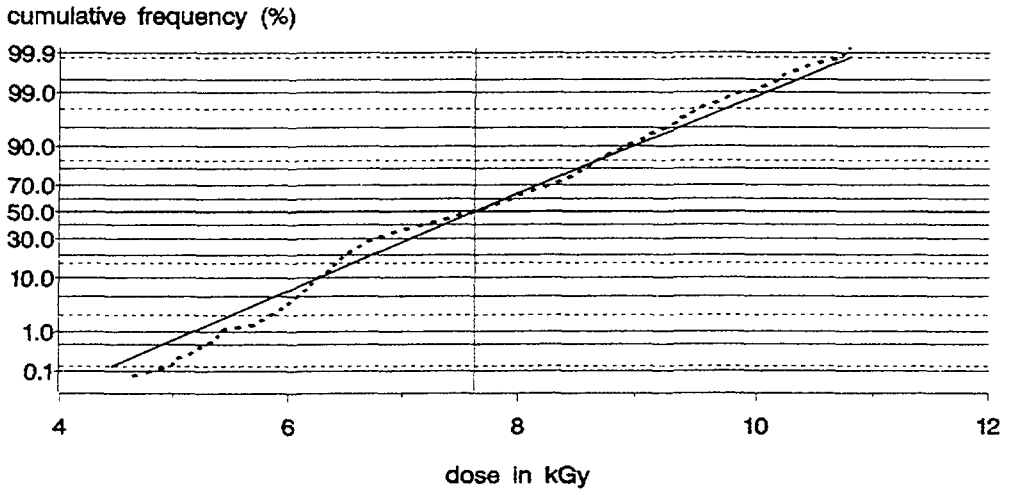

FIG. 5. Electron-processing of pistachio: 10 MeV electrons, double-sided; fine vertical line: mean value (experiment with 23 repetitions and 1400 individual dosimeter readings)

Especially in the light of the statistical approach taken above, the value of such devices - if available at suitable dose threshold values - remains disputable, even after they have been proven to be real dosimeters: securing a specific dose value at an easily accessible position outside a consignment not necessarily ensures that a minimum dose throughout the product load has been met even at positions not accessible for verification. To ensure that, other measures are indispensable.

TABLE I. RELATIONSHIP BETWEEN SOURCE-PRODUCT GEOMETRY AND THE DOSE VALUE REQUIRED AT THE REFERENCE POSITION WHERE THE LABEL RESIDES FOR A GENERIC MINIMUM DOSE OF 300 GY AND 99.5 %-CONFIDENCE LEVEL (ONE-TAILED, TOLERANCE FACTOR=2.6)

Geometry	Mean dose (Gy)	Std. Dev.	Required reference dose (Gy)
apples on crate [x]	363	24.2	416 [1]
grains on pallets [x] (gamma)	680	146	938 [1]
pistachio in bags/boxes			
(electrons [e])	489	68.1	430 [2]
(X-rays [b,x])	497	75.8	489 [2]

notes: [1] reference = maximum, position accessible;
[2] reference ≠ maximum, position not accessible
[x] observed minimum was larger than corresponding tolerance limit, data adjusted to assure tolerance limit
[e] 10 MeV electrons, double-sided;
[b] 5 MeV bremsstrahlung, one-sided

REFERENCES

[1] LEWIS, D.F., LISTL, C.A. (1992) Radiation Dose Indicator, US Patent No. 5084623

[2] EHLERMANN, D.A.E. (1997) Validation of a Label Dosimeter for Food Irradiation Applications by Subjective and Objective Means, Appl. Radiat. Isot. **48**, 1197-1201

[3] RAZEM, D. (1997) Dosimetric Performance of and Environmental Effects on STERIN Irradiation Indicator Labels, Radiat. Phys. Chem. **49**, 491-495

[4] EHLERMANN, D.A.E., BAUER, B. A Simple Reader for Dose Indicators in Quarantine and Other Applications, These Procedings, paper no: IAEA-SM-356/39

[5] K. CHADWICK, D.A.E. EHLERMANN, W.L. McLAUGHLIN, Manual of Food Irradiation Dosimetry, Techn. Report Series No. 178, IAEA, Vienna, 1977

[6] EHLERMANN, D.A.E. (to be published) Process control and dosimetry applied to establish a relation between reference dose measurements and actual dose distribution, in: Final report of FAO/IAEA Co-ordinated Research Programme on 'Standardized Methods to Verify Absorbed Dose of Irradiated Fresh and Dried Fruits and Tree Nuts in Trade'

DOSE ESTIMATION IN THIN PLASTIC TUBINGS AND WIRES IRRADIATED BY ELECTRON BEAM

A. DODBIBA
Institute of Nuclear Physics,
Tirana, Albania

Abstract

High energy ionising radiation can be used to beneficially change the properties of plastic materials used in the manufacture of coated wires, cables and extruded tubings. For realisation of this process it is preferable to use electron accelerators as radiation sources. In the present study a scanned 2-MeV electron beam was used to irradiate the simulated objects and the real products. The determination of absorbed dose distribution in the irradiated objects was performed by using the thin polyethylene film equivalent to the insulating material. Equations of dose evaluations for "figure eight" irradiation technique for the real products (thin wires and tubes) are given.

1. INTRODUCTION

For irradiation of long products like wires, cables and tubes it is suitable to use an electron accelerator as a radiation source. It allows to organise a continuous irradiation process by way of transportation of long cylindrical products (wires or tubes) through the zone of the scanned electron beam extracted into atmosphere.

During the irradiation process the main objectives are :

- To prevent the waste of electron beam power.
- To provide the distribution of the absorbed dose in the plastic material as uniform as possible.

The realisation of the two above-mentioned objectives mostly depend on the chosen irradiation technique. An efficient way to irradiate a tubular product is a multiple pass system (handling system) using a sets of sheaves or drums. This system allows the product to make a number of passes through the electron beam zone, with a turn (two opposite sides irradiation) to optimise the dose uniformity and the efficiency of electron beam utilisation.

A variant of above - mentioned irradiation technique, which is used in the present work for irradiation of thin wires and tubes, is a "figure eight" technique [1-4].

2. METHODS AND RESULTS

2.1. The distribution of electron beam along the scanning direction

All parts of the product, irradiated using the "figure eight" technique, will pass through the identical irradiation zone of scanned electron beam. It means that the product will absorb the same average dose.

Multiple successive passing of the product under the scanner allows to accumulate the required absorbed dose in separate cycles. It is also known that the dose absorbed (D) is in direct proportion to the electron beam current I and in inverse proportion to the product running speed V ($D \sim I/V$). As V is constant, for evaluation of the absorbed dose it is necessary to measure the electron beam energy deposited in the product for each of its pass through the irradiation zone. More precisely, it is necessary to know the electron beam distribution along the scanning direction.

Firstly, a qualitative estimation of this distribution was made. An aluminium collector with dimensions 10 × 5 ×250 mm was moved along the scanning direction Z (Fig. 1). The distance between the collector and scanner was 35 mm.

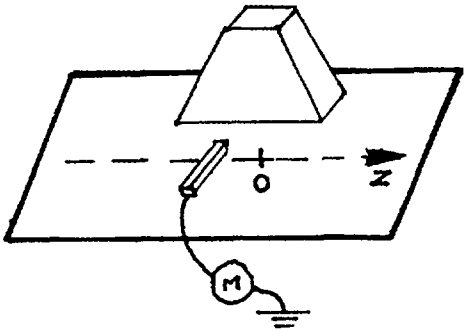

FIG. 1. The position of the collector under the scanner

The electron current I_K in the collector, as it passes along the scanner, was measured by the microamperemeter M. It is observed that the I_K had two maxima, at Z = −135 mm and Z = 145 mm, and a minimum at Z = −3 mm. Outside the zone -135≤ Z ≤ 145 mm, the electron beam current I_K decreased very rapidly.

The zone −135 mm ≤ Z ≤ 145 mm was considered as the optimal irradiation field (OIF). For the quantitative estimation of the electron beam along the scanning direction, the electrical scheme given in Fig. 2 was used.

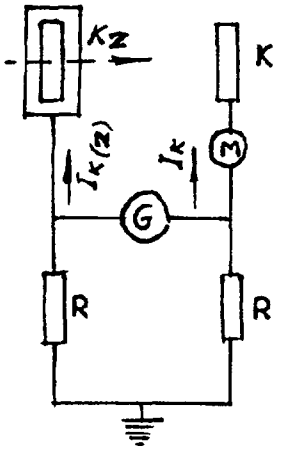

FIG. 2. Electrical scheme for measuring the electron beam distribution along the scanning direction

The aluminium collector K is placed in a fixed position (Z=80 mm) at a distance of 20 mm under the scanner. K and M are respectively the collector and the microampermeter shown in Fig. 1. A hollow collector K_z, placed at a distance 35 mm under the scanner, moves forward and backward (see the arrows in Fig. 2) along the OIF. It is a combination of an aluminium slab (with gap dimensions 10 × 250 mm) with a Faraday cup, isolated from each other. The wall thickness of the Faraday cup and slab are thicker than the maximal range of the electrons with energy 1.81 MeV(electron energy used in

this work). G is a galvanometer (5.3×10^{-3} μA/division) with internal resistance 280 Ω. R are ohmic resistances with value of 1500 Ω.

For each pass of the collector K_z along the OIF the indications N (Nmin and Nmax) of the galvanometer G in different zones of OIF were measured. The accelerator parameters were kept constant during these measurements.

The ratio $I_K(z)/I_K$, based on [5], can be calculated by Eq. (1):

$$\frac{I_K(z)}{I_K} = 1 + 0.0116\frac{N}{I_K} \quad (1)$$

where: $I_K(z)$: is the electron beam current in the collector K_z, and
I_K : is the electron beam current in the collector K.

Taking into account Eq. (1), the OIF was separated in five zones, in such a way that the uniformity of electron beam current $I_K(z)$ in each zone , calculated as the ratio $[I_K(z)]min / [I_K(z)]max$ to be ≥ 90 %. These zones are:

Zone 1	-50mm ≤ z ≤ 50 mm
Zone 2	50mm ≤ z ≤ 110 mm
Zone 3	110mm ≤ z ≤ 145 mm
Zone 4	-90mm ≤ z ≤ -50 mm
Zone 5	-135mm ≤ z ≤ -90 mm

The data for the nine passes of the collector K_z along the OIF are given in Table I.

TABLE I. THE RATIO $[I_K(z)]min / Imin$ and $[I_K(z)]max / Imin$ FOR EACH ZONE "i" (i=1-5) [a]

Number	Zone 1		Zone 2		Zone 3		Zone 4		Zone 5	
of passes	A/C	B/C	A/C	B/C	A/C	B/C	A/C	B/C	A/C	B/C
1	1.00	1.10	1.01	1.05	1.04	1.09	1.11	1.17	1.17	1.27
2	1.00	1.11	1.01	1.05	1.05	1.11	1.11	1.17	1.17	1.27
3	1.00	1.11	1.01	1.09	1.09	1.13	1.10	1.17	1.17	1.27
4	1.00	1.12	1.00	1.07	1.07	1.10	1.12	1.17	1.17	1.28
5	1.00	1.12	1.01	1.09	1.09	1.14	1.12	1.17	1.18	1.28
6	1.00	1.09	1.03	1.07	1.06	1.13	1.08	1.16	1.17	1.27
7	1.00	1.14	1.03	1.07	1.08	1.13	1.14	1.18	1.18	1.27
8	1.00	1.12	1.02	1.11	1.10	1.15	1.12	1.20	1.21	1.30
9	1.00	1.11	1.02	1.09	1.10	1.15	1.10	1.19	1.19	1.30
Average	1.00	1.11 ± 0.02	1.02 ± 0.01	1.08 ± 0.02	1.08 ± 0.02	1.13 ± 0.02	1.11 ± 0.02	1.18 ± 0.01	1.18 ± 0.01	1.28 ± 0.01

[a] The letters A and B represent respectively: the minimal and the maximal value of electron beam current $I_K(z)$ for each zone "i", while C represents the minimal value of $I_K(z)$ for each pass of the hollow collector along the OIF.

2.2 Dosimetry of irradiation

Before irradiation of the real product (thin wire and tube), the distribution of the absorbed dose in the simulated objects for two-sided irradiation was measured. A thin polyethylene dosimeter film is used for simulation of tube and wire[6]. The dosimeters consist of strips 0.221 mm thick and 25 mm wide.

The irradiation geometry of the simulated objects is given in Fig. 3. The simulated objects (1), are placed under the scanner (3) on the wood holder(4), along the OIF. The collectors (2) are aluminium parallelepipeds with dimensions 5×5×250 mm. They are fixed at the extremities of the OIF. The wood holder and the simulated objects are on the moving table. All they, during the irradiation move with a constant speed, forward and backward, perpendicular to the scanning direction(see the arrows in Fig. 3).

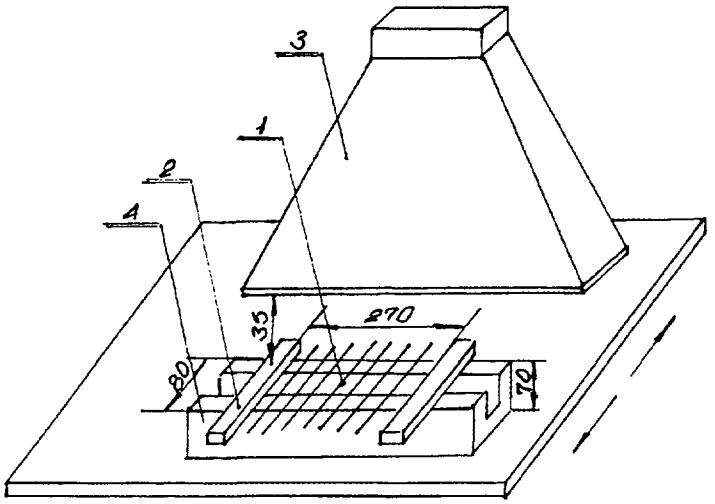

FIG. 3 Irradiation geometry of simulated objects (dimensions in mm)

The irradiation parameters for the simulated objects, tube (insulation wall thickness w =1.5 mm, outer diameter OD = 6mm) and wire (w = 0.9 mm and OD = 4.6 mm) are given in Table II. T, Io, Vo, N given in Table II are : electron energy, electron beam current in collectors, moving speed of the simulated objects, and the number of their passes under the scanner.

TABLE II. IRRADIATION PARAMETERS OF THE SIMULATED OBJECTS

Simulated objects	T (MeV)	Io (μA/cm)	Vo(cm/s)	N
Tube	1.81± 0.02	6.36 ± 0.04	0.721± 0.01	14
Wire	1.81± 0.02	4.35 ± 0.04	0.635 ± 0.01	18

After irradiation the film was unwrapped and the change of the optical density trace ΔOD at 250 nm wavelength was measured along the centre of the film. By using the calibration curve shown in [5] it was possible to calculate the distribution of the absorbed dose. The data for average absorbed dose (minimal and maximal), $D_i$min and $D_i$max in each zone "i", are given in Table III.

TABLE III. THE VALUES (MINIMAL AND MAXIMAL) OF DOSE ABSORBED IN THE SIMULATED OBJECTS FOR EACH ZONE OF THE OIF

Simulated object	Absorbed dose(kGy)	Zone 1	Zone 2	Zone 3	Zone 4	Zone 5
Tube	Dimin.	185	196	202	213	223
	Dimax.	235	248	256	264	283
Wire	Dimin.	139	143	146	157	169
	Dimax.	252	255	258	281	313

The distributions of absorbed dose in the simulated objects for the zone 1 are given in Fig. 4.

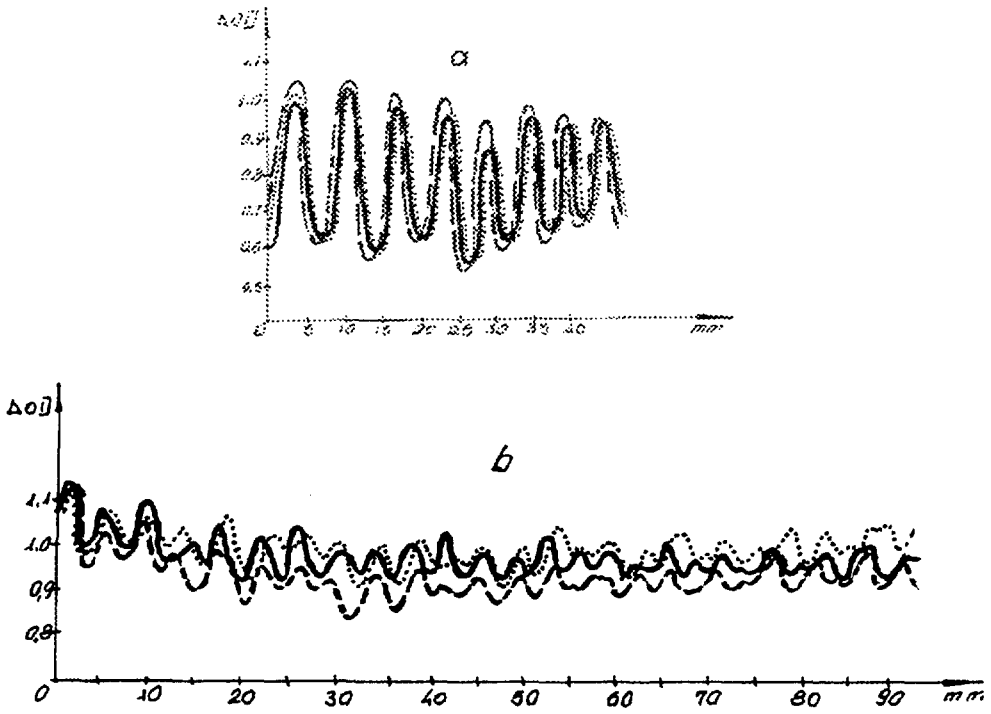

FIG. 4. Dose distributions for the two simulated objects(a-wire, b-tube) in the first zone of OIF.

2.2.1. *Product handling system*

The evaluation of the absorbed dose in the real product is related with the type of the product handling system used. For irradiation of the real products (wire and tube) the "figure eight" irradiation technique was chosen. The design of the product handling system, which can provide the realisation of the above-mentioned technique is given in Fig. 5.

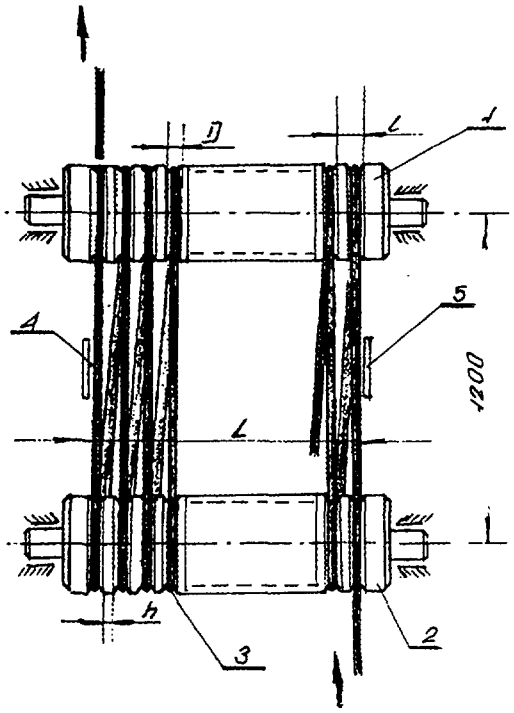

FIG. 5. The design of the product handling system .

If the number of the circular canals (3 in Fig. 5) along the OIF (L) is n_1, then:

$$L = n_1 D + (n_1 - 1) h \quad \text{or} \quad n_1 = (L+h) / (D+h), \text{ and} \tag{2}$$

$$n = 2 n_1 - 1 \tag{3}$$

where, D : is the diameter of the circular canal on the drum (1and 2 in Fig. 5)
h : is the distance between two successive canals, and
n : is the number of passes, along the OIF, of the real product.

For measuring of the electron beam current, two collectors (5 in Fig.5) (which are the collectors shown in Fig. 3) are put at the extremities of the OIF. This technique has some limitations that were taken into consideration during the irradiation of the real product. The main limitations are :

-the outer diameter of the product may not exceed the half of the centre-line spacing *l* of the circular canals on the drum.

-The accelerator voltage must be equal or higher than the critical value Vc [4].

$$V(kV) = 197 p \sqrt{w(OD - w)} + 325 \tag{4}$$

p is the specific gravity of isolated material; w and OD are given in millimetres.

- The relations between duration of the irradiation cycles and interval between them ought to be chosen (by varying the parameters of the handling system) so that the insulation has time to cool.

2.2.2 *Evaluation of dose absorbed from the real product*

The variation of the dose (minimal and maximal) in the first zone (Fig. 4) indicate that the differences between them(for the two simulated objects) are smaller than 10% . The same situation is also valid for the other zones [7-8]. In consequence of that, the data given in Table III where chosen as the representative of the absorbed dose (minimal or maximal) from the simulated products in each zone. Two methods were used for the evaluation of the average dose (minimal or maximal) for the real product.

a) First method

The dose is evaluated as the sum of the average doses (minimal or maximal) absorbed from the real product in each zone "i". If the parameters during the irradiation of the simulated object and the real product are respectively: T, Io, Vo, N (Table II) and T, I, V, n_i then:

$$D\min = \frac{I}{I_o}\frac{V_o}{V}\sum_{i=1}^{5}\frac{D_i \min}{N} n_i \tag{5}$$

$$D\max = \frac{I}{I_o}\frac{V_o}{V}\sum_{i=1}^{5}\frac{D_i \max}{N} n_i \tag{6}$$

where, V, I, n_i and D_i min, D_i max are, respectively, the moving speed of the real product, electron beam current in the collectors, number of passes of the real product in each zone "i" and the average dose (minimal and maximal) absorbed in each zone "i" for the simulated object during N passes under the scanner.

b) Second method

Dose is evaluated based on the average (minimal or maximal) dose absorbed by the simulated object in the first zone and the fact that the dose is in direct proportion to the electron beam current. The distribution of electron beam current along the scanning direction (Table I) indicate that the difference between the extremal values in each zone "i" is smaller than 10%. Therefore, the average values I_i (i=1-5) of this distribution were chosen as the representative values for each zone "i". As the absorbed dose is in direct proportion to the electron beam current, the dose absorbed for the real product is :

$$D\min = \frac{I}{I_0}\frac{V_0}{V}\frac{D_1\min}{N}\sum_{i=1}^{5}\partial_i n_i \tag{7}$$

$$D\max = \frac{I}{I_0}\frac{V_0}{V}\frac{D_1\max}{N}\sum_{i=1}^{5}\partial_i n_i \tag{8}$$

where, parameters I, I_o, V, V_o, n_1, N are those given in Eqs (5) and (6). D_1min and D_1max are minimal and maximal dose absorbed by the simulated object, in the first zone, during N passes under the scanner. The coefficient ∂_i is the ratio I_i / I_1, where I_1 is the average value of the electron beam distribution in the first zone. The values of coefficient ∂_i for each zone "i" are respectively: 1, 1.028, 1.072, 1.106 and 1.193. For irradiation of the real product (wire and tube) the handling system used (Fig. 5) has the dimensions : l=12 mm, D=6 mm and h=6mm.

Using Eqs (2) and (3), the number of passes of the real product in each zone "i", beginning from the first zone, are: 16, 10, 5, 6 and 8.

Eqs (5) and (7) or (6) and (8) can be rewritten as Eqs (9) and (10):

$$\frac{(D\min)_I}{(D\min)_{II}} = \frac{\sum_{i=1}^{5} n_i D_i\min}{D_1\min\sum_{i=1}^{5} n_i\partial_i} \tag{9}$$

$$\frac{(D\max)_I}{(D\max)_{II}} = \frac{\sum_{i=1}^{5} n_i D_i\max}{D_1\max\sum_{i=1}^{5} n_i\partial_i} \tag{10}$$

The numbers I and II in Eqs (9) and (10) refer to the first and the second method of dose evaluation. After substitution of the quantities given in Eqs (9) and (10) with their respective values, the ratio of the doses estimated by the two methods was 98%.

Two simulations were made directly on the wire before irradiating it using the polyethylene film dosimeter. The irradiation parameters were: T=1.81 MeV, I=6.66μA/cm and V=1.64cm/s. The minimal (230 kGy and 218 kGy) and the maximal dose value (≈ 390 kGy) were determined by measuring the change of the optical density of the irradiated film dosimeters. The corresponding values estimated from Eqs (5) and (6) or (7) and (8) were Dmin=220 kGy and Dmax= 397 kGy. It means that there is a very good agreement between the dose values estimated by "theoretical" equations and those determined "experimentally". The maximal difference between them was about 5%.

3. CONCLUSIONS

The primary conclusions drawn from this work are:

- Based on the measurements and calculations, the two methods for dose evaluations and their respective equations are given,
- there is a very good agreement between the two methods of dose evaluation. The ratio is 98%, but for practical use the second method is more appropriate. In this case, it is necessary to know the dose distribution only in the first zone,
- the dose values (minimal and maximal) measured directly on the irradiated wire agreed well with those evaluated theoretically. The maximal difference was 5%. It means that the selected method for the dose evaluation is the proper one.

REFERENCES

[1] FINKEL, E.E, et al., Radiation processing in electroinsulating and cable engineering state and prospects, J. of Industr. Irradiation Tech., 2(2),155-187,1984.

[2] SIMONIS, P.J.C.A., The use of electron irradiation to crosslink cable and wire insulations, High Voltage Engineering (Europa) N.V., 1972.

[3] SVENDSEN, E.B., Plant design and beam utilisation, Radiation Physics Chemistry, Vol.22,No.1/2,pp.41-54,1983.

[4] BLY, J.H., Choosing an accelerator for the irradiation of wire and cable, Radiation Physics Chemistry, Vol.9,pp. 596-611,1977.

[5] DODBIBA, A., Dosimetry and electron irradiation technique of polyethylene tubes and sheets, Thesis, INP,1983.

[6] DODBIBA, A., Research on polyethylene film dosimeter, Bulletin of INP, No.2, 1985.

[7] DODBIBA, A., HOXHAJ, E., Technical Report, INP, 1988

[8] DODBIBA, A., HOXHAJ, E., Technical Report, INP, 1989.

BIBLIOGRAPHY

CHEEK, C.H., LINNENBON, V.J., Calculation of absorbed dose , NLR Report 5448, U.S. Nav. Res.Lab. Washington, February 24, 1960.

HARRIS, K.K., PRICE,W.E., A thin plastic dosimeter, International Journal of applied radiation and isotopes, Vol.II, No. 2/3, 1961.

MILLER, A., et al., Absorbed dose distribution in small copper wire insulation due to multi-sided irradiations by 0.4 MeV electrons, Radiation Physics Chemistry, Vol.13, pp.181-186, 1979.

MILLER, A., McLAUGHLIN, W.L., Absorbed dose distributions in irradiated plastic tubing and wire insulation, Radiation Physics Chemistry, Vol.14, pp. 523-533, 1979.

MILLER, A., PEDERSON, B.W., Dose distribution in electron irradiated plastic tubing , Radiation Physics Chemistry, Vol.18, No.5-6, pp. 967-973, 1981.

CALIBRATION AND TRACEABILITY

(Session 7)

Chairperson

R.D. CHU
Canada

Invited Paper

CALIBRATION AND TRACEABILITY IN HIGH DOSE DOSIMETRY

P.H.G. SHARPE
Centre for Ionising Radiation Metrology,
National Physical Laboratory,
Teddington, United Kingdom

Abstract

Accurate dose measurements, traceable to recognized national standards, are an essential component of industrial irradiation processing. Applications such as the sterilization of medical devices and the irradiation of foodstuffs are both highly regulated and international in nature. In order to ensure both the safety of the process, and to facilitate international trade, it is essential that a widely accepted system of calibration and traceability is in place. Mutual equivalence and recognition of high dose dosimetry standards are achieved both by experimental intercomparisons, and by the adoption of standard procedures and methods, including formal accreditation of calibration laboratories by independent third parties. Dose measurements in industrial irradiation plants pose particular difficulties because the behaviour of many dosimetry systems is influenced by the environmental conditions in the plant. In particular, it is not possible to accurately mimic in a calibration laboratory the variable dose rates and temperatures characteristic of industrial plants. Calibration protocols have to be carefully designed to avoid the introduction of significant systematic errors. In this paper, the current status of industrial dosimetry standards and calibration methods are reviewed. Potential sources of error and uncertainty will be discussed, and estimates made of the accuracy achievable in industrial dosimetry.

1. INTRODUCTION - NATIONAL AND INTERNATIONAL MEASUREMENT SYSTEMS

Coordination of measurements at an international level is undertaken under the framework of an international treaty, known as the "Convention of the Metre". This treaty dates from 1875 and currently has 48 countries as signatories. The treaty establishes a number of bodies which are charged with various functions relating to the establishment and maintenance of a unified international system of measurement. Figure 1 shows the principal bodies established under the Treaty, the most important of which, from a practical point of view, are the International Committee for Weights and Measures (CIPM) and its associated laboratory the International Bureau of Weights and Measures (BIPM), located in Paris.

An important role of the BIPM is to act as a focal point for the intercomparison of standards held by individual countries, known as *national standards*. Ideally, each member state will possess only one designated *national standard* for each quantity of interest, and a system of calibrations will exist within that country to ensure that all measurements can be related to the *national standard* through an unbroken chain. Such a chain is known as a *traceability chain* and is discussed in more detail below. The relationships between BIPM, *national standards laboratories* and the "end users" of a measurement are shown schematically in Fig. 2. In some instances BIPM holds physical standards with which individual *national laboratories* can compare, and in other instances BIPM acts as a coordinator of comparisons between one or more *national laboratories*. The "end users" of measurements within a country will either derive their calibrations direct from the *national standards laboratory* or from a *secondary calibration laboratory*. A significant development in recent years has been the development of formal third party accreditation schemes to ensure the competence of the *secondary calibration laboratories*. Increasingly, regulatory bodies demand documented *traceability* to *national standards*

and this requirement is often most easily satisfied by obtaining calibrations from a laboratory having formal accreditation.

In this paper, the specific aspects of traceability and calibration applicable to high dose dosimetry will be discussed. Significant sources of uncertainty will be considered and estimates made of the accuracy achievable.

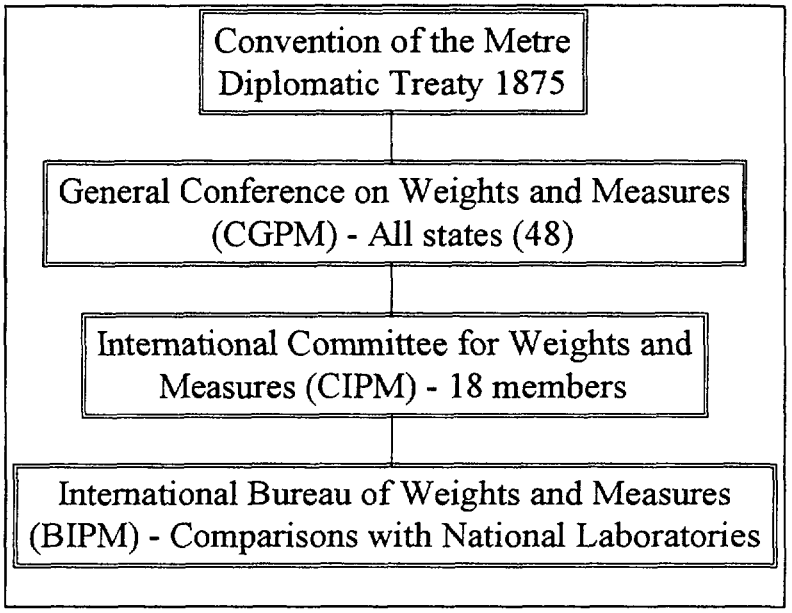

FIG. 1. Structure of bodies set up under the Convention of the Metre.

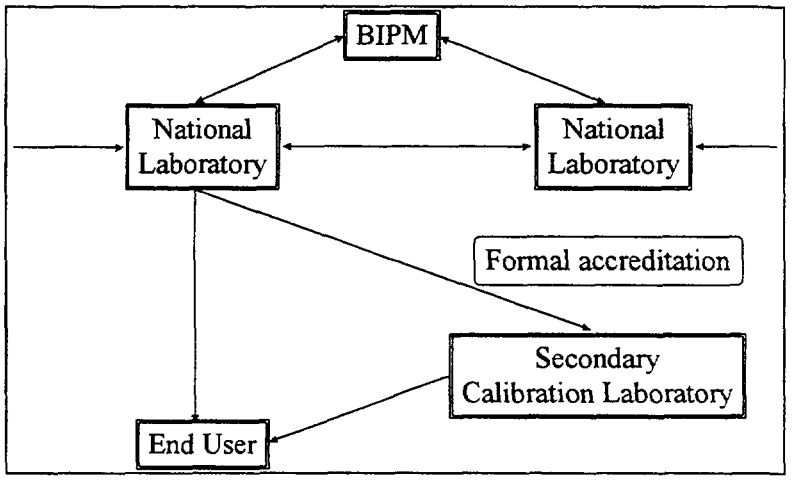

FIG. 2. Relationships between bodies within the International Measurement System

2. NATIONAL TRACEABILITY CHAINS

It is useful to classify dosimeters into a hierarchy according to their intrinsic accuracy. Such a classification is shown in Fig.3 and includes dosimeters classified as *primary*, *reference* and *routine*. The figure also represents a *traceability chain* in that it outlines how *primary standard* dosimeters are used to calibrate *reference standard* dosimeters, which in turn are used to calibrate the *routine* dosimeters, used for day-to-day measurement. Each class of dosimeter is described in more detail below.

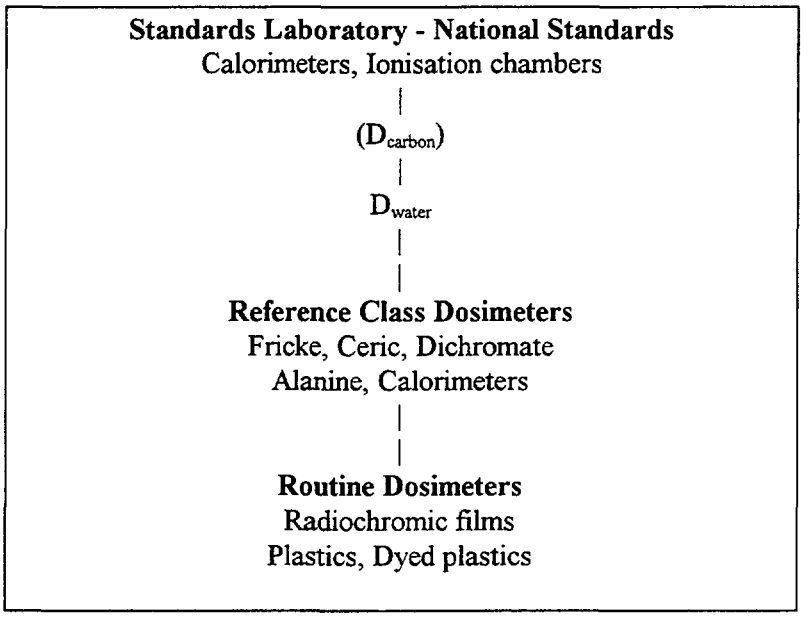

FIG. 3. A typical national traceability chain for high dose dosimetry.

A *primary standard* dosimeter is one which enables an absolute measurement of absorbed dose to be made with reference only to the SI base units (mass, length, time, electric current etc) and fundamental physical constants. This type of dosimeter is generally operated by *national standards laboratories* and is used to provide the basic standard for use in a particular country. There are two main types of *primary standard* dosimeter, ionisation chambers and calorimeters. The quantity normally used in high dose dosimetry is *absorbed dose to water* (D_{water}), but many *primary standards* actually measure *absorbed dose to carbon* (D_{carbon}). This is shown for completeness in Fig. 3, but in this paper the term *dose* is taken to mean *absorbed dose to water*.

A *reference dosimeter* is defined as a dosimeter of high metrological quality that can be used as a reference standard to calibrate other dosimeters. To be of use it must satisfy well-established criteria. It must have a radiation signal that is accurately measurable, and this signal must have a well- defined functional relationship with absorbed dose. The effect of parameters, such as irradiation temperature, post-irradiation stability, etc must be well characterised and capable of expression in terms of simple correction factors. Examples of commonly used *reference dosimeters* include chemical dosimeters, such as the Fricke, ceric-cerous, dichromate and alanine dosimeters.

Several calibration laboratories operate mailed dosimetry services in which dosimeters are shipped from the calibration laboratory to the industrial facility for irradiation and subsequently returned to the calibration laboratory for readout and certification of the dose received. These services are essential in enabling traceable calibrations of routine dosimeters, as described below. The dosimeters used in such services are known as *transfer dosimeters* and, in terms of the hierarchy in

Fig.3, are usually *reference class dosimeters*. However, under certain well defined conditions, it may also be possible to use *routine class dosimeters* as *transfer dosimeters*.

A *routine dosimeter* is a dosimeter whose performance is not as good as that of a *reference dosimeter*, but whose cost and ease of use make it suitable for day-to-day measurements in a radiation processing facility. The effects of factors such as irradiation temperature and dose rate on a *routine dosimeter* tend to be complex, and it is often not possible to apply straightforward correction factors. This means the calibration of a *routine dosimeter* is often specific to a particular environment (see below). Examples of commonly used routine dosimeters are systems based on polymethylmethacrylate (both dyed and un-dyed), cellulose tri-acetate and thin radiochromic films.

Examples of actual *traceability chains* for high dose dosimetry of Co-60 and high energy electron beams are given in Figs 4 and 5. In both cases the starting point is a *primary standard* graphite calorimeter, whose response has been compared with that of the standards maintained at BIPM. This calorimeter operates at therapy level dose rates of the order of 1 Gy/min, and a transfer dosimeter of some type is, therefore, required to step up to the high dose (kilogray) dose region. In the case of ^{60}Co radiation, this transfer is carried out using Fricke dosimeters, and in the case of electron beams by using an intermediate calorimeter, which is capable of operating over a wide range of dose rates. The overall uncertainty at each stage is also shown in the Figures.

System	**Overall uncertainty in calibration (2σ)**
Primary Standard Graphite Microcalorimeter (1 Gy / min)	1.3%
Fricke Transfer Dosimeter	1.4%
High Dose Co-60 Irradiator (100 Gy / min)	1.8%
Reference Dosimeters (Alanine & Dichromate)	2.1%

FIG. 4. UK National Traceability Chain Cobalt-60 Absorbed Dose to Water

System	**Overall uncertainty in calibration (2σ)**
Primary Standard Graphite Microcalorimeter	0.6% (to graphite)
16 MeV	
High Dose Graphite Calorimeter	0.7% (to graphite)
10 MeV	
Water Phantom	2.3% (to water)

FIG. 5. UK National Traceability Chain Electron Beam Absorbed Dose to Water

3. CALIBRATION OF HIGH DOSE DOSIMETERS

One of the major problems associated with high dose dosimeter calibration is the effect that environmental factors such as temperature (both before and after irradiation), dose rate, humidity etc can have on the response of the dosimeter. In the case of the relatively "well behaved" *reference dosimeters*, it is necessary to state under what conditions a calibration was carried out in order that corrections can be made subsequently if the dosimeter is used to measure dose in different conditions. In the case of *routine dosimeters* it is necessary to calibrate the dosimeter under the conditions of final use, as post-calibration corrections are generally not possible. Before starting to calibrate a dosimeter it is necessary to have detailed knowledge of what environmental factors are likely to influence the particular system and to then devise a scheme which will allow any important factors to be taken into account.

For both *reference* and *routine* systems, it is generally necessary to generate a separate calibration for each identifiable "batch" of dosimeters. This is because small variations in component concentrations and production methods can alter both the response under reference conditions, and the effect of environmental factors.

Only a very few dosimeters exhibit a strict linear relationship between the readout signal and absorbed dose. This means that it is generally not possible to define a single *calibration factor* for a dosimeter, and a curved *calibration function* has to be used instead. The form of the function is somewhat arbitrary, and can be any mathematical expression that is capable of reproducing the observed response. In general, the best expression will be the simplest one that will adequately reproduce the observed response.

The curved nature of most dosimeter *calibration functions* has implications both for the dose range over which a system must be calibrated, and also for the number of discrete calibration dose points that must be used. A dosimeter must be calibrated over a dose range significantly wider than the dose range of subsequent use. A curved *calibration function* cannot be extrapolated outside the dose range over which it was derived; there is simply not the information available to do this. Polynomial based calibration functions, in particular, may exhibit totally unexpected behaviour outside the dose range of preparation. The number of discrete calibration dose points required will depend both on the dose range and also the degree of curvature of the calibration function. As a guide, at least five calibration dose points distributed arithmetically (i.e. spaced at a fixed dose apart) will generally be required for irradiations spanning less than one decade of dose. For irradiations spanning more than one decade of dose, at least five dose points will generally be required for each decade, and these should be distributed geometrically (i.e. spaced at fixed multiples of each other). There must always be more dose points than there are coefficients in the mathematical expression used to represent the observed response. It is also good practice to use several replicate dosimeters at each dose point, in order that a full statistical analysis can be carried out on the calibration data. In order not to bias the calibration line, the same number of replicates should be used at each dose point.

3.1. Calibration of reference dosimeters

The calibration of *reference dosimeters* is relatively straightforward in that the response of the dosimeter to environmental conditions is, by definition, well defined and corrections can therefore be applied to relate the response under one set of conditions to those under another. Nevertheless, such corrections are subject to uncertainty, and for the highest accuracy, the reference dosimetry system should be calibrated under conditions as close as possible to those of eventual use. The calibration process consists of measuring the response of the dosimetry system when irradiated to a series of known doses under well defined conditions. The conditions that need defining vary according to the properties of the dosimetry system, but are likely to include temperature, dose rate and radiation spectrum. Humidity during irradiation, and environmental storage conditions after irradiation, may also need to be either controlled, or monitored to ensure they are within acceptable limits.

3.2. Calibration of routine dosimeters

Because the response of *routine dosimeters* cannot, in general, be easily corrected for variations in environmental factors, the dosimeters must be calibrated in the same conditions as those of eventual use. There are two main ways of achieving this, both of which have advantages and disadvantages:

3.2.1. Calibration in the irradiation plant

The best method of ensuring all relevant environmental influence factors have been taken properly into account is to calibrate *routine dosimeters* in the plant in which they will be used. The usual method of achieving this is to irradiate the dosimeters to be calibrated alongside *reference dosimeters* supplied and measured by an accredited calibration laboratory. To ensure both types of dosimeter receive the same dose, it is good practice to irradiate in a specially designed *calibration phantom*, in which the dosimeters are surrounded by material having approximately the same radiation absorption properties and density as themselves. In the case of electron beam irradiation, this phantom also ensures that all dosimeters are irradiated at the same point on the depth dose curve. The calibration phantom needs to be large enough to ensure that dosimeters do not shield each other, but not so large that errors are introduced because of non-uniformity of the radiation field.

The response of the *reference dosimeters* used in the calibration will need to be corrected for irradiation temperature. In an industrial irradiation plant, the temperature is unlikely to be constant, and some means has to be devised to determine an *effective temperature* for the *reference dosimeters*. For electron beam irradiations this is fairly straightforward as the dose will be delivered in a short time compared to the rate of heat loss, and the *effective temperature* can be taken as the average temperature during irradiation. The situation in an industrial gamma ray plant is far more complex as the irradiation is delivered over a relatively long time, and the dosimeter has time to exchange heat with the surroundings. It is reasonable to expect that the highest temperatures will be experienced close to the source, where the dose rate is highest, and the *effective irradiation temperature* would, therefore, be expected to be somewhere between the average and maximum temperatures experienced. In situations where the temperature range is large enough for uncertainties in *effective temperature* to make a significant contribution to the overall uncertainty, consideration should be given to using more than one type of *reference dosimeter*. If the chosen systems have different irradiation temperature coefficients, for example alanine and dichromate, it is possible to factor out the effect of irradiation temperature by analysing the difference in apparent doses measured by the two systems.

The principal disadvantage of the *in-plant* calibration method is that it may be difficult to achieve the required range of doses in some designs of industrial gamma irradiators. This can sometimes be overcome by irradiating calibration dosimeters to only part of the full irradiation cycle, but care needs to be taken to ensure that such dosimeters experience the same environmental conditions as dosimeters completing the full cycle.

3.2.2. Irradiation at a calibration facility followed by in-plant verification

It is possible to calibrate *routine dosimeters* by performing a set of irradiations at a remote calibration facility, provided steps are taken to verify the applicability of the calibration to the plant in which the routine dosimeters will be used. Without this verification step, systematic errors in the calibration may go undetected, and it is not possible to apply any meaningful uncertainty estimates to the calibration.

Calibration verification can be carried out by comparing the doses measured by *routine* and *reference* dosimeters irradiated alongside each other in the irradiation plant. In contrast to the full range of doses required for the *in-plant* calibration described above, the calibration verification need only be carried out at a small number of dose points (usually 3) spread along the dose range of the *routine*

dosimeters. If both *reference* and *routine* dosimeters give the same dose, within the uncertainty of the systems involved, then the calibration of the *routine dosimeters* is verified and can be used without further correction. If the verification shows a difference between the two systems that is essentially constant over the dose range, then a correction factor can be applied to bring the readings of the *routine dosimeters* into agreement with the readings of the *reference dosimeters*. Differences between *reference* and *routine* dosimeters that vary significantly across the dose range indicate a major discrepancy between environmental conditions in the plant and those used for the calibration irradiation. In such situations it is generally not possible to correct the calibration line, and a full *in-plant* calibration is required.

The purpose of the *calibration verification* is to detect small errors arising from differences between the conditions of calibration and final use of *routine dosimeters*. In order to minimise the size of potential errors, the calibration irradiation should be carried out using conditions of dose rate and temperature as close as possible to those which will be experienced in the industrial plant. Estimates of irradiation temperature for both the calibration irradiation, and the subsequent verification can be made using the same philosophy as outlined above. It may also be possible to use two types of reference dosimeter with differing temperature coefficients to correct for irradiation temperature.

4. UNCERTAINTY OF HIGH DOSE MEASUREMENTS

In order to establish the accuracy of a dose measurement, it is necessary to first identify and then quantify all possible sources of uncertainty. This is most easily done by considering in turn each step in the calibration and use of a dosimeter, and assessing what uncertainties are likely to be associated with each stage. The uncertainty associated with a dose measurement can then be calculated by combining the individual components. An example of this is given in Fig. 4, where uncertainties for the calibration of alanine and dichromate *reference dosimeters* in a Co-60 beam are given as 2.1% (2σ). Uncertainties in *routine dosimetry* measurements are more difficult to assess, as they are influenced significantly by environmental factors. A detailed discussion of uncertainties is outside the scope of this paper, but some of the principle components of uncertainty that affect high dose measurements are listed below.

4.1. Uncertainties in the Preparation of a Calibration Function

Uncertainty in calibration doses - The certificates supplied by calibration laboratories in connection with their *reference dosimeters* or calibration irradiations will contain statements about uncertainties and the *traceability* to *national standards*. Consideration also has to be given to dose variation arising from the relative positioning of dosimeters during calibration irradiations.

Uncertainty due to fit of calibration function - The process of fitting a *calibration function* to measured data will be subject to uncertainty. Statistical software packages may provide this information, but a detailed analysis is complex for anything except a straight line. Approximations of this uncertainty can be obtained from the differences between the original data and the calculated values.

Uncertainty due to environmental influence factors - Environmental factors such as temperature, humidity and dose rate can influence the response of high dose dosimeters. Calibration procedures should be designed to correct as much as possible for these effects, but uncertainties will still remain. Typical examples are uncertainties arising from the difficulties in assessing *effective temperatures and dose rates* in ^{60}Co plants.

4.2. Uncertainties in the Use of Dosimeters

Uncertainty due to dosimeter-to-dosimeter scatter - This is the statistical scatter observed between replicate dosimeters irradiated to the same dose under the same conditions.

Uncertainty due to variation in plant environmental conditions - Environmental conditions in industrial plants are often not well controlled. Variations, for example from summer to winter, may cause additional uncertainties in dose measurements.

Uncertainty due to instability of dosimeter reading - The readings of many dosimeters change with time after irradiation. Variations in readout times will, therefore, introduce uncertainties in dose measurements.

Uncertainty due to instability of instrumentation - Instrumental instabilities will translate directly into uncertainties in dose measurement. The effect of variations in, for example, the wavelength settings of spectrophotometers needs to be assessed.

BIBLIOGRAPHY

ASTM STANDARD E1261, "Guide for Selection and Calibration of Dosimetry Systems for Radiation Processing", Annual Book of ASTM Standards, vol **12.02**, American Society for Testing and Materials, 100 Barr Harbor Drive, West Conshohocken, PA 19428, USA (1998).

ASTM STANDARD E1707, "Standard Guide for Estimating Uncertainties in Dosimetry for Radiation Processing.", Annual Book of ASTM Standards, vol **12.02**, American Society for Testing and Materials, 100 Barr Harbor Drive, West Conshohocken, PA 19428, USA (1998).

BUREAU INTERNATIONAL DES POIDS ET MESURES (BIPM), "The International System of Units (SI)", Pavillon de Breteuil, F-92312 Sèvres Cedex, France (1998)

HIGH-DOSE DOSIMETRY AT ANSTO: QUALITY ASSURANCE, CALIBRATION & TRACEABILITY

G.J. GANT
Physics Division,
Australian Nuclear Science & Technology Organisation,
Menai, Australia

Abstract

A overview of the techniques used by ANSTO's high-dose dosimetry laboratory is given, commencing with a description of the facilities operated and the nature of the services provided. The dosimetry systems used by ANSTO are detailed along with their applications. Techniques used for calibration of dosimeters and radiation sources are given, including traceability and measurement uncertainty considerations. Quality assurance aspects of the dosimetry service are discussed.

1. INTRODUCTION

The Radiation Technology Group at ANSTO is part of the Physics Division and provides services and advice in the areas of gamma irradiation and high-dose dosimetry.

The Group maintains and operates a number of irradiation facilities. The cobalt-60 used in the gamma irradiation facilities is produced in ANSTO's HIFAR research reactor. ANSTO's underwater facility consists of seven cobalt-60 sources configured in annular arrays with a range of activities and dose rates. The pond is approximately 5 m deep and is filled with de-ionised water. Water-tight stainless steel canisters with capacities of up to 30 litres are used in the processing of customer goods.

The main irradiation facility is GATRI – the Gamma Technology Research Irradiator – a research and small scale batch irradiator commissioned in 1969. The source is a cobalt-60 plaque source with a maximum capacity of 100 000 Ci. It is stored in a deionised water tank 5-m deep and is raised into a concrete shielded cell for irradiations.

Materials commonly irradiated at ANSTO include medical and other materials requiring processing for sterilisation or verification of sterilisation dose, items requiring decontamination and disinfestation for quarantine purposes, frozen bone and tissue samples for transplant surgery, monomers and polymers for modification of properties, virus samples, and Queensland fruit fly pupae used in the Sterile Insect Technique. The GATRI facility has been loaded with cobalt to provide the largest possible uniform radiation field, rather than for efficiency, so that we can provide the required doses as precisely as possible. We can offer irradiations at a range of dose rates and at frozen and elevated temperatures. During the past twelve months, client demand for target doses ranged from 10 Gy to 6000 kGy, at temperatures from -80 °C to 270 °C.

In order to provide a comprehensive irradiation service, Radiation Technology is licensed by Australia's Therapeutic Goods Administration (TGA) and the Australian Quarantine and Inspection Service (AQIS). Obtaining these licences meant implementing a Quality System complying with the ISO 9000 series of documents. In addition, the GATRI facility is required to comply with the National Health and Medical Research Council's (NH&MRC) Code of Practice for the Design and Safe Operation of Non-medical Irradiation Facilities. All radiation facilities are licensed by ANSTO's Safety Assessment Committee. An external regulatory

body, the Australian Radiation Protection and Nuclear Safety Agency (ARPANSA), is proposed to be formed in 1998 and will also licence these facilities.

Radiation Technology makes and sells reference and transfer standard dosimeters which are purchased by users and suppliers of commercial irradiation services in Australia and the Asia-Pacific region. A calibration service is also provided for dosimeters made by or purchased from other organisations.

2. DOSIMETRY SYSTEMS

ANSTO's dosimetry practices are based on the standards published by the American Society for Testing and Materials (ASTM). Dosimetry systems in use are Fricke, ceric-cerous sulfate, Harwell Red and Amber Perspex and alanine/EPR.

2.1. Fricke

The Fricke dosimeter is used as a transfer standard to calibrate ANSTO's Underwater Calibration Facility with reference to the Secondary Standard Dosimetry Laboratory; for dose-mapping and calibration checks of self-shielded laboratory irradiators, such as blood irradiators; and to monitor irradiations for the Sterile Insect Technique and other low dose applications.

The methods used for preparation, measurement and calculation of results are essentially as described in ASTM Standard E 1026 [1], except that the solution is not air saturated and is dispensed into 5 mL polyethylene ampoules as required. These ampoules are conditioned prior to their initial use by irradiating them to a dose of approximately 1 kGy, and are reused many times. To avoid pre- and post-irradiation effects, the ampoules are filled immediately before use and are measured within one hour. The dose response of each new batch of dosimeter solution is verified before use by irradiation to several dose levels in the known radiation field of the Underwater Calibration Facility.

2.2. Ceric-Cerous sulfate

The ceric-cerous dosimeter is used by ANSTO during product dose mapping studies for critical process parameter determination; during sterilisation dose determination for product qualification studies; and for routine process control where a high degree of accuracy is required. These dosimeters are sold on a supply and measurement basis to users and suppliers of commercial irradiation services in Australia and the Asia-Pacific region wishing to verify the response of their routine dosimetry systems or confirm the dose delivered to their products. The dosimeters are also used as a transfer standard during the in-plant calibration of the routine dosimetry system used by Australia's only commercial irradiation company.

The methods used for preparation, measurement and calculation of results are essentially as described in ASTM Standard E 1205 [1] using the potentiometric method except for the following. A low range dosimeter is prepared and calibrated over the range 1-12 kGy using concentrations of 3.75×10^{-3} mol·L^{-1} ceric sulfate and cerous sulfate, and a high range dosimeter is prepared and calibrated over the range 10-35 kGy using concentrations of 0.01 mol·L^{-1} ceric sulfate and cerous sulfate. Each batch of dosimeters is calibrated by irradiating five samples to each of at least six dose levels in the known radiation field of the Underwater Calibration Facility. Following calculation of the dose using the Matthew's equation, a plot is made using curve-fitting software to determine the relationship between calculated dose and delivered dose. All subsequent measurements using this batch are then corrected according to this mathematical relationship.

2.3. Harwell Perspex

Harwell Red 4034 and Amber 3042 dyed Perspex dosimeters are used during dose mapping studies for relative dose determinations and for routine process control for non-critical items. They are calibrated in the Underwater Calibration Facility as described in ASTM Standard E 1276 [1].

2.4. Alanine-EPR

ANSTO has recently acquired a Bruker EMS104 EPR analyser and is in the process of developing protocols for the use and calibration of alanine dosimeters using this instrument for inclusion in our Quality System. It is not yet ready for routine use, but it is anticipated that it will be used as a transfer and reference standard.

3. CALIBRATION

All dosimetry calibrations performed at ANSTO either for internal use or for external clients are carried out in the known radiation field of the Underwater Calibration Facility (UCF). Calibration of this radiation field is described in section 4.

The source consists of 12 cobalt-60 pencils in an annular arrangement, stored at the bottom of ANSTO's underwater facility. All items for irradiation are loaded into a water-tight stainless steel canister which is in series with a continuous stainless steel roller chain driven by an electric motor which lowers it reproducibly into the centre of the source. The dosimeters for calibration are mounted onto a turntable fitted with a polyethylene holder with locations for up to 12 dosimeters. The turntable is sited in a fixed position within the irradiation canister and the dosimeters are continuously rotated to ensure an even dose.

The facility is controlled by a computer which provides for independent confirmation of irradiation time, irradiation temperature and rotation of the turntable. Temperature is monitored using a thermocouple.

4. TRACEABILITY

At ANSTO, measurement traceability to the national standard is obtained by the following approach. The Australian Standard for Absorbed Dose, formerly held by ANSTO but now residing in Melbourne at the Australian Radiation Laboratories, consists basically of a cobalt gamma source whose dose rate at a fixed point is measured using a graphite calorimeter. This primary standard is then disseminated by the Secondary Standard Dosimetry Laboratory or SSDL which is in the process of being re-established at ANSTO. The SSDL ionisation chamber is calibrated against the primary standard and this chamber is then used to calibrate a collimated beam from a teletherapy gamma source. ANSTO's Fricke dosimeters are then irradiated in this calibrated beam to a range of doses so that the response of this solution is well characterised. This dosimeter solution is then used to determine the dose rate in a fixed geometry on the turntable in the Underwater Calibration Facility in the pond. Routine and transfer standard dosimeters are then calibrated as required in the UCF, with the dose rate calculated according to the decay of the cobalt-60 source. Doses are routinely expressed in terms of the dose absorbed in water.

This process has a shortcoming that I suspect is common to other calibration labs around the world. That is, the calibrated collimated beams used in primary and secondary standard labs have very low dose rates because they are usually teletherapy units. Obviously, the dosimeters used in the traceability irradiations are selected because their response is as affected as little as possible by dose rate, but if it takes 12 or 24 hours to achieve a dose in the SSDL

that will take a couple of minutes to get in the calibration facility, then this is obviously far from ideal.

In conjunction with this calibration process, ANSTO has confirmed the dose rate in the UCF through irradiation of dosimeters supplied and measured by the National Physical Laboratories in the UK and via the IAEA's International Dose Assurance Scheme (IDAS). The dose rate measured in these instances agrees within 0.5% with ANSTO's calibrated dose rate.

5. MEASUREMENT UNCERTAINTY

As with the result of any analysis, the absorbed dose measurement obtained after reading a dosimeter is somewhat meaningless without an expression of the uncertainty associated with the result. In principle ANSTO follows the guidelines set out in ISO's 1993 "Guide to the Expression of Uncertainty in Measurement" and ASTM Standard E 1707 [1]. Uncertainties are reported as a percentage at the 95% confidence interval and are in the process of being fully incorporated into our Quality System.

6. QUALITY ASSURANCE

Radiation Technology performs all its functions according to the requirements of its ISO 9001 Quality System. This system requires that each dosimetry system, which includes the appropriate measuring instruments and written procedures for the system's use, is calibrated and maintained within specified accuracy limits. Extensive log books are maintained and stored to record such things as

- irradiation processes and dosimeter measurements,
- dosimeter batch preparation and calibration records,
- dose mapping details,
- calibration records for all measure and test equipment,
- maintenance records for facilities and
- non-conformances.

All services offered by Radiation Technology are initiated by completion of our Agreement for Service Work, which serves as an order form but also sets out ANSTO's Terms of Business and the responsibilities of both the customer and ANSTO according to Australia's Code of Good Manufacturing Practice.

Radiation Technology's activities are regularly audited by external regulatory bodies, by clients as part of their accreditation requirements and by ANSTO's Manager, Quality.

ACKNOWLEDGEMENT

The author would like to acknowledge the assistance and support provided to him by his colleagues in the Radiation Technology Group, and to thank ANSTO for providing funds to make attendance at this Symposium possible.

REFERENCE

[1] American Society for Testing and Materials, Annual Book of ASTM Standards, Volume 12.02, West Conshohocken, PA (1997)

SOME RADIATION-INDUCED EFFECTS IN TYPICAL CALORIMETRIC MATERIALS AND SENSORS

P.P. PANTA, W. GLUSZEWSKI
Institute of Nuclear Chemistry and Technology,
Warsaw, Poland

Abstract

The radiation-induced effects of the electron beams (EB) generated by accelerators in typical calorimetric materials and sensors have been surveyed and investigated. These effects influence the useful lifetime of the materials and sensors at high doses of about 4,000 to 5,000 kGy.

1. INTRODUCTION

There are increasing needs to accept calorimetry as an absolute dosimetry method for radiation processing. As a result of long term development of radiation calorimetry, three materials have been found to be of practical use: water, graphite and recently also polystyrene. Problems of radiation induced heat defects in H_2O, C and $(C_8H_8)_n$ were the subject of previous paper [1].

On the other hand, there are also some radiolytic and radiation damage effects in liquid and solid state materials which can influence dosimetric responses and moreover life span of calorimetric system. Radiation can break chemical bonds in water and polystyrene and involve short term effects which usually can be estimated and taken into account. Contrary to it, atomic displacement induced by fast electrons in temperature sensors, mainly thermistors, cause long term effects gradually changing resistance/temperature characteristics of thermistors as dose increases to its critical level. Principally, thermistors which are made of semiconductor materials are more radiation sensitive in comparison to electronic conductors (graphite and metals) and radiation resistant dielectrics such as polystyrene. However, thermistors are ten times as sensitive (4 %/ ^{0}C) as thermocouples and platinum resistance thermometers.

Some calculations of the atomic displacement cross section induced by fast electrons for the quantitative estimation of the long-term changes in thermistors and typical calorimetric materials are presented in the present paper.

2. CALCULATIONS OF ATOMIC DISPLACEMENT CROSS SECTIONS IN CALORIMETRIC MATERIALS AND SENSORS INDUCED BY FAST ELECTRONS

Only several elements i.e. hydrogen, carbon, oxygen and some metals (Mn, Ni, Co, Ti) are important for estimation of radiation damage in calorimetric materials and sensors.

EB irradiation of graphite and other materials are convenient for the determination of the threshold energy for atomic displacements. Simple or primary atom displacement occurs if the energy given to the primary knock-on is between E_d and 3 E_d. Multiple (secondary) atom displacements take place if energy imparted to a primary knock-on atom exceeds three time the threshold energy. Maximum energy imparted to an atomic nucleus by fast electrons with kinetic energy of E_e and rest mass m_0 is given by Eq. (1).

$$E_{max} = \frac{2\left(E_e + 2m_0c^2\right)}{Mc^2} E_e \qquad (1)$$

where, M = mass of the target atom, c = velocity of light in vacuum.

The cross section σ_d for an atomic displacement is, according to Vavilov [2], as follows:

$$\sigma_d = 8\pi\sigma_o\left[\frac{1}{2}\left(\frac{1}{x_o^2}-1\right)+\pi\alpha\beta\left(\frac{1}{x_o}-1\right)+\left(\beta^2+\pi\alpha\beta\right)\ln x_o\right] \quad (2)$$

where,

$$\sigma_o = \left(\frac{2e^2}{2m_o c}\right)^2\left(\frac{1-\beta^2}{\beta^4}\right) \quad (3)$$

$$\alpha = \frac{Ze^2}{hc} = \frac{Z}{137} \quad (4)$$

$$x_o = \sqrt{\frac{Ed}{E_{\max}}} \quad (5)$$

$$\beta = \frac{V_o}{C} = \sqrt{1-\frac{m_o c^2}{\left(E_e+m_o c^2\right)}} \quad (6)$$

Z = atomic number, and h = Planck's constant.

This formula is relatively simple in comparison to very complex method of Oen's [3], which employed the Mott series with Kinchin and Pease model. Comprehensive Oen's work reports displacement cross section of 37 different elements for incident electron energies ranging from threshold to about 150 MeV (see Fig. 1).

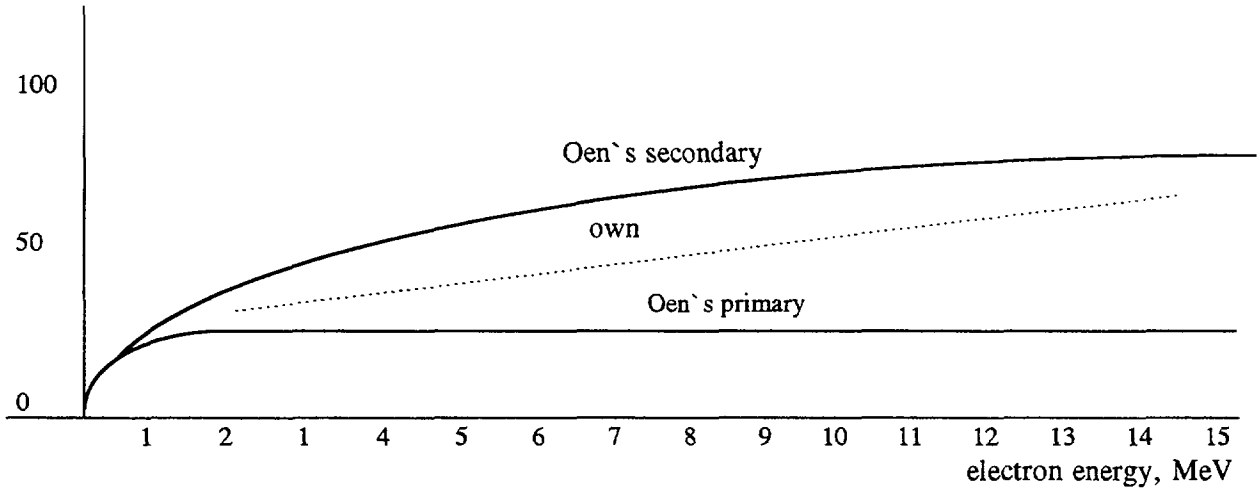

FIG. 1.Present atomic displacement cross sections of oxygen for incident electron energies in range from 2 to 13 MeV

3. EXPERIMENTAL

3.1. Materials and sensors

- Nuclear grade graphite, density of 1,670 kg/m^3, Russian production.
- Transparent polystyrene (PS) commercially available, manufactured mainly for building applications, density of 1,050 kg/m^3.
- Expandable polystyrene (EPS) foam also commercially available, produced as thermo-insulating material, density of 20 to 40 kg/m^3.
- Purified water, distilled from alkaline solution of $KMnO_4$.
- NTC - glass coated bead thermistors of Philips, VECO, Siemens and Polish production of two kinds:
  High resistance (20-40 kΩ) - low temperature (up to 200 ^{0}C)
  Low resistance (1-2 kΩ) - higher temperature (over 300^{0}C)

3.2. Radiation sources

- UHF electron linac, type LAE 13/9, (5 -19 MeV, 9 kW average beam power, 0.5, 2.5, and 5.5 μs pulse duration),
- UHF electron linac, type UELV-10-10-70-1, (10 MeV, 10 kW average beam power, 4.5 μs pulse duration)
- HF pulsed resonant electron accelerator, type ILU-6M2, (0.7 -2 MeV, 20 kW average beam power, 400 μs pulse duration).

4. RESULTS AND DISCUSSION

4.1. Graphite

Synthetic, very pure graphite is widely used as a moderator material in nuclear reactors. Heavily irradiated nuclear graphites were tested in research and commercial reactors as early as Manhattan Project times. On the other hand, reactor grade graphites are certainly very good materials for calorimetric applications because of its excellent mechanical, thermal and radiation properties and also chemical purity. It is important to be careful during mechanical treatment of graphite because there is possibility of contamination of this very pure material.

According to our experiments and literature data the bulk nuclear graphite samples showed very high radiation resistance, without any property changes even above 10,000 kGy. It is enough for ensuring the long-term life time of the calorimetric body.

On the other hand, powdered graphite samples, irradiated in contact with air exhibited some physiochemical effects (wettability with water, insignificant oxidation) at about 800-1000 kGy. Assuming a threshold energy, E_d, of carbon atom in elastic collision with fast electron as equal to 24.7 eV, we calculated cross section of displacement of about 17 b at 10 MeV [4]. Several Japanese authors [5-6] report displacement damage in local electronic structure of graphite lattice irradiated using high voltage electron microscopy with energy > 0.12 MeV. At this incident energy, the cross section of carbon atom displacement is one order of magnitude smaller than for 10-MeV electrons. The stored energy of atomic displacement in crystalline lattice of graphite can be released only at dose level of 10^6 kGy (so called Wigner effect, observable in nuclear reactors).

4.2. Polystyrene

The bulk polystyrene (PS) appears to have a considerable resistance to ionizing radiation because of the radiation protection effect of the benzene ring. Also, some styrene copolymers (for example with acrylonitrile) are highly resistant to radiation, having a small G-value for cross-linking [G(C) = 0.77] and chain scission [G(S) =0.055] [7]. The energy dissipated per cross-link in polystyrene is 1400 to 1800 eV, about thirty times the 45 to 60 eV per cross-link in polyethylene [8].

We used commercially available transparent PS as a possible pure polymer without dyes. As well known, the mechanical properties of polystyrene are changed very little by irradiation. The tensile strength elongation at break of unmodified polystyrene is reduced by only 5 to 10% by exposure of 50,000 kGy. High-impact polystyrene, which contains modifiers, show greater susceptibility to radiation damage. The samples of transparent polystyrene were irradiated on a conveyor belt by 10 MeV electrons analogically as during sterilization procedure of medical supplies. After several sterilisation doses (25 - 35 kGy) the yellowish colour was observed. Also, polystyrene disks in PS calorimeters show the change of colour, without worsening of mechanical properties at very high dose of 5,000 kGy.

4.3. Water

Water has been used nearly as extensively as graphite as a moderator in nuclear reactors. Radiation effects on water are complex and have been investigated extensively since fifties [4]. The primary effect of radiation on water is probably excitation and ionization of the molecules and to a lesser extent dissociation into free radicals, hydrogen atoms and hydrogen peroxide.

The value of water as a calorimetric body is due to its stability toward radiation. Our experiments with irradiation of distilled water encapsulated inside sealed glass vessels show that the G-value of formation of gaseous hydrogen is equal to 0.4. This value agrees very well with the literature data [9,10]. Also, water calorimeters containing water inside glued Petri dishes show weight losses of about 1-2% after dose close to 2,000 kGy. This result depends on the purity of the used polystyrene vessel.

4.4. Thermistors

Negative temperature-coefficient (NTC) bead thermistors are manufactured mainly from the metallic oxide semiconductor materials sintered on platinum-iridium thin lead wires. A glass coating applied to these beads provides them with an effective hermetic seal against conductive, corrosive and other hostile environment. Most of the commercially available thermistor beads are made from transition metal oxides with spinel structure, sintered at temperature close to 1300 ^{0}C.

It is often assumed that the activation energy, B of thermistor material is constant, and the plot of lnR vs. 1/T, where R is thermistor resistance in ohms at the temperature T in Kelvin, is approximately linear, and is described by Eq. (7):

$$R = A \bullet e^{B/T} \tag{7}$$

Radiation tolerance of the thermistors used in calorimeters depend on chemical composition, structure and manufacturing technology. We statistically observed some stages of thermistor radiation damage on absorption of high doses from fast electrons:

- several percent resistance rise (at about 1,000 kGy)
- characteristic drift of resistance readout (at about 3,000 - 4,000 kGy), see Fig. 2.
- lack of resistance readout, caused by break of electrical circuit of thermistor.

Sometimes a single thermistor can be damaged on absorption of several sterilization doses. However, average radiation tolerance is worse in the case of high resistance and lower permissible temperature and is better for low resistance and higher permissible temperature of thermistor.

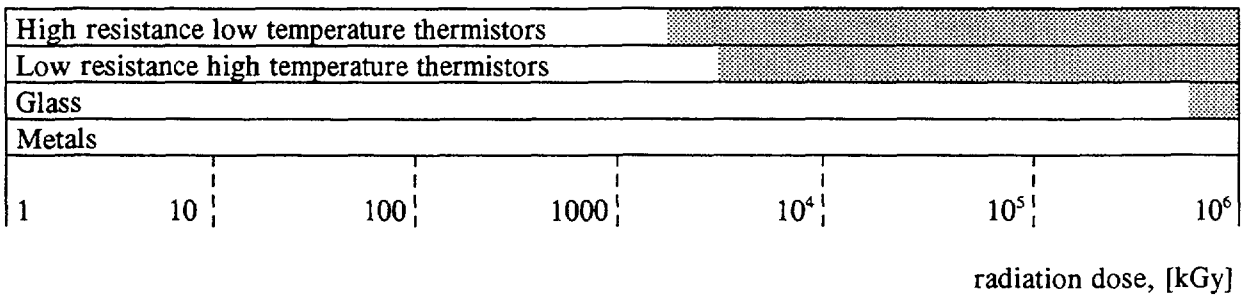

FIG. 2. Approximate tolerance of calorimetric materials to EB irradiation

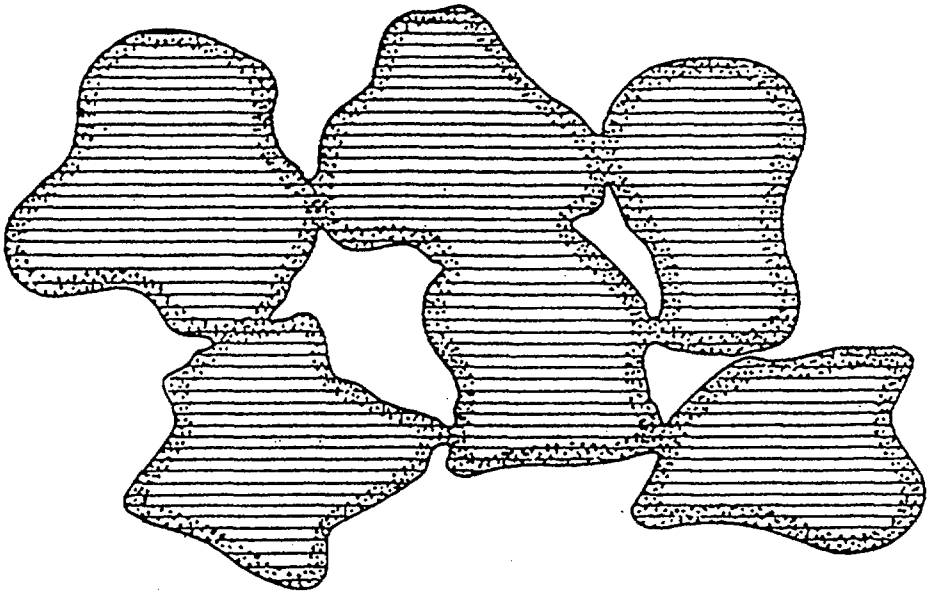

FIG 3. Cross section of a sintered sample

On the other hand, we also observed long term degradation of thermistor parameters without any irradiation. Some thermistor manufacturers state that their products are stable over period of about 10^8s (roundly 3 years). A small sample of ten thermistors was stored in dark, at room temperature during over twenty years. All thermistors of this sample were out of order [11].

In the light of these experiments we try to interpret some important aspects of complex mechanism of irradiation damage of NTC bead thermistors. On the one hand, semiconductor sintered material of beads have some tendency to long term recrystallization, which reduces its starting electrical conductivity. In effect, constant B (so called material constant) rises slowly with the absorbed dose. Just 2% change of B involves about 5% rise of resistance at the same temperature. The bead material is prepared by sintering the microcrystalline powder of metallic oxides mixtures. The individual microcrystallites have dimension of the order 10^{-3}-10^{-4} cm.

A schematic magnified cross section of sintered powder specimen is show in Fig.3. There are clearly seen sprinkling of voids and mutual contacts of individual microcrystallites grains.

On the other hand, radiation worsens the quality of the electrical contacts of bead sintered microcrystallites with thin platinum-iridium lead wires. Pulsating EB induces thermal microstrain cracks, which cause fatigue of surface contact of sintered material with wires. There is an additional possibility that the oxygen atoms of the oxides knocked on by fast electrons can generate some volatile platinum oxides which reduce conductivity of contacts. The old model of radiation induced "thermal spikes" suggested in fifties by Seitz becomes an argument for possibility of surface oxidation of Pt-Ir wires.

5. CONCLUSION

Transient and delayed radiation effects in calorimetric materials and sensors have been surveyed and interpreted.

Commercially available nuclear grade graphite and polystyrene and also re-distilled water can be used as durable materials of calorimeters for doses of 4,000 to 5,000 kGy without observable damage.

Carefully selected NTC bead thermistors with resistance of 1 to 2 kΩ (at 25 ^{0}C) and permissible work temperature above 300 ^{0}C exhibit average radiation tolerance at the similar dose range.

ACKNOWLEDGEMENT

The authors acknowledge discussions with Eugeniusz KuŸma.

REFERENCES

[1]. PANTA P.P., ZAGÓRSKI Z.P., GLUSZEWSKI W.J., Thermal defects of water, graphite and polystyrene affecting calorimetric response, IAEA TECDOC-1023, IAEA Viena (1998), 499-509
[2]. VAVILOV V.S., Destviye izlucheniy na poluprovodniki, Atomizdat, Moskwa, 1963, 264 pp
[3]. OEN O.S., Cross sections for atomic displacements in solids by fast electrons, ORNL - 4897, Oak-Ridge (1973), 207 pp.
[4]. ETHERINGTON M., Nuclear Engineering Handbook, Mc Graw Hill, New York 1958, 10.099 - 10.101 pp.
[5]. MUTO S., TANABE T., Damage process in electron irradiation graphite studied by transmission electron microscopy., I, High resolution observation of highly graphitized carbon fibres, Philos. Mag.A., **76**, 679 (1997)
[6]. TAKEUCHI M., MUTO S., TANABE T., ARAI S. AND KUROYANAGI T., Damage process in electron irradiation graphite studied by transmission electron microscopy., II, Analysis of extended energy-loss fine structure of highly oriented pyrolytic graphite, Philos. Mag.A., **76**, 691 (1997)
[7]. T.Q. NGUYEN, H.H. KAUSCH., Protective effect of the phenyl group in γ- irradiated compatible blends of Poly(methyl methacrylate) and poly(styrene-Co-acrylonitrile), Journal of Applied Polymer Science, Vol. **29**, 455-460 (1984)
[8]. BOLT R.Q., CARROLL J.G., Radiation effects on organic materials, Academic Press, New York - London 1963, 576 pp
[9]. SPINKS. J.W.T., Wood R.J., Introduction to radiation chemistry, J.Wiley New York 1976, p. 258
[10]. BUGAENKO. V.L., BYAKOV. V.M., Quantitative model for the radiolisis of liquid water and dilute aqueous solutions of hydrogen, oxygen , and hydrogen peroxide: I. Statement of the model, High Energy Chemistry, **32**, 411 (1998), (In Russian: Journal „Khimiya Vysokikh Energii)
[11]. P.PANTA., unpublished results, Warsaw 1996

IAEA REFERENCE DOSIMETER: ALANINE–ESR

K. MEHTA, R. GIRZIKOWSKY
Dosimetry and Medical Radiation Physics Section,
International Atomic Energy Agency,
Vienna

Abstract

Since 1985, the IAEA has been using alanine-ESR as a transfer dosimeter for its dose quality audit service, namely the International Dose Assurance Service. The alanine dosimeters are rod-type containing 70 wt% DL-α-alanine and 30 wt% polystyrene. We have two self-shielded gamma facilities for the calibration of the dosimetry system, where the temperature within the irradiation chamber can be controlled by a specially designed unit. A 4^{th} order polynomial is fitted to the 16 data points in the dose range of 100 Gy to 50 kGy. The measured value of the irradiation temperature coefficient at two dose values (15 and 45 kGy) is 0.23 %/°C. Also, the ESR-response was followed for several dosimeters for about 8 months to study the post-irradiation effect. A value of 0.008 %/day was observed for the fading of the response for two dose values (15 and 45 kGy) and three irradiation temperatures (15, 27 and 40 °C). The effect of the analysis temperature on the ESR response was also studied. The combined relative uncertainty for the IAEA alanine-ESR dosimetry system is 1.5% (k=1). This includes that transferred from the primary laboratory for the dose rate measurements of the gamma facilities, dosimetry system calibration uncertainties, batch variability and uncertainty in the curve fitting procedure. This value however does not include the contribution due to the irradiation temperature correction which is applied when it differs from that during calibration; this component being specific for each dose measurement.

1. INTRODUCTION

Several guidelines and standard practices have been developed by international and regional organisations, such as ISO, WHO, FAO, CAC, CEN, ASTM and AAMI (for example, Refs [1-4]). One of the principal concerns of all guidelines is process validation – the objective of which is to establish documentary evidence that the radiation process will reliably achieve the desired results. The key element in process validation is a well characterised, reliable and accurate dosimetry system that is traceable to a primary standard dosimetry laboratory (PSDL). To help developing Member States to establish such a dosimetry system, the IAEA started the "High-dose dosimetry programme" in 1977 [5,6]. One of the principal elements of this programme is the dose quality audit service (International Dose Assurance Service, IDAS) for gamma radiation which was initiated in 1985 [6].

The transfer dosimetry system used for the IDAS is alanine-ESR. The selection of alanine was based on several intercomparisons that were conducted by the IAEA in early 1980s for this specific purpose [6]. Amongst the dosimeters tested, alanine-ESR was judged to be the most suitable dosimeter for the IDAS for the following reasons: near-tissue equivalency, insensitivity to ambient environment, broad useful dose range, non-destructive analysis, and little fading of response with time. At that time, this was a 'new' system used by hardly any standard laboratories. Today, almost every PSDL and SSDL is using alanine-ESR as a reference or a transfer system.

2. DOSIMETRY SYSTEM

The IAEA reference dosimetry system consists of rod-type DL-α-alanine dosimeters, Bruker ESR spectrometer, an in-house ^{60}Co calibration facility, and documented procedure for the use of the system.

2.1. Alanine dosimeter

The alanine dosimeters presently in use at the IAEA dosimetry laboratory are 'Aminogray' purchased commercially[1] and are rod type: 30 mm long and 3 mm in diameter. The dosimeter consists of polystyrene (30 wt%) as the binder material and DL-α-alanine as the radiation sensor (70 wt%). The dosimeter is placed inside a sealed polystyrene capsule which provides the required buildup material to achieve secondary electron equilibrium for ^{60}Co photons and also provides a controlled humidity environment. Some of the relevant characteristics of the dosimeter are given in Table I.

TABLE I. CHARACTERISTICS OF AMINOGRAY DOSIMETER

Property	Value
Composition	
dosimeter	70 wt% alanine + 30 wt% polystyrene
capsule	polystyrene
Dimensions	
dosimeter	30 mm long, 3 mm diameter
capsule	50 mm long, 12 mm diameter, 4 mm wall
Background response	equivalent to about 5 Gy
Density	1.30 g/cm^3
Effective atomic number (Z)	6.2
Irradiation-temperature coefficient	+ 0.23 %/°C
Post-irradiation response fading	0.008 %/day

2.2. Spectrometer

The ESR spectrometer in use at the IAEA dosimetry laboratory is the Bruker X-band ESP-3-9/2.7 with a rectangular cavity. The spectrometer is housed in a room where the temperature is maintained within ±2 °C. The peak-to-peak height of the central line of the first derivative of the ESR absorption spectrum is used as the radiation-induced response.

Details of the spectrometer and measurement parameters are given below:

Spectrometer - Bruker ESP 300, X-band with 9" magnet;
Cavity - TMH8808 rectangular cavity;
Microwave power - 1.3 mW;
Modulation amplitude - 2.0 G;
Field sweep - 150 G;
modulation frequency - 12.5 kHz.

2.3. Calibration

The dosimetry system is calibrated over the full range of the IDAS, namely 100 Gy to 100 kGy of the absorbed dose in water. The dosimeters were irradiated in the two in-house self-shielded ^{60}Co facilities (Gammacell 220 from Nordion) to cover the total dose range. The dose rate in the central region of the irradiation chamber of each Gammacell was measured by transfer dosimeters from the National Physical Laboratory of U.K. The values of the dose rate in this location are 1.96 and 41.4 Gy/min (01-01-1998) for the two Gammacells. Also, film (GafChromic DM-1260) dosimeters were used to establish the isodose contours within the irradiation chamber.

[1] These are supplied by Hitachi Cable International, Ltd.

Sixteen dose points (equally spaced on the log-scale) from 100 Gy to 100 kGy were selected for the calibration of the system. Three dosimeters were irradiated simultaneously at each dose level in a specially designed polystyrene holder. The temperature of the dosimeters was controlled within ±1 °C for all irradiation using a Peltie device. A fourth-order polynomial function provides the best fit to the data.

2.4. Procedure

The IAEA dosimetry laboratory operates under a quality assurance programme that is based on Guide 25 of the ISO [7]. Under this QA programme, we have established a standard operating procedure for the use of our alanine-ESR dosimetry system, which is consistent with the relevant ASTM standard [8].

3. INFLUENCE PARAMETERS

The ESR response of Aminogray dosimeters is affected by several influence quantities. We have studied this effect for four parameters: angular orientation of the dosimeter in the cavity, irradiation temperature, time after irradiation and analysis temperature.

3.1. Angular orientation

A goniometer was used to measure the ESR response as a function of the angular position of the dosimeter in the cavity. The response was measured every 10° for two dosimeters irradiated at 1 and 40 kGy (see Fig.1). The periodicity for both the cases is about 180°. Thus, every dosimeter is measured at two angles orthogonal to each other, and the mean value is taken as the response for further analysis.

3.2. Irradiation temperature

The value for the irradiation-temperature coefficient for alanine dosimeter as reported by various users varies between 0.15 and 0.30 %/°C. We have measured this influence for Aminogray dosimeters at 15 and 45 kGy over the temperature range of 5 - 45 °C. The value of the irradiation-temperature coefficient based on these data is 0.23 %/°C for both the dose levels [9].

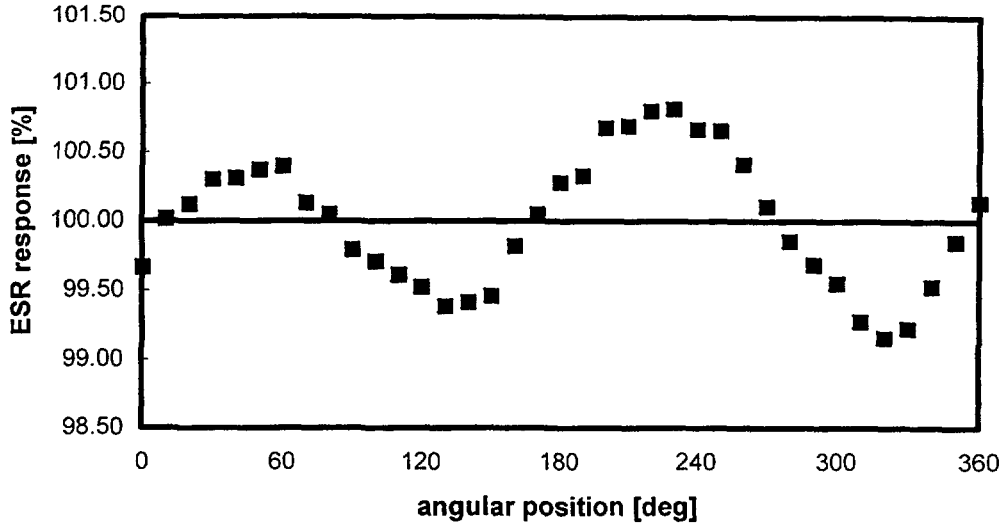

FIG.1. ESR response of Aminogray dosimeter (irradiated to 40 kGy) as a function of angular position. The results are similar for 1 kGy.

3.3. Time evolution

We measured the ESR response of several dosimeters over a period of about 8 months after irradiation for different irradiation conditions: two dose values (15 and 45 kGy) and three irradiation temperatures (15, 27 and 40 °C). The time evolution of the ESR response for all the six cases was very similar. The first measurement was about 12-24 hours after the end of irradiation. We observed a small increase of the response (0.5-1 %) over the first few days. The response was then almost constant for 10-15 days after which time it started to decrease very slowly. The average fading rate for all the irradiation conditions was about 0.008 %/day [9]. The initial rise is statistically significant and was present for all the six cases studied. This phenomenon is explained by Dolo *et al.* [10] by assuming that the creation of the alanine radical is a two-step reaction proceeding through a transient species. In all cases, the dosimeters were pre-treated at 25-40 % r.h. for 2-3 months before irradiation, and the temperature of storage before and after irradiation was 20-25 °C. This is the normal procedure according to our SOP.

3.4. Analysis temperature

We also studied the effect of the temperature of the cavity on the ESR response. The temperature was measured by a mercury thermometer placed very close to the cavity. The cavity temperature was varied between 15 and 26 °C by varying the room temperature. The analysis-temperature coefficient was -0.75 %/°C based on this limited set of data.

4. DOSE MEASUREMENT UNCERTAINTY

To determine the total uncertainty of the dosimetry system, the dose measurement system is divided into various components, sub-components and activities following the ASTM standard E1707 [11]. The contribution to the uncertainty in the measured value from each of these activities was identified and the values for type A and type B evaluated as suggested by ISO [12]. These contributions are then combined to yield the total estimate of the uncertainty value. These values are given in Table II.

4.1. Reference dose rate

The uncertainty in the dose rate value at the reference location in the Gammacell is largely transferred from the PSDL that measured the dose rate using their transfer dosimeters. The dose rate for the high dose-rate Gammacell was measured by the NPL using dichromate transfer dosimeters. Adding a small contribution for the timing of the irradiation period to their stated value, the uncertainty in the dose rate value is 1.1 % (k=1).

4.2. Calibration of alanine-ESR dosimetry system

The dosimetry system is calibrated as mentioned above by irradiating the dosimeters in the known reference field. This procedure consists of four sub-components: irradiation of the dosimeters, ESR analyses of the irradiated dosimeters, intra-batch variability, and polynomial fit of these data. Type A and type B uncertainties for each of these four sub-components were evaluated and combined to give the value of 0.90 % (k=1) for this component.

Combining this value with the uncertainty in the dose rate value (1.1 %), the total uncertainty of the dosimetry system is 1.5 % (k=1).

4.3. Dose measurement

When the calibrated dosimetry system is used for the measurement of an unknown dose at a point, there are further contributions to uncertainty. The two sub-components here are: irradiation of

TABLE II. ALANINE-ESR DOSIMETRY UNCERTAINTY

Component	type A (k=1, %)	type B
1. DETERMINATION OF THE GAMMACELL DOSE RATE		
Transferred mainly from PSDL	0.86	0.64
Combined uncertainty for 1.	*1.1*	
2. CALIBRATION OF THE DOSIMETRY SYSTEM		
Irradiation	.....	0.44
ESR measurement	0.21	-----
Intra-batch variability	0.25	-----
Polynomial fit	0.7	-----
Total of 2.	*0.78*	*0.44*
Combined uncertainty for 2.	*0.90*	
Combined uncertainty of the calibrated system (1+2)	*1.5*	
3. DOSE MEASUREMENT USING THE SYSTEM(3 dosimeters)		
Irradiation :		
Irradiation temperature	.....	$0.23 \times \delta T/\sqrt{3}$ [a]
Temperature coefficient	.....	$0.02 \times \Delta T$ [b]
Fading correction	.....	$0.002 \times \delta D$ [c]
ESR measurement	0.21	.....

[a] δT is the uncertainty in the irradiation temperature, assumed to have a rectangular probability distribution.

[b] ΔT is the temperature difference between the calibration temperature and the estimated temperature during dose measurement, and 0.02 is the uncertainty in the value of the temperature coefficient.

[c] δD is the number of days representing the time interval between irradiation and ESR analysis less 20, and 0.002 is the uncertainty in the value of the fading rate.

dosimeters and ESR analyses of the irradiated dosimeters. If the irradiation conditions are not the same as those during calibration, it is necessary to apply certain corrections (for example, for irradiation temperature and the time interval between irradiation and analysis). However, application of these corrections add further to the total uncertainty. These corrections and the associated uncertainty in the corrections are case specific but could amount to about 1.4 % (if the irradiation temperature is known within ±10 °C only).

5. MAINTENANCE OF QUALITY

To maintain the dosimetry system at a high level of quality, several special activities besides the routine ones are followed at the IAEA dosimetry laboratory. These include: frequent traceability exercises, proficiency tests and intercomparisons.

As mentioned above, our dose measurements are traceable to a PSDL through the dose rate measurements of our in-house calibration facilities using the transfer dosimeters from them. This is accomplished regularly at an interval of 3-4 years or if there is any significant change in the calibration facility, such as the dosimeter holder geometry.

Proficiency test is performed once a year where our dosimeters are sent to a PSDL to be exposed at three dose levels, which are then analysed by the IAEA dosimetry laboratory and the results compared with the PSDL values. Any discrepancy greater than the uncertainties of the two systems is investigated. This is a 'blind' exercise.

Also, the IAEA dosimetry laboratory participates in intercomparisons between calibration laboratories organised by, for example, the International Bureau of Weights and Measures (BIPM).

6. CONCLUSION

The alanine-ESR has performed well as a reference dosimeter for the radiation processing dose levels for the IAEA's dose quality audit service for ^{60}Co gamma radiation.

REFERENCES

[1] INTERNATIONAL ORGANISATION FOR STANDARDISATION, 'Sterilisation of health care products – requirements for validation and routine control – radiation sterilisation', ISO 11137, 1995.

[2] AMERICAN SOCIETY FOR TESTING AND MATERIALS, Standard practice for dosimetry in irradiation facilities for food processing, ASTM E 1204, Annual Book of ASTM Standards, **12.02**, ASTM, 1998.

[3] AMERICAN SOCIETY FOR TESTING AND MATERIALS, Standard practice for dosimetry in an electron beam facility for radiation processing at energies between 300 keV and 25 MeV, ASTM E 1649, Annual Book of ASTM Standards, **12.02**, ASTM, 1998.

[4] ASSOCIATION FOR THE ADVANCEMENT OF MEDICAL INSTRUMENTATION, 'Guideline for gamma radiation sterilisation', ANSI/AAMI ST32, USA, 1991.

[5] K. MEHTA, IAEA high-dose dosimetry programme. These proceedings, paper no: IAEA-SM-356/R2.

[6] NAM J.W., Standardization and assurance of high doses: an IAEA activity on dosimetry for radiation processing. Proceedings of the international symposium on 'High dose dosimetry for radiation processing', 5-9 November 1990, Vienna, 1991.

[7] INTERNATIONAL ORGANISATION FOR STANDARDISATION, 'General requirements for the competence of calibration and testing laboratories', Guide 25, 3rd edn., 1990.

[8] AMERICAN SOCIETY FOR TESTING AND MATERIALS, Practice for use of the alanine-ESR dosimetry system, ASTM E 1607, Annual Book of ASTM Standards, **12.02**, ASTM, 1998.

[9] K. MEHTA, High-dose standardization service of the IAEA, Appl. Radiat. Isot. **47**, pp 1155-1159, 1996.

[10] J.M. DOLO, ESR/alanine dosimetry: study of the kinetics of free radical formation - evaluation of its contribution to the evolution of the signal after irradiation, These proceedings, paper no: IAEA-SM-356/54.

[11] AMERICAN SOCIETY FOR TESTING AND MATERIALS, Standard guide for estimating uncertainties in dosimetry for radiation processing, ASTM E 1707, Annual Book of ASTM Standards, **12.02**, ASTM, 1998.

[12] INTERNATIONAL ORGANISATION FOR STANDARDISATION, 'Guide to the expression of uncertainty in measurement', 1995.

DOSIMETRY STANDARDS AND INTERCOMPARISIONS

(Session 8)

Chairperson

B.WHITTAKER
United Kingdom

Invited Paper

DOSIMETRY STANDARDS FOR RADIATION PROCESSING

H. FARRAR IV
Bell Canyon, California,
United States of America

Abstract

For irradiation treatments to be reproducible in the laboratory and then in the commercial environment, and for products to have certified absorbed doses, standardized dosimetry techniques are needed. This need is being satisfied by standards being developed by experts from around the world under the auspices of Subcommittee E10.01 of the American Society for Testing and Materials (ASTM). In the time period since it was formed in 1984, the subcommittee has grown to 150 members from 43 countries, representing a broad cross-section of industry, government and university interests. With cooperation from other international organizations, it has taken the combined part-time effort of all these people more than 13 years to complete 24 dosimetry standards. Four are specifically for food irradiation or agricultural applications, but the majority apply to all forms of gamma, x-ray, bremsstrahlung and electron beam radiation processing, including dosimetry for sterilization of health care products and the radiation processing of fruits, vegetables, meats, spices, processed foods, plastics, inks, medical wastes and paper. An additional 6 standards are under development. Most of the standards provide exact procedures for using individual dosimetry systems or for characterizing various types of irradiation facilities, but one covers the selection and calibration of dosimetry systems, and another covers the treatment of uncertainties. Together, this set of standards covers essentially all aspects of dosimetry for radiation processing. The first 20 of these standards have been adopted in their present form by the International Organization of Standardization (ISO), and will be published by ISO in 1999.

1. INTRODUCTION

Today, radiation processing is an expanding technology with numerous applications in, for example, health care products sterilization, sewage and hospital waste treatment, polymer modification, and food processing. In the time since dosimetry standards were discussed at the previous IAEA High-Dose Symposium in 1990 [1], public perception and media coverage about food irradiation have shifted dramatically from *generally negative* to *usually positive*, and it appears increasingly likely that large amounts of meat (to reduce the possibility of contamination) and fruits (to inactivate insects) will be processed in the next few years. The effectiveness of the irradiation process depends, however, on the proper application of dose and its measurement. Regulatory authorities generally require the processor to control the irradiation process so that all parts of the product receive an absorbed dose within certain prescribed limits. This required absorbed dose range will depend on the product and the desired effect, such as total sterilization of medical products, extended shelf-life of food, or insect disinfestation. The lower limit must be high enough to accomplish this desired effect, but the upper limit should not be so high as to cause adverse effects. Adequate dosimetry with proper statistical controls and documentation is the key part of the Quality Control (QC) process which is necessary to assure the products are properly treated.

Recognizing the importance of standards, several national and international organizations such as ISO, CEN, and the Association for the Advancement of Medical Instrumentation (AAMI) have been involved in the development of guidelines and standards related to various aspects of radiation processing. Amongst them, ASTM is the principal player for the development of standards for dosimetry.

2. ASTM SUBCOMMITTEE E10.01 ON DOSIMETRY FOR RADIATION PROCESSING

To address the needs of industry, ASTM Subcommittee E10.01 "*Dosimetry for Radiation Processing*" was formed in 1984 with the principal objective of developing dosimetry standards. Membership has grown to about 150 individuals from 43 countries, representing industry, government laboratories, radiation equipment manufacturers, dosimeter manufacturers, regulatory agencies, universities, medical companies, food companies, and irradiator operators. This membership includes most groups in the world known to be active in the development of dosimetry for radiation processing. The international composition of this subcommittee is reflected in the fact that 14 of the 32 task groups that are writing or revising these standards are chaired by individuals from countries ***other*** than the United States of America.

Individual ASTM standards are developed by task groups consisting of both members and non-members, including anyone in the world who wants to participate. The standards pass through a series of ballot steps where all members have the individual power to cast a negative vote, which can be overridden only by the subcommittee providing a persuasive written explanation. The results of this consensus process are *standard practices* and *standard guides* that represent state-of-the-art thinking, and that have the technical consensus and support from all interested parties. This gives the standards particular credibility for specifying how research or production operations should be done properly, and makes them ideal for use in government regulations. ASTM has a policy where standards may undergo a technical review at any time, but must undergo this review at least every 5 years.

3. DOSIMETRY STANDARDS

Table I lists the 24 standards that have completed the ASTM ballot process with unanimous approval, and that are published in Volume 12.02 of the Annual Book of ASTM Standards [2]. There are plans to publish this set of standards also as a separate handbook.

Four of the standards are specifically for food irradiation or agricultural applications, but the majority apply to all forms of gamma, x-ray, bremsstrahlung and electron-beam radiation processing. Twelve of them are "vertical" standards that provide exact procedures for implementing 12 different dosimetry systems. The remaining twelve "horizontal" standards, which can be used with any of the individual dosimetry systems, include seven standards for characterizing and operating various types of gamma, x-ray, bremsstrahlung and electron beam irradiation facilities. The remaining horizontal standards include Guide E1261, which provides detailed information and criteria for selecting an optimum dosimetry system, and describes the three ways of calibrating dosimetry systems; and Guide E1707, which covers the treatment of uncertainties in absorbed dose measurements using the new ISO Type A and Type B evaluations. The remaining three standards are for specific applications on how to perform dosimetry while irradiating blood products or irradiating insects for sterile release programs, and on how to perform dosimetry during research on food and agricultural products. The latter standard was originally considered to be unnecessary, but the subcommittee, after examining some recent research papers in which there was inadequate dosimetry, and after noting that detailed dosimetry information is often not reported in the literature, decided that such a standard was very much needed.

Table II lists six draft standards that are currently being developed. The first, for the use of a label dosimetry system, has until recently been dormant due to the unavailability of label dosimeters. Some research is being undertaken by Ehlermann [3] to develop a label system, but more work still needs to be done to determine how his "dose meters" can be commercially implemented. Draft standard E10.01-N on dosimetry for small self-contained dry-storage irradiators of the type used widely for blood irradiation and for insect sterilization, is in its final ballot stage. Guide E10.01-S for dose mapping has been worked on for more than five years and is now in its seventh draft. Dose mapping is covered to some extent in some of the other existing dosimetry standards, but this standard is intended to treat the subject much more comprehensively.

TABLE I. COMPLETED DOSIMETRY STANDARDS

E1204 - 97	Practice for Dosimetry in Gamma Irradiation Facilities for Food Processing
E1205 - 93	Practice for Use of a Ceric-Cerous Sulfate Dosimetry System
E1261 - 94	Guide for Selection and Calibration of Dosimetry Systems for Radiation Processing
E1275 - 93	Practice for the Use of a Radiochromic Film Dosimetry System
E1276 - 96	Practice for the Use of a Polymethylmethacrylate Dosimetry System
E1310 - 94	Practice for the Use of a Radiochromic Optical Waveguide Dosimetry System
E1400 - 95a	Practice for Characterization and Performance of a High-Dose Radiation Dosimetry Calibration Laboratory
E1401 - 96	Practice for Use of a Dichromate Dosimetry System
E1431 - 98	Practice for Dosimetry in Electron and Bremsstrahlung Irradiation Facilities for Food Processing
E1538 - 93	Practice for Use of the Ethanol-Chlorobenzene Dosimetry System
E1539 - 93	Guide for Use of Radiation-Sensitive Indicators
E1540 - 98	Practice for Use of a Radiochromic Liquid Dosimetry System
E1607 - 94	Practice for Use of the Alanine-EPR Dosimetry System
E1608 - 94	Practice for Dosimetry in an X-Ray (Bremsstrahlung) Facility for Radiation Processing
E1631 - 96	Practice for Use of Calorimetric Dosimetry Systems for Electron Beam Dose Measurements and Dosimeter Calibrations
E1649 - 94	Practice for Dosimetry in an Electron-Beam Facility for Radiation Processing at Energies between 300 keV and 25 MeV
E1650 - 97	Practice for Use of Cellulose Acetate Dosimetry Systems
E1702 - 95	Practice for Dosimetry in a Gamma Irradiation Facility for Radiation Processing
E1707 - 95	Guide for Estimating Uncertainties in Dosimetry for Radiation Processing
E1818 - 96	Practice for Dosimetry in an Electron Beam Facility for Radiation Processing at Energies Between 80 and 300 keV
E1900 - 97	Guide for Dosimetry in Radiation Research on Food and Agricultural Products
E1939 - 98	Practice for Blood Irradiation Dosimetry
E1940 - 98	Guide for Dosimetry for Irradiation of Insects for Sterile Release Programs
E1956 - 98	Practice for Thermoluminescence Dosimetry (TLD) Systems for Radiation Processing

TABLE II. DOSIMETRY STANDARDS BEING DEVELOPED

E10.01-J	Practice for Use of a Label Dosimetry System
E10.01-N	Practice for Dosimetry for a Self-Contained Dry-Storage Irradiator
E10.01-S	Guide for Dose Mapping Product in Radiation Processing Facilities
E10.01-ß	Practice for Dosimetry in Radiation Processing of Fluidized Beds and Fluid Streams
E10.01-Δ	Guide for Using Mathematical Models for Predicting Absorbed Dose in Radiation Processing
E10.01-ζ	Guide for Performance Testing of Dosimetry Systems

The final three draft standards listed in Table II have not yet reached the ballot stage but are being worked on by their respective task groups. Significant progress on developing the guide for performance testing of dosimetry systems, including a discussion of influence quantities, was made at the ASTM meeting following the present symposium in Vienna.

4. COORDINATION WITH OTHER INTERNATIONAL ORGANIZATIONS

Over the past few years, there have been significant international movements to coordinate various national regulations and procedures. Accordingly, concurrent with the development of new

dosimetry standards, and to minimize overlapping or conflicting efforts, Subcommittee E10.01 has been coordinating its standards development activities with other international groups having similar or complementary interests. As a result of this effort, many of the 24 standards that have been completed and published are presently being used by a number of national and international groups and regulatory bodies. For example, some of the standards are regularly referred to (and have methodology that is consistent with) documents issued by AAMI. Others are referenced in documents issued by the International Consultative Group on Food Irradiation (ICGFI), a group established under the ægis of the United Nations' FAO, IAEA, and WHO to evaluate global developments in the field of food irradiation. Several of these dosimetry standards are quoted in US government regulations on food irradiation, and are being considered for inclusion or are already included in regulations issued by other countries. Also, several are relied upon and referred to extensively in international standards being developed for the radiation sterilization of health care products by ISO's Technical Committee 198 (ISO/TC198), or are utilized as the basis for dosimetry equipment Recommendations being developed by the International Organization of Legal Metrology (OIML).

Two other ASTM groups are responsible for closely related standards. Subcommittee F02.40 on "*Food Processing and Packaging*" is developing standard guides on good irradiation practice for food commodities as well as standards for the selection and use of packaging materials. Subcommittee E10.07 on "*Radiation Dosimetry for Radiation Effects on Materials and Devices*" is developing a number of standards on dosimetry for "radiation hardness" testing, and is responsible for Standard E1026 "*Practice for Using the Fricke Reference Standard Dosimetry System*", which is not included in Table I. Finally, ASTM Subcommittee E10.01 will cooperate with the International Commission on Radiation Units and Measurements (ICRU) should that organization decide to develop a report on dosimetry for radiation processing. All these coordination efforts are being helped by the fact that the experts writing the standards come from many different countries, and many are active in more than one of these organizations. The goals of these various organizations are all similar: to develop consensus standards that have the solid technical support of the worldwide radiation processing community.

5. ADOPTION BY ISO USING THE "FAST TRACK" PROCESS

An effort started in 1995 to transform 20 of the completed ASTM standards into ISO standards using the "fast track" process completed its final ballot stage in 1998. In 1996, ISO Technical Committee TC85 (Nuclear Energy) took responsibility for making this happen, and a new Working Group-3 (WG3) "*High-Level Dosimetry for Radiation Processing*" was formed. In a subsequent 1997 ISO ballot, all 20 dosimetry standards (then classified as Draft International Standards) were approved, but WG3 nevertheless decided to accommodate negative votes on three of the draft standards. The negative votes were made because the three standards contained technical information that overlapped with requirements in the existing Standard ISO 11137 "*Sterilization of health care products - Requirements for validation and routine control - Radiation sterilization.*" Although the overlapping requirements are technically consistent at the present time, there was concern that this might not always be the case in the future. As a result, compromise wording in the scopes of the three draft standards was worked out to everyone's satisfaction, including the membership of ISO/TC198/WG2, which is responsible for ISO 11137. Specifically, to satisfy the overlap problem, the scopes of the three Standards E1608, E1649, and E1702 were modified in the ISO versions to include the words "*In those areas covered by ISO 11137, that standard takes precedence.*" Except for the scope changes to these three standards, the contents of the 20 new ISO standards are identical to the ASTM versions that were submitted for ISO consideration in 1995. The first 20 standards listed in Table I have ISO designations starting with ISO 15554 (for E1204) and continuing consecutively to ISO 15573 (for E1818).

The main problem with this adoption by ISO of the first 20 dosimetry standards listed in Table I is that 9 have since been revised, and the ISO versions that have just been balloted are therefore already out of date! Working Group 3 of ISO/TC85 is aware of this issue, and has devised a strategy to minimize this problem in the future. The working group also knows that there are four new dosimetry standards that have not yet been considered for ISO adoption. The decision

was made at the biennial ISO/TC85 meeting in Paris in March 1998 to take one step at a time, and first get the 20 fast-tracked standards established. Now that this has been done, the working group is expected to request permission from ISO to update the standards, but not using the "fast track" process. For this effort, the working group will require additional technical manpower, and so an effort will be made to encourage more people from additional ISO member countries to join.

6. FINAL OBSERVATIONS

An enormous amount of work has been expended by many experts from around the world to generate this set of consensus standards that cover essentially all aspects of dosimetry for radiation processing. These *standard practices* and *standard guides* represent the state-of-the-art thinking and have the technical consensus and support from all who helped put them together. They are now published and available for use by the radiation processing community and national authorities for incorporation into harmonized regulations to avoid trade barriers and to facilitate international trade.

REFERENCES

[1] FARRAR, IV, H., "Efforts to obtain international consensus on dosimetry standards for radiation processing", High Dose Dosimetry for Radiation Processing (Proc. Symp. Vienna, 1990), IAEA, Vienna (1991).

[2] ANNUAL BOOK OF ASTM STANDARDS, Vol. 12.02, The American Society for Testing and Materials, West Conshohocken, Pennsylvania (1998).

[3] EHLERMANN, D.A.E., "Validation of a label dose meter with regard to dose assurance in critical applications as quarantine control", these Proceedings, paper number: IAEA-SM-356/38.

THE NIM ALANINE–EPR DOSIMETRY SYSTEM: ITS APPLICATION IN NDAS PROGRAMME AND OTHERS

Jun-Cheng GAO
Ionizing Radiation Division,
National Institute of Metrology,
Beijing, China

Abstract

In 1983, National Institute of Metrology (NIM) began to study alanine–EPR dosimetry system. From 1988 on, the system has been used as a transfer standard to launch into the National Dose Assurance Service (NDAS) programme for cobalt-60 facilities in China. In this paper, the eleven years implementation of NDAS programme are presented by statistics. In 1991, under an IAEA coordinated research programme, NIM had studied to extend the range of the system to therapy level. In recent years, the NIM in cooperation with other institutes has been developing film–alanine dosimeter for electron beam dosimetry.

1. INTRODUCTION

In order to suit the rapid development in radiation processing in China, NIM initiated a research project, having the name of "to establish metrological standards for dosimetry of ^{60}Co gamma-rays used in medicine, industrial irradiation and agriculture" in 1983. The key section of the project is to develop primary, secondary and transfer standards at processing level. At that time, the standardization on dosimetry of industrial radiation processing made the first step in China. When the research was fulfilled in 1988, several new primary and secondary dosimetric standards had been established in China. These standards are water calorimetry system, Fricke system, alanine-EPR system, potassium (silver) dichromate system, silver dichromate system and ceric-cerous sulfate system. Together with the old standards, graphite calorimetry and ionization chamber systems, there is a more complete group of metrology systems for high-dose dosimetry at NIM.

The idea that the alanine-EPR system had been placed on the project at that time, was affected by the IAEA report[1] and Regulla's work[2].

2. NIM ALANINE -EPR DOSIMETRY SYSTEM

The NIM alanine-EPR dosimetry system under the research project had been developed independently by ourselves. The comprehensive study on the system was summarized in a NIM final research report in 1987[3].

The system consists of alanine dosimeters, an EPR spectrometer, a precision balance, a fused quartz tube with high quality, a dose calibration curve and a national documentary standard.

The cylindrical alanine samples, having the size of ø3mm×8mm and the mass of about 68mg, are prepared with mixture of DL-α-alanine powder and paraffin in the weight ratio of 4 to 1. A sartoris electronic analytical balance with 0.1mg resolution is used for weighing the samples. Three samples are placed into a Perspex capsule to form an alanine dosimeter. There is fixed number on one end of the capsule, however, another end is sealed with a Perspex screw and paraffin to protect the samples from moisture. The outer size of the capsule is the same as that of NIM Fricke ampoule to make the calibration of alanine dosimeters convenient. Its wall thickness can meet secondary electron equilibrium for ^{60}Co gamma-rays.

The EPR instrument at NIM is a JES-FE1XG ESR spectrometer. EPR spectra of alanine samples are recorded under x-band at room temperature. The parameter of modulation width is selected as 0.63 mT to obtain higher spectrum amplitude in spite of its distortion, as the system belongs to relative measurement method. The ESR amplitude of the central peak for irradiated alanine sample is proportional to the absorbed dose.

Among the NIM primary standards, the Fricke system is chosen to make dose calibration for NIM alanine dosimeters. The calibration is carried out within a water phantom placed in a ^{60}Co irradiation field with substitution method. Since the NIM does not have its own standardization gamma-ray field, the calibration has to be performed in a user's field. Therefore, it is important to keep the same scattering condition and the same position for both Fricke and alanine dosimeters in the irradiation field throughout the calibration.

After the calibration of the field, a set of alanine dosimeters which had received accurate doses ranging from 1 to 10kGy, is applied to establish a dose calibration curve. In this dose range, the relationship between dose D and its response h, the peak amplitude of ESR spectrum of the calibrated alanine dosimeter, shows a good logarithmic linearity with a linear correlation coefficient of more than 0.9999 generally.

$$ln h = a + b ln D \quad (1)$$

The calibration of the dosimetry system should be made once a year.

A China national documentary standard with the name of "Alanine-EPR dosimetry system for radiation processing" was drafted by NIM and put into effect in June 1. 1997[4]. The standard is refereed to ASTM E1607-94 "Standard practice for use of the alanine-EPR dosimetry system" and made some appropriate changes. One of them is that the section of "Precision and bias" has been replaced with "uncertainty in measurement" which is refereed to the ISO Guide.

3. THE NDAS PROGRAMME FOR ^{60}CO FACILITIES

There is no doubt that the idea of the NDAS programme was inspired by the IDAS programme and had come true in 1988 in China. The procedure of the NDAS is similar to that of IDAS [5,6].

Each participant in NDAS gets a set of two alanine transfer dosimeters from the NIM every half an year. The NIM dosimeters and the participant dosimeters are bunched up together. Then the bundle of dosimeters is put in between irradiated articles for irradiation. The nominal dose D_1 of NIM dosimeters determined by the participant is based on the dose measurements of its own dosimeters.

The irradiated alanine dosimeters are returned to NIM to measure the response value h_0. According to the formation (1), the NIM evaluated dose D_0 can be obtained,

$$D_0 = \exp[(ln h_0 - a) / b] \quad (2)$$

The expanded uncertainty of D_0 is not more than 4% (2σ, or k=2). The percent deviation δ given in the NIM certificate is calculated as follows:

$$\delta = (D_1 - D_0) / D_0 \quad (3)$$

In 1990, a China national metrological norm, Monitoring method of dose assurance for radiation processing with gamma rays, had been put into force[7]. The norm explains the purpose, the significance, the method, the procedure and the result evaluation of NDAS programme. The norm established the role and the position of NDAS programme in dissemination of absorbed dose at processing levels in China.

The NDAS programme, with a scale of sixty participants now, has performed for more than ten years. By the end of August 1998, all together 798 dose checks had been carried out under the frame of NDAS.

Table I lists the distribution of the dose check results in different deviation ranges. It can be seen from the Table that 526 checks are within ±5%, accounting for 65.9% of the total number. However 161 (20.2%) and 111(13.9%) checks on the ranges between 5% and 10% and more than 10%, respectively. That is to say, the deviations for 86.1% dose checks are less than 10%.

TABLE I. THE DISTRIBUTION OF THE DEVIATIONS FOR NDAS DOSE CHECKS (1988–1998)

Deviation range (%)	< -20	-20 to -15	-15 to -10	-10 to -5	-5 to 0
Number of dose checks	21	16	26	110	305
Percentage (%)	2.6	2.0	3.3	13.8	38.2

Deviation range (%)	0 to +5	+5 to +10	+10 to +15	+15 to +20	>+20
Number of dose checks	221	51	14	7	27
Percentage (%)	27.7	6.4	1.7	0.9	3.4

Table II lists the number of dose checks, the corresponding averages of the percentage deviations and the standard deviations of the averages in chronological order. The result of last five years (1994–1998) in a general way, is better than that of the first six years (1988–1993) from the statistics in Table II. The mean value of all deviations for 798 checks is -0.88%. In other words, the mean ratio of users nominal doses to NIM evaluated doses is 0.9912.

TABLE II. THE ANNUAL MEAN VALUES AND CORRESPONDING STANDARD DEVIATIONS OF THE THE DEVIATIONS δ FOR ALL 798 DOSE CHECKS BY THE END OF AUGUST 1998

Year	1988	1989	1990	1991	1992	1993
Number of dose checks	7	64	64	52	90	53
Mean value of δ (%)	+1.85	-0.99	+7.30	-3.57	-4.58	+1.19
Standard deviation (%)	3.8	1.7	3.3	1.5	1.6	1.9

Year	1994	1995	1996	1997	1998
Number of dose checks	89	127	89	95	68
Mean value of δ (%)	+0.74	-1.75	-1.19	-1.56	-2.56
Standard deviation (%)	1.0	0.62	0.87	0.74	0.87

4. *RESEARCHES IN RADIOTHERAPY DOSIMETRY*

In 1991, NIM had participated in the IAEA coordinated research programme of therapy level dosimetry with the alanine-ESR system[8]. The main task of the research is to study the metrological properties of NIM alanine-EPR system in dose range of 1 to 100Gy, especially bellow 10Gy to enable the system to suit radiotherapy dosimetry.

The contribution of each component and their combination of the system to the background signal has been studied. They are: empty resonance cavity, cavity plus quartz tube, raw material of pure alanine powder, mixture of alanine and paraffin powders and shaped sample made of the mixture. Some parameters of the system has been changed or adjusted in order to increase its detective sensitivity, reduce the dose equivalent of noise and finally increase the signal–to–noise ratio. The main changes are as

follows: the outer size of alanine sample has been enlarged from ⌀3.0mm×8mm to ⌀4.5mm×10mm; the microwave power and the modulation width adjusted to 5mW and 1.25mT, respectively. In addition, the batch homogeneity of samples, the angular dependence of readout, the measurement repeatability and the influence of storage humidity have also been studied.

The dose comparisons between IAEA and NIM have been carried out by using NIM alanine dosimeters as the transfer elements. The mean dose ratio for 28 dosimeters in the range of 2.5 to 100 Gy is 0.974, which is within the uncertainty of NIM exposure standard.

The conclusion of the research is that the NIM alanine-EPR system can be used for therapy dosimetry for more than 5 Gy dose at present. We wish it could have a chance to try the system on a hospital ^{60}Co therapy unit.

5. RESEARCHES IN ELECTRON BEAM DOSIMETRY

In recent years, NIM has developed film-alanine dosimeter for electron beam (EB) dosimetry, in cooperation with Beijing Normal University and China Institute of Atomic Energy respectively[9,10]. The research is related to preparation technology of film samples, batch homogeneity of samples, angular dependence of readout, measurement repeatability, short-term and long-term stability, dose response curve, influence of irradiation temperature, influence of storage humidity and so on. Part of the research had been accomplished in 1996 and a preliminary plan for dissemination of absorbed dose value in EB dosimetry is drawing up. Since there would be a high degree of difficulty in realizing this dissemination, it is impossible to start the desired NDAS programme for EB dosimetry in a couple of years.

6. OTHER RELATED WORKS

The NIM alanine dosimeters were used to determine the technological irradiation dose ranges in drawing up China national hygienic standards of irradiated foodstuffs. In this application, two alanine samples are sealed in a plastic tube with a thickness of 1mm to become a dosimeter, which can be placed in any position of the foodstuffs. In this situation, there is no need to consider the electron equilibrium.

The dosimeters were also applied to check and accept the irradiation field of a new ^{60}Co facility according to the norm JJG591-89 "gamma ray irradiation source for radiation processing"[11]. In the meantime, several NIM alanine dosimeters were matched with GSF ones one by one by the user to be irradiated in the field while NIM know nothing about it. Then the NIM and the GSF dosimeters were sent to the institutes they belong to separately and measured by the institutes individually. The results evaluated by NIM are within 3% with those by GSF for more than ten pairs of dosimeters.

7. CONCLUSION AND DISCUSSION

NIM started to develop alanine-EPR dosimetry system in 1983 independently and initiated the NDAS programme by mailing alanine dosimeters in 1988. NIM is one of the institutes which have developed and applied the system earlier.

Up to now, there has been a dose dissemination and comparison network centered in the NIM under the frame of NDAS programme for high-dose dosimetry in China. The network possesses a scale of 60 participants and has the national regulations to support its validity.

The NDAS programme has been implemented for eleven years in China and 798 dose checks in all have been performed by the end of August 1998. Most checks, 526(65.9%), have a deviation less than 5%. The total mean value of all deviations is -0.88%.

The statistics in Table I do not obey normal distribution. For one thing 48 deviations are more than ±20%, making up 8%, and it shows that the ability in dosimetry has yet to be improved for a few

participants. For another thing, of the deviations less than ±10%(687), the negative ones are near to 60%(415). the reasons of unsymetrical distribution should be sought from both participants and NIM.

NIM possesses several kinds of dosimetry systems, however does not have its own standardization irradiation field at processing level.

For conducting dissemination of dose value in EB dosimetry, more difficult works have to be done for us.

We hope it is possible to make cooperations and intercomparisons between the NIM, the organization and the institute in the range of high-dose dosimetry.

REFERENCES

[1] INTERNATIONAL ATOMIC ENERGY AGENCY, High-dose Measurement in Industrial Radiation Processing, IAEA Technical Reports Series, No. 205, Vienna(1981).

[2] REGULLA, D., DEFFENER, U., Dosimetry by ESR Spectroscopy of Alanine, Int. J. Appl. Radiat. Isot. 33(1982)1101.

[3] GAO JUN-CHENG, et al., Alanine/ESR Dosimeter—The Transfer Standard for ^{60}Co Rays at Radiation Processing level, NIM Final Research Report(1987) (in Chinese).

[4] CHINA STATE BUREAU OF TECHNICAL SUPERVISION, Alanine-EPR Dosimetry System for Radiation Processing, China National Documentary standard, GB/T 16639-1996, China Standard Publishing House, Beijing(1996).

[5] NAM, J., REGULLA, D., The Significance of the International Dose Assurance Service for Radiation Processing, Appl. Radiat. Isot. 40(1989) 953.

[6] MEHTA. K., GIRZIKOWSKY, R., IAEA Activities on High–Dose Measurements, SSDL Newsllett. 31(1992)31.

[7] CHINA STATE BUREAU OF TECHNICAL SUPERVISION, Monitoring Method of Dose Assurance for Radiation Processing with Gamma Rays, China National Metrology Norm, JJG1020-90, China Metrology Publishing House, Beijing(1990).

[8] GAO JUN-CHENG, WANG ZAIYONG, The Extension of the Range of NIM Alanine/ESR Dosimetric System to Therapy Level, Appl. Radiat. Isot. 47(1996)1193-1196.

[9] GAO JUN-CHENG, et al., Alanine/ESR Dosimetry System for Radiation Processing with Electron Beams, NIM Final Research Report (1996) (in Chinese).

[10] LIN M., et al., A Set of Dosimetry Systems for Electron Beam Irradiation, These Proceedings.

[11] CHINA STATE BUREAU OF TECHNICAL SUPERVISION, Gamma Ray Irradiation Source for Radiation Processing, China National Metrology Norm, JJG591–89,China Metrology Publishing House, Beijing (1989).

DEVELOPMENT AND CURRENT STATE OF DOSIMETRY IN CUBA

E.F. PRIETO MIRANDA, G. CUESTA FUENTE
Research Institute for Food Industry

A. CHAVEZ ARDANZA
Center of Applied Studies for Nuclear Development

Havana, Cuba

Abstract

In Cuba, the application of the radiation technologies has been growing in the last years, and at present there are several dosimetry systems with different ranges of absorbed dose. Diverse researches were carried out on high dose dosimetry with the following dosimetry systems: Fricke, ceric-cerous sulfate, ethanol-chlorobenzene, cupric sulfate and Perspex (Red 4034 AE and Clear HX). In this paper the development achieved during the last 15 years in the high dose dosimetry for radiation processing in Cuba is presented, as well as, the current state of different dosimetry systems employed for standardization and for process control. The paper also reports the results of dosimetry intercomparison studies that were performed with the Ezeiza Atomic Center of Argentine and the International Dose Assurance Service (IDAS) of IAEA.

1. INTRODUCTION

As part of the Cuban nuclear programme and the applications of the nuclear techniques, particularly the employment of the gamma sources in radiation processing, a number of studies have been realized and different dosimetry systems applied which insure the radiation processing quality.

At present, Cuba has two laboratory irradiators located in the Center of Applied Studies for Nuclear Development, and a laboratory irradiator in the Laboratory for Irradiation Techniques. Cuba also has a semi-industrial irradiation plant belonging to the Research Institute for Food Industry, in which different applications have been developed in the field of radiation processing, such as food preservation, sterilization of medical and pharmaceutical products, treatment of biological products, radiobiology and treatment of polymers. To obtain the desired technological effect, it is necessary to know the absorbed dose value by means of accurate and reliable dosimetry systems employed during the commissioning of the facility, during process qualification and for process control, and also to have appropriate documented procedures.

The present paper describes the studies carried out for different dosimetry systems employed in high dose dosimetry in Cuba, as well as the results obtained in the dose intercomparison exercises.

2. FRICKE DOSIMETRY SYSTEM

In radiation processing, Fricke is a generally accepted reference standard dosimeter for in-house absorbed dose calibration. We have employed this dosimeter for calibration of other dosimetry systems, for process control and commissioning of different irradiators in our country.

The influence of different factors on the molar extinction coefficient value was studied, as well as, the effect of the measurement wavelength, the oxygen concentration in the dosimetric solution and the measurement equipment to obtain a good precision and accuracy in the absorbed dose value with this dosimeter [1,2].

2.1. Molar extinction coefficient (ε)

The molar extinction coefficient value of any system generally depends on several factors, such as the preparation procedure, quality of the ingredients, dissolvent, wavelength and temperature. We found that for a set preparation procedure [3], the temperature, measurement wavelength and the quantity of hydrogen peroxide (H_2O_2) in the solution were the most influential factors.

A factorial plan 2^3 was followed in which the above factors were taken into account at two measurement levels as independent variables (see Table I).

TABLE I. MEASUREMENT LEVELS OF THE INDEPENDENT VARIABLES.

	Low level	High level
Temperature (°C)	24	25
Wavelength (nm)	303	305
H_2O_2 quantity (mL)	4	10

The experimental results showed that the measurement temperature and the quantity of hydrogen peroxide in the solution had significant influence on the ε value, whereas the wavelength and the interaction of the tested parameters do not have significant effect. Thus, the mathematical model is given by:

$$y = 219.4 + 1{\cdot}0\ \{(T - 24.5)/\ 0.5\ \} - 1.6\ \{(H_2O_2 - 7)\ /\ 3\ \}$$

Substituting different values of temperature and hydrogen peroxide in this expression, the calculated ε value is in the range of 216.8 – 222.0 ($m^2 \cdot mol^{-1}$). The results agree with the values reported in the literature [4,5].

This model is appropriate for this range of the variables and for our spectrophotometer, as the ε value is different for each spectrophotometer.

2.2. Measurement wavelength

The ferric ion concentrations were determined at 224 and 304 nm in the spectrophotometer, Busch & Lomb Spectronic 1001 type, for seven different radiation times to determine the influence of the measurement wavelength on the absorbed dose value.

Table II shows the absorbed dose values obtained for the two wavelength values. A linear regression analysis is made in which it is obtained for the measurement at 224 nm a functional relation of D(Gy)=10.07+11.36 t(min), and the correlation coefficient value (r) of 0.9997, and for 304 nm the relation is D(Gy)=9.18+11.55 t(min) and r= 0.9998. Finally a Duncan test was made and it was determined that there is no significant difference between these two expressions. It shows that it is not necessary to make the measurements at 224 nm when the equipment of high precision and a control of measurement temperature are used, although the temperature coefficient for 224 nm is only 0.13 % $°C^{-1}$ between 20 and 30 °C, in comparison with 0.7 % $°C^{-1}$ at 304 nm [6].

TABLE II. ABSORBED DOSE VALUES (Gy) AND THE STANDARD DEVIATIONS FOR WAVELENGTH (λ) OF 224 AND 304 nm

Radiation time (min)	λ=224 nm	λ=304 nm
1.4	26.10 ± 3.68	24.62 ± 3.36
2.8	40.24 ± 1.36	38.62 ± 1.29
7.05	92.61 ± 2.51	93.15 ± 2.60
14.11	167.74 ± 5.36	170.56 ± 5.17
21.21	254.61 ± 11.23	260.04 ±11.27
28.26	329.43 ± 11.02	336.65 ±11.52
35.60	404.50 ± 16.75	417.07 ±19.66

2.3. Oxygen concentration in the dosimetric solution

The ferric ion concentrations of the un-saturated and saturated solutions with oxygen were determined at 304 nm in a spectrophotometer, type Sf-4, for five different irradiation times. The absorbed dose values are given in Table III, as well as, the standard deviations for each irradiation time for the two Fricke solutions. The data show that the relation between the absorbed dose and the irradiation time is linear for both solutions; the expressions are D(Gy)=9.68+11.59 t(min), r=0.9989 and D(Gy)=9.71+11.52 t(min), r=0.9998, respectively.

TABLE III. ABSORBED DOSE VALUES (Gy) AND THE STANDARD DEVIATIONS FOR THE UN-SATURATED AND SATURATED FRICKE SOLUTIONS.

Radiation time(min)	Un-saturated O_2 Fricke	Saturated O_2 Fricke
2.80	37.82 ± 6.31	39.57 ± 1.42
7.05	90.40 ± 6.66	92.67 ± 4.87
14.11	182.25 ± 9.22	173.75 ± 6.69
21.21	256.60 ±10.24	255.04 ± 3.93
28.26	332.97 ±12.20	333.96 ±11.71

A Duncan test was carried out for this exercise also, and it showed that there is no significant difference between the two solutions (un-saturated and saturated). For this reason, it is not necessary to saturate the solution with oxygen in the working range of Fricke dosimeter (40 - 330 Gy).

2.4. Measurement equipment

To determine the influence of the measurement equipment on the absorbed dose value, the un-saturated solution was irradiated and the measurements were made with Sf-4 and Bausch & Lomb Spectronic 1001 spectrophotometers, the molar extinction coefficient value of each equipment is 219.6 and 213.8 $m^2 \cdot mol^{-1}$, respectively for the wavelength of 304 nm.

The absorbed dose values obtained for different irradiation times are presented in Table IV. By means of a Duncan test it is determined that there is no significant difference between the results for the dose range studied, although some researchers have reported that there are differences when the measurements are made with different equipment [4,7]; this could be possible when the molar extinction coefficient value is not determined for each spectrophotometer separately.

TABLE IV. ABSORBED DOSE VALUES (Gy) AND THE STANDARD DEVIATIONS FOR DIFFERENT MEASUREMENT EQUIPMENT AT 304 nm.

Radiation time(min)	Sf-4	Bausch &Lomb Spectronic 1001
2.80	37.82 ± 6.31	38.62 ± 1.29
7.05	90.40 ± 6.66	93.15 ± 2.60
14.11	182.25 ± 9.22	170.56 ± 5.17
21.21	256.60 ± 10.24	260.04 ± 11.24
28.26	332.97 ± 12.20	336.65 ± 11.52

3. CERIC-CEROUS SULFATE DOSIMETRY SYSTEM

Ceric-cerous sulfate is a reference standard dosimeter which can be used for the measurement of radiation dose in kGy range. It is particularly well suited for the measurements of dose in the range of about 20 to 30 kGy which is the important range for sterilization [8].

This dosimetry system has been studied to understand the influence of: ceric concentration, molar extinction coefficient, dilution factor of the sample and stability of the dosimetric solution before and after irradiation (diluted and un-diluted) [9]. The measurement of the cerous ion concentration is made in Pye Unicam 8600 spectrophotometer at wavelength of 320 nm.

3.1. Influence of ceric concentration

A stock solution was prepared of 100-mM ceric sulfate. From this stock solution were made ceric and ceric-cerous solution of 1.5 mM for the dose range of 0.6-5 kGy, and another one of 10 mM for the dose range of 5-40 kGy; the radiation yield value (G-value) is 2.32×10^{-7} and 2.26×10^{-7} $mol \cdot J^{-1}$, respectively.

For the 1.5-mM solution, the measured dose rate was 0.036 kGy/min (r=0.999) as compared to 0.035 kGy/min (r=0.997) determined by Fricke; this represents a relative error of 2.7 %, which agrees with the values reported in other papers [10].

For the 10-mM solution, the measured dose rate was 0.70 kGy/h (r=0.999) as compared to 0.715 kGy/h determined by the Fricke dosimeter; this represents a relative error of 2 %. Similarly, for the ceric-cerous solution, the estimated dose rate value was of 0.315 kGy/h while the value with Fricke was 0.318 kGy/h (r = 0.999) which represents a relative error of 0.9 %. This demonstrates that with high concentration values of ceric ions the system is more stable.

3.2. Influence of molar extinction coefficient

We have determined the ε values for the concentrations of 1.5 and 10 mM; these are 562.2 ± 4 and 564.5± 2 $m^2 \cdot mol^{-1}$ respectively. This represents a relative error of 0.6 % for the higher of the two values with relation to the value of 561.0 $m^2 \cdot mol^{-1}$ reported in the literature [11,12].

3.3. Dilution factor

Dilution of unirradiated and irradiated solutions is needed to bring the optical density within the measurement range of the spectrophotometer (0.04-0.2 mM). Dilution factors as high as 250 are reported [12], although we did not obtain good results with these values. By means of a study, dilution factors of 12.5 and 100 for the 1.5 and 10 mM concentrations were determined.

3.4. Stability before irradiation

With good preparation, clean glassware and an appropriate storage, the stock ceric solution is stable for six months and the solution of 10-mM concentration is stable for four months, in agreement with the reported values [10,13]. On the other hand, the stock ceric-cerous solution is stable for one year and its dilutions, 1.5 and 10 mM prepared immediately, showed a stability of eight months. Since ceric sulfate solution is sensitive to light, which is more significant at low concentrations, care should be taken to avoid errors in dosimetry by photo-reduction.

3.5. Stability after irradiation

Table V shows the variation in the evaluated dose values for the solution diluted immediately after the radiation process and the solution diluted at the time of measurement for different times. In the first case, a relative error of −14.2% could occur if measured after 24 hours, and this error increases with time. However in the second case, the error is less than 10% for one week and this value does not increase as quickly as in the first case. Besides, in the first case the dose value increases, while for the second case the dose value decreases with time.

TABLE V. VARIATION OF ABSORBED DOSE WITH MEASUREMENT TIME.

Measurement time	Solution diluted immediately after irradiation			Solution diluted at the time of measurement		
	Dose(kGy)	Variation coefficient	Relative error(%)	Dose(kGy)	Variation coefficient	Relative error(%)
Immediately	10.893 ± 0.104	0.0096	---	10.960 ± 0.212	0.0193	----
3 hours	11.613 ± 0.291	0.0250	- 6.1	10.746 ± 0.115	0.0107	1.9
24hours	12.696 ± 0.052	0.0041	-14.2	10.672 ± 0.035	0.0032	2.6
1 week	13.102 ± 0.104	0.0079	-16.86	10.084 ± 0.081	0.0080	7.9
2 week	13.357 ± 0.050	0.0037	-18.44	9.272 ± 0.062	0.0066	15.3
3 week	14.978 ± 0.052	0.0034	-27.27	9.274 ± 0.071	0.0076	15.3
4 week	17.002± ---	---	-35.93	8.023 ± 0.047	0.0058	26.7

4. ETHANOL-CHLOROBENZENE DOSIMETRY SYSTEM

We use ethanol-chlorobenzene dosimeters for routine control in radiation processing due to the following properties: appropriate accuracy, quick evaluation, dosimeter solution and dosimeters can be easily prepared and stored for a long time, and chemicals are inexpensive [14]. The evaluation of the absorbed dose is made by measuring the electrical conductivity of the irradiated solution in an oscillotitrator equipment, OK-302/2 type, at a frequency of 48 MHz.

The calibration curve was obtained by means of a regression analysis with the following functional dependence: $D\ (kGy)=a \cdot x^b$ for 2-40 kGy, and another of $D\ (kGy)= a + b \cdot x$ for 1-2 kGy, where a and b are coefficients and x is the deflection of the needle in the equipment. The dosimeters prepared in our laboratory were intercompared with the dosimeters supplied by the Institute of Isotopes of the Hungarian Academy of Sciences, where a good agreement was found. To study the effect of storage, a few dosimeters were stored for six months in dark at a temperature of 25±1 °C; the maximum variations of ±10 % with relation to the value measured immediately after irradiation were found [15] .

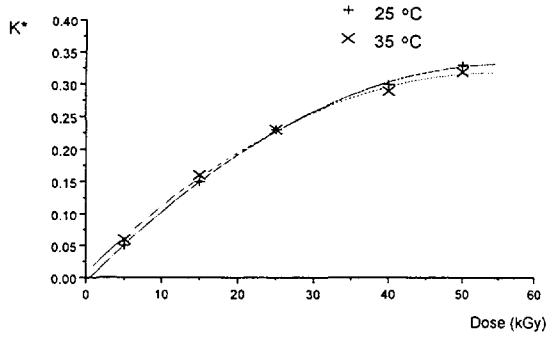

FIG. 1. Calibration curves of the Red Perspex irradiated at 27 °C. Storage temperatures are 25 and 35 °C (λ = 640 nm).

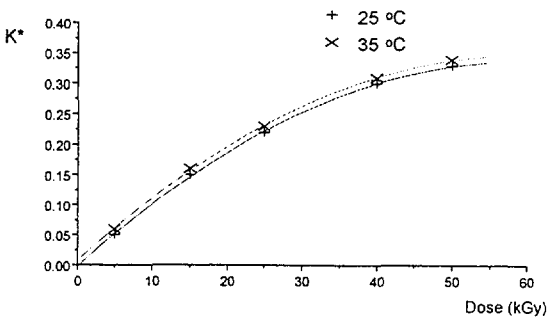

FIG. 2. Calibration curves of the Red Perspex irradiated at 40 °C. Storage temperatures are 25 and 35 °C (λ = 640 nm).

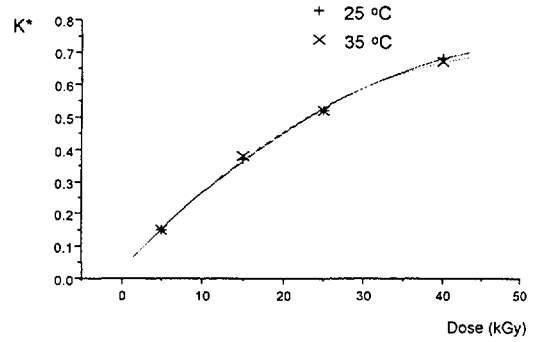

FIG. 3. Calibration curves of the Clear Perspex irradiated at 27 °C. Storage temperatures are 25 and 35 °C (λ = 315 nm).

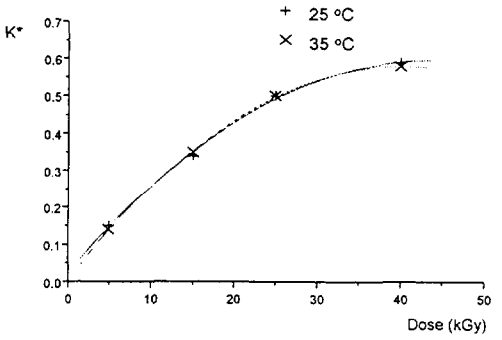

FIG. 4. Calibration curves of the Clear Perspex irradiated at 40 °C. Storage temperatures are 25 and 35 °C (λ = 315 nm).

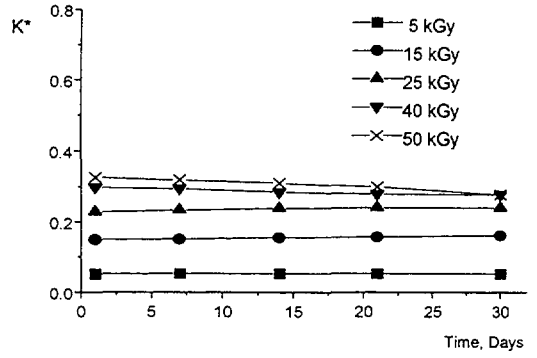

FIG. 5. Post-irradiation K variations for different absorbed dose values for the Red Perspex irradiated at 27 °C and stored at 25 °C (λ = 640 nm).*

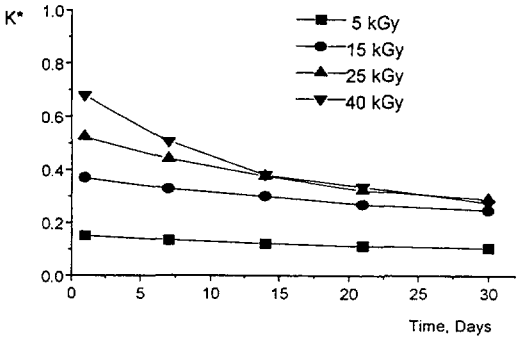

FIG. 6. Post-irradiation K variations for different absorbed dose values for the Clear Perspex irradiated at 27 °C and stored at 25 °C (λ = 315 nm).*

5. CUPRIC SULFATE DOSIMETRY SYSTEM

Cupric sulfate dosimeters have been employed for radiation process control of several products, but much less often compared to other dosimeters because of the instability of the dosimetric solution. For this reason, it is necessary to employ fresh solution for each irradiation [16]. The dosimeter was calibrated, using the Pye Unicam 8600 spectrophotometer and analysis wavelength of 305 nm, in the dose range of 1-8 kGy, where the following functional relation was obtained:
D(kGy)= 0.27 + 0.64 t(min), r=0.997, as well as good results for radiation process control.

6. PERSPEX DOSIMETERS (RED 4034 AE AND CLEAR HX)

The Perspex dosimeters are inexpensive, tissue equivalent, accurate and easy to handle, that can be used for industrial applications such as radiation sterilization of medical products and food irradiation [17].

The red Perspex dosimeters were irradiated for the dose range 5 – 50 kGy and the absorbance change was measured at 640 nm wavelength, while the clear Perspex dosimeters were irradiated between 5 – 40 kGy and the absorbance was measured at 315 nm. The irradiations were carried out at 27±1 and 40±1 °C. After irradiation, the dosimeters were stored at two temperature values (25 and 35 °C) [18]. Figures 1 and 2 show, for the red Perspex dosimeters, the relationship between the induced specific absorbance value (K*) and absorbed dose for irradiation temperature of 27 and 40 °C and different storage temperatures (25 and 35 °C), where it is observed that the behaviour is different. On the other hand, the results obtained with the clear Perspex HX (Batch No.7) dosimeters, as shown in Figs 3 and 4, show similar behavior for the two storage temperatures up to about 30 kGy; there is some influence of the storage temperature for higher dose values.

In Fig. 5, the variation of K* is presented for red Perspex dosimeter with relation to post-irradiation time for different absorbed dose values. It shows that K* decreases significantly for high dose values with time. However, for doses below 25 kGy, K* is reasonably stable over 30 days. The behavior of the clear Perspex dosimeters is shown in the Fig. 6, where the K* value decreases with time for all dose values investigated. This places a very severe restriction on the use of this dosimeter.

7. QUALITY ASSURANCE PROGRAMME

We have developed a Dosimetry Good Practice Manual which constitutes the first step for a Quality Assurance Program. This manual has the following aspects: dosimetry procedures, equipment control, laboratory techniques manual and reported results. It is very important for process control for our irradiation facility.

8. DOSE INTERCOMPARISON EXERCISES

We had participated in two dose intercomparison exercises in 1996, where ceric-cerous sulfate dosimeters were employed. One exercise was carried out at three different dose values in the range of 10-50 kGy with the Dosimetry Laboratory for Radiation Processing of Ezeiza Atomic Center, Argentina. They employed their silver/potassium dichromate dosimeters for this exercise. The minimum relative error between the two dosimetry systems was 4.4 % and the maximum error was 5.8%.The other intercomparison exercise was with the International Dose Assurance Service (IDAS) of the IAEA for two dose values using alanine dosimeter, where the relative errors were –1.77 and –2.85 %. This indicates that our dosimetry system is suitable and accurate for the measurement of medium and high doses.

9. CONCLUSION

The gained experience has allowed us during these years of work in Cuba to understand and characterise suitable and accurate dosimetry systems for the radiation process quality control. Also, we have developed appropriate methodologies to improve the available materials. Besides, we have studied the influence of different factors on the behaviour of the dosimeters for our conditions, which allow us to obtain more accuracy in the absorbed dose values.

REFERENCES

[1] PRIETO, E.F., CAÑET, F., LÓPEZ, R., Algunos factores que influyen en la determinación del coeficiente de extinción molar en el dosímetro Fricke, Tecnología Química, Año X, No. 3 (1989) 9-15.

[2] PRIETO, E.F., CAÑET, F., Aspectos a conciderar en el dosimetro Fricke, Tecnología Química, Año XI, No. 2 (1990) 19-28.

[3] HOLM, N., Dosimetry in radioesterilization of medical products. PhD Thesis. Danish AEC Research Establishment Riso, Denmark (1968).

[4] BRYANT, T.H.E., RIDLER, T.P., Health Physics, **15** (1968) 263.

[5] EGGERMONT, G., BUYSSE, J., JANSSENS, A., National and International Standardization of Radiation Dosimetry. Vol II, Vienna (1978) 317.

[6] FRICKE, H., HART, E.J., Chemical Dosimetry. Radiation Dosimetry. Vol II, Ed. Attix, Roesch, Tocholin. Academic Press, N.Y. and London (1966).

[7] KUME, T., TACHIBANA, H., TAKEHISA, M., Fricke Dosimetry in Low Dose Range for Sprout Inhibition. Radioisotopes, **30**, No. 10 (1981) 560-562.

[8] MATTHEWS, R.W., Effect of solute concentration and temperature on the ceric-cerous dosimeter. Radiation Research, **55**, No. 2 (1963) 242-255.

[9] PRIETO, E.F., El sistema dosimétrico sulfato cérico (cérico-ceroso). Desarrollo y aplicación en Cuba. Proceedings 4th Meeting on Nuclear Application, MG, Brazil (1997) 24.

[10] MATTHEWS, R.W., Use of Pre-irradiated solutions in Ceric Dosimetry, Int. J. Appl. Radiat. Isot. **33** (1981) 53-55.

[11] MATTHEWS, R.W., An evaluation of the ceric-cerous system as a impurity-insensitive Megarad Dosimeter, Int. J. Appl. Radiat. Isot. **22** (1971) 199-207.

[12] DRAGANIC, I.G., et al., Laboratory Manual for some High-Level Chemical Dosimeters. Riso. Report No. 22 (1961).

[13] MATTHEWS, R.W., Aqueous Chemicals Dosimetry. Int. J. Appl. Radiat. Isot. **33** (1982) 1159-1170.

[14] STENGER, V., et al., Long term experience in using the ethanol chlorobenzene dosimeter system. STI/PUB/846. IAEA, Vienna (1991) 277-288.

[15] DOMÍNGUEZ, L., et al., Aplicación del sistema etanol clorobenceno para dosimetría de altas dosis en la irradiación de alimentos. Informe Técnico. IIIA. C. Habana (1989).

[16] INTERNATIONAL ATOMIC ENERGY AGENCY, Manual of Food Irradiation Dosimetry. Tech. Report. Series No. 178, IAEA, Vienna (1977).

[17] CHADWICK, K.H., et al., The accuracy of the calibration curve of the Clear Perspex dosimeters. Food Preservation by Irradiation, Vol II, Vienna (1978) 327-334.

[18] PRIETO, E.F., CHÁVEZ, A., Efecto de la temperatura durante la calibración y el almacenamiento de los dosímetros Perspex (Red y Clear). Proceedings Int. Sym. on Nuclear and Related Techniques in Agriculture, Industry, Health and Enviroment. Cuba (1997).

THE IMPACT OF EUROPEAN STANDARDS CONCERNING RADIATION STERILIZATION ON THE QUALITY ASSURANCE OF MEDICAL PRODUCTS IN POLAND

I. KALUSKA, Z. ZIMEK
Department of Radiation Chemistry and Technology,
Institute of Nuclear Chemistry and Technology,
Warsaw, Poland

Abstract

The ISO 11137 and EN 552 standards were issued in the mid-90's. These documents have been devoted to the requirements regarding the sterile medical devices offered on the market. The implementation of those standards by Polish manufacturers of medical devices is discussed in this paper. The currently introduced national regulations effectively stimulated this process. The activities of the Institute of Nuclear Chemistry and Technology (INCT) in the field of radiation sterilization standardization and its radiation sterilization commercial service are described.

1. INTRODUCTION

Radiation sterilization has been applied at the Institute of Nuclear Chemistry and Technology (INCT) since 1973. Till today the only facilities in Poland, where the radiation sterilization is performed in a large scale commercial process, have been built in INCT. The radiation sterilization service was preceded by our investigation of the irradiation conditions (characteristics of the electron beam i.e. beam energy, average beam current, scan width and scan uniformity, conveyor speed) [1] and evaluation of the ionizing radiation dose to obtain sterile medical devices [2]. Our activities in the 80's were supported by the IAEA (through the regional training courses) and based on the AAMI guidelines. After some years of experience, the procedures were written and they became the basis upon which the radiation sterilization process has been carried out. Standardization of the radiation sterilization process in Poland has been initiated recently. This effort is also led by the members of the INCT staff.

2. REGULATORY DOCUMENTS

Our internal procedures were for a long time adequate for us as the contractor and for our customers, but in the mid-90's the international standards concerning radiation sterilization were published (ISO 11137 [3] and EN 552 [4]). It significantly influenced our activity. Also our customers have started to demand service in accordance with these international regulations. All medical devices which are being marketed in Europe must comply with the Medical Device Directive (MDD) [5] and display the CE mark since June 14th 1998. The CE mark provides the assurance to the patients and the users that the products perform as intended by the manufacturer and they are safe when used as intended. The CE mark must be placed visibly, legibly and indelibly not only on all devices or their packaging, but also on the instructions for use and sale packaging. Since the CE mark is mandatory in the countries belonging to Common Market, the Polish products must have the CE mark when they are sold in Western Europe. There are also known examples that some importers from non European Community countries require this mark on Polish products, even if this is not needed by law in both countries. The new regulations have stimulated the effort towards process certification and changed the attitude of the staff at all levels to the quality of the service.

The basic requirement for all sterile products is that they are safe for use according to MDD. It is not related to a specific definition of sterility. It may be SAL of 10^{-6}, 10^{-3} or any other level. The label 'sterile' means that there is no risk of infection from the prospective of the users (physicians or patients). In addition, the process of achieving SAL of 10^{-6} is not defined as the method for obtaining a

safe product. The dose required to achieve SAL of 10^{-6} can cause in some cases the material to become brittle, and therefore unsafe for use.

Most medical device manufacturers have adopted a quality system based on EN 46001 or EN 46002, but in addition they must incorporate the requirements of MDD into their procedures. The link between EN 46000 and the MDD is clarified in the note within the clause 4.2.1 of EN 46001, which states that "if this European standard is used for compliance with regulatory requirements, the relevant requirements of the regulations should be included in the specified requirements". Therefore, a Notified Body will require a manufacturer to meet the requirements of the MDD as well as those of EN 46000 before the CE mark is used.

Sterilization is viewed by EN 46000 and the MDD as a high-risk special process which requires validation. The wide use of the harmonized standards, EN 550, EN 552 and EN 554, to show the conformance to the essential requirements also implies that the control and validation techniques must yield the same level of assurance as the harmonized standards, although the standards are not mandatory. Therefore, it became obvious to the INCT staff and our customers that sterilization which has not been validated or when updated procedures or processes have not been used, this may lead to major non-compliance and delay in CE-marking; that was also observed in UK [6]. When a subcontractor is used for a critical process, it is essential that the controls are the same as those for the processes carried out at the manufacturer's site.

Many medical devices manufactures already follow Good Manufacturing Practice (GMP). Also, several ISO 9000 procedures have been applied, in particular, document control, inspection and testing, calibration and most process controls. The manufacturers should follow the procedure of assessing compliance of the products to different standards. These include the standards dealing with validation of the sterilization processes. In the case of radiation sterilization there are two basic documents ISO 11137 [3] and EN 552 [4].

There is only one major difference between these two standards - the definition of sterility. CEN allows only the level of 10^{-6} for the probability of finding a viable microorganism on a sterilized product. Thus, according to EN 556 [7], which describes the requirements for medical devices to be labeled sterile, the product is sterile only when the sterility assurance level (SAL) of 10^{-6} is achieved. On the other hand, ISO supports the notion of dual SALs for sterile health care product depending on the product use: SAL of 10^{-3} for topically applied medical devices and SAL of 10^{-6} for implantable devices. It should mean from a product point of view that there is no risk of infection when the patient uses the product. Based on this definition, ISO 11137 declares a product sterile with SAL of 10^{-6} or 10^{-3}, depending on its use.

The standards concerning radiation sterilization appeared in the mid 90's. These standards give the guidelines on how the validation and the routine control of sterilization using ionizing radiation should be performed. Taking into account already mentioned requirements and different regulations about sterility, it was necessary to establish our national regulations concerning radiation sterilization. Polish Committee of Standardization (PCS) has decided that a Polish representative would participate in ISO/TC 198 Working Group 2 concerning Radiation Sterilization as an observer to have a world wide perspective of the field. The Standardization Working Group for Sterilization, Disinfection and Antiseptics, with the above-mentioned observer as one of the members, has been appointed. Although ISO 11137 covers wider range of products which can be sterilized by radiation and that its implementation would be less expensive than EN 552, it was decided that the Polish translation of EN 552 would become our national standard. The main reason for selecting EN 552 as a Polish standard was our membership in the European Union. This standard has already been translated into Polish and is under the standardization process in PCS. EN 552 provides two approaches for establishing the sterilization dose to achieve compliance with EN 556 and hence provide a SAL of 10^{-6}:

- selection of the sterilization dose capable of achieving compliance with EN 556 by identifying the number of the innate microbial population present on or in the medical devices and its resistance to radiation, or
- the product is treated with a minimum dose of 25 kGy [8].

In the second case, the manufacturer must substantiate the effectiveness of 25 kGy as a sterilization dose. This is a new requirement; in the past, 25 kGy was generally accepted as adequate for the purpose of sterilization and no further investigations were needed. For both approaches, the manufacturer must have an access to a microbiology laboratory.

3. VALIDATION OF RADIATION PROCESS AT INCT

Till now the Polish Authority responsible for the medical devices distribution allows only the traditional approach; the product has to be treated with the minimum dose of 25 kGy. It is obvious that such an approach increases the costs for the manufacturer and decreases the INCT sterilization capacity.

The main issues that need to be resolved are the validation procedure and the traceability of the product. If the manufacturer follows the standardized methods for sterilization validation, the required calculation and the appropriate statistics are automatically considered. If the validation is followed in this way, the sterilization process will result in a sterile product [9]. The traceability of the irradiated product being sterilized is achieved at INCT by through computer that records the data of the irradiation parameters. Special software was designed by the INCT staff to automatically collect the values of the parameters, such as the beam current, energy and conveyor speed, and the data about the customer and product are also entered. The data are printed on the label which is put on each sterilized package. Also, routine dosimeters used during processing are kept for the period of the shell-life of the product.

The release of the radiation-sterilized products relies on dosimetry. Therefore, it is important for our customers that we have dosimetry procedures well documented. Different types of dosimeters are available. Their responses are traceable to national or international standards [10]. The polystyrene calorimeters and the aluminum-wedge energy measurement device were purchased from the High Dose Reference Laboratory (Riso National Laboratory, Denmark) as reference instruments.

The validation of sterilization process also involved much paper work. In the past, many procedures were done without documentation or were not documented properly. At INCT, much effort was placed for changing the attitude of the staff towards establishing the validation process. They had to understand the importance of following the procedures strictly and for documentation. We have organized internal training for all levels of employees to achieve this. Those efforts are still on going. We have established internal audits to ensure that we meet requirements for validation. They also help us to improve our sterilization process procedures. Finally, we validated our sterilization process in the middle of this year. We are aware that it is a 'never ending story'. The manufacturers of the medical devices increase their investment in validation each year; this means that INCT must revise and upgrade the existing instructions and procedures. It will allow us to be in accord with the requirements of EN 552 and have our process of radiation sterilization really validated and in control.

4. CONCLUSIONS

Today we can say that 25 years of INCT activity in radiation sterilization has been very fruitful. Polish manufacturers of medical devices can compete with the products from all over the world. Still much effort must be put to achieve a full compliance with EN 552.

REFERENCES

[1] BULHAK Z., KOLYGA S., PANTA P., STACHOWICZ W., Fifteen years of experience in the sterilization of medical products with the linear electron accelerator LAE-13/9, Radiat. Phys. Chem., Vol.**34**, No.3 (1989) 395-397.

[2] CZERNIAWSKI E., STOLARCZYK L., Attempt to establish the ionizing radiation dose to be used in the sterilization of one-use medical equipment units, Acta microbiologica polonica, Series **B6** (1974) 177-83.

[3] ISO 11137, Sterilization of health care products – Requirements for validation and routine control – Radiation sterilization, (International Organization for Standardization, Geneva, Switzerland), 1995.

[4] EN 552, Sterilization of medical devices - Validation and routine control of sterilization by irradiation (CEN, European Committee for Standardization, Brussels, Belgium), 1994.

[5] Council Directive 93/42/EEC of 14 June 1993 concerning medical devices, Official Journal of the European Communities, No.L 169, 12 July 1993.

[6] JEPSON CH., Achieving the CE mark: Getting it right first time, Medical Device Technology, Vol.**8**, No.7 (1997) 16-19

[7] EN 556, Sterilization of medical devices - Requirement for terminally sterilized devices to be labeled sterile (CEN, European Committee for Standardization, Brussels, Belgium), 1995.

[8] RICHARDS S., EN 552: Validating 25 kGy as a sterilization dose, Medical Device Technology, Vol.7, No.6 (1996) 22-25.

[9] WINCKELS H.W., DORPEMA J.W., Risk assessment a basic for the definition of sterility, Medical Device Technology, Vol.5, No.9 (1994) 38-43.

[10] MEHTA K., KOVACS A., MILLER A., Dosimetry for quality assurance in electron-beam sterilization of medical devices, Medical Device Technology Vol.4, No.4 (1993) 24-29.

PERFORMANCE OF DICHROMATE DOSIMETRY SYSTEMS IN CALIBRATION AND DOSE INTERCOMPARISON

XA9949744

E.S. BOF, E. SMOLKO
Comisión Nacional de Energía Atómica,
Centro Atómico Ezeiza,
Buenos Aires, Argentina

Abstract

This report presents the results of the High Dose Dosimetry Laboratory of Argentina during ten years of international intercomparisons for high dose with the International Dose Assurance Service(IDAS) of the IAEA, using the standard high dose dichromate dosimetry system, and the results of a high dose intercomparison regional exercise in which our Laboratory acted as a reference laboratory, using the standard high dose and low dose dichromate dosimetry system.

1. INTRODUCTION

To promote the application of radiation processing in environmentally sustainable industrial development, it is very important to have the knowledge of process control in accordance with the international standards. In this context high dose dosimetry is fundamental in industrial applications of radiation technology. Irradiation facilities management are expected to give evidence of accurate and precise dose in the products they have to treat. For that purpose, the traceability of the dose measurements whereby, it can be related to appropriate standards, generally international, through an unbroken chain of comparisons must be encouraged [1]. In the present work we show the results of the dichromate dosimetry systems obtained by the High Dose Dosimetry Laboratory of Argentina, using the high dose dichromate systems (HDDS) and the low dose dichromate systems (LDDS) in two different experiments:

- A. Participation in the International Dose Assurance Service (IDAS) of the IAEA.
- B. Participation in a High Dose Intercomparison Regional Exercise.

2. MATERIALS AND METHODS

2.1 Dosimetry Systems

The High Dose Dosimetry Laboratory of Argentina uses the following dosimetry systems:

- Fricke as a reference standard dosimeter for the dose range 30 to 400 Gy.
- low dose dichromate dosimeter as a transfer standard dosimeter for the dose range 1 to10 kGy.
- high dose dichromate dosimeter as a transfer standard dosimeter for the dose range 10 to 50 kGy.
- Potassium Nitrate, dry dosimeter for routine irradiation at extreme temperatures and for the dose range 10 to 50 kGy.

All the dosimeters we use are prepared in our laboratory according to the Refs [2, 3, 4], respectively.

2.2. Apparatus

- The absorbance measurements are obtained using a Beckman Model 25, Double Beam UV-V (Wavelength range 190-700 nm) Spectrophotometer and quartz cuvettes 1-cm path length.
- Mettler H35, Analytical balance.
- Glassware, Borosilicate glass

2.3. Reagents

- All reagents we use are Merck, analytical reagent grade, except Silver Dichromate 99% from Pfaltz & Bauer,
- Three-times distilled water, conductivity 0.7 μS is obtained using single distillation apparatus, Rolco 81 and Quartz double distillation apparatus, Heraeus Bi-18

2.4. Calibrations

- The spectrophotometer wavelength calibration is performed using a Standard holmium-oxide filter. The spectrophotometer absorbance calibration is done using NIST SRM 2031a metal on quartz filters.
- he Analytical balance is calibrated periodically, according to Mettler Standards.

2.5. Methods

2.5.1. Experiment A

Our high dose gamma radiation dosimetry system has been checked since 1986 by the International Dose Assurance Service (IDAS) of the IAEA; their calibration is traceable to a Primary Standard Dosimetry Laboratory (NPL in U.K.). The IAEA sends us periodically alanine dosimeters; we irradiate our dichromate dosimeters and the IAEA alanine dosimeters together in a PMMA phantom specially designed for that purpose and monitor the irradiation temperature with a thermocouple. The intercomparison with IDAS are carried out at the semi-industrial irradiation facility. The irradiation room dimensions are 12 m x 6 m, the Co-60 source dimensions are 90 cm high and 150 cm wide, and the phantom dimensions are high 6 cm, length 20 cm an wide 2.8 cm. It is located on a special aluminium device, 60 cm away from the source and at its geometrical center (see Fig.1).

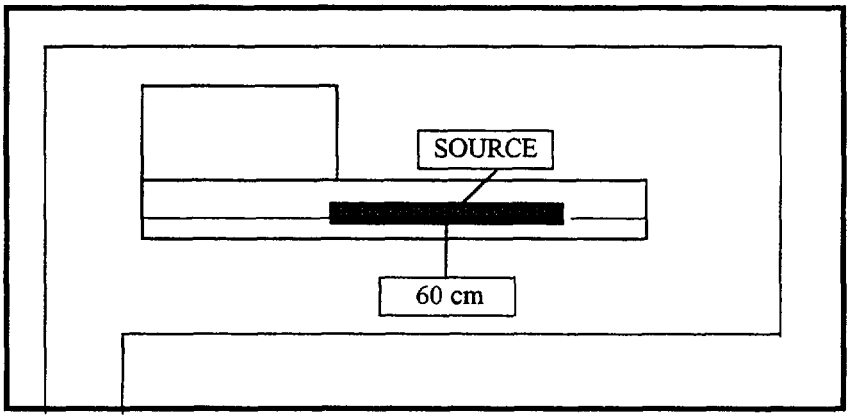

FIG. 1. Irradiation geometry.

2.5.2. Experiment B

Our laboratory organised the high dose intercomparison regional exercise which was carried out during the Regional Workshop on High Dose Dosimetry and Process and Quality Control in Industrial Radiation Processing, held at Buenos Aires during 22 to 26 July 1996, and in which our laboratory acted as the Reference Laboratory. The following countries participated in this exercise employing their own dosimeters: Brazil, Chile, Colombia, Cuba, Ecuador and Austria (IAEA).

3. TRACEABILITY

Our traceability is to:
- Primary Laboratory N. P. L. (U. K.) using calorimeter or Fricke
- Primary Laboratory N. P. L.(U. K.) using dichromate for Co-60 gamma field
- Laboratory I.A.E.A. (Austria) using alanine and High Dose Laboratory (Argentina) using dichromate and Fricke

Also our Laboratory is reference for:
- the irradiation plant at CNEA (Argentina), that uses Perspex Red-Amber as routine dosimeters
- the private irradiation plant Ionics (Argentina) that uses Perspex Red-Amber as routine dosimeters
- a mobile irradiator that uses Fricke
- blood irradiators that use Fricke
- Gammacell 220 that uses Fricke.

4. RESULTS

The results of the Experiment A are given in Table I.

TABLE I. TEN YEARS OF DOSE INTERCOMPARISONS BY IDAS

Year	Source Activity (kCi)	Estimated Irr. Temperature (°C)	IAEA Estimated Dose Alanine (kGy)	CNEA Estimated Dose HDDD (kGy)	Relative Deviation (%)
1986	243	25	25,2	25,35	0,60
1987	213	25	23,5	23,54	0,17
1990	500	22	24,40	24,51	0,45
1992	340	30	24,24	24,00	0,97
1993	290	30	23,46	23,41	0,23
1994	410	44	24,32	24,92	2,46
1996	340	35	26,44	25,67	2,93
1997	277	30	26,56	26,60	0,15

The source activity and the estimated irradiation temperature are shown in columns 2 and 3. The estimated dose of high dose dichromate dosimeter at CNEA and the corresponding estimated dose given by IDAS alanine dosimeter are shown in columns 4 and 5. Both estimated doses are corrected for the irradiation temperature. The relative deviation of the two estimated doses are given in column 6.

The results of the Experiment B are given in Table II and Table III.

TABLE II. COMPARATIVE ESTIMATED DOSES BETWEEN DIFFERENT DOSIMETRY SYSTEMS EMPLOYED BY PARTICIPATING COUNTRIES AND THE CNEA HDDD SYSTEM TAKEN AS REFERENCE FOR THE DOSE RANGE 10 kGy - 50 kGy

Country	$K_2 Cr_2 O_7$ - $Ag_2 Cr_2 O_7$ Dosimeter (HDDD) Estimated Dose (kGy)	Dosimeter Country Estimated Dose (kGy)	Relative Deviation (%)
1	15.17 (3)	15.00	1.2
	25.46 (3)	25.00	1.8
2	25.24 (3)	23.60	6.5
	28.55 (3)	27.40	4.0
3	14.39 (2)	15.02	4.4
	28.75 (2)	30.15	4.9
	42.80 (2)	45.27	5.8
4	27.48 (6)	23.70	13.7
5	24.38 (6)	21.07	13.6
6	11.91 (1)	10.00	16.0

TABLE III. COMPARATIVE ESTIMATED DOSES BETWEEN DIFFERENT DOSIMETRY SYSTEMS EMPLOYED BY PARTICIPATING COUNTRIES AND THE CNEA LDDD SYSTEM TAKEN AS REFERENCE FOR THE DOSE RANGE 1 kGy - 10 kGy.

Country	$Ag_2 Cr_2 O_7$ (LDDD) Dosimeter Estimated Dose (kGy)	Dosimeter Country Estimated Dose (kGy)	Relative Deviation (%)
1	3.01 (3)	3.00	0.33
	8.07 (3)	8.00	0.87
2	4.59 (6)	4.60	0
3	1.87 (2)	2.04	9.1
	4.64 (2)	4.85	4.5
	7.61 (2)	8.54	12.2
4	6.59 (6)	7.07	7.3
5	6.36 (6)	5.71	10.2
6	1.11 (1)	1.00	9.9

5. CONCLUSIONS

Experiment A - In column 6 of Table I, the relative deviation of the two estimated doses are given, where it has been observed that the relative deviations are less than 3% in all the cases, but within 1% in 75 % of the experiments.

Experiment B -The regional intercomparison exercise showed that about 50 % of the cases were well within 5% of the relative deviation .

We conclude that experiments A and B showed a good behaviour for the dichromate dosimetry system. More than ten years of experience in this field show, in our opinion, that a simple, reliable cheap and outstanding dosimetry system, **the dichromate dosimetry systems,** can be adopted without losing accuracy and reproducibility for the industrial dose radiation applications.

REFERENCES

[1] McLAUGHLIN, W.L. et al (1989). Dosimetry for Radiation Processing. Taylor & Francis, London pp 81 - 87.

[2] FRICKE, H. and HART, E. J. (1966). Chemical Dosimetry. In Radiation Dosimetry, Vol II. Attix and Roesch, (New York: Academic Press), Chapter 12.

[3] SHARPE, P. H. G. (1996). ASTM Standard E 1401 (Draft). Dosimetry for Radiation Processing, Progress Report 40, pp 49 - 62, February 29, 1996.

[4] DORDA, E. M. et al (1984). Potassium Nitrate Dosimeter for High Dose. IAEA, Austria, SM 272 / 1) pp 193 - 202, (1984).

[5] BOF E. S. and E. E. SMOLKO (1997). Ejercicio Regional de Intercomparación de Dosimetría de Altas Dosis, International Symposium on Nuclear and Related Techniques in Agriculture, Industry, Health and Environment. Havana, Cuba.

DOSE INTERCOMPARISON STUDY INVOLVING FRICKE, ETHANOL CHLOROBENZENE, PMMA AND ALANINE DOSIMETERS

L.G. LANUZA, E.G. CABALFIN
Philippine Nuclear Research Institute,
Quezon City, Philippines

T. KOJIMA, H. TACHIBANA
Takasaki Radiation Chemistry Research Establishment,
Japan Atomic Energy Research Institute,
Takasaki, Japan

Abstract

A dose intercomparison study was carried out between the Philippine Nuclear Research Institute (PNRI) and Takasaki Radiation Chemistry Research Establishment, Japan Atomic Energy Research Institute (JAERI) to determine reliability of the dosimetry systems being used by PNRI employing ethanol chlorobenzene (ECB), Fricke and alanine dosimeters. The Fricke and ECB dosimeters were prepared at PNRI while the alanine-polystyrene dosimeter was provided by JAERI. Fricke or ECB dosimeters were irradiated together with alanine at PNRI gamma irradiation facilities. Analyses of the Fricke and ECB dosimeters were performed at PNRI while alanine dosimeters were analyzed at JAERI. A comparison study between alanine and polymethylmethacrylate (PMMA, Radix RN15) dosimeters was also undertaken at JAERI. The dosimeters were irradiated together under different irradiation conditions using the gamma irradiation facilities of JAERI and Radia Industry Co. Ltd. (Japan). Evaluations of PMMA and alanine dosimeters were both performed at JAERI. Result of the dose intercomparison of PNRI with the International Atomic Energy Agency through the International Dose Assurance Service (IDAS) is also presented.

1. INTRODUCTION

The Philippine Nuclear Research Institute (PNRI) with the technical assistance of the International Atomic Energy Agency (IAEA) has set up a pilot scale multipurpose gamma irradiation facility to introduce and demonstrate radiation technology to the local industry. The facility was commissioned in 1989 with an initial loading of about 1 PBq ^{60}Co [1]. To increase the capacity of the facility, additional ^{60}Co were loaded in 1993 and in 1996. At present, the total ^{60}Co loading of the facility is about 4.4 PBq.

The batch type irradiator, a Gammabeam 651PT from Nordion International Co. Ltd., is designed for research and pilot scale studies. Effectively, the source configuration can be considered as a plane or source plaque, 112 cm wide by 140 cm high.

The availability of the irradiation facility has opened the door for the local industries to become aware of radiation sterilization, radiation decontamination and food irradiation. Though still in a limited scale, some local industries are now using radiation for the sterilization or decontamination of their products, such as empty aluminum tubes, empty gelatin capsules, orthopedic implants, spices and dehydrated vegetables.

Radiation processes like sterilization of medical products and food irradiation are directly concerned with public health and safety. Dosimetric control of these processes has implications for the

regulatory acceptance of the irradiated product [2]. In other radiation processes, it is used to confirm the reliability of the process and quality assurance of the irradiated product. Dosimetry combined with control of operational parameters will give satisfactory assurance that each process is carried out such that the minimum dose received by the product will give the desired effect, while the maximum dose will not have adverse effect on the product.

An informal dose intercomparison study was carried out between PNRI and Takasaki Radiation Chemistry Research Establishment (TRCRE), Japan Atomic Energy Research Institute (JAERI) to check the reliability of the dosimetry systems at PNRI. The dosimeters used in the study were Fricke, ethanol chlorobenzene (ECB) and JAERI alanine dosimeters. A comparison between JAERI alanine and polymethylmethacrylate (PMMA) dosimeters was also undertaken while one of the authors was undergoing an on-the-job training at JAERI.

PNRI has also participated in the International Dose Assurance Service (IDAS) of IAEA.

2. EXPERIMENTAL PROCEDURES

2.1. Preparation of dosimeters

The dosimeters being used at PNRI for food irradiation and radiation sterilization and decontamination are Fricke and ECB. Both dosimeters are prepared at PNRI.

ECB dosimeter [3] consisted of an alcoholic solution of monochlorobenzene. The solution contained 24 vol% monochlorobenzene, 4 vol% water, 0.04 vol% acetone, 0.04 vol% benzene and 71.92 vol% absolute ethanol. The ECB solution was flame-sealed in 2-ml borosilicate glass ampoules (10 mm diameter, Ampullagyar, Type 2) obtained from Hungary.

Fricke dosimeter containing 1×10^{-3} mol·L^{-1} ferrous ammonium sulfate and 1×10^{-3} mol·L^{-1} sodium chloride in 0.4 mol·L^{-1} sulfuric acid was prepared according to standard procedures [4]. Polyethylene vials (15 mm diameter and 55 mm length) were filled with the Fricke solution just before irradiation. Before using the vials, they were conditioned by irradiating them filled with the dosimetric solution.

Alanine-PS dosimeter [5], commercially known as Aminogray, was developed by Hitachi Cable Ltd. in cooperation with JAERI. This dosimeter was molded from a mixture of 70 wt% DL-α-alanine and 30 wt% polystyrene into 3 mm diameter by 30 mm length. Each dosimeter is sealed in a polystyrene case (12 mm diameter and 40 mm length and 4 mm thick wall).

Clear PMMA dosimeters, Radix RN15, are manufactured by Radia Industry, Co. Ltd. Radix, in its commercially available form (40×10×1.5 mm in size) is sealed under conditions of 25 °C and 40% relative humidity in aluminum-coated PE pouches [6]. The outside dimensions of the pouch are 20x50 mm. The optical density of the unirradiated dosimeters was measured at 314 nm using a UV spectrophotometer. The dosimeters were sandwiched between 3 mm of used PMMA dosimeters to achieve approximate electron equilibrium conditions during irradiation.

2.2. Irradiation and calibration of dosimeters

2.2.1. Comparison between Fricke, ECB and JAERI alanine dosimeters

In this intercomparison, Fricke or ECB dosimeters were irradiated together with alanine dosimeters from JAERI in a Gammacell 220 (9.1 TBq ^{60}Co), a self-shielded gamma irradiator from Nordion International Co. Ltd. or in the Gammabeam 651PT irradiator.

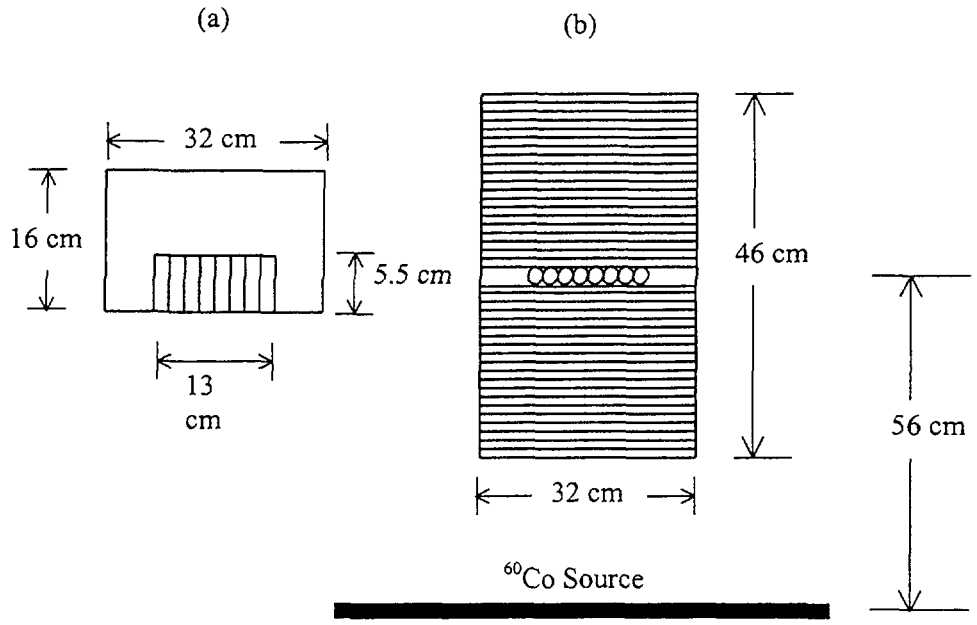

FIG.1. Irradiation setup using Gammabeam 651PT: (a) frontview and (b) topview

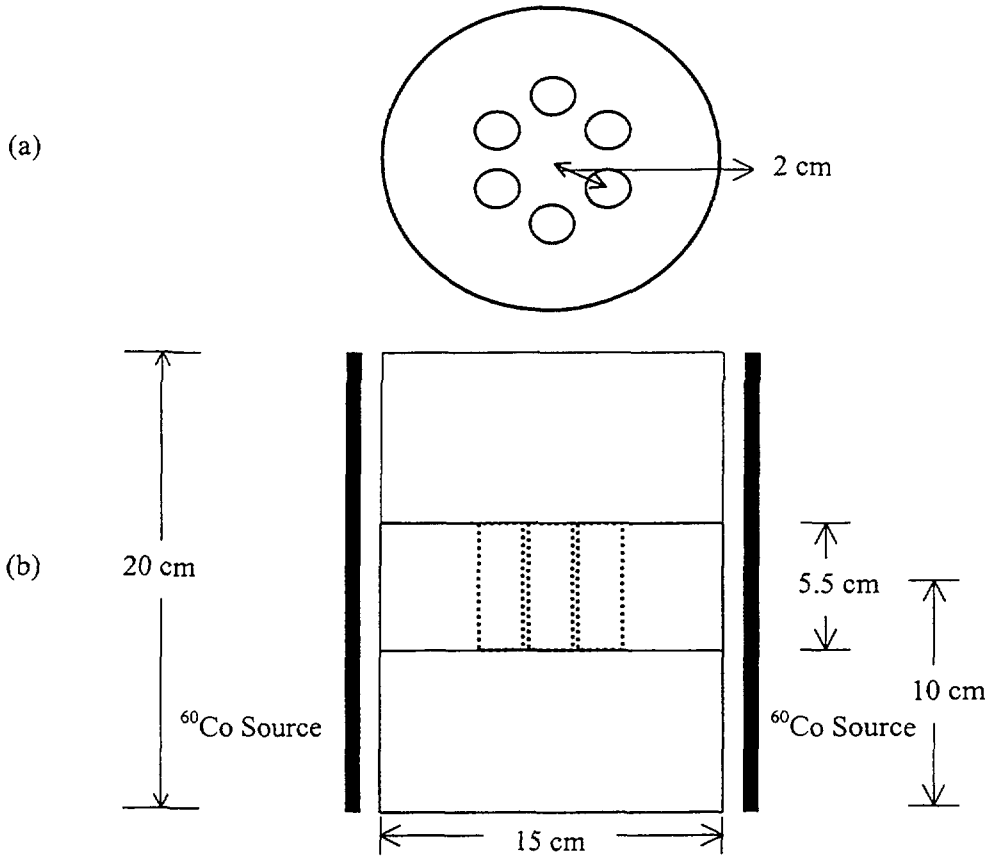

FIG. 2. Irradiation setup using Gammacell 220: (a) topview and (b) frontview

When using the Gammabeam 651PT, the dosimeters were placed at the center of a product box, 46 cm×32 cm×16 cm, containing dummy products having a density of about 295 $kg \cdot m^{-3}$. Dosimeters were placed at the center of the box as shown in Fig. 1. The variation of dose in this position is within ±1 %. The product box was placed at the centerline of the source plaque, 56 cm from the source and 73 cm from the floor.

For irradiation using Gammacell 220, the dosimeters were placed in the center of a cylindrical polystyrene container with a diameter of 15 cm and a height of 20 cm. Dosimeters were placed in six positions 2 cm from the central axis and 10 cm from the bottom (Fig. 2). The variation of dose in these six positions is within ±1 %.

The Gammacell 220 is also used for calibration of ECB dosimeter. The dose rate at the calibration position was determined using Fricke dosimeter. ECB dosimeters were irradiated at the calibration position of the Gammacell 220 to at least five known doses. Three dosimeters were irradiated at each dose. The relationship of the absorbed dose versus the oscillotitrator reading is fitted using a third order polynomial.

2.2.2. Comparison between alanine and PMMA (Radix RN15) at JAERI

Radix RN15 (Batch 3) and alanine dosimeters were irradiated together under different irradiation conditions in the gamma irradiation facilities of JAERI and Radia Industry Co. Ltd. Two boxes measuring 40 cm×34 cm×40 cm filled with dummy products with density of 220 $kg \cdot m^{-3}$ were used. Fifteen packets containing alanine and PMMA dosimeters were placed in each box as shown in Fig. 3. Stationary irradiation was done at TRCRE (5.8 PBq ^{60}Co). The box was rotated at half the irradiation time. Irradiation using conveyor was done at RIC-2 facility of Radia Industry Co. Ltd. (36.6 PBq ^{60}Co).

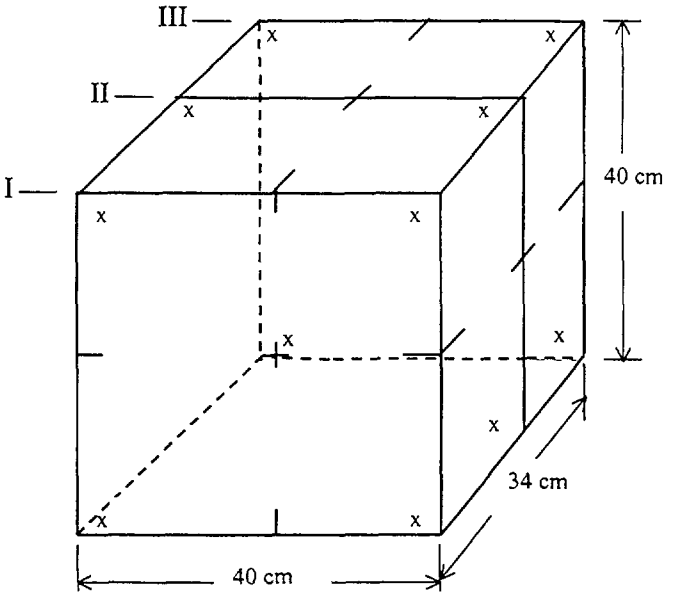

x– packets of dosimeters containing alanine and PMMA

FIG.3. Position of dosimeters in dummy product box

2.3. Measurement

Fricke and ECB dosimeters were measured in PNRI while alanine and PMMA dosimeters were measured in JAERI. The absorbance of Fricke dosimeters were measured immediately after irradiation at 304 nm using a Jasco Model 7800 UV-VIS double beam spectrophotometer. The wavelength and absorbance scale of the spectrophotometer were periodically checked using holmium oxide glass filter and absorbance standards (Pye Unicam Ltd.), respectively. The bandwidth of the spectrophotometer is 2 nm. The response of the ECB dosimeters was measured using a high frequency oscillotitrator, Radelkis OK 302/1 from Hungary.

The optical density at 314 nm of the PMMA dosimeters was measured immediately after irradiation using a Hitachi UV spectrophotometer, Model 220A. Before irradiation the optical density of the unirradiated PMMA dosimeters was also measured at 314 nm. The thickness of the dosimeter was measured using a Mitutuyo digimatic micrometer, HDC series 293 [6]. JAERI alanine dosimeter was measured using a compact ESR spectrometer, JEOL, Model JES 3000S [5].

2.4. Intercomparison with IDAS

ECB or Fricke dosimeters, prepared at PNRI, were irradiated together with alanine dosimeters provided by the International Dose Assurance Service (IDAS) of IAEA [7] using the Gammabeam 651PT irradiator. The positions of the dosimeters during irradiation were as described earlier. After irradiation, the response of the Fricke and ECB dosimeters was measured at PNRI. The results of the absorbed dose measurement were sent to IAEA together with the irradiated alanine dosimeters for analysis and evaluation.

3. DISCUSSION OF RESULTS

3.1. Comparison between Fricke, ECB and JAERI alanine dosimeters

The result of the intercomparison between Fricke and JAERI alanine is shown in Table I. The average ratio between dose determined by Fricke (PNRI) to that determined by alanine (JAERI) dosimeters was 0.948. These results showed that on the average, the PNRI Fricke dosimeter give an absorbed dose about 5% lower than that obtained by JAERI alanine. An intercomparison [8] with the National Physical Laboratory (NPL), Teddington, U.K., showed that the JAERI alanine agreed with NPL measurement to within ±2%. It should be mentioned that dose measured by JAERI alanine lay within ±2% that of IDAS alanine.

TABLE I. DOSE INTERCOMPARISON BETWEEN FRICKE (PNRI) AND ALANINE (JAERI)

	PNRI Fricke (kGy)[a]	JAERI Alanine (kGy)[a]	Ratio PNRI/JAERI
1990	0.218	0.228	0.956
1991	0.202	0.218	0.927
1993	0.222	0.226	0.982
	0.057	0.060	0.950
	0.098	0.106	0.924
	0.200	0.212	0.943
	0.297	0.314	0.946
	0.395	0.425	0.929
1994	0.123	0.126	0.976
Average			0.948
SD			0.021

[a] absorbed dose in water

Table II shows the result of the intercomparison between ECB (PNRI) and alanine (JAERI). On the average, the ratio of absorbed dose determined by PNRI ECB to that determined by JAERI alanine dosimeter was 1.00.

TABLE II. DOSE INTERCOMPARISON BETWEEN ECB (PNRI) AND ALANINE (JAERI)

	PNRI ECB (kGy)[a]	JAERI Alanine (kGy)[a]	Ratio PNRI/JAERI
1990	17.73	17.34	1.02
1991	11.70	12.00	0.98
	32.20	32.40	0.99
1996	1.00	1.04	0.96
	5.05	5.13	0.98
	14.96	14.72	1.02
	24.64	23.45	1.05
	34.10	33.30	1.02
	48.83	49.98	0.98
Average			1.00
SD			0.03

[a] absorbed dose in water

3.2. Comparison between alanine and PMMA (Radix) at JAERI

The intercomparison between PMMA (Radix) and JAERI alanine dosimeters showed that the average ratio of dose determined by Radix to dose determined by alanine dosimeters using stationary irradiation was 1.01 while the ratio using conveyor irradiation was 1.02 as shown in Table III. There is good agreement between the results using stationary and conveyor irradiation although geometry conditions and irradiation parameters (dose rate, source to product distance, source activity, etc.) in JAERI and Radia Industry, Co. Ltd. are different.

TABLE III. COMPARISON BETWEEN PMMA AND ALANINE DOSIMETERS USING STATIONARY AND CONVEYOR IRRADIATION

Irradiation Condition	Ratio [a] PMMA/Alanine
Stationary Irradiation	1.01 ± 0.02
Conveyor Irradiation	1.02 ± 0.02

[a] average of 30 dosimeters

3.3. Intercomparison with IDAS

The results of the intercomparison with IDAS are shown in Table IV. The results from 1989 to 1998 showed that dose measured by PNRI Fricke agreed to within ±1.7% of the IDAS estimated dose. On the other hand, results obtained from PNRI ECB were in agreement within ±4.4% that of alanine of IDAS.

TABLE IV. RESULTS OF INTERCOMPARISON WITH IDAS

	Dosimeter	PNRI Nominal Dose (kGy)	IDAS Estimated Dose (kGy)	Deviation (%)
1989	ECB	14.50	13.80	5.07
	Fricke	0.2147	0.2095	2.48
1990	ECB	12.3	11.8	4.24
	Fricke	0.16311	0.161	1.31
1991	ECB	20.45	19.4	5.41
	Fricke	0.214	0.216	-0.93
1993	ECB	6.00	5.701	5.24
	ECB	26.32	24.958	5.46
1994	ECB	26.9	25.83	4.14
	Fricke	0.2	0.2047	-2.3
1995	ECB	24.47	25.13	-2.63
	Fricke	0.203	0.207	-1.93
1996	Fricke	0.2004	0.202	-0.79
1997	ECB	5.4	5.58	-3.4
	ECB	25.4	26.94	-5.7
1998	ECB	6.006	6.069	-1.04
	ECB	24.00	25.68	-6.54
	Fricke	0.1997	0.2043	-2.25

4. CONCLUSION

Good agreement between dosimetry systems was obtained from the dose intercomparison studies. On the average the PNRI Fricke dosimeter gave an absorbed dose about 5% lower than that obtained by JAERI alanine. The average ratio of absorbed dose determined by PNRI ECB to that determined by JAERI alanine dosimeter was 1.00.

The results of the intercomparison with IDAS showed that dose measured by Fricke agreed to within ±1.7% of the IDAS estimated dose. On the other hand, results obtained from ECB were in agreement within ±4.4% that of alanine of IDAS.

The intercomparison between PMMA (Radix) and JAERI alanine dosimeters showed that there is good agreement (within ±2%) between the results using stationary and conveyor irradiation although geometry conditions and irradiation parameters are different.

These intercomparison studies have shown the reliability of the dosimetry systems of PNRI using ECB and Fricke dosimeters. The performance of the dosimetry systems being used by PNRI is acceptable for routine dose measurements in radiation processing in the Philippines.

ACKNOWLEDGEMENT

Part of this work was done while one of the authors (L.G. Lanuza) was on an IAEA on-the-job training in TRCRE, JAERI. The support of IAEA and JAERI during this fellowship is gratefully acknowledged. We also thank the Secondary Standards Dosimetry Laboratory of PNRI for their assistance.

REFERENCES

[1] CABALFIN, E.G., LANUZA, L.G., VILLAMATER, D.T., KOVACS, A., "Dose Measurements at the Philippine Multipurpose Gamma Irradiation Facility", High Dose Dosimetry for Radiation Processing (Proc. Symp. Vienna, 1990), IAEA, Vienna (1991) 357-370.

[2] McLAUGHLIN, W.L., BOYD, A.W., CHADWICK, K.H., McDONALD, J.C., MILLER, A., Dosimetry for Radiation Processing, Taylor and Francis, London (1989).

[3] AMERICAN SOCIETY FOR TESTING AND MATERIALS, Standard Practice for Use of the Ethanol-Chlorobenzene Dosimetry System, ASTM-E-1538-93, ASTM, Philadelphia, PA.

[4] AMERICAN SOCIETY FOR TESTING AND MATERIALS, Standard Practice for Using the Fricke Reference Standard Dosimetry System, ASTM-E-1026-95, ASTM, Philadelphia, PA.

[5] KOJIMA, T., TANAKA, R. "Polymer-Alanine Dosimeter and Compact Reader", Appl. Radiat. Isot. **40** (1989) 851-857.

[6] KOJIMA, T., HANEDA, N., MITOMO, S., TACHIBANA, H., TANAKA, R..,"The Gamma-ray Response of Clear Polymethylmethacrylate Dosimeter Radix RN15", Appl. Radiat. Isot. **43** (1992) 1197-1202.

[7] MEHTA, K., GIRZIKOWSKY, R. "Reference Dosimeter System of the IAEA", Radiat. Phys. Chem. **46** (1995) 1247-1250.

[8] KOJIMA, T., TACHIBANA, H., HANEDA, N., KAWASHIMA, I., SHARPE, P., "Uncertainty Estimation in ^{60}Co Gamma Ray Dosimetry at JAERI Involving a Two Way Dose Intercomparison Study with NPL in the Dose Range 1-50 kGy", accepted by Radiat. Phys. Chem. (1998).

DOSE INTERCOMPARISON STUDIES FOR STANDARDIZATION OF HIGH-DOSE DOSIMETRY IN VIET NAM

Hoang Hoa MAI , Nguyen Dinh DUONG
Irradiation Center,
Vietnam Atomic Energy Commission,
Hanoi, Viet Nam

T. KOJIMA
Japan Atomic Energy Research Institute,
Takasaki, Gunma,
Japan

Abstract

The Irradiation Center of the Vietnam Atomic Energy Commission (IC-VAEC) is planning to establish a traceability system for high-dose dosimetry and to provide high-dose standards as a secondary standard dosimetry laboratory (SSDL) level in Vietnam. For countries which do not have a standard dosimetry laboratory, the participation in the International Dose assurance Service(IDAS) operated by the International Atomic Energy Agency(IAEA) is the most common means to verify own dosimetry performance with a certain uncertainty. This is, however, only one-direction dose intercomparison with evaluation by IAEA including unknown parameter at participant laboratories. The SSDL level laboratory should have traceability as well as compatibility, ability to evaluate uncertainties of its own dosimetry performance by itself. In the present paper, we reviewed our dosimetry performance through two-way dose intercomparison studies and self-evaluation of uncertainty in our dosimetry procedure. The performance of silver dichromate dosimeter as reference transfer dosimeter in IC-VAEC was studied through two-way blind dose intercomparison experiments between the IC-VAEC and JAERI. As another channel of dose intercomparison with IAEA, alanine dosimeters issued by IDAS were simultaneously irradiated with the IC-VAEC dichromate dosimeters at IC-VAEC and analyzed by IAEA. Dose intercomparison between IC-VAEC and JAERI results into a good agreement (better than ±2.5%), and IDAS results also show similar agreement within ±3.0%. The uncertainty was self-estimated on the basis of the JAERI alanine dosimetry, and a preliminary value of about 1.86% at a 68% confidence level is established. The results from these intercomparisons and our estimation of the uncertainty are consistent. We hope that our experience is valuable to other countries which do not have dosimetry standard laboratories and/or are planning to establish them.

1. INTRODUCTION

A semi-commercial scale ^{60}Co gamma-ray irradiator, the first one in Vietnam, has been operated at IC-VAEC since 1991 for food irradiation and radiation sterilization of medical products. The facility is equipped with a plaque source (120 cm height × 60 cm width, 2.8×10^{15} Bq, 1997) and a hanger-type conveyor system. High-dose dosimetry techniques have been developed in IC-VAEC for the dose-rate profile measurements in the irradiation field and the product boxes, for optimization of processing parameters, and for validation and commissioning procedures. Since the national standards laboratory for high-dose is not yet established in Vietnam, the Fricke dosimetry was chosen as a tentative reference dosimetry on the basis of its G-value. The dichromate dosimetry was successively developed as a reference transfer system for high-dose[1,2], also see Refs [3,4,5]. Other routine dosimeters such as perspex dosimeters and ethanolchlorobenzene (ECB) dosimeter have also been tested.

IC-Vietnam is now expected to be a SSDL level laboratory in Vietnam in radiation processing and reliability check of dichromate dosimetry is required for high-dose dosimetry. The SSDL level laboratory should have traceability/compatibility not only one-way comparison through IDAS, but also through two-way comparison with a sort of SSDL level laboratories, besides demonstrating its ability to estimate uncertainty in dosimetry performance by itself.

For evaluation of the potentiality of IC-VAEC as a SSDL level laboratory, dose intercomparison studies were performed with JAERI involving JAERI alanine and IC-VAEC dichromate dosimeters, and with IDAS as yet another channel. Also, self-evaluation of the uncertainties for IC-VAEC dichromate reference transfer dosimetry system was carried out.

2. EXPERIMENTAL PROCEDURES

2.1. Dosimeter systems for dose intercomparison

The silver dichromate dosimeters prepared at IC-VAEC and commercially available alanine dosimeters were used for the present studies. Silver dichromate with two different initial concentration of Cr^{+6} ions according to useful dose range, Type(a) and Type(b), were prepared following the ASTM standard E1401-96 [5]:

Type(a) : dichromate dosimeter for dose range 1-12 kGy
0.5mM $Ag_2Cr_2O_7$ in 0.1M $HClO_4$
Type(b) : dichromate dosimeter for dose range 3-50 kGy
2.0mM $K_2Cr_2O_7$+0.5mM $Ag_2Cr_2O_7$ in 0.1M $HClO_4$.

Dosimeter bulk solution was oxygen-bubbled for one hour and irradiated with gamma rays up to a dose of 1 kGy before flame-sealing in 3 ml Pyrex glass ampoules.

The alanine-PS dosimeters (Aminogray, HITACHI Cable Ltd.) prepared with 70 wt% of DL-α-alanine and 30 wt% of polystyrene were provided by JAERI or IAEA for these dose intercomparison studies. The alanine dosimeter is a rod of 3 mm dia. and 30 mm length, which is put in a capped polystyrene capsule with 4-mm thick wall. The ESR-spectrometry analysis of irradiated alanine dosimeters were performed using a compact ESR reader at the JAERI [6,7] or a ESR spectrometer ESP-300 (Bruker) at IAEA.

2.2. ^{60}Co Gamma-ray irradiation

The irradiation of dosimeters was carried out using the above-described γ-ray irradiation facility at IC-VAEC under electron equilibrium condition. The dose rate at the calibration position was estimated by air-saturated Fricke dosimeters, which were prepared in 2.5 ml sealed glass ampoules (10 mm dia and 25 mm solution length). Fricke dosimeter at IC-VAEC is well-characterized and satisfies the requirements stated in the ASTM Standard Practice E1026-95 [8]. An absorbed dose (to water) rate at the calibration position was 34.54 Gy/min (February 1997), and transient dose was 0.023 kGy. The irradiation of dosimeters at JAERI was performed using a plaque ^{60}Co γ-ray source (3.8×10^{15} Bq, 37.4 cm in width and 45.0 cm in height). The dose rate at the irradiation point was estimated using the parallel-plate free-air ionization chamber periodically calibrated at the Electrotechnical Laboratory, the primary standard laboratory in Japan [9].

2.3. Traceability and its verification plan in Vietnam

There are different channels for traceability check with the national and/or international standard laboratory[4]. Traceability checks and calibration chain of different class dosimeters in Vietnam is

under the planning stage as shown in Fig.1, involving two different dose intercomparisons. As one channel, dichromate as a tentative reference transfer dosimeter is used to compare with alanine transfer dosimeters calibrated by the ionization chamber which maintains traceability to the Japan national standard laboratory [9]. The dose rate at the calibration position in the in-house irradiation facility of the IC-VAEC was measured using Fricke dosimeter and then verified by JAERI alanine transfer dosimetry. In another rout to maintain traceability and performance check of local reference dosimeters, the intercomparison experiments have been performed with the IAEA through the IDAS [10,11].

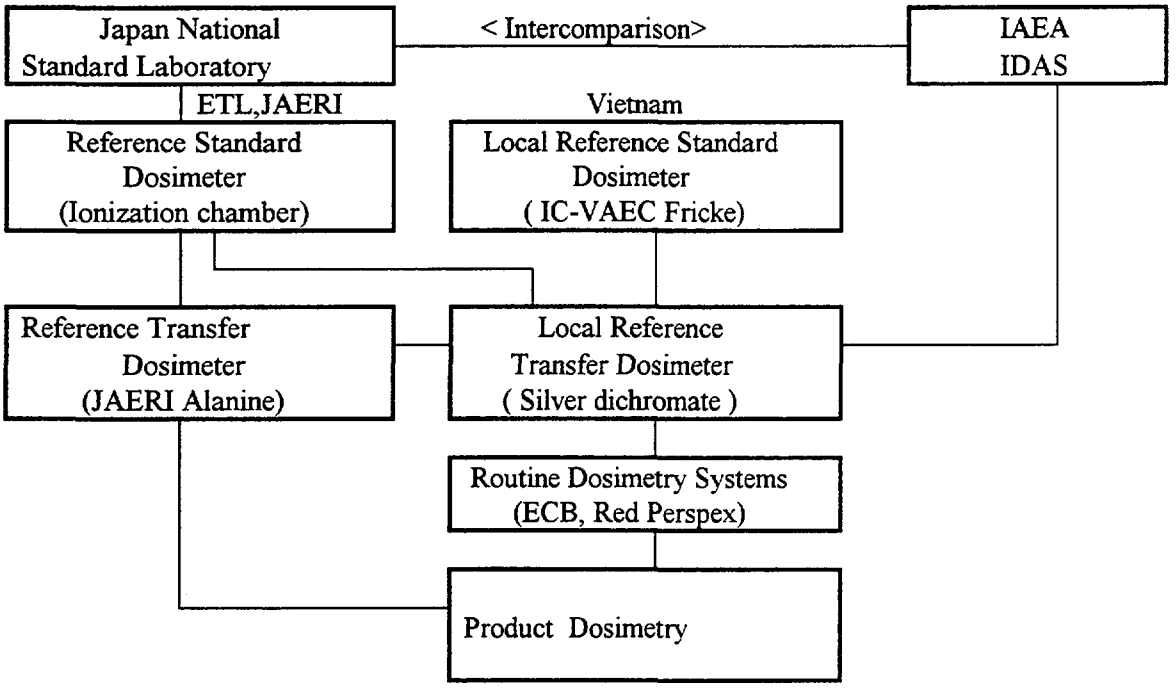

FIG. 1. The schematic diagram of traceability and international calibration chains of high-dose dosimetry at IC-VAEC under planning.

3. RESULTS AND DISCUSSION

3.1. Dose Intercomparison between IC-VAEC and JAERI

The gamma ray dose intercomparison experiments have been periodically carried out between IC-VAEC and JAERI since 1994 [2]. Dichromate dosimeters of the IC-VAEC were mailed to JAERI and then returned after irradiation for spectrophotometry analysis at IC-VAEC. While the JAERI alanine dosimeters were mailed to the in-house facility at the IC-VAEC and returned after irradiation to JAERI for ESR analysis.

The results of the dose intercomparison experiments carried out in March 1997 and May 1998 with JAERI alanine are listed in Table I. The relative deviations between the absorbed dose values quoted by IC-VAEC and those estimated at JAERI are within ± 2.5% in the dose range of 5-25 kGy. The results of the dose intercomparison experiments of March 1997 using IC-VAEC dichromate dosimeters are shown in Table II. The dose values estimated at the IC-VAEC are in agreement with dose values quoted by JAERI within ±2.3% for both types of dichromate dosimeters, type(a) and (b).

TABLE I. DOSE INTERCOMPARISON EMPLOYING JAERI ALANINE DOSIMETERS WHICH WERE IRRADIATED AT IC-VAERC

Irradiation Laboratory	Readout Laboratory	Quoted dose (kGy)	Estimated dose (kGy)	Relative deviation, %
IC-VAEC	JAERI	5.0	4.97	+0.6
		10.0	9.89	+1.1
		15.0	14.80	+1.3
		25.0	24.39	+2.4

TABLE II. DOSE INTERCOMPARISON EMPLOYING IC-VAEC DICHROMATE DOSIMETERS WHICH WERE IRRADIATED AT JAERI

Dosimeter	Irradiation laboratory	Readout laboratory	Quoted dose, kGy	Estimated dose, kGy	Relative deviation, %
Type (a)	JAERI	IC-VAEC	10.0	9.84	-1.6
Type (b)	JAERI	IC-VAEC	10.0	10.18	+1.8
			30.0	30.69	+2.3

3.2. Dose intercomparison through IAEA-IDAS

As another channel, IC-VAEC applied to IDAS for the verification of its dosimetry performance. The measurements were carried out in March 1997 and in May 1998. The two alanine dosimeter sets provided by the IDAS and three IC-VAEC dichromate dosimeters were irradiated with ^{60}Co gamma rays for 10 and 15 kGy in the IC-VAEC irradiation field at a dose rate of about 2 kGy/h. The IC-VAEC dichromate dosimeters were readout at IC-VAEC to quote absorbed doses given to IDAS alanine dosimeters, while the alanine dosimeters after irradiation were returned to the IAEA for analysis. The results of the IDAS measurements are summarized in Table III. The relative deviations between the dose values estimated by IDAS and that quoted by IC-VAEC were -2.9% and -2.78%. These deviations are within the acceptance limit of the IDAS, ±5%, although the values given by IC-VAEC dichromate system seems to have a tendency of a lower value than those given by IDAS.

TABLE III. DOSE INTERCOMPARISON STUDY THROUGH IDAS

Dosimeter	Irradiation laboratory	Readout laboratory	Date of study	Estimated dose, kGy	Relative deviation, %
IDAS alanine	IC-VAEC	IDAS	Mar.1997	11.02	-2.90
IC-VAEC dichromate	IC-VAEC	IC-VAEC	Mar.1997	10.70	
IDAS alanine	IC-VAEC	IDAS	May.1998	15.03	-2.78
IC-VAEC dichromate	IC-VAEC	IC-VAEC	May.1998	14.46	

3.3. Uncertainty estimation on performance of silver-dichromate dosimetry at IC-VAEC

To be recognised as a SSDL-level laboratory, IC-VAEC should have an ability to estimate the uncertainty of its dichromate reference transfer dosimetry. The following is the preliminary estimation of the uncertainties for each component of the IC-VAEC dosimetry procedure on the basis of the JAERI alanine transfer dosimetry. Each uncertainty component is classified as either "Type A" and "Type B",

which are respectively defined as uncertainty estimated by experiments and that cited from published report or based on other information, according to the ASTM standard 1707-95 [12].

The dichromate dosimetry system at IC-VAEC has the major uncertainty components as follows:
- uncertainty arising from the characterization of the irradiation field and calibration point;
- uncertainty arising from the calibration procedure of the dosimetry system; and
- uncertainty arising from the dose estimation using the calibrated dosimetry system.

The dichromate dosimetry system consists of the dosimeter ampoules, the spectrophotometer and the calibration curve with mathematical fitting. The uncertainties in the absorbance measurement and wavelength setting of the spectrophotometer were determined by repeating measurements using a standard holmium filter. These uncertainty components are regarded as negligible. The uncertainty due to intra-batch absorbance variation of dichromate dosimeters was estimated from measured values for 30 dosimeters that were randomly picked from the same batch. The uncertainties associated with calibration of dosimeters and curve fittings were evaluated as per the ASTM standard guide E 1707-95. Table IV lists the uncertainty components in the calibration procedure of the dichromate dosimetry system, including that transferred from JAERI [13]. All components of uncertainty are expressed in percentage (%) at 1σ (approximating at a 68% confidence level), and combined to determine the overall uncertainty, which is the square root of the sum of their squares.

TABLE IV. UNCERTAINTY IN THE CALIBRATION OF DICHROMATE DOSIMETRY

	Component of uncertainty	Type A, %	Type B, %
4.1	Dose rate at IC-VAEC given by JAERI alanine	0.63	1.60
4.2	Source decay correction (every two days)	0.02	0.01
4.3	Irradiation timing(1sec)	0.03	
4.4	Positioning of dosimeters	0.19	
4.5	Averaging of response of three dosimeter replicates	0.23	
4.6	Temperature effect during irradiation ($\leq \pm 1°C$)	0.20	
4.7	Absorbance variation in one batch of dosimeter sol.	0.36	
4.8	Fitting goodness of calibration curve		0.47
4.9	Type A and Type B combined, separately	0.81	1.67
4.10	Overall uncertainty: combined A & B in quadrature	1.86	

The quoted uncertainty of the JAERI alanine transfer dosimetry was 1.72 % at 1σ. The variation of the irradiation timing was estimated to be 0.7 s, and its contribution is about 0.03 % in case of 1 kGy when the irradiation time is about 2,000 s. The precision of positioning of the JAERI alanine and the dichromate dosimeters at the same calibration point was estimated to be 0.19% according to the scattering of the center of the effective volume within ±2 mm. The uncertainty in averaging of dose response of three dosimeter replicates is 0.23 % including dose rate distribution in the effective volume. The variation of temperature during irradiation for calibration is $\leq \pm 1$ °C and results into uncertainty of 0.20 % in correction of temperature dependence of alanine and dichromate dosimeters, with the temperature coefficients of 0.2 % [7] and -0.2 % [3,14], respectively. Variation of the absorbance in the same batch of solution is 0.36 % including uncertainty of spectrophotometry. The uncertainty related to the calibration curve fitting with the first-order function is 0.47 %. From combination of these uncertainty components in quadrature, overall uncertainty in dichromate dosimetry at IC-VAEC is estimated to be 1.86 % at a 68 % confidence level. This preliminary estimate of the uncertainty value is, however, smaller than the difference in the dose intercomparison studies. It might be necessary to seek more uncertainty components in dichromate dosimetry with more careful reviewing of our dosimetry procedure.

4. SUMMARY

The dose intercomparison studies were carried out at IC-VAEC through two different channels. Relatively good agreement (within ±3%) was obtained for both dose intercomparison studies with JAERI and IDAS. The uncertainty in dichromate dosimetry as a local reference transfer dosimetry at IC-VAEC was estimated to be 1.86% by reviewing dosimetry procedures. The combination of the results of the dose intercomparison and the preliminary study of the uncertainties in dichromate dosimetry demonstrates a potentiality to establish a SSDL level laboratory at IC-VAEC which has also maintain compatibility with other SSDL level laboratories as well as metrological ability of self-evaluation of uncertainty in own dosimetry.

This kind of dose intercomparison study and self-evaluation study of uncertainty for own reference transfer dosimetry should contribute towards establishing the SSDL level laboratory in Vietnam, as well as other countries without domestic dosimetry standard laboratories.

ACKNOWLEDGEMENTS

This study is partly supported by the International Atomic Energy Agency. The authors appreciate the financial support provided by the IAEA, and would like to thank Dr. Kishor Mehta of the IAEA for his continuous interest and discussion on this paper.

REFERENCES

[1] MAI H.H., DUONG NG. D., "Silver dichromate – a suitable dosimeter for radiation processing" Preprint (Vietnam Atomic Energy Commission) VAEC-E-26 (1995).

[2] MAI H.H., DUONG NG. D., KOJIMA T., "γ-Ray dose intercomparison in absorbed dose range, 5-50 kGy, using dichromate and alanine dosimeters" Int. J.Appl.Radiat.Isot., **47**(1996)259-261.

[3] SHARPE P. H. G., BARRET J. H., BERKLY A. M. "Acidic aqueous dichromate solution as reference dosimeter in the 10-40 kGy range", Int.J.Appl.Radiat.Isot. **36**(1985)647-652.

[4] MCLAUGHLIN W. L. et al., "Dosimetry for radiation processing", (1989) pp. 81-87, pp. 148-149, pp.173-175, Taylor & Francis, London.

[5] ASTM Standard Practice E1401-91 (1997). "Standard practice for use of the dichromate dosimetry system", Annual Book of the ASTM standards, Vol. 12.02, Nuclear (II), Solar, and Geothermal Energy, pp.801-805 (American Society for Testing and Materials, Philadelphia)

[6] KOJIMA T., TANAKA R. "Polymer-alanine dosimeter and compact reader", Int. J. Appl. Radiat.Isot. **40**(1989) 851-857.

[7] KOJIMA T. et al., "Recent progress in JAERI alanine/ESR dosimetry system", Radiat.Phys. Chem.,40(1993)813-816.

[8] ASTM Standard Practice E1026-95 (1997). "Standard practice for using the Fricke reference standard dosimetry system", Annual Book of the ASTM standards, Vol. 12.02, Nuclear (II), Solar, and Geothermal Energy, pp.801-805 (American Society for Testing and Materials, Philadelphia)

[9] TANAKA R. et al., "Standard measurement of processing level gamma ray dose rates with parallel-plate ionization chamber. Proceedings of the International Symposium on High-Dose Dosimetry for Radiation Processing (IAEA, 1984), **STI/PUB/67** (1985) 203-320(IAEA, Vienna)

[10] MEHTA K. K., GIRZIKOWSKY R., "IAEA activities on high-dose measurements", IAEA SSDL Newsletter **31**(1992), 31-37.

[11] MEHTA K. K., GIRZIKOWSKY R., "Reference dosimeter system of the IAEA", Radiat. Phys.Chem.**35**(1995)757-761.

[12] ASTM Standards Guide E1707-95(1997), "Standard Guide for Estimating Uncertainties in Dosimetry for Radiation Processing, Annual Book of the ASTM standards, Vol. 12.02, Nuclear (II), Solar, and Geothermal Energy, pp.853-872 (American Society for Testing and Materials, Philadelphia)

[13] KOJIMA T. et al., "Uncertainty estimation in ^{60}Co gamma-ray dosimetry at JAERI involving a two- way dose intercomparison study with NPL in the dose range 1-50 kGy", accepted by Radiat.Phys.Chem., to be published (1999).

[14] MAI H.H., TACHIBANA H., KOJIMA T., "Effects of temperature during irradiation and spectrophotometry analysis on the dose response of aqueous dichromate dosimeters", **53**(1998) 85-91

LIST OF PARTICIPANTS

Andreo, P.
Dosimetry and Medical Radiation Physics Section,
International Atomic Energy Agency,
P.O. Box 100, A-1400 Vienna,
Austria

Benny, P.G.
Isotope Division,
Bhabha Atomic Research Centre,
Trombay, Mumbai 400 085,
India

Bhuiyan, N.U.
Institute of Nuclear Science & Technology,
AERE,
G.P.O. Box 3787, Dhaka-1000,
Bangladesh

Biramontri, S.
Office of Atomic Energy for Peace,
Vibhavadi Rangsit Road,
Chatuchak, Bangkok 10900,
Thailand

Bof, E.S.
Comisión Nacional de Energía Atómica,
Avenida del Libertador 8250,
1429 Buenos Aires, Argentina

Bugay, O.
Institute of Semiconductor Physics,
Prospekt Nauki, 45,
252650 Kiev, Ukraine

Calvert, G.W.
ISOMEDIX,
11 Apollo Drive,
Whippany, New Jersey 07981,
United States of America

Chu, R.D.H.
MDS Nordion,
447 March Road,
Kanata, Ontario K2K 1X8,
Canada

de Lima, W.
Instituto de Pesquisas Energéticas e Nucleares,
Travessa "R", no. 400, Cidade Universitária,
05508-900 Sao Paulo, Brazil

Desai, R.
The Gujarat Cancer and Research Institute,
Compound of Civil Hospital,
Asarwa, Ahmedabad 380016, India

Dodbiba, A.
Institute of Nuclear Physics,
Tirana, Albania

Dolo, J.-M.	Commissariat à l'énergie atomique, CEA Centre d'études de Saclay, F-91191 Gif-sur-Yvette Cedex, France
Ebraheem, S.	National Center for Radiation Research and Technology, P.O. Box 29, Nasr City, Cairo, Egypt
Ehlermann, D.	Institute of Process Engineering, Federal Research Centre for Nutrition, Haid-und-Neu-Strasse 9, D-76131 Karlsruhe, Germany
El-Assaly, F.M.	Radiation Protection Department, Ministry of Health, P.O. Box 1853, Dubai, United Arab Emirates
Emi-Reynolds, G	National Nuclear Research Institute, Ghana Atomic Energy Commission, Box 80, Legon, Accra, Ghana
Falvi, L.	Institute of Isotopes Co. Ltd., Konkoly Thege M. út 29-33, H-1121 Budapest, Hungary
Farrar IV, H.	18 Flintlock Lane, Bell Canyon, California 91307-1127, United States of America
Fassbender, A.G.	Sunna Systems Corporation, 3100 George Washington Way, Richland, Washington 99352, United States of America
Fathony, M.	Centre for Standardization and Radiological Safety Research, PSPKR-Batan, Jl. Cinere Pasar Jumat, P.O.Box 7043 JKSKL, Jakarta 12070, Indonesia
Fuochi, P.	Istituto di Fotochimica e Radiazioni d'alta energia, Via P. Gobetti 101, I-40129 Bologna, Italy
Gant, G.J.	Australian Nuclear Science and Technology Organization, Private Mail Bag 1, Menai, NSW 2234, Australia

Gao, Jun-Cheng.	Ionizing Radiation Division, National Institute of Metrology, No. 18, Bei San Huan Dong Lu, Beijing 100013, China
Girzikowsky, R.	Dosimetry and Medical Radiation Physics Section, International Atomic Energy Agency, Agency's Laboratories, A-2444 Seibersdorf, Austria
Ilijaš, B	Ruder Bošković Institute, c/o D. Ražem, Bijenička Cesta 54, P.O. Box 1016, HR-41000 Zagreb, Croatia
Inokuti, Mitio	International Commission on Radiation Units and Measurements Physics Division, Argonne National Laboratory, 9700 South Cass Avenue, Argonne, Illinois 60439-4843, United States of America
Janovsky, I.	Institut für Oberflächenführung, Permoserstrasse 15, D-04303 Leipzig, Germany
Jia, Haishun	Department of Chemistry, Beijing Normal University, Beijing 100875, China
Jurina, V.	Ministry of Health, Limbová 2, P.O. Box 52, SK-833 43 Bratislava, Slovakia
Kałuska, I.	Institute of Nuclear Chemistry and Technology, Dorodna 16, PL-03-195 Warsaw, Poland
Kawamata, T.	Radia Industry Co. Ltd., 168 Ooyagi, Takasaki, Gunma 370-0072, Japan
Khan, Hasan M.	National Centre of Excellence in Physical Chemistry, University of Peshawar, Peshawar 25120, Pakistan
Kojima, T.	Japan Atomic Energy Research Institute, Takasaki Radiation Chemistry Establishment, 1233 Watanuki-machi, Takasaki-shi, Gunma 370-1292, Japan

Kovács, A.	Institute of Isotopes and Surface Chemistry, Chemical Research Center, Hungarian Academy of Sciences, Konkoly Thege M. út 29-33, H-1121 Budapest, Hungary
Kuntz, F.	Aérial, 19 rue de Saint-Junien, B.P. 23, F-67305 Schiltigheim, Cedex, France
Lanuza, L.G.	Philippine Nuclear Research Institute, Commonwealth Avenue, Diliman, Quezon City, Philippines
Lee, Chin-Min	World Health Organization, c/o United Nation System, Vienna International Centre, Wagramerstrasse 5, A-1400 Vienna, Austria
Lin, Min	Radiometrology Centre, China Institute of Atomic Energy, P.O. Box 275 (20), Beijing 102413, China
Linares, M.A.	Instituto Peruano de Energía Nuclear, Avda. Canada 1470, San Borja, Lima, Peru
McEwen, M.R.	National Physical Laboratory, Queens Road, Teddington, TW11 0LW, United Kingdom
McLaughlin, W.L.	Ionizing Radiation Division, National Institute of Standards and Technology, Building 245/C229, Gaithersburg, Maryland 20899-0001, United States of America
Mehta, K.	Dosimetry and Medical Radiation Physics Section, International Atomic Energy Agency, P.O. Box 100, A-1400 Vienna, Austria
Miller, S.D.	Sunna Systems Corporation, 3100 George Washington Way, Richland, Washington 99352, United States of America

Mittendorfer, J.	Mediscan GmbH, Bad Hallerstrasse 34, A-4550 Kremsmünster, Austria
Mod Ali, N.	Radiation Processing Group, Malaysian Institute for Nuclear Technology Research, 43000 Kajang, Selangor, Malaysia
Nikolova, M.	Elgatech Ltd., "Atanas Kirchev" Str. 76, A, BG-1330 Sofia, Bulgaria
Panta, P.	Institute of Nuclear Chemistry and Technology, Dorodna 16, PL-03-195 Warsaw, Poland
Pivovarov, S.	Institute of Nuclear Physics, National Nuclear Center, 13 Republic Square, Almaty 480013, Kazakhstan
Poli, D.C.R.	Instituto de Pesquisas Energéticas e Nucleares, Travessa "R", no. 400, Cidade Universitária, 05508-900 Sao Paulo, Brazil
Prieto Miranda, E.F.	Instituto de Investigaciones para la Industria Alimenticia, c/o Calle 121 # 4518 entre 45 y 49, Marianao, Ciudad de la Habana, Cuba
Ražem, D.	Ruder Bošković Institute, Bijenička Cesta 54, P.O. Box 1016, HR-41000 Zagreb, Croatia
Regulla, D.F.	Institute of Radiation Protection, GSF- National Research Center for Environment and Health, Postfach 1129, D-85764 Neuherberg, Germany
Roginets, L.P.	Radiation Physics and Chemistry Problems Institute, Belarus Academy of Sciences, Minsk-Sosny 220109, Belarus

Saravi, M.	División Dosimetría, Comisión Nacional de Energía Atómica, Avenida del Libertador 8250, AR-1429 Buenos Aires, Argentina
Saylor, M.C.	Special Process Services L.C., 2203 Cedar Mill Court, Vienna, Virginia 22182, United States of America
Sharpe, P.H.G.	Division of Radiation Science and Acoustics, National Physical Laboratory, Queens Road, Teddington, Middlesex TW11 0LW, United Kingdom
Slezsák, I.	Z. Bay Applied Research Foundation, Budapest, Hungary
Stenger, V.	Institute of Isotopes Co. Ltd., Konkoly Thege M. út 29-33, H-1121 Budapest, Hungary
Stuglik, Z.	Institute of Nuclear Chemistry and Technology, Dorodna 16, PL-03-195 Warsaw, Poland
Vanhavere, F.	CEN-SCK, Belgian Nuclear Research Centre, Boeretang 200, B-2400 Mol, Belgium
Wagner, M.	Abteilung für Medizinische Physik, Landeskrankenhaus Feldkirch, Carinagasse 47, A-6800 Feldkirch, Austria
Watts, M.F.	Harwell Dosimeters Ltd, 10-30 Harwell, Didcot, Oxfordshire OX11 ORA, United Kingdom
Whittaker, B.	3 Mayfield Avenue, Grove, Wantage, Oxfordshire OX12 7PU, United Kingdom
Wilcott, T.	Becton Dickinson and Company, 1 Becton Drive, Franklin Lakes, New Jersey 07417, United States of America

Yordanov, N.
Institute of Catalysis,
Bulgarian Academy of Sciences,
BG-1113 Sofia, Bulgaria

Zagórski, Z.P.
Department of Radiation Chemistry,
Institute of Nuclear Chemistry and Technology,
Dorodna 16,
PL-03-195 Warsaw, Poland